

## REPORT DOCUMENTATION PAGE

Form Approved  
OMB NO. 0704-0188

Public reporting burden for this collection of information is estimated to average 1 hour per response, including the time for reviewing instructions, searching existing data sources, gathering and maintaining the data needed, and completing and reviewing the collection of information. Send comment regarding this burden estimate or any other aspect of this collection of information, including suggestions for reducing this burden, to Washington Headquarters Services, Directorate for Information Operations and Reports, 1215 Jefferson Davis Highway, Suite 1204, Arlington, VA 22202-4302, and to the Office of Management and Budget, Paperwork Reduction Project (0701-0188), Washington, DC 20503.

1. AGENCY USE ONLY (Leave blank)		2. REPORT DATE 9/14/97	3. REPORT TYPE AND DATES COVERED Technical Report	
4. TITLE AND SUBTITLE Two-phase Flow in Microchannels			5. FUNDING NUMBERS DAAH04-94-G-0348	
6. AUTHOR(S) Roger S. Stanley Timothy A. Ameel Randall F. Barron			8. PERFORMING ORGANIZATION REPORT NUMBER	
7. PERFORMING ORGANIZATION NAME(S) AND ADDRESS(ES) Louisiana Tech University P.O. Box 7923 T.S. Ruston, LA 71272				
9. SPONSORING / MONITORING AGENCY NAME(S) AND ADDRESS(ES) U.S. ARMY RESEARCH OFFICE P.O. BOX 12211 RESEARCH TRIANGLE PARK, NC 27709-2211			10. SPONSORING / MONITORING AGENCY REPORT NUMBER  ARO 33844.3-PH-DPS	
11. SUPPLEMENTARY NOTES  The views, opinions and/or findings contained in this report are those of the author(s) and should not be construed as an official Department of the Army position, policy, or decision, unless so designated by other documentation.				
12a. DISTRIBUTION / AVAILABILITY STATEMENT  Approved for public release; distribution unlimited.			12b. DISTRIBUTION CODE	
13. ABSTRACT (Maximum 200 words)  The purpose of this study was to investigate fluid mechanic and heat transfer characteristics of two-phase two-component flow in rectangular microchannels. Experiments were conducted using rectangular aluminum channels with hydraulic diameters ranging between 56 $\mu\text{m}$ and 256 $\mu\text{m}$ and aspect ratios which varied from 0.5 to 1.5. Both single- and two-phase tests were conducted using water and gaseous argon, helium, and nitrogen as the working fluids. The Reynolds number for both types of experiments ranged from approximately 50 to nearly 10,000. The Nusselt number ranged between 0.0002 and 70. The single- and two-phase experimental data were empirically correlated, using parameters derived from a dimensional analysis. Experimental data were also used to correlate the unknown variables in derived analytical expressions.  Both single- and two-phase tests yielded excellent correlations of the friction factor. For Nusselt number, the correlations were fair to poor. Reynolds number and the combination of Reynolds number and Prandtl number were the dominant parameters in the prediction of pressure drop and heat transfer rate, respectively, in both single- and two-phase flows. The pressure drop predictions based on the semi-empirical relations by Martinelli for two-phase flows were shown to substantially over-predict the pressure drop measured in these experiments.				
14. SUBJECT TERMS Convection heat transfer, microchannel flow, two-phase fluids			15. NUMBER OF PAGES 348	
			16. PRICE CODE	
17. SECURITY CLASSIFICATION OR REPORT UNCLASSIFIED	18. SECURITY CLASSIFICATION OF THIS PAGE UNCLASSIFIED	19. SECURITY CLASSIFICATION OF ABSTRACT UNCLASSIFIED	20. LIMITATION OF ABSTRACT  UL	

DTC QUALITY IMPROVING

TWO-PHASE FLOW AND HEAT TRANSFER IN MICROCHANNELS

TECHNICAL REPORT

ROGER S. STANLEY  
TIMOTHY A. AMEEL

MARCH, 1997

U.S ARMY RESEARCH OFFICE

CONTRACT/GRANT NUMBER  
DAAH04-94-G-0348

LOUISIANA TECH UNIVERSITY  
P.O. BOX 7923 T.S.  
RUSTON, LA 71272

APPROVED FOR PUBLIC RELEASE;  
DISTRIBUTION UNLIMITED.

THE VIEWS, OPINIONS, AND/OR FINDINGS CONTAINED IN THIS REPORT ARE  
THOSE OF THE AUTHOR(S) AND SHOULD NOT BE CONSTRUED AS AN OFFICIAL  
DEPARTMENT OF THE ARMY POSITION, POLICY, OR DECISION, UNLESS SO  
DESIGNATED BY OTHER DOCUMENTATION

19971007 119

## ABSTRACT

The purpose of this study was to investigate fluid mechanic and heat transfer characteristics of two-phase two-component flow in rectangular microchannels. Experiments were conducted using rectangular aluminum channels with hydraulic diameters ranging between 56  $\mu\text{m}$  and 256  $\mu\text{m}$  and aspect ratios which varied from 0.5 to 1.5. Both single- and two-phase tests were conducted using water and gaseous argon, helium, and nitrogen as the working fluids. The Reynolds number for both types of experiments ranged from approximately 50 to nearly 10,000. The Nusselt number ranged between 0.0002 and 70. The single- and two-phase experimental data were empirically correlated, using parameters derived from a dimensional analysis. Experimental data was also used to correlate the unknown variables in derived analytical expressions.

Both single- and two-phase tests yielded excellent correlations of the friction factor. For Nusselt number, the correlations were fair to poor. Reynolds number and the combination of Reynolds number and Prandtl number were the dominant parameters in the prediction of pressure drop and heat transfer rate, respectively, in both single- and two-phase flows. The pressure drop predictions based on the semi-empirical relations by Martinelli for two-phase flows were shown to substantially over predict the pressure drop measured in these experiments.

Other findings showed that for single-phase flow, the transition from laminar to turbulent regimes of the friction factor was suppressed as the channel hydraulic diameter decreased. For gases, the suppression occurred in varying degrees between hydraulic diameters of 80  $\mu\text{m}$  and 150  $\mu\text{m}$ , with no transition seen below 80  $\mu\text{m}$  . For water, no transition was seen for any of the channel configurations tested. Two-phase friction factor data showed a definite transition from laminar to turbulent regimes at a Reynolds number of 3,000 for all channel configurations tested. It is believed that the transition was due to the intense pressure fluctuations associated with two-phase flows. For the Nusselt number, both single- and two-phase data was seen to parallel, though lower, the macroscale turbulent regime predictions. Also, no transition from laminar to turbulent regimes was seen in the Nusselt number data over the range of Reynolds numbers tested.



## TABLE OF CONTENTS

ABSTRACT .....	iii
LIST OF TABLES .....	ix
LIST OF FIGURES .....	x
ACKNOWLEDGMENTS .....	xiii
CHAPTER 1: INTRODUCTION .....	1
CHAPTER 2: LITERATURE SURVEY .....	4
Single Phase Flow in Microchannels .....	5
Friction Factor .....	5
Nusselt Number .....	7
Two-Phase Flow Boiling in Microchannels .....	8
Experimentation and Findings .....	8
Experimental Data Comparison .....	13
Two-Phase Two-Component Flow in Channels .....	17
Macroscale .....	17
Microscale .....	22
CHAPTER 3: GOVERNING EQUATIONS AND FLOW REGIMES .....	24
Homogeneous Flow .....	25
Conservation of Mass .....	26
Conservation of Momentum .....	28
Conservation of Energy .....	34
Separated Flow .....	36

Conservation of Mass .....	37
Conservation of Momentum .....	37
Conservation of Energy .....	44
Two-Phase Two-Component Flow Regimes .....	45
Macroscale .....	45
a) Bubble Flow .....	45
b) Plug Flow .....	45
c) Stratified Flow .....	45
d) Wavy Flow .....	47
e) Slug Flow .....	47
f) Annular Flow .....	47
g) Mist Flow .....	47
Microscale .....	48
a) Bubble Flow .....	48
b) Slug Flow .....	50
c) Plug Flow .....	50
d) Annular Flow .....	50
e) Mist Flow .....	51
CHAPTER 4: DIMENSIONAL AND EMPIRICAL ANALYSIS .....	52
Dimensional Analysis .....	52
Pressure Drop .....	53
Heat Transfer .....	56
Separated Flow Model and Other Considerations .....	59
Empirical Relations .....	62

## CHAPTER 5: EXPERIMENTAL APPARATUS, PROCEDURE, AND

CALCULATIONS .....	68
Experimental Apparatus .....	68
Test Section .....	68
Test Fixture .....	84
Flow Loop .....	86
Experimental Procedure .....	93
Experimental Calculations .....	101
CHAPTER 6: ANALYSIS OF RESULTS .....	112
Single-Phase Flow Results .....	113
Friction Factor .....	115
Nusselt Number .....	121
Two-Phase Flow results .....	124
Two-Phase Friction Factor .....	125
Homogeneous Flow .....	125
Separated Flow .....	127
Nusselt Number .....	128
Analytical Flow Models .....	129
Homogeneous Flow .....	129
Separated Flow .....	131
Flow Regimes .....	134
Other Heat Transfer Comparisons .....	134
Error Analysis .....	136
Final Summary of Equations .....	142

CHAPTER 7: CONCLUSION AND RECOMMENDATIONS .....	178
Study Summary .....	178
Recommendations for Future Research .....	181
APPENDIX A: FORTRAN program to solve for correlation coefficients .....	182
APPENDIX B: Manufactures addresses and products .....	198
APPENDIX C: Measured data .....	201
APPENDIX D: Reduced data .....	286
BIBLIOGRAPHY .....	343
VITA .....	348

## LIST OF TABLES

Table 1: Martinelli Constants .....	19
Table 2: Values of Constant C .....	19
Table 3: Measured Channel Dimensions .....	71
Table 4: Bias and precision error for experimental measured values. ....	137
Table 5: Single-phase Nusselt number uncertainty .....	141
Table 5: Two-phase Nusselt number uncertainty .....	141

## LIST OF FIGURES

Figure 2.1: Critical heat flux comparison for mini- and microgeometries .....	14
Figure 2.2: Heat transfer coefficient comparison for mini- and microgeometries ...	14
Figure 2.3: Critical heat flux ranges .....	16
Figure 2.4: Flow Regime Map by Baker (1954) .....	21
Figure 3.1: Homogeneous flow model control volume .....	27
Figure 3.2: Separated flow model control volume .....	38
Figure 3.3: Macroscale two-phase flow regimes .....	46
Figure 3.4: Microscale two-phase flow regimes .....	49
Figure 5.1: Test Section; a) Dimensions, b) Cross-section, c) Component description, and d) Thermocouple numbering and locations, approximately 0.01" beneath channels. ....	69
Figure 5.2: Model for determining channel spacing. ....	78
Figure 5.3: Test fixture assembly. ....	85
Figure 5.4: Schematic of experimental flow loop. ....	87
Figure 5.5: General layout of flow loop apparatus (flow loop components). ....	88
Figure 5.6: General layout of flow loop apparatus (entire apparatus). ....	88
Figure 5.7: Test fixture components. ....	90
Figure 5.8: Test fixture. ....	90
Figure 5.9: Detail of test fixture components without test section installed. ....	91
Figure 5.10: Detail of test fixture without test section installed. ....	91
Figure 6.1: All single-phase friction factor data. ....	146
Figure 6.2: All single-phase Nusselt number data. ....	147

Figure 6.3:	Water friction factor data with channel configuration indicated. ....	148
Figure 6.4:	Friction factor correlation of water in all channel sizes. ....	149
Figure 6.5:	Nitrogen gas friction factor data for specified channels showing transition suppression. ....	150
Figure 6.6:	Friction factor correlation of all gas data for channels with hydraulic diameter between 150 $\mu\text{m}$ and 250 $\mu\text{m}$ . ....	151
Figure 6.7:	Friction factor correlation of all gas data for channels with hydraulic diameter between 50 $\mu\text{m}$ and 150 $\mu\text{m}$ . ....	152
Figure 6.8:	Comparison of friction factor data with correlations of Chapter 2. ....	153
Figure 6.9:	Nusselt number correlation of all gases for all channel sizes. ....	154
Figure 6.10:	Correlation of Nusselt number data for all fluids and all channel sizes. ....	155
Figure 6.11:	Comparison of Nusselt number data with correlations from Chapter 2. ....	156
Figure 6.12:	All two-phase friction factor data for all channel sizes. ....	157
Figure 6.13:	All two-phase Nusselt number data for all channel sizes. ....	158
Figure 6.14:	Correlation of two-phase friction factor data for all channel sizes. ....	159
Figure 6.15:	Modified correlation of laminar two-phase friction factor data for all channel sizes. ....	160
Figure 6.16:	Correlation of Turbulent two-phase friction factor data for all channel sizes using the separated flow model parameters. ....	161
Figure 6.17:	Correlation of two-phase Nusselt number data for all channel sizes using the homogeneous flow model parameters. ....	162
Figure 6.18:	Regions of friction factor $f_{fa}$ calculated by equation (6.12). ....	163
Figure 6.19:	Correlation of $f_{fa}$ data for $f_{fa} < 0.005$ . ....	164
Figure 6.20:	Correlation of $f_{fa}$ data for $f_{fa} > 0.005$ . ....	165
Figure 6.21:	Correlation of $\phi_f^2$ over the lower range of $f_{fa}$ . ....	166

Figure 6.22: Correlation of $\phi_f^2$ over the upper range of $f_{fa}$ . .....	167
Figure 6.23: Pressure drop prediction based on $f_{fa}$ . .....	168
Figure 6.24: Pressure drop prediction based on $\phi_f^2$ . .....	169
Figure 6.25: Pressure drop prediction based on Martinelli's equations. ....	170
Figure 6.26: Flow Regime map by Baker (1954) with two-phase data. ....	171
Figure 6.27: Flow regime map by Sou and Griffith (1964) with two-phase data. ..	172
Figure 6.28: Heat flux comparisons with Figure 3.3. ....	173
Figure 6.29: Heat transfer coefficient comparisons with typical values from Incropera and DeWitt (1985). ....	174
Figure 6.30: Typical Nusselt number uncertainty associated with gas flow. ....	175
Figure 6.31: Typical Nusselt number uncertainty associated with water flows. ....	176
Figure 6.32: Typical Nusselt number uncertainty associated with two-phase flows. ....	177



## ACKNOWLEDGMENTS

I would like to thank my parents, Dr. Patricia D. Stanley and Larry R. Stanley. Your untiring and loving support, for all the endeavors I have chosen to undertake, has made all my dreams come true. I love you both. To Dr. Randall F. Barron. Thank you for being my mentor, educator, and most importantly, a role model for every engineer. To all of the mechanical engineering professors at Louisiana Tech University. Those of you that have touched my life have shaped me as an engineer and a person. My years at Tech will not ever be forgotten. Last, but not least, to Theresa. Thank you for your love and support, through good times and bad, as I achieve the goals I have set for myself. I love you and look forward to the adventures in our life together.

## CHAPTER 1

### INTRODUCTION

The area of two-phase forced convection heat transfer in microtubes and microchannels is a burgeoning field. Though extensive work has been done in the area of single-phase liquid and gas flow through microgeometries [Choi (1991), Yu (1995), Harley et al. (1989a and 1989b), Pfahler et al. (1991, 1990a, and 1990b)], the only area where detailed analysis of two-phase heat transfer in microgeometries has taken place is in the specialized area of micro heat pipes. As the field of microfluidics continues to grow, it is becoming increasingly important to understand the mechanisms involved with heat transfer in two-phase flow through microgeometries. This importance is reiterated by the increasing number of applications which use phase change as the principal mechanism to conduct or remove heat. These fields include bioengineering and biotechnology, aerospace, mini heaters, and mini heat exchangers, electronics and microelectronics, material processing and thin film deposition technology, etc.[Peng and Wang (1993)]. Other areas of research include cooling of laser diode arrays, micro Joule-Thompson cooling devices, and the evaporator and condenser sections of micro vapor compression cycles [Drost et al. (1994)]. Much work has been done by Little (1990a, 1990b, and 1984) in developing a commercially available mini Joule-Thompson cooling device capable

of dissipating 0.25W over a few square centimeters at cryogenic temperatures. In addition, the development of a microscale Joule-Thompson cooling device is currently underway at the Institute for Micromanufacturing. This program seeks to design, fabricate using LIGA technology, package, and test a complete microscale device which may have applicability toward electronic chip cooling. A micro heat pump concept has been proposed by researchers from Battelle (Pacific Northwest National Laboratories) [Drost et al. (1994)]. The PNNL concept incorporates a sheet architecture in which the various processes of a vapor compression refrigeration system are divided into individual unit operations and sheets of material with embedded micro mechanical systems are developed that can perform each unit operation. The sheet unit operations could then be combined together to form more complex systems. The major advantage of two-phase flow is that the temperature gradient along the length of the channel is much smaller than in single-phase flow, due to the phase change phenomena. This results in larger values of the heat transfer coefficient and reduces the requirement of large liquid flow rates.

This research is intended to help bridge the gap between the existing, mainly empirical, research on single-phase flow and two-phase flow boiling of fluids in microchannels. Two component flow was used in this research instead of boiling flow. This allowed the controlling hydrodynamic and heat transfer mechanisms to be more easily identified. Governing equations for two-phase flow, both homogeneous and separated, were developed. The different flow regimes (plug, slug, etc.) were defined and discussed. The resulting equations were compared with existing experimental data and empirical

formulas. Also, new empirical formulas were derived from data that were taken as part of this research. These results were compared to the widely accepted macro scale two-phase pressure drop equations by Lockhart and Martinelli (1949), Martinelli et al. (1944), and Martinelli and Nelson (1948) and a flow regime map developed by Baker (1954).

Because this research was mainly empirical, testing of several fluids flowing through various channel configurations was carried out. To help answer some conflicting results reported previously, single-phase tests were conducted. The single-phase tests were conducted because the two-phase predictions of Martinelli rely entirely on single-phase coefficients and equations. The data that were taken were used, along with a dimensional analysis, to derive empirical formulas for pressure drop and rate of heat transfer rate in microchannels. It was intended that these experiments would shed light on the dominant mechanisms present in single and two-phase flow. Also, it was intended that a quantitative expression could be developed that would help distinguish macro- and microscale flow regimes in two-phase flow.

## CHAPTER 2

### LITERATURE SURVEY

Because the main area of focus of this research was two phase flows, a comprehensive review of single phase flow will not be given. Only a few of the papers used for comparisons will be discussed. However, excellent reviews of this area can be found in Bailey (1996), Choi (1991), and Yu (1995). To date, only one paper considering two-phase two-component flow (with no phase change) in capillary tubes was found, Suo and Griffith (1964). However, there exist several empirical studies of flow boiling in microchannels. For completeness, a review of these articles is given below. Though not usually considered with flow boiling, a large volume of empirical and analytical studies have been conducted on micro heat pipes. The research on micro heat pipes has produced many insights into the mechanics of phase change and will be very useful in future research of flow boiling in microchannels. For more information on micro heat pipes, please see Babin et al. (1990), Badran et al. (1993), Cao et al. (1993), Cotter (1984), Duncan and Peterson (1994), Gerner et al. (1992), Khrustalev and Faghri (1994), Longtin et al. (1992), Mallik et al. (1992), Peterson (1992), Peterson et al. (1993), Peterson et al. (1991), Swanson and Peterson (1995), Swanson and Peterson (1993), and Wu and Peterson (1991a and 1991b). For comparisons made later in this section, some definitions are

necessary: 1) Open-channel flow boiling is forced convection boiling over external microstructure enhanced surfaces. 2) Closed-channel flow boiling is forced convection through enclosed tubes or channels. And, 3) Pool boiling is boiling on external microstructure enhanced surfaces with no forced movement of the fluid.

### Single Phase Flow in Microchannels

Because of the reviews mentioned above, only the pertinent information on friction factors and Nusselt numbers will be presented.

#### Friction Factor

For fluid flow in macroscale rectangular channels, Hartnett and Kostic (1989) gave a relation for the Manning friction factor as

$$f \cdot Re = 94(1 - 1.3553AR + 1.9467AR^2 - 1.7012AR^3 + 0.9564AR^4 - 0.2537AR^5) \quad (2.1)$$

where AR is the aspect ratio of the rectangular channel (height /width). Though this is a macroscale equation, it provides a useful comparison.

Wu and Little (1993) have done extensive investigations of small to medium aspect ratio glass channels. Correlations for laminar, transition, and turbulent flow regimes were

given as

$$f = \frac{(110 \pm 8)}{Re} \quad Re \leq 900 \quad (2.2a)$$

$$f = 0.165(3.48 - \log(Re))^{2.4} + (0.081 \pm 0.007) \quad 900 \leq Re \leq 3,000 \quad (2.2b)$$

$$f = \frac{(0.195 \pm 0.017)}{Re^{0.11}} \quad 3,000 \leq Re \leq 15,000 \quad (2.2c)$$

Pfahler et al. (1991, 1990a, and 1990b) and Harley et al. (1989a and b) tested very low aspect ratio channels and compared their experimental findings with the Navier-Stokes predictions. For hydraulic diameters of nearly 40 microns or below, the measured pressure drop showed larger deviation from the Navier-Stokes predictions than did the channels with hydraulic diameters larger than 40 microns. This work seems to have indicated that there may exist a lower limit to macroscale theory and that below this theory, microscopic effects must be considered for accurate predictions of a pressure drop.

Choi (1991) was one of the first investigators to test gas flow in microtubes instead of microchannels. The results show that not only is the friction factor lower than predicted, but it is Reynolds number dependent in both laminar and turbulent regimes. The expressions for friction factor developed by Choi (1991) were given as

$$f = \frac{64}{Re} \left[ 1 + (30 \pm 7) \frac{u}{DC_a} \right] \quad Re \leq 2,300 \quad (2.3a)$$

$$f = 0.140 Re^{-0.182} \quad 4,000 \leq Re \leq 18,000 \quad (2.3b)$$

where  $\nu$  is the kinematic viscosity,  $D$  is the inside diameter of the microtubes, and  $C_a$  is the acoustic velocity.

Yu (1995) continued the work of Choi (1991) by considering flow of water and nitrogen gas through microtubes. The expressions developed for friction factor were

$$f = \frac{50.13}{Re} \quad Re \leq 2,000 \quad (2.4a)$$

$$f = 0.302 Re^{-0.25} \quad 6,000 \leq Re \leq 20,000 \quad (2.4b)$$

#### Nusselt Number

Choi (1991) also conducted heat transfer experiments in micro tubes. Choi (1991) concluded that Reynolds analogy does not hold for microchannel flow and that this may be due to suppression of the turbulent eddies in the small channels [Bailey (1996)]. Correlations given for the Nusselt number were

$$Nu = 0.000972 Re^{1.17} Pr^{1/3} \quad Re < 2,000 \quad (2.5a)$$

$$Nu = (3.82 \times 10^{-6}) Re^{1.96} Pr^{1/3} \quad 2,500 \leq Re \leq 20,000 \quad (2.5b)$$

For Nusselt number predictions in turbulent regimes, Wu and Little (1983) and Yu (1995) developed these expressions, respectively,

$$Nu = 0.00222 Re^{1.09} Pr^{0.4} \quad Re \leq 3,000 \quad (2.6a)$$

$$Nu = 0.0007 Re^{1.2} Pr^{0.2} \quad 6,000 \leq Re \leq 20,000 \quad (2.6b)$$



### Two-Phase Flow Boiling in Microchannels

The amount of theoretical development in closed-channel flow boiling is very limited. In fact the only general analytical developments found in this area were equations for the pressure drop in flow boiling given by Bowers and Mudawar (1994). However, these equations were based on macroscale theory. These pressure drop equations included the contributions of single-phase flow, boiling flow, and outlet conditions of the channel, where the boiling pressure drop consisted of acceleration and friction effects. Other than these equations, only heat flux correlations and experimental data were given.

### Experimentation and Findings

Zhukov and Yarmak (1990) presented a strictly empirical look at the boiling behavior of superconducting magnet windings. The experimental apparatus consisted of a 0.8 mm diameter tube 1 m long with the first 150 mm heated. For nitrogen and helium respectively, "The heat generation was up to 35 W or 20 W," the mass flow rates varied from 35 - 520 kg/m<sup>2</sup>s or 40 - 237 kg/m<sup>2</sup>s, and the inlet qualities varied from 0.0 - 0.58 or 0.0 - 0.22. The experiment considered the onset of boiling crisis from a timed heat pulse of known power. The duration of the rectangular heating pulse varied from 1 ms to 12.5 s. The change in wall temperature resulting from the heat pulse duration was measured and shown in graphical form. Though the data given were not conducive to the critical heat flux (CHF) comparisons made later, several important observations were made. First, "the onset of boiling under heat pulse should bring about an abrupt pressure rise in the heated section. The pressure rise can cause the flow to stop quickly and may even result in

reverse flow." Second, "the vapor phase growth rate in channels with pulse heat should be much lower than that corresponding to the steady state boiling regime." And third, "helium heat transfer crisis appears to be due to the pressure jump over the critical point at the onset of boiling."

Peng and Wang (1993) experimentally investigated the transition between the regions of forced convection and nucleate boiling. The experimental apparatus utilized a split flow system to control the flow rate accurately through the test section. The fluid used for testing was deionized water with an inlet temperature varied from 30°C - 60°C. For water at ambient pressure, boiling ensued "at a little over 100°C." Three channels were machined into a stainless steel plate with a width of 15 mm, a length of 60 mm, and a thickness of 2 mm. The flow channels were 0.6 mm wide and 0.7 mm high. The channels were heated by electrically heating the stainless steel. Because of this heating configuration, nonuniform spacing of the channels was chosen to provide uniform heat flux to all three sides of the channels. The top surface of the test section was Pyrex glass so that the flow could be viewed. Thermocouples were located at each end of each channel and their average value taken as the wall temperature in the data presented.

Experimental observation yielded two important events; 1) the boiling regime was fully developed nucleate boiling, and 2) bubbles did not grow in microchannel boiling. Peng and Wang (1993) mention "that the bubble growth in liquid might be concerned with the scale of the liquid bulk. If the scale of liquid bulk is large enough, bubbles grow, otherwise, no bubbles grow and exist in liquid" flowing in microchannels. What this is

saying is that in microchannel flow, the fluid properties vary enough from the bulk properties to provide a noticeable change in flow behavior. The experimental results show a dramatic increase in the slope of the heat flux when the transition to boiling is reached. Before the transition, the data was spread as would be expected. However, after the transition, the values of the heat flux for all tests were very close. Peng and Wang (1993) conclude that in this region, "heat flux may be affected by other factors besides flow velocity and liquid subcooling" and that further study is warranted to determine the mechanisms involved. Peng and Wang (1993) also compare existing macro scale Nusselt number correlations to their experimental data. For a given Reynolds number, the forced convection data was much higher than that predicted analytically. The nucleate boiling data, on the other hand was slightly lower than that predicted analytically but does show a similar trend near the region where the equations intersect. Peng and Wang (1993) do not try to explain this behavior and simply state that, "The reasons promoting the transitions and the behaviors are not recognized or understood." Peng and Wang (1993) then compared their data to experimental data of flow boiling in a 9 mm tube. There were two items of importance drawn from these comparisons; 1) before transition, the heat flux was about the same or lower for the microchannel than for the 9 mm tube; and, 2) after transition, the heat flux was markedly higher for the flow in microchannels. Other conclusions Peng and Wang (1993) reached were; 1) flow "velocity and liquid subcooling appears to have no obvious effect on the flow nucleate boiling" and, 2) "No partial (nucleate) boiling ... (is) observed or inspected for the transition from single-phase liquid

convection to nucleate boiling." Peng and Wang (1993) mention that number two above was "very strange," but no explanation was given. However, this either was an optical effect, or the experimental configuration was such that the flow transitioned past the regime of partial nucleate boiling. Finally, an observation made by Peng and Wang (1993) was "that no bubble(s) grow for flow boiling of liquid flowing through microchannels." This, also, was probably an optical effect caused by the combination of the tendency of the bubble size to decrease as it condensed back to a liquid and the tendency of the bubble size to increase with the decreasing pressure in the channel.

Bowers and Mudawar (1994) presented an experimental comparison of mini- (2.54 mm) and microchannel (510  $\mu\text{m}$ ) heat sinks with a 1 cm heated length. The 1 cm square test sections were able to accommodate three minichannels and 17 microchannels across their width. The working fluid used was R-113 with a flow rate of 19 - 95 ml/min, an inlet subcooling of 10 - 32°C, and a constant inlet pressure of 1.38 bar. Assuming a homogeneous two-phase flow model, Bowers and Mudawar (1994) used a macroscale pressure drop equation accounting for frictional and acceleration losses. The expression, considering acceleration losses, was not applicable to this research. However, the expression, considering frictional losses, was applicable. From Collier (1981),

$$-\left(\frac{dP}{dz}\right)_F = \left(\frac{2f_{TP}G^2}{\rho_f D}\right) \left[1.0 + x \left(\frac{v_{fg}}{v_f}\right)\right] \quad (2.7)$$

Integrating over the exit length (unheated) of the channel, Bowers and Mudawar (1994) obtained

$$\Delta P_o = \left( \frac{2 f_{TP} G^2 L_o}{\rho_f D} \right) \left[ 1.0 + x_L \left( \frac{v_{fg}}{v_f} \right) \right] \quad (2.8)$$

where  $\Delta P_o$  is the pressure drop through the unheated section,  $f_{TP}$  is the two-phase friction factor,  $G$  is the total mass velocity,  $L_o$  is the length of the unheated section,  $\rho_f$  is the density of the liquid,  $x_L$  is the quality at the entrance to the unheated section,  $v_{fg}$  is the difference in specific volume of the liquid and gas, and  $v_f$  is the specific volume of the liquid. Collier (1981) gave a range of  $f_{TP}$  as 0.0029 to 0.005. Bowers and Mudwar (1994) used the conservative estimate of 0.005. Equation (2.8) is directly applicable to this study. It can be used to both predict a pressure drop, given a correlation for the two-phase friction factor, or to help correlate the two-phase friction factor, given a measured pressure drop. It is shown, in Chapter 3, that equation (2.8) is virtually identical to the macroscale expression for the pressure drop derived for this study.

Besides the pressure model, a CHF correlation was given and both were shown to be in good agreement with the experimental data. The effect on heat transfer on several variables was discussed, including pressure drop (extensive), inlet subcooling, superheated exit conditions, and size. One problem associated with boiling heat transfer is "the production of vapor bubbles that lead not only to increased heat transfer but also to increased pressure drop." This problem is magnified, as would be expected, as the size of

the channel decreases. The inlet subcooling is shown to have little or no effect on the CHF. This agrees with the findings of Peng and Wang (1993). Some other features highlighted by the experimental results were; 1) "The two heat sinks demanded minimal flow rates..." (to allow complete evaporation); 2) "The small diameters of mini- and microchannels suggest an increased frequency and effectiveness of droplet impact with the channel wall in regions of high  $x_L$  (quality) values"; and, 3) "The small overall size of the heat sink seems to greatly contribute to delaying CHF by conducting heat away from the downstream region undergoing either partial or total dryout to the boiling region of the channel."

#### Experimental Data Comparison

Figures 2.1 and 2.2 are graphs of the CHF and resulting heat transfer coefficient ( $h$ ) versus the temperature difference ( $T_{\text{wall}} - T_{\text{inlet}}$ ) as compiled from Peng and Wang (1993) and Bowers and Mudawar (1994). The data points of He (1988) were referenced by Peng and Wang (1993). One important point shown in Figure 2.1 is the lack of dependency of the CHF on the liquid velocity. For the data given by Peng and Wang (1993), the CHF value of  $1.3 \text{ MW/m}^2$  corresponds to a liquid velocity of  $2.32 \text{ m/s}$  whereas the CHF value of  $0.9 \text{ MW/m}^2$  has the highest velocity of  $3.6 \text{ m/s}$ . Comparing the rectangular channel to the  $9 \text{ mm}$  tube shows the inefficiency of the  $9 \text{ mm}$  tube. A much larger temperature difference was required to achieve the same heat flux. It should be pointed out that the liquid velocity in the  $9 \text{ mm}$  tube was much lower than in the rectangular channels. Looking at the data for the micro- and minichannels, one can see

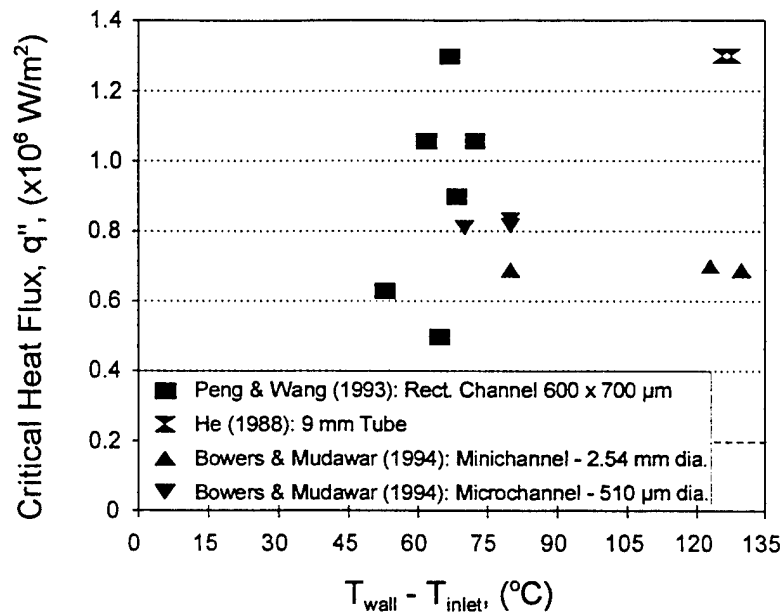


Figure 2.1: Critical heat flux comparison for mini- and microgeometries.

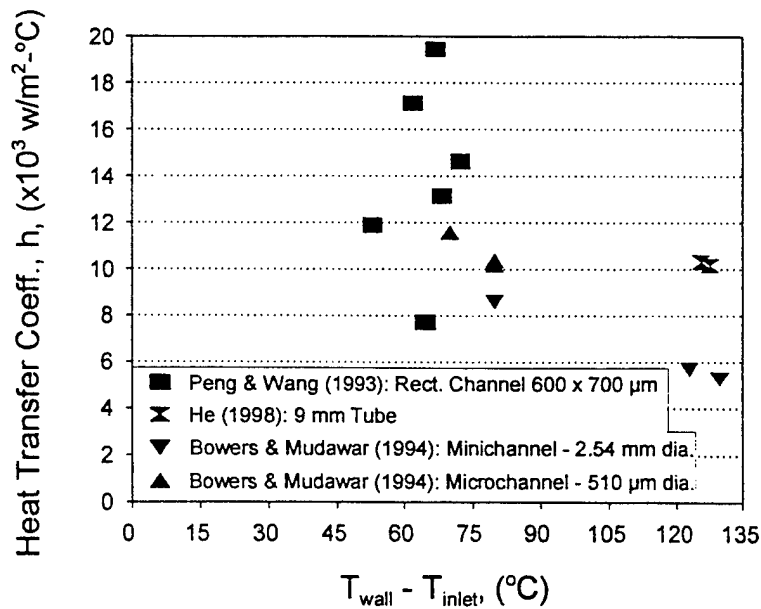


Figure 2.2: Heat transfer coefficient comparison for mini- and microgeometries.

that though there is more heat transfer per channel for the mini channels, the increased density of the microchannels make them a more effective system. Again, the one drawback to microchannels is the high pressure drop. In Figure 2.2, the same trends are seen and the effectiveness of the different configurations is more pronounced.

As a final comparison, Figure 2.3 presents the range of critical heat flux achieved for various flow configurations. The pool boiling range was developed from Anderson and Mudawar (1989), Marto and Lepere (1982), Mudawar and Anderson (1993 and 1990), and Wright and Gebhart (1982). For more information on the open-channel flow boiling, micro heat pipes, and pool boiling included in this figure, see Stanley et al.(1996). Also shown in Figure 2.3 is the ultra-high CHF achieved by Mudawar and Bowers (1995) using very high flow rates and pressures in microtubes. Figure 2.3 raises some interesting points. First, open-channel micro flow boiling achieves the highest practical CHF. However, it is the least researched of these areas and one of the most practical. Second, micro heat pipes which are the most practical and most researched, do not achieve the level of CHF possible with the other flow configurations. Third, pool boiling can achieve reasonably high values of CHF over a wide range of temperatures. And Fourth, the data from Mudawar and Bowers (1995) is offered to show what values of CHF can be achieved in closed-channel micro flow boiling. Unfortunately, this value is not currently practical in microsystems due to the high pressure and high flow rate required. However, as new and more powerful micropumps are developed, this limit will be met and even raised.



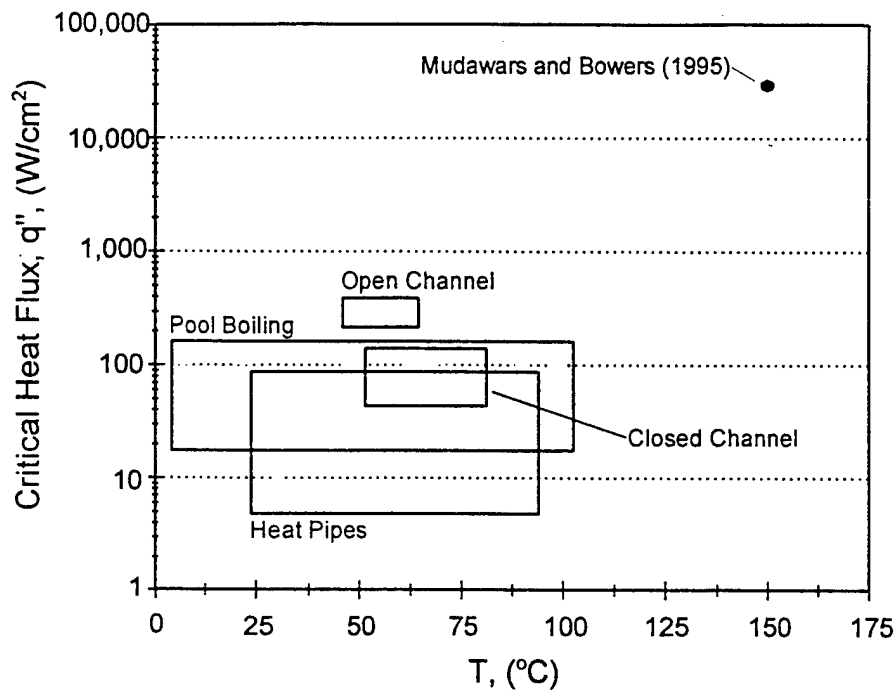


Figure 2.3: Critical heat flux ranges.

Though heat pipes will not be discussed in detail, as mentioned, one particular finding is worth noting. Swanson and Peterson (1993) found that when the operating radius of the micro heat pipes reached nearly 20 microns or below, molecular effects such as the Margoni effect must be considered to accurately model the heat pipes. That is, they found a quantifiable limit to the macroscale theory of heat pipes. This seems to indicate, along with some of the work done on single-phase gas flow in microchannels, that there is a definite lower limit to the usual macroscale theory of fluid flow. However, what this definite limit is and how to predict it for various types of fluid flow is still under debate and will require much more research in this area.

## Two-Phase Two-Component Flow in Channels

### Macroscale

By far, the most widely used and accepted correlation for the prediction of pressure drop in two-phase, two-component, flow without heat transfer are the semi-empirical correlations of Lockhart and Martinelli (1949), Martinelli et al. (1944), and Martinelli and Nelson (1948). The correlations are based on the pressure drop that occurs when only liquid flowing through the channel is multiplied by a factor which accounts for two-phase effects. Or,

$$\left( \frac{\Delta p}{\Delta L} \right)_{TP} = \phi_f^2 \left( \frac{\Delta p}{\Delta L} \right)_f \quad (2.9)$$

where  $(\Delta p/\Delta L)_{TP}$  is the pressure drop for the two-phase flow, and  $(\Delta p/\Delta L)_f$  is the pressure drop if only the liquid was flowing through the channel. The friction-pressure-drop parameter  $\phi_f$  is based on  $X$ , termed the Martinelli parameter. This parameter is

$$X^2 = \frac{(\Delta p/\Delta L)_f}{(\Delta p/\Delta L)_g} = \frac{C_f (Re_g)^m \rho_g}{C_g (Re_f)^n \rho_f} \left( \frac{1-x}{x} \right)^2 \quad (2.10)$$

where  $x$  is the fluid quality,  $\rho$  is the density of the liquid (f) and gas (g) phases respectively, and  $Re_f$  and  $Re_g$  are the liquid and gas Reynolds numbers. The Reynolds numbers are calculated from

$$Re = \frac{\dot{m}D}{A\mu} \quad (2.11)$$

where the mass flow rate is of each fluid separately and viscosity is determined for each fluid at the measured temperature and pressure of the two-phase flow. The other coefficients  $C_l$ ,  $C_g$ ,  $m$ , and  $n$  in the Martinelli parameter are based on macroscale single phase correlations. The values of these coefficients are given in Table 1. From Barron (1985), the Martinelli parameter is related to the frictional pressure drop parameter by

$$\phi_f = \frac{(X^2 + CX + 1)^{1/2}}{X} \quad (2.12)$$

where the values of  $C$  are given in Table 2. The pressure drop of only the liquid flowing through the channel is found, from macroscale theory, as

$$\left( \frac{\Delta p}{\Delta L} \right)_f = \frac{f (\dot{m}_f/A)^2}{2 g_c \rho_f D} \quad (2.13)$$

where  $f$ , the friction factor, is also determined using macroscale theory.

Table 1: Martinelli Constants

Constant	Laminar Regime Re < 2,500	Turbulent Regime 2,500 < Re < 50,000
$C_f$	64	0.316
$C_g$	64	0.316
m	1	0.25
c	1	0.25

Table 2: Values of Constant C

Liquid Flow Regime	Gas Flow Regime	C
Laminar	Laminar	5
Turbulent	Laminar	10
Laminar	Turbulent	12
Turbulent	Turbulent	20

Martinelli and Nelson (1948) also developed expressions for boiling two-phase flow. Because of the phase change involved, both friction and momentum pressure drops must be considered. Though the frictional pressure drop is not applicable to the proposed research, the momentum pressure drop is applicable. From Barron (1985),

$$\Delta p_m = \frac{\phi_m (\dot{m}_f + \dot{m}_g)^2}{g_c \rho_f A^2} \quad (2.14)$$

with the momentum-pressure-drop parameter given by

$$\phi_m = \frac{(1-x_{out})^2}{\alpha_{f,out}} - \frac{(1-x_{in})^2}{\alpha_{f,in}} + \left( \frac{x_{out}^2}{1-\alpha_{f,out}} - \frac{x_{in}^2}{1-\alpha_{f,in}} \right) \left( \frac{\rho_f}{\rho_g} \right) \quad (2.15)$$

where  $\alpha$  is the volume fraction of liquid at the entrance and exit of the channel. Similar to before, the Martinelli parameter,  $X$ , and the momentum-pressure-drop parameter are related by

$$\phi_m = \frac{X}{(X^2 + CX + 1)^{1/2}} \quad (2.16)$$

where the coefficient  $C$  is given in Table 2. This equation is applicable even though the quality does not change between the inlet and outlet. This is because the volume fraction of liquid does change. The reason is that the volume of the gas increases as it flows through the channel due to the local pressure decreasing. Therefore, these relations can be compared directly to the data taken in this research by combining the frictional and momentum pressure drop equation. Or,

$$\Delta p = \Delta p_f + \Delta p_m \quad (2.17)$$

Also of interest in this area is the flow regime map developed by Baker (1954). Using two parameters,  $G/\lambda$  and  $\lambda L\psi/G$ , Baker (1954) was able to plot seven different flow regimes on one graph, as seen in Figure 2.4. For the two parameters,  $G$  and  $L$  are the gas

and liquid mass flow rates per unit area, respectively. The units for  $G$  and  $L$  in Figure 2.4 are  $\text{lbm/hr-ft}^2$ .  $\psi$  and  $\lambda$  are defined by

$$\lambda = [(\rho_g/\rho_a)(\rho_f/\rho_w)]^{1/2} \quad (2.18)$$

$$\psi = (\sigma_w/\sigma_f)[(\mu_f/\mu_w)(\rho_w/\rho_f)^2]^{1/3} \quad (2.19)$$

where the subscripts refer to air (a), water (w), the particular liquid (f), and the particular gas (g). The values of the properties of the air and water are taken at standard atmospheric conditions.

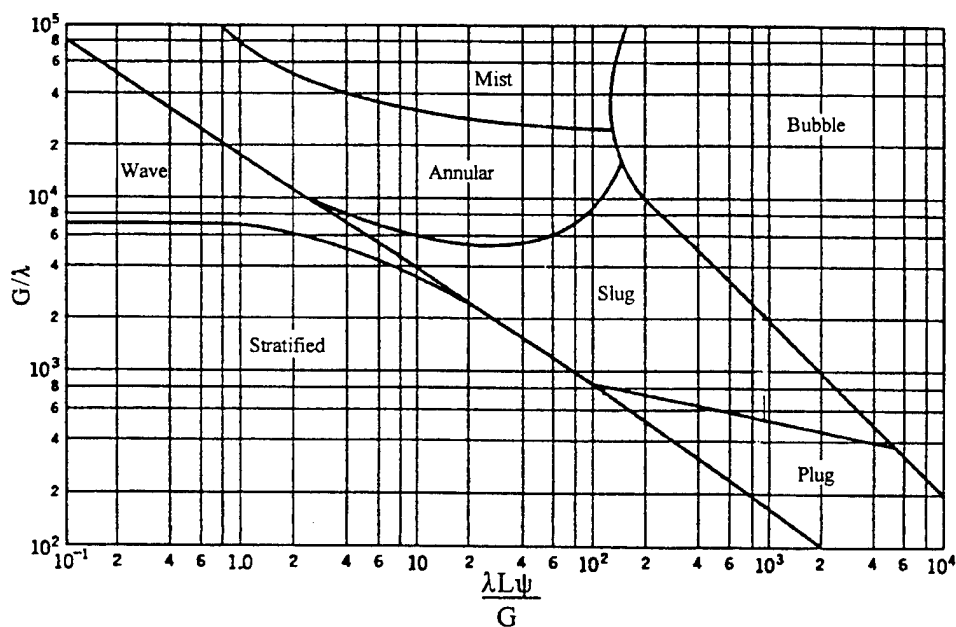


Figure 2.4: Flow Regime Map by Baker (1954).

### Microscale

The only work found concerning two-phase two-component flow was that conducted by Suo and Griffith (1964), mainly an analytical study of two-phase gas-liquid flows in capillary tubes. Though a flow regime map for annular, slug, and bubbly-slug flow was developed, the work centered on analyzing the velocities associated with long bubble motion. A dimensional analysis was conducted along with a small amount of experimentation. Some of the more important findings of the research were: 1) Surface tension and viscosity dominate over gravity. 2) For large liquid to gas viscosity ratios, the liquid film around the bubble did not move. 3) For small liquid to gas viscosity ratios, the liquid film around the bubble did move. 4) The original seven dimensionless parameters were reduced to three,  $\lambda$ ,  $\psi$ , and  $L_s/r_o$  (slug length/ radius of tube). The parameters  $\lambda$  and  $\psi$  were defined as

$$\lambda \equiv \frac{\mu_f^2}{\rho_f^2 \sigma r_o} \quad ; \quad \psi \equiv \frac{\mu_f U_B}{\sigma} \quad (2.20)$$

where  $\mu_f$  and  $\rho_f$  are the liquid viscosity and density, respectively,  $\sigma$  is the surface tension,  $U_B$  is the bubble velocity, and  $r_o$  is the tube inside diameter. For the flow regime map, the transition from slug flow was not characterized by an explicit mathematical expression. However, it was plotted on a graph of  $\psi$  versus the volume rate fraction of liquid

$(Q_f / Q_g + Q_f)$ . The transition between slug flow and bubbly-slug flow was more rigorously defined by

$$\frac{\psi^2}{\lambda^2} = Re \cdot We = 2.8 \times 10^5 \quad (2.21)$$

where  $Re$  and  $We$  are the Reynolds number and Weber number, respectively.



## CHAPTER 3

### GOVERNING EQUATIONS AND FLOW REGIMES

One of the main purposes of this research is to compare existing two-phase macroscale equations to experimental data on two-phase flow in microchannels. In this chapter, the governing equations for macroscale two-phase flow will be developed. These governing equations consist of the Conservation of Mass, Momentum, and Energy. Governing equations will be presented for both the homogeneous flow model and the separated flow model. The homogeneous flow model assumes average fluid properties based on the ratio of the liquid and gas components. The separated flow model, on the other hand, develops governing equations based on the individual behavior of each component. The one assumption that will be utilized in both models is one-dimensional flow. That is, any changes in properties across the height or width of the channel are very small compared to any changes along the length of the channel. Additionally, in this chapter, the various possible two-phase two-component flow regimes (slug flow, bubble flow, etc.) for macroscale and microscale will be defined and described.

### Homogeneous Flow

In homogeneous flow, the average properties of the combined components are based on either the volume fraction or the mass fraction of the fluid. The volume fraction, or void fraction, is defined by

$$\alpha = \frac{Q_g}{Q_g + Q_f} \quad (3.1)$$

where  $Q$  is the volumetric flow rate of the gas (g) and liquid (f). Similarly, the mass fraction, or quality, is defined as

$$x = \frac{\dot{m}_g}{\dot{m}_g + \dot{m}_f} \quad (3.2)$$

where  $\dot{m}$  is the mass flow rate of the gas (g) and liquid (f). Quality is the more commonly used variable and will be used throughout this derivation. Typical average values of a property, specific volume ( $1/\rho$ ) for example, can be calculated using the quality by

$$v_m = v_g x + (1 - x) v_f \quad (3.3)$$

where  $v_m$  is the mean value of the specific volume, and  $v_g$  and  $v_f$  are the gas and liquid specific volumes, respectively. When calculating other properties, the equation will have the same form as equation (3.3).

In addition to the one-dimensional assumption mentioned previously, the following assumptions will be used with the homogeneous flow model:

- 1) Steady flow.
- 2) Constant properties.
- 3) Both components are flowing at the same average velocity ( $\bar{u}$ ).
- 4) Thermodynamic equilibrium exists between phases.
- 5) The use of a suitably defined single-phase friction factor for two-phase flow.

The last three assumptions, as outlined by Collier (1981), are used in the more general derivation of the two-phase flow equations and apply for this investigation. The first two assumptions are specific to this derivation.

### Conservation of Mass

From Figure 3.1, summing the mass flow rate in the x-direction yields

$$\rho \bar{u} dy dz = \left[ \rho \bar{u} + \frac{\delta}{\delta x} (\rho \bar{u}) dx \right] dy dz \quad (3.4)$$

Integrating over the cross-sectional area  $dy dz$  and noting that the partial derivative term is zero because of the steady flow assumption, we obtain

$$\rho \bar{u} A)_{in} = \rho \bar{u} A)_{out} \quad (3.5)$$

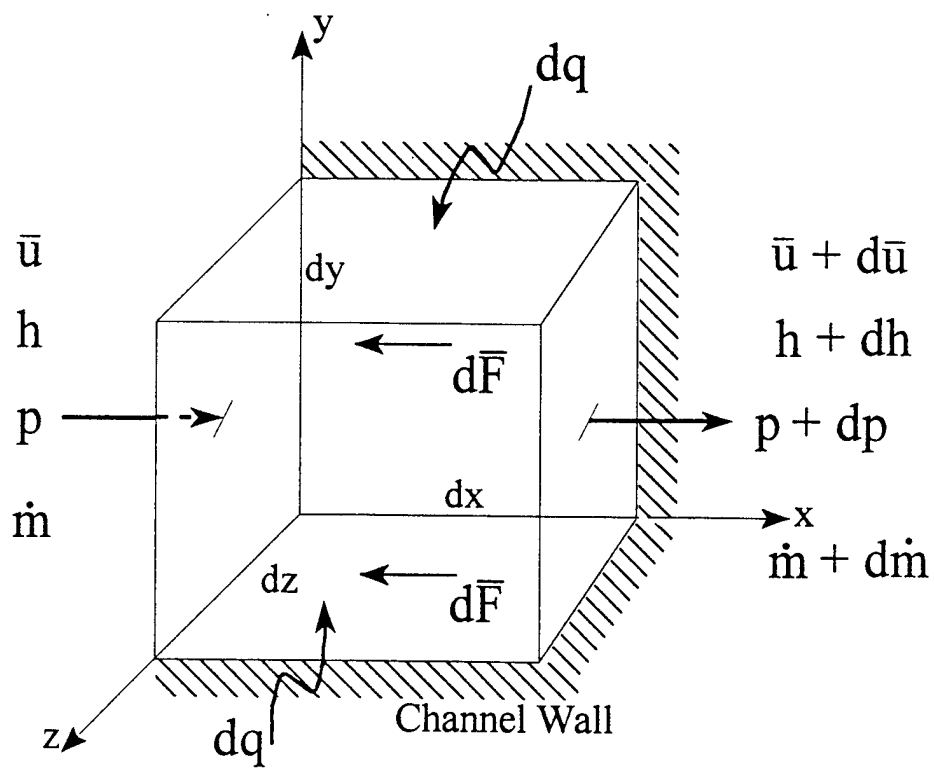


Figure 3.1: Homogeneous flow model control volume.

or, simply stated,

$$\dot{m} = \rho \bar{u} A = \text{constant} \quad (3.6)$$

Putting this equation in terms of mean properties, yields the final form of the conservation of mass equation.

$$\dot{m} = \rho_m \bar{u} A = \text{constant} \quad (3.7)$$

where  $\rho_m$  is the mean density, and  $A$  is the cross-sectional area of the channel.

### Conservation of Momentum

The forces present in the x-direction of a differential control volume of fluid are shown in Figure 3.1. Summing the forces in the x-direction, dividing by the cross-sectional area, and multiplying by the differential length ( $A dx$ ) yields

$$\rho g_x - \frac{dp}{dx} - \frac{1}{A} \frac{d\bar{F}}{dx} = \rho \frac{d\bar{u}}{dt} + \rho \bar{u} \frac{d\bar{u}}{dx} \quad (3.8)$$

where  $d\bar{F}$  is the force exerted to overcome friction. For a horizontal tube,  $g_x = 0$ . Therefore, the first term on the left-hand side can be neglected. The first term on the right-hand side can also be neglected due to the steady flow assumption. Making these substitutions, multiplying through by the cross-sectional area ( $A$ ), and noting that  $\rho_m \bar{u} A$  is the mass flow rate ( $\dot{m}$ ), the final form of the conservation of momentum equation

becomes

$$\dot{m} \frac{d\bar{u}}{dx} = -A \frac{dp}{dx} - \frac{d\bar{F}}{dx} \quad (3.9)$$

The term  $d\bar{F}$  is the total wall shear force and can be expressed in terms of the wall shear stress  $\tau_w$ . Or,

$$\frac{d\bar{F}}{dx} = \tau_w P \quad (3.10)$$

where  $P$  is the perimeter of the channel. Also,  $\tau_w$  may be expressed in terms of a friction factor,

$$\tau_w = f_{tp} \left( \frac{\rho_m \bar{u}^2}{2} \right) \quad (3.11)$$

As Collier (1981) notes, the total wall shear force ( $d\bar{F}$ ) can be expressed as a part of the overall static pressure gradient required to overcome friction, or

$$-\left( \frac{dp}{dx} \right)_F = \frac{1}{A} \frac{d\bar{F}}{dx} = \frac{\tau_w P}{A} = \frac{f_{tp} P}{A} \left( \frac{\rho_m \bar{u}^2}{2} \right) \quad (3.12)$$

This is the well-known Fanning friction equation. For a known geometry, equation (3.12) reduces to

$$-\left(\frac{dp_F}{dx}\right)_{tp} = \frac{2f_{tp} G^2 v_m}{D_h} \quad (3.13)$$

where  $G$  is the mass flux,  $v_m$  is the specific volume of the fluid mixture, and  $D_h$  is the hydraulic diameter.

The left-hand term of equation (3.9) involves the acceleration of the fluid through the control volume due to expansion of the gas phase as the local pressure drops. Putting this expression in terms of the static pressure gradient yields

$$\frac{\dot{m}}{A} \left( \frac{d\bar{u}}{dx} \right) = - \left( \frac{dp_a}{dx} \right)_{tp} \quad (3.14)$$

From Collier (1981),

$$-\left(\frac{dp_a}{dx}\right)_{tp} = G \frac{d\bar{u}}{dx} = G^2 \frac{dv_m}{dx} \quad (3.15)$$

where, neglecting the compressibility of the liquid phase,

$$\frac{dv_m}{dx} = v_{fg} \frac{d(\text{quality})}{dx} + x \frac{dv_g}{dp} \left( \frac{dp}{dx} \right) = x \frac{dv_g}{dp} \left( \frac{dp}{dx} \right) \quad (3.16)$$

Substituting equations (3.13), (3.15), and (3.16) into equation (3.9) yields, after simplifying

$$-\frac{dp}{dx} = -\left(\frac{dp}{dx}\right)_p = \frac{\frac{2f_p G^2 v_f}{D} \left[ 1 + x \left( \frac{v_{fg}}{v_f} \right) \right]}{1 + G^2 x \left( \frac{dv_g}{dp} \right)} \quad (3.17)$$

To solve (3.17), one must either use stepwise integration or some simplifying assumptions. The first assumption that can be made is that  $v_{fg}/v_f$  is approximately constant. This assumption is valid because of the large difference in specific volumes. A second assumption is that the compressibility of the gas can be neglected, or that

$$\left| G^2 x \left( \frac{dv_g}{dp} \right) \right| \ll 1 \quad (3.18)$$

This second assumption can be checked using some experimental data. For example, the following data is taken from data point 30 for water and nitrogen flowing together through five -  $134.64\mu\text{m} \times 121.83\mu\text{m}$  channels. We have;  $G = 466.128 \text{ kg/m}^2\text{-s}$ ,  $x = 0.03525$ ,  $dv_g = 0.8071 \text{ m}^3/\text{kg}$ , and  $dp = 432.7 \text{ psi} = 2.983351 \text{ MPa}$ . Putting these numbers into equation (3.18), we have

$$G^2 x \left( \frac{dv_g}{dp} \right) = (466.128 \text{ kg/m}^2\text{s})^2 (0.03525) \left( \frac{0.8071 \text{ m}^3/\text{kg}}{2.983351 \times 10^6 \text{ Pa}} \right) = 0.00207 \ll 1$$



Therefore, the second assumption is also valid. Employing these assumptions, equation (3.17) reduces to

$$-\left(\frac{dp}{dx}\right)_{tp} = \frac{2f_{tp} G^2 v_f}{D_h} \left[ 1 + x \left( \frac{v_{fg}}{v_f} \right) \right] \quad (3.19)$$

To evaluate the two-phase friction factor, Collier (1981) outlines two different approaches. The first approach assumes  $f_{tp}$  equal to the friction factor that would occur if the total flow was assumed to be all liquid. Denoting this friction factor as  $f_{fa}$  gives

$$-\left(\frac{dp_F}{dx}\right)_{tp} = \frac{2f_{fa} G^2 v_f}{D_h} \left[ 1 + x \left( \frac{v_{fg}}{v_f} \right) \right] = -\left(\frac{dp_F}{dz}\right)_{fa} \left[ 1 + x \left( \frac{v_{fg}}{v_f} \right) \right] \quad (3.20)$$

where  $-\left(\frac{dp_F}{dx}\right)_{fa}$  is the frictional pressure gradient, from the Fanning equation, for the flow assumed to be all liquid. Unfortunately, this method does not allow extrapolation to the correct value at a quality of 100%. To overcome this problem, a second method must be used to evaluate the two-phase friction factor. This method evaluates the two-phase friction factor by using a mean two-phase viscosity in the normal friction factor relationship. The most popular form of the two-phase viscosity equation, given as

$$\frac{1}{\mu_m} = \frac{x}{\mu_g} + \frac{(1-x)}{\mu_f} \quad (3.21)$$

was proposed by McAdams et al. (1942). The next assumption is that the friction factor may be expressed in terms of the Reynolds number, by the Blasius equation

$$f_{fa} = 0.079 \left[ \frac{GD}{\mu} \right]^{-\frac{1}{4}} \quad (3.22)$$

Using equations (3.21) and (3.22) in equation (3.20), one obtains Collier's (1981) result of

$$-\left( \frac{dp_F}{dx} \right)_{tp} = -\left( \frac{dp_F}{dx} \right)_{fa} \left[ 1 + x \left( \frac{v_{fg}}{v_f} \right) \right] \left[ 1 + x \left( \frac{\mu_{fg}}{\mu_f} \right) \right]^{-\frac{1}{4}} \quad (3.23)$$

Therefore, we have a two-phase pressure gradient expressed as a single-phase (liquid) pressure gradient multiplied by a term that accounts for two-phase effects. Or, defined in general,

$$-\left( \frac{dp_F}{dx} \right)_{tp} = -\left( \frac{dp_F}{dx} \right)_{fa} \phi_{fa}^2 \quad (3.24)$$

where  $\phi_{fa}^2$  is known as the two-phase friction multiplier and is defined, from above, as

$$\phi_{fa}^2 = \left[ 1 + x \left( \frac{v_{fg}}{v_f} \right) \right] \left[ 1 + x \left( \frac{\mu_{fg}}{\mu_f} \right) \right]^{-\frac{1}{4}} \quad (3.25)$$

Applying these results to equation (3.19) gives

$$-\left(\frac{dp}{dx}\right)_{tp} = -\left(\frac{dp}{dx}\right)_F \phi_{fa}^2 = \frac{2f_{fa} G^2 v_f}{D_h} \left[1 + x \left(\frac{v_{fg}}{v_f}\right)\right] \left[1 + x \left(\frac{\mu_{fg}}{\mu_f}\right)\right]^{-\frac{1}{4}} \quad (3.26)$$

Integration over the length of the channel gives the final result of

$$\Delta p_{tp} = \frac{2f_{fa} G^2 v_f L}{D_h} \left[1 + x \left(\frac{v_{fg}}{v_f}\right)\right] \left[1 + x \left(\frac{\mu_{fg}}{\mu_f}\right)\right]^{-\frac{1}{4}} \quad (3.27)$$

### Conservation of Energy

From the First Law of Thermodynamics

$$\dot{E}_{in} = \dot{E}_{out} \quad (3.28)$$

From Figure 3.1, assuming steady flow with no work done on the system, equation (3.28) becomes

$$dq = \dot{m} \left( dh_m + \frac{d\bar{u}^2}{2} \right) \quad (3.29)$$

where  $q$  is in watts and  $h_m$  is the mean enthalpy of the fluid. Integrating yields

$$q_{in} = \dot{m} \left( h_{m,out} - h_{m,in} + \frac{\bar{u}_{out}^2}{2} - \frac{\bar{u}_{in}^2}{2} \right) \quad (3.30)$$

Note, if kinetic effects can be neglected, this equation reduces to

$$q_{in} = \dot{m}(h_{m,out} - h_{m,in}) \quad (3.32)$$

Also, for constant properties, equation (3.32) further reduces to

$$q_{in} = \dot{m}c_{pm}(T_{out} - T_{in}) \quad (3.33)$$

where  $\dot{m}c_{pm}$  is the capacity rate of the fluid.

The main nondimensional parameter used for comparisons in convection heat transfer is the Nusselt number. The average Nusselt number is defined as

$$\overline{Nu} = \frac{\bar{h}D_h}{k_m} \quad (3.34)$$

where  $\bar{h}$  is the overall heat transfer coefficient,  $D_h$  is the hydraulic diameter, and  $k_m$  is the mean thermal conductivity of the fluid. The overall heat transfer coefficient is defined by Newton's law of cooling as

$$q = \bar{h}A(T_s - T_\infty) \quad (3.35)$$

where  $A$  is the cross-sectional area of the channel,  $T_s$  is the channel surface temperature, and  $T_\infty$  is the bulk fluid temperature. Solving equation (3.35) for the overall heat transfer coefficient and substituting into the definition for the average Nusselt number, we have

$$\overline{Nu} = \frac{\left( \frac{q}{A(T_s - T_\infty)} \right) D_h}{k_m} \quad (3.36)$$

Substituting the expressions for the heat transfer ( $q$ ), found in equations (3.30) and (3.33), we obtain the final expressions for the Nusselt number. Combining equation (3.30), with constant properties, and equation (3.36) yields

$$\overline{Nu} = \frac{D_h \dot{m} \left[ c_p (T_{out} - T_{in}) + \frac{1}{2} (\bar{u}_{out}^2 - \bar{u}_{in}^2) \right]}{A k_m (T_s - T_\infty)} \quad (3.37)$$

Similarly, combining equation (3.33) with (3.36) gives

$$\overline{Nu} = \frac{D_h \dot{m} [c_p (T_{out} - T_{in})]}{A k_m (T_s - T_\infty)} \quad (3.38)$$

### Separated Flow

The separated flow model, as mentioned previously, develops governing equations based on the individual behavior of each component. The assumptions for this model are similar to the ones used for the homogeneous model. Along with the one-dimensional assumption mentioned earlier, the assumptions used with the separated flow model are as follows:

- 1) Steady flow.
- 2) Constant properties.

- 3) Liquid and gas velocities not necessarily equal.
- 4) Thermodynamic equilibrium between phases.
- 5) The use of empirical correlations to relate the two-phase friction multiplier ( $\phi^2$ ) to the independent variables of the flow.

As before, the last three assumptions by Collier (1981) are used in the more general derivation of the two-phase flow equations and apply for this investigation. The first two assumptions are specific to this derivation.

### Conservation of Mass

Following the same procedure as for the homogeneous flow model, equations can be developed for each component of the fluid. From Figure 3.2, summing the mass flow rates in the x-direction for each component and simplifying gives

$$\dot{m}_g = \rho_g \bar{u}_g A_g = \text{constant} \quad (3.39)$$

$$\dot{m}_f = \rho_f \bar{u}_f A_f = \text{constant} \quad (3.40)$$

with the additional constraints

$$\dot{m}_{\text{total}} = \dot{m}_g + \dot{m}_f \quad (3.41)$$

$$A_{\text{total}} = A_g + A_f \quad (3.42)$$

### Conservation of Momentum

The momentum equation for each component of the fluid can be found by summing the forces in the x-direction of Figure 3.2. Neglecting gravity and acceleration of the flow

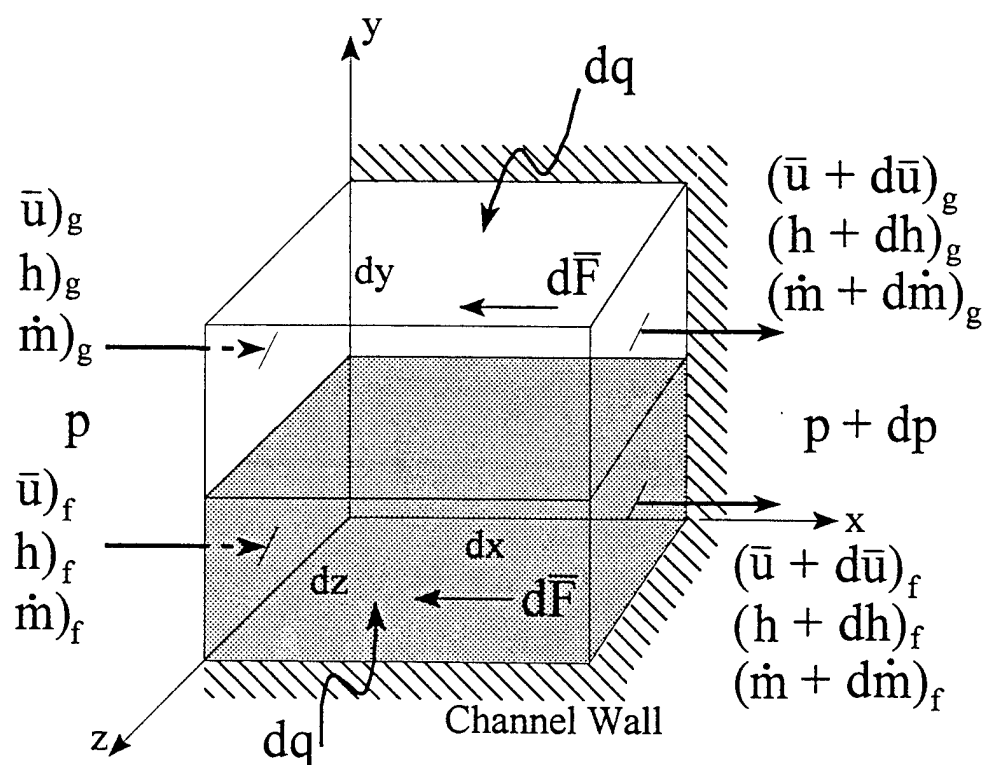


Figure 3.2: Separated flow model control volume.

with respect to time gives

$$-A_g dp - dF_g - I_F = \rho_g \bar{u}_g A_g d\bar{u}_g = \dot{m}_g d\bar{u}_g \quad (3.43)$$

$$-A_f dp - dF_f + I_F = \rho_f \bar{u}_f A_f d\bar{u}_f = \dot{m}_f d\bar{u}_f \quad (3.44)$$

where  $I_F$  is the interface friction force acting between the gas and liquid. Adding equations (3.43) and (3.44) gives

$$-Adp - dF_g - dF_f = d(\dot{m}_g \bar{u}_g + \dot{m}_f \bar{u}_f) \quad (3.45)$$

Using the area of each component to express the net friction force acting on each component, Collier (1981) gives

$$(dF_g + I_F) = -A_g \left( \frac{dp}{dx} F_g \right)_{\text{tp}} dx \quad (3.46)$$

$$(dF_f - I_F) = -A_f \left( \frac{dp}{dx} F_f \right)_{\text{tp}} dx \quad (3.47)$$

$$\text{or, } (dF_g + dF_f) = -A \left( \frac{dp}{dx} F \right)_{\text{tp}} dx \quad (3.48)$$

Substituting equation (3.48) into equation (3.45) and dividing by  $A dx$  yields

$$-\left( \frac{dp}{dx} \right)_{\text{tp}} = -\left( \frac{dp}{dx} F \right)_{\text{tp}} + \frac{1}{A} \frac{d}{dx} (\dot{m}_g \bar{u}_g + \dot{m}_f \bar{u}_f) \quad (3.49)$$



where the first and second terms on the right-hand side are the static pressure gradients due to friction and acceleration, respectively. In Collier's (1981) derivation, he considers the acceleration of the fluid and finds that

$$\frac{1}{A} \frac{d}{dx} (\dot{m}_g \bar{u}_g + \dot{m}_f \bar{u}_f) = G^2 \frac{d}{dx} \left[ \frac{x^2 v_g}{\alpha} + \frac{(1-x)^2 v_f}{1-\alpha} \right] \quad (3.50)$$

Therefore, equation (3.49) becomes

$$-\left( \frac{dp}{dx} \right)_{tp} = -\left( \frac{dp_F}{dx} \right)_{tp} + G^2 \frac{d}{dx} \left[ \frac{x^2 v_g}{\alpha} + \frac{(1-x)^2 v_f}{1-\alpha} \right] \quad (3.51)$$

It should be noted that the acceleration term is presented for completeness. In the final expression for the pressure drop, these terms drop out because of either the steady state assumption or through the use of simplifying assumptions.

As for homogeneous flow, the friction pressure gradient may be expressed in terms of a single-phase pressure gradient ( $f_{fa}$ ) with the total flow considered to be liquid.

$$-\left( \frac{dp_F}{dx} \right)_{tp} = -\left( \frac{dp_F}{dx} \right)_{fa} \phi_{fa}^2 = \left[ \frac{2 f_{fa} G^2 v_f}{D_h} \right] \phi_{fa}^2 \quad (3.52)$$

The fiction pressure gradient may also be expressed in terms a single-phase pressure gradient ( $f_f$ ) with the liquid phase considered to flow alone in the channel.

$$-\left( \frac{dp_F}{dx} \right)_{tp} = -\left( \frac{dp_F}{dx} \right)_f \phi_f^2 = \left[ \frac{2 f_f G^2 (1-x)^2 v_f}{D_h} \right] \phi_f^2 \quad (3.53)$$

This is the preferred form used in calculating pressure drop. Substituting equation (3.53) back into equation (3.51) and simplifying yields,

$$-\left(\frac{dp}{dx}\right)_{tp} = \frac{\left[\frac{2f_f G^2 (1-x)^2 v_f}{D_h}\right] \Phi_f^2}{1 + G^2 \left[ \frac{x^2}{\alpha} \left( \frac{dv_g}{dp} \right) + \frac{d\alpha}{dp} \left\{ \frac{(1-x)^2 v_f}{(1-\alpha)^2} - \frac{x^2 v_g}{\alpha^2} \right\} \right]} \quad (3.54)$$

As with the homogeneous model, equation (3.54) requires stepwise integration unless simplifying assumptions are made. These assumptions are similar to those made for the homogeneous flow model; 1) the specific volumes,  $v_g$  and  $v_f$ , along with the friction factor ( $f_f$ ) remain constant over the length of the channel, and 2) the second term in the denominator is much less than one. With these assumptions, equation (3.54) reduces to a form very similar to equation (3.26)

$$-\left(\frac{dp}{dx}\right)_{tp} = \left[ \frac{2f_f G^2 (1-x)^2 v_f}{D_h} \right] \Phi_f^2 \quad (3.55)$$

The difference with this model is that no expression has been derived for the two-phase multiplier ( $\Phi_f^2$ ). Therefore, to apply equation (3.55) one must develop an expression for the two-phase multiplier in terms of the independent variables. This expression was first developed by Martinelli et al.(1944). This material was presented in Chapter 2. As a brief

summary, expressions for  $\phi_f^2$  and  $\phi_g^2$  were given as

$$\phi_f^2 = 1 + \frac{C}{X} + \frac{1}{X^2} \quad (2.12)$$

$$\phi_g^2 = 1 + CX + X^2 \quad (3.56)$$

where the constant  $C$  is given in Table 2, pg.17, and the Martinelli parameter,  $X$ , was given by

$$X^2 = \frac{(\Delta p / \Delta L)_f}{(\Delta p / \Delta L)_g} = \frac{C_f (Re_G)^m \rho_G}{C_g (Re_f)^n \rho_f} \left( \frac{1-x}{x} \right)^2 \quad (2.10)$$

where the values of the coefficients  $C_f$ ,  $C_g$ ,  $m$ , and  $n$  were given in Table 1, pg. 17. The literature survey also discussed Martinelli and Nelson (1948) who developed an expression for boiling two-phase flow. Again, as a summary, only the pertinent equations are repeated here. From Barron (1985),

$$\Delta p_m = \frac{\phi_m (\dot{m}_f + \dot{m}_g)^2}{g_c \rho_f A^2} \quad (2.14)$$

with the momentum-pressure-drop parameter given by

$$\phi_m = \frac{(1-x_{out})^2}{\alpha_{f,out}} - \frac{(1-x_{in})^2}{\alpha_{f,in}} + \left( \frac{x_{out}^2}{1-\alpha_{f,out}} - \frac{x_{in}^2}{1-\alpha_{f,in}} \right) \left( \frac{\rho_f}{\rho_g} \right) \quad (2.15)$$

where  $\alpha_f$  is the volume fraction of liquid at the entrance and exit of the channel. Similar to before, the Martinelli parameter,  $X$ , and the momentum-pressure-drop parameter are related by

$$\phi_m = \frac{X}{(X^2 + CX + 1)^{1/2}} \quad (2.16)$$

where the coefficient  $C$  was given in Table 2.

To now obtain the final expression for the pressure drop, we must combine the above equations such that

$$\Delta p = \Delta p_f + \Delta p_m \quad (2.17)$$

Integrating equation (3.55) over the length of the channel, and combining with equation (2.14) gives

$$\Delta p_{tp} = \left[ \frac{2L f_f G^2 (1-x)^2 v_f}{D_h} \right] \phi_f^2 + \frac{\phi_m (\dot{m}_f + \dot{m}_g)^2}{g_c \rho_f A^2} \quad (3.57)$$

After simplification, the final result is obtained as

$$\Delta p_{tp} = G^2 v_f \left( \frac{2L f_f (1-x)^2 \phi_f^2}{D_h} + \phi_m \right) \quad (3.58)$$

where  $\phi_f^2$  and  $\phi_m$  are given in equations (2.12) and (2.16), respectively.

### Conservation of Energy

The analysis of the conservation of energy is virtually identical to the derivation for the homogeneous model. Each component of the fluid is considered separately and the resulting equations are then combined using the definition of quality. The results are the same equations as found for the homogenous flow model. This conclusion is only possible because of the assumption of thermodynamic equilibrium between the two phases. To help reduce redundancy, the final equations are simply restated. When considering kinetic effects, we have

$$\overline{Nu} = \frac{D_h \dot{m} \left[ c_p (T_{out} - T_{in}) + \frac{1}{2} (\bar{u}_{out}^2 - \bar{u}_{in}^2) \right]}{A k_m (T_s - T_\infty)} \quad (3.37)$$

When neglecting kinetic effects, we have

$$\overline{Nu} = \frac{D_h \dot{m} [c_p (T_{out} - T_{in})]}{A k_m (T_s - T_\infty)} \quad (3.38)$$

It should be noted that if phase change was present or thermodynamic equilibrium between the phases was not assumed, a detailed analysis would be necessary to account for the interaction between the phases.

## Two-Phase Two-Component Flow Regimes

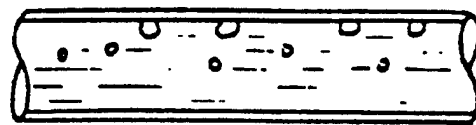
### Macroscale

Though many types of two component flow geometries exist, the generally accepted macroscale flow regimes for two-phase two-component horizontal flow are shown graphically in Figure 3.3. A general description is as follows.

a) *Bubble Flow*. Here the main continuum is liquid with bubbles of various sizes flowing along with the liquid. For macroscale channels, the bubbles tend to flow at or near the top of the channel. This regime is characterized by a low quality. The bubble size will vary depending of the quality of the flow. As the quality and, hence, the bubble size increases, the bubbles will tend to coalesce into larger and larger bubbles which provides the transition to the next regime.

b) *Plug Flow*. In this regime the bubble size is large enough to occupy the upper part of the channel so that the liquid no longer surrounds the bubble. Hence the descriptive name changes from a bubble to a plug of gas. The liquid does, however, still separate each plug of gas. As the size of the plug (quality of the flow) continues to increase, the amount of liquid separating the plugs decreases until it no longer exists. This is the transition to the next regime.

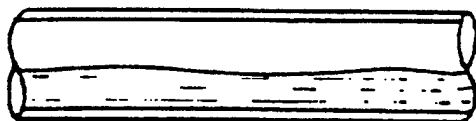
c) *Stratified Flow*. For this regime, the gas and liquid are flowing as two separate entities. Therefore, the flow rates are much more independent than in any other flow regime. However, for this regime to exist, the overall flow rate of both components must



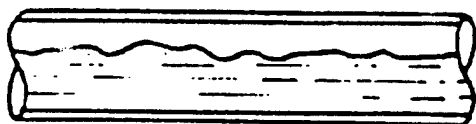
Bubble Flow



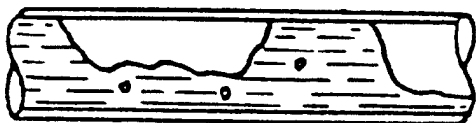
Plug Flow



Stratified Flow



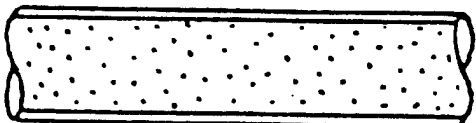
Wavy Flow



Slug Flow



Annular Flow



Mist Flow

Figure 3.3: Macroscale two-phase flow regimes (Barron, 1985).

be relatively low. As the gas flow rate increases, relative to the liquid flow rate, the viscous interaction between the two components causes the transition to the next regime.

d) *Wavy Flow*. Here the gas flow rate is large enough, relative to the liquid flow rate, to cause waves to form. As the flow rate of the gas continues to increase, the amplitude of the waves will increase. The size of these waves can vary from ripples up to the height of the channel. When the liquid waves reach the top of the channel, the next regime is attained.

e) *Slug Flow*. In this regime the slug of liquid, for the most part, is actually being pushed by the gas. Though this regime is easily mistaken for plug flow, it generally occurs at a much higher overall flow rate. As the quality and overall flow rate continue to increase, the gas will reach a point that its flow rate, relative to the liquid, becomes large enough to actually start pushing the liquid to all sides of the channel. At this point the next regime is reached.

f) *Annular Flow*. For this regime the flow of the liquid is mainly restricted to a thin layer around the perimeter of the channel. The gas flows through the center of the liquid and can contain some entrained droplets of liquid. This flow regime is characterized by high values of quality and gas flow rate. As the quality continues to increase, the thickness of the liquid layer decreases until it can no longer exist. This is the transition to the last regime.

g) *Mist Flow*. This regime exists only for the highest values of quality and flow rates. The gas flowing through the channel contains entrained droplets of liquid, as in the

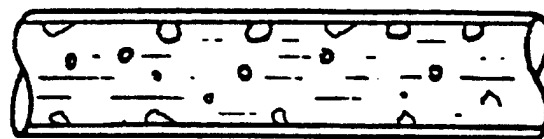


last regime. However, the liquid flow rate is so low that the droplets have virtually no chance to coalesce. The size of the droplets will vary but will decrease with increasing quality. This will continue until only gas is flowing thorough the channel.

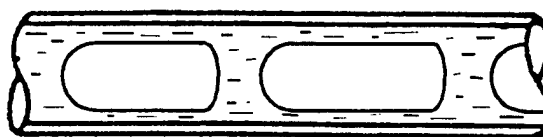
### Microscale

For microscale, the flow regimes are not as well defined. The regimes proposed below are based on literature reviews and experimental observation. One of the biggest differences between macroscale and microscale regimes is the role of surface tension. For macroscale, gravity dominates over surface tension even though they both play important roles. In microscale, however, surface tension is not only dominant but gravity has been shown [Suo and Griffith (1964)] not to be a factor. The flow regimes to be discussed are shown graphically in Figure 3.4.

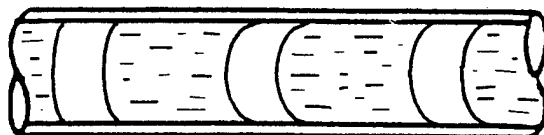
a) *Bubble Flow*. Like macroscale, this regime is made up of a continuum of liquid with bubbles of various size flowing along with the liquid. For microscale, however, the bubbles do not tend to flow near the top of the channel. Instead, they are present throughout the entire depth of the channel. Also, bubbles of various sizes will tend to adhere to the channel walls and be pushed through the channel by the liquid and other bubbles. As before, as the quality increases, the average bubble size increases. This will continue until the bubble size approaches the size of the channel. At this point, increasing the quality will only increase the bubbles length. And, depending on the flow rate of each component, one of the next two regimes will occur.



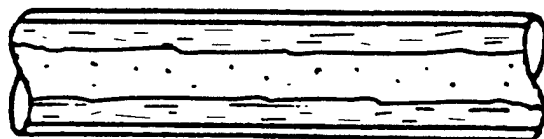
Bubble Flow



Slug Flow



Plug Flow



Annular Flow



Mist Flow

Figure 3.4: Microscale two-phase flow regimes.

b) *Slug Flow*. In this regime the gas forms long bubbles separated from the channel walls by a thin layer of liquid. The long bubbles are separated from each other by liquid filling the entire cross-section. It is easy to see, for this regime, that as the quality increases the bubble length increases. This can continue until the bubble length actually becomes longer than the channel itself. At this point we have transitioned to annular flow.

c) *Plug Flow*. For this regime the bubble occupies the entire cross section of the channel and is not separated from the channel wall by a thin layer of liquid. Therefore, the liquid and gas components are virtually completely separate at a given cross section. As with slug flow, the bubble length will increase with increasing quality. This can continue until either the bubble length becomes longer than the channel itself or the liquid plug becomes so thin that surface tension will not maintain a film across the channel cross-section. In the former case, one would have only gas flowing through the channel. In the latter case, the flow will have transitioned to mist flow. How and when this regime will occur, and how it will transition between the other regimes, is unclear at this point. However, one detail about the pressure drop in this unique regime is worth mentioning. As with the other regimes, the pressure drop will be dependent on the viscous interaction of each component with the channel wall. In addition, because the interface of the two components meets at the wall, the pressure drop will also be highly dependent on the surface tension produced by the two fluids.

d) *Annular Flow*. As with macroscale, this regime is characterized by the liquid flow being restricted to a thin layer around the perimeter of the channel with the gas

flowing through the center. Though possible, it is not expected that small liquid droplets will be entrained in the gas flow. For small channels, if any liquid is entrained it will not travel far before contacting and becoming part of the thin liquid layer. With increasing quality, the liquid layer will continue to decrease until surface tension is not able to maintain a continuous fluid around the entire perimeter of the channel. At this point, we have the transition to the next regime.

e) *Mist Flow*. Analogous to macroscale, this regime is made up of gas flowing through the channel with some entrained liquid droplets. Though some droplets may stay entrained in the gas, it is anticipated most of the droplets will adhere to the channel wall and be pushed through the channel by the gas while coalescing with other droplets. As before, the size of the droplets will decrease with increasing quality until only gas is flowing thorough the channel.

## CHAPTER 4

### DIMENSIONAL AND EMPIRICAL ANALYSIS

The empirical equations used to interpret the experimental data of this study will be derived in this chapter. A dimensional analysis will be the main source of this derivation. The first section of this chapter (Dimensional Analysis) will present the dimensional analysis for both single-phase and two-phase flow. As discussed in chapter two, single-phase flow is only being considered because of two interrelated reasons; one, the macroscale and microscale two-phase relations are based on single-phase coefficients, and two, there is no general agreement on the values of these coefficients in microscale flow. The second section (Empirical Relations) will discuss the form of the empirical equations and present the procedure to solve for the empirical coefficients. Also, the computational method used to determine the empirical coefficients, correlation coefficient, and the standard deviation will be presented.

#### Dimensional Analysis

The method used in this section is the Buckingham Pi Theorem. This method, like other methods, reduces a number of dimensional variables into smaller dimensionless groups (White, 1986). The MLT (mass, length, and time) system is used for the pressure drop analysis, while the MLTH (mass, length, time, and heat transfer) system is used for

the heat transfer analysis. Analysis of this type is mainly based on the homogeneous flow model, or average fluid properties. The separated flow model, which involves ratios of variables ( $\rho_g / \rho_f$ , for example) and quality, will be considered in the last part of this section.

### Pressure Drop

The following variables can be used to describe the pressure drop per unit length in two-phase flow.

$$\frac{\Delta p}{L} = f(\rho_m, \mu_m, \sigma, D_H, V, \epsilon) \quad (4.1)$$

From White (1986), for the MLT system,

$\Delta p/L$	$\rho_m$	$\mu_m$	$\sigma$	$D_H$	$V$	$\epsilon$
$ML^{-2}T^{-2}$	$ML^{-3}$	$ML^{-1}T^{-1}$	$MT^{-2}$	$L$	$LT^{-1}$	$L$

The maximum number of variables that can be combined and not form a pi group is three.

The combination that will be used here is  $(\mu_m V D_H)$ . Therefore, we have  $7 - 3 = 4$

dimensionless pi groups to be found. For the first pi group

$$\Pi_1 = [\mu_m D_H V] \rho_m = (ML^{-1}T^{-1})^a (L)^b (LT^{-1})^c (ML^{-3})^1 = M^0 L^0 T^0$$

$$M: 0 = a + 1 \quad (4.2)$$

$$L: 0 = -a + b + c - 3$$

$$T: 0 = -a - c$$

Solving gives,  $a = -1$ ,  $b = c = 1$ . Substituting the values of the coefficients into the above equation gives

$$\Pi_1 = \mu_m^{-1} D_H V \rho_m = \frac{\rho_m D_H V}{\mu_m} = \text{Re} \quad (4.3)$$

where Re is the Reynolds number based on average properties of the fluid. Using the same method for the other variables yields

$$\begin{aligned} \Pi_2 &= \frac{\text{We}}{\text{Re}} \\ \Pi_3 &= \frac{D_H^2 \Delta p}{\mu_m V L} \\ \Pi_4 &= \frac{\varepsilon}{D_H} \end{aligned} \quad (4.4)$$

For the third pi group, we can substitute in the definition of the friction factor

$$f = \frac{\Delta p D_H}{2 \rho_m V^2 L} \quad (4.5)$$

Making this substitution and simplifying gives

$$\Pi_3 = 2 f Re \quad (4.6)$$

Therefore, the friction factor may be described by

$$2 f Re = f \left\{ Re, \frac{We}{Re}, \frac{\varepsilon}{D_H} \right\} \quad (4.7)$$

Or, eliminating redundancy

$$f = f \left\{ Re, We, \frac{\varepsilon}{D_H} \right\} \quad (4.8)$$

For single-phase flow, the dimensional analysis follows exactly the same procedure. The only differences are that the fluid properties are based on a single component and surface tension need not be considered. The results are the same that are found for macroscale flow. From White (1988),

$$f = f \left\{ Re, \frac{\varepsilon}{D_H} \right\} \quad (4.9)$$

If the pressure term, at the start of the analysis, was taken as  $\Delta p$  instead of  $\Delta p/L$ , then a  $L/D_H$  pi group would be found. This applies to both single and two-phase.



Therefore, including the  $L/D_H$  term in the above analysis, the final description of pressure drop is

$$\text{Two-Phase: } f = f\left\{\text{Re}, \text{We}, \frac{\epsilon}{D_H}, \frac{L}{D_H}\right\} \quad (4.10)$$

$$\text{Single-Phase: } f = f\left\{\text{Re}, \frac{\epsilon}{D_H}, \frac{L}{D_H}\right\} \quad (4.11)$$

The  $L/D_H$  ratio was included for completeness and to help show if any entrance effects are present in the experimental data. Entrance effect pi groups will be discussed in more detail in the last part of this section.

### Heat Transfer

Using the MLT $\theta$  (mass, length, time, and temperature) system, the heat transfer of two-phase flow in an enclosed channel can be described by the following variables

$$q = f(h, k_m, C_{p_m}, \Delta T, D_H, \mu_m, V, \rho_m, \sigma, L, \epsilon) \quad (4.12)$$

For the MLT $\theta$  system, the basic units for these variables are

q	h	k	C <sub>p</sub>	$\Delta T$	$D_H$	$\mu_m$	V	$\rho_m$	$\sigma$	L	$\epsilon$
ML <sup>-2</sup> T <sup>-2</sup>	MT <sup>-2</sup> $\theta^{-1}$	MLT <sup>-3</sup> $\theta^{-1}$	L <sup>2</sup> T <sup>-2</sup> $\theta^{-1}$	$\theta$	L	ML <sup>-1</sup> T <sup>-1</sup>	LT <sup>-1</sup>	ML <sup>-3</sup>	MT <sup>-2</sup>	L	L

As Schenck (1968) describes, the MLT $\theta$  system can be changed to the MLTH (mass,

length, time, and heat transfer) system by making the substitution

$$H = \frac{q}{L\Delta T} = MLT^{-2}\theta^{-1} \quad (4.13)$$

Or,

$$\theta^{-1} = \frac{H}{MLT^{-2}} \quad (4.14)$$

Substituting for  $\theta^{-1}$ , the basic dimensions on each of the variables becomes

h	k	C <sub>p</sub>	D <sub>H</sub>	$\mu_m$	V	$\rho_m$	$\sigma$	$\epsilon$
HL <sup>-1</sup> T <sup>-5</sup>	HT <sup>-5</sup>	HMLT <sup>-4</sup>	L	ML <sup>-1</sup> T <sup>-1</sup>	LT <sup>-1</sup>	ML <sup>-3</sup>	MT <sup>-2</sup>	L

thereby eliminating  $\Delta T$ , L, and q from the analysis. We now have

$$h = f(k_m, C_{p_m}, D_H, \mu_m, V, \rho_m, \sigma, \epsilon) \quad (4.15)$$

Schenck (1968) mentions this substitution is done because the resulting system (MLTH) is more applicable to heat transfer systems and the pi groups are more easily found. The maximum number of variables that can be combined and not form a pi group is four. The combination that will be used here is ( $D_H$  V  $\rho_m$   $k_m$ ). Therefore, we have  $9 - 4 = 5$  dimensionless pi groups to be found. For the first pi group

$$\Pi_1 = [D_H V \rho_m k_m] h = (L)^a (L T^{-1})^b (M L^{-3})^c (H T^{-5})^d (H L^{-1} T^{-5})^1 = M^0 L^0 T^0$$

$$M: 0 = c$$

$$L: 0 = a + b + 3c - 1 \quad (4.16)$$

$$T: 0 = -b - 5d - 5$$

$$H: 0 = d + 1$$

Solving gives,  $a = 1$ ,  $b = c = 0$ , and  $d = -1$ . Substituting these values into equation (4.16)

yield

$$\Pi_1 = D_H k_m^{-1} h = \frac{h D_H}{k_m} = Nu \quad (4.17)$$

where  $Nu$  is the Nusselt number based on average fluid properties. Using the same method for the other variables yields

$$\Pi_2 = Re$$

$$\Pi_3 = We$$

$$\Pi_4 = RePr \quad (4.18)$$

$$\Pi_5 = \frac{\epsilon}{D_H}$$

Therefore, the heat transfer between the channel and the fluid may be described by

$$Nu = f \left\{ Re, We, RePr, \frac{\epsilon}{D_H} \right\} \quad (4.19)$$

As before, the dimensional analysis for single-phase flow follows exactly the same procedure. Basing the fluid's properties on a single component and neglecting surface tension, we have

$$\text{Nu} = f\left\{\text{Re}, \text{RePr}, \frac{\varepsilon}{D_H}\right\} \quad (4.20)$$

Reducing redundancy with regard to the Reynolds number, and including  $L/D_H$ , the final description of heat transfer becomes

$$\text{Two-Phase: } \text{Nu} = f\left\{\text{Re}, \text{We}, \text{Pr}, \frac{\varepsilon}{D_H}, \frac{L}{D_H}\right\} \quad (4.20)$$

$$\text{Single-Phase: } \text{Nu} = f\left\{\text{Re}, \text{Pr}, \frac{\varepsilon}{D_H}, \frac{L}{D_H}\right\} \quad (4.21)$$

### Separated Flow Model and Other Considerations

By definition, the separated flow model is concerned with the individual properties of each component. This has led to many researchers [Lockhart and Martinelli (1949), Martinelli et al. (1944), Martinelli and Nelson (1948), and Suo and Griffith (1964)] using the ratio of the fluid properties as pi groups. Though a dimensional analysis could be done with all properties of each fluid present, this would be exceedingly lengthy. One would soon find out that the ratios of specific properties do naturally fall out of such an analysis. However, by not including them directly in the analysis, many unnecessary terms are eliminated. For example, a Reynolds number type expression based on the density of the

liquid and the viscosity of the gas. The ratios to be used as pi groups in this analysis are based on the preceding analysis as well as the studies just mentioned. They are

$$\frac{k_f}{k_g}, \frac{Cp_f}{Cp_g}, \frac{\rho_f}{\rho_g} \text{ or } \frac{v_g}{v_f}, \text{ and } \frac{\mu_f}{\mu_g}$$

Another natural pi group that arises in the study of two-phase flow is quality. Quality itself is nondimensional and therefore can be used as a pi group. However, most often it is not. The term involving quality, used by Martinelli and Nelson (1948), is based on the ratio of the mass flow rates. Quality is defined as

$$x = \frac{\dot{m}_g}{\dot{m}_f + \dot{m}_g} \quad (4.22)$$

Solving this expression for the ratio of the mass flow rate of the gas to the mass flow rate of the liquid yields the pi group based on quality

$$\frac{\dot{m}_g}{\dot{m}_f} = \frac{1-x}{x} \quad (4.23)$$

This pi group applies to both pressure drop and heat transfer analysis.

When considering entrance effects in heat transfer, two other pi groups come about from the Seider-Tate equation. The Seider-Tate equation considers the thermal and velocity entry lengths, and has shown to be a good correlation. From Incropera and

DeWitt (1985), the Seider-Tate equation is given as

$$\overline{Nu}_D = 1.86 \left( \frac{Re_D Pr}{L/D} \right)^{1/3} \left( \frac{\mu}{\mu_s} \right)^{0.14} \quad (4.24)$$

The pi groups of interest are  $L/D$  and  $\mu/\mu_s$ , where  $\mu$  is evaluated at the mean fluid temperature and  $\mu_s$  is evaluated at the mean wall temperature. These pi groups can be used for two-phase flow if the following substitutions are made: 1) The channel hydraulic diameter ( $D_H$ ) replaces the tube inside diameter ( $D$ ), and 2) The viscosity terms are the mean values as found by the homogeneous flow model.

As will be discussed in Chapter 5, channel configurations with various aspect ratios were tested to determine the effect, if any, of the aspect ratio. The consideration of the aspect ratio applies for each flow model. To conclude this section, the various pi groups discussed above can be combined to give a final description of the pressure drop and heat transfer, in single- and two-phase flow, for each flow model. For two-phase flow we have:

Homogeneous Flow Model:

$$f = f \left\{ Re, We, \frac{\epsilon}{D_H}, \frac{L}{D_H}, \frac{1-x}{x}, \alpha \right\} \quad (4.25)$$

$$Nu = f \left\{ Re, We, Pr, \frac{\mu_m}{\mu_{ms}}, \frac{\epsilon}{D_H}, \frac{L}{D_H}, \frac{1-x}{x}, \alpha \right\} \quad (4.26)$$

Separated Flow Model:

$$f = f \left\{ \frac{k_f}{k_g}, \frac{Cp_f}{Cp_g}, \frac{v_g}{v_f}, \frac{\mu_f}{\mu_g}, \frac{\varepsilon}{D_H}, \frac{L}{D_H}, \frac{1-x}{x}, \alpha \right\} \quad (4.27)$$

$$Nu = f \left\{ \frac{k_f}{k_g}, \frac{Cp_f}{Cp_g}, \frac{v_g}{v_f}, \frac{\mu_f}{\mu_g}, \frac{\varepsilon}{D_H}, \frac{L}{D_H}, \frac{1-x}{x}, \alpha \right\} \quad (4.28)$$

Similarly, for single-phase flow, we have

$$f = f \left\{ Re, \frac{\varepsilon}{D_H}, \frac{L}{D_H}, \alpha \right\} \quad (4.29)$$

$$Nu = f \left\{ Re, Pr, \frac{\mu_m}{\mu_{ms}}, \frac{\varepsilon}{D_H}, \frac{L}{D_H}, \alpha \right\} \quad (4.30)$$

### Empirical Relations

The form that the empirical correlation equations will take is that of a multidimensional power equation. Or, an equation of the form

$$y = A x_1^b x_2^c x_3^d \dots \quad (4.31)$$

where the  $x_i$ 's are nondimensional parameters (Re, Nu, etc.) and A, b, c, etc. are empirical constants to be calculated. Putting equations (4.25) through (4.30) into this form gives:

Homogeneous Two-Phase Flow Model:

$$f = A (Re)^b (We)^c \left( \frac{\mu_m}{\mu_{ms}} \right)^d \left( \frac{\varepsilon}{D_H} \right)^e \left( \frac{L}{D_H} \right)^f \left( \frac{1-x}{x} \right)^g (\alpha)^h \quad (4.32)$$

$$Nu = A (Re)^b (We)^c (Pr)^d \left( \frac{\mu_m}{\mu_{ms}} \right)^e \left( \frac{\varepsilon}{D_H} \right)^f \left( \frac{L}{D_H} \right)^g \left( \frac{1-x}{x} \right)^h (\alpha)^i \quad (4.33)$$

Separated Two-Phase Flow Model:

$$f = A \left( \frac{k_f}{k_g} \right)^b \left( \frac{Cp_f}{Cp_g} \right)^c \left( \frac{v_g}{v_f} \right)^d \left( \frac{\mu_f}{\mu_g} \right)^d \left( \frac{\varepsilon}{D_H} \right)^e \left( \frac{L}{D_H} \right)^f \left( \frac{1-x}{x} \right)^g (\alpha)^h \quad (4.34)$$

$$Nu = A \left( \frac{k_f}{k_g} \right)^b \left( \frac{Cp_f}{Cp_g} \right)^c \left( \frac{v_g}{v_f} \right)^d \left( \frac{\mu_f}{\mu_g} \right)^d \left( \frac{\varepsilon}{D_H} \right)^e \left( \frac{L}{D_H} \right)^f \left( \frac{1-x}{x} \right)^g (\alpha)^h \quad (4.35)$$

Single-Phase:

$$f = A (Re)^b \left( \frac{\mu_m}{\mu_{ms}} \right)^c \left( \frac{\varepsilon}{D_H} \right)^d \left( \frac{L}{D_H} \right)^e (\alpha)^f \quad (4.36)$$

$$Nu = A (Re)^b (Pr)^c \left( \frac{\mu_m}{\mu_{ms}} \right)^d \left( \frac{\varepsilon}{D_H} \right)^e \left( \frac{L}{D_H} \right)^f (\alpha)^g \quad (4.37)$$

Solving for the empirical coefficients is accomplished by using multiple linear regression. The equation for multiple linear regression takes the form

$$y = a + bx_1 + cx_2 + dx_3 + \dots \quad (4.38)$$

Equations (4.32) through (4.37) can be put into this form by taking the natural log of the equation. For example, equation (4.36) can be put into the form of equation (4.38) by



making the following substitutions:

$$\begin{aligned}
 y &= \ln(f) \\
 x_1 &= \ln(\text{Re}) \\
 x_2 &= \ln\left(\frac{\mu_m}{\mu_{ms}}\right) \\
 x_3 &= \ln\left(\frac{\varepsilon}{D_H}\right) \\
 x_4 &= \ln\left(\frac{L}{D_H}\right) \\
 x_5 &= \ln(\alpha)
 \end{aligned} \tag{4.39}$$

Once these substitutions are made, the resulting equation can then be solved for the empirical coefficients using the standard numerical methods for multiple linear regression.

The method of solving a multiple linear regression equation, as outlined by Chapra and Canale (1985), is to minimize the sum of the square of the residuals. The sum of the

square of the residuals is given by the expression

$$S = \sum_{i=1}^n (y_i - a - bx_{1,i} - cx_{2,i} - dx_{3,i} - \dots)^2 \tag{4.40}$$

Differentiating equation (4.40) with respect to each of the coefficients (a, b, c, etc.) and setting each equation equal to zero, generates a system of equations. This system of equations, when solved, yields the coefficients that minimize the sum of the squares of the

residuals. For the general case of multiple linear regression, the matrix to be solved is given by Chapra and Canale (1985) as

$$\begin{bmatrix} n & \sum x_{1,i} & \sum x_{2,i} & \dots & \sum x_{m,i} \\ \sum x_{1,i} & \sum x_{1,i}^2 & \sum x_{2,i}x_{1,i} & \dots & \sum x_{1,i}x_{m,i} \\ \sum x_{2,i} & \sum x_{2,i}x_{1,i} & \sum x_{2,i}^2 & \dots & \sum x_{2,i}x_{m,i} \\ \vdots & \vdots & \vdots & \ddots & \vdots \\ \sum x_{m,i} & \sum x_{m,i}x_{1,i} & \sum x_{m,i}x_{2,i} & \dots & \sum x_{m,i}^2 \end{bmatrix} \begin{bmatrix} a_0 \\ a_1 \\ a_2 \\ \vdots \\ a_m \end{bmatrix} = \begin{bmatrix} \sum y_i \\ \sum x_{1,i}y_i \\ \sum x_{2,i}y_i \\ \vdots \\ \sum x_{m,i}y_i \end{bmatrix} \quad (4.41)$$

where 'n' is the number of data points, 'i' is incremented from one to 'n', 'm' is the number of dimensionless numbers or ratios used in the correlation minus one,  $a_i$ 's are the coefficient values (a, b, c, d, etc.), and  $x_i$ 's and  $y_i$ 's are the natural logs of the dimensionless numbers or ratios as described in equation (4.39). The only post computational manipulation required is to calculate the correct value of the constant 'A.' Because the natural log of the original equation was taken before solving, the computed value of the constant 'a' is not equal to 'A.' The relationship is  $a = \ln(A)$ . Therefore, the correct value of 'A' is given by  $A = e^a$ .

An important issue when using empirical correlation is to know how well the resulting correlation fits the data points. The rating, or value, of the correlation is determined by using a correlation coefficient. From Holman (1984), the correlation coefficient (r) is defined as

$$r = \left[ 1 - \frac{\sigma_{y,x}^2}{\sigma_y^2} \right]^{1/2} \quad (4.42)$$

where  $\sigma_y$  is the standard deviation of  $y$  given as

$$\sigma_y = \left[ \frac{\sum_{i=1}^n (y_i - y_m)^2}{n-1} \right]^{1/2} \quad (4.43)$$

and

$$\sigma_{y,x} = \left[ \frac{\sum_{i=1}^n (y_i - y_{ic})^2}{n-2} \right]^{1/2} \quad (4.44)$$

In these equations,  $y_i$  are the measured values,  $y_m$  is the mean of the measured values, and  $y_{ic}$  are the values calculated using the correlation equation. The standard deviation is also helpful in evaluating the success of the correlation equation, as it is a measure of the variability of the data around the correlation equation. The coefficient of determination ( $r^2$ ) is a measure of how well the computed correlation explains the variability of the data. A value of  $r^2 = 1$  signifies that the computed correlation explains 100% of the variability and a value of  $r^2 = 0$  represents no improvement [Chapra and Canale (1985)].

The calculation methods described above are very easily incorporated into a computer program. For this study, a FORTRAN program was written that calculates the empirical coefficients, the standard deviation, and the correlation coefficient for a given

set of dimensionless numbers and ratios. The program, listed in Appendix A, also does these calculations for each unique combination of the given dimensionless numbers and ratios in the input data file. For example, if one wishes to correlate equation (4.36), the following procedure should be followed:

- 1) Generate a data file listing the values calculated for the dimensionless numbers and ratios shown in equation (4.36) ( $f$ ,  $Re$ ,  $\mu_m/\mu_{ms}$ ,  $\epsilon/D_H$ , and  $L/D_H$ ) for each data point. One data point per line.
- 2) Determine the number of dimensionless numbers (columns) and data points (rows). These will be the constants  $m$  and  $n$ , respectively, used in the computer program. For this example,  $m$  has a value of five.
- 3) Change the computer program to reflect the correct values of  $m$  and  $n$ .
- 4) Make sure the name and path of the file containing the data is listed correctly in the program. Also check the output file name.
- 5) Run the program.

The output file will list all the pertinent information for each unique combination on a separate line. Each line will list the following for each combination; correlation coefficient, standard deviation, value of coefficients  $A$ ,  $b$ ,  $c$ , etc. These results can easily be transferred into a spread sheet for further analysis. As will be discussed in chapter six, using this computer program along with a spreadsheet allows for a much more thorough analysis. Not only can one determine which particular correlation gives the best fit to the data, but one can also determine the relative importance of each dimensionless term.

## CHAPTER 5

### EXPERIMENTAL APPARATUS, PROCEDURE, AND CALCULATIONS

#### Experimental Apparatus

##### Test Section

The basic test section configuration was designed by the author and Darin Bailey (1996). Shown in Figure 5.1, the test section consisted of an aluminum blank in which the microchannels were machined and a glass cover plate (not shown) epoxied on top to seal the tops of the microchannels and the manifold areas. Detailed information on milling the aluminum blank to the dimensions shown in Figure 5.1, along with program listings of all CNC G-Code is given in Bailey (1996). The test section used in this study differed from Bailey's (1996) in that there were seven small thermocouples mounted in the aluminum just beneath the channels to measure the wall temperature along the channel length.

In this study, liquid water was used along with gaseous argon, helium, and nitrogen. Each fluid was tested as a single phase and then combinations of water and each gas were tested. The fluids were chosen to give a range of viscosity, density, specific heat, and surface tension. The channel sizes were chosen to range from approximate 254  $\mu\text{m}$  square down to 50  $\mu\text{m}$  square. This range was chosen to encompass macroscopic

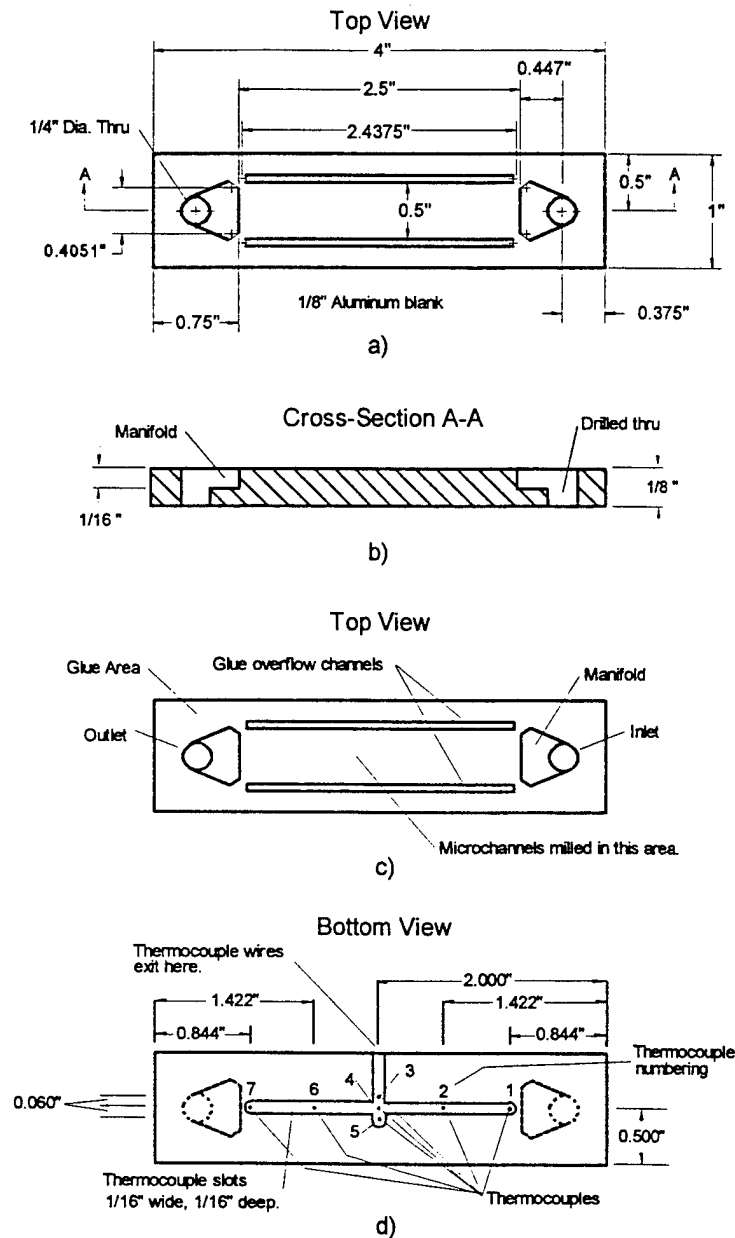


Figure 5.1: Test Section; a) Dimensions, b) Cross-section, c) Component description, and d) Thermocouple numbering and locations, approximately 0.01" beneath channels.

effects for the larger channels as well as microscopic effects for the smaller channels. Table 3, below, lists the measured channel height, width, aspect ratio, surface roughness, and number of channels for each configuration. A majority of the channels had an aspect ratio of approximately 1:1. However, for configurations C1-4, several aspect ratios were considered to determine the effect, if any, of the aspect ratio. Numbers in parentheses indicate the size of the end-mill used in cutting the channels. Variations from the size of the end-mill were caused by the end-mill being slightly out of round, build up of material on the end-mill during machining, and build up of material on the channel wall during machining. The channels were machined on the Ultra Precision Milling Machine of the Institute of Micromanufacturing using commercially available micro end-mills. The micro end-mills are available from McMaster-Carr and Mini Tool, Inc. A complete listing of companies and products mentioned in this study are given in Appendix B. The channel dimensions and surface characteristics were measured on a WYKO - RST surface profilometer. This device gave accurate and detailed information of depth and surface roughness using white light interferometry. Widths of the channel were measured using a microscope/video camera system with interpolating software. The system was calibrated using micrommeasurement slides from Edmond Scientific. The accuracy of all measurements will be discussed in the Error Analysis section of the next chapter.

Table 3: Measured Channel Dimensions

Channel Designation	Avg. Roughness, nm	Avg. Depth, $\mu\text{m}$	Avg. Width, $\mu\text{m}$	Aspect Ratio	Hydraulic Diameter, $\mu\text{m}$	Num. of Channels
A	102.7	255.8	258.0 (254)	0.991	256.9	3
B	154.7	211.1	208.9 (203)	1.010	210.1	3
C1	290.4	134.6	121.8 (127)	1.105	127.9	5
C2	1,846.2	263.73	170.4 (127)	1.548	170.4	3
C3	156.5	71.3	144.8 (127)	0.492	95.6	7
C4	202.8	19.3	150.7 (127)	0.128	34.2	9
D	183.9	111.3	112.4 (90)	1.010	111.9	7
E	1,334.7	74.9	85.8 (70)	1.145	80.0	9
F	427.6	54.1	58.0 (50)	1.073	56.0	11

Channel spacing and the number of channels to be used in each configuration were given great consideration. The number of channels in each configuration was selected considering the desired range of Reynolds numbers, the available pressures and flow rates from the flow loop apparatus, and the pressure restriction on the channels themselves. Though a larger number of configurations would ensure an adequate range of Reynold number, machining time was an important limiting factor. The largest channels (configuration A) took only about one hour to machine. However, the smallest channels (configuration F) took over 33 hours of machine time, not including setup. Unfortunately, there is no set formula for determining which number of channels is best for the wide variation of fluid properties between liquid s and gases. However, as one will see in the



next chapter, the data for both the single- and two-phase flow experiments yield a good range of Reynolds numbers. These ranges will be discussed in detail in the next chapter. The channels were spaced five widths of the cutting end-mill (on center) apart. Assumptions of equal heat flux from each wall of the channel was used to determine this spacing. Details of how the channel spacing was calculated, and verification of the heat flux assumption using the macroscale fin theory is given at the end of this section.

Originally, the test sections were to be covered with a glass plate bonded directly on the aluminum blank. However, residual stresses in the aluminum from machining caused the blank to warp. Also, the glass plates were not perfectly flat and therefore made sealing the channels impossible. During the initial testing with water, one could see the water traveling between the glass and the aluminum even for very low flow rates. The problem was solved using a Loctite-UV cure adhesive. The following procedure was used to sealing the channels:

- 1) Thin the UV adhesive with acetone (~50/50 by volume).
- 2) Pour this mixture on the polished side of a clean 4" silicon wafer.
- 3) Allow the acetone to evaporate leaving a thin layer of adhesive.
- 4) Place wafer in direct sunlight for about one hour.
- 5) Carefully remove the thin layer of adhesive, being sure not to stretch the partially cured adhesive. The adhesive has a rubbery consistency at this point. One may need to use a small sharp knife around the edge of the wafer to start the removal.

- 6) Lay the side of the adhesive that was exposed to the atmosphere on top of the aluminum blank. This side will still be slightly tacky. Be sure that all the channels and the manifold areas are completely covered. Press only hard enough to ensure contact. Too much pressure can press the film into the channel or cause sagging in the manifold areas.
- 7) Tape the glass cover plate on top of the blank/adhesive combination and let cure in direct sunlight for 10 - 12 hours. The cover plate will keep the adhesive from curling up along its edges and possibly lifting off the channels and manifolds.
- 8) Carefully remove the glass cover plate and, using a sharp knife, remove the excess adhesive from around the channels and manifolds. Be sure to leave the channel and manifold completely covered.
- 9) Finally, clean the glass cover plate thoroughly and bond to the aluminum blank with epoxy. Lay the assembly flat and allow to dry using no pressure to maintain contact (i.e. do not clamp). When the glue is completely cured, the test section is ready for use. It is recommended that one install the seven thermocouples in the backside of the blank before sealing the channels.

The channels were covered and recovered several times, while perfecting the above procedure, before satisfactory results were achieved. Obviously, the more experience and practice one has using the above procedure the sooner satisfactory results will be achieved. In addition, two tips are worth noting. First, use an epoxy that will not soften in the

slightest for the temperatures that the test section will experience. And second, be sure the epoxy melt temperature is low enough so that the cover can be removed, if needed, without damaging the thermocouples installed in the back of the test section.

This method was successful because of the properties of the UV-adhesive. After one-hour of cure time, the adhesive was still tacky on the side exposed to the atmosphere. This side was placed against the aluminum blank before final cure. The initial one-hour of cure time allowed the adhesive to be stiff enough to handle, and not be pressed into the micro channels, but pliable enough to conform to any unflatness of the aluminum blank. When assembling the glass cover plate and the aluminum blank, two points were crucial. First, do not use the same UV adhesive to bond the cover plate. The uncured adhesive will slightly dissolve the cured adhesive and cause the channels to become clogged. Second, any pressure, due to clamping of the glass cover plate to the aluminum while bonding, has been seen to push the cured adhesive into the channels and partially or completely clog them. It should also be noted that the above method proved unsuccessful in sealing the shallow channels of configuration C4 (20  $\mu\text{m}$  depth). The problem seemed to be the adhesive film sagging into the manifold areas, even with no pressure applied during assembly. Many attempts were made without success. Also, the diffusion bonding machine at Louisiana Tech University was not operational during this study. Therefore, configuration C4 was not used in this study.

From the experiments run for this study, the maximum pressure restriction on the test section assemblies described above was approximately 600 psi. However, if necessary

in future studies, the apparatus is capable of providing up to 1000 psi liquid pressures and 1500 psi gas pressures. It is not recommended to run the test sections, previously described, above a pressure of 200 psi without wearing safety goggles. Though the single-phase tests can be run at maximum pressure indefinitely, the two-phase tests cannot. It was seen that the intense pressure fluctuation associated with two-phase flow would eventually fatigue the epoxy bonding the glass cover plate to the aluminum. On more than one occasion during the two-phase tests, the epoxy did not hold. The results were quite explosive. Therefore, it is recommended that high pressure ( $> 300$  psi) two-phase flows not be run for more than a few minutes at a time. This recommendation is restated for a lower maximum pressure if one uses an epoxy that softens (even slightly) at the operating temperature of the test section.

The seven small thermocouples placed beneath the microchannels are shown in Figure 5.1. The thermocouples were type-T (copper-constantan) and are constructed from 36-gage wire coated with Teflon<sup>®</sup>. Small channels were machined on the back of the aluminum so the thermocouple wires could be routed out of the test section without interfering with the heater. The thermocouples were glued in the channel with a high temperature, high thermal conductivity epoxy. Thermocouple locations were symmetrical about the center of the channels and the end thermocouples were placed as near the channel ends as possible without the thermocouple slot cutting into the manifold area. From Figure 5.1, the end thermocouples are located  $0.844'' - 0.75'' = 0.094$  inches (2.39 mm) from the end of the channels. The thermocouples were numbered, as shown in Figure

5.1. Note that thermocouple numbers three, four, and five were placed lateral to the direction of the microchannels. Though not expected, any lateral heat conduction present during testing would be indicated by thermocouples number three through five having unequal readings. Small holes were drilled in the bottom of the thermocouple slots to a depth of approximately 0.01 inches (254  $\mu\text{m}$ ) from the backside of the channels using a #70 (0.028" diameter) drill. The welded bead of the thermocouple was then carefully inserted into the small hole and glued in place with a high temperature, high thermal conductivity epoxy. Care was taken to assure that no air bubbles were left in the epoxy. The distance from the microchannel wall to the thermocouple was chosen so that an assumption of a constant wall temperature between the wall and the thermocouple would be valid. This assumption may be checked with a simple calculation. For 6060-T6 aluminum, the thermal conductivity at 300 K is approximately 177 W/m-K. In this study the maximum heat dissipated was about 100 W and the smallest area was for 11 - 50  $\mu\text{m}$  wide channels. The channels were spaced five channel widths apart (on center). For conduction through a solid

$$q = kA \frac{dT}{dx} \doteq kA \frac{\Delta T}{\Delta x} \quad (5.1)$$

Solving for  $\Delta T$  gives

$$\Delta T = \frac{q \Delta x}{kA} \quad (5.2)$$

For  $\Delta x = 0.01$  inches (0.25 mm) and a channel length of 2.5 inches (0.0635 m)

$$\Delta T = \frac{(100 \text{ W})(2.54 \times 10^{-4} \text{ m})}{(177 \text{ W/m-K})[(11)(5) + 1](5 \times 10^{-5} \text{ m})(6.35 \times 10^{-2} \text{ m})} = 0.81^\circ \text{C} \quad (5.3)$$

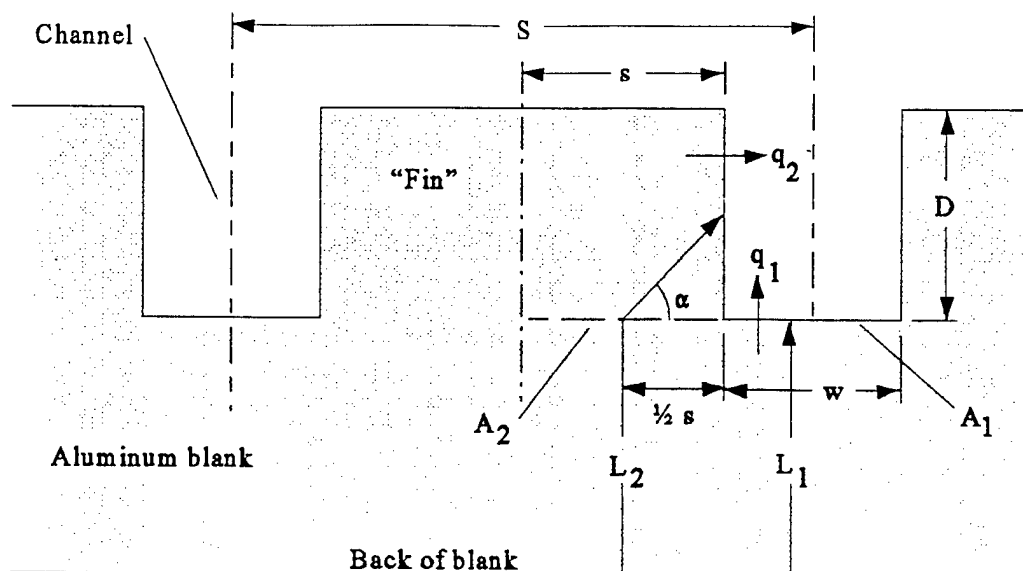
The accuracy of type-T thermocouples is  $\pm 1.0^\circ \text{C}$ . Therefore, the assumption of constant wall temperature is valid because the change in temperature within the aluminum wall is too small to be measured accurately.

The model for determining the spacing of the channels is shown in Figure 5.2. All variables used in the spacing model are defined in Figure 5.2. It is assumed that the heat transferred to area one and area two are equal. Or,

$$q_1 = q_2 \quad (5.4)$$

$$\frac{k_1 A_1 \Delta T_1}{L_1} = \frac{k_2 A_2 \Delta T_2}{L_2} \quad (5.5)$$

Since the blank material (aluminum) is homogeneous,  $k_1 = k_2$ . Also, assuming a constant wall temperature,  $\Delta T_1 = \Delta T_2$ . Define  $A_1 = wl$ ,  $A_2 = sl$ , and  $L_2 = L_1 + D/(2 \sin 45^\circ)$ . The angle of  $\alpha = 45^\circ$  is assumed and will be checked later in the analysis. Replacing the



Definition of variables:

$w$  = width of channel

$D$  = depth of channel

$s = \frac{1}{2}$  distance between edge of  
channels

$S = 2s + w$

$A_1$  = heat transfer area for bottom  
of channel

$A_2$  = horizontal heat transfer area  
for  $\frac{1}{2}$  width of "fin"

$L_1$  = thickness from back of blank to  
bottom of channel.

$L_2$  = distance from back of blank to  
center of side wall through angle  $\alpha$

$l$  = length of channel between manifolds

$q_1$  = heat transfer through bottom of  
channel

$q_2$  = heat transfer through side of channel

Figure 5.2: Model for determining channel spacing.

variables in equation (5.5) gives

$$sl = wl \left( \frac{L_1 + \frac{D}{2 \sin 45^\circ}}{L_1} \right) \quad (5.6)$$

Simplifying yields the final expression

$$s = w \left( 1 + \frac{D}{2 L_1 \sin 45^\circ} \right) \quad (5.7)$$

Because the area between the channels behaves as a fin, the worst case condition for this study is the channel configuration with the largest aspect ratio (configuration C2). However, to make sure, this analysis was also conducted for all other configurations. Configuration C2 was machined with a 127  $\mu\text{m}$  (0.005") diameter end-mill. Therefore, the expected dimensions are 127  $\mu\text{m}$  x 254  $\mu\text{m}$ . For the aluminum blanks,  $L_1 \approx 1/8" = 3,175 \mu\text{m}$ . Substituting these values into equation (5.7) yields

$$s = (1.25 \times 10^{-4} \text{m}) \left( 1 + \frac{2.5 \times 10^{-4} \text{m}}{2 (3.175 \times 10^{-4} \text{m}) \sin 45^\circ} \right) = 1.139 \times 10^{-4} \text{m} = 132 \mu\text{m} \quad (5.8)$$

Or, in terms of the channel width,

$$s = \frac{134}{127} w = 1.057 w \quad (5.9)$$



To add in a slight factor of safety, this number is rounded up to  $s = 1.5 w$ . Now, the spacing between the centers of the channels can be defined as

$$S = 2s + w \quad (5.10)$$

Substituting in the above expression for  $s$  gives

$$S = 2(1.5w)s + w = 4w \quad (5.11)$$

Or,

$$S \geq 4w \quad (5.12)$$

for the assumptions in this analysis to be valid. Again adding a slight factor of safety, the channel spacing was set at

$$S = 5w \quad (5.13)$$

Or, the spacing of the channels is five (5) widths of the end-mill used to machine the channels, on center. Using the actual dimensions of configuration C2, the assumed angle of  $\alpha = 45^\circ$  may be checked. For configuration C2,  $D = 263.7$  m,  $S = 5(127 \text{ m}) = 635$  m, and  $s = (S - 127 \text{ m})/2 = 254$  m. Then,

$$\alpha = \tan^{-1}\left(\frac{D}{s}\right) = \tan^{-1}\left(\frac{263.7}{254}\right) = 46.1^\circ$$

Therefore, the assumption of  $\alpha = 45^\circ$  is reasonable. The validity of the spacing can be checked using macroscale fin theory.

The analysis of the channel spacing using macroscale fin theory is based on two assumptions. First, a constant wall temperature. And second, equal heat fluxes from each wall of a given channel. For a given fin with an adiabatic tip, the temperature distribution is given by Incropera and DeWitt (1985) as

$$\frac{\theta}{\theta_b} = \frac{\cosh m(L-x)}{\cosh mL} \quad (5.14)$$

where  $\theta = T_{\text{fin}} - T_{\infty}$ ,  $\theta_b = T_{\text{wall}} - T_{\infty}$ ,  $m = hP/kA_c$ ,  $L$  = fin height (depth of channel),  $x = 0 \rightarrow L$  from base of fin,  $h$  = heat transfer coefficient,  $k$  = thermal conductivity of the fin material,  $P = 2w + 2t$  (perimeter of fin),  $A_c = wt$  (cross-sectional area of fin),  $w$  = width of fin (length of channel), and  $t$  = the thickness of the fin (distance between edges of channels). Again, the worst case scenario occurs for configuration C2. For the aluminum,  $k = 177 \text{ W/m-K}$ . The measured dimensions of configuration C2, based on the definitions above, are;  $L = 263.7 \text{ } \mu\text{m}$ ,  $t = 4(170.4) = 681.6 \text{ } \mu\text{m}$ , and  $w = 63,500 \text{ } \mu\text{m}$ . From the experimental data, the maximum values of  $h$  and  $\theta$  were found to be  $133,000 \text{ w/m}^2\text{-K}$  and  $10^\circ\text{C}$ , respectively. Substituting these values into the definitions above yield

$$P = 2(6.35 \times 10^{-2} \text{ m}) + 2(6.816 \times 10^{-4} \text{ m}) = 0.128363 \text{ m}$$

$$A_c = (6.35 \times 10^{-2} \text{ m})(6.816 \times 10^{-4} \text{ m}) = 4.32816 \times 10^{-5} \text{ m}^2$$

$$m = \left[ \frac{(133,000 \text{ W/m}^2\text{-K})(0.128363 \text{ m})}{(177 \text{ W/m-K})(4.32816 \times 10^{-5} \text{ m}^2)} \right]^{1/2} = 1,492.8 \text{ m}^{-1}$$

$$mL = (1,492.8 \frac{1}{\text{m}})(2.637 \times 10^{-4} \text{ m}) = 0.393657$$

The largest variation of the fin temperature from the base temperature will occur at the fin tip. Substituting into equation (5.14) at  $x = L$  (the tip of the fin) gives

$$\frac{\theta}{\theta_b} = \frac{\cosh(0)}{\cosh(0.393657)} = \frac{1}{1.078489} = 0.9272 \quad (5.15)$$

For  $\theta_b = 10^\circ\text{C}$ ,  $\theta$  becomes

$$\theta = 10^\circ\text{C}(0.9272) = 9.27^\circ\text{C} \quad (5.16)$$

Or, the maximum temperature drop within the fin is  $10 - 9.27 = 0.73^\circ\text{C}$ . As mentioned earlier, the wall temperature thermocouples have an accuracy of  $\pm 1.0^\circ\text{C}$ . Therefore the maximum temperature drop in the fin is too small to be measured accurately and hence, our assumption of constant wall temperature is valid.

The second assumption, constant heat flux from each wall of a given channel, can be examined by determining the heat flux for a given fin and comparing it to the heat flux from the channel bottom. Incropera and DeWitt (1985) give the heat transfer from a fin

with an adiabatic tip as

$$q_f = M \tanh mL \quad (5.17)$$

where  $M = [hPkA_c]^{1/2} \theta_b$ , and all other variables are defined below equation (5.14).

Substituting the values used in the temperature distribution yields

$$\begin{aligned} M &= [(133,000 \text{ W/m}^2\text{-K})(0.128363 \text{ m})(177 \text{ W/m-K})(4.32816 \times 10^{-5} \text{ m}^2)]^{1/2} (10 \text{ K}) \\ &= 114.36 \text{ W} \end{aligned}$$

and

$$q_f = (114.36 \text{ W}) \tanh (0.393657) = (114.36 \text{ W}) (0.3745) = 42.8 \text{ W} \quad (5.18)$$

Considering the heat loss though the bottom of the channel, for the same conditions give

$$\begin{aligned} q_b &= h A_b (T_b - T_\infty) \\ &= (133,000 \text{ W/m}^2\text{-K})(1.704 \times 10^{-4} \text{ m})(0.0635 \text{ m})(10 \text{ K}) \\ &= 14.39 \text{ W} \end{aligned} \quad (5.19)$$

where  $A_b$  is the channel width times its length. Equations (5.18) and (5.19) can seem deceiving until one puts them in terms of the wall area over which they occur. Considering the aspect ratio of configuration C2, one can see that a single vertical wall has an area 1.548 times that of the bottom wall. Also, the fin equation is based on the area of both sides of the fin. Therefore, the fin wall area is actually  $2(1.548) = 3.096$  times larger than the area of the wall bottom. Taking both these points under consideration, we find the

maximum difference in the heat transferred from each wall is

$$\frac{14.39 - \frac{42.8}{3.096}}{14.39} = \frac{14.39 - 13.82}{14.39} = 0.0396 = 3.96\% \quad (5.20)$$

Considering other inaccuracies, such as the accuracy of the thermocouples, a maximum difference of 4% in the amount heat flux from each wall is acceptable.

### Test Fixture

The test section will be held in a test fixture, shown in Figure 5.3. Inlet and outlet temperatures and pressures of the test section are measured, as well as the heater temperature. Also shown in Figure 5.3 is the position of a heater which will provide the necessary heating of the channels for heat transfer analysis. A OMEGA (1" x 2.5") Kapton heater, rated at 121 Ohms and a maximum heat flux of 6 Watts, was mounted between a piece of silicon wafer and a high temperature epoxy/fiberglass material. The silicon wafer helped distribute the heat evenly over the back of the test section and the epoxy/fiberglass material provided rigidity. The epoxy/fiberglass material also provided a location to mount the heater thermocouple without actually touching the heater. Teflon<sup>®</sup>, beneath the heater, provided high temperature thermal insulation for the heater while Lexan<sup>®</sup> (polycarbonate) insulated the entire test fixture from the surroundings. Note that the test section did not touch any metal which would conduct heat away and possibly affect the experiment. However, one must be careful when mounting the test section so as not to over compress the o-rings. This would allow the test section to come in contact

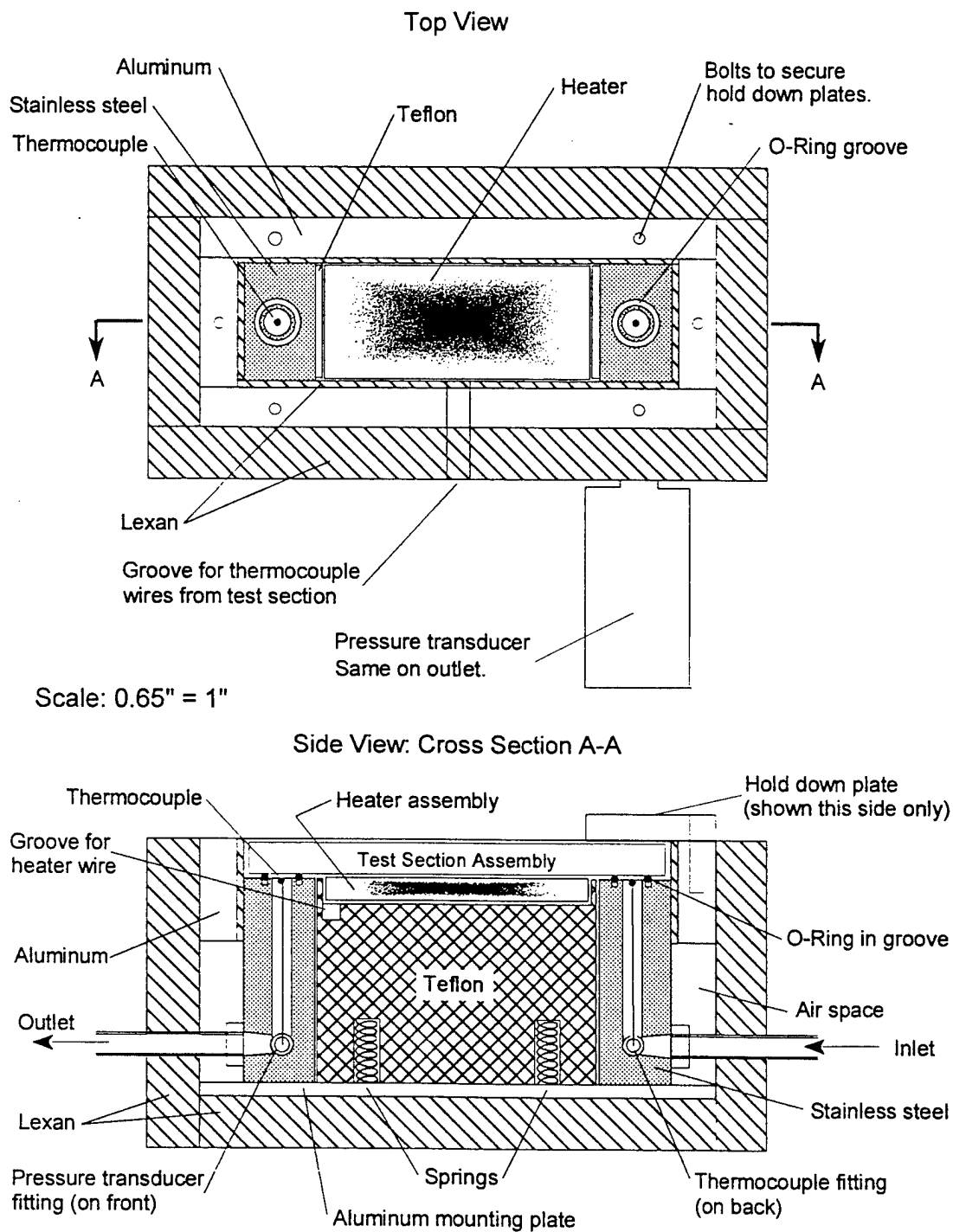


Figure 5.3: Test fixture assembly.

with the stainless steel. One must also be sure not to under compress the o-rings. The high inlet pressure can cause the o-rings to blow out of their grooves. Also note that the heater and test section maintain contact through the use of springs mounted in the lower part of the Teflon<sup>®</sup>.

One can see the location of the temperature and pressure measurements of the test fixture in Figure 5.3. The temperature is measured very near the entrance to the channels. Though the pressure is measured below the entrance to the channels, the pressure drop for the maximum flow rates of this study is negligible (less than 2%). The value of 2% was determined from the calculations of Bailey (1996) at a maximum water flow rate of 100 cc/min. More details on the layout of the test fixture will be given in the next section.

### Flow Loop

The apparatus on which the experimental study will be carried out was designed and built by the author and Darin Bailey. A schematic of the flow loop is given in Figure 5.4. The flow loop is designed to be a generic test bed for microscale fluid and heat transfer experiments here at Louisiana Tech University and the Institute for Micromanufacturing. For a thorough quantitative description of the apparatus and a complete list of components and manufacturers, please see Bailey (1996). The flow loop is mounted on a 4' x 6' air suspension table to dampen out any vibration from outside sources. Figure 5.5 and Figure 5.6 show the general layout of the actual system. All temperatures, pressures, and flow rates of the flow loop are monitored real time with a computer and data acquisition system. All wiring from the various components is routed

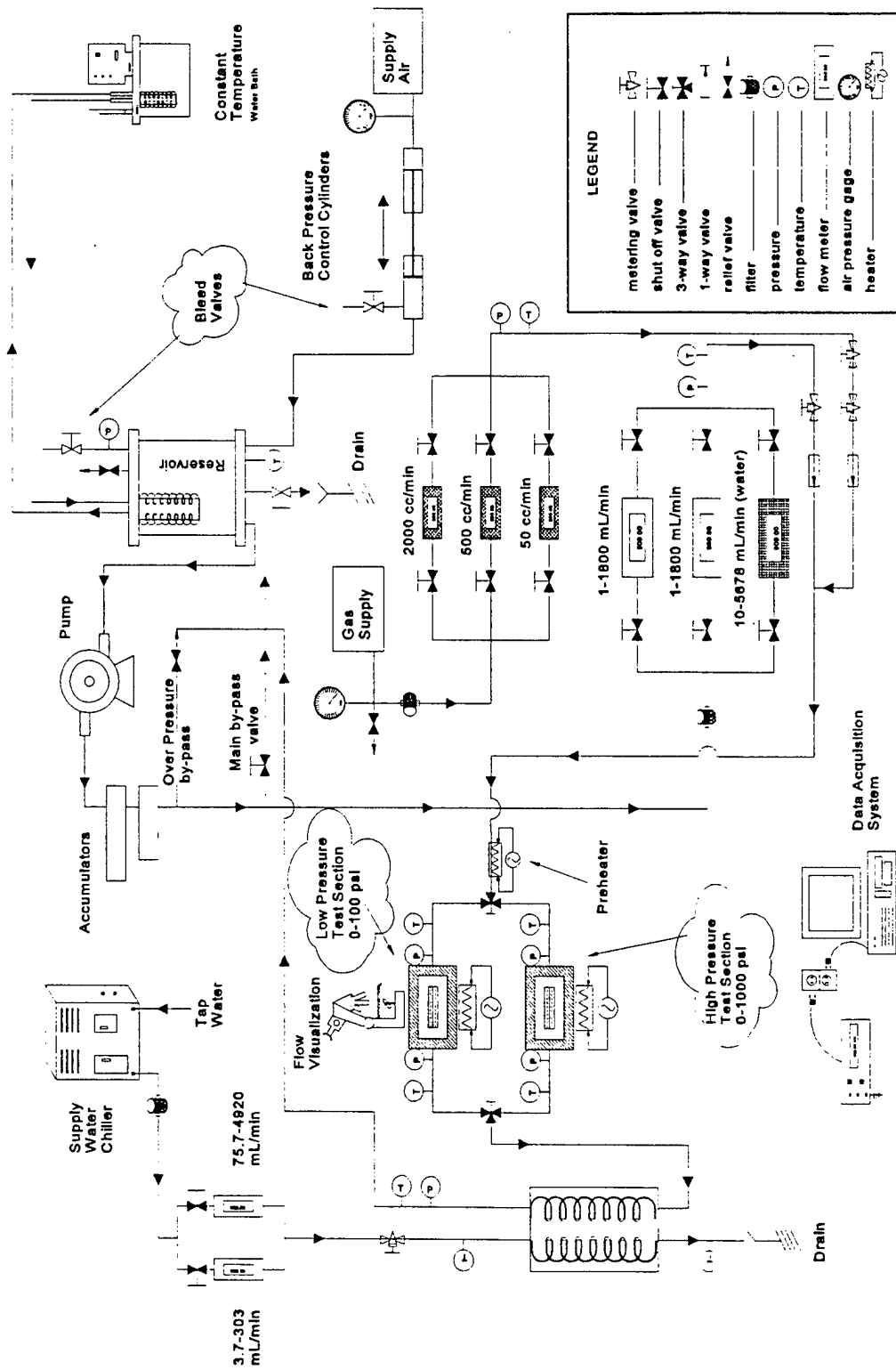


Figure 5.4: Schematic of experimental flow loop.



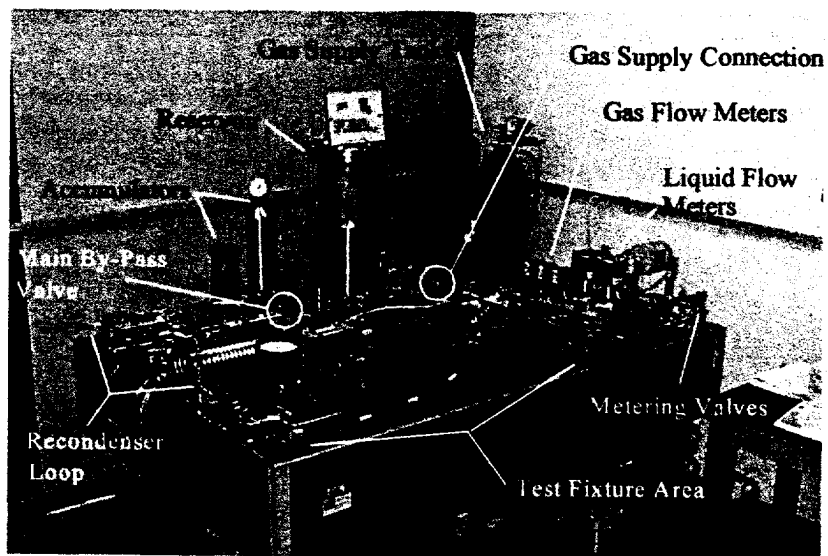


Figure 5.5: General layout of flow loop apparatus (flow loop components).

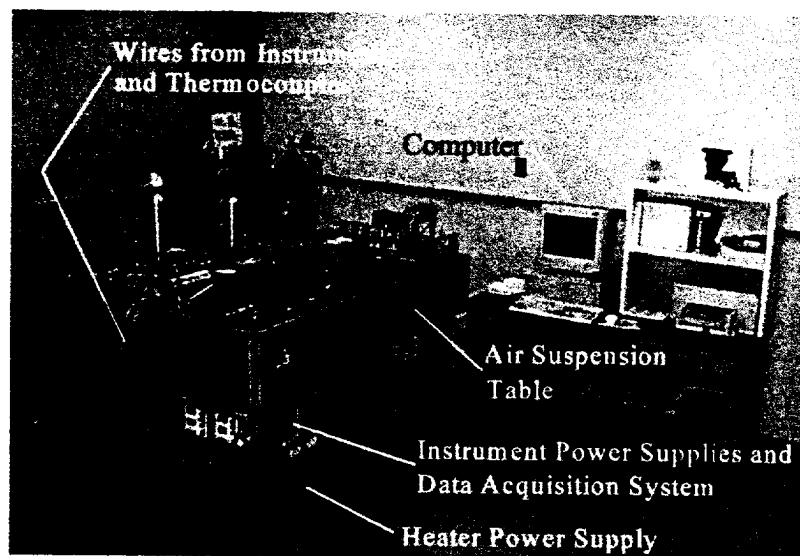


Figure 5.6: General layout of flow loop apparatus (entire apparatus).

off the table to the data acquisition chassis and power supplies underneath the air table. Shielded cable then connects the data acquisition chassis to the computer. The data acquisition system also monitors all temperatures and pressures of the test fixture and test section. Currently the data acquisition system is set up to measure all quantities 512 times each second. The data output to the screen, or written to a data file, is updated an average of every 250 readings. That is, the data screen is updated approximately twice per second. With only a click of a mouse button, the various information displayed on the computer screen can be stored to a spreadsheet or data file.

The test section and test fixture are incorporated into the flow loop as shown in Figures 5.7 and 5.8. In Figure 5.7, one can see the connections where the liquid and gas are mixed prior to entering the test fixture. Also shown in Figure 5.7 are the pressure transducers, test section thermocouple wires, the inlet and outlet thermocouple connections, and the test section being held in place by the aluminum cover plates. The bracket supporting the test fixture (seen more clearly in Figure 5.8) above the table can be removed. Removing the bracket will allow the test section to be mounted to the video/microscope system (used to measure the channel width) for flow visualization studies. Currently these studies are not being conducted pending the purchase of a high-speed video camera. Figures 5.9 and 5.10 show more detail of the test fixture with the test section removed. One can clearly see the o-ring grooves, heater, test section thermocouple wire slot, and the heater power wires and thermocouple. Also, one can see how the test fixture is bolted to the support bracket.

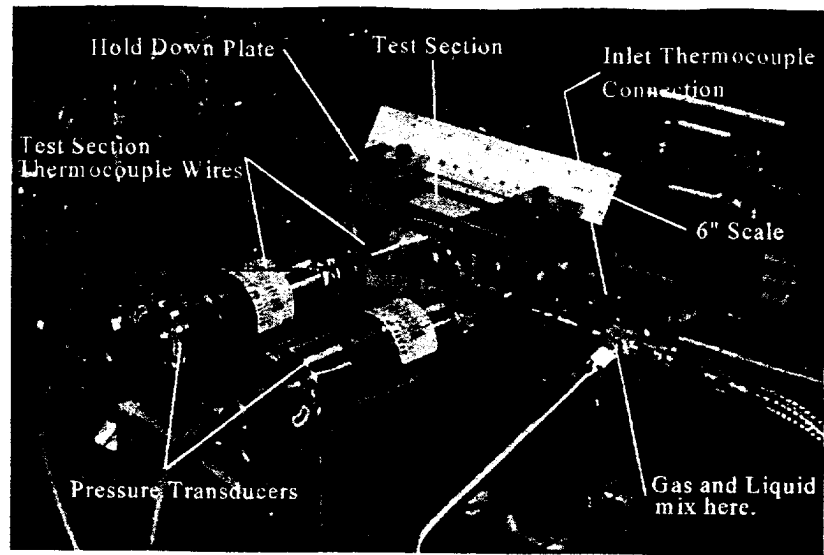


Figure 5.7: Test fixture components.

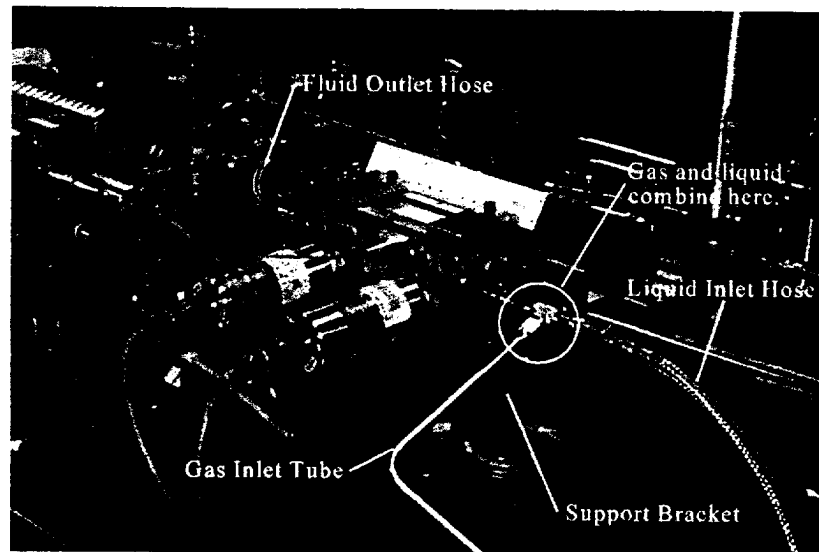


Figure 5.8: Test fixture.

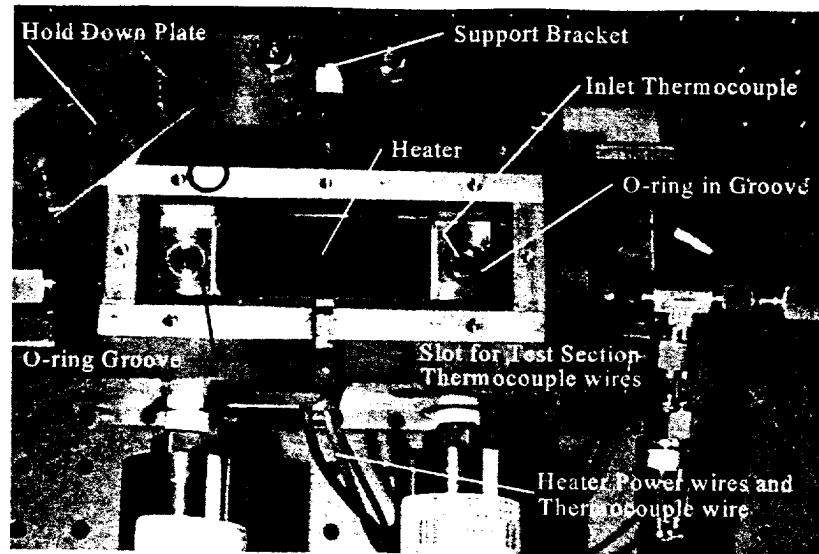


Figure 5.9: Detail of test fixture components without test section installed.

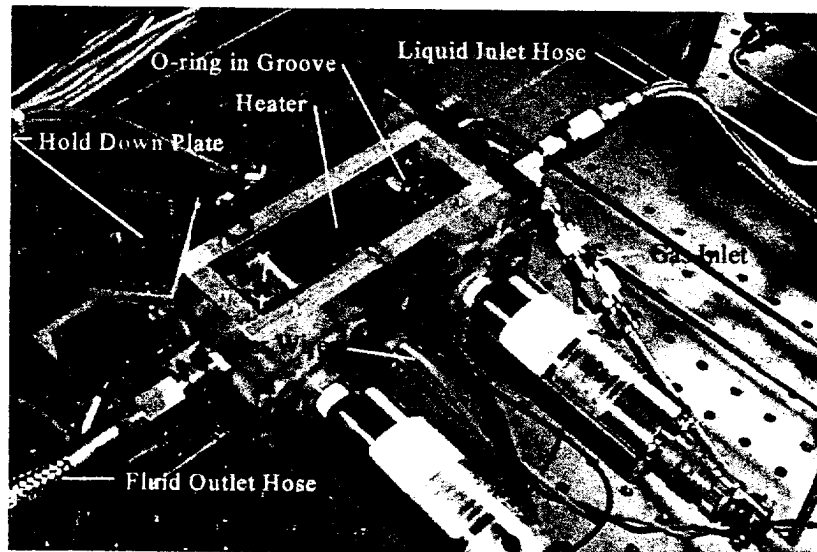


Figure 5.10: Detail of test fixture without test section installed.

The flow meters used for this study can also be seen in Figure 5.5. For the water, a flow meter from Max Machinery was used which has a flow rate range from approximately 5 cc/min to 4000 cc/min (based on the density of water at one atmosphere and 20°C). The upper end of the liquid flow meter (4000 cc/min) was well above the pressure restrictions of the test sections. For gases, the flow meters used were produced by Omega. A combination of three flow meters, with different ranges, allowed flow rates ranging from approximately 1 cc/min to approximately 2500 cc/min (based on the density of nitrogen at one atmosphere and 20°C). Though the gas flow meters were calibrated using nitrogen, a conversion factor could be used when the gas or pressure changed. This calibration factor will be discussed in the calculation section of this chapter. As can be seen in Figure 5.3, the gas was introduced from outside the main liquid flow path. The two components could be mixed at any point between the flow meters and the test section. Once through the test section, the gas was vented out the top of the reservoir.

### Experimental Procedure

Material in this section is a description of how the experimental apparatus used for this study was operated. The detailed instructions are applicable to both single- and two-phase flow experiments. One needs only to leave out the appropriate steps for their particular situation. Also included in this section is a discussion on the order of the fluids and channel configurations tested, along with information on the data files generated during the tests.

Start by turning on the computer, data acquisition system, and all power supplies. Allow approximately 30 minutes for the instruments to come up to operating temperature. During this wait, start the data acquisition program and monitor all pressures and temperatures. Monitoring of these values will help one determine if all instruments are functioning properly. Also, by not having the test section installed in the test fixture at this point, and making sure all pressure transducers are vented to atmosphere, one can determine if the pressure transducers have drifted since the previous calibration. Calibration (or signal conversion) of the transducers and the gas flow meters is conducted within the data acquisition program.

Next, install a test section into the test fixture. First, make sure the test section and test fixture are clean, dry, and free of debris. Second, coat the heater with a thin layer of Omegatherm high-thermal-conductivity grease. The grease will assure an even distribution of heat energy to the test section. Third, place new o-rings in the o-ring grooves of the test fixture. It is best to use new o-rings each time a test section is removed. Once o-rings are used, they develop ridges from being compressed between the test section and the test fixture and are unreliable. Fourth, lay the test section in the test fixture making sure the inlet and outlet holes of the manifolds are lined up with those of the test fixture and the thermocouple wires of the test section clear the test fixture. Fifth, press the test section down firmly and bolt on the hold down plates. Be sure to only finger tighten (as tight as possible with only your fingers) the bolts. Using any assistance such as an allen wrench or screw driver risks over compressing the o-rings and breaking the glass cover plates.

**The glass cover plates are very fragile.** Sixth, connect the test section thermocouples and check the data acquisition readout to make sure the thermocouples are functioning properly.

Now it is time to start the liquid flow loop. Before turning on the pump, make sure the main by-pass valve (see Figure 5.4) is open and the metering valve down stream of the liquid flow meter is closed. Also, make sure that the valves on the flow meters are set so that the liquid will flow only through the meter(s) you designate. This will prevent any unexpected flow through a flow meter not meant to handle the current liquid. Turn on the pump and let it run for a few minutes. Next, warm up the entire flow loop. For this next step, an additional by-pass line (a straight pipe between the multi-way valves) around the test fixtures was installed though it is not shown in the schematic of Figure 5.4. Switch the multi-way valves so that the liquid will go through the test section by-pass. Completely open the metering valve down stream of the liquid flow meters and slowly start closing the main by-pass valve. As the valve closes, the accumulators will slowly begin to fill and the flow rate and pressure to the flow meter will start to increase. For this system, the maximum flow rate and pressure from the pump is below the limits of the flow meter. Therefore, one does not have to worry about damaging the flow meter as long as no sudden changes are made. Continue to close the main by-pass valve until it is completely closed. During this time, however, monitor the pressure down stream of the liquid flow meter. If this pressure is higher than expected then the microfilter is becoming clogged and the element needs to be replaced. Note that there is an over pressure relief valve

installed, around the main by-pass valve, in case the flow is obstructed for any reason. With the main by-pass valve closed, let the system run for a few minutes while monitoring the system temperatures and pressures. Once the system has warmed up, slowly open the main by-pass valve and let the system return to normal.

The gas flow meters are ready to be prepared at this point. Start by connecting the air regulator and hose to the desired gas supply tank. Before opening the supply tank main valve, make sure the pressure regulator is set so that no gas will flow into the hose when the main valve is opened. Second, open the supply tank main valve and connect the gas supply hose to the apparatus. We use a quick disconnect fitting. Third, slowly open the valves upstream of the gas flow meters. The gas flow meters are very susceptible to sudden increases in pressure and flow. Also, flow rates beyond a given flow meters range will damage the flow meter. Fourth, open the valve down stream of the highest range flow meter (flow meter number 6). Opening this valve will allow all down stream piping to fill without running the risk of damaging the lower flow range meters. Fifth, very slowly start turning the pressure regulator knob to increase pressure and start the gas flowing. Monitor the data acquisition output to make sure one does not allow the flow to become greater than the range of each flow meter. Again, it is very easy to over range the flow meters and damage them. Proceed until the desired flow meter pressure is reached. Typically, this pressure will be 50 - 200 psi higher than the maximum pressure experienced at the inlet of the test section during maximum flow rate of a given gas. Sixth, once the pressure downstream of the flow meters has stabilized, open the remaining ball valves for



the other two flow meters. The gas flow meters can be used in any combination to achieve the desired flow range for testing. One final note. Be sure that the reservoir vent is open to allow the gas to escape. Having it closed will allow the pressure to build up in the test section and reservoir. At low flow meter pressures this will only result in a stoppage of the gas flow. However, for higher flow meter pressures the test section and, more easily, the reservoir can be damaged.

As with the gas, the maximum liquid pressure at the flow meter can now be set. Start by making sure the metering valve down stream of the liquid flow meter is closed and that the main by-pass valve is completely open. Next, while monitoring the pressure of the liquid at the flow meter, slowly start closing the main by-pass valve. Close the main by-pass valve until the desired pressure is achieved at the liquid flow meter. Just like the gas flow meters, this pressure will be approximately 50 - 200 psi higher than the maximum pressure to be experienced in the test section. However, be sure that the pressure at the flow meter does not go higher than approximately 1100 psi. Any higher risks tripping the over pressure safety relief valve.

Now one is ready to start running the fluid(s) through the test section. Before opening the metering valves, switch the multi-way valves so that the fluid flow will proceed through the test section. Due to the unsteady readout of the liquid flow meter at low flow rates, it was found to be easier to set the test section inlet pressure using the metering valve, and then measure the liquid flow rate. Adjustments of the liquid metering valve should proceed slowly because there is moderate lag time between adjusting the

valve and the test section inlet pressure stabilizing. Too large of an adjustment will very quickly result in excess pressure in the test section which may cause damage. For this particular apparatus, the inlet pressure could be controlled within  $\pm 0.5$  psi. A similar procedure is followed when adjusting the gas flow meters. Here, however, one monitors and controls the flow rate through the flow meters. As will be discussed in the Experimental Calculations section of this chapter, the gas flow meter reading on the screen is not the actual flow rate of the gas. Instead the reading is a relative flow rate based on the maximum range of the flow meter. For this particular apparatus, the gas flow rate could be controlled within  $\pm 1\%$  of the maximum range of the largest flow meter being used at a given time. While setting the gas flow rate, one should also monitor the inlet pressure of the test section. In two-phase flow, the gas and liquid flow meters tend to work against each other. That is, when one flow meter is adjusted, the flow rate from the other flow meter will change. This is not as big a problem as it may seem because the system equalizes fairly quickly. The worst case that may occur is that increasing the flow rate in one flow meter will actually stop the flow from the other flow meter. However, this only occurs when one or both of the flow meters are at the low end of their flow range and small adjustments will quickly fix the problem.

Once the fluid is flowing through the test section, the heater power supply may be turned on and the voltage output adjusted. It is very important to make sure fluid is flowing through the test section before turning on the heater. If no fluid is passing through the test section when the heater is turned on, damage to the test section, heater, or even

the test fixture may result. The heater for this study was powered by a 150 V, 35 Amp, DC power supply. It is recommend that one use a DC power supply and not an AC power supply. The AC power supply generates a slight induction voltage that will interfere with any thermocouple if its wires are located near the heater or heater wires. While adjusting the power supply, one must monitor the temperatures of the heater, test section wall, and test section inlet and outlet. To prevent any damage to any part of the test apparatus, the following maximum temperatures are recommended; 1) The heater temperature should not exceed  $160^{\circ}\text{C}$  ( $320^{\circ}\text{F}$ ), and 2) the test section wall, inlet, and outlet temperatures should not exceed  $60^{\circ}\text{C}$  ( $140^{\circ}\text{F}$ ). Once the heater is set, the system must be allowed to come to steady-state before the first data point is taken.

Typically the system takes ten to twenty minutes to come to steady-state for the first data point depending on how high one sets the heater voltage. During the initial time period, the channels as well as the entire test fixture are warming-up to operating temperature. The state of all test section and test fixture temperatures can be monitored on the computer screen. Once all temperatures have stabilized, the system data is ready to be recorded. The data is stored to computer disk using the data acquisition software. A virtual switch on the computer screen starts the data recording when it is triggered by "clicking" on it with the computers mouse. The data is recorded at a rate of approximately two measurements per second. As will be discussed in the next chapter, for statistical purposes, sixty data points are recorded for each fluid flow rate/heater setting. One stops the data recording after about 35 seconds by again "clicking" the virtual switch with the

computer's mouse. The fluid flow rates can now be adjusted for the next data point.

For the next data point, adjust the liquid and/or gas flow rate as described above. The heater voltage may also be adjusted. Reaching steady-state takes much less time, now that the test fixture is at its operating temperature. However, the amount of time required to reach steady-state depends on the magnitude of the changes in the flow rates and/or heater voltages. For the experiments run with this study, the time between taking data varied from three to seven minutes. One advantage of the data acquisition system was being able to view the temperature and pressure variations with respect to time. Continuous graphs show a history for a given number of data points up to the present, not just current tabulated numbers. When all desired data points have been taken, the system may be shut down.

Shutting down the flow loop is basically the reverse of the start up. However, precautions should be taken. First, with the fluid continuing to flow through the test section, turn the heater supply voltage off and allow the test section and fixture to cool. Second, when the test section and fixture are cool, close the liquid metering valve and slowly open the main by-pass valve. The increased pressure to the flow meter will be reduced to its starting value. Third, at this point the liquid pump can be turned off and the ball valves on either side of the flow meter closed. Fourth, as for the gas, it is best to turn off the gas supply tank main valve and allow the pressure to bleed down slowly through the test section. Slowly bleeding the pressure down eliminates the risk of damaging the flow meters by a quick pressure release at the quick disconnect. Fifth, when the flow has

completely stopped, close the gas metering valves and all the ball valves on both sides of the gas flow meters. Also, disconnect the gas supply hose from the flow loop. Sixth, switch the multi-way valves on either side of the test section so that no back flow of liquid will escape through the test fixture when the test section is removed. One may now either change test sections and/or gas supply tanks and start the process over. Finally, if done for the day, turn off the computer and all the power supplies.

In the experiments conducted for this study, the various fluids were tested in a relatively specific order. First, the gases were tested for a given test section. Next, water was tested. Finally, the two-phase tests were conducted with water and each of the three gases. Therefore, seven sets of data were generated for each test section. Test sections were changed in a similar manner. The largest test section (configuration A) was tested first. Subsequently, the various configurations B, C1, C2, ..., F were tested. Obviously the experiments did not go as well as the preceding statements suggest. On several occasions the test sections ruptured and the glass cover plates had to be replaced. Other times, certain configurations were reinstalled to collect additional data. The data files generated from these experiments are discussed in the next paragraph. The calculations used in converting the raw data and determining other fluid mechanic and heat transfer parameters are presented in the last section of this chapter.

The data files generated from the experiments of this study are given in appendices C and D. Appendix C contains the measured data and Appendix D contains the reduced data. Though the data acquisition system records all the pressures, temperatures and flow

rates shown in Figure 5.4, not all of these values are needed. Only the pressures and temperatures of the test section, test fixture, and flow meters are used in the calculations. The raw data files were copied into a spreadsheet to allow easy conversion (pressures and flow rates) of the data and parameter calculation. Each data file is listed on several pages. The first page lists the measured values as converted from the raw data. The second list all reduced or calculated fluid mechanic and heat transfer parameters.

### Experimental Calculations

The raw data collected from the data files discussed in the previous section, were used in determining all fluid properties, material properties, fluid mechanic parameters, and heat transfer parameters. The equations used in all of these conversions and calculations will be presented in this section. Raw data values stored by the data acquisition system were in the default units of the software. All temperatures were internally converted from millivolts and stored in units of degrees Celsius. Pressure and gas flow meter readings, however, were stored as the measured output voltages from the various instruments. The liquid flow meter has a pulsed output and its values were stored in hertz. The values recorded consisted of the following; 1) the fluid inlet and outlet temperatures of the test section, 2) the test section wall temperatures, 3) the gas and liquid flow meter temperatures, 4) the inlet and outlet pressures of the test section, 5) the gas and liquid flow meter pressures, and 6) the gas and liquid flow meter flow rates. All together, nineteen values were used for the calculations and described as follows.

All equations used to determine liquid and gas properties are given by Reid et al. (1987). Due to the extent of the equations, they will not be listed. The liquid and gas properties calculated for this study were the density, specific heat, absolute viscosity, thermal conductivity, Prandtl number, and surface tension. The calculated values were compared to tabulated values given by White (1986) (surface tension, viscosity, density), Barron (1985) (density, specific heat, absolute viscosity, thermal conductivity, Prandtl number), Incropera and DeWitt (1985) (thermal conductivity, Prandtl number, absolute viscosity), Hayduk (1981) (surface tension), and Sonntag and Van Wylen (1991) (density, specific heat). For a temperature range of 20 °C - 80 °C and a pressure range of 0 psig - 600 psig, all calculated fluid properties were found to be accurate to within 1%, or better, of the tabulated values. Thermal conductivity of the aluminum test section was curve-fit from the tabulated values given in Incropera and DeWitt (1985). The resulting equation was also accurate to within 1% for the temperature range considered.

Most of the measuring instruments used on this apparatus had output signals in volts or hertz, which required conversion of units. For example, the pressure transducers give an output of 0.0 vdc - 5 vdc or 0.5 vdc to 5.5 vdc depending on the model. The voltage signal was converted to the corresponding pressure by the equation

$$\text{Pressure (gage)} = \frac{\text{voltage} - \text{offset}}{5.0} (\text{max. pressure range}) \quad (5.21)$$

where *voltage* is the value recorded by the data acquisition system, *offset* is the calibration voltage measured with the transducer open to atmospheric pressure, and *max. pressure*

*range* is the maximum pressure range to which the transducer is calibrated (measured in gage pressure). The transducer was calibrated by measuring the output voltage when the transducer was open to the atmosphere and substituting this value into equation (5.21) for offset.

A similar equation was used for the gas flow meters which also had an output of 0.0 vdc - 5.0 vdc.

$$\text{Flow Rate (cc/min)} = \frac{\text{voltage} - \text{offset}}{5.0} (\text{max. flow range}) \quad (5.22)$$

where *voltage* is the value recorded by the data acquisition system, *offset* is the calibration voltage measured with no flow, and *max. flow range* is the maximum range of the given flow meter. Because the density of the gas was dependent on the pressure and temperature in the flow meter, the readout of the gas flow meters was actually a relative flow based on the maximum range of a given flow meter. That is, for a constant mass flow rate, as the temperature and density of the gas changed, so did the output voltage. To calculate the actual flow rate through a given flow meter, Omega gives the correction factor

$$CF = \frac{(\rho C_p)_{\text{calibration}}}{(\rho C_p)_{\text{flow meter}}} \quad (5.23)$$



where  $(\rho C_p)_{\text{calibration}}$  are the density and specific heat for the calibration gas at calibration conditions, and  $(\rho C_p)_{\text{actual}}$  are the density and specific heat of the actual gas flowing through the flow meter. The calibration gas for the three gas flow meters was nitrogen at one standard atmosphere and 20 °C. The properties for the actual gas were determined using the measured pressure and temperature at the flow meter. Therefore, multiplying equation (5.23) by (5.22) will give the actual flow rate (cc/min) of a given gas through the flow meters. The correction factor applied for all of the gas flow meters and this feature made them versatile. Any gas could be used with the flow meter without having to recalibrate. Equation (5.23) could be modified to yield the flow rate at the test section. From the continuity equation, the mass flow rate at the flow meter is simply the measured volumetric flow rate times the density of the gas at the flow meter. Assuming steady-flow, the mass flow rate at the flow meter is the same as at the test section. Therefore, by then dividing equation (5.23) by the density at the test section, one finds the volumetric flow rate at the test section. Or, in equation form

$$CF = \frac{(\rho C_p)_{\text{calibration}}}{(\rho C_p)_{\text{flow meter}}} * \frac{\rho_{\text{flow meter}}}{\rho_{\text{test section}}} = \frac{(\rho C_p)_{\text{calibration}}}{\rho_{\text{test section}} C_{p \text{ flow meter}}} \quad (5.24)$$

Now, equation (5.22) and (5.24) can be used to determine the volumetric flow rate at the test section directly. Note that the fluid properties in the test section are based on the average temperature and pressure of the test section. Because of the extremely small mass

flow rates, the liquid and gas flow rates are listed in Appendix C and D as the volumetric flow rates.

The liquid flow meter conversion was easier to carry out because of the incompressibility of the water and because the meter was calibrated using water. Max Machinery gave an equation for the flow rate based on an average K-factor times the hertz output of the flow meter. The accuracy of the equation was listed as +2%/-4% over the entire range of the flow meter (5 - 4,000 cc/min). However, for better accuracy, the calibration specifications that came with the flow meter were curve-fit. The resulting equations are

$$5 - 100 \text{ cc/min: Flow Rate, (cc/min)} = 87.596 (\text{output})^{3.118696\text{E-}04} \quad (5.25)$$

$$100 - 4000 \text{ cc/min: Flow Rate, (cc/min)} = 89.343 (\text{output})^{-2.400849\text{E-}06} \quad (5.26)$$

where the flow meter output is in hertz. Equations (5.25) and (5.26) agree with the tabulated calibration information to within  $\pm 1 \%$ .

For the analysis to be presented in the next chapter, several fluid mechanic and heat transfer parameters need to be calculated. The equations presented below are used in the calculation of all variables and parameters listed in Appendix C and D. Because the parameters are overall or average values, the fluid properties will be determined from the average temperature and pressure measured between the inlet and outlet of the test section. Any exceptions will be noted as needed.

In considering pressure drop in a channel, the relevant fluid mechanic parameters are the Reynold number and the Darcy-Weisbach friction factor. To calculate these parameters, one needs several fluid properties, channel dimensions, measured pressure drop, and velocity. Velocity is easily found from the continuity equation as

$$\bar{V} = \frac{\dot{V}}{A} \quad (5.27)$$

where  $\dot{V}$  is the measured volumetric flow rate, and  $A$  is the cross-sectional area of the channel {(width)(depth)}. Another variable that must be calculate at this point is the channel hydraulic diameter. White (1986) defines the hydraulic diameter as

$$D_h = \frac{4A}{P} \quad (5.28)$$

where  $A$  is the cross-sectional area of the channel and  $P$  is the wetted perimeter {2(width) + 2(depth)}. With equations (5.27) and (5.28), the Reynolds number can be calculated from

$$Re = \frac{\rho \bar{V} D_h}{\mu} \quad (5.29)$$

where  $\rho$  and  $\mu$  are the average fluid density and absolute viscosity, respectively. For the

Darcy-Weisbach friction factor, White (1986) gives

$$h_f = f \frac{L}{D_h} \frac{\bar{V}^2}{2g} \quad (5.30)$$

where  $h_f$  is the pipe-head loss,  $L$  is the length of the channel, and  $g$  is the local acceleration due to gravity. The pipe-head loss is also given as

$$h_f = \frac{\Delta p}{\rho g} \quad (5.31)$$

Combining equations (5.30) and (5.31) and solving for the friction factor yields

$$f = \frac{2 \Delta p D_h}{\rho L \bar{V}^2} \quad (5.32)$$

where  $\Delta p$  is the measured pressure drop of the fluid flowing through the channels.

When considering forced convection heat transfer inside channels, the most useful parameters are the Nusselt number, Reynolds number, and the Prandtl number. The Reynolds number is given in equation (5.29), and the Prandtl is a fluid property ( $\mu c_p/k$ ) calculated as previously discussed. In order to calculate the Nusselt number, one needs to know the heat transferred to the fluid and the overall heat transfer coefficient. For a fluid being heated as it flows through a channel, the amount of heat transferred to the fluid is given by Incropera and DeWitt (1985) as

$$q = \dot{m} C_p (T_{\text{outlet}} - T_{\text{inlet}}) \quad (5.33)$$

Or, in terms of volumetric flow rate,

$$q = \dot{V} \rho C_p (T_{\text{outlet}} - T_{\text{inlet}}) \quad (5.33)$$

Now, equating the amount of heat transferred to the fluid to the amount of heat transferred from the channels, one can determine the overall heat transfer coefficient. The heat transfer coefficient is defined by Newton's law of cooling as

$$q = h A_w (T_w - T_\infty) \quad (5.34)$$

where  $T_w$  is average channel wall temperature,  $T_\infty$  is the bulk fluid temperature, and  $A_w$  is the wall area of the channel over which the heat is transferred. Several correlations used in next chapter's comparisons contain fluid properties evaluated at the channel wall temperature. For these properties, the channel wall temperature was determined by averaging the test section wall thermocouple readings. Only the test section thermocouples numbered 1, 2, 4, 6, and 7 were averaged for this purpose. These thermocouples were used because they were located down the center of the channels. Because of the glass cover plate used in construction of the test section, the top channel wall was considered adiabatic. Therefore, the wall area over which heat energy is transferred to the fluid is given by

$$A_w = L (2 \text{ Depth} + \text{Width}) \quad (5.35)$$

Solving equation (5.34) for the heat transfer coefficient gives

$$h = \frac{q}{A_w (T_w - T_\infty)} \quad (5.36)$$

The Nusselt number can now be calculated from

$$Nu = \frac{h D_h}{k} \quad (5.37)$$

where  $k$  is the average thermal conductivity of the fluid. Another parameter that will be used in the comparisons of the next chapter is the heat flux. To determine the heat flux, one simply divides the amount of heat transferred from the channel wall by the channel wall area. Or,

$$q'' = \frac{q}{A_w} \quad (5.38)$$

For two-phase flow, the parameters presented above are essentially the same. The only difference is how one determines the fluid properties for a mixture of fluids. As mentioned in Chapter 3, average properties in two-component gas-liquid flows are

determined using the quality or mass fraction of gas in the mixture. The quality is defined by

$$x = \frac{\dot{m}_g}{\dot{m}_g + \dot{m}_f} \quad (5.39)$$

Putting equation into terms of the volumetric flow rate, gives

$$x = \frac{\dot{V}_g \rho_g}{\dot{V}_g \rho_g + \dot{V}_f \rho_f} \quad (5.40)$$

From basic thermodynamics, average properties of two-component gas-liquid mixtures take the form

$$v_{\text{mix}} = x v_g + (1 - x) v_f \quad (5.41)$$

where  $v_{\text{mix}}$  is the specific volume of the mixture,  $v_g$  is the specific volume of the gas, and  $v_f$  is the specific volume of the liquid. Other properties ( $\mu$ ,  $c_p$ ,  $k$ , etc.) take exactly the same form. Along with the fluid mechanic and heat transfer parameters discussed above, in two-phase flow another parameter arises when considering surface tension between the liquid and gas, the Weber number. The Weber number is the ratio of the liquid inertia to

the surface tension at the gas-liquid interface. White (1986) gives the Weber number as

$$We = \frac{\rho \bar{V}^2 L}{\Upsilon} \quad (5.42)$$

where  $\Upsilon$  is the surface tension.



## CHAPTER 6

### ANALYSIS OF RESULTS

In this chapter, the experimental data taken for both single- and two-phase flow will be presented and analyzed. The resulting empirical correlations based on the dimensional analysis of Chapter 4 will be presented along with the empirical solutions of the analytical flow models developed in Chapter 3. At the end of each respective single- and two-phase flow section, the new correlations will be compared with the correlations listed in chapter two. The two-phase data will then be compared to Baker's (1954) flow regime map. Also, comparisons will be made of other heat transfer quantities such as heat flux and forced convection heat transfer coefficient. Finally, in the last section, an analysis of the amount of uncertainty present in the experimental data will be developed and discussed.

As mentioned in Chapter 4, the empirical correlations presented in this chapter were chosen from a list of sometimes hundreds of correlations determined by the parameters derived using the dimensional analysis. The empirical correlations will most frequently be discussed and compared based on their correlation coefficients ( $r$ ) and the standard deviation ( $\sigma$ ) of the data. To follow the discussion, it is important that one understand the definition of the correlation coefficient. The correlation coefficient is a

description of the relative worth of the resulting empirical correlation. As Schenck (1968) states, a correlation coefficient value of 1.0 means that 100% of the variability is explained by the correlation. For a correlation coefficient value of 0.0, no improvement is seen. Also, there will virtually always be some combination of parameters that yield a higher correlation coefficient than those presented in this chapter. However, this can be likened to the number of terms used to estimate an infinite series. For example, five terms may give an estimate that is accurate to within 1% of the actual series value. An additional ten terms may increase the accuracy to within 0.75% but very little insight is gained using the extra terms. As with all empirical correlations, a large number of parameters can be correlated against experimental data to give a relatively high correlation coefficient. However, the larger the number of parameters correlated, the more difficult it becomes to understand which parameters are important to help to describe the behavior of the data. Now, all this is to say that the correlations presented in this chapter were not simply chosen based on how high their correlation coefficients were, but, more importantly, on how well they aided in describing the behavior of the fluid.

### Single-Phase Flow Results

For the single-phase experiments, liquid water and gaseous argon, helium, and nitrogen were tested in each of the channel configurations. The Reynolds numbers ranged from around 2 to just under 10,000 with most of the data between 100 and 5000. Figure 6.1 shows the friction factor data for all single-phase tests. For convenience, all figures are located together at the end of this chapter. As can be seen, there is a great deal of

scatter at the larger Reynolds numbers. The correlations presented in this section should help clarify the fluid's behavior in the various channel configurations. As will be shown, the friction factor for the gases has a strong, virtually complete, dependence on the Reynolds number. For the water, on the other hand, the friction factor will be shown also to be dependent on other parameters such as the ratio  $L/D_h$  and the viscosity ratio  $(\mu/\mu_s)$ .

As discussed in chapter four, the test section was electrically heated during all tests so that a heat transfer analysis could be conducted along with the fluid mechanic analysis. Figure 6.2 shows the resulting single-phase Nusselt number data. The laminar Nusselt number ( $Nu = 2.98$ ) and turbulent macroscale correlation are also shown for comparison. For this study, the turbulent macroscale correlation is given by the Dittus-Boelter equation, for the fluid being heated, as

$$Nu = 0.023 Re^{4/5} Pr^{0.4} \quad (6.1)$$

where the Reynolds number is based on the hydraulic diameter of the channel. As can be seen, there is even more scatter in these results than in the data for friction factor. The scatter is mainly due to inaccuracies in the temperature's measurement. However, considering the gas data separately did help in determining which parameters are important in single-phase heat transfer.

### Friction Factor

To analyze the friction factor data shown in Figure 6.1, one needs to break it down into several areas of consideration. The break down consists of considering the water and gases separately, and further breaking down the gases into two groups based on the channel's hydraulic diameter. The group with the largest hydraulic diameters is also broken down into two groups based on Reynolds number. Therefore, we have four groups to analyze. The reason for this particular break down is based on the fluid's behavior in the transition from laminar to turbulent regimes in the various channel configurations. The water showed virtually no transition in any size channel at any Reynolds number. For gases, transition did occur in the larger channels (configurations A - C2) but not in the smaller channels (configurations C3 - F).

The friction factor data for water in the various channel configurations are shown in Figure 6.3. As one can see there is a large amount of scatter associated with this data. For channel configuration C2, it is difficult to tell if the flow undergoes transition. All data points for channel C2 were well above both macroscale correlations. The increased pressure drop for this set of channels may be due to the very rough surface finish of these channels (see Table 3). However, pressure restriction did not allow higher Reynolds numbers data to be obtained for this set of channels which may have clarified the question of transition. Unlike what will be shown with gases, the friction factor for water is dependent on parameters in addition to Reynolds number. Correlating the data against the parameters discussed in Chapter 4, the empirical correlation which best describes the

fluid's behavior is

$$f = 3.9 \times 10^{11} \text{ Re}^{-1.862} \left( \frac{\mu}{\mu_s} \right)^{0.7845} \left( \frac{L}{D_h} \right)^{-2.762} \quad (6.2)$$

This correlation is a good fit to the data, as shown in Figure 6.4, with  $r = 0.983$  and  $\sigma = 0.033$ . The dependence on the Reynolds number was expected from classical fluid mechanics. Also, the various correlations of this data indicate that the Reynolds number is, by far, the parameter of primary importance. However, though the dependence of the friction factor on the other two terms was not expected, it does reveal some interesting fluid behavior. The viscosity term is important because the flow was also being heated. As the fluid flows through the channel and is warmed, the viscosity decreases which tends to also decrease the pressure drop. Because  $(\mu/\mu_s)$  was found to be important, it seems to emphasize that the change in the viscosity due to temperature increase is more important than the Reynold number alone considers. In addition, this particular viscosity ratio  $(\mu/\mu_s)$  is used in heat transfer analysis to take into account thermal and viscous boundary layer development [Incropera and DeWitt (1985)]. The final parameter, the  $L/D_h$  ratio, is an indication of entrance effects or viscous boundary layer development. Though for the smaller channels the entrance length may be no more than 10% of the channel's length, for the largest channel (configuration A) the entrance length can cover over 55% of the channel's length. The negative exponent on the  $L/D_h$  ratio is also an indication of the importance of this parameter as the channel size increases. Examination of the

different correlation combinations indicated that the viscosity ratio is the least important of the three parameters and that  $L/D_h$  ratio, though important, is less important than the Reynolds number.

For gases, the lack of transition was seen only in the smaller channel sizes. To show this difference, Figure 6.5 compares channel configurations B, E, and F with nitrogen gas as the fluid. As one can see, configuration B shows a well defined transition from laminar to turbulent regimes, configuration E shows a possible (slight) transition, and configuration F shows no transition. The transition behavior was seen to fall into several groups based on the channel's hydraulic diameter. Channels with hydraulic diameters greater than  $150\text{ }\mu\text{m}$  (A - C2) show a definite predictable transition. Between the hydraulic diameters of  $80 - 150\text{ }\mu\text{m}$ , suppression of the transition behavior is seen to take place in varying degrees. Below a hydraulic diameter of  $80\text{ }\mu\text{m}$ , the transition behavior is almost completely suppressed.

For the larger channels (A - C2), transition was seen to occur between a Reynolds number of 1,500 and 2,000. Therefore, the data below a Reynolds number of 1,500 and above a Reynolds number of 2,000 were correlated separately. From the resulting correlations, both regions were found to be completely dependent on the Reynolds number. Also, the exponents on the Reynolds number were all found to be close to -1.0 for the laminar region and -0.25 for the turbulent. Both of these values are as macroscale theory predicts. Therefore, each region was re-correlated based on these exponents to determine the appropriate constants. The resulting expressions for the friction factor are

Laminar Region ( $Re < 1,500$ ):

$$f = \frac{74}{Re} \quad (6.3)$$

Turbulent Region ( $Re > 2000$ ):

$$f = \frac{0.39}{Re^{0.25}} \quad (6.4)$$

These correlations are shown in Figure 6.6. In both cases the correlation for the data of this study are above the macroscale correlations. From equations (6.3), the laminar constant of 74 is approximately 15% higher than the macroscale constant of 64. Similarly, for equation (6.4), the turbulent constant of 0.39 is approximately 23% higher than the macroscale constant of 0.316. Equations (6.3) and (6.4) have correlation coefficients of 0.994 and 0.516, respectively. As can be seen in Figure 6.6, equation (6.3) does only a fair job of reducing the data. This is due to the scatter associated with the transition region. More data taken at higher Reynolds numbers would help clarify the gases' behavior in the turbulent region. Unfortunately, the experimental apparatus described in Chapter 4 was not capable of higher gas flow rates. It should be noted that correlations were also calculated over the entire range of Reynolds numbers. However, due to the two distinct regions, no useful correlation was found.

For the channels with a hydraulic diameter less than 150  $\mu\text{m}$ , the resulting correlations also showed a complete dependence on the Reynolds number. Because little or no transition from the laminar to the turbulent region was seen, these correlations were

calculated for the entire range of Reynolds numbers. As with the channels that had a hydraulic diameter larger than 150  $\mu\text{m}$ , the Reynolds number exponent was approximately -1.0. Therefore, the data was re-correlated as before. The resulting expression for the friction factor is

$$f = \frac{66}{\text{Re}} \quad (6.5)$$

with a correlation coefficient value of 0.995. Note that the value of the constant in equation (6.5) (66) is close to the value of the macroscale constant (64). This almost insignificant difference can be entirely due to slight error in the data measurements. Equation (6.5) is shown in Figure 6.7. The macroscale correlation is not shown because one would have a hard time distinguishing it from equation (6.5). Of the most interest in this figure is the lack of the transition from laminar to turbulent regimes. Though it can be argued that the maximum Reynolds number in this figure is still in or near the transition region, the behavior of the gas is almost identical to that of the water which had Reynolds numbers as high as 10,000 with no transition. It is believed that this behavior can be explained by some ideas from the work of Yu (1995). Yu (1995) discusses how in microchannel flow, the size of the channel suppresses the formation of turbulent eddies. That is, the size of the channels is at, or below, the size of an eddie required for the fluid to transition from laminar to turbulent regions. These ideas are also based on the assumption that an eddie must be of a certain size to cause complete transition. Now, this suppression can clarify two points about the data taken for this study. First, as can be seen



in Figure 6.7, the behavior of the fluid does show some change in the area where transition is thought to start. What is possibly occurring at this point is that small eddies are forming and trying to develop into larger eddies; eddies large enough to cause the fluid to transition. However, the size of the channel restricts their growth and does not allow them to develop into a size that is large enough to cause the flow to transition to the turbulent region. This is why that even though the flow is seen to be less stable than turbulent flow, the friction factor is still a function of  $1/Re$ . Second, there is a noticeable difference between where the transition starts to be suppressed for liquids and gases. In this study, the water shows no transition, even at the largest channel size. For the gases, on the other hand, the suppression started at approximately  $150\text{ }\mu\text{m}$ . It is believed that because of the higher density and viscosity of a liquid, the size of an eddie required to cause transition is larger than for a gas. Therefore, a larger channel is required to have transition. A study of eddie formation and behavior on a very small scale may clarify this point.

A comparison between the experimentally measured friction factor data of this study and the friction factor correlations listed in Chapter 2, is shown in Figure 6.8. Note that the equations have been normalized and plotted as the ratio of the measured friction factors over the correlated friction factors ( $f_{\text{meas}}/f_{\text{corr}}$ ) versus Reynolds number. As one can see, most of the experimentally measured data is less than that predicted by the correlations. Note that all the correlations derived by considering microchannel flow give fairly good descriptions of the pressure drop, particularly the work by Yu (1995).

### Nusselt Number

To aid in the analysis of the Nusselt number, the gas data were analyzed in several steps. First, each channel configuration was correlated for all gases. Next, all channel configurations were correlated for all gases. Finally, all channel configurations were correlated with all single-phase data (both gas and water). The water was also correlated separately for all channel configurations. However, the maximum correlation coefficient was found to be less than 0.4 with a standard deviation on the order of 10.0. These correlations offered no insight into the behavior of the water in the microchannels and therefore will not be presented. However, the water data is included in the final analysis, as mentioned above, for completeness. The problem associated with the water data can be traced back to the inaccuracies of the temperature measurements. During the tests, the water dissipated much more heat than the gases, as would be expected. Unfortunately, even trying to compensate with higher heater powers, this higher heat dissipation of the water still usually resulted in a much lower change in temperature between the inlet and outlet of the channels. Also, the kinetic energy effects discussed in chapter three were found to effect the data by no more than 5%. As will be shown, this is considerably less than the error due to the thermocouples. Therefore, kinetic energy effects were not considered in the following gas correlations.

To start the analysis, each channel configuration was correlated against all the gas flow data taken for that particular channel. The correlation coefficients ranged from 0.826 to 0.998 with only one configuration (F) being below 0.95. The resulting correlations

revealed several interesting findings. First, as in most cases of the friction factor, no transition between laminar and turbulent regions was seen. This is evident in Figure 6.2 and will be seen in the graphs that follow. Even more interesting, the flow behaved slightly opposite to the friction factor. That is the Nusselt number data was which seen to be a function of the Reynolds number and Prandtl number (a turbulent flow profile) and not constant as macroscale laminar correlations predict. However, this finding agrees with the study by Choi (1991). Second, as with macroscale flow, the Reynolds number and the Prandtl number were found to be the most important parameters. For these correlations the Reynolds number was seen to be slightly more important than the Prandtl number. Third, the measured Nusselt number was considerably below the macroscale prediction. Fourth, and finally, the viscosity ratio ( $\mu/\mu_s$ ) was also found to be an important parameter. As mentioned in the previous section, the viscosity parameter is an indication of entrance effects. For each channel configuration, as the hydraulic diameter decreased, the importance of this viscosity parameter diminished. In fact, for the two smallest channels, the parameter vanished altogether. For a fixed length channel, these results were as would be expected. As the hydraulic diameter decreases so does the percentage of the channel with developing flow.

Next, the Nusselt number data for all channel configurations and gases were correlated. The resulting empirical correlation, seen in Figure 6.9, is

$$Nu = 3.47 \times 10^{-6} Re^{1.639} Pr^{-0.6858} \quad (6.6)$$

With a correlation coefficient of 0.925, equation (6.5) is a very good correlation for a Nusselt number. As one can see in Figure 6.7, the scatter in the Nusselt number data decreases as the Nusselt number, or temperature difference, increases. Again pointing towards the importance of the temperature measurement, the correlations computed for this set of data revealed two more interesting findings. First, the Reynolds number was, by far, the most important parameter. The Reynolds number combined with any other parameter(s) yielded a correlation of at least 0.85. Without the Reynolds number, the highest correlation coefficient achieved was 0.52. Second, the viscosity term ( $\mu/\mu_s$ ) and the term  $L/D_h$  indicated a slight dependence of the correlation on entrance effects. However, these effects were too small to include the terms in equation (6.5).

Finally, the Nusselt number data for all single-phase data (gases and water) were correlated for all channel configurations. The resulting empirical correlation is

$$Nu = 1.5 \times 10^{-8} Re^{1.812} Pr^{2.38} \quad (6.7)$$

Shown in Figure 6.10, with an correlation coefficient of only 0.616, equation (6.6) is not a very good correlation of the Nusselt number. However, as with the all gas correlations, ( $\mu/\mu_s$ ) and  $L/D_h$  again indicated the presence of entrance effects.

A comparison between the experimentally measured Nusselt number data of this study and the Nusselt number correlations listed in Chapter 2 are shown in Figure 6.11. As mentioned earlier, the equations have been normalized and plotted as the ratio of the

measured Nusselt number over the correlated Nusselt number ( $Nu_{meas}/Nu_{corr}$ ) versus the Reynolds number times the Prandtl number. As one can see, most of the experimental data is considerably less than that predicted by the correlations. However, between the values of  $Re \cdot Pr = 2,000$  to  $10,000$ , the correlations of Yu (1995) and Choi (1991) predict the observed Nusselt number well.

### Two-Phase Flow Results

For the two-phase experiments, a combination of water and each gas (argon, helium, and nitrogen) were tested in each of the channel configurations. The Reynolds numbers ranged from around 30 to just under 10,000 with the data distributed slightly more heavily near the lower Reynolds numbers. The quality ranged from very low values (on the order of 0.01%) up to approximately 45%. However, most of the data had a quality of less than 10%. Figure 6.12 shows the friction factor data for all two-phase tests. As one can see, this data is well behaved and the laminar and turbulent regions are well defined. As will be discussed, the friction factor of the two-phase tests showed no dependence on channel size. The heat transfer results are given in Figure 6.13. Here the data show a large amount of scatter, as with the single phase results. Also, the two-phase Nusselt number data show the same trend as the single-phase in that no transition is indicated. In the following sections it will be shown that neither the homogeneous flow model nor the separated flow model parameters correlate the heat transfer data well.

### Two-Phase Friction Factor

Homogeneous Flow Model. Because of the two distinct regions that are shown in Figure 6.12, the two-phase data was analyzed in each region separately. Discussed in Chapter 4 was the fact that the flow parameters are calculated based on average fluid properties. As with the single-phase data, the two-phase data for friction factor was correlated starting with each individual channel configuration. Then, more and more general correlations were performed until all two-phase data were correlated for all channel configurations. Though the specifics of each of these correlations need not be presented, several interesting details were found. First, the friction factor data show two distinct regions for all channel sizes. Or, in two-phase flow we did not see the suppression of the turbulent tendencies, as with the single-phase data. It is believed that this behavior is due to the intense pressure fluctuations associated with two-phase flow. These pressure fluctuations, present over almost the entire range of quality, provide enough induced turbulence to overcome any suppression tendencies. Second, there is virtually no scatter around the Reynolds number of 3,000. There is literally only one point, in the turbulent region, that has a Reynolds number less than 3,000. The lack of scatter is probably also due to the pressure fluctuations associated with two-phase flow. It is believed that the transition Reynolds number of 3,000 is dependent on the test section and test fixture. In other words, a different test section may show a similar definite transition Reynolds number, but the value of this number most likely will not be exactly 3,000. Third, as with single-phase correlations, all two-phase correlations showed a complete dependence on

the Reynolds number. For the laminar and turbulent regions, the Reynolds number exponent has values of approximately -1.0 and -0.25, respectively, just as macroscale theory predicts. Therefore, the resulting equations will have the same form as equations (6.3, 4 and 5). The resulting empirical correlations are

Laminar Region ( $Re < 3,000$ ):

$$f_{tp} = \frac{97}{Re} \quad (6.8)$$

Turbulent Region ( $Re > 3,000$ ):

$$f_{tp} = \frac{0.3384}{Re^{0.25}} \quad (6.9)$$

The correlation coefficients are 0.931 and 0.907 for the laminar and turbulent regions, respectively. Equations (6.8) and (6.9) are shown in Figure 6.14. As one can see, both correlations are exceptional, particularly in the turbulent regime. Equation (6.9) fits the data to within +2.4% to - 0.8%. Note the change in range of the error bars provided in Figure 6.14. There is a slight indication that entrance effects from the correlations are probably what is causing the scatter at the lower Reynolds numbers. As the error analysis will show, the uncertainty of the pressure measurements was very small and did not change with changing pressure. To better fit the laminar data at the higher Reynold numbers, the coefficient in Equation (6.7) can be changed to a value of 87. The resulting equation is shown in Figure 6.15. The fourth, and final detail that was learned from the empirical correlations was that the two smallest channels, configurations E and F, indicated a

dependence of the quality and surface tension parameters (  $(1-x)/x$  and  $We$ ), respectively. No other channel configurations showed this dependence. However, the quality for these channels also covered a larger range and was higher than the other channels (10 - 40%). The last point seems to indicate that the quality and surface tension parameters become more important as the quality increases.

Separated Flow Model. The parameters presented in Chapter 4 for the separated flow model were correlated in the same manner as the homogeneous parameters. However, the resulting correlations were very poor ( $r < 0.45$ ) in almost all cases. Also, the correlations provided no insight into which parameters were important. For the turbulent regime ( $Re > 3,000$ ), the empirical correlation

$$f_{tp} = 0.0487 \left( \frac{v_g}{v_f} \right)^{0.0644} \left( \frac{\mu_f}{\mu_g} \right)^{-0.0667} \left( \frac{\epsilon}{D_h} \right)^{-0.0189} \left( \frac{L}{D_h} \right)^{-0.0751} \left( \frac{1-x}{x} \right)^{0.00868} \alpha^{0.2809} \quad (6.10)$$

does, to some degree, reduce the scatter in the data. Equation (6.10) is shown in Figure 6.16. However, because so many parameters are contained in equation (6.10) it can really only be applied to this particular set of data. That is, because no insight can be determined from the parameters on the behavior of the fluid, there is no reason to believe that this equation would apply to data other than that of this study.



### Nusselt Number

The Nusselt number data taken during the two-phase tests is shown in Figure 6.13. As with the previous sections, the data was analyzed based on each channel configuration first and then by more general correlations. Unfortunately, the resulting correlations for both the homogeneous and separated flow models were very poor. However, the numerous empirical correlations did provide some insight into the dominant parameters in two-phase heat transfer. When each channel configuration was considered separately, the Reynolds number and the Prandtl number were found to be most important in describing the behavior of the flow. This agrees with the Dittus-Boelter equation. As one can see in Figure 6.13, the behavior of the data parallels that of the Dittus-Boelter equation. Also, as with the single-phase heat transfer results, no transition is seen to occur. Note the data in Figure 6.13 labeled channel D. The data appears to be in a transition to a higher Nusselt number. However, no other channel was seen to behave in this manner. Extensive physical inspection was conducted on channel configuration D, but nothing was found that would explain the jump in the Nusselt number. Based on the Reynolds number and the Prandtl number, the empirical correlation for the Nusselt number is

$$\text{Nu} = 0.00166 \text{Re}^{0.6268} \text{Pr}^{2.293} \quad (6.11)$$

Equation (6.11), with a correlation coefficient of only 0.434, is shown in Figure 6.17. As one can see, this correlation does not fit the data well and has a large standard deviation. Again, error in the measurement of the temperatures has made any analysis very difficult. Correlation of the separated flow parameters gave even less information about the behavior of the fluid. The best separated flow correlation had a correlation coefficient of 0.4 and a standard deviation on the order of 10.

### Analytical Models

This section presents empirical correlations based on the analytical equations developed in Chapter 3. It will be shown that the separated flow model can make use of the correlation derived from the homogeneous flow model.

Homogeneous Flow Model. Looking at equation (3.27), one can see that the two-phase pressure drop is a function of a friction factor ( $f_{fa}$ ) and frictional flow parameter ( $\Phi_{fa}^2$ ). For the homogeneous flow model, the parameter  $\Phi_{fa}^2$  is expressed quantitatively by equation (3.25). Therefore, the friction factor can be computed directly for each pressure measurement. Solving equation (3.37) for the friction factor gives

$$f_{fa} = \frac{\Delta P_{tp} D_h}{2 G^2 v_f L \Phi_{fa}^2} \quad (6.12)$$

The friction factor in equation (6.12) was correlated against both the homogeneous and separated flow model parameters. Both sets of parameters were utilized because of the

difficulty in finding an adequate correlation. As can be seen in Figure 6.18, there are two regimes which need to be considered. One for  $f_{fa}$  larger than 0.005 and the other for  $f_{fa}$  less than 0.005. The apparent jump in the friction factor does not appear to be due to the lack of data in that area. For channel configurations E and F, which makeup the data for  $f_{fa} < 0.005$ , several data points for these channels are above  $f_{fa} = 0.005$ . Also, inspecting the measured flow rates show no jumps in either the gas or liquid flow rates that might account for this jump in the data. Unfortunately, virtually no dimensionless combination of parameters gave a correlation coefficient greater than 0.4. The resulting empirical correlations are

$$(f_{fa} < 0.005): \quad f_{fa} = 43,940 \, G^{-3.885} \, \text{Re}^{2.732} \left( \frac{\dot{m}_f}{m_g} \right)^{-0.1137} \quad (6.13)$$

$$(f_{fa} > 0.005): \quad f_{fa} = 6,791 \, G^{-1.495} \, \text{Re}^{0.2466} \, x^{-1.571} \left( \frac{\dot{m}_f}{m_g} \right)^{-1.731} \quad (6.14)$$

As one can see, both equations are dimensional. This, unfortunately, could not be avoided. The correlations indicated that by far the most important parameter in determining  $f_{fa}$  was the mass velocity ( $G$ ). Even though dimensionless parameters containing  $G$  were tried, none were remotely successful. Only a correlation containing  $G$  gave reasonable results. On the positive side, however, in macroscale two-phase flow the mass velocity is a common and important parameter. Equations (6.13) and (6.14) are shown in Figures 6.19 and 6.20 for the different  $f_{fa}$  regimes. As one can see, the correlations give good results.

Equations (6.13) and (6.14) will be used in the next section to predict the two-phase friction coefficient. Comparisons will be made at that time.

Separated Flow Model. For the separated flow model, the pressure drop through a channel is given by equation (3.57). In equation (3.57), the pressure drop is a function of a friction factor ( $f_f$ ), a frictional pressure drop coefficient ( $\phi_f^2$ ), and a momentum pressure drop parameter ( $\phi_m$ ). The friction factor ( $f_f$ ) is based on a single phase pressure gradient with the liquid assumed to flow alone in the channel. The momentum pressure drop parameter is described by equation (2.15) and is particularly important in two-phase flow involving phase change. However, preliminary calculations indicated that the momentum pressure drop parameter changed the pressure calculation by less than 3% and was therefore neglected. Therefore, equation (3.57) was only a function of the liquid friction factor and the frictional pressure drop parameter. To solve equation (3.57), one can make use of the correlation of  $f_{fa}$  determined in the previous section. By using the Baisius equation (3.22), Collier (1981) showed that

$$f_f = f_{fa} (1 - x)^{-1/4} \quad (6.15)$$

Substituting this expression into equation (3.57) and neglecting the momentum pressure drop parameter, equation (3.57) becomes

$$\Delta P_{tp} = \frac{2 G^2 v_f L f_{fa} (1-x)^{-1.75}}{D_h} \Phi_f^2 \quad (6.16)$$

Note that equation (6.16) is now a function  $\Phi_f^2$  and the friction factor ( $f_{fa}$ ) that was correlated in the last section. Therefore, values of  $\Phi_f^2$  can be determined for each pressure measurement directly and correlated against the homogeneous and separated flow parameters. Solving equation (6.16) for the frictional pressure drop parameter gives

$$\Phi_f^2 = \frac{D_h \Delta P_{tp}}{2 G^2 v_f L f_{fa} (1-x)^{-1.75}} \quad (6.17)$$

The resulting empirical correlations of equation (6.17), over the two ranges of  $f_{fa}$ , yielded some interesting results. By far the most important parameters in predicting  $\Phi_f^2$  were found to be  $e/D_h$ ,  $L/D_h$ ,  $(1-x)/x$ , and  $\alpha$  (aspect ratio). Interestingly, the empirical correlation is dominated by the channel's physical dimensions more than any other parameter. Only one fluid parameter was shown to be important, the quality. Any correlation of parameters that contained these four parameters had a correlation coefficient of 0.91 or higher. To help reduce the standard deviation, the final correlation of  $\Phi_f^2$  also related some parameters which have been shown to be important in earlier correlations; Reynolds number, Weber number, Prandtl number, and the viscosity ratio ( $\mu/\mu_s$ ). The frictional pressure parameter is predicted well by the expressions

( $f_{fa} < 0.005$ ):

$$\Phi_f^2 = 0.011 \text{Re}^{0.325} \text{We}^{-0.0162} \text{Pr}^{-0.1803} \frac{\mu}{\mu_s}^{1.989} \frac{\epsilon}{D_h}^{0.231} \frac{L}{D_h}^{-0.113} \frac{1-x}{x}^{0.0541} \alpha^{7.94} \quad (6.18)$$

( $f_{fa} > 0.005$ ):

$$\Phi_f^2 = 1.0x^{-10} \text{Re}^{0.0834} \text{We}^{0.056} \text{Pr}^{2.932} \frac{\mu}{\mu_s}^{1.367} \frac{\epsilon}{D_h}^{-0.01795} \frac{L}{D_h}^{2.865} \frac{1-x}{x}^{0.0277} \alpha^{1.214} \quad (6.19)$$

Figures 6.21 and 6.22 show equations (6.18) and (6.19) which have correlations coefficients of 0.979 and 0.971, respectively.

The accuracy of the pressure drops predicted by empirical solution compared to the two analytical flow models can be seen in Figures 6.23 and 6.24. As one can see in Figure 6.23, the predicted pressure drop is reasonably accurate, particularly for the higher pressure drops where Martinelli's equations will be shown to fail. From Figure 6.24, one can see that the separated flow model does not provide a good estimate of the pressure drop. However, this could be for several reasons. First the separated flow model is essentially a correlation of a correlation. That is, the correlation for  $\Phi_f^2$  can not be expected to be any better than the correlation of  $f_{fa}$  on which it is based. Second, the separated flow model is not a good model for fluid flow at the scale of these experiments. For most macroscale developments, the correlation of  $\Phi_f^2$  is based on the assumption of a constant value for  $f_{fa}$ . As shown in these experiments,  $f_{fa}$  is definitely not a constant. Other reasons for the inaccuracy of the separated flow model can be seen when comparing the pressure prediction of Martinelli to the experimental data.

Figure 6.25 shows the data taken for this study plotted with the predicted pressure drop of Martinelli. As one can see, Martinelli's equations substantially over predict the measured pressure drop except at lower values of the measured pressure drop. This over prediction is due to two reasons. First, as Collier (1981) states, the semi-empirical equations developed by Martinelli are only good for low-to-moderate pressure drops over the length of the channel. For the data taken in this study, the calculated values of  $\Delta P/L$  were several orders of magnitude higher than Martinelli's equations would predict. Second, Martinelli's equations are based on the macroscale constants which predict the friction factor in laminar and turbulent regimes for the individual components. Not only have we shown that in some cases these constants are different, but also that there is no transition in the smaller channels for single-phase flow.

### Flow Regimes

To compare the flow regimes present for this study, the data of this study are plotted on Baker's (1954) flow regime map given in Figure 6.26. As one can see, the data extend past the regions given by Baker. The data are mainly concentrated in the mist flow and bubble flow regimes. Also, some data lie along the transition lines to annular and slug flow. The jump in the data about  $f_{fa} = 0.005$  is also seen in this figure. From what could be observed during the experimentation, the regimes predicted by Baker's flow regime map seem reasonable. Though the specific regimes could not be verified without a high-speed camera, the behavior of the two fluids in the manifold area of the test section indicated that the flow regimes were mainly slug flow with some annular flow. With such

low qualities seen during the experiments, it is also reasonable to believe that bubble flow occurred. However, this could not be confirmed. The large amount of data shown in the mist flow regime is not believed to have actually been mist flow. For mist flow to occur, the quality needs to be relatively high. The only data with high qualities are those points shown to have a  $f_{fa}$  value less than 0.005. These points can be seen to be the upper right grouping of data. Some of this contradiction is clarified by the flow regime map given by Suo and Griffith (1964) in Figure 6.27. Figure 6.27 shows the separation between bubbly-slug flow and slug flow. As can be seen, most of the data is in the region of bubbly-slug flow. It is believed that this figure is a better representation of what is actually occurring in the microchannels. For data points generated by this study, the mist flow regime on Baker's (1954) map are probably more like the bubbly-slug flow described by Suo and Griffith (1964).

#### Other Heat Transfer Comparisons

As some final comparisons, the heat flux data measured in this study, and the calculated heat transfer coefficients are compared with the information given in Chapter 2 for forced convection flow boiling. Figure 6.28 compares the measured heat flux in both the single- and two-phase data to the critical heat flux ranges given in Figure 3.3. As one can see, the heat flux dissipated by the water and all two-phase data approach the levels present in micro heat pipes for a lower temperature difference.

Figure 6.29 given the ranges of the calculated heat transfer coefficients for both the single- and two-phase flow data of this study. Typical ranges for the heat transfer



coefficient in various types of convection are listed on the left side of the graph. As can be seen the water and the two-component two-phase data have heat transfer coefficients on the order of, and higher, than convection involving phase change. It would therefore be expected to see higher heat transfer coefficients for microchannel flow boiling. The comparison indicates that heat transfer through microchannels does have advantages over macroscale channels.

### Error Analysis

For the results presented above to be used to their fullest, an uncertainty analysis of the experimental measurements must be considered. The uncertainty ( $\pm U$ ), or the 95% confidence limit, of the measurements are made up of the precision error (P) and the Bias error (B). Precision error is the lack of repeatability due to random error and unsteadiness. The Bias error is a measure of fixed or constant error. A list of the precision and bias limits for the equipments used in this error analysis is given in Table 4. For a detailed description of the experimental flow loop, please see the work by Bailey (1996).

For the experimental data taken during this study, only two expressions need to be analyzed. The friction factor, defined by

$$f = \frac{2 \Delta P D_h}{\rho L \bar{V}^2} \quad (6.20)$$

Table 4: Bias and precision error for measured experimental variables.

Variable	Bias Error	Precision Error
Pressures	0.1 %	0.15 %
Volumetric Flow Rates	0.25 %	1.0 %
Thermocouples	0.1 °C	1.0 °C
Channel Height (Depth)	0.01 %	0.01 %
Channel Length	0.04 %	0.04 %
Channel Width	0.01 %	0.01 %
Density	0.0	1.0 %
Specific Heat	0.0	1.0 %
Thermal Conductivity	0.0	1.0 %

and the Nusselt number, defined by

$$Nu = \frac{h D_h}{k} \quad (6.21)$$

To break these equations down into forms that contain only measured variables, requires the use of the equations

$$D_h = \frac{4 A}{P} = \frac{4 W H}{2 W + 2 H} \quad (6.22)$$

$$\bar{V} = \frac{\dot{V}}{A} = \frac{\dot{V}}{WH} \quad (6.23)$$

$$h = \frac{q}{A_w(T_w - T_\infty)} \quad (6.24)$$

$$A_w = L(W + 2H) \quad (6.25)$$

$$q = \dot{m} C_p (T_{in} - T_{out}) \quad (6.26)$$

Substituting equations (6.22) through (6.26) into equations (6.21) and (6.22) yield

$$f = \frac{2(P_{in} - P_{out})W^3H^3}{\rho L \bar{V}^2(W + H)} \quad (6.27)$$

$$Nu = \frac{2\rho \dot{V} C_p (T_{in} - T_{out})WH}{kL(T_w - T_\infty)(W + 2H)(W + H)} \quad (6.28)$$

Equations (6.27) and (6.29) can now be used to determine the experimental uncertainty due to the instruments used with the experimental flow loop.

Consider the friction factor. The square of the precision error for the friction factor can be found by summing the square of the partial derivative with respect to each variable multiplied by the square of the precision error for that variable. Or,

$$\begin{aligned}
 (P f)^2 = & \left( \frac{\partial f}{\partial P_{in}} \right)^2 (P_{P_i})^2 + \left( \frac{\partial f}{\partial P_{out}} \right)^2 (P_{P_o})^2 + \left( \frac{\partial f}{\partial W} \right)^2 (P_w)^2 + \left( \frac{\partial f}{\partial H} \right)^2 (P_H)^2 + \\
 & \left( \frac{\partial f}{\partial \rho} \right)^2 (P_\rho)^2 + \left( \frac{\partial f}{\partial L} \right)^2 (P_L)^2 + \left( \frac{\partial f}{\partial \dot{V}} \right)^2 (P_{\dot{V}})^2
 \end{aligned} \tag{6.29}$$

The bias error is determined using an equation of the same form by substituting the bias error for the precision error. Once the bias and precision error have been determined using equation (6.30), the uncertainty can be determined by the expression

$$U = (B^2 + P^2)^{1/2} \tag{6.30}$$

where  $U$  is the +/- percentage applied to the friction factor or Nusselt number for which it was calculated. The uncertainties for both the friction factor and the Nusselt number data are listed with the reduced data in Appendix D. Because of all the bias and precision error terms used in determining the friction factor being related as percentages, the final equations reduced down to the square root of the sum of the squares of the error terms. Therefore, the uncertainty calculated for the friction factor was a constant for all flow situations. The uncertainty of all friction factor measurements was found to be  $\pm 3.06\%$ . For the Nusselt number calculations, the bias and precision errors for the thermocouples were given a  $0.1^\circ\text{C}$  and  $1.0^\circ\text{C}$ , respectively. Therefore, the uncertainty of the Nusselt number measurements changed with each temperature measurement. Figures 6.30, 31, and 32 are samples of the uncertainty seen in the Nusselt number calculations. One can see in Figure 6.30 that the uncertainty in Nusselt number for gas flow is largest at the

lowest Reynolds numbers. Here the temperature differences are the smallest. Figure 6.30 also shows that the large error associated with the low Reynolds number quickly diminishes to a relatively constant value as Reynolds number increases. The ranges of the Nusselt number uncertainties are given for each channel configuration and flow combination in Table 5 and 6. A trend just opposite to Figure 6.30 can be seen in Figure 6.31 for water flows. Here the smaller temperature differences occur at the high end of the Reynolds numbers. Because of the temperature limitations on the test section and heater, the amount of power used to heat the channels was not adequate to maintain a larger temperature difference. A similar trend is seen in Figure 6.32 for two-phase flows. The uncertainty of the Nusselt number increases with average Reynolds number. Also, the Nusselt number is seen to be fairly constant within the different ranges of liquid and gas Reynolds numbers. As discussed through the previous sections, the medium to large amount of error in the Nusselt number measurements played a major role in the large amount of scatter observed in the various single- and two-phase tests conducted for this study.

Table 5: Single-phase Nusselt number uncertainty.

Channel Configuration	Uncertainty ( $\pm U$ , %)							
	Argon Min. Max.		Helium Min. Max.		Nitrogen Min. Max.		Water Min. Max.	
A	7.82	22.5	9.25	30.5	8.42	14.5	12.6	21.3
B	7.32	23.2	7.97	62.5	7.27	16.1	14.7	42.4
C1	9.03	172	10.2	136	8.77	252	10.2	20.3
C2	12.1	95.6	14.0	119	12.3	196	13.0	31.2
C3	10.4	186	11.9	73.7	11.0	857	13.3	24.9
D	43.5	11.7	17.9	91.3	14.6	220	14.1	165
E	13.4	122	15.7	9,329	25.7	500	12.7	22.2
F	13.3	113	12.5	303	13.8	267	15.2	23.6

Table 6: Two-phase Nusselt number uncertainty.

Channel Configuration	Uncertainty ( $\pm U$ , %)					
	Water-Argon Min. Max.		Water-Helium Min. Max.		Water-Nitrogen Min. Max.	
A	13.3	16.3	15.8	23.9	13.4	19.6
B	7.90	25.2	10.1	17.7	11.2	16.1
C1	10.1	19.6	10.1	17.9	11.3	19.2
C2	10.1	35.8	10.9	19.4	25.3	69.2
C3	13.8	17.7	15.3	17.8	13.9	18.0
D	18.2	123	22.4	88.9	23.0	494
E	33.4	49.7	15.8	25.1	16.2	23.8
F	14.4	19.3	14.0	19.3	14.1	19.3

### Final Summary of Equations

To conclude Chapter 6, the empirical relations developed in this chapter are summarized below with details for which flow regimes and conditions apply.

Single-Phase Flow:

Water: ( $50 \mu\text{m} < D_h < 250 \mu\text{m}$ )

$$(\text{Re} < 10,000) \quad f = 3.9 \times 10^{11} \text{Re}^{-1.862} \left( \frac{\mu}{\mu_s} \right)^{0.7845} \left( \frac{L}{D_h} \right)^{-2.762} \quad (6.2)$$

All Gases: ( $150 \mu\text{m} < D_h < 250 \mu\text{m}$ )

$$(\text{Re} < 1,500) \quad f = \frac{74}{\text{Re}} \quad (6.3)$$

$$(\text{Re} > 2000) \quad f = \frac{0.39}{\text{Re}^{0.25}} \quad (6.4)$$

All Gases: ( $50 \mu\text{m} < D_h < 150 \mu\text{m}$ )

$$(\text{Re} < 5,000) \quad f = \frac{66}{\text{Re}} \quad (6.5)$$

All Gases: ( $50 \mu\text{m} < D_h < 250 \mu\text{m}$ )

$$(\text{Re} < 5,000) \quad \text{Nu} = 3.47 \times 10^{-6} \text{Re}^{1.639} \text{Pr}^{-0.6858} \quad (6.6)$$

All Single-Phase: ( $50 \mu\text{m} < D_h < 250 \mu\text{m}$ )

$$(Re < 5,000) \quad Nu = 1.5 \times 10^{-8} Re^{1.812} Pr^{2.38} \quad (6.7)$$

Two-Phase Flow:

All Two-Phase: ( $50 \mu\text{m} < D_h < 250 \mu\text{m}$ )

$$(Re < 3,000) \quad f_{tp} = \frac{97}{Re} \quad (6.8)$$

$$(Re > 3,000) \quad f_{tp} = \frac{0.3384}{Re^{0.25}} \quad (6.9)$$

( $Re > 3,000$ )

$$f_{tp} = 0.0487 \left( \frac{v_g}{v_f} \right)^{0.0644} \left( \frac{\mu_f}{\mu_g} \right)^{-0.0667} \left( \frac{\epsilon}{D_h} \right)^{-0.0189} \left( \frac{L}{D_h} \right)^{-0.0751} \left( \frac{1-x}{x} \right)^{0.00868} \alpha^{0.00868} \quad (6.10)$$

$$(Re < 10,000) \quad Nu = 0.00166 Re^{0.6268} Pr^{2.293} \quad (6.11)$$

Homogeneous Flow Model:

$$(f_{fa} < 0.005): \quad f_{fa} = 43,940 G^{-3.885} Re^{2.732} \left( \frac{m_f}{m_g} \right)^{-0.1137} \quad (6.13)$$

$$(f_{fa} > 0.005): \quad f_{fa} = 6,791 G^{-1.495} Re^{0.2466} x^{-1.571} \left( \frac{m_f}{m_g} \right)^{-1.731} \quad (6.14)$$



Separated Flow Model:

$$(f_{fa} < 0.005)$$

$$\Phi_f^2 = 0.011 \text{Re}^{0.325} \text{We}^{-0.0162} \text{Pr}^{-0.1803} \frac{\mu}{\mu_s}^{1.989} \frac{\epsilon}{D_h}^{0.231} \frac{L}{D_h}^{-0.113} \frac{1-x}{x}^{0.0541} \alpha^{7.94} \quad (6.18)$$

$$(f_{fa} > 0.005)$$

$$\Phi_f^2 = 1.0x^{-10} \text{Re}^{0.0834} \text{We}^{0.056} \text{Pr}^{2.932} \frac{\mu}{\mu_s}^{1.367} \frac{\epsilon}{D_h}^{-0.01795} \frac{L}{D_h}^{2.865} \frac{1-x}{x}^{0.0277} \alpha^{1.214} \quad (6.19)$$

where  $f_{fa}$  and  $\Phi_f^2$  are used in

$$\Delta p_{tp} = \frac{2f_{fa} G^2 v_f L}{D_h} \left[ 1 + x \left( \frac{v_{fg}}{v_f} \right) \right] \left[ 1 + x \left( \frac{\mu_{fg}}{\mu_f} \right) \right]^{-\frac{1}{4}} \quad (3.27)$$

$$\Delta P_{tp} = \frac{2 G^2 v_f L f_{fa} (1-x)^{-1/75}}{D_h} \Phi_f^2 \quad (6.16)$$

respectively.

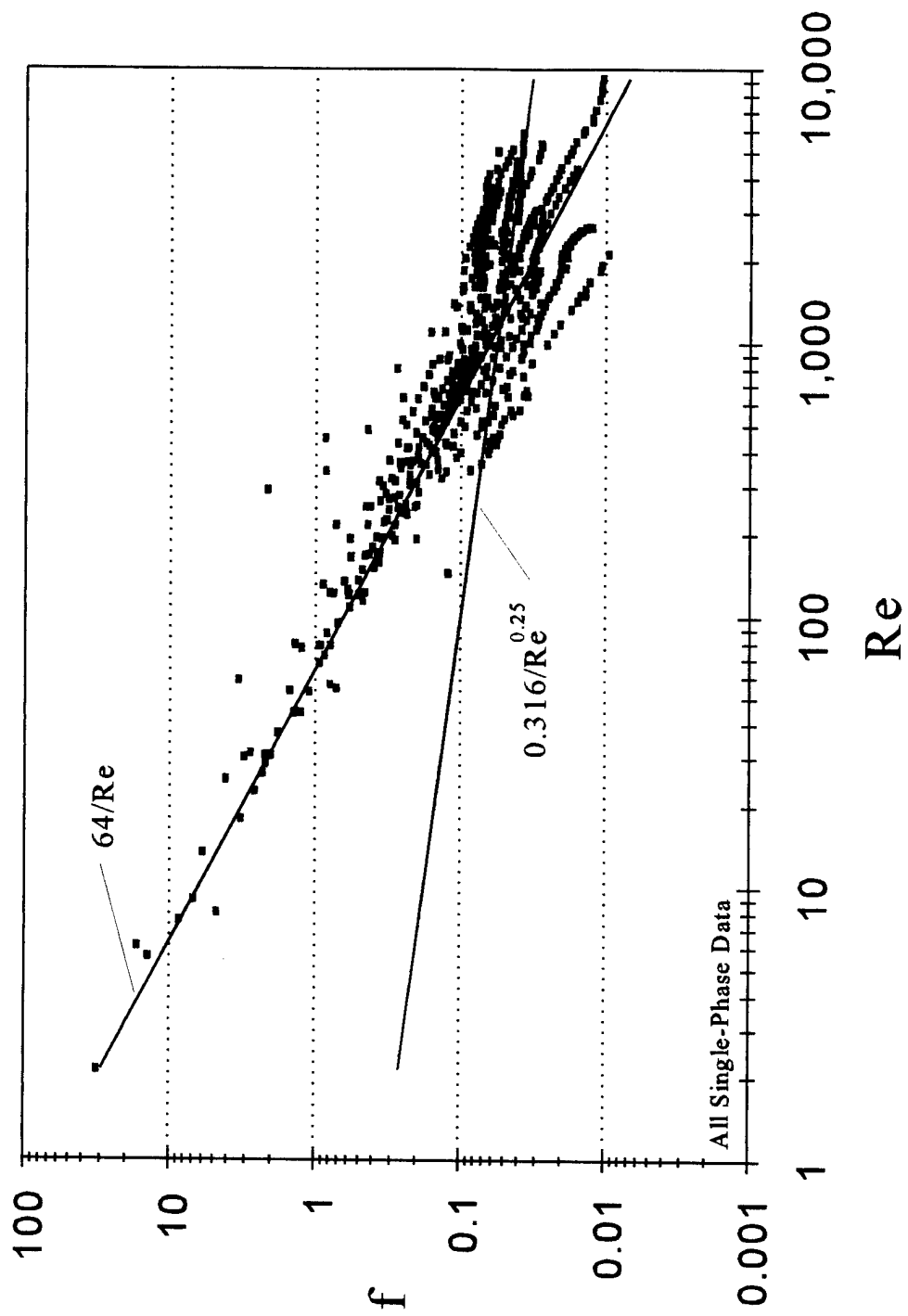


Figure 6.1: All single-phase friction factor data.

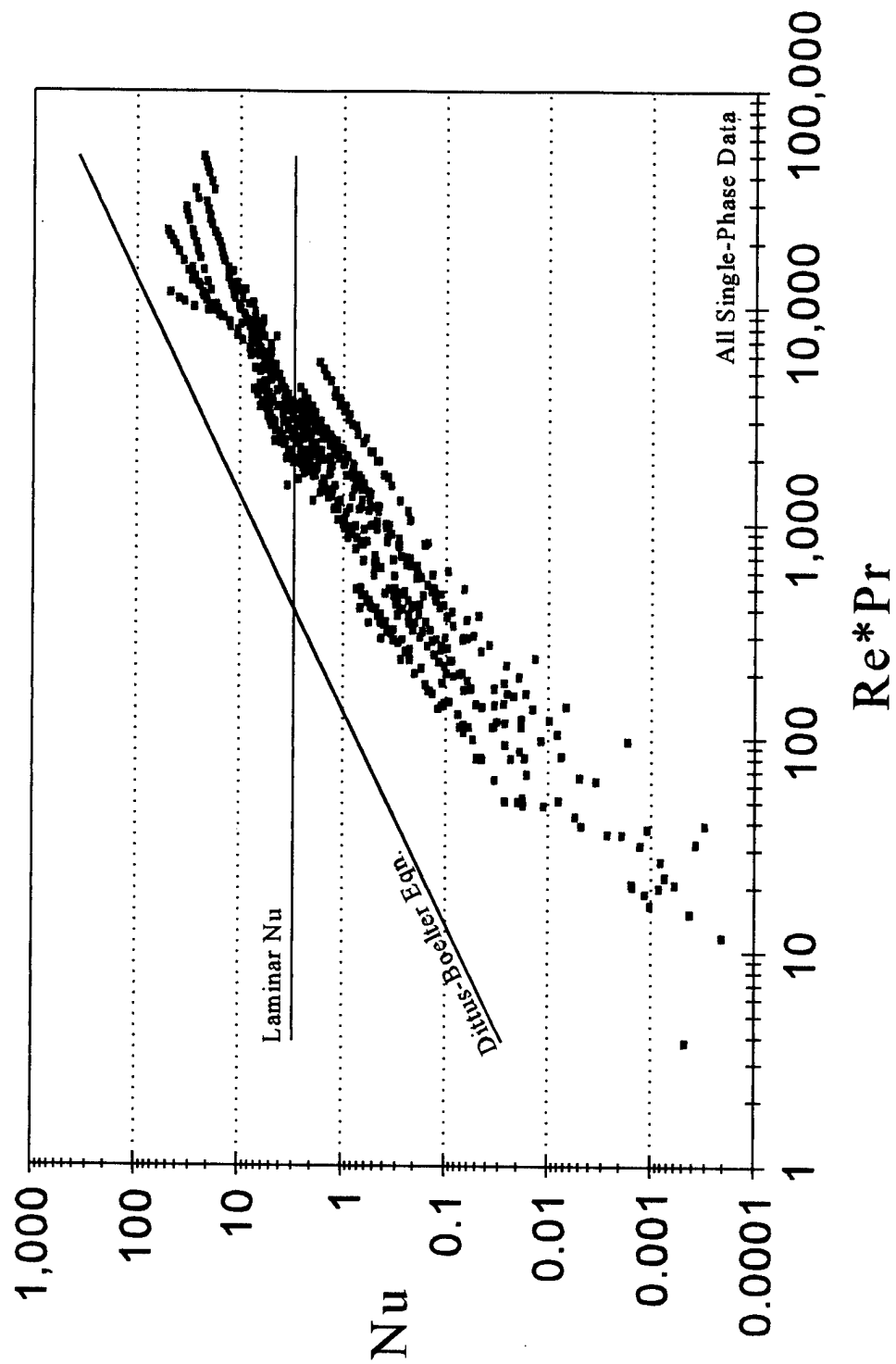


Figure 6.2: All single-phase Nusselt number data.

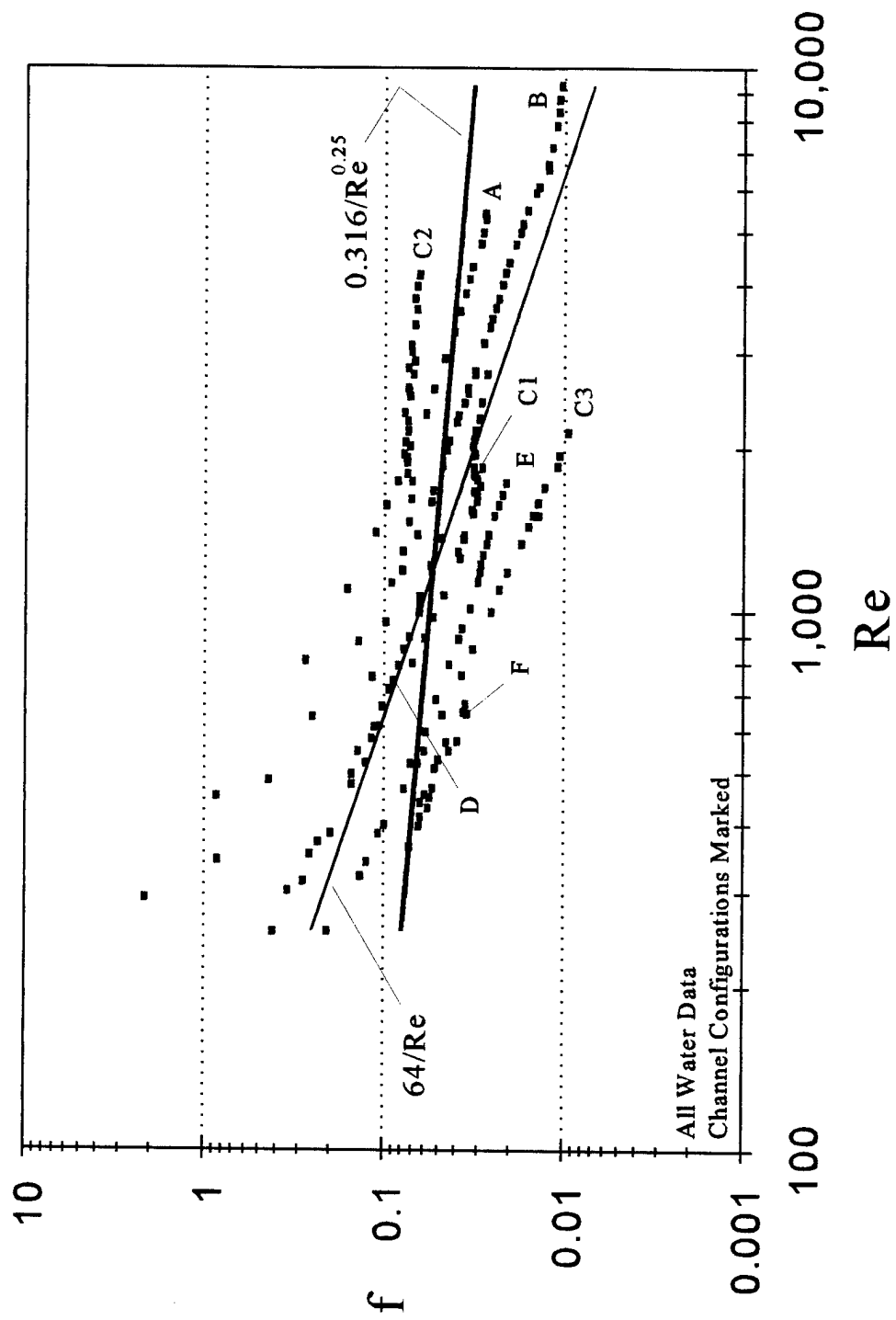


Figure 6.3: Water friction factor data with channel configurations indicated.

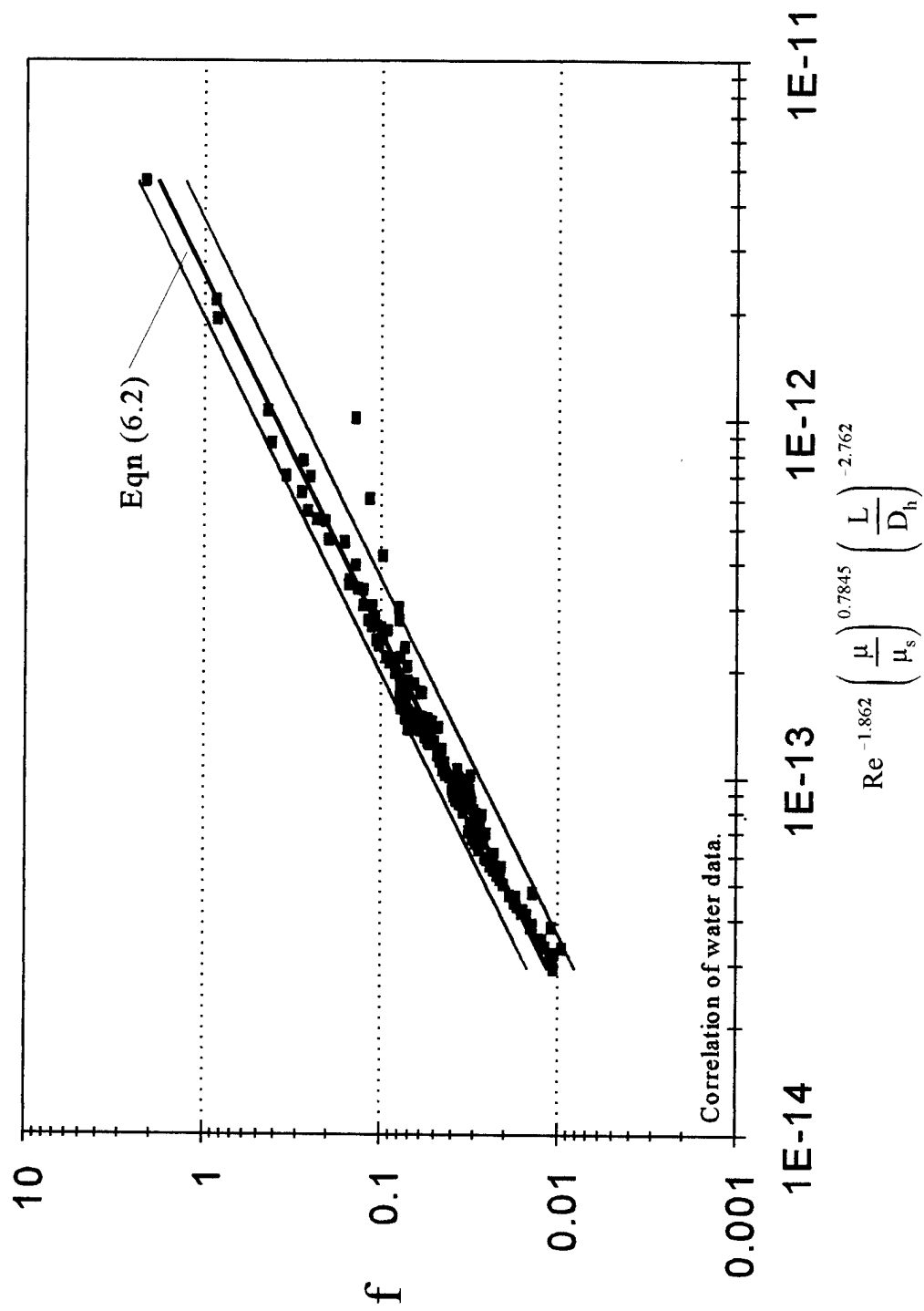


Figure 6.4: Friction factor correlation for water in all channel sizes.

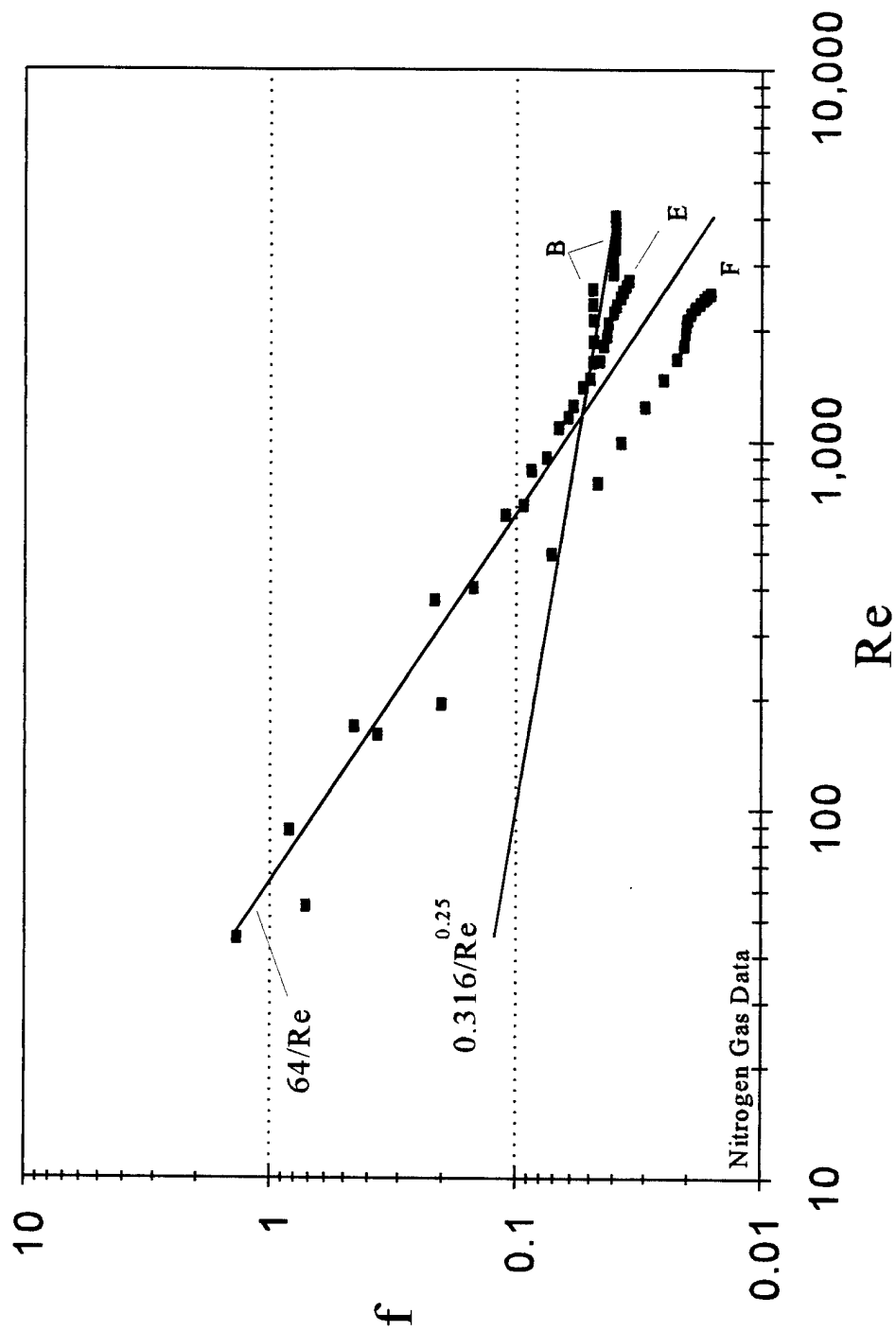


Figure 6.5: Nitrogen gas friction factor data for specified channels showing transition suppression.

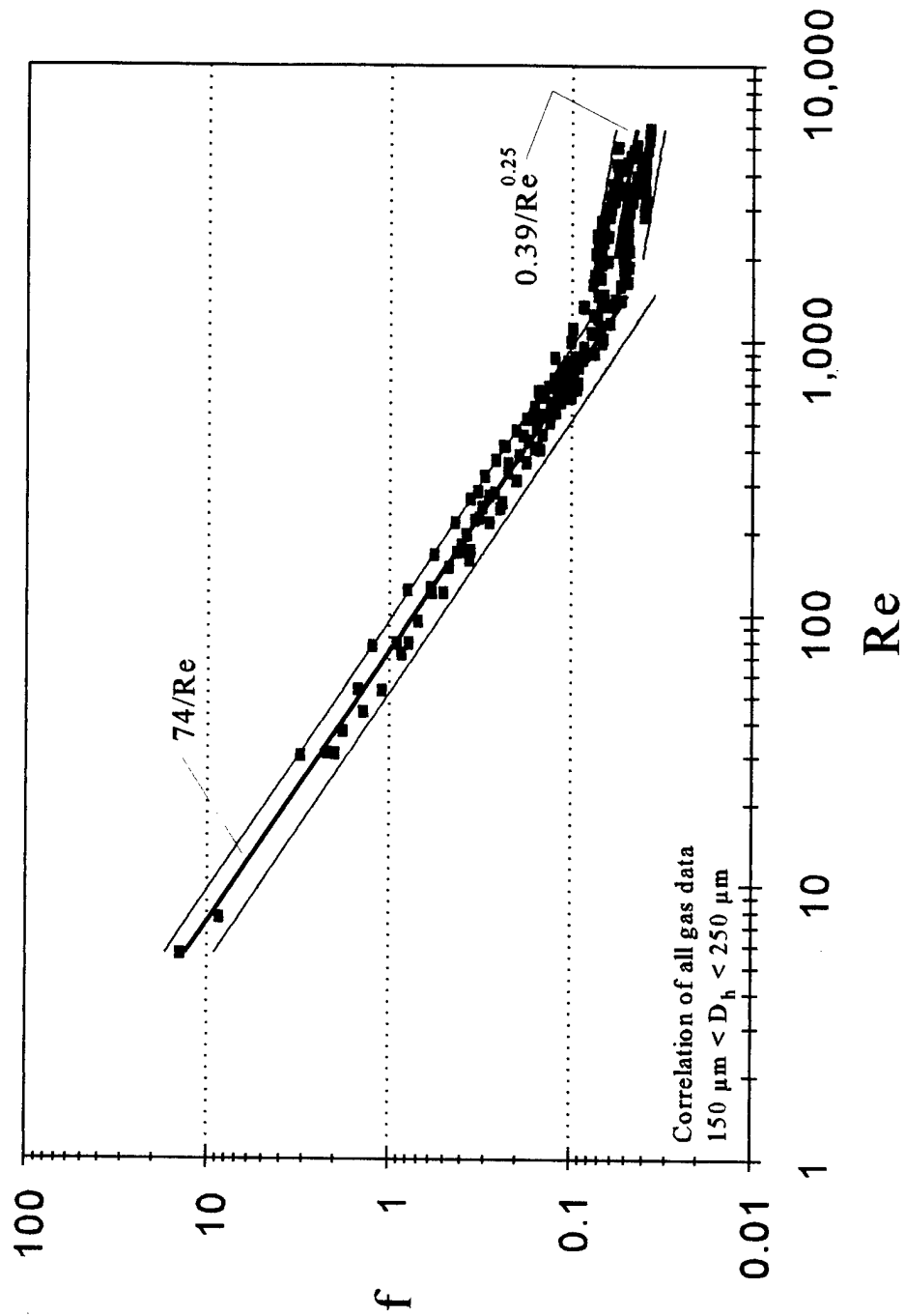


Figure 6.6: Friction factor correlation of all gas data for channels with hydraulic diameter between  $150 \mu\text{m}$  and  $250 \mu\text{m}$ .

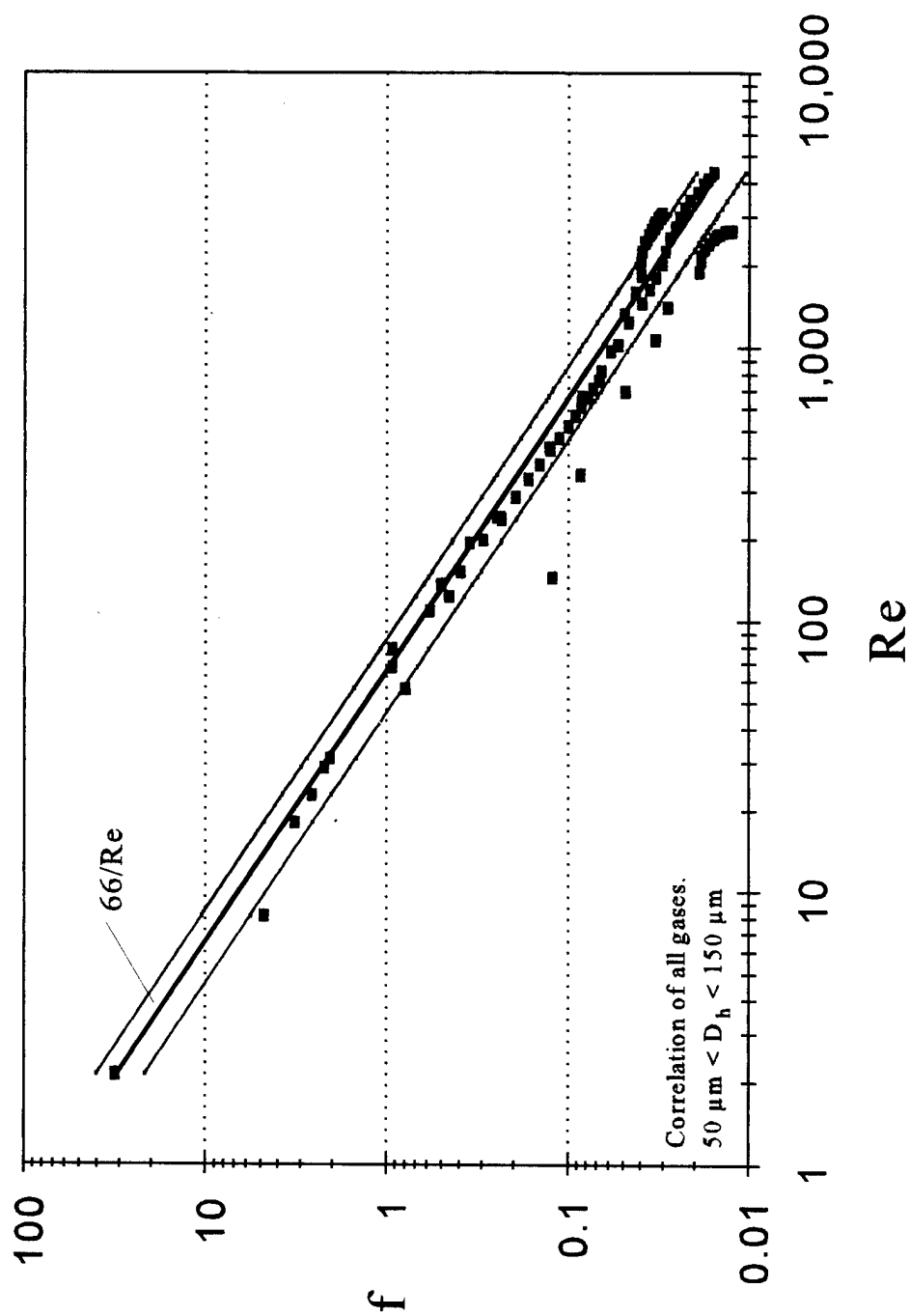


Figure 6.7: Friction factor correlation of all gas data for channel with hydraulic diameters between  $50 \mu\text{m}$  and  $150 \mu\text{m}$ .



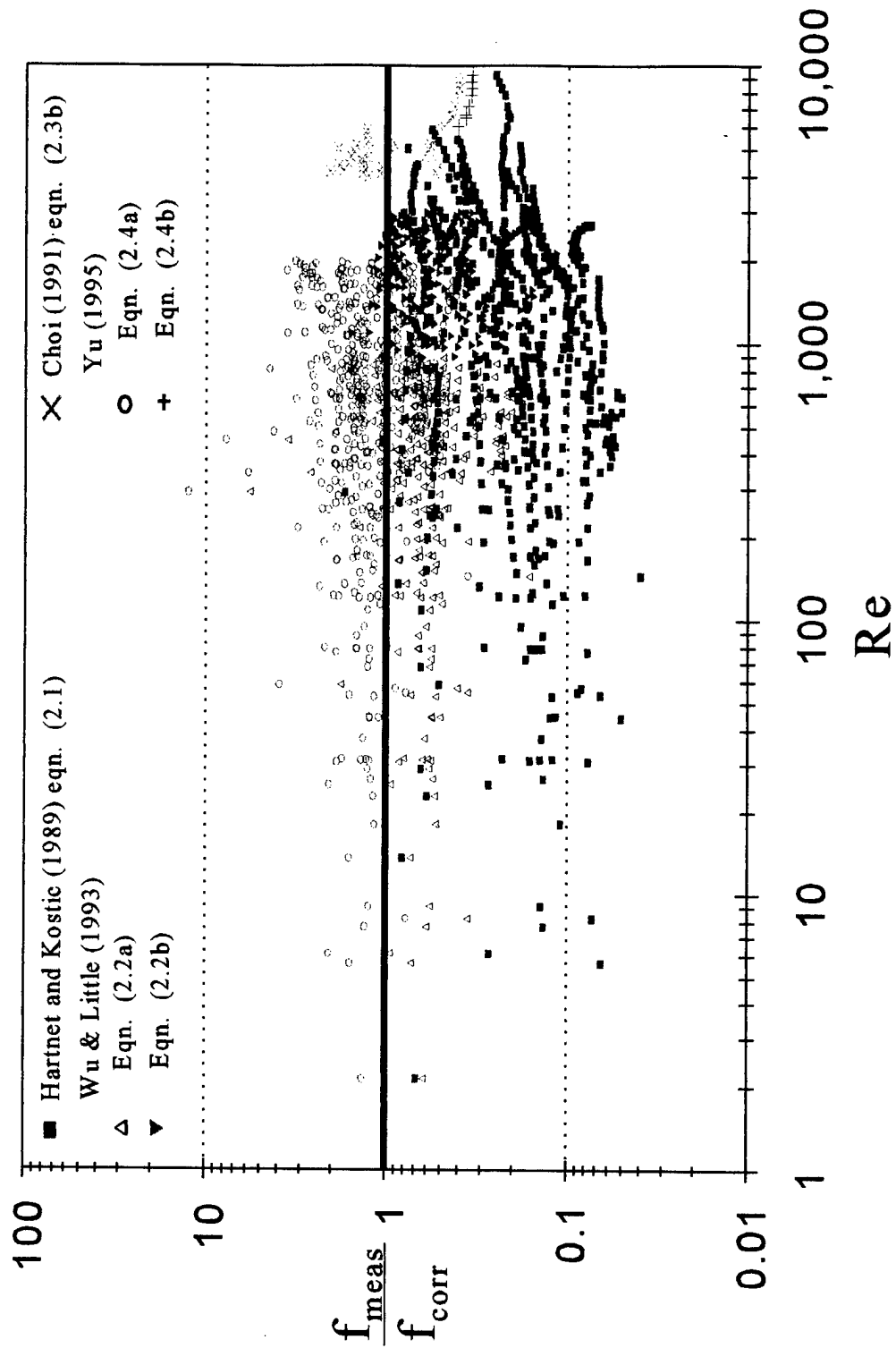


Figure 6.8: Comparison of friction factor data with correlations from Chapter 2.

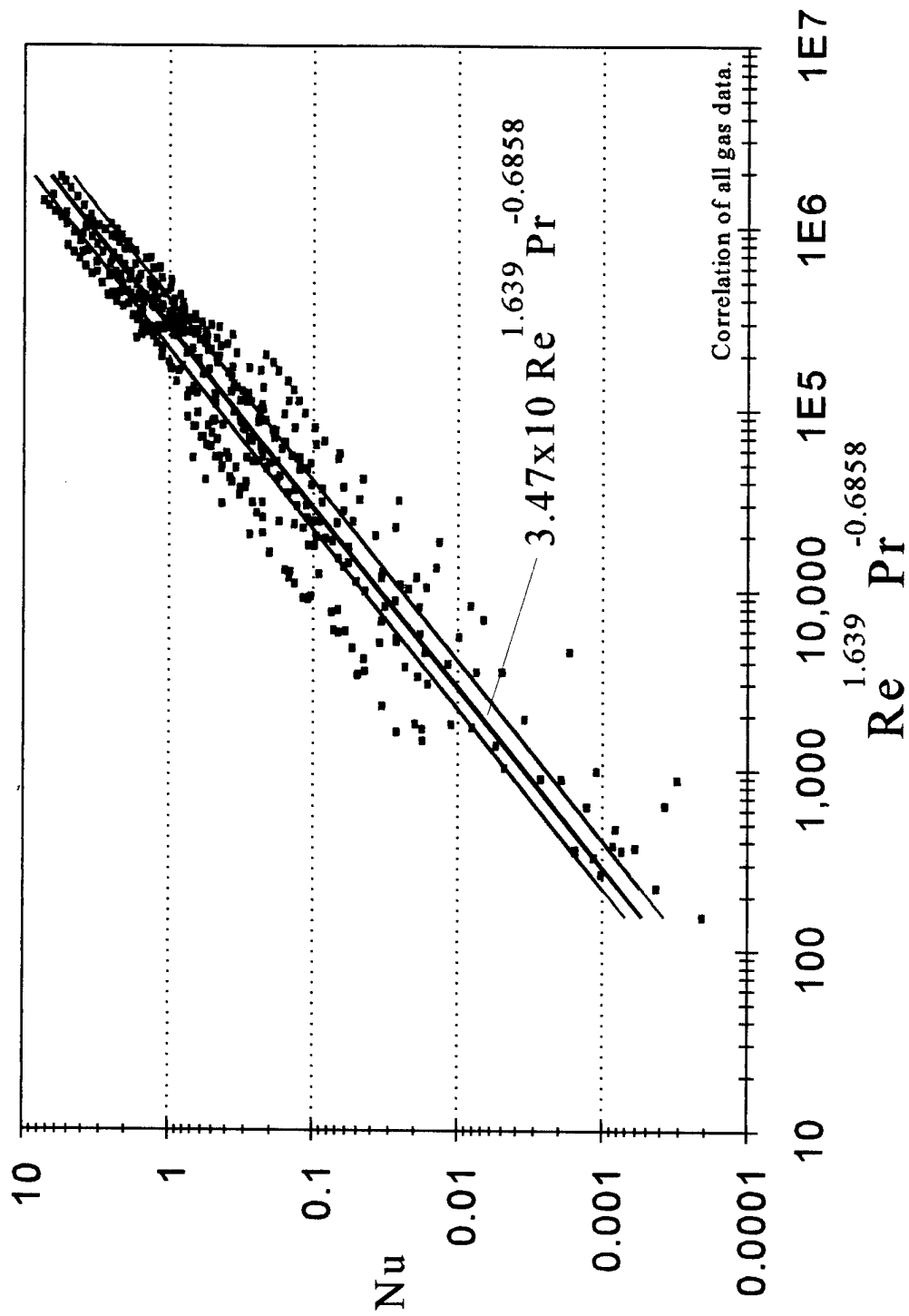


Figure 6.9: Nusselt number correlation of all gases for all channel sizes.

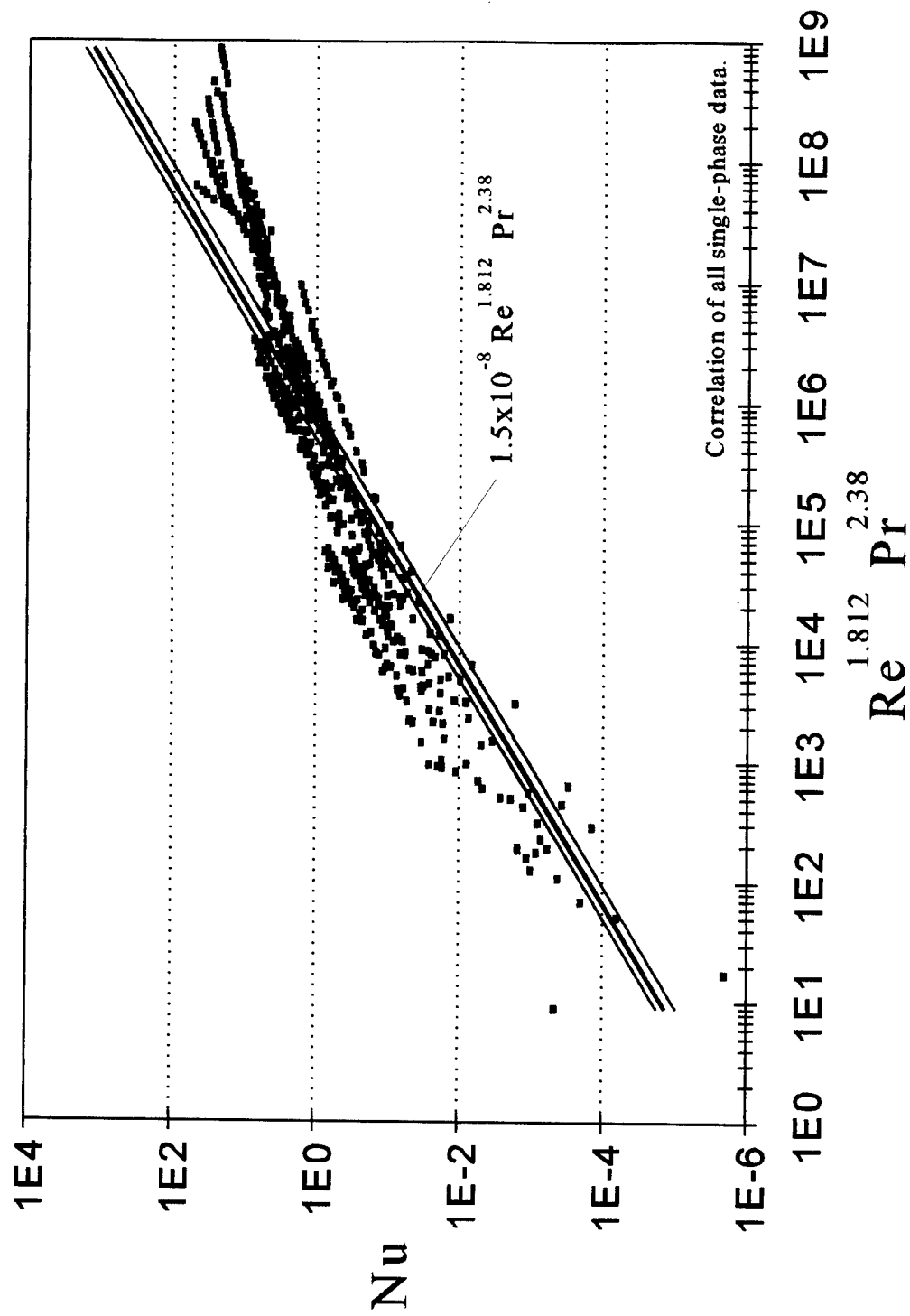


Figure 6.10: Correlation of Nusselt number data for all fluids and all channel sizes.

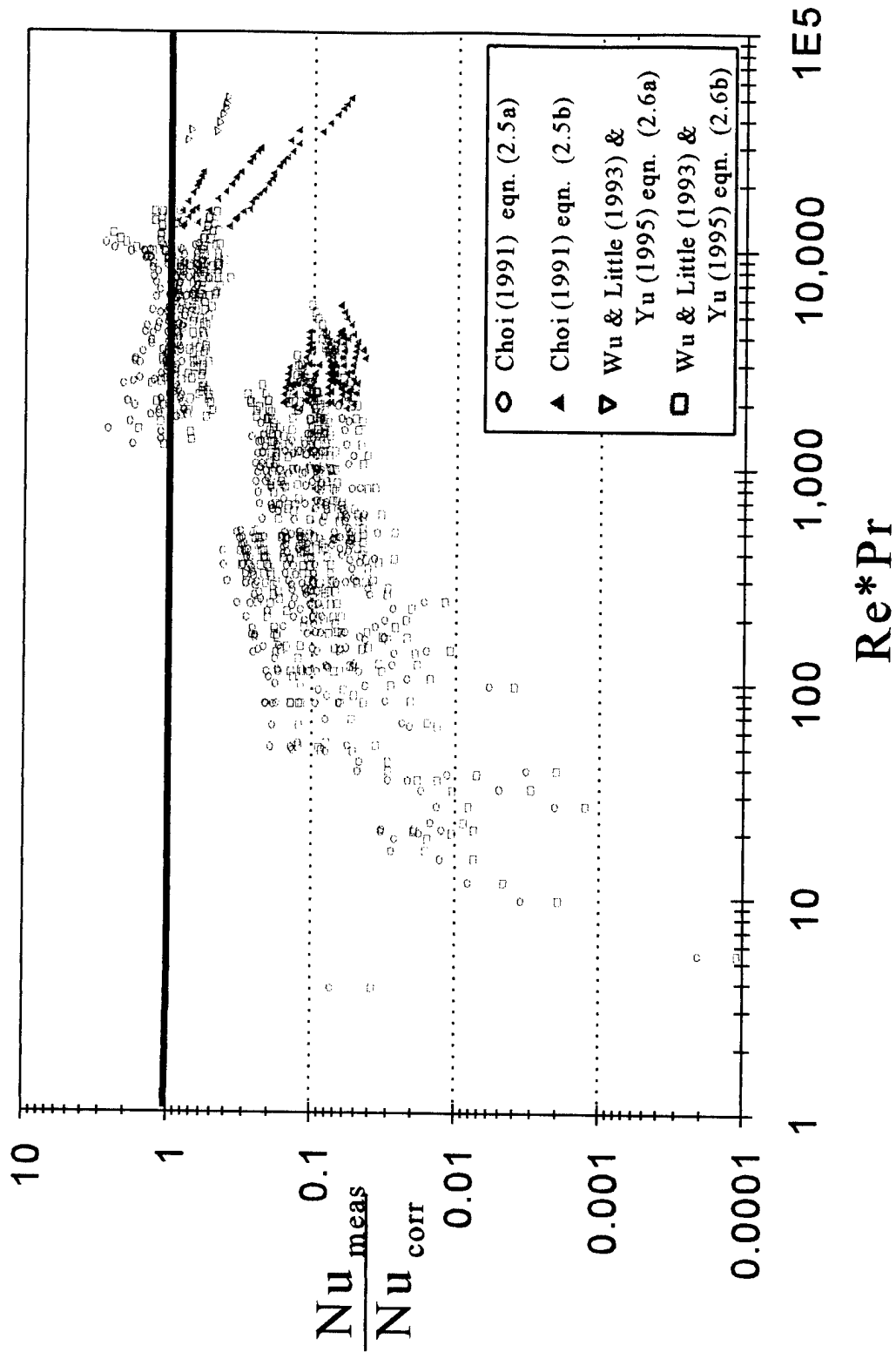


Figure 6.11: Comparison of Nusselt number data with correlations from Chapter 2.

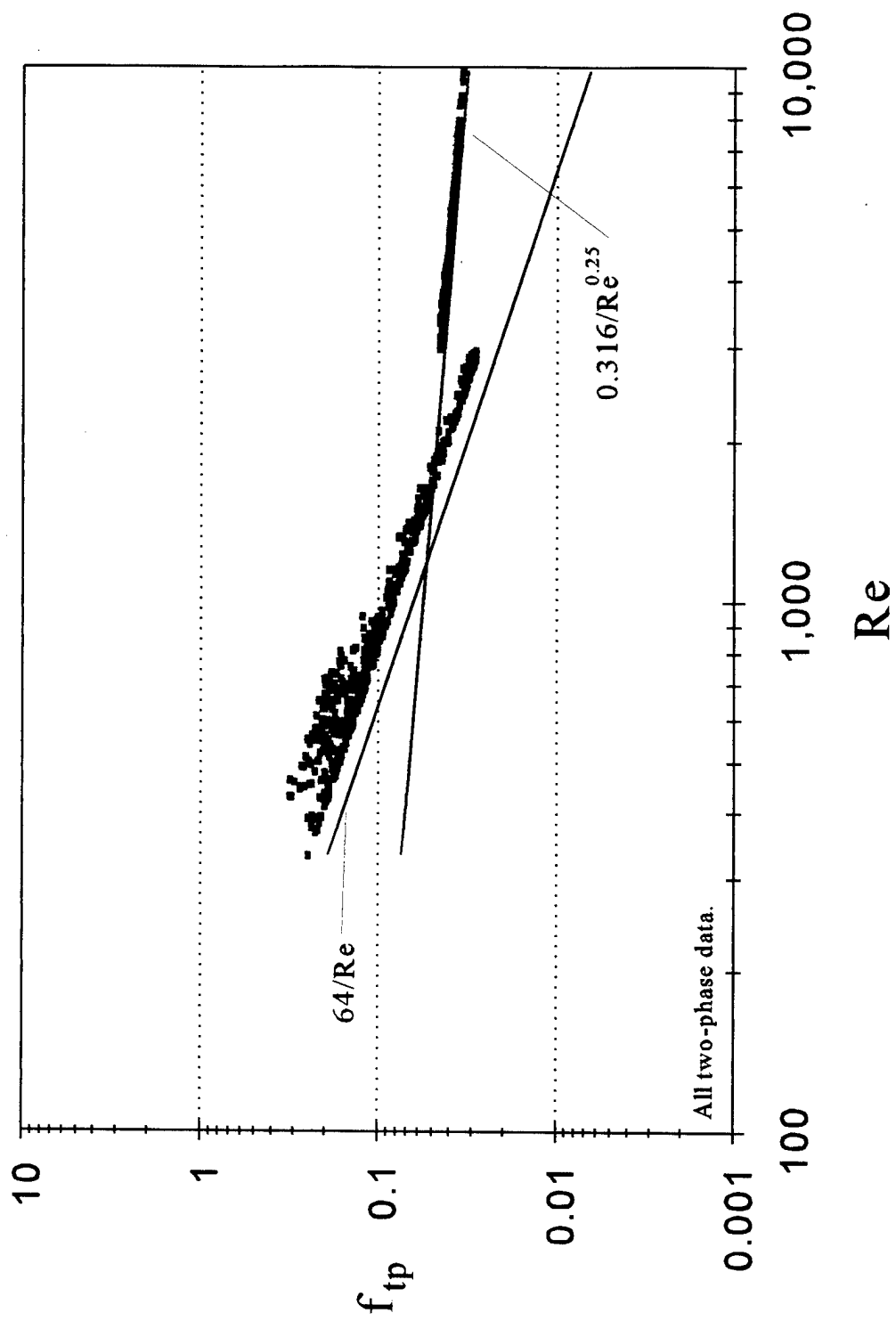


Figure 6.12: All two-phase friction factor data for all channel sizes.

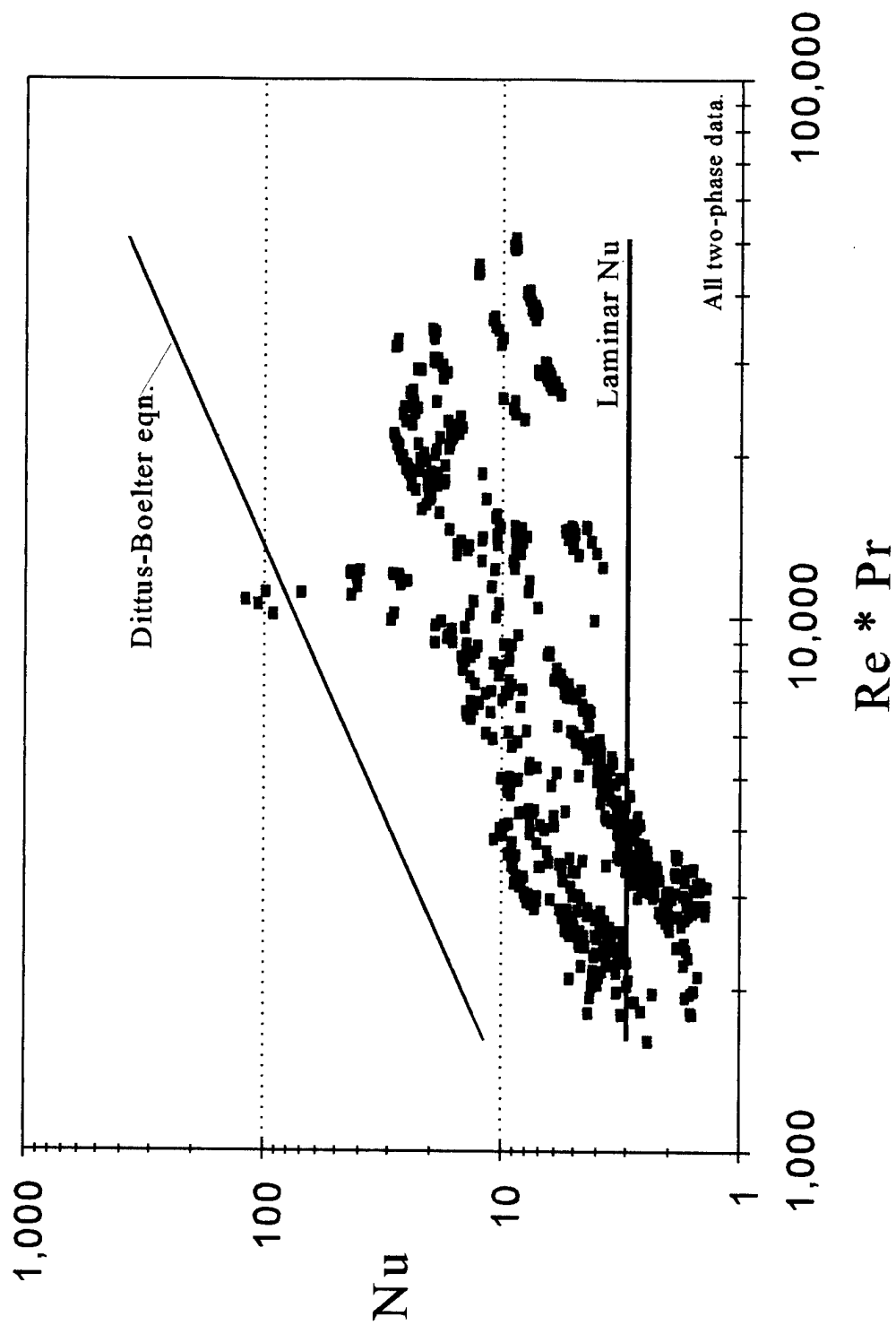


Figure 6.13: All two-phase Nusslet number data for all channel sizes.

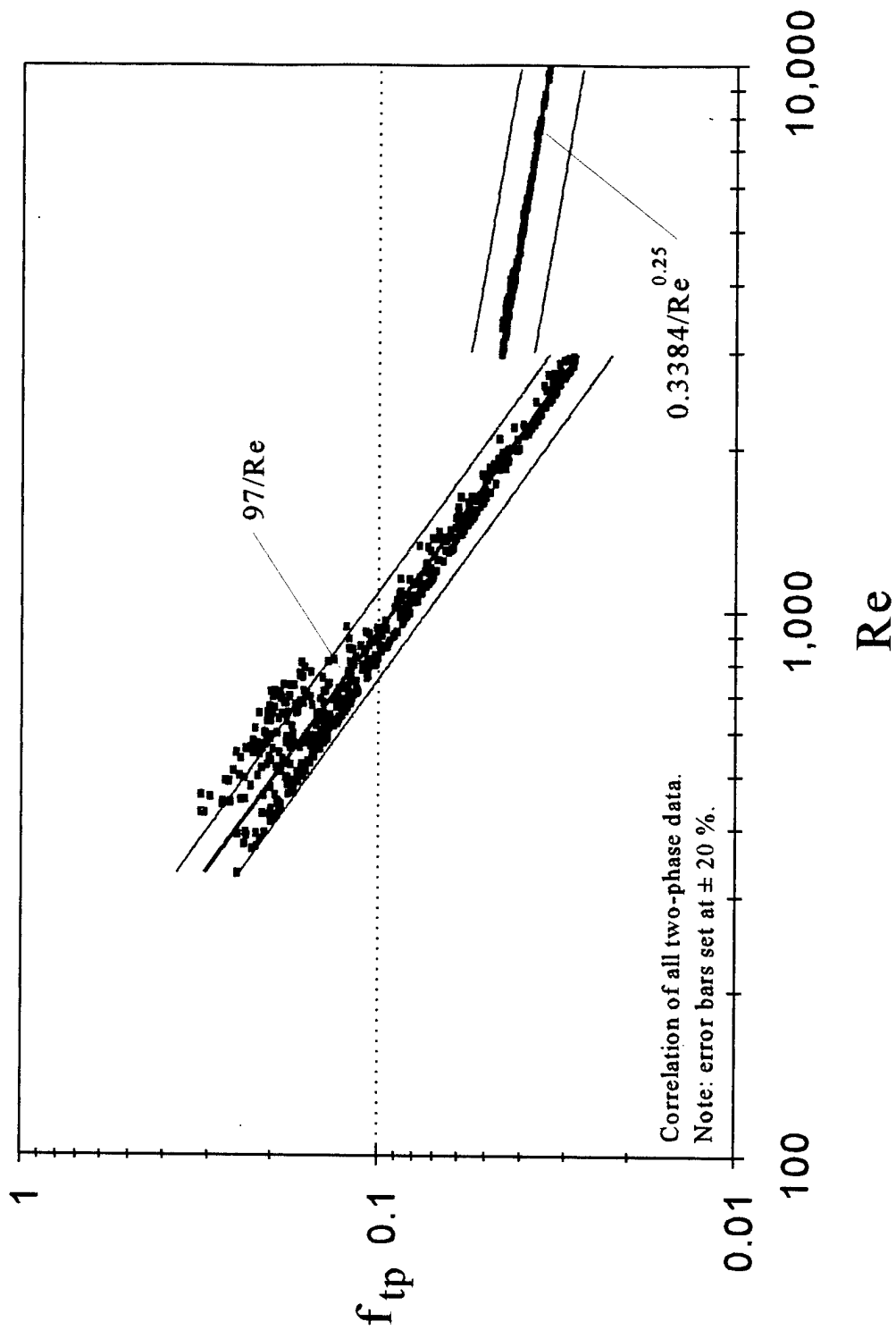


Figure 6.14: Correlation of all two-phase friction factor data for all channel sizes.

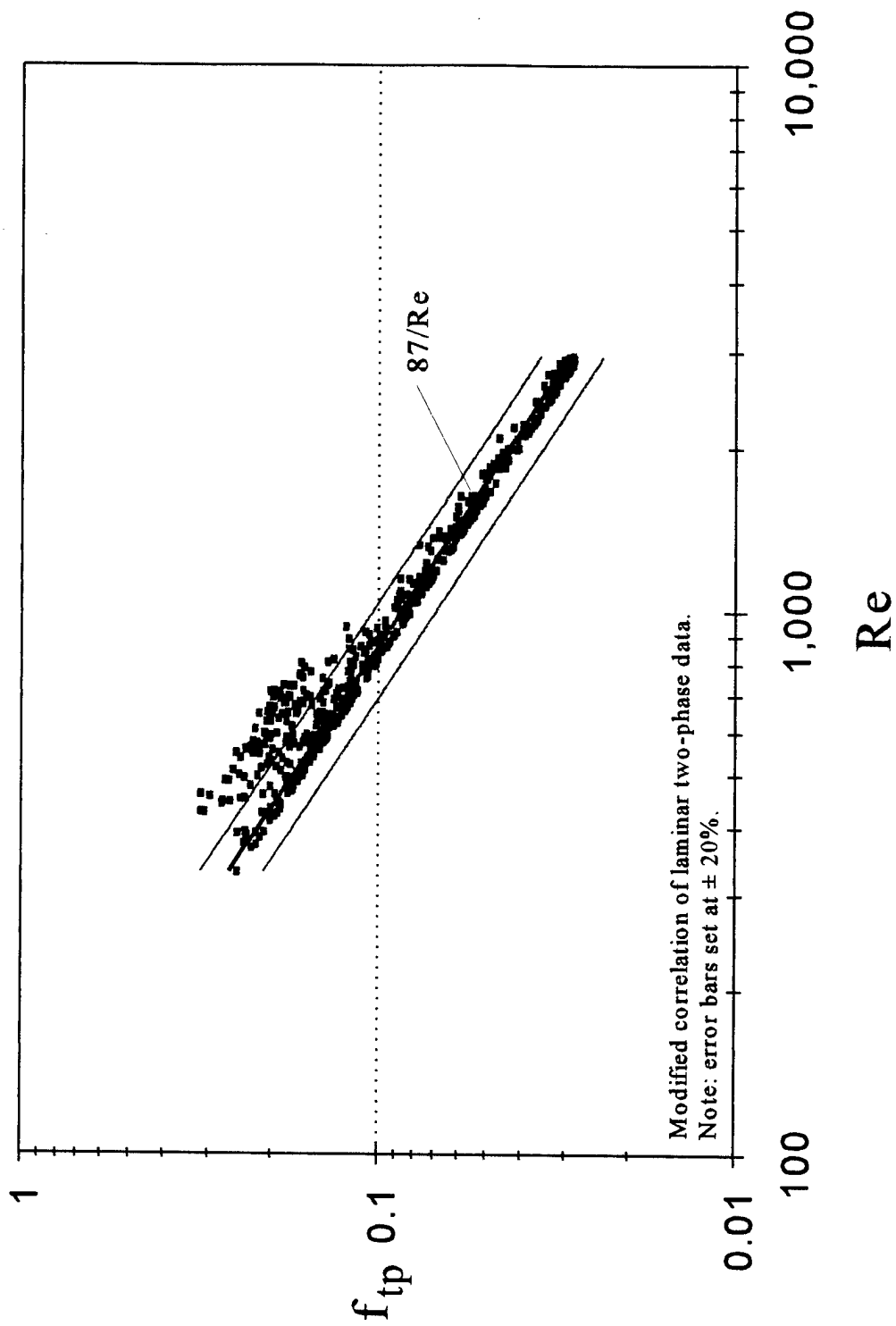


Figure 6.15: Modified correlation of laminar two-phase friction factor data for all channel sizes.



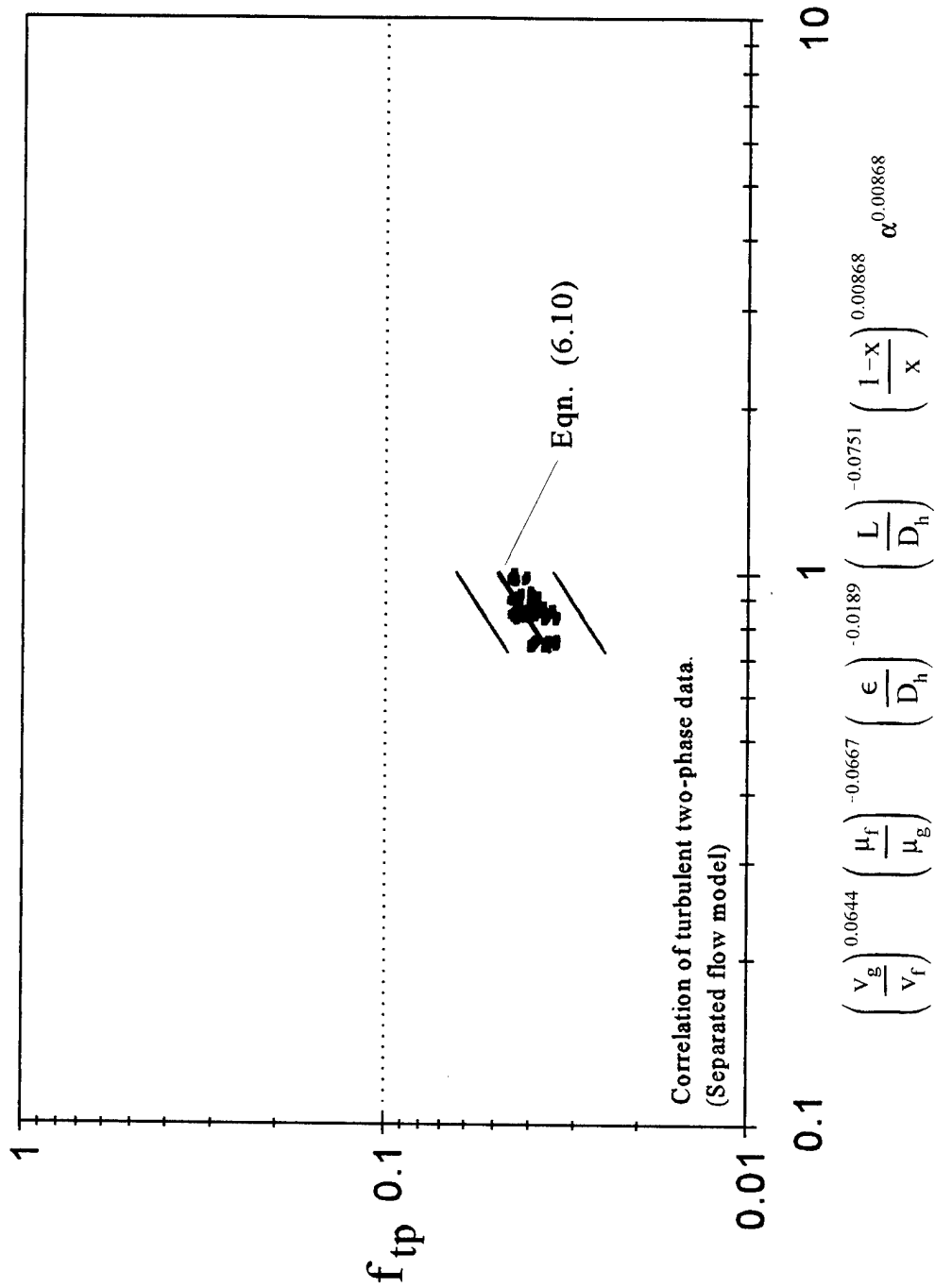


Figure 6.16: Correlation of turbulent two-phase friction factor data for all channel sizes using separated flow model parameters.

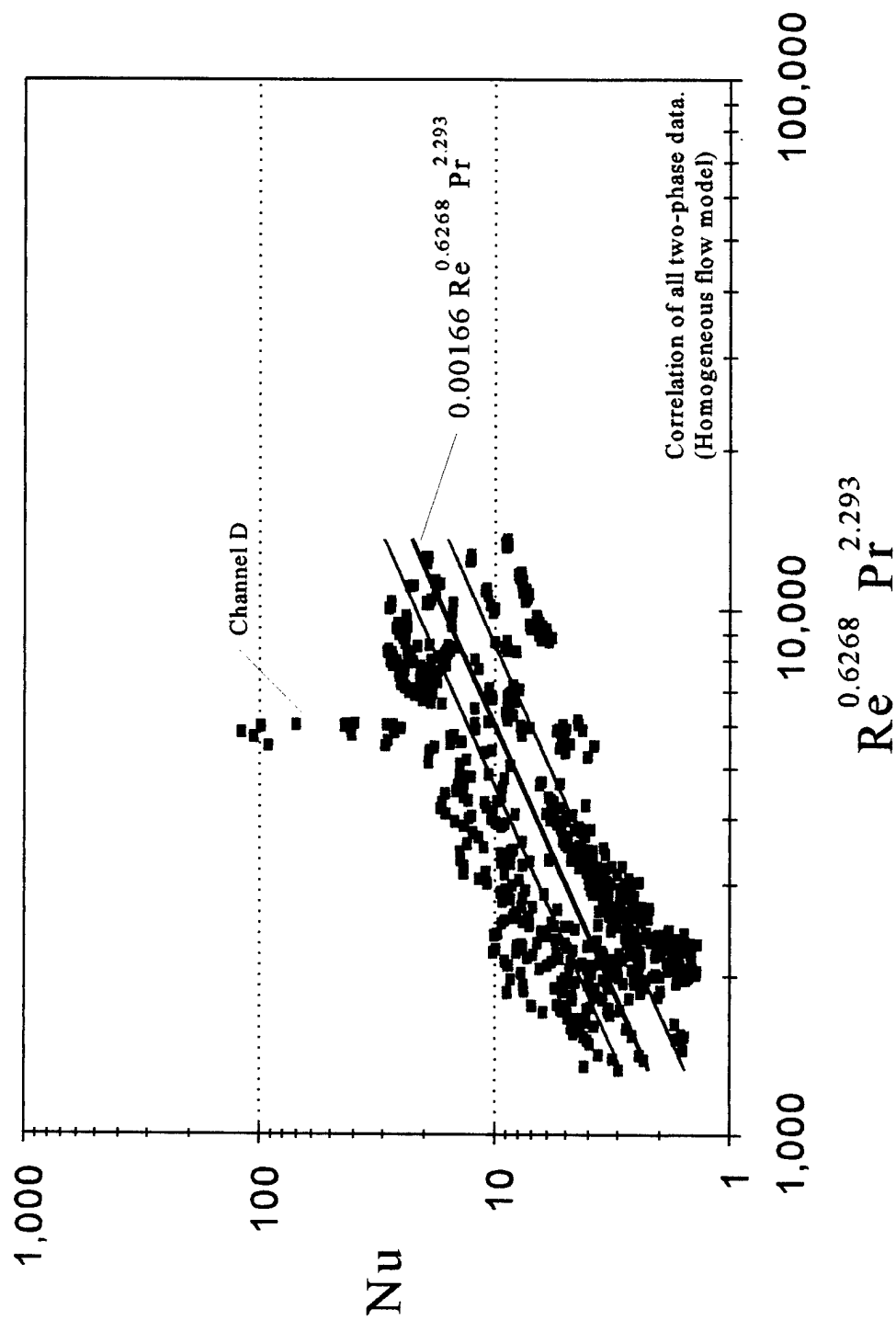


Figure 6.17: Correlation of two-phase Nusselt number data for all channel sizes using homogeneous flow model parameters.

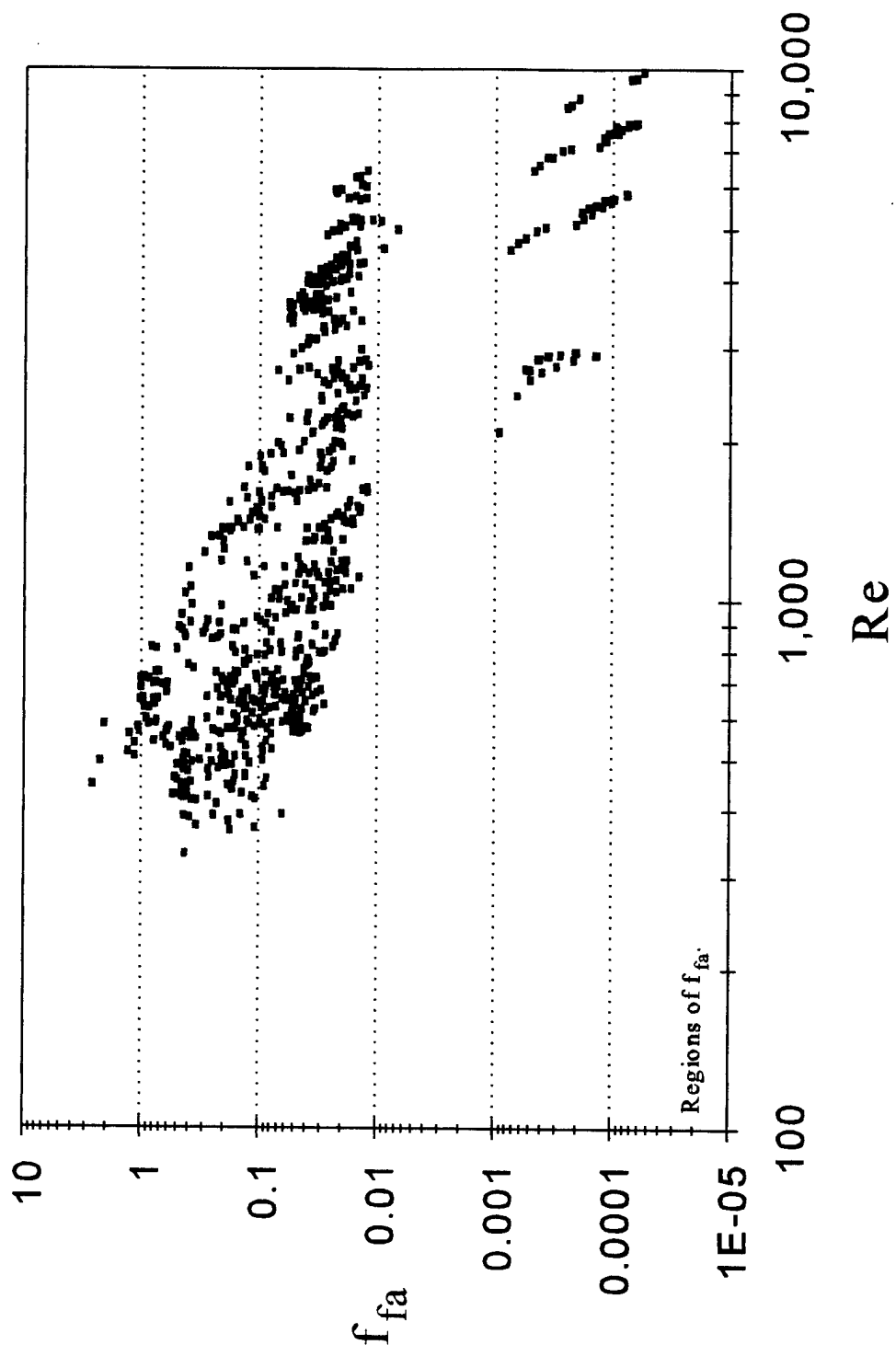


Figure 6.18: Regions of friction factor  $f_{fa}$  calculated by equation (6.12).

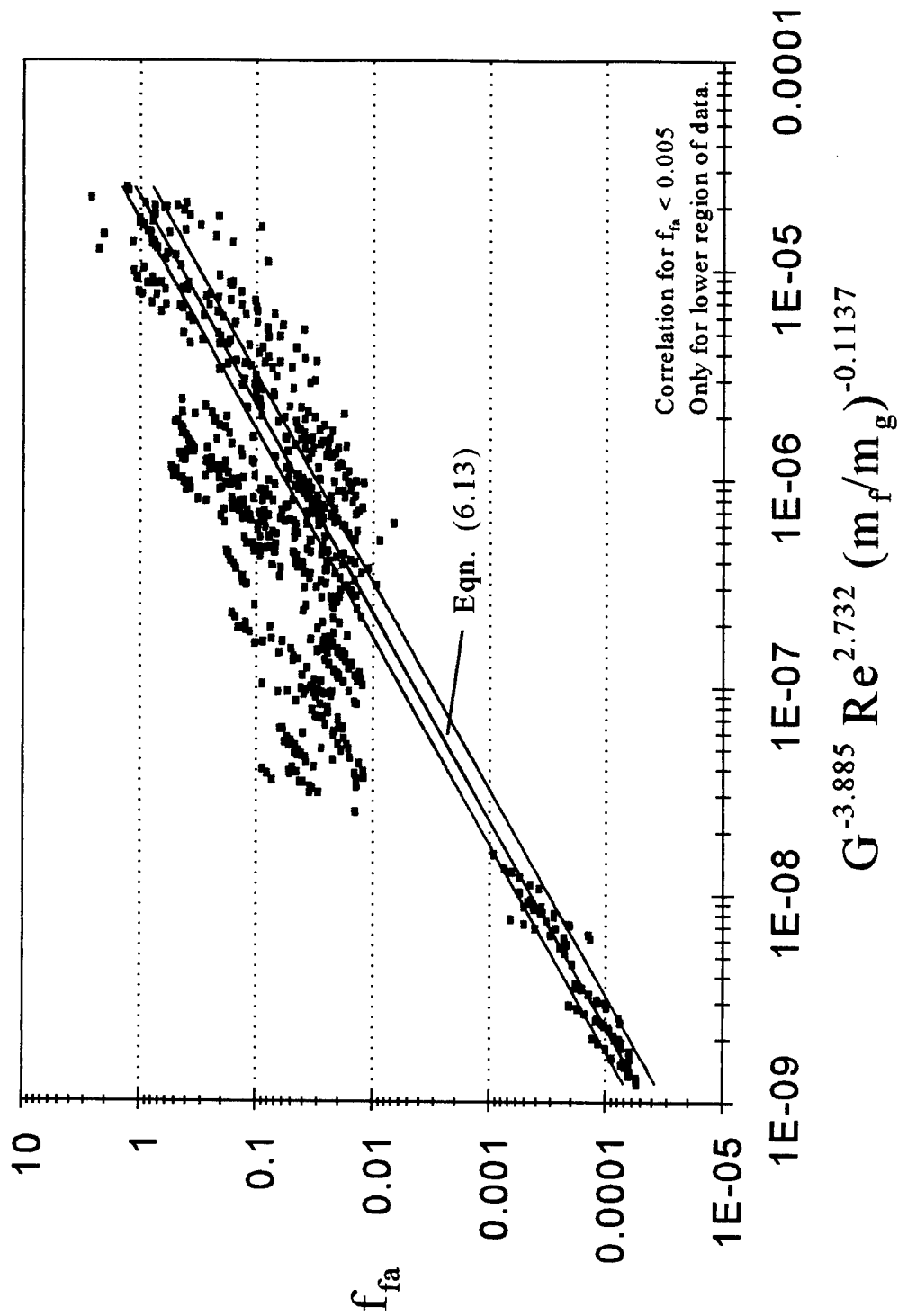


Figure 6.19: Correlation of  $f_{fa}$  data for  $f_{fa} < 0.005$ .

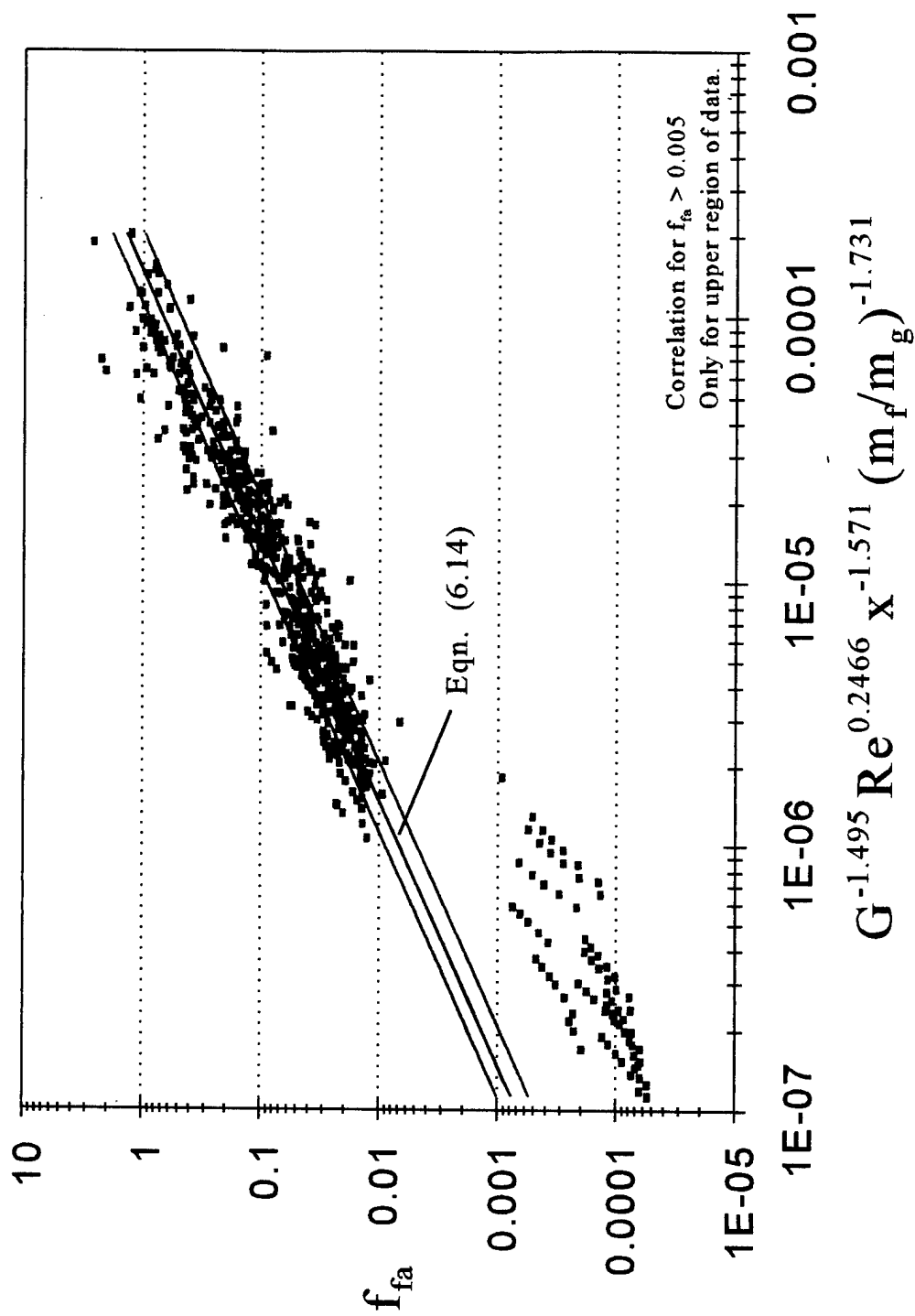
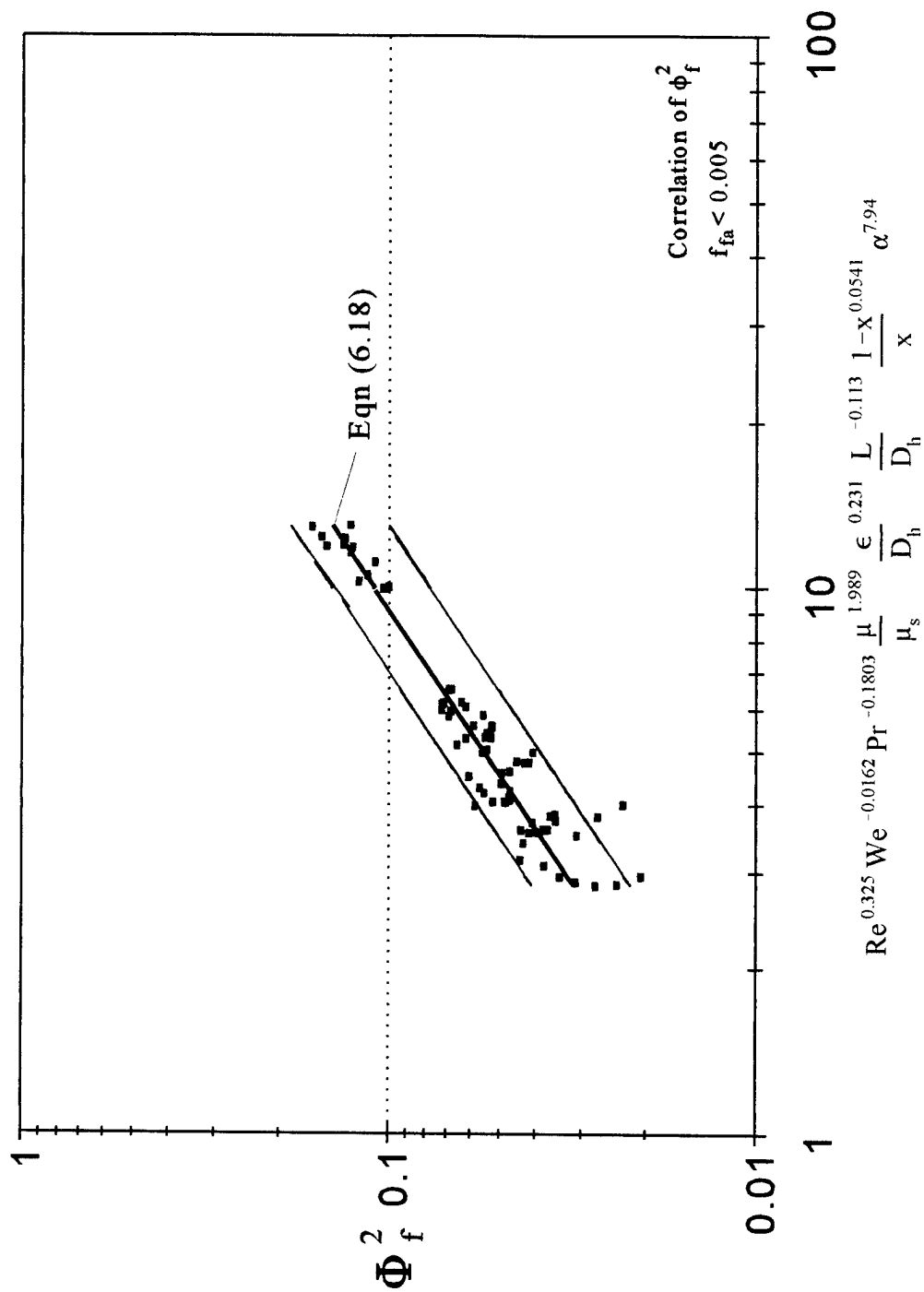
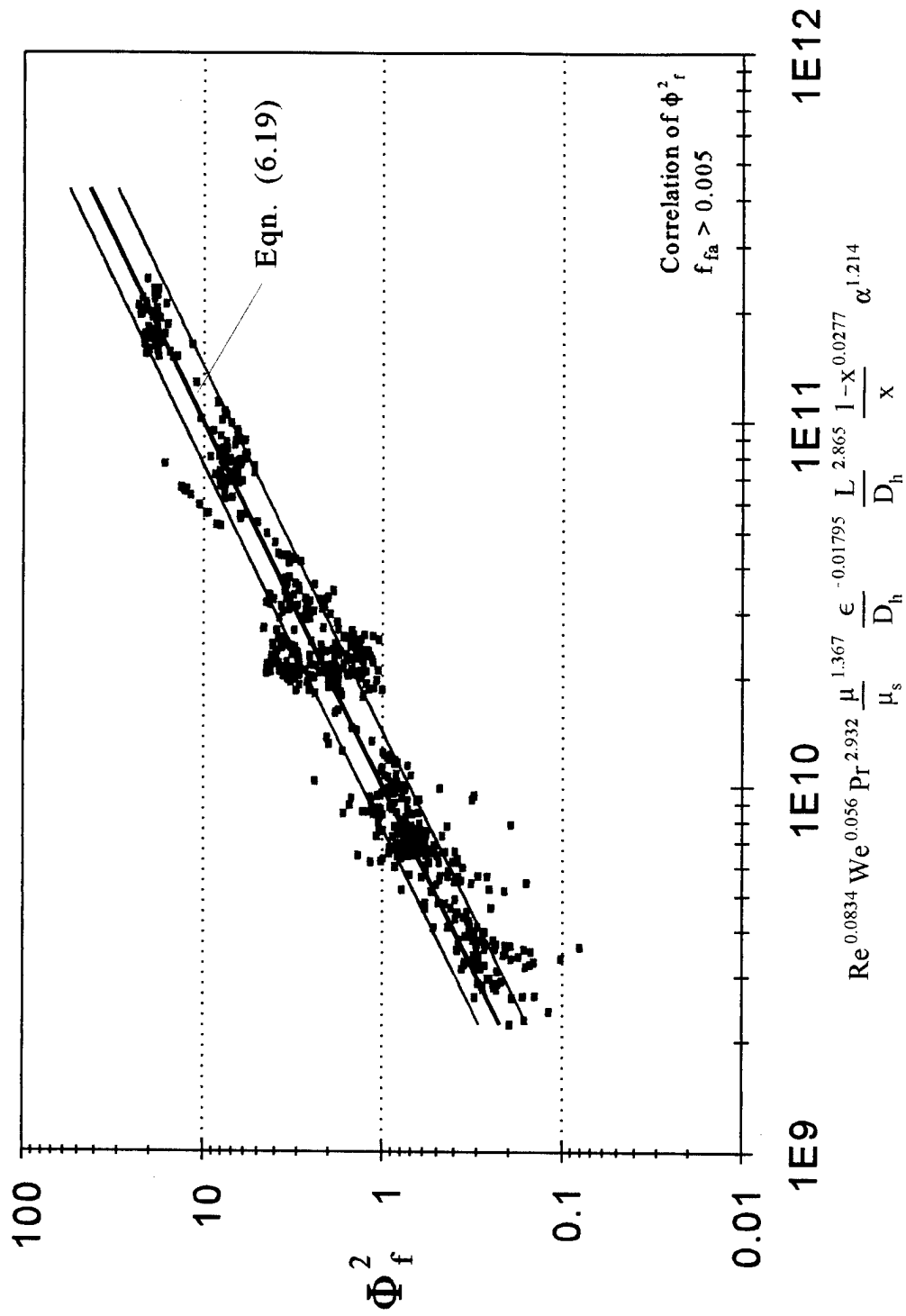


Figure 6.20: Correlation of  $f_{fa}$  data for  $f_{fa} > 0.005$ .

Figure 6.21: Correlation of  $\Phi_f^2$  over lower range of  $f_{fa}$ .

Figure 6.22: Correlation of  $\Phi_f^2$  over upper range of  $f_{fa}$ .

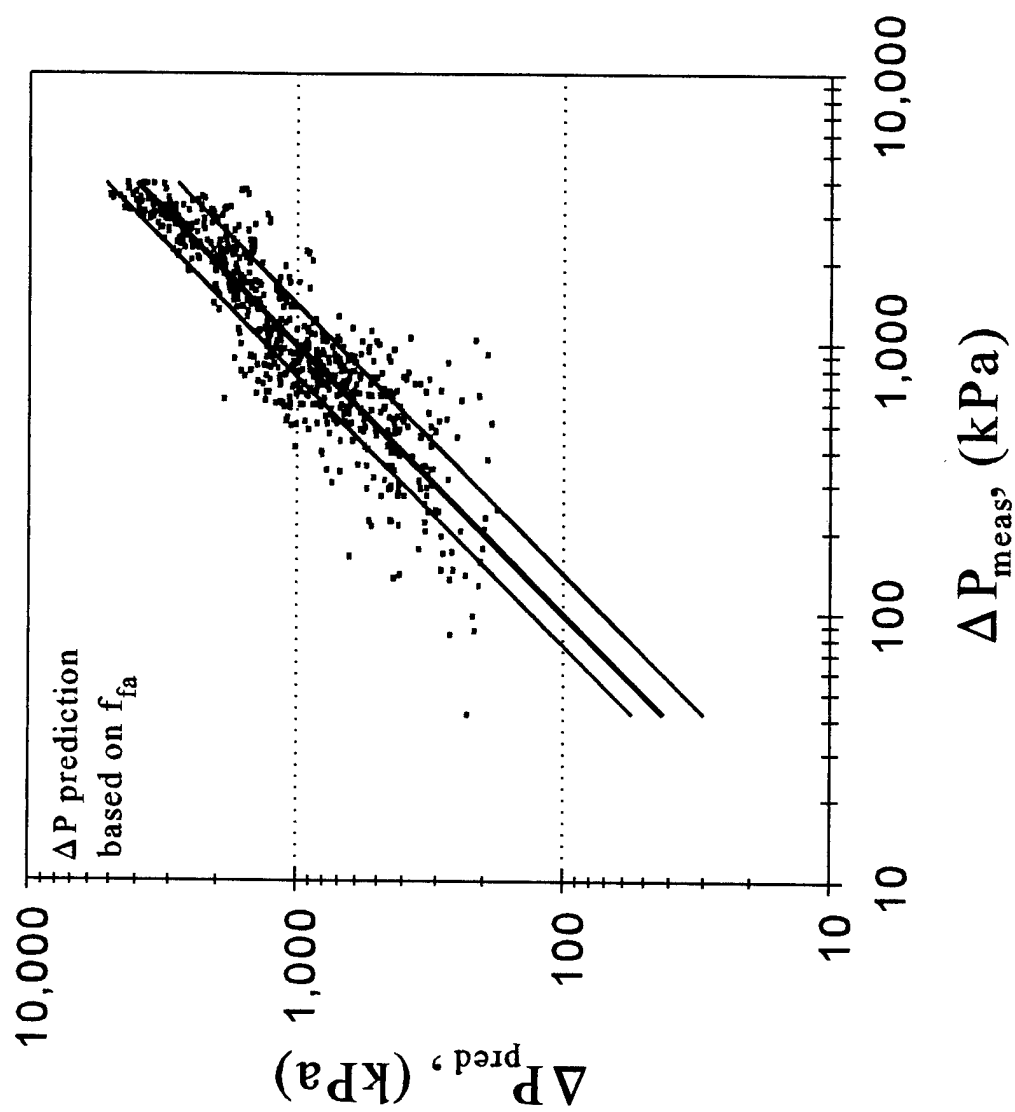


Figure 6.23: Pressure drop prediction based on  $f_{fa}$ .



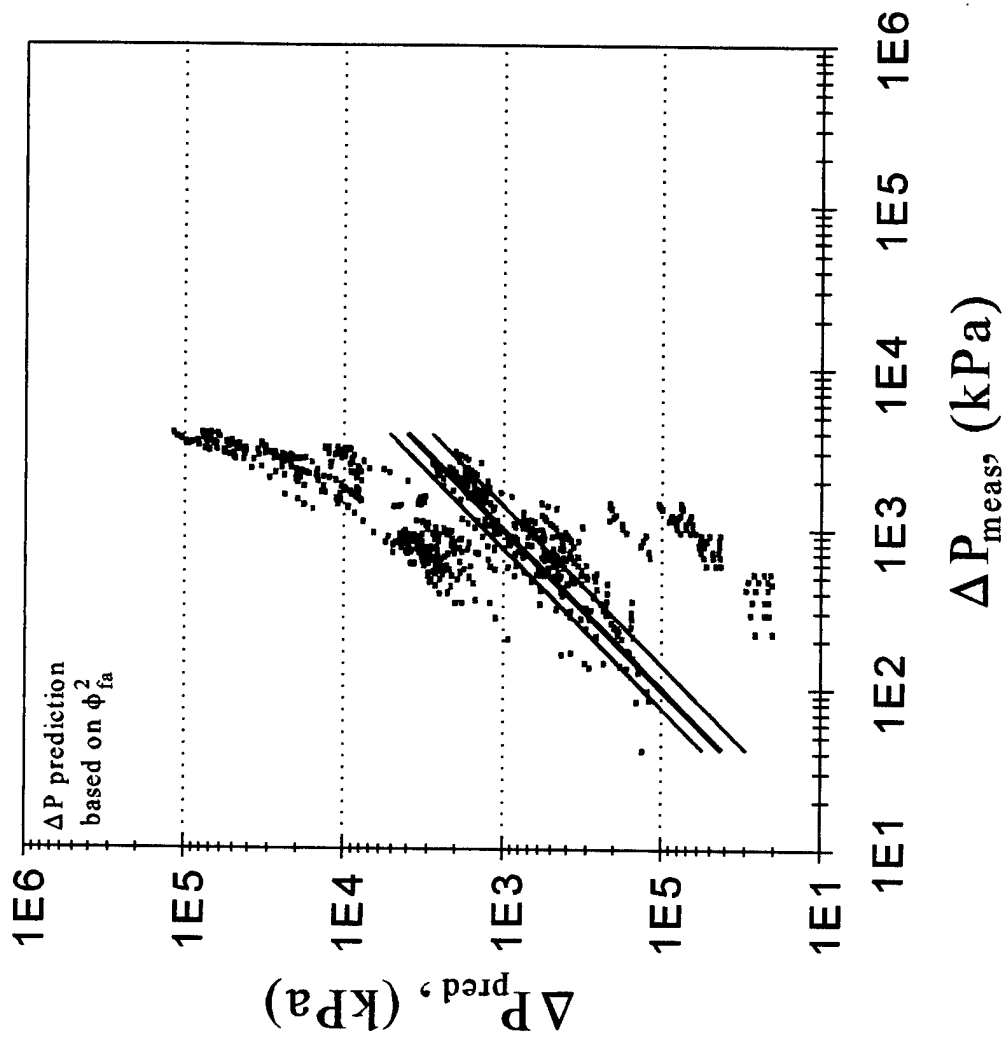


Figure 6.24: Pressure drop prediction based on  $\phi_f^2$ .

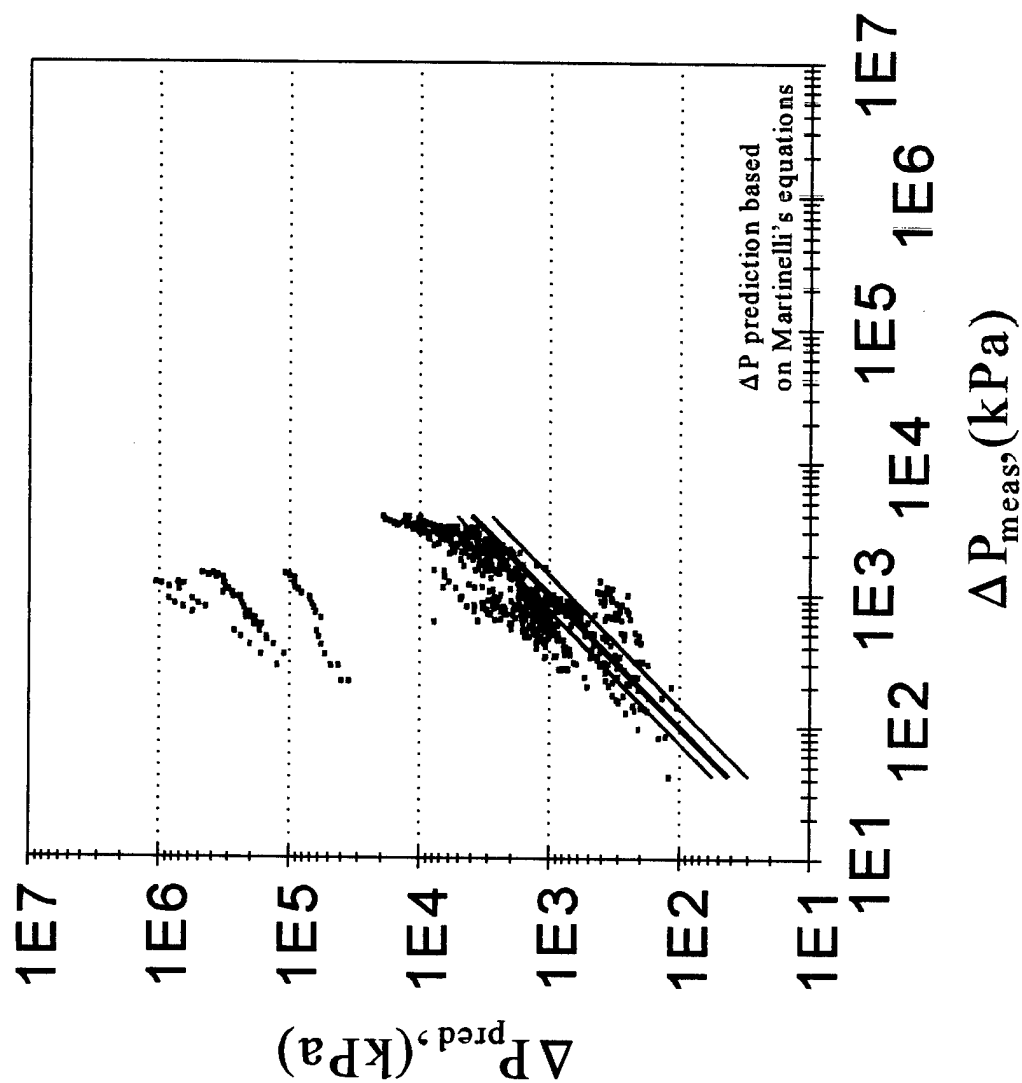


Figure 6.25: Pressure drop prediction based on Martinelli's equations.

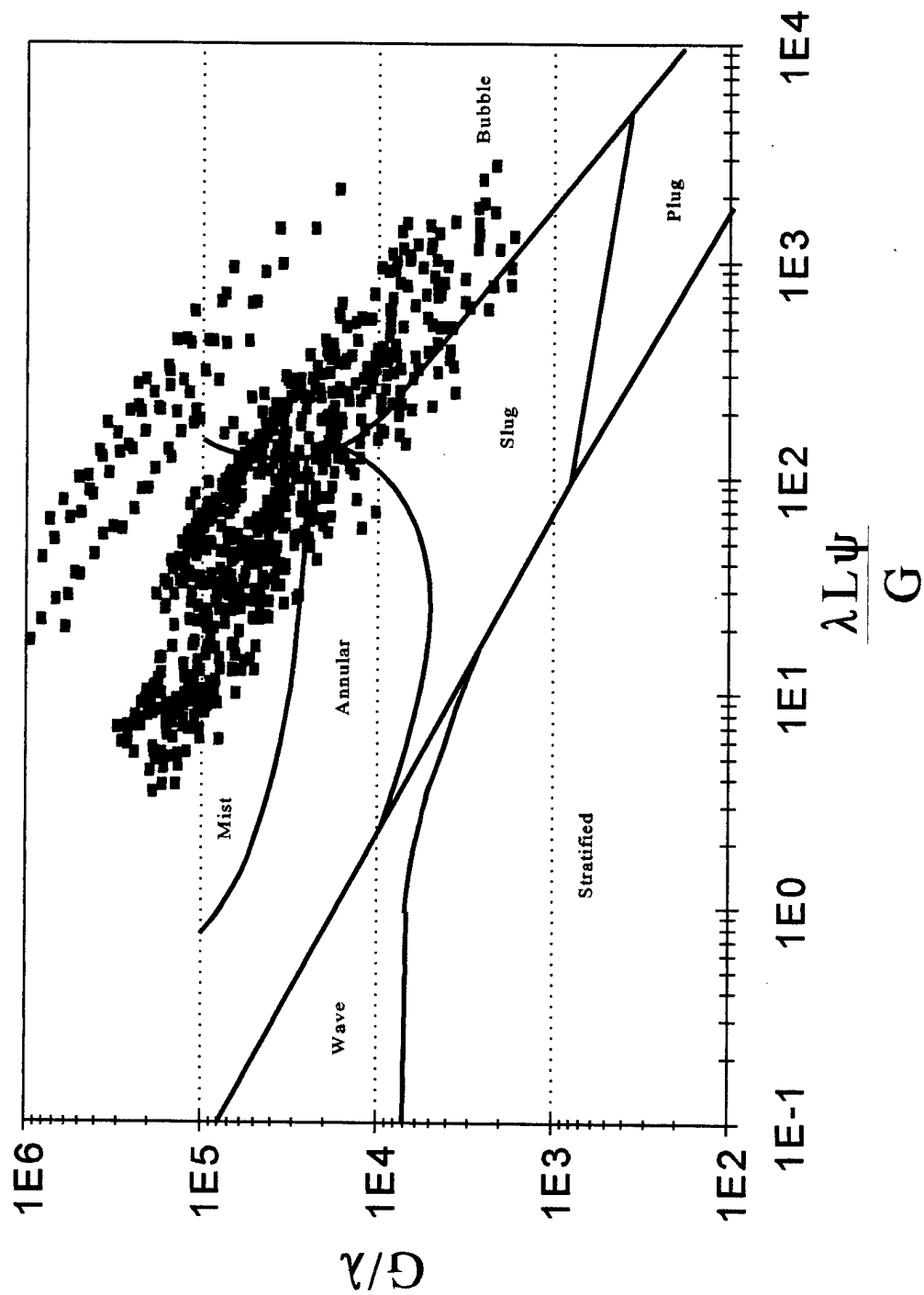


Figure 6.26: Flow regime map by Baker (1954) with two-phase data.

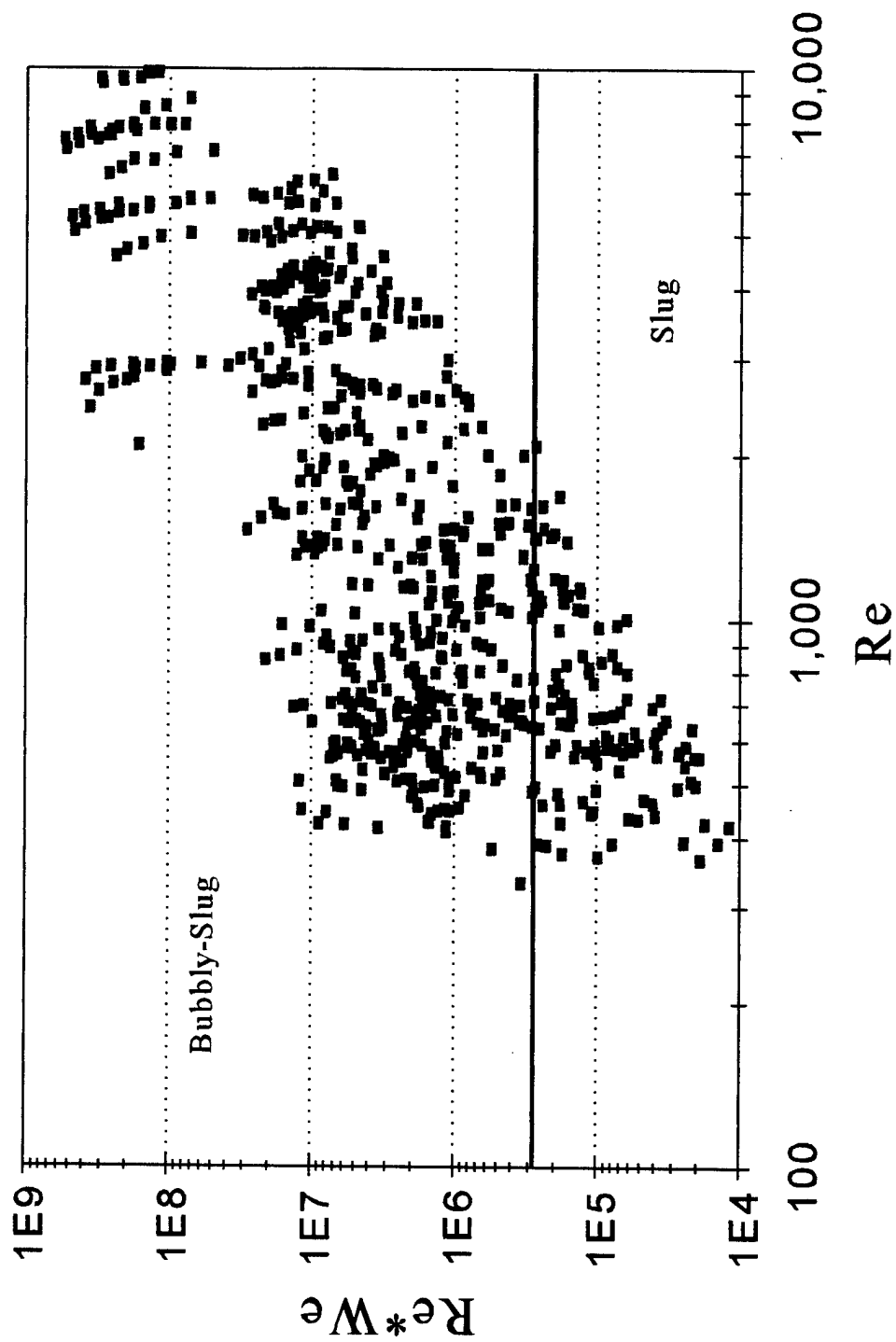


Figure 6.27: Flow regime map by Suo and Griffith (1964) with two-phase data.

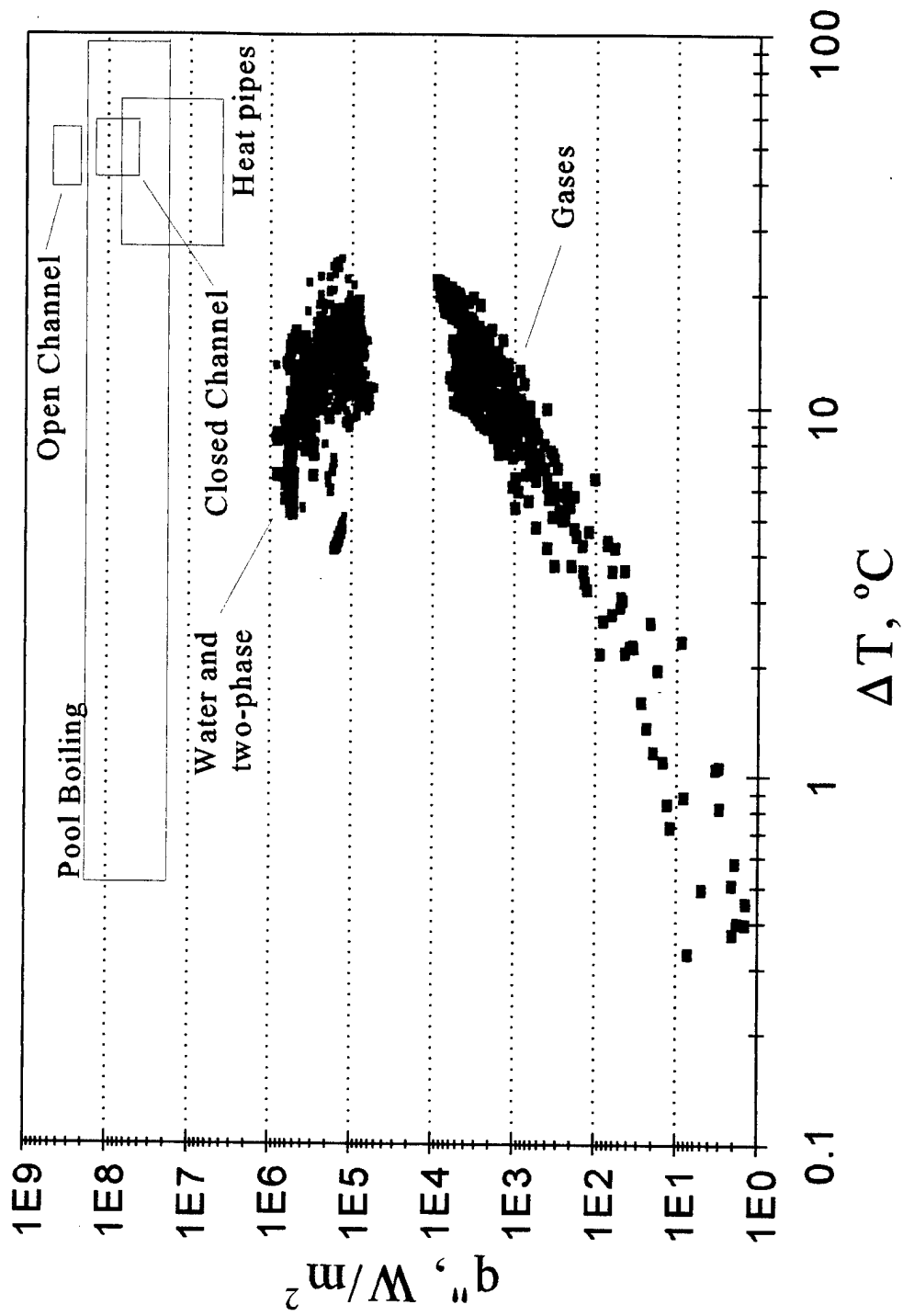


Figure 6.28: Heat flux comparisons with Figure 3.3.

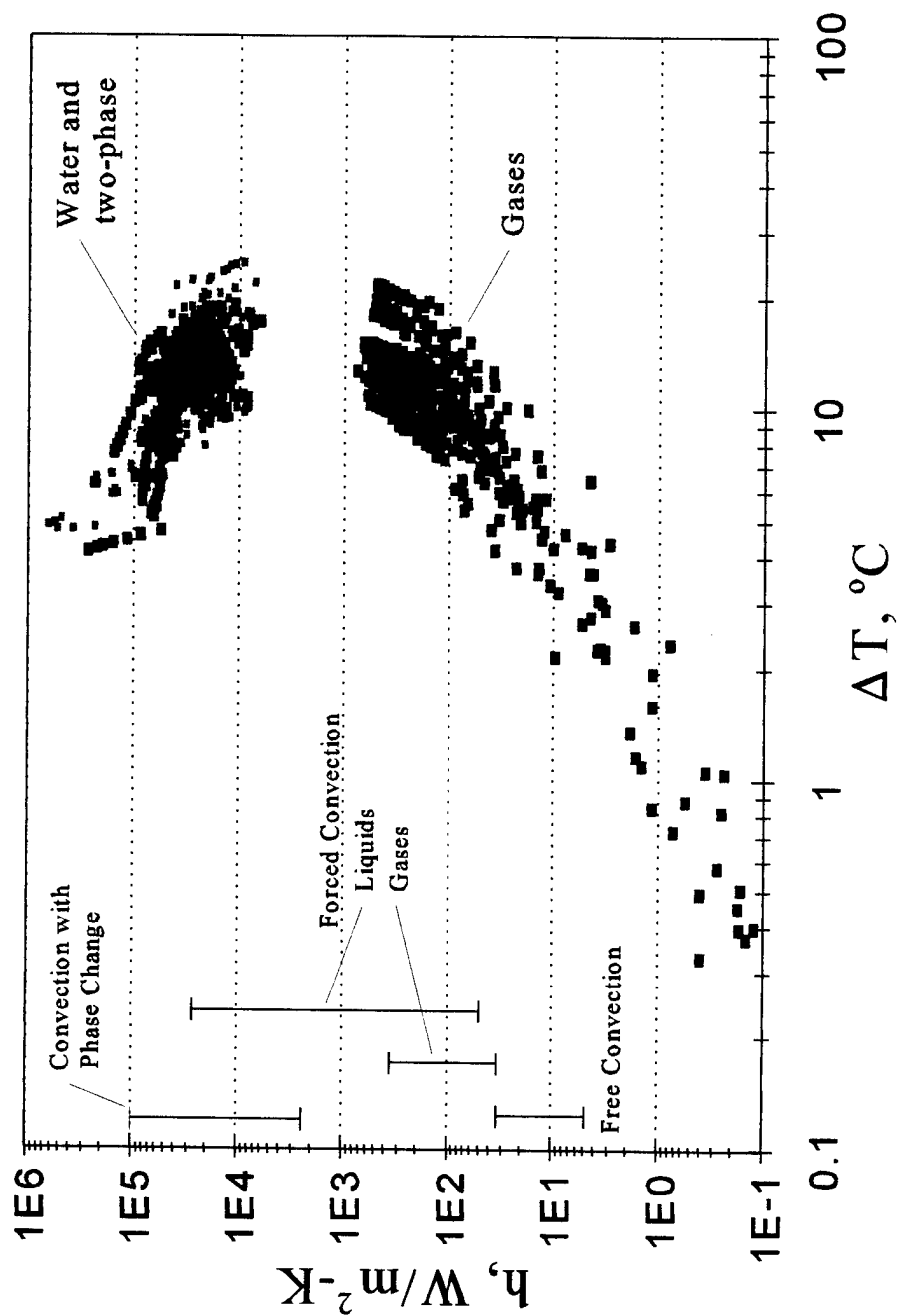


Figure 6.29: Heat transfer coefficient comparisons with typical values from Incropera and DeWitt (1985). Note: The temperature differences do not apply for the typical values.

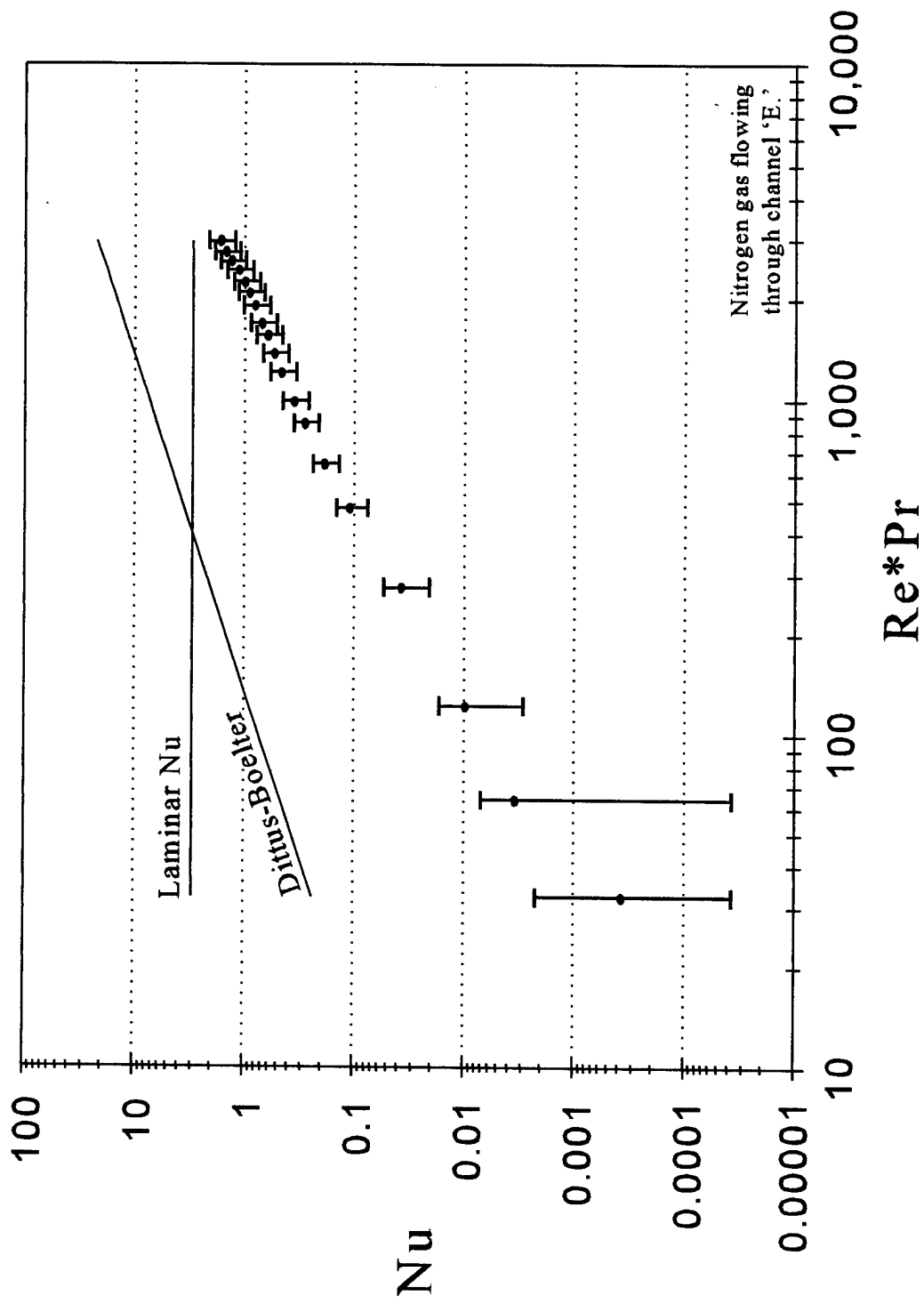


Figure 6.30: Typical Nusselt number uncertainty associated with gas flows.

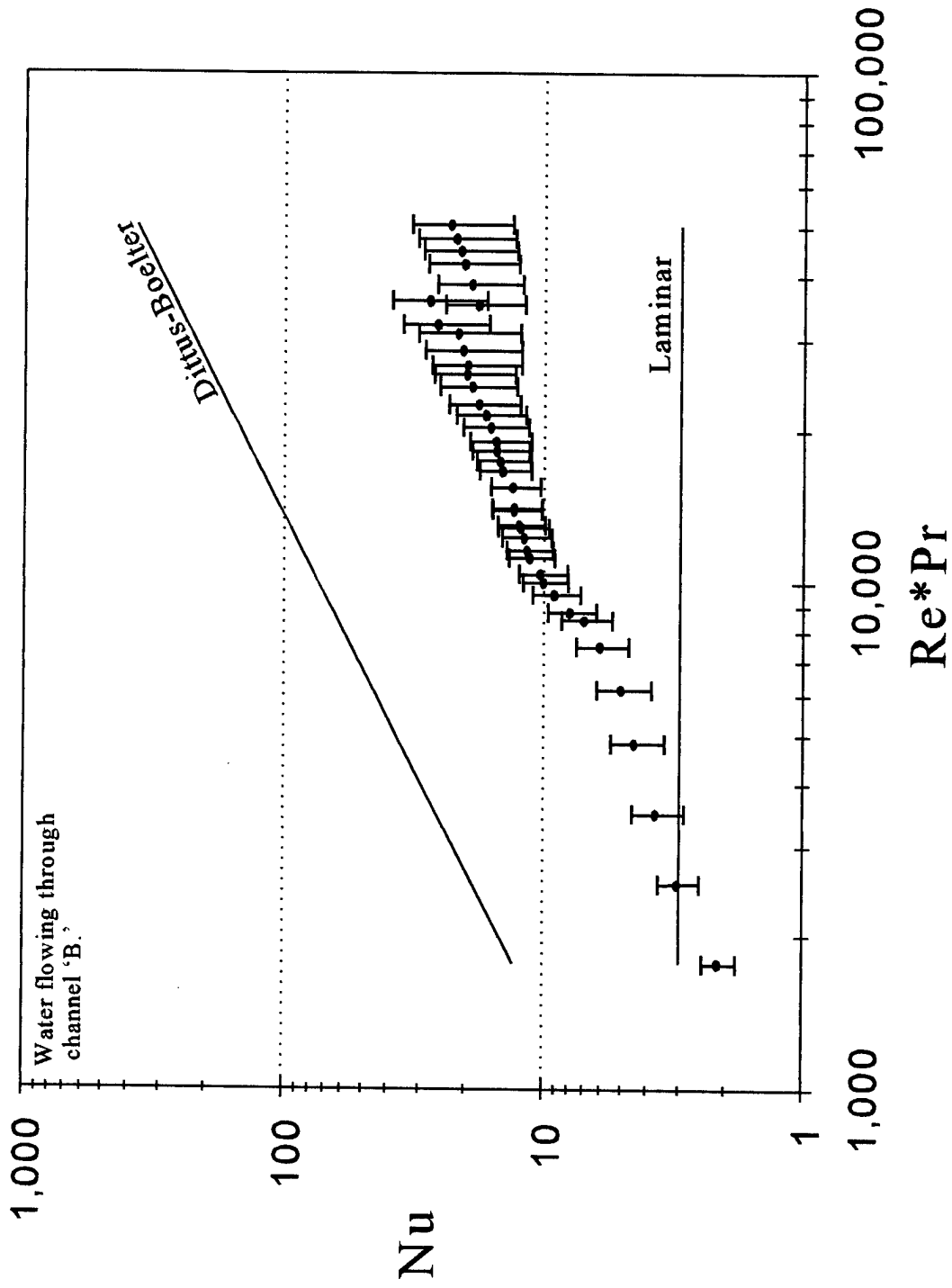


Figure 6.31: Typical Nusselt number uncertainty associated with water flows.



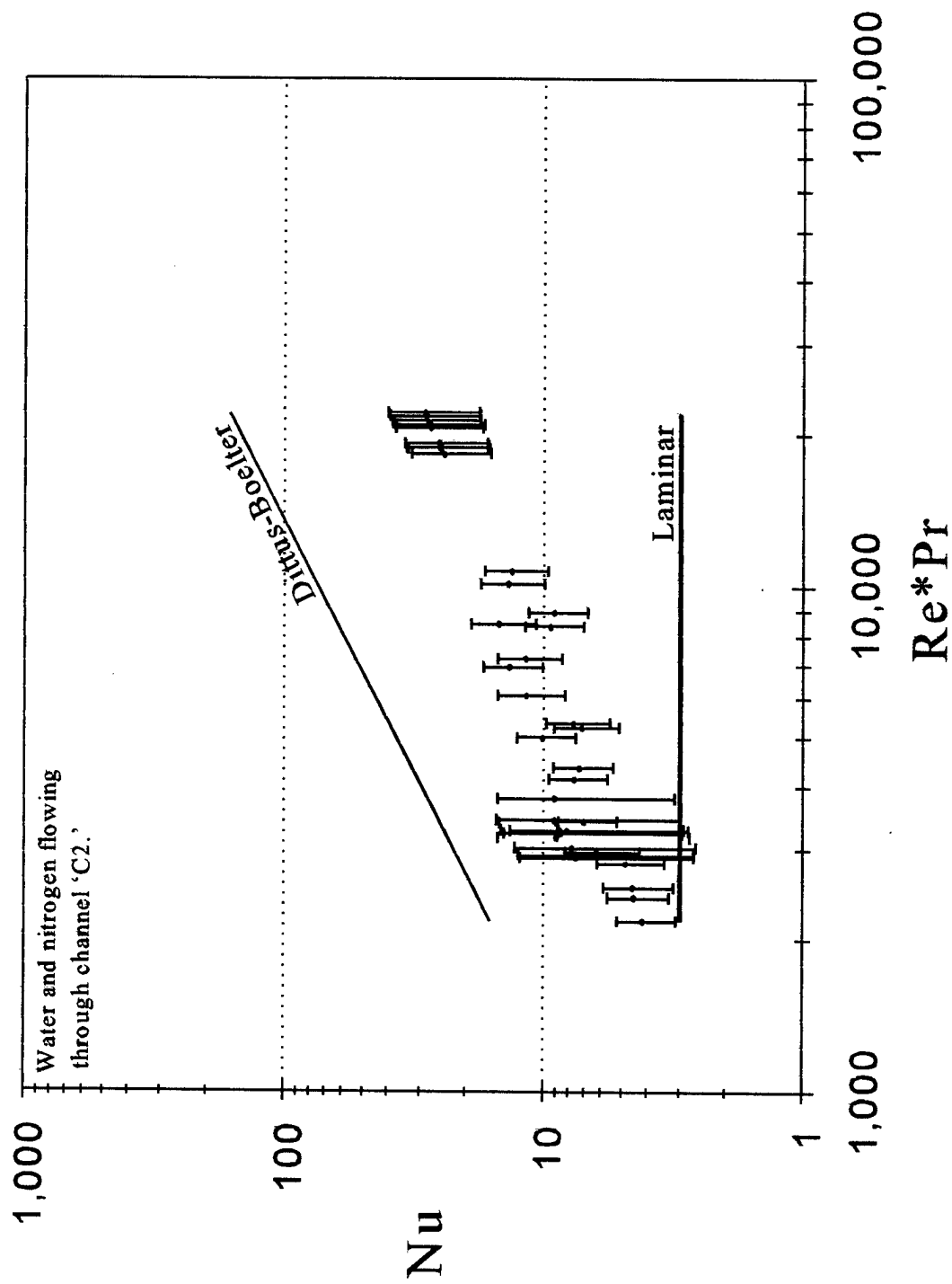


Figure 6.32: Typical Nusselt number uncertainty associated with two-phase flows.

## CHAPTER 7

### CONCLUSIONS AND RECOMMENDATIONS

#### Study Summary

The focus of the study was an empirical investigation of two-component two-phase flow being heated. Because of the dependence of existing two-phase relationships on single-phase equations, single-phase tests were also conducted. A dimensional analysis was used to determine the important pressure drop and heat transfer parameters. The resulting parameters were curve-fit against experimental data using multiple linear regression techniques. A FORTRAN program was developed to compute all of the necessary parameter coefficients. Governing equations based on the Conservation of Mass, Momentum, and Energy were considered for two flow models. The first of the flow models was the homogeneous flow model which consider the fluid properties to be averages based on the quality of the two components. Second, was the separated flow model which considered each component of the flow separately. Because neither of the flow models for pressure drop could be solved directly, they were solved empirically with the techniques mentioned above. Also, the flow regimes in macroscale and microscale two-phase flow were defined and discussed. Correlations of the single- and two-phase experimental data were presented and compared with other correlations and equations.

The flow experiments were conducted on an apparatus built by the author and Darin Bailey (1996). The hydraulic diameter of the microchannels tested varied from  $50\mu\text{m}$  to  $250\mu\text{m}$ . Most of the channels had an aspect ratio of approximately one, but several different aspect ratios were tested. Glass covers were used on the microchannels to allow flow visualization during the experiments. However, no available camera was found to be fast enough to provide any useful information. For the two-phase experiments, deionized water along with either argon, helium, or nitrogen were tested. Single-phase tests were conducted using the same four fluids separately. During the tests a data acquisition system was employed in the monitoring and storage of the flow information.

For both single- and two-phase tests, the Reynolds number was found to be the most important parameter in determining the friction factor. Considering heat transfer, the combination of Reynolds number and Prandtl were found to be the dominant parameters. These results are as were expected from macroscale theory. Other parameters also indicated the presence of entrance effects, particularly in the larger channels. However, what was found to be most interesting about the experimental results was not which flow parameters were important, but how the fluids behaved in microchannels. In single-phase flow, the transition from laminar to turbulence regimes was seen to be suppressed in certain situations. For gas flows, the suppression the did not occur above a hydraulic diameter of  $150\mu\text{m}$ . Between  $150\mu\text{m}$  and  $80\mu\text{m}$ , the suppression was seen in varying degrees. Below  $80\mu\text{m}$  the suppression seemed complete and no transition was seen. For

the water, no transition was seen even for the largest channels tested. These results indicate that the presence of laminar to turbulent transition is dependent on the fluid properties as well as the channel dimensions. A study of microscale turbulent eddy formation should help clarify these observations. For two-phase flow, a clear and well defined transition was seen for all channel sizes at a Reynolds number of 3,000. It is believed that the transition is caused by the intense pressure fluctuations associated with two-phase flows. Though some suppression tendencies may be present at the smaller channel sizes, the turbulence induced by the pressure fluctuations of two-phase flow is more than enough to ensure transition. It will be interesting to see in future research if two-phase flow sees any suppression tendencies in much smaller channels

The friction factor correlations developed for both single- and two-phase flows were seen to be in excellent agreement with the various flow situations considered. The analytical two-phase pressure drop models yielded mixed results. Pressure predictions based on the total flow assumed to be all liquid, gave reasonable results over the pressure ranges seen in the two-phase tests. However, pressure prediction based on the separated flow model were seen to give very poor result, particularly for the high pressure drops present in these tests.

Nusselt number data yielded very few reasonable correlations for either single- or two-phase data. The only Nusselt number correlation found to be useful was the correlation for gases only. All other combination of fluids could not be correlated well. Most of the problems associated with correlating the Nusselt number were traced back to

the inaccuracies associated with the thermocouple measurement. However, correlating the various fluid combinations did indicate several things. One, no transition from laminar to turbulent Nusselt values was seen. Two, opposite to the friction factor, the fluids paralleled the Nusselt predictions of turbulent flow correlations which is in agreement with the work of Choi (1991). Finally, the Reynolds number and the Prandtl number are the dominant flow parameters in closed channel forced convection heat transfer.

#### Recommendations for Future Research

Though this study may have helped understand the behavior of single and two-phase fluids in microchannels, much more research is needed in this area. In particular, studies of single- and two-phase flow using localized pressure and temperature measurements. On this scale, the only way to make sure that the inlet pressure, for example, is being accurately measured, is to have the pressure instrument in or very near the channel entrance. Temperature measurements are even more critical. As was seen in this study, the inaccuracies in the thermocouples themselves some times accounted for measurement uncertainties of well over 200%. The increasing number of fabrication techniques being used and developed today will allow localized instrumentation to become common place over the next few years. Along with the increasing need for heat dissipation from electronic components, micro refrigeration cycles, and other microfluidic devices, the need for basic research in the micro thermal fluids area will continue to have far reaching implication for all areas of micro technologies.

## APPENDIX A

# APPENDIX A: FORTRAN program to solve for correlation coefficients.

```

C Program to calculate empirical coefficients from experimental values.
C Program Name: 2-PHS-2.FOR
C By: Roger S. Stanley
C Written: 9/30/96; Modified: 10/18/96
C
C
C Define double precision variables, integers N and M, and dimension arrays
  INTEGER N, M, L2, L3, L4, L5, L6, L7, L8, L9, NC
  DIMENSION YMDATA(800), YC(800), X(800,11), XDATA(800,11)
  DIMENSION M1(11,11), A(11)
  DOUBLE PRECISION YMDATA, YC, X, A, YMEAN, XDATA, ST, SR, R
  DOUBLE PRECISION M1, SIGMAXY, SIGMAY
C
C N are the number of data points for the specified file.
C M are the number of coefficients to be found (order of multiple regression).
C Value of M should not exceed 10.
C
  N = 678
  M = 7
C
C Open input and output data files.
C
  OPEN (UNIT=1,FILE='c:\disert\correla\dph2-3.txt')
  OPEN (UNIT=2,FILE='c:\disert\correla\dph2-3.dat')
C
C Read in entire data file
C
  DO 10 I = 1,N
10  READ(1,*) YMDATA(I),(XDATA(I,J),J=2,M)
C
C Take natural log of X-values and YM-values (Entire data file.).
C
  DO 20 I=1,N
    YMDATA(I) = LOG(YMDATA(I))
  DO 30 J=2,M
    XDATA(I,J) = LOG(XDATA(I,J))
30  CONTINUE
20  CONTINUE
C
C Start coefficient selection here.

```

APPENDIX A: FORTRAN program to solve for correlation coefficients (continued).

C Set NC (number of coefficients. currently being solved for) equal to 2.

C

NC = 2

C

C The following loops find all unique combinations of coefficients.

C

C Two Coefficients:

C

IF (M.LT.2) THEN

GOTO 999

ENDIF

L2 = 2

200 IF (L2.GT.M) THEN

GOTO 310

ENDIF

DO 210 I=1,N

210 X(I,2) = XDATA(I,L2)

GOTO 998

C

C Three Coefficients

C

310 NC = 3

IF (M.LT.3) THEN

GOTO 999

ENDIF

L3 = 2

320 L2 = L3+1

300 IF (L3.GT.M) THEN

GOTO 410

ENDIF

IF (L2.GT.M) THEN

L3 = L3 + 1

GOTO 320

ENDIF

DO 330 I=1,N

X(I,2) = XDATA(I,L3)

330 X(I,3) = XDATA(I,L2)

GOTO 998

C

C Four Coefficients



APPENDIX A: FORTRAN program to solve for correlation coefficients (continued).

C

```

410 NC = 4
    IF (M.LT.4) THEN
        GOTO 999
    ENDIF
    L4 = 2
420 L3 = L4+1
430 L2 = L3 +1
400 IF (L4.GT.M) THEN
        GOTO 510
    ENDIF
    IF (L3.GT.M) THEN
        L4 = L4 + 1
        GOTO 420
    ENDIF
    IF (L2.GT.M) THEN
        L3 = L3 + 1
        GOTO 430
    ENDIF
    DO 440 I=1,N
        X(I,2) = XDATA(I,L4)
        X(I,3) = XDATA(I,L3)
440   X(I,4) = XDATA(I,L2)
        GOTO 998

```

C

C Five Coefficients

C

```

510 NC = 5
    IF (M.LT.5) THEN
        GOTO 999
    ENDIF
    L5 = 2
520 L4 = L5 + 1
530 L3 = L4 + 1
540 L2 = L3 +1
500 IF (L5.GT.M) THEN
        GOTO 610
    ENDIF
    IF (L4.GT.M) THEN
        L5 = L5 + 1

```

APPENDIX A: FORTRAN program to solve for correlation coefficients (continued).

```
      GOTO 520
ENDIF
IF (L3.GT.M) THEN
  L4 = L4 + 1
  GOTO 530
ENDIF
IF (L2.GT.M) THEN
  L3 = L3 + 1
  GOTO 540
ENDIF
DO 550 I=1,N
  X(I,2) = XDATA(I,L5)
  X(I,3) = XDATA(I,L4)
  X(I,4) = XDATA(I,L3)
550  X(I,5) = XDATA(I,L2)
  GOTO 998
C
C Six Coefficients
C
610  NC = 6
      IF(M.LT.6) THEN
        GOTO 999
      ENDIF
      L6 = 2
620  L5 = L6 + 1
630  L4 = L5 + 1
640  L3 = L4 + 1
650  L2 = L3 + 1
600  IF (L6.GT.M) THEN
        GOTO 710
      ENDIF
      IF (L5.GT.M) THEN
        L6 = L6 + 1
        GOTO 620
      ENDIF
      IF (L4.GT.M) THEN
        L5 = L5 + 1
        GOTO 630
      ENDIF
      IF (L3.GT.M) THEN
```

APPENDIX A: FORTRAN program to solve for correlation coefficients (continued).

```

        L4 = L4 + 1
        GOTO 640
    ENDIF
    IF (L2.GT.M) THEN
        L3 = L3 + 1
        GOTO 650
    ENDIF
    DO 660 I=1,N
        X(I,2) = XDATA(I,L6)
        X(I,3) = XDATA(I,L5)
        X(I,4) = XDATA(I,L4)
        X(I,5) = XDATA(I,L3)
660    X(I,6) = XDATA(I,L2)
        GOTO 998
C
C Seven Coefficients
C
710  NC = 7
        IF(M.LT.7) THEN
            GOTO 999
        ENDIF
        L7 = 2
720  L6 = L7 + 1
730  L5 = L6 + 1
740  L4 = L5 + 1
750  L3 = L4 + 1
760  L2 = L3 + 1
700  IF (L7.GT.M) THEN
            GOTO 810
        ENDIF
        IF (L6.GT.M) THEN
            L7 = L7 + 1
            GOTO 720
        ENDIF
        IF (L5.GT.M) THEN
            L6 = L6 + 1
            GOTO 730
        ENDIF
        IF (L4.GT.M) THEN
            L5 = L5 + 1

```

APPENDIX A: FORTRAN program to solve for correlation coefficients (continued).

```

      GOTO 740
    ENDIF
    IF (L3.GT.M) THEN
      L4 = L4 + 1
      GOTO 750
    ENDIF
    IF (L2.GT.M) THEN
      L3 = L3 + 1
      GOTO 760
    ENDIF
    DO 770 I=1,N
      X(I,2) = XDATA(I,L7)
      X(I,3) = XDATA(I,L6)
      X(I,4) = XDATA(I,L5)
      X(I,5) = XDATA(I,L4)
      X(I,6) = XDATA(I,L3)
770   X(I,7) = XDATA(I,L2)
      GOTO 998
C
C Eight Coefficients
C
810  NC = 8
      IF (M.LT.8) THEN
        GOTO 999
      ENDIF
      L8 = 2
820  L7 = L8 + 1
830  L6 = L7+1
840  L5 = L6 + 1
850  L4 = L5 + 1
860  L3 = L4 + 1
870  L2 = L3 +1
800  IF (L8.GT.M) THEN
        GOTO 910
      ENDIF
      IF (L7.GT.M) THEN
        L8 = L8 + 1
        GOTO 820
      ENDIF
      IF (L6.GT.M) THEN

```

APPENDIX A: FORTRAN program to solve for correlation coefficients (continued).

```

      L7 = L7 + 1
      GOTO 830
    ENDIF
    IF (L5.GT.M) THEN
      L6 = L6 + 1
      GOTO 840
    ENDIF
    IF (L4.GT.M) THEN
      L5 = L5 + 1
      GOTO 850
    ENDIF
    IF (L3.GT.M) THEN
      L4 = L4 + 1
      GOTO 860
    ENDIF
    IF (L2.GT.M) THEN
      L3 = L3 + 1
      GOTO 870
    ENDIF
    DO 880 I=1,N
      X(I,2) = XDATA(I,L8)
      X(I,3) = XDATA(I,L7)
      X(I,4) = XDATA(I,L6)
      X(I,5) = XDATA(I,L5)
      X(I,6) = XDATA(I,L4)
      X(I,7) = XDATA(I,L3)
880   X(I,8) = XDATA(I,L2)
      GOTO 998
    C
    C Nine Coefficients
    C
910   NC = 9
      IF(M.LT.9) THEN
        GOTO 999
      ENDIF
      L9 = 2
920   L8 = L9 + 1
930   L7 = L8 + 1
940   L6 = L7+1
950   L5 = L6 + 1

```

APPENDIX A: FORTRAN program to solve for correlation coefficients (continued).

```
960 L4 = L5 + 1
970 L3 = L4 + 1
980 L2 = L3 + 1
900 IF (L9.GT.M) THEN
      GOTO 1010
ENDIF
IF (L8.GT.M) THEN
      L9 = L9 + 1
      GOTO 920
ENDIF
IF (L7.GT.M) THEN
      L8 = L8 + 1
      GOTO 930
ENDIF
IF (L6.GT.M) THEN
      L7 = L7 + 1
      GOTO 940
ENDIF
IF (L5.GT.M) THEN
      L6 = L6 + 1
      GOTO 950
ENDIF
IF (L4.GT.M) THEN
      L5 = L5 + 1
      GOTO 960
ENDIF
IF (L3.GT.M) THEN
      L4 = L4 + 1
      GOTO 970
ENDIF
IF (L2.GT.M) THEN
      L3 = L3 + 1
      GOTO 980
ENDIF
DO 990 I=1,N
      X(I,2) = XDATA(I,L9)
      X(I,3) = XDATA(I,L8)
      X(I,4) = XDATA(I,L7)
      X(I,5) = XDATA(I,L6)
      X(I,6) = XDATA(I,L5)
```

APPENDIX A: FORTRAN program to solve for correlation coefficients (continued).

```

          X(I,7) = XDATA(I,L4)
          X(I,8) = XDATA(I,L3)
990      X(I,9) = XDATA(I,L2)
          GOTO 998
C
C Ten Coefficients
C
1010 NC = 10
      IF(M.LT.10) THEN
          GOTO 999
      ENDIF
      L10 = 2
1020 L9 = L10 + 1
1030 L8 = L9 + 1
1040 L7 = L8 + 1
1050 L6 = L7 + 1
1060 L5 = L6 + 1
1070 L4 = L5 + 1
1080 L3 = L4 + 1
1095 L2 = L3 + 1
1000 IF (L10.GT.M) THEN
      GOTO 999
  ENDIF
  IF (L9.GT.M) THEN
      L10 = L10 + 1
      GOTO 1020
  ENDIF
  IF (L8.GT.M) THEN
      L9 = L9 + 1
      GOTO 1030
  ENDIF
  IF (L7.GT.M) THEN
      L8 = L8 + 1
      GOTO 1040
  ENDIF
  IF (L6.GT.M) THEN
      L7 = L7 + 1
      GOTO 1050
  ENDIF
  IF (L5.GT.M) THEN

```

APPENDIX A: FORTRAN program to solve for correlation coefficients (continued).

```

      L6 = L6 + 1
      GOTO 1060
ENDIF
IF (L4.GT.M) THEN
      L5 = L5 + 1
      GOTO 1070
ENDIF
IF (L3.GT.M) THEN
      L4 = L4 + 1
      GOTO 1080
ENDIF
IF (L2.GT.M) THEN
      L3 = L3 + 1
      GOTO 1095
ENDIF
DO 1090 I=1,N
      X(I,2) = XDATA(I,L10)
      X(I,3) = XDATA(I,L9)
      X(I,4) = XDATA(I,L8)
      X(I,5) = XDATA(I,L7)
      X(I,6) = XDATA(I,L6)
      X(I,7) = XDATA(I,L5)
      X(I,8) = XDATA(I,L4)
      X(I,9) = XDATA(I,L3)
1090   X(I,10) = XDATA(I,L2)
      GOTO 998
C
C Start calculations of matrix (NC x NC+1) coefficients here.
C
998  CONTINUE
C
C Set J=1 values of X(I,J) equal to 1.0
C
      DO 40 I = 1,N
          X(I,1) = 1.0
40   CONTINUE
C
C Set matrix (M1) values equal to zero.
C
      DO 50 J = 1,NC

```



APPENDIX A: FORTRAN program to solve for correlation coefficients (continued).

```

      DO 60 K = 1,NC+1
        M1(J,K) = 0.0
60    CONTINUE
50    CONTINUE

C
C Calculate matrix coefficient values for M1.
C
      DO 70 J=1,NC
        DO 80 K=1,NC
          DO 90 I=1,N
            M1(J,K) = M1(J,K) + X(I,K)*X(I,J)
90    CONTINUE
80    CONTINUE
70    CONTINUE
C
C Calculate right hand side coefficients (M1 (I, NC + 1)).
C
      DO 95 J=1,NC
        K = NC + 1
        DO 97 I=1,N
          M1(J,K) = M1(J,K) + YMDATA(I)*X(I,J)
97    CONTINUE
95    CONTINUE
C
C Set A(J) values equal to zero.
C
      DO 85 J=1,M
        A(J) = 0.0
85    CONTINUE
C
C Solve matrix M1 (subroutine Gauss).
C
      CALL GAUSS(NC,M1,A)
C
C Find values for Y-calc (YC).
C
      DO 100 I=1,N
        YC(I) = 0.0
      DO 110 J=1,NC

```

APPENDIX A: FORTRAN program to solve for correlation coefficients (continued).

```

      YC(I) = YC(I) + A(J)*X(I,J)
110  CONTINUE
      YC(I) = EXP(YC(I))
100  CONTINUE
C
C Take exponential of YM(I) for computing error.
      DO 115 I=1,N
          YMDATA(I) = EXP(YMDATA(I))
115  CONTINUE
C
C Calculate mean of measured values.
C
      YMEAN = 0.0
      DO 120 I=1,N
          YMEAN = YMEAN + YC(I)
120  CONTINUE
      YMEAN = YMEAN/N
C
C Calculate ST and SR.
C
      ST = 0.0
      SR = 0.0
      DO 130 I=1,N
          ST = ST + (YMDATA(I) - YMEAN)**2
          SR = SR + (YMDATA(I) - YC(I))**2
130  CONTINUE
C
C Calculate standard error (standard deviation), SIGMAY.
C
      SIGMAY = (ST/(N-1))**(0.5)
C
C Calculate SIGMAXY.
C
      SIGMAXY = (SR/(N-2))**(0.5)
C
C Calculate correlation coefficient, (R).
C
      IF((1-(SIGMAXY**2)/(SIGMAY**2)).LT.0.0) THEN
          R = 0.0
          GOTO 140

```

APPENDIX A: FORTRAN program to solve for correlation coefficients (continued).

```

      ENDIF
C
      R = (1 - (SIGMAXY**2)/(SIGMAY**2))**(0.5)
C
140  CONTINUE
C
C Output data to file.
C
      A(1) = EXP(A(1))
2000 WRITE(2,145) R,SIGMAXY,A(1),(A(J),J=2,NC)
145  FORMAT (F6.4,"",F7.4,10("","E12.4))
C
C Get YMDATA ready for the next set.
      DO 150 I=1,N
          YMDATA(I) = LOG(YMDATA(I))
150  CONTINUE
C
C Determine next set of coefficients, if any, and send back to start.
C
      IF(NC.EQ.2) THEN
          L2 = L2 + 1
          GOTO 200
      ELSE IF(NC.EQ.3) THEN
          L2 = L2 + 1
          GOTO 300
      ELSE IF(NC.EQ.4) THEN
          L2 = L2 + 1
          GOTO 400
      ELSE IF(NC.EQ.5) THEN
          L2 = L2 + 1
          GOTO 500
      ELSE IF(NC.EQ.6) THEN
          L2 = L2 + 1
          GOTO 600
      ELSE IF(NC.EQ.7) THEN
          L2 = L2 + 1
          GOTO 700
      ELSE IF(NC.EQ.8) THEN
          L2 = L2 + 1
          GOTO 800

```

APPENDIX A: FORTRAN program to solve for correlation coefficients (continued).

```

      ELSE IF(NC.EQ.9) THEN
        L2 = L2 + 1
        GOTO 900
      ELSE IF(NC.EQ.10) THEN
        L2 = L2 + 1
        GOTO 1000
      ENDIF
C
C All possibilities have been calculated.
C
999 CONTINUE
      PRINT*, 'ALL POSSIBLE COMBINATIONS OF PARAMETERS HAVE'
      PRINT*, 'BEEN CALCULATED!!!'
C
C Close files
C
      CLOSE(UNIT=1)
      CLOSE(UNIT=2)
C
C Stop and end program
C
      PRINT *, 'PROGRAM IS FINISHED'
      STOP
      END
C
C Subroutine Gauss to solve matrix.
C
      SUBROUTINE GAUSS(N1,A1,X1)
      DIMENSION A1(11,11),X1(11)
      DOUBLE PRECISION A1,X1,QT1,SUM
C forward substitution
      M2 = N1 + 1
      L1 = N1 - 1
      DO 1140 K1=1,L1
        KK1 = K1 + 1
        DO 1100 I1=KK1,N1
          QT1 = A1(I1,K1)/A1(K1,K1)
          DO 1090 J1=KK1,M2
            A1(I1,J1) = A1(I1,J1) - QT1*A1(K1,J1)
          1090 CONTINUE

```

APPENDIX A: FORTRAN program to solve for correlation coefficients (continued).

```
1100 CONTINUE
      DO 1130 I1=KK1,N1
        A1(I1,K1)=0.0
1130 CONTINUE
1140 CONTINUE
C
C Back substitution
C
      X1(N1) = A1(N1,M2)/ A1(N1,N1)
      DO 1240 NN1=1,L1
        SUM = 0.0
        I1 = N1 - NN1
        II1 = I1 + 1
        DO 1220 J1=II1,N1
          SUM = SUM + A1(I1,J1)*X1(J1)
1220 CONTINUE
        X1(I1) = (A1(I1,M2) - SUM)/ A1(I1,I1)
1240 CONTINUE
C
      RETURN
      END
```

## APPENDIX B

APPENDIX B: Manufacturers addresses and products.

Manufactures addresses:	Manufactures products:
<p>Capital Valve &amp; Fitting Co. (Swagelok Companies) 224 North Service Highway Sulphur, LA. 70669 TEL: (318) 625-5136 FAX: (318) 625-2419</p>	<p>All valves, filters, and fittings for flow loop and test fixture.</p>
<p>Max Machinery, Inc. 1420 Healdsburg Ave. Healdsburg, CA. 95548-3298 TEL: (707) 433-7281 FAX: (707) 433-0571</p>	<p>Liquid Flow Meters</p>
<p>McMaster - Carr, Inc. P.O. Box 740100 Atlanta, Ga. 30374-0100 TEL: (404) 346-7000 FAX: (404) 349-9091</p>	<p>Miniature end mills, aluminum and Lexan<sup>®</sup> for test sections and test fixture, electrical wiring, glass cover plates, Teflon<sup>®</sup>, epoxy/fiberglass, Loctite-UV cure adhesive, and o-rings.</p>
<p>Mini Tool, Inc. 634 University Ave. Los Gatos, CA. 95030 TEL: (408) 395-1585 FAX: (408) 395-1605</p>	<p>Micro end mills</p>

## APPENDIX B: Manufacturers addresses and products (continued).

National Instrument, Inc. Corporate Headquarters 6504 Bridge Point Pkwy. Austin TX. 78730-5039 TEL: (512) 795-8284 FAX: (512) 794-5678	Data acquisition system
OMEGA Engineering, Inc. World Wide Headquarters One OMEGA Dr. Stamford, CT. 06907-0047 TEL: (800) 826-6342 FAX: (203) 359-7700	Gas flow meters, pressure transducers, thermocouple wire and fittings, Omega- therm high thermal conductivity paste, Kapton <sup>®</sup> heaters.

For a complete list and description of all products used in the construction of the experimental flow loop, please Bailey (1996).



## APPENDIX C

### Appendix C: Single- and two-phase measured data.

Channel A: Argon gas tests.

Number of channels: 3

Channel Dimensions:

Depth ( $\mu\text{m}$ ): 255.80      Hyd. Diameter ( $\mu\text{m}$ ): 256.91

Width ( $\mu\text{m}$ ): 258.03      Channel Length (m): 0.0635

Data Point	Test Fixture Temperature		Test Section Temperature, ( $^{\circ}\text{C}$ )						
	Inlet	Outlet	Pos #1	Pos #2	Pos #3	Pos #4	Pos #5	Pos #6	Pos #7
1									
2									
3	30.16	34.82	46.87	47.87	48.45	50.14	49.97	50.03	49.44
4	30.23	35.67	46.85	47.84	48.43	50.12	49.96	50.02	49.44
5	30.16	36.30	47.01	48.01	48.61	50.30	50.14	50.21	49.65
6	30.39	39.98	52.78	54.19	55.04	56.70	56.46	56.56	55.79
7	30.74	41.33	54.69	56.18	57.07	58.72	58.48	58.60	57.82
8	30.89	42.51	55.43	56.94	57.87	59.52	59.28	59.40	58.62
9	30.83	43.47	55.98	57.52	58.47	60.12	59.87	60.01	59.25
10	30.75	43.69	56.33	57.90	58.86	60.51	60.26	60.41	59.63
11	30.76	44.64	56.61	58.18	59.16	60.80	60.56	60.70	59.91
12	30.98	45.67	56.78	58.37	59.38	61.02	60.77	60.94	60.16
13	30.40	47.76	56.28	57.92	58.98	60.63	60.38	60.59	59.86
14	30.13	50.33	55.64	57.32	58.45	60.09	59.85	60.11	59.43
15	29.98	50.97	55.05	56.77	57.96	59.60	59.36	59.66	59.04
16	29.83	51.36	54.49	56.24	57.49	59.13	58.89	59.24	58.65

Data Point	Gas Flow Meter		Test Fixture Press., (Pa)		Gas Flow Rates, (cc/min)		
	Temp. ( $^{\circ}\text{C}$ )	Press. (Pa)	Inlet	Outlet	F.M. #4	F.M. #5	F.M. #6
1							
2							
3	23.94	800.748	18.684	3.865	0.00	248.76	0.00
4	23.96	780.606	27.785	3.931	0.00	367.59	0.00
5	23.97	765.438	38.127	4.010	0.00	483.28	0.00
6	23.95	755.786	49.660	4.168	0.00	581.35	0.00
7	23.95	1,017.780	62.672	4.370	0.00	0.00	647.10
8	23.98	1,007.156	78.116	4.458	0.00	0.00	726.47
9	23.96	999.854	93.422	4.686	0.00	0.00	792.78
10	23.94	994.339	110.972	4.860	0.00	0.00	849.29
11	23.96	990.202	126.846	4.998	0.00	0.00	887.29
12	23.97	987.444	143.614	5.337	0.00	0.00	932.41
13	23.91	983.194	200.978	6.022	0.00	0.00	1063.20
14	23.93	984.686	259.828	6.687	0.00	0.00	1159.02
15	23.96	986.065	314.840	7.471	0.00	261.17	976.83
16	24.00	983.488	375.162	8.163	0.00	270.10	1024.29

## Appendix C: Single- and two-phase measured data (continued).

Channel A: Helium gas tests. Number of channels: 3

Channel Dimensions:

Depth ( $\mu\text{m}$ ): 255.80 Hyd. Diameter ( $\mu\text{m}$ ): 256.91Width ( $\mu\text{m}$ ): 258.03 Channel Length (m): 0.0635

Data Point	Test Fixture Temperature		Test Section Temperature, ( $^{\circ}\text{C}$ )						
	Inlet	Outlet	Pos #1	Pos #2	Pos #3	Pos #4	Pos #5	Pos #6	Pos #7
1									
2									
3									
4	36.76	40.16	49.46	50.46	51.07	52.75	52.59	52.66	52.11
5	37.09	42.08	50.64	51.69	52.33	54.00	53.83	53.90	53.34
6	37.09	42.81	50.74	51.81	52.45	54.13	53.96	54.03	53.46
7	37.64	44.27	55.34	56.80	57.67	59.32	59.09	59.18	58.42
8	38.22	45.16	57.16	58.69	59.62	61.26	61.01	61.12	60.34
9	38.57	46.16	57.91	59.48	60.43	62.07	61.83	61.96	61.18
10	38.82	47.89	58.41	60.00	60.98	62.61	62.36	62.51	61.74
11	39.02	49.35	58.77	60.39	61.39	63.03	62.78	62.94	62.19
12	39.10	49.96	58.94	60.58	61.60	63.24	62.99	63.17	62.44
13	38.59	52.30	58.69	60.39	61.48	63.11	62.87	63.10	62.41
14	37.99	53.99	58.30	60.07	61.23	62.86	62.62	62.92	62.30
15	37.36	54.49	57.72	59.55	60.77	62.41	62.17	62.53	61.96
16	36.75	54.32	57.03	58.88	60.17	61.80	61.56	61.96	61.46

Data Point	Gas Flow Meter		Test Fixture Press., (Pa)		Gas Flow Rates, (cc/min)		
	Temp. ( $^{\circ}\text{C}$ )	Press. (Pa)	Inlet	Outlet	F.M. #4	F.M. #5	F.M. #6
1							
2							
3							
4	23.93	1,184,653.07	23,373.15	3,779.67	0.00	383.51	0.00
5	23.94	1,158,453.08	30,697.39	3,838.44	0.00	491.01	0.00
6	23.94	1,140,526.78	39,093.14	3,913.04	0.00	602.48	0.00
7	24.00	1,132,253.10	45,895.19	3,994.42	0.00	0.00	723.44
8	23.99	1,125,358.36	52,251.91	4,014.77	0.00	0.00	807.31
9	24.00	1,118,463.63	59,539.98	4,096.15	0.00	0.00	907.09
10	24.00	1,112,947.84	66,629.12	4,175.27	0.00	0.00	1,003.78
11	24.01	1,108,811.00	72,877.33	4,267.95	0.00	0.00	1,088.79
12	23.99	1,106,053.11	79,607.04	4,299.60	0.00	0.00	1,177.65
13	24.00	1,097,101.26	99,215.21	4,645.47	0.00	0.00	1,443.36
14	24.01	1,089,505.75	119,766.04	4,955.17	0.00	0.00	1,701.12
15	24.00	1,085,368.91	140,032.03	5,576.82	0.00	398.66	1,506.98
16	23.99	1,081,232.07	159,262.69	5,992.77	0.00	434.03	1,667.99

Appendix C: Single- and two-phase measured data (continued).

Channel A: Nitrogen gas tests.

Number of channels: 3

Channel Dimensions:

Depth ( $\mu\text{m}$ ): 255.80

Hyd. Diameter ( $\mu\text{m}$ ): 256.91

Width ( $\mu\text{m}$ ): 258.03

Channel Length (m): 0.0635

Data Point	Test Fixture Temperature		Test Section Temperature, ( $^{\circ}\text{C}$ )						
	Inlet	Outlet	Pos #1	Pos #2	Pos #3	Pos #4	Pos #5	Pos #6	Pos #7
1									
2									
3									
4									
5	36.39	44.41	52.71	53.72	54.33	56.00	55.83	55.90	55.35
6	35.85	44.38	52.54	53.57	54.19	55.86	55.69	55.77	55.22
7	35.29	44.41	52.32	53.36	54.00	55.67	55.50	55.59	55.05
8	34.83	44.51	52.03	53.08	53.73	55.40	55.24	55.33	54.81
9	34.48	44.54	51.76	52.82	53.48	55.15	54.99	55.09	54.58
10	34.16	44.71	51.51	52.57	53.24	54.92	54.75	54.87	54.37
11	34.02	47.04	55.74	57.17	58.09	59.73	59.50	59.65	58.99
12	34.09	48.54	57.30	58.81	59.79	61.43	61.19	61.36	60.67
13	33.94	49.62	57.18	58.74	59.77	61.41	61.17	61.36	60.67
14	33.82	51.10	56.89	58.50	59.58	61.22	60.98	61.22	60.57
15	33.55	52.03	56.50	58.16	59.30	60.94	60.70	60.99	60.38
16	33.06	52.36	55.86	57.56	58.76	60.40	60.17	60.50	59.94

Data Point	Gas Flow Meter		Test Fixture Press., (Pa)		Gas Flow Rates, (cc/min)		
	Temp. ( $^{\circ}\text{C}$ )	Press. (Pa)	Inlet	Outlet	F.M. #4	F.M. #5	F.M. #6
1							
2							
3							
4							
5	23.93	1,450,405.50	23,282.04	3,899.48	0.00	370.21	0.00
6	23.95	1,424,589.80	28,959.01	3,942.43	0.00	451.98	0.00
7	23.97	1,406,663.50	35,645.77	4,030.59	0.00	0.00	533.93
8	23.92	1,397,010.90	41,563.94	4,078.07	0.00	0.00	610.47
9	23.91	1,388,918.00	46,939.57	4,179.79	0.00	0.00	674.55
10	23.93	1,383,877.00	53,020.50	4,286.04	0.00	0.00	741.77
11	23.92	1,379,152.40	60,432.90	4,399.07	0.00	0.00	803.31
12	23.91	1,376,326.70	67,906.34	4,460.10	0.00	0.00	859.98
13	23.91	1,368,053.00	101,283.60	4,835.36	0.00	0.00	1,022.14
14	23.97	1,362,537.20	136,690.90	5,018.46	0.00	0.00	1,137.21
15	23.99	1,358,400.30	170,809.70	5,353.03	0.00	258.51	970.86
16	23.96	1,352,884.60	209,069.80	5,633.34	0.00	271.86	1,037.14

### Appendix C: Single- and two-phase measured data (continued).

Channel A: Water tests. Number of channels: 3

Channel Dimensions:

Depth ( $\mu\text{m}$ ): 255.80 Hyd. Diameter ( $\mu\text{m}$ ): 256.91

Width ( $\mu\text{m}$ ): 258.03 Channel Length (m): 0.0635

Data Point	Test Fixture Temperature		Test Section Temperature, ( $^{\circ}\text{C}$ )						
	Inlet	Outlet	Pos #1	Pos #2	Pos #3	Pos #4	Pos #5	Pos #6	Pos #7
1	24.64	40.38	36.84	39.97	43.06	44.60	44.26	45.52	45.72
2	24.30	36.96	34.86	38.04	41.26	42.74	42.33	43.20	43.10
3	24.45	34.68	34.03	37.67	41.63	42.99	42.41	42.95	42.45
4	25.11	34.53	34.13	38.07	42.46	43.76	43.08	43.27	42.32
5	25.65	36.08	34.53	38.75	44.52	45.64	44.75	45.00	44.02
6	26.06	37.58	35.27	39.93	46.69	47.69	46.61	46.64	45.52
7	26.54	37.24	34.73	38.99	45.31	46.25	45.14	44.78	43.96
8	26.82	38.47	35.60	40.09	47.03	47.75	46.42	46.10	45.47
9	26.81	37.95	35.20	39.40	46.14	46.85	45.54	45.19	44.69
10	26.95	36.97	34.49	38.32	44.81	45.50	44.22	43.78	43.40
11	27.11	37.77	35.21	39.39	46.76	47.24	45.71	45.10	44.78
12	27.36	38.13	35.68	40.02	48.26	48.50	46.71	45.88	45.62
13	27.49	37.26	35.11	39.08	47.21	47.41	45.62	44.68	44.51
14	27.77	37.28	35.17	39.22	47.85	47.92	45.99	44.90	44.76
15	27.82	36.64	34.73	38.56	47.04	47.10	45.18	44.03	43.93
16	27.63	36.11	34.34	38.01	46.43	46.48	44.57	43.33	43.27
17	27.64	35.59	33.92	37.46	45.84	45.86	43.96	42.67	42.65
18	27.62	35.01	33.48	36.96	45.15	45.17	43.29	41.92	41.94
19	27.51	34.51	33.04	36.41	44.50	44.51	42.66	41.26	41.31
20	27.50	34.10	32.66	35.91	43.97	43.98	42.14	40.71	40.80
21	27.57	33.76	32.32	35.46	43.54	43.54	41.70	40.26	40.38

# Appendix C: Single- and two-phase measured data (continued).

## Channel A: Water tests (continued).

Data Point	Liquid Flow Meter		Test Fixture Press., (Pa)		liquid Flow Rate
	Temp.(°C)	Press.(Pa)	Inlet	Outlet	F. M. #1, (cc/min)
1	24.10	2,788,887.96	116,374.06	100,862.04	10.69
2	24.27	2,734,136.99	133,757.83	99,290.94	17.17
3	24.90	2,681,171.88	169,406.99	98,832.05	31.52
4	25.96	2,647,376.38	201,122.76	98,253.34	42.51
5	26.63	2,636,796.92	239,348.97	98,526.87	52.86
6	27.11	2,638,854.04	271,788.12	99,180.17	58.31
7	27.49	2,633,315.65	307,595.53	99,128.18	64.65
8	27.76	2,627,935.49	343,222.08	99,177.91	70.28
9	27.95	2,634,468.54	380,634.49	99,914.86	74.16
10	28.17	2,585,775.90	446,010.12	98,920.21	85.77
11	28.43	2,552,251.67	511,182.31	98,823.00	94.29
12	28.62	2,532,607.33	613,631.26	99,139.48	106.80
13	28.72	2,524,491.89	726,320.59	99,706.89	120.56
14	28.79	2,503,152.13	827,322.78	99,695.58	130.90
15	28.85	2,492,233.58	933,840.76	100,095.70	142.14
16	28.88	2,501,162.83	1,042,980.99	101,092.61	152.24
17	28.89	2,436,985.29	1,165,707.25	99,984.94	161.25
18	28.89	2,449,124.54	1,314,949.96	101,241.81	178.93
19	28.87	2,388,676.95	1,447,396.66	100,529.73	188.83
20	28.87	2,391,706.11	1,601,047.49	100,755.79	200.92
21	28.84	2,326,036.60	1,733,109.88	99,573.51	205.93

# Appendix C: Single- and two-phase measured data (continued).

Channel A: Water and argon tests. Number of channels: 3

Channel Dimensions:

Depth ( $\mu\text{m}$ ): 255.80 Hyd. Diameter ( $\mu\text{m}$ ): 256.91

Width ( $\mu\text{m}$ ): 258.03 Channel Length (m): 0.0635

Data Point	Test Fixture Temperature		Test Section Temperature, ( $^{\circ}\text{C}$ )						
	Inlet	Outlet	Pos #1	Pos #2	Pos #3	Pos #4	Pos #5	Pos #6	Pos #7
1	24.83	39.90	34.16	38.34	42.33	43.83	43.37	44.94	45.10
2	25.02	41.10	33.59	37.45	41.53	42.97	42.50	44.33	45.04
3	24.65	41.46	33.68	37.44	41.51	42.91	42.40	44.26	44.99
4	24.73	41.59	33.86	37.58	41.66	43.04	42.51	44.39	45.06
5	24.82	41.73	34.08	37.79	41.86	43.24	42.73	44.59	45.19
6	24.97	42.01	34.57	38.34	42.40	43.79	43.27	45.07	45.52
7	24.67	37.23	32.53	36.81	42.13	43.22	42.44	43.40	43.97
8	24.94	37.98	32.60	36.64	41.85	42.93	42.12	43.11	43.89
9	26.74	39.74	34.21	38.08	42.83	44.03	43.33	44.37	44.96
10	25.12	37.99	32.95	37.02	42.34	43.39	42.53	43.77	44.41
11	25.14	37.30	33.10	37.24	42.66	43.70	42.83	44.19	44.82
12	25.10	38.80	33.22	37.45	42.98	43.99	43.11	44.61	45.21
13	25.83	34.59	32.84	36.76	43.76	44.21	42.79	42.60	43.85
14	25.94	35.52	33.03	37.04	44.12	44.55	43.13	43.04	44.22
15	25.98	35.77	33.20	37.27	44.43	44.86	43.42	43.45	44.58
16	25.96	36.30	33.35	37.56	44.84	45.27	43.82	44.04	45.09
17	25.93	36.57	33.57	37.96	45.45	45.85	44.36	44.86	45.85
18	25.85	36.74	33.77	38.32	46.05	46.46	44.93	45.74	46.65
19	26.18	34.73	33.15	37.08	45.81	45.78	43.84	43.18	44.83
20	26.19	34.96	33.26	37.31	46.14	46.09	44.14	43.64	45.22
21	26.12	35.34	33.39	37.57	46.55	46.49	44.50	44.15	45.68
22	26.12	35.99	33.48	37.79	46.92	46.85	44.82	44.70	46.12
23	26.08	36.56	33.70	38.25	47.63	47.56	45.46	45.67	47.01
24	26.01	37.03	33.71	38.36	47.96	47.88	45.73	46.28	47.68

# Appendix C: Single- and two-phase measured data (continued).

## Channel A: Water and argon tests (continued).

Data Point	Gas Flow Meter		Liquid Flow Meter		Test Fixture Press., (Pa)		Flow Meter/Flow rates, (cc/min)			
	Temp.(°C)	Press.(Pa)	Temp.(°C)	Press.(Pa)	Inlet	Outlet	F.M. #4	F.M. #5	F.M. #6	F.M. #1
1	23.82	1,529,390	24.00	1,998,789	200,558	113,543.8	0.00	0.00	210.68	14.27
2	24.17	1,517,070	24.41	1,962,868	295,705	124,489.5	0.00	0.00	382.10	14.82
3	24.14	1,515,600	24.37	1,904,274	374,079	131,978.8	0.00	0.00	504.21	13.33
4	24.12	1,511,124	24.36	1,892,180	455,889	140,797.2	0.00	0.00	597.35	12.74
5	24.08	1,510,062	24.36	1,900,138	539,643	149,672.2	0.00	142.34	529.95	11.98
6	24.06	1,510,740	24.34	1,903,528	621,679	157,719.8	0.00	153.68	581.78	9.80
7	23.99	1,536,284	25.66	1,871,835	326,132	111,719.5	0.00	0.00	163.90	47.20
8	23.96	1,521,116	25.98	1,845,748	445,309	121,849.2	0.00	0.00	306.69	42.30
9	25.15	2,460,179	27.79	3,280,102	406,315	130,055.0	0.00	0.00	485.60	35.72
10	23.94	1,515,035	26.17	1,849,908	641,075	140,937.4	0.00	0.00	483.30	37.72
11	23.94	1,513,340	26.17	1,855,175	732,288	148,892.3	0.00	117.19	436.43	35.41
12	23.92	1,516,278	26.10	1,860,713	825,944	156,458.5	0.00	127.16	481.47	32.45
13	23.94	1,536,284	27.34	1,775,784	716,578	113,301.9	0.00	0.00	110.20	101.44
14	23.91	1,523,806	27.42	1,785,029	779,941	120,922.3	0.00	0.00	168.84	99.65
15	23.92	1,516,979	27.43	1,784,962	842,582	127,566.1	0.00	0.00	221.67	95.38
16	23.94	1,518,358	27.34	1,779,242	935,694	136,913.6	0.00	0.00	305.58	89.27
17	23.98	1,515,035	27.25	1,780,893	1,040,788	147,635.5	0.00	0.00	390.94	82.00
18	24.01	1,515,691	27.14	1,788,918	1,149,951	158,624.1	0.00	99.99	378.51	74.49
19	23.98	1,538,296	27.64	1,705,277	1,067,260	112,978.7	0.00	0.00	80.26	140.78
20	24.00	1,523,580	27.62	1,703,649	1,111,951	119,868.9	0.00	0.00	129.16	137.60
21	24.03	1,521,116	27.57	1,695,059	1,146,651	125,807.4	0.00	0.00	173.79	131.03
22	24.10	1,520,619	27.51	1,718,433	1,223,510	136,850.3	0.00	0.00	247.05	123.35
23	24.16	1,518,223	27.42	1,724,876	1,299,533	148,573.6	0.00	0.00	332.86	111.96
24	24.12	1,523,603	27.31	1,739,456	1,365,542	157,812.5	0.00	85.02	320.90	103.54



Appendix C: Single- and two-phase measured data (continued).

Channel A: Water and helium tests. Number of channels: 3

Channel Dimensions:

Depth ( $\mu\text{m}$ ): 255.80 Hyd. Diameter ( $\mu\text{m}$ ): 256.91

Width ( $\mu\text{m}$ ): 258.03 Channel Length (m): 0.0635

Data Point	Test Fixture Temperature		Test Section Temperature, ( $^{\circ}\text{C}$ )						
	Inlet	Outlet	Pos #1	Pos #2	Pos #3	Pos #4	Pos #5	Pos #6	Pos #7
1	25.62	34.75	31.74	35.17	38.46	39.91	39.49	40.34	40.15
2	25.96	35.22	31.30	34.60	37.95	39.40	38.99	39.98	40.04
3	26.11	35.21	30.81	33.90	37.19	38.63	38.23	39.26	39.55
4	25.99	34.85	30.56	33.53	36.76	38.19	37.80	38.80	39.12
5	25.65	34.67	30.25	33.11	36.27	37.70	37.31	38.28	38.65
6	25.57	34.41	30.11	32.94	36.09	37.51	37.12	38.06	38.44
7	26.10	36.91	32.80	37.21	42.60	43.67	42.90	43.83	44.40
8	26.14	37.08	32.45	36.60	41.75	42.81	42.03	42.75	43.45
9	26.41	37.18	32.32	36.37	41.45	42.50	41.71	42.47	43.33
10	26.31	37.27	32.24	36.24	41.29	42.32	41.54	42.36	43.26
11	26.04	37.32	32.13	36.09	41.10	42.13	41.36	42.21	43.10
12	26.03	37.28	32.21	36.19	41.21	42.24	41.47	42.32	43.15
13	26.48	34.69	31.99	35.69	41.97	42.47	41.25	41.08	42.48
14	26.51	34.84	31.95	35.70	42.04	42.53	41.30	41.24	42.56
15	26.80	36.08	32.76	36.97	44.11	44.43	43.03	43.03	44.50
16	26.76	36.24	32.75	36.97	44.15	44.47	43.06	43.14	44.56
17	26.49	36.50	32.71	36.94	44.18	44.48	43.05	43.24	44.62
18	26.41	36.88	32.65	36.91	44.20	44.49	43.05	43.38	44.67
19	26.61	34.76	32.28	35.98	44.04	44.04	42.30	41.86	43.51
20	26.61	35.09	32.26	36.03	44.17	44.17	42.42	42.09	43.70
21	26.85	35.22	32.27	36.07	44.23	44.25	42.47	42.30	43.85

# Appendix C: Single- and two-phase measured data (continued).

Channel A: Water and helium (continued).

Data Point	Gas Flow Meter		Liquid Flow Meter		Test Fixture Press., (Pa)		Flow Meter/Flow rates, (cc/min)			
	Temp.(°C)	Press.(Pa)	Temp.(°C)	Press.(Pa)	Inlet	Outlet	F.M. #4	F.M. #5	F.M. #6	F.M. #1
1	24.06	1,707,274	26.22	1,876,650	207,995	109,432	0.00	0.00	222.88	28.54
2	24.08	1,687,969	26.14	1,872,084	249,341	120,511	0.00	0.00	415.60	27.30
3	24.09	1,675,558	26.06	1,867,631	287,341	129,913	0.00	0.00	583.54	26.80
4	24.10	1,667,284	25.96	1,863,856	315,078	138,797	0.00	0.00	745.18	26.13
5	24.06	1,666,335	25.85	1,870,637	354,887	146,826	0.00	182.43	685.84	25.55
6	24.03	1,667,058	25.77	1,874,684	383,799	153,655	0.00	204.85	784.96	25.05
7	24.06	1,725,200	26.26	1,816,045	284,312	108,864	0.00	0.00	193.59	48.80
8	24.07	1,696,242	26.36	1,815,683	341,594	120,943	0.00	0.00	358.26	46.54
9	24.08	1,683,832	26.39	1,820,114	390,739	130,674	0.00	0.00	501.23	46.60
10	24.07	1,678,316	26.37	1,818,667	434,956	138,711	0.00	0.00	634.19	45.52
11	24.08	1,674,224	26.34	1,835,192	478,201	147,421	0.00	155.36	583.82	44.56
12	24.08	1,675,558	26.30	1,813,535	500,512	153,314	0.00	177.81	681.28	42.29
13	24.11	1,737,859	27.05	1,732,019	621,001	109,977	0.00	0.00	118.75	98.64
14	24.14	1,710,032	27.06	1,737,851	683,980	123,009	0.00	0.00	234.41	97.01
15	24.18	1,692,874	27.01	1,743,412	731,927	132,417	0.00	0.00	343.05	94.26
16	24.19	1,685,211	26.93	1,746,849	775,465	141,381	0.00	0.00	436.14	91.35
17	24.19	1,678,452	26.85	1,767,329	828,634	150,592	0.00	109.31	410.99	89.16
18	24.17	1,679,695	26.73	1,773,501	872,918	157,546	0.00	122.52	468.92	87.28
19	24.17	1,745,884	27.02	1,669,040	964,336	110,992	0.00	0.00	88.06	136.17
20	24.16	1,712,790	26.99	1,675,776	1,019,516	124,218	0.00	0.00	179.10	132.29
21	24.18	1,697,825	26.96	1,680,026	1,065,655	134,246	0.00	0.00	261.70	128.19

# Appendix C: Single- and two-phase measured data (continued).

Channel A: Water and nitrogen tests. Number of channels: 3

Channel Dimensions:

Depth ( $\mu\text{m}$ ): 255.80 Hyd. Diameter ( $\mu\text{m}$ ): 256.91

Width ( $\mu\text{m}$ ): 258.03 Channel Length (m): 0.0635

Data Point	Test Fixture Temperature		Test Section Temperature, ( $^{\circ}\text{C}$ )						
	Inlet	Outlet	Pos #1	Pos #2	Pos #3	Pos #4	Pos #5	Pos #6	Pos #7
1	25.62	34.75	31.74	35.17	38.46	39.91	39.49	40.34	40.15
2	25.96	35.22	31.30	34.60	37.95	39.40	38.99	39.98	40.04
3	26.11	35.21	30.81	33.90	37.19	38.63	38.23	39.26	39.55
4	25.99	34.85	30.56	33.53	36.76	38.19	37.80	38.80	39.12
5	25.65	34.67	30.25	33.11	36.27	37.70	37.31	38.28	38.65
6	25.57	34.41	30.11	32.94	36.09	37.51	37.12	38.06	38.44
7	26.10	36.91	32.80	37.21	42.60	43.67	42.90	43.83	44.40
8	26.14	37.08	32.45	36.60	41.75	42.81	42.03	42.75	43.45
9	26.41	37.18	32.32	36.37	41.45	42.50	41.71	42.47	43.33
10	26.31	37.27	32.24	36.24	41.29	42.32	41.54	42.36	43.26
11	26.04	37.32	32.13	36.09	41.10	42.13	41.36	42.21	43.10
12	26.03	37.28	32.21	36.19	41.21	42.24	41.47	42.32	43.15
13	26.48	34.69	31.99	35.69	41.97	42.47	41.25	41.08	42.48
14	26.51	34.84	31.95	35.70	42.04	42.53	41.30	41.24	42.56
15	26.80	36.08	32.76	36.97	44.11	44.43	43.03	43.03	44.50
16	26.76	36.24	32.75	36.97	44.15	44.47	43.06	43.14	44.56
17	26.49	36.50	32.71	36.94	44.18	44.48	43.05	43.24	44.62
18	26.41	36.88	32.65	36.91	44.20	44.49	43.05	43.38	44.67
19	26.61	34.76	32.28	35.98	44.04	44.04	42.30	41.86	43.51
20	26.61	35.09	32.26	36.03	44.17	44.17	42.42	42.09	43.70
21	26.85	35.22	32.27	36.07	44.23	44.25	42.47	42.30	43.85

Appendix C: Single- and two-phase measured data (continued).

Channel A: Water and nitrogen (continued).

Data Point	Gas Flow Meter		Liquid Flow Meter		Test Fixture Press., (Pa)		Flow Meter/Flow rates, (cc/min)			
	Temp.(°C)	Press.(Pa)	Temp.(°C)	Press.(Pa)	Inlet	Outlet	F.M. #4	F.M. #5	F.M. #6	F.M. #1
1	24.06	1,707,274	26.22	1,876,650	207,995	109,432	0.00	0.00	222.88	28.54
2	24.08	1,687,969	26.14	1,872,084	249,341	120,511	0.00	0.00	415.60	27.30
3	24.09	1,675,558	26.06	1,867,631	287,341	129,913	0.00	0.00	583.54	26.80
4	24.10	1,667,284	25.96	1,863,856	315,078	138,797	0.00	0.00	745.18	26.13
5	24.06	1,666,335	25.85	1,870,637	354,887	146,826	0.00	182.43	685.84	25.55
6	24.03	1,667,058	25.77	1,874,684	383,799	153,655	0.00	204.85	784.96	25.05
7	24.06	1,725,200	26.26	1,816,045	284,312	108,864	0.00	0.00	193.59	48.80
8	24.07	1,696,242	26.36	1,815,683	341,594	120,943	0.00	0.00	358.26	46.54
9	24.08	1,683,832	26.39	1,820,114	390,739	130,674	0.00	0.00	501.23	46.60
10	24.07	1,678,316	26.37	1,818,667	434,956	138,711	0.00	0.00	634.19	45.52
11	24.08	1,674,224	26.34	1,835,192	478,201	147,421	0.00	155.36	583.82	44.56
12	24.08	1,675,558	26.30	1,813,535	500,512	153,314	0.00	177.81	681.28	42.29
13	24.11	1,737,859	27.05	1,732,019	621,001	109,977	0.00	0.00	118.75	98.64
14	24.14	1,710,032	27.06	1,737,851	683,980	123,009	0.00	0.00	234.41	97.01
15	24.18	1,692,874	27.01	1,743,412	731,927	132,417	0.00	0.00	343.05	94.26
16	24.19	1,685,211	26.93	1,746,849	775,465	141,381	0.00	0.00	436.14	91.35
17	24.19	1,678,452	26.85	1,767,329	828,634	150,592	0.00	109.31	410.99	89.16
18	24.17	1,679,695	26.73	1,773,501	872,918	157,546	0.00	122.52	468.92	87.28
19	24.17	1,745,884	27.02	1,669,040	964,336	110,992	0.00	0.00	88.06	136.17
20	24.16	1,712,790	26.99	1,675,776	1,019,516	124,218	0.00	0.00	179.10	132.29
21	24.18	1,697,825	26.96	1,680,026	1,065,655	134,246	0.00	0.00	261.70	128.19

## Appendix C: Single- and two-phase measured data (continued).

Channel B: Argon gas tests.

Number of channels: 3

Channel Dimensions:

Depth ( $\mu\text{m}$ ): 211.14 Hyd. Diameter ( $\mu\text{m}$ ): 210.05Width ( $\mu\text{m}$ ): 208.97 Channel Length (m): 0.0635

Data Point	Test Fixture Temperature		Test Section Temperature, ( $^{\circ}\text{C}$ )						
	Inlet	Outlet	Pos #1	Pos #2	Pos #3	Pos #4	Pos #5	Pos #6	Pos #7
1	30.56	34.95	55.12	56.54	57.39	59.11	58.71	59.01	58.26
2	31.01	38.56	56.15	57.57	58.43	60.15	59.75	60.05	59.30
3	30.75	40.90	57.24	58.64	59.50	61.21	60.81	61.12	60.37
4	32.10	45.26	58.66	60.03	60.87	62.58	62.17	62.46	61.69
5	32.50	46.69	59.18	60.58	61.44	63.15	62.74	63.05	62.28
6	31.57	47.51	59.42	60.86	61.76	63.47	63.05	63.38	62.62
7	31.80	47.72	59.47	60.92	61.83	63.56	63.13	63.46	62.68
8	31.39	48.36	59.41	60.90	61.86	63.59	63.16	63.52	62.77
9	31.51	49.00	59.30	60.81	61.80	63.53	63.10	63.48	62.75
10	31.49	49.59	59.11	60.63	61.64	63.37	62.94	63.34	62.64
11	31.41	51.45	58.81	60.35	61.39	63.12	62.69	63.12	62.44
12	31.23	51.66	58.56	60.12	61.19	62.93	62.49	62.95	62.29
13	31.08	51.97	58.33	59.92	61.02	62.76	62.32	62.80	62.17
14	31.04	52.36	58.16	59.76	60.89	62.64	62.20	62.71	62.11
15	30.87	52.49	57.82	59.44	60.60	62.35	61.90	62.45	61.87
16	30.72	52.55	57.51	59.15	60.33	62.09	61.64	62.21	61.66
17	30.65	52.58	57.24	58.88	60.08	61.83	61.38	61.97	61.44

Data Point	Gas Flow Meter		Test Fixture Press., (Pa)		Gas Flow Rates, (cc/min)		
	Temp. ( $^{\circ}\text{C}$ )	Press. (Pa)	Inlet	Outlet	F.M. #4	F.M. #5	F.M. #6
1	23.92	1,199.822	20,194	3,472	0.00	127.76	0.00
2	23.88	1,043.840	46,751	3,560	0.00	314.41	0.00
3	23.82	1,028.832	66,088	3,633	0.00	427.89	0.00
4	23.76	1,015,043	98,457	3,859	0.00	0.00	539.87
5	23.74	994,358	127,001	4,001	0.00	0.00	626.06
6	23.71	989,069	175,678	4,320	0.00	0.00	690.27
7	23.69	983,779	205,047	4,514	0.00	0.00	722.48
8	23.68	976,025	247,686	4,831	0.00	0.00	770.98
9	23.68	982,920	282,076	5,242	0.00	0.00	808.80
10	23.67	983,327	313,597	5,511	0.00	0.00	838.94
11	23.68	984,706	349,563	5,837	0.00	0.00	869.38
12	23.70	985,226	362,575	6,097	0.00	0.00	931.54
13	23.76	986,062	397,584	6,402	0.00	0.00	946.50
14	23.84	985,135	426,377	6,748	0.00	207.01	769.11
15	23.90	987,464	468,284	7,157	0.00	209.22	783.04
16	23.90	988,504	503,040	7,408	0.00	211.10	794.77
17	23.94	994,517	529,387	7,573	0.00	212.55	803.83

## Appendix C: Single- and two-phase measured data (continued).

Channel B: Helium gas tests.                      Number of channels:                      3  
Channel Dimensions:  
Depth ( $\mu\text{m}$ ):                      211.14                      Hyd. Diameter ( $\mu\text{m}$ ):                      210.05  
Width ( $\mu\text{m}$ ):                      208.97                      Channel Length (m):                      0.0635

Data Point	Test Fixture Temperature		Test Section Temperature, ( $^{\circ}\text{C}$ )						
	Inlet	Outlet	Pos #1	Pos #2	Pos #3	Pos #4	Pos #5	Pos #6	Pos #7
1	33.40	35.00	55.76	57.02	57.68	59.44	59.04	59.27	58.47
2	34.06	40.97	57.87	59.18	59.85	61.63	61.23	61.47	60.68
3	33.83	45.53	58.42	59.76	60.46	62.24	61.83	62.09	61.29
4	34.69	46.57	58.71	60.07	60.77	62.55	62.14	62.39	61.57
5	35.10	48.65	58.97	60.36	61.09	62.87	62.46	62.72	61.91
6	35.31	50.35	59.24	60.67	61.42	63.21	62.79	63.07	62.28
7	35.24	51.79	59.34	60.81	61.61	63.39	62.98	63.30	62.54
8	35.14	51.48	59.34	60.87	61.72	63.50	63.08	63.45	62.73
9	35.04	50.18	59.34	60.91	61.81	63.59	63.17	63.59	62.92
10	34.88	50.69	59.18	60.78	61.71	63.49	63.06	63.50	62.85
11	34.63	51.48	58.90	60.52	61.49	63.27	62.84	63.30	62.66
12	34.44	52.26	58.77	60.43	61.44	63.21	62.78	63.27	62.67
13	34.32	52.74	58.57	60.25	61.29	63.07	62.63	63.16	62.59
14	34.19	52.98	58.31	60.02	61.10	62.88	62.44	63.00	62.45
15	33.99	53.44	58.06	59.79	60.90	62.68	62.24	62.83	62.31
16	33.89	53.69	57.77	59.52	60.65	62.44	62.00	62.61	62.12
17	33.96	53.96	57.44	59.19	60.34	62.13	61.68	62.32	61.86

Data Point	Gas Flow Meter		Test Fixture Press., (Pa)		Gas Flow Rates, (cc/min)		
	Temp.( $^{\circ}\text{C}$ )	Press.(Pa)	Inlet	Outlet	F.M. #4	F.M. #5	F.M. #6
1	23.67	1,119,119	19,167	3,988	0.00	0.00	133.85
2	24.35	1,051,930	39,557	4,015	0.00	0.00	315.67
3	24.30	1,031,590	55,443	4,103	0.00	0.00	457.78
4	24.27	1,013,935	72,490	4,227	0.00	0.00	608.86
5	24.24	1,004,667	86,795	4,517	0.00	0.00	733.79
6	24.21	999,083	98,579	4,453	0.00	0.00	836.84
7	24.19	992,957	113,487	4,471	0.00	0.00	962.24
8	24.18	987,532	126,680	4,600	0.00	0.00	1065.42
9	24.17	984,954	138,555	4,673	0.00	0.00	1153.04
10	24.16	984,367	150,730	4,885	0.00	0.00	1241.82
11	24.14	981,948	163,389	5,315	0.00	0.00	1329.82
12	24.15	981,903	174,534	5,681	0.00	0.00	1404.29
13	24.14	981,948	185,491	5,495	0.00	0.00	1478.67
14	24.14	981,948	197,296	5,613	0.00	323.60	1213.30
15	24.09	981,948	210,667	6,180	0.00	337.74	1277.48
16	24.03	982,445	220,632	5,830	0.00	349.01	1328.83
17	23.96	983,327	233,406	6,370	0.00	362.00	1389.52

Appendix C: Single- and two-phase measured data (continued).

Channel B: Nitrogen gas tests.

Number of channels: 3

Channel Dimensions:

Depth ( $\mu\text{m}$ ): 211.14

Hyd. Diameter ( $\mu\text{m}$ ): 210.05

Width ( $\mu\text{m}$ ): 208.97

Channel Length (m): 0.0635

Data Point	Test Fixture Temperature		Test Section Temperature, ( $^{\circ}\text{C}$ )						
	Inlet	Outlet	Pos #1	Pos #2	Pos #3	Pos #4	Pos #5	Pos #6	Pos #7
1	37.88	44.36	62.52	63.73	64.37	66.10	65.70	65.94	65.17
2	37.53	47.57	63.89	65.16	65.84	67.57	67.16	67.42	66.64
3	37.04	49.70	64.39	65.70	66.42	68.15	67.73	68.00	67.23
4	36.61	51.84	64.45	65.79	66.55	68.28	67.86	68.16	67.41
5	36.24	52.47	64.45	65.81	66.58	68.32	67.89	68.21	67.45
6	36.00	54.86	64.33	65.70	66.51	68.25	67.81	68.15	67.42
7	35.78	55.45	64.23	65.63	66.44	68.19	67.75	68.10	67.37
8	35.91	55.13	64.04	65.45	66.30	68.05	67.60	67.96	67.23
9	35.77	55.08	63.67	65.10	65.98	67.73	67.28	67.66	66.94
10	35.59	55.49	63.37	64.83	65.75	67.49	67.04	67.45	66.76
11	35.23	55.71	63.13	64.62	65.58	67.33	66.88	67.32	66.65
12	35.10	55.60	62.76	64.28	65.27	67.02	66.57	67.04	66.40
13	34.89	55.57	62.34	63.88	64.89	66.65	66.19	66.69	66.07
14	34.74	55.61	61.93	63.49	64.55	66.30	65.84	66.36	65.76
15	34.54	55.61	61.58	63.16	64.24	66.00	65.54	66.07	65.50
16	34.28	55.58	61.19	62.79	63.90	65.66	65.20	65.76	65.21
17	33.96	55.46	60.61	62.24	63.39	65.15	64.68	65.28	64.76

Data Point	Gas Flow Meter		Test Fixture Press., (Pa)		Gas Flow Rates, (cc/min)		
	Temp. ( $^{\circ}\text{C}$ )	Press. (Pa)	Inlet	Outlet	F.M. #4	F.M. #5	F.M. #6
1	23.84	1,073,704	12,962	3,653	0.00	94.98	0.00
2	23.84	935,845	26,614	3,663	0.00	227.52	0.00
3	23.83	906,106	41,782	3,734	0.00	358.57	0.00
4	23.79	895,074	56,675	3,850	0.00	0.00	458.12
5	23.79	885,535	71,983	3,979	0.00	0.00	558.73
6	23.79	880,991	86,736	4,092	0.00	0.00	644.17
7	23.79	877,103	101,895	4,137	0.00	0.00	715.23
8	23.79	871,723	122,310	4,311	0.00	0.00	764.32
9	23.81	870,253	147,672	4,413	0.00	0.00	812.20
10	23.81	867,744	171,121	4,551	0.00	0.00	843.05
11	23.83	866,772	194,782	4,589	0.00	0.00	874.12
12	23.83	864,466	193,823	4,842	0.00	0.00	960.88
13	23.82	864,737	212,704	5,321	0.00	0.00	984.45
14	23.84	861,980	236,706	5,129	0.00	215.20	803.93
15	23.86	861,414	256,502	5,224	0.00	218.51	821.38
16	23.86	861,980	278,778	5,550	0.00	221.43	837.81
17	23.90	871,632	308,348	5,816	0.00	224.42	856.46

Appendix C: Single- and two-phase measured data (continued).

Channel B: Water tests.

Number of channels: 3

Channel Dimensions:

Depth ( $\mu\text{m}$ ): 211.14

Hyd. Diameter ( $\mu\text{m}$ ): 210.05

Width ( $\mu\text{m}$ ): 208.97

Channel Length (m): 0.0635

Data Point	Test Fixture Temperature		Test Section Temperature, ( $^{\circ}\text{C}$ )						
	Inlet	Outlet	Pos #1	Pos #2	Pos #3	Pos #4	Pos #5	Pos #6	Pos #7
1	24.33	41.75	41.46	45.41	49.01	51.39	50.05	52.37	53.11
2	25.03	39.39	38.67	42.12	45.35	47.75	46.43	48.35	48.90
3	24.57	35.43	35.37	38.41	41.21	43.67	42.39	43.83	43.98
4	25.14	35.17	35.31	38.94	42.16	44.85	43.31	44.92	45.15
5	25.57	35.20	36.27	40.16	43.61	46.55	44.69	46.16	45.84
6	25.78	35.75	36.92	41.04	44.49	47.76	45.65	47.25	46.97
7	26.47	36.84	37.63	41.77	45.53	49.18	46.71	48.57	48.68
8	26.64	37.82	37.89	41.38	45.76	49.62	46.73	49.07	49.87
9	27.65	38.99	38.40	41.87	46.61	50.83	47.50	49.43	49.29
10	27.80	39.94	39.04	42.64	47.60	52.17	48.38	50.16	50.44
11	28.14	39.46	38.51	41.92	46.77	51.29	47.51	49.21	49.65
12	27.98	40.27	39.10	42.60	47.88	52.75	48.44	50.34	51.08
13	28.00	39.82	38.70	42.09	47.34	52.21	47.88	49.75	50.54
14	28.26	39.24	38.15	41.43	46.58	51.38	47.11	48.95	49.76
15	28.16	38.78	37.72	40.97	46.07	50.87	46.60	48.39	49.24
16	28.13	39.62	38.42	41.95	47.53	52.73	47.93	49.87	50.86
17	28.12	39.05	37.91	41.37	46.89	52.09	47.30	49.19	50.20
18	28.14	38.85	37.75	41.18	46.67	51.88	47.08	48.95	49.98
19	29.47	40.02	38.81	42.55	48.65	54.32	48.92	51.29	53.98
20	29.32	39.51	38.35	41.96	47.81	53.53	48.10	49.99	51.35
21	29.33	38.98	37.94	41.38	47.11	52.81	47.41	49.23	50.64
22	29.37	38.59	37.54	40.93	46.59	52.28	46.90	48.68	50.13
23	29.62	38.18	37.17	40.44	46.02	51.70	46.36	48.08	49.59
24	29.60	37.58	36.43	39.61	45.03	50.68	45.39	47.15	48.78
25	29.62	37.18	35.86	38.91	44.32	49.93	44.61	46.52	48.26
26	29.55	36.95	35.44	38.43	43.79	49.31	43.97	46.00	47.88
27	29.59	36.45	34.77	37.69	42.94	48.43	43.04	45.17	47.23
28	29.58	36.11	34.31	37.17	42.31	47.81	42.40	44.59	46.77
29	29.80	35.67	33.90	36.60	41.56	47.03	41.64	43.87	46.15
30	29.73	35.23	33.56	36.12	40.93	46.33	40.91	43.18	45.54
31	29.67	34.87	33.33	35.77	40.49	45.80	40.41	42.55	45.06
32	28.37	34.61	33.14	35.40	39.93	45.33	39.84	42.13	44.73
33	28.30	34.00	32.81	34.79	39.06	44.43	38.97	41.15	43.85
34	27.75	34.41	33.38	35.83	40.76	45.91	41.26	43.56	43.65
35	27.89	34.07	33.19	35.46	40.24	45.38	40.78	42.97	43.11
36	27.98	33.82	33.05	35.18	39.88	45.01	40.43	42.58	42.75
37	28.03	33.64	32.96	35.01	39.66	44.80	40.21	42.34	42.59
38	28.03	33.46	32.81	34.77	39.37	44.53	39.93	42.02	42.27
39	28.03	33.29	32.68	34.57	39.12	44.28	39.69	41.76	42.05



## Appendix C: Single- and two-phase measured data (continued).

## Channel B: Water tests (continued).

Data Point	Liquid Flow Meter		Test Fixture Press., (Pa)		liquid Flow Rate
	Temp.(°C)	Press.(Pa)	Inlet	Outlet	F. M. #1, (cc/min)
1	23.19	2,718,923	120,945	92,025	10.20
2	23.83	2,832,133	141,322	95,025	14.60
3	24.49	2,882,114	175,076	96,131	20.02
4	25.48	2,881,159	204,380	95,834	27.64
5	26.33	2,859,915	238,189	95,211	35.26
6	26.93	2,861,317	271,921	95,667	42.95
7	27.40	2,888,037	310,186	96,413	48.53
8	27.60	2,885,550	342,784	96,359	50.37
9	27.78	2,910,552	376,450	97,198	54.76
10	27.89	2,926,082	411,448	97,763	57.96
11	27.98	2,936,933	446,119	98,084	60.27
12	28.03	2,937,453	489,752	98,228	64.86
13	28.06	2,887,788	521,176	96,696	67.13
14	28.11	2,891,247	554,696	97,080	70.98
15	28.13	2,885,120	590,714	96,850	74.28
16	28.17	2,886,545	616,154	97,033	75.17
17	28.20	2,891,224	661,508	97,421	80.48
18	28.23	2,864,459	682,475	96,707	81.45
19	29.29	2,874,292	762,331	97,525	89.72
20	29.42	2,885,731	839,959	98,323	96.44
21	29.49	2,871,308	907,709	98,339	100.54
22	29.54	2,860,277	967,704	98,176	105.57
23	29.58	2,833,941	1,030,797	97,670	110.11
24	29.65	2,813,076	1,140,276	97,749	117.52
25	29.70	2,795,353	1,243,946	97,749	124.02
26	29.88	2,751,272	1,326,162	96,786	130.06
27	29.94	2,744,626	1,450,584	97,290	140.99
28	29.94	2,709,474	1,534,813	96,843	148.58
29	29.93	2,675,995	1,633,758	96,488	154.87
30	29.94	2,712,142	1,766,363	98,378	165.15
31	29.93	2,670,935	1,855,684	98,470	178.25
32	29.93	2,657,029	1,958,918	98,296	185.20
33	29.92	2,673,418	2,175,594	100,729	205.77
34	29.24	4,135,622	2,084,419	103,394	134.52
35	29.45	4,128,049	2,424,228	104,280	147.70
36	29.64	4,093,959	2,777,329	104,737	161.82
37	29.78	4,037,332	3,092,294	104,775	172.04
38	29.86	4,011,449	3,445,213	104,673	181.40
39	29.93	4,009,640	3,811,290	105,510	192.81

# Appendix C: Single- and two-phase measured data (continued).

Channel B: Water and argon tests. Number of channels: 3

Channel Dimensions:

Depth ( $\mu\text{m}$ ): 211.14 Hyd. Diameter ( $\mu\text{m}$ ): 210.05

Width ( $\mu\text{m}$ ): 208.97 Channel Length (m): 0.0635

Data Point	Test Fixture Temperature		Test Section Temperature, ( $^{\circ}\text{C}$ )						
	Inlet	Outlet	Pos #1	Pos #2	Pos #3	Pos #4	Pos #5	Pos #6	Pos #7
1	28.71	50.87	46.87	52.31	56.80	59.35	57.71	60.45	60.99
2	29.09	54.08	46.92	52.42	57.11	59.65	57.96	61.02	61.87
3	29.29	54.03	45.81	50.91	55.65	58.19	56.45	59.69	60.84
4	29.51	53.99	45.84	50.80	55.55	58.07	56.33	59.52	60.46
5	29.93	53.78	46.08	50.88	55.55	58.08	56.32	59.40	60.04
6	29.01	49.63	41.82	46.04	50.57	53.15	51.39	54.54	55.45
7	27.44	39.30	37.78	42.68	47.10	50.23	48.01	50.27	50.75
8	28.08	41.49	36.73	40.35	44.38	47.56	45.37	47.65	48.99
9	28.33	40.08	35.34	38.43	42.36	45.46	43.26	45.59	46.97
10	28.37	40.17	35.19	38.18	42.17	45.23	42.99	45.50	46.91
11	28.09	40.52	35.31	38.27	42.38	45.42	43.13	45.85	47.29
12	28.04	39.62	34.54	37.20	41.24	44.26	41.94	44.74	46.30
13	28.54	38.89	36.75	39.60	44.13	48.21	44.87	47.11	48.95
14	28.95	40.36	36.60	39.62	44.28	48.35	44.96	47.50	49.56
15	28.67	40.08	36.15	38.98	43.66	47.70	44.28	46.92	49.00
16	28.62	39.78	35.63	38.17	42.91	46.91	43.42	46.33	48.57
17	28.55	39.78	35.27	37.69	42.40	46.36	42.84	45.92	48.32
18	28.41	40.02	35.13	37.58	42.32	46.24	42.67	45.89	48.42
19	29.04	38.12	36.29	38.33	43.90	49.44	44.19	47.00	50.43
20	29.11	39.40	36.43	38.60	44.36	49.90	44.51	47.64	51.16
21	28.91	40.04	36.47	38.68	44.43	49.96	44.41	47.74	51.56
22	28.89	39.96	36.29	38.40	43.92	49.33	43.56	46.93	51.06
23	25.92	34.31	31.46	33.76	37.55	41.42	38.38	35.55	42.56
24	26.37	31.79	30.76	32.33	35.58	37.00	36.59	35.74	40.44
25	26.53	31.90	30.67	32.18	35.32	39.22	36.23	33.08	40.37
26	25.42	35.31	33.48	36.16	41.10	45.58	41.84	38.48	44.86
27	25.77	36.33	33.95	36.62	41.74	46.11	42.23	39.49	45.83
28	26.71	37.46	34.81	37.57	42.48	46.96	43.23	40.87	47.17
29	27.09	40.15	40.48	44.69	50.16	53.35	50.01	50.10	54.66
30	27.80	36.21	34.29	37.45	42.98	48.22	43.41	46.20	46.85
31	27.78	36.26	34.23	37.39	42.93	48.16	43.35	46.15	46.84
32	27.75	36.58	34.30	37.55	43.18	48.41	43.58	46.43	47.15
33	27.68	36.78	34.29	37.60	43.27	48.48	43.65	46.55	47.29
34	27.62	37.13	34.40	37.79	43.55	48.78	43.89	46.87	47.62
35	27.99	37.44	34.68	38.01	43.72	48.92	44.07	47.05	47.83
36	27.94	37.77	34.75	38.17	43.96	49.13	44.29	47.35	48.13
37	27.85	37.78	34.71	38.18	43.99	49.14	44.31	47.40	48.17
38	27.77	37.94	34.73	38.27	44.13	49.26	44.43	47.59	48.37

## Appendix C: Single- and two-phase measured data (continued).

## Channel B: Water and argon (continued).

Data Point	Gas Flow Meter		Liquid Flow Meter		Test Fixture Press.. (Pa)		Flow Meter/Flow rates. (cc/min)			
	Temp.(°C)	Press.(Pa)	Temp.(°C)	Press.(Pa)	Inlet	Outlet	F.M. #4	F.M. #5	F.M. #6	F.M. #1
1	24.87	2,154,550	24.71	2,441,499	145,400	103188.2	0.00	0.00	64.36	8.86
2	24.88	2,065,800	24.74	2,403,950	261,073	114371.2	0.00	0.00	294.24	8.06
3	24.87	2,029,947	24.77	2,397,485	402,607	125479.6	0.00	0.00	419.11	8.06
4	24.87	2,014,756	24.84	2,399,000	548,934	136425.3	0.00	0.00	505.95	8.06
5	24.86	2,014,010	24.83	2,383,967	666,845	145203.1	0.00	122.57	455.49	8.06
6	24.86	2,018,486	24.86	2,379,762	847,917	153741.2	0.00	125.61	475.69	8.51
7	24.82	2,185,814	26.45	2,408,539	270,409	106038.7	0.00	0.00	50.37	34.59
8	25.31	2,068,558	27.22	2,403,476	456,680	115250.6	0.00	0.00	216.18	33.47
9	25.33	2,028,636	27.45	2,365,182	674,441	126413.2	0.00	0.00	300.23	34.66
10	25.33	2,009,241	27.57	2,387,494	843,531	138430.4	0.00	0.00	379.40	32.70
11	25.34	2,006,505	27.61	2,378,994	963,906	147447.8	0.00	94.91	353.06	30.70
12	25.39	2,010,100	27.66	2,384,736	1,121,129	155549.7	0.00	101.54	384.39	31.60
13	25.36	2,192,618	28.61	2,398,751	527,571	107248.1	0.00	32.92	0.00	63.81
14	25.38	2,053,389	28.70	2,396,174	712,870	117551.8	0.00	0.00	160.18	60.69
15	25.42	2,033,836	28.67	2,417,288	903,300	130816.8	0.00	0.00	245.29	58.44
16	25.44	2,012,496	28.66	2,380,938	1,087,040	140731.7	0.00	0.00	313.26	59.45
17	25.45	2,007,183	28.60	2,381,706	1,221,204	149651.9	0.00	79.05	293.97	57.58
18	25.45	2,007,274	28.51	2,388,353	1,320,262	159731.8	0.00	91.01	345.18	53.60
19	25.37	2,190,629	29.08	2,372,958	1,007,987	108448.5	0.00	0.00	22.04	105.46
20	25.37	2,070,118	29.10	2,328,244	1,130,691	119342.2	0.00	0.00	112.70	97.16
21	25.39	2,032,728	29.07	2,328,131	1,235,921	132080.5	0.00	0.00	197.08	91.10
22	25.39	2,012,699	28.98	2,283,960	1,284,930	141111.5	0.00	0.00	276.96	88.01
23	24.50	1,938,349	27.51	2,131,891	1,705,260	154107.5	0.00	61.68	230.12	86.16
24	24.42	1,905,842	28.15	2,100,786	1,583,347	105955.1	0.00	18.58	0.00	130.09
25	24.40	1,919,948	28.31	2,050,488	1,726,125	119536.6	0.00	18.09	63.33	129.17
26	23.52	2,746,706	27.10	1,950,955	1,203,911	109350.5	0.00	18.86	0.00	86.08
27	23.57	2,722,359	27.38	1,927,739	1,251,428	114583.7	0.00	73.78	0.00	80.18
28	24.24	2,685,286	28.20	1,885,467	1,243,335	120897.5	0.00	0.00	127.67	78.76
29	24.21	2,646,337	28.28	1,850,043	927,217	296229.4	0.00	0.00	269.74	111.88
30	24.06	4,016,783	29.04	4,060,111	1,617,725	118679.8	0.00	0.00	87.55	100.89
31	24.10	3,985,090	29.02	4,072,092	1,700,982	122075.2	0.00	0.00	107.52	101.57
32	24.08	3,980,795	28.94	4,014,538	1,760,412	126033.5	0.00	0.00	139.63	98.78
33	24.04	3,985,113	28.84	3,966,003	1,826,692	129135	0.00	0.00	164.99	96.70
34	24.01	3,944,739	28.75	3,930,738	1,919,059	134065.3	0.00	0.00	214.33	93.43
35	24.50	3,952,199	29.18	3,927,438	2,014,342	136549.6	0.00	0.00	211.35	93.67
36	24.49	3,970,171	29.10	3,854,489	2,109,150	141186.1	0.00	53.38	179.01	90.27
37	24.51	3,953,013	29.01	3,840,135	2,196,136	145564.8	0.00	58.00	196.37	89.52
38	24.52	3,943,699	28.92	3,836,224	2,271,843	150131.1	0.00	62.38	214.19	87.63

# Appendix C: Single- and two-phase measured data (continued).

Channel B: Water and helium tests. Number of channels: 3

Channel Dimensions:

Depth ( $\mu\text{m}$ ): 211.14 Hyd. Diameter ( $\mu\text{m}$ ): 210.05

Width ( $\mu\text{m}$ ): 208.97 Channel Length (m): 0.0635

Data Point	Test Fixture Temperature		Test Section Temperature, ( $^{\circ}\text{C}$ )						
	Inlet	Outlet	Pos #1	Pos #2	Pos #3	Pos #4	Pos #5	Pos #6	Pos #7
1	24.95	40.90	38.12	42.63	46.29	48.98	47.51	49.86	50.15
2	25.15	42.90	38.45	43.05	46.80	49.41	48.00	50.45	50.58
3	25.09	43.68	38.20	42.61	46.50	49.09	47.64	50.33	50.69
4	25.19	43.53	38.30	42.38	46.15	48.73	47.27	49.93	50.29
5	24.02	34.55	34.70	38.87	42.43	45.43	43.66	45.45	45.17
6	24.40	37.14	34.84	39.33	43.19	46.18	44.39	46.37	46.35
7	24.63	39.45	35.45	39.70	43.57	46.51	44.68	46.93	47.29
8	25.17	42.44	37.14	41.45	45.56	48.46	46.58	49.34	49.86
9	24.57	34.26	34.58	38.46	42.10	45.59	43.23	44.14	44.59
10	24.96	37.00	34.90	38.88	42.62	46.10	43.73	45.17	46.07
11	25.23	40.22	36.28	40.54	44.72	48.17	45.73	47.86	48.89
12	25.52	44.60	38.73	43.63	48.58	51.96	49.39	52.26	53.34
13	25.13	34.21	33.75	36.47	39.79	43.52	40.95	42.36	43.27
14	25.40	35.71	34.01	37.09	40.76	44.48	41.88	43.57	44.62
15	25.56	37.32	34.54	38.01	42.02	45.71	43.06	45.04	46.07
16	23.67	31.90	32.00	34.96	39.25	44.29	40.05	41.39	42.24
17	24.08	32.62	32.46	35.49	39.85	44.92	40.63	41.99	42.88
18	24.38	33.12	32.79	35.87	40.28	45.36	41.06	42.45	43.35
19	24.55	33.45	32.92	36.01	40.47	45.54	41.22	42.65	43.63
20	24.69	33.63	33.05	36.15	40.65	45.71	41.38	42.83	43.82
21	24.91	32.56	32.93	35.59	40.03	45.50	40.75	41.95	43.14
22	25.08	32.65	32.86	35.49	39.94	45.39	40.65	41.85	43.08
23	25.11	32.85	32.94	35.63	40.15	45.61	40.84	42.07	43.31
24	25.16	33.09	33.04	35.80	40.40	45.85	41.06	42.33	43.58
25	25.09	33.22	33.04	35.85	40.50	45.95	41.14	42.45	43.71
26	25.21	31.98	32.52	34.83	39.14	44.61	39.89	40.93	42.22
27	25.26	32.16	32.56	34.91	39.27	44.75	40.00	41.07	42.39
28	25.28	32.25	32.57	34.94	39.33	44.80	40.04	41.14	42.46
29	25.24	32.33	32.56	35.01	39.45	44.91	40.14	41.29	42.62
30	25.20	32.27	32.48	34.92	39.37	44.82	40.05	41.21	42.54

## Appendix C: Single- and two-phase measured data (continued).

Channel A: Water and helium (continued).

Data Point	Gas Flow Meter		Liquid Flow Meter		Test Fixture Press., (Pa)		Flow Meter/Flow rates, (cc/min)			
	Temp.(°C)	Press.(Pa)	Temp.(°C)	Press.(Pa)	Inlet	Outlet	F.M. #4	F.M. #5	F.M. #6	F.M. #1
1	23.36	1,016,919	23.64	1,208,652	251,414	111,249	0.00	55.58	0.00	15.54
2	23.41	988,797	23.70	1,185,549	370,659	124,449	0.00	0.00	298.01	11.54
3	23.45	984,683	23.69	1,171,805	518,229	140,960	0.00	0.00	521.33	12.47
4	23.46	979,122	23.66	1,151,392	670,297	156,386	0.03	152.05	583.36	10.93
5	23.42	1,025,080	24.09	1,064,134	388,630	103,195	0.00	42.68	0.00	32.95
6	23.44	994,358	24.46	1,048,875	504,190	115,404	0.00	0.00	254.98	28.05
7	23.48	985,497	24.62	1,039,426	631,686	131,113	0.00	0.00	471.80	22.84
8	23.51	981,292	24.63	1,041,416	770,644	145,126	0.00	135.39	517.73	15.33
9	23.49	1,031,590	25.72	970,140	587,221	97,399	0.00	31.73	0.00	50.20
10	23.46	997,320	25.89	974,164	687,251	110,499	0.00	0.00	207.04	41.76
11	23.46	988,278	25.90	987,388	791,011	127,424	0.01	0.01	406.06	32.90
12	23.43	987,712	25.75	1,004,365	892,420	142,459	0.08	124.20	475.82	21.44
13	23.40	1,208,050	26.53	1,348,333	812,668	96,176	0.00	26.29	0.00	61.57
14	23.41	1,157,323	26.64	1,370,215	916,563	111,652	0.00	0.00	164.45	55.23
15	23.40	1,134,220	26.62	1,396,687	1,036,306	129,305	0.00	0.00	326.95	47.59
16	22.45	4,589,069	25.00	3,803,988	1,499,926	117,889	0.00	0.00	65.19	105.87
17	22.51	4,145,161	25.49	3,822,502	1,615,644	130,112	0.00	0.00	155.62	103.02
18	22.48	4,110,484	25.76	3,820,468	1,678,330	137,160	0.00	0.00	216.78	101.46
19	22.42	4,076,304	25.96	3,832,358	1,842,876	149,623	0.00	59.61	211.55	100.30
20	22.40	4,036,315	26.07	3,850,194	1,926,630	156,440	0.00	69.51	252.23	98.16
21	22.32	4,208,728	26.50	3,784,118	2,141,882	120,167	0.00	0.00	59.07	128.55
22	22.32	4,126,218	26.64	3,830,573	2,346,531	131,974	0.00	0.00	112.84	132.61
23	22.27	4,084,917	26.68	3,828,244	2,421,898	140,551	0.00	0.00	164.54	132.26
24	22.25	4,084,623	26.70	3,825,305	2,510,128	150,246	0.00	45.61	161.36	127.41
25	22.22	4,027,770	26.68	3,840,655	2,600,302	158,172	0.00	53.74	194.77	124.86
26	22.17	4,401,057	26.94	3,774,510	2,771,156	121,313	0.00	0.00	43.44	153.17
27	22.24	4,083,402	26.99	3,834,529	2,898,607	134,832	0.00	0.00	99.99	154.23
28	22.25	4,071,625	26.99	3,836,721	2,981,999	142,117	0.00	0.00	136.60	150.69
29	22.23	4,070,517	26.97	3,847,482	3,083,092	153,269	0.00	39.14	139.29	148.14
30	22.21	4,029,262	26.95	3,844,046	3,214,341	159,370	0.00	43.87	159.28	149.82

Appendix C: Single- and two-phase measured data (continued).

Channel B: Water and nitrogen tests. Number of channels: 3

Channel Dimensions:

Depth ( $\mu\text{m}$ ): 211.14 Hyd. Diameter ( $\mu\text{m}$ ): 210.05

Width ( $\mu\text{m}$ ): 208.97 Channel Length (m): 0.0635

Data Point	Test Fixture Temperature		Test Section Temperature, ( $^{\circ}\text{C}$ )						
	Inlet	Outlet	Pos #1	Pos #2	Pos #3	Pos #4	Pos #5	Pos #6	Pos #7
1	25.10	38.06	36.55	40.67	43.98	26.57	45.23	46.81	47.26
2	25.23	40.73	36.42	40.51	44.16	26.58	45.32	47.34	48.34
3	25.50	42.26	36.69	40.59	44.39	26.57	45.46	47.93	49.19
4	25.52	42.90	37.04	40.94	44.80	26.56	45.83	48.36	49.54
5	25.56	42.70	36.88	40.74	44.61	26.61	45.62	48.13	49.25
6	24.53	32.54	32.93	36.08	39.13	25.61	40.38	41.30	41.93
7	25.05	36.92	33.74	37.03	40.54	25.69	41.71	43.67	45.09
8	25.21	38.86	34.64	38.25	42.11	45.28	43.17	45.40	46.73
9	25.21	40.15	35.36	39.21	43.30	46.46	44.28	46.69	47.96
10	25.24	41.51	36.21	40.28	44.56	47.66	45.46	48.03	49.21
11	24.93	33.46	32.95	35.58	38.80	42.35	40.00	41.51	42.93
12	25.28	36.13	33.66	36.74	40.34	43.86	41.44	43.25	44.72
13	25.30	38.03	34.59	38.12	42.08	45.57	43.10	45.17	46.47
14	25.41	39.07	35.18	38.94	43.10	46.56	44.05	46.28	47.54
15	25.30	33.40	33.01	35.54	38.90	42.69	40.01	41.47	43.00
16	25.39	35.67	33.79	36.83	40.55	44.33	41.60	43.30	44.69
17	25.38	37.69	34.79	38.36	42.54	46.28	43.48	45.54	46.90
18	27.44	35.20	35.30	37.85	42.28	47.69	42.97	44.12	45.40
19	27.44	35.45	35.32	37.93	42.41	47.79	43.08	44.28	45.56
20	27.39	35.41	35.23	37.83	42.35	47.75	43.00	44.22	45.52
21	27.36	35.41	35.12	37.72	42.25	47.62	42.88	44.13	45.43
22	27.90	35.79	34.08	37.09	42.55	47.82	42.98	45.79	46.36
23	27.99	36.31	34.27	37.37	42.93	48.26	43.30	46.25	46.84
24	27.96	36.52	34.31	37.45	43.02	48.30	43.39	46.37	46.97
25	27.87	36.77	34.27	37.45	43.08	48.32	43.44	46.46	47.12
26	27.76	37.04	34.32	37.63	43.34	48.56	43.70	46.77	47.46

## Appendix C: Single- and two-phase measured data (continued).

Channel B: Water and nitrogen (continued).

Data Point	Gas Flow Meter		Liquid Flow Meter		Test Fixture Press., (Pa)		Flow Meter/Flow rates, (cc/min)			
	Temp.(°C)	Press.(Pa)	Temp.(°C)	Press.(Pa)	Inlet	Outlet	F.M. #4	F.M. #5	F.M. #6	F.M. #1
1	23.62	1,216,369	25.43	1,326,157	237,671	100,731	0.00	42.61	0.00	22.58
2	23.61	1,214,990	25.39	1,315,668	415,329	111,249	0.00	0.00	243.71	18.38
3	23.59	1,202,195	25.30	1,309,609	589,121	124,105	0.00	0.00	365.99	17.00
4	23.56	1,196,883	25.16	1,316,527	671,677	130,966	0.00	89.09	332.00	13.22
5	23.59	1,195,526	25.06	1,332,871	787,735	138,657	0.00	97.06	369.18	14.94
6	23.51	1,226,722	25.67	1,323,987	415,148	103,952	0.00	30.09	0.00	46.43
7	23.56	1,220,754	25.92	1,308,276	629,043	113,361	0.00	0.00	190.18	36.81
8	23.54	1,205,270	25.94	1,319,827	785,045	127,168	0.00	0.00	301.20	31.49
9	23.54	1,201,200	25.89	1,323,015	865,046	132,942	0.00	74.77	278.81	27.89
10	23.58	1,195,798	25.83	1,334,363	952,010	140,680	0.00	85.50	325.70	24.22
11	23.55	1,232,916	26.49	1,305,043	623,323	100,561	0.00	23.94	0.00	63.56
12	23.56	1,221,885	26.60	1,294,305	793,838	114,147	0.00	0.00	163.97	56.00
13	23.57	1,206,083	26.54	1,302,285	930,128	127,681	0.00	0.00	274.60	42.82
14	23.59	1,201,472	26.45	1,314,221	993,763	133,758	0.00	68.23	254.69	37.35
15	23.50	1,236,126	26.88	1,298,307	802,835	101,701	0.00	19.51	0.00	74.00
16	23.52	1,225,343	26.86	1,294,238	928,523	115,339	0.00	0.00	143.88	61.24
17	23.53	1,207,281	26.70	1,301,268	1,040,624	128,794	0.00	0.00	255.47	48.91
18	24.24	4,288,956	29.03	3,886,883	2,273,764	116,051	0.00	0.00	42.86	135.46
19	24.20	3,934,363	29.03	3,888,262	2,379,898	124,435	0.00	0.00	81.73	132.77
20	24.18	3,929,661	29.01	3,885,097	2,577,223	131,106	0.00	0.00	111.28	134.30
21	24.15	3,905,360	29.00	3,874,224	2,822,291	139,995	0.00	30.79	106.53	131.93
22	23.92	4,604,034	29.50	4,067,186	1,447,165	112,454	0.00	0.00	47.59	101.24
23	24.09	3,724,741	29.48	4,083,508	1,677,178	125,333	0.00	0.00	124.06	100.68
24	24.08	3,711,810	29.37	4,091,397	1,765,928	130,604	0.00	0.00	152.60	99.76
25	24.05	3,740,316	29.21	4,048,898	1,926,993	138,076	0.00	42.01	145.15	98.58
26	24.06	3,697,885	29.01	4,015,532	2,006,475	144,154	0.00	50.57	178.35	93.37

## Appendix C: Single- and two-phase measured data (continued).

Channel C1: Argon gas tests.

Number of channels:

5

Channel Dimensions:

Depth ( $\mu\text{m}$ ): 134.64Hyd. Diameter ( $\mu\text{m}$ ): 127.92Width ( $\mu\text{m}$ ): 121.83

Channel Length (m): 0.0635

Data Point	Test Fixture Temperature		Test Section Temperature, ( $^{\circ}\text{C}$ )						
	Inlet	Outlet	Pos #1	Pos #2	Pos #3	Pos #4	Pos #5	Pos #6	Pos #7
1	32.79	33.37	39.13	39.37	39.40	41.18	41.13	41.15	40.84
2	32.13	34.42	42.01	42.41	42.49	44.26	44.17	44.17	43.67
3	31.86	37.64	48.79	49.56	49.73	51.48	51.31	51.30	50.43
4	31.87	40.47	51.56	52.41	52.63	54.37	54.19	54.20	53.27
5	31.77	43.86	52.51	53.42	53.66	55.40	55.22	55.25	54.32
6	31.73	45.13	52.92	53.86	54.14	55.87	55.69	55.74	54.82
7	31.78	45.10	53.18	54.16	54.47	56.20	56.01	56.08	55.17
8	31.93	44.51	53.47	54.49	54.83	56.56	56.37	56.46	55.56
9	31.80	44.57	53.61	54.66	55.03	56.77	56.58	56.68	55.79
10	31.70	45.10	53.68	54.77	55.16	56.89	56.70	56.82	55.94
11	31.63	45.55	53.66	54.77	55.20	56.93	56.74	56.88	56.01
12	31.56	47.79	53.50	54.64	55.09	56.83	56.64	56.80	55.95
13	31.55	48.69	53.32	54.48	54.96	56.69	56.50	56.68	55.85
14	31.66	49.09	53.11	54.29	54.80	56.53	56.34	56.54	55.72
15	31.59	49.30	52.98	54.19	54.72	56.45	56.26	56.47	55.66
16	31.51	49.51	52.76	53.99	54.54	56.27	56.08	56.30	55.51
17	31.39	49.52	52.46	53.71	54.29	56.02	55.84	56.07	55.29
18	31.29	49.46	52.06	53.33	53.93	55.66	55.48	55.73	54.96

Data Point	Gas Flow Meter		Test Fixture Press., (Pa)		Gas Flow Rates, (cc/min)		
	Temp. ( $^{\circ}\text{C}$ )	Press. (Pa)	Inlet	Outlet	F.M. #4	F.M. #5	F.M. #6
1	23.78	1,216,866	17,972	3,538	26.96	0.00	0.00
2	23.76	1,184,065	62,053	3,520	0.00	104.62	0.00
3	23.75	1,189,016	131,000	3,585	0.00	216.51	0.00
4	23.65	1,179,137	191,674	3,723	0.00	295.15	0.00
5	23.61	1,184,676	270,274	3,997	0.00	0.00	349.69
6	23.54	1,187,841	335,084	4,137	0.00	0.00	390.93
7	23.49	1,183,387	424,716	4,365	0.00	0.00	407.25
8	23.52	1,181,895	510,210	4,551	0.00	0.00	418.16
9	23.50	1,178,708	591,568	4,700	0.00	0.00	432.75
10	23.50	1,175,000	673,152	4,994	0.00	0.00	446.74
11	23.51	1,178,550	739,952	5,240	0.00	0.00	458.40
12	23.54	1,177,012	824,339	5,561	0.00	0.00	471.21
13	23.60	1,178,595	895,682	5,875	0.00	0.00	480.14
14	23.64	1,425,313	976,226	6,006	0.00	0.00	487.01
15	23.64	1,427,687	1,033,826	6,352	0.00	105.73	393.36
16	23.64	1,431,259	1,113,850	6,264	0.00	106.32	398.19
17	23.63	1,430,496	1,195,616	6,647	0.00	106.49	401.29
18	23.68	1,427,777	1,288,298	6,958	0.00	106.62	404.40



## Appendix C: Single- and two-phase measured data (continued).

Channel C1: Helium gas tests. Number of channels: 5  
 Channel Dimensions:  
 Depth ( $\mu\text{m}$ ): 134.64 Hyd. Diameter ( $\mu\text{m}$ ): 127.92  
 Width ( $\mu\text{m}$ ): 121.83 Channel Length (m): 0.0635

Data Point	Test Fixture Temperature		Test Section Temperature, ( $^{\circ}\text{C}$ )						
	Inlet	Outlet	Pos #1	Pos #2	Pos #3	Pos #4	Pos #5	Pos #6	Pos #7
1	31.14	30.87	43.55	44.68	45.06	40.68	46.63	46.64	45.50
2	32.10	32.83	47.44	48.64	49.02	44.61	50.56	50.57	49.41
3	30.43	32.60	39.35	39.91	40.09	35.88	41.78	41.84	41.34
4	31.02	37.20	46.55	47.66	48.03	43.73	49.58	49.63	48.61
5	31.81	39.21	49.89	51.11	51.52	47.34	53.05	53.12	52.04
6	32.73	40.59	51.38	52.62	53.03	54.76	54.55	54.62	53.54
7	33.05	41.73	52.57	53.87	54.32	56.05	55.84	55.93	54.84
8	33.58	42.98	53.25	54.57	55.03	56.77	56.55	56.65	55.56
9	33.89	43.89	53.73	55.08	55.55	57.28	57.07	57.18	56.09
10	34.10	44.98	54.22	55.59	56.08	57.81	57.59	57.71	56.62
11	34.16	45.97	54.53	55.94	56.44	58.17	57.95	58.09	57.01
12	33.98	45.98	52.86	54.16	54.65	56.38	56.18	56.33	55.37
13	33.74	46.14	52.29	53.59	54.09	55.82	55.63	55.78	54.85
14	33.45	46.45	52.07	53.37	53.88	55.61	55.42	55.58	54.66
15	33.20	46.88	51.79	53.11	53.64	55.38	55.19	55.36	54.45
16	32.95	47.00	51.53	52.88	53.45	55.18	54.99	55.20	54.33
17	32.82	47.11	51.46	52.84	53.44	55.18	54.99	55.22	54.38
18	32.60	47.24	51.29	52.68	53.32	55.05	54.86	55.12	54.30

Data Point	Gas Flow Meter		Test Fixture Press., (Pa)		Gas Flow Rates, (cc/min)		
	Temp. ( $^{\circ}\text{C}$ )	Press. (Pa)	Inlet	Outlet	F.M. #4	F.M. #5	F.M. #6
1	23.64	1,235,561	20,684	3,757	32.72	0.00	0.00
2	24.10	1,069,364	63,432	3,549	0.00	111.63	0.00
3	24.06	1,042,622	126,863	3,626	0.00	223.11	0.00
4	24.00	1,023,316	177,884	3,721	0.00	307.99	0.00
5	23.97	1,012,285	217,874	3,825	0.00	0.00	394.83
6	23.94	1,006,769	251,873	3,888	0.00	0.00	458.17
7	23.90	1,002,700	286,798	4,001	0.00	0.00	521.29
8	23.89	1,001,253	315,847	4,135	0.00	0.00	579.36
9	23.88	999,874	346,116	4,220	0.00	0.00	632.78
10	23.87	999,852	372,316	4,408	0.00	0.00	681.42
11	23.83	1,000,869	397,137	4,758	0.00	0.00	725.73
12	23.81	999,874	423,337	4,982	0.00	0.00	768.19
13	23.81	999,874	448,158	5,202	0.00	0.00	808.93
14	23.81	1,001,253	472,979	5,274	0.00	0.00	850.85
15	23.82	1,002,632	496,421	5,186	0.00	184.87	693.43
16	23.83	1,004,011	522,621	5,480	0.00	191.43	723.99
17	23.83	1,005,390	543,305	5,450	0.00	197.14	750.71
18	23.85	1,006,769	565,368	5,627	0.00	202.66	777.16

## Appendix C: Single- and two-phase measured data (continued).

Channel C1: Nitrogen gas tests.      Number of channels:      5

Channel Dimensions:

Depth ( $\mu\text{m}$ ):      134.64      Hyd. Diameter ( $\mu\text{m}$ ):      127.92

Width ( $\mu\text{m}$ ):      121.83      Channel Length (m):      0.0635

Data Point	Test Fixture Temperature		Test Section Temperature, ( $^{\circ}\text{C}$ )						
	Inlet	Outlet	Pos #1	Pos #2	Pos #3	Pos #4	Pos #5	Pos #6	Pos #7
1	32.18	32.58	39.83	40.18	40.25	42.03	41.95	41.95	41.49
2	31.77	34.04	41.76	42.19	42.27	44.04	43.95	43.95	43.43
3	31.29	34.92	42.19	42.64	42.74	44.51	44.42	44.43	43.91
4	31.16	37.47	48.46	49.29	49.50	51.25	51.08	51.08	50.19
5	31.28	40.72	51.31	52.25	52.51	54.25	54.06	54.09	53.13
6	31.37	42.85	52.40	53.37	53.66	55.40	55.21	55.25	54.28
7	31.45	44.81	53.00	54.01	54.32	56.05	55.86	55.92	54.97
8	31.45	45.92	53.32	54.36	54.69	56.43	56.24	56.32	55.39
9	31.52	46.51	53.63	54.71	55.08	56.81	56.62	56.72	55.79
10	31.54	44.62	53.76	54.88	55.28	57.01	56.82	56.93	56.02
11	31.55	45.82	53.83	54.98	55.42	57.15	56.96	57.10	56.19
12	31.44	47.90	53.76	54.95	55.42	57.14	56.95	57.12	56.25
13	31.31	47.47	53.78	55.00	55.51	57.23	57.04	57.22	56.36
14	31.21	48.73	53.63	54.88	55.41	57.14	56.95	57.16	56.32
15	31.29	49.24	53.51	54.78	55.34	57.06	56.87	57.11	56.29
16	31.14	49.50	53.42	54.72	55.30	57.03	56.84	57.09	56.29
17	31.05	49.53	53.10	54.41	55.02	56.75	56.56	56.84	56.06
18	30.93	49.72	52.90	54.24	54.89	56.62	56.43	56.72	55.97

Data Point	Gas Flow Meter		Test Fixture Press., (Pa)		Gas Flow Rates, (cc/min)		
	Temp. ( $^{\circ}\text{C}$ )	Press. (Pa)	Inlet	Outlet	F.M. #4	F.M. #5	F.M. #6
1	23.67	1470095	13789.47	3447.367	0.00	21.51	0.00
2	23.66	1311516.2	44126.29	3510.663	0.00	87.59	0.00
3	23.68	1282942.6	86873.64	3503.881	0.00	177.41	0.00
4	23.66	1267389.9	128762	3585.261	0.00	249.42	0.00
5	23.60	1261761.1	175126.2	3711.853	0.00	0.00	308.54
6	23.54	1257737.2	213736.7	3813.579	0.00	0.00	360.26
7	23.54	1252221.5	248210.4	3885.917	0.00	0.00	400.52
8	23.56	1253600.4	288199.9	3998.945	0.00	0.00	437.51
9	23.56	1250842.5	330947.2	4132.319	0.00	0.00	460.10
10	23.57	1250842.5	384726.1	4161.706	0.00	0.00	469.21
11	23.56	1249463.6	439884	4412.629	0.00	0.00	479.66
12	23.60	1249463.6	495041.8	4532.439	0.00	0.00	491.80
13	23.64	1250842.5	540547.1	4690.679	0.00	0.00	502.12
14	23.72	1249463.6	588810.2	4803.708	0.00	0.00	513.94
15	23.80	1250842.5	631557.6	4857.961	0.00	111.41	415.73
16	23.86	1249802.6	678600	5088.539	0.00	112.58	422.94
17	23.91	1252198.8	729462.8	5348.505	0.00	113.34	428.67
18	23.94	1252221.5	780325.6	5506.744	0.00	114.10	434.49

# Appendix C: Single- and two-phase measured data (continued).

Channel C1: Water tests.

Number of channels: 5

Channel Dimensions:

Depth ( $\mu\text{m}$ ): 134.64Hyd. Diameter ( $\mu\text{m}$ ): 127.92Width ( $\mu\text{m}$ ): 121.83

Channel Length (m): 0.0635

Data Point	Test Fixture Temperature		Test Section Temperature, ( $^{\circ}\text{C}$ )						
	Inlet	Outlet	Pos #1	Pos #2	Pos #3	Pos #4	Pos #5	Pos #6	Pos #7
1	26.75	43.76	40.53	43.47	46.13	47.85	47.50	49.24	49.48
2	26.49	41.80	38.45	41.04	43.44	45.17	44.85	46.36	46.49
3	26.33	38.92	35.87	38.07	40.13	41.89	41.59	42.80	42.74
4	26.47	40.39	37.45	40.40	42.96	44.72	44.27	45.71	45.33
5	26.55	42.35	39.62	43.45	46.55	48.32	47.69	49.38	48.62
6	26.45	41.48	39.17	42.90	45.90	47.69	47.06	48.63	47.71
7	26.61	40.44	38.53	42.12	44.95	46.76	46.14	47.57	46.55
8	26.75	39.58	37.99	41.46	44.15	45.97	45.36	46.65	45.48
9	26.96	41.74	40.09	44.50	47.76	49.61	48.78	50.20	48.51
10	27.13	41.22	39.75	44.11	47.31	49.17	48.33	49.57	47.66
11	27.38	40.52	39.50	43.80	46.86	48.74	47.91	48.88	46.95
12	27.52	43.01	41.35	46.50	50.10	52.03	50.95	51.87	48.94
13	27.49	42.84	41.09	46.21	49.92	51.86	50.76	51.59	48.60
14	27.61	42.44	40.73	45.80	49.46	51.42	50.33	51.06	47.95
15	27.68	42.13	40.55	45.49	49.08	51.04	49.96	50.62	47.50
16	27.68	42.13	40.55	45.50	49.08	51.04	49.96	50.62	47.50
17	27.79	41.61	39.91	44.59	47.89	49.85	48.77	49.26	46.65
18	27.89	41.29	39.54	44.11	47.45	49.38	48.27	48.68	46.22
19	25.18	36.95	36.38	41.64	45.36	46.96	46.27	48.03	46.77
20	25.48	36.18	35.15	39.58	42.36	44.05	43.43	44.25	43.47
21	25.80	36.00	34.49	38.32	40.52	42.21	41.64	42.61	42.03
22	26.05	35.69	33.74	37.05	39.45	41.06	40.48	41.87	41.41
23	26.28	35.68	33.34	36.39	38.87	40.46	39.86	41.12	40.06
24	26.46	35.28	33.05	36.00	38.41	40.02	39.42	40.59	39.60
25	26.62	35.01	32.90	35.78	38.12	39.73	39.14	40.25	39.29
26	26.77	34.50	32.59	35.34	37.57	39.19	38.61	39.64	38.70

# Appendix C: Single- and two-phase measured data (continued).

## Channel C1: Water tests (continued).

Data Point	Liquid Flow Meter		Test Fixture Press., (Pa)		liquid Flow Rate
	Temp.(°C)	Press.(Pa)	Inlet	Outlet	F. M. #1, (cc/min)
1	25.20	2,258,019	227,526	95,035	8.71
2	25.26	2,231,771	267,945	93,716	10.41
3	25.37	2,225,893	351,044	93,628	15.89
4	25.61	2,190,063	423,789	92,708	18.32
5	25.89	2,194,313	484,010	93,092	23.56
6	26.28	2,188,911	548,097	92,875	26.49
7	26.66	2,179,574	617,859	92,652	29.16
8	27.02	2,181,632	685,540	92,166	32.25
9	27.28	2,200,100	748,361	92,686	36.96
10	27.57	2,214,658	837,201	93,377	38.00
11	27.78	2,198,088	897,287	92,604	40.35
12	27.97	2,202,592	954,760	92,311	43.90
13	28.14	2,185,994	1,030,525	91,858	46.39
14	28.28	2,213,754	1,113,556	93,307	48.00
15	28.39	2,194,823	1,165,486	92,222	49.71
16	28.39	2,194,878	1,165,504	92,220	49.63
17	28.54	2,239,751	1,318,296	93,886	51.16
18	28.58	2,217,190	1,376,573	93,217	53.90
19	26.68	4,734,604	1,055,228	103,758	43.43
20	27.01	4,706,460	1,396,641	103,780	52.23
21	27.37	4,680,599	1,719,021	103,692	56.38
22	27.67	4,649,381	2,084,487	103,317	61.27
23	27.94	4,644,724	2,429,405	103,464	65.28
24	28.18	4,623,950	2,775,294	103,209	71.40
25	28.41	4,605,029	3,130,475	103,170	76.75
26	28.71	4,571,504	3,812,804	103,281	87.08

## Appendix C: Single- and two-phase measured data (continued).

Channel C1: Water and argon tests. Number of channels: 5

Channel Dimensions:

Depth ( $\mu\text{m}$ ): 134.64 Hyd. Diameter ( $\mu\text{m}$ ): 127.92Width ( $\mu\text{m}$ ): 121.83 Channel Length (m): 0.0635

Data Point	Test Fixture Temperature		Test Section Temperature, ( $^{\circ}\text{C}$ )						
	Inlet	Outlet	Pos #1	Pos #2	Pos #3	Pos #4	Pos #5	Pos #6	Pos #7
1	26.97	39.98	36.53	39.72	42.24	44.05	43.63	45.05	44.81
2	27.16	41.60	38.01	41.57	44.19	46.00	45.55	46.98	46.44
3	27.44	43.24	39.77	43.59	46.27	48.08	47.62	49.03	48.25
4	27.53	43.14	39.80	43.66	46.34	48.15	47.69	49.03	48.09
5	28.38	46.47	43.26	47.46	50.25	52.03	51.52	52.89	51.75
6	26.88	38.17	35.67	39.07	41.64	43.49	42.97	44.15	43.11
7	27.01	39.26	36.44	40.09	42.78	44.63	44.09	45.33	44.12
8	27.00	40.57	37.54	41.51	44.32	46.16	45.60	46.87	45.55
9	27.16	41.91	38.66	42.86	45.74	47.58	47.00	48.25	46.85
10	26.90	40.87	37.97	42.33	45.47	47.35	46.65	48.01	46.32
11	27.09	42.08	38.73	43.30	46.57	48.44	47.72	49.11	47.36
12	27.56	43.28	39.73	44.58	47.92	49.79	49.06	50.42	48.61
13	27.67	44.71	40.85	45.95	49.39	51.25	50.49	51.86	50.05
14	27.79	46.12	41.97	47.32	50.87	52.73	51.95	53.37	51.54
15	26.39	37.36	34.80	37.52	39.44	41.17	40.93	42.04	41.74
16	26.37	37.39	34.98	37.73	39.61	41.36	41.12	42.18	41.76
17	26.23	37.03	34.80	37.50	39.34	41.08	40.84	41.84	41.30
18	25.85	35.87	33.59	36.13	37.95	39.66	39.40	40.41	39.89
19	25.60	35.09	32.99	35.45	37.16	38.89	38.65	39.56	39.02
20	25.54	34.96	32.99	35.40	37.07	38.80	38.56	39.45	38.89
21	25.51	35.03	33.11	35.53	37.20	38.93	38.69	39.58	38.98
22	25.64	33.05	31.36	34.21	36.45	38.04	37.53	38.78	38.27
23	25.93	33.76	31.88	34.76	37.06	38.65	38.14	39.38	38.89
24	26.12	33.92	32.04	34.91	37.22	38.82	38.30	39.53	39.06
25	26.22	34.36	32.32	35.27	37.60	39.20	38.67	39.92	39.40
26	26.35	34.57	32.50	35.53	37.90	39.50	38.96	40.21	39.64
27	26.39	35.07	32.83	35.97	38.43	40.02	39.47	40.77	40.14
28	26.43	35.55	33.14	36.38	38.93	40.52	39.96	41.30	40.65
29	26.45	36.35	33.65	37.10	39.80	41.40	40.82	42.26	41.53

Appendix C: Single- and two-phase measured data (continued).

Channel C1: Water and argon (continued).

Data Point	Gas Flow Meter		Liquid Flow Meter		Test Fixture Press., (Pa)		Flow Meter/Flow rates, (cc/min)			
	Temp.(°C)	Press.(Pa)	Temp.(°C)	Press.(Pa)	Inlet	Outlet	F.M. #4	F.M. #5	F.M. #6	F.M. #1
1	24.89	1,321,508	26.34	1,245,070	499,088	92,826	0.00	38.75	0.00	16.29
2	24.86	1,305,458	26.24	1,223,391	608,296	94,069	0.00	102.79	0.00	15.41
3	24.85	1,297,546	26.12	1,201,328	693,588	97,672	0.00	148.09	0.00	12.91
4	24.90	1,303,265	26.12	1,227,799	868,985	104,888	0.00	0.00	172.41	11.07
5	24.89	1,308,238	26.01	1,233,293	1,049,763	114,570	0.00	0.00	234.71	7.77
6	24.85	1,316,218	26.20	1,580,742	713,051	94,810	0.00	31.58	0.00	25.60
7	24.89	1,308,012	26.33	1,624,054	823,163	97,657	0.00	74.42	0.00	23.24
8	24.93	1,301,705	26.39	1,645,892	925,070	102,872	0.00	117.25	0.00	22.17
9	24.91	1,310,002	26.38	1,634,476	1,048,813	110,210	0.00	0.00	149.65	19.12
10	24.82	1,324,831	26.68	1,692,957	774,765	100,907	0.00	28.20	0.00	28.68
11	24.81	1,307,379	26.78	1,690,832	849,205	101,023	0.00	60.60	0.00	26.32
12	24.82	1,306,000	26.82	1,690,470	932,055	104,572	0.00	96.45	0.00	24.45
13	24.88	1,304,395	26.79	1,701,253	1,016,238	109,091	0.00	0.00	121.38	22.58
14	24.94	1,307,967	26.75	1,684,525	1,081,117	112,097	0.00	0.00	147.28	20.48
15	23.38	3,885,919	26.15	4,471,398	843,435	123,976	0.00	54.31	195.25	11.45
16	23.33	3,731,070	26.01	4,412,691	966,681	127,652	0.00	61.37	223.20	9.60
17	23.38	3,798,978	25.85	4,396,890	1,097,116	131,154	0.00	66.52	244.68	11.33
18	23.36	3,733,919	25.73	4,337,912	1,261,844	134,526	0.00	68.03	252.71	11.96
19	23.36	3,827,823	25.63	4,292,972	1,411,697	137,436	0.00	69.75	261.60	12.76
20	23.34	3,739,140	25.57	4,303,370	1,525,923	140,987	0.00	72.77	275.57	12.53
21	23.35	3,755,688	25.47	4,283,568	1,673,764	146,657	0.00	75.59	289.62	10.29
22	23.32	4,567,074	27.10	4,430,595	2,510,830	110,510	0.00	11.23	0.00	66.80
23	23.22	4,305,458	27.43	4,385,022	2,762,861	119,340	0.00	38.35	0.00	63.70
24	23.44	4,360,183	27.69	4,442,254	2,923,344	122,556	0.00	13.93	49.39	64.47
25	23.35	4,283,576	27.89	4,389,882	3,094,916	127,512	0.00	18.71	67.36	63.80
26	23.33	4,389,958	28.04	4,364,926	3,411,373	135,686	0.00	25.33	93.26	62.22
27	23.33	4,264,858	28.06	4,324,597	3,405,111	140,702	0.00	30.70	114.64	59.23
28	23.32	4,344,611	28.06	4,266,704	3,400,341	143,652	0.00	34.94	131.91	55.12
29	23.36	4,284,344	28.01	4,205,149	3,382,144	149,394	0.00	41.90	160.98	47.42

## Appendix C: Single- and two-phase measured data (continued).

Channel C1: Water and helium tests. Number of channels: 5

Channel Dimensions:

Depth ( $\mu\text{m}$ ): 134.64 Hyd. Diameter ( $\mu\text{m}$ ): 127.92Width ( $\mu\text{m}$ ): 121.83 Channel Length (m): 0.0635

Data Point	Test Fixture Temperature		Test Section Temperature, ( $^{\circ}\text{C}$ )						
	Inlet	Outlet	Pos #1	Pos #2	Pos #3	Pos #4	Pos #5	Pos #6	Pos #7
1	26.28	44.08	39.00	42.92	45.87	47.62	47.17	49.05	48.98
2	27.77	46.14	41.31	45.32	48.20	49.97	49.50	51.25	50.98
3	27.70	46.12	41.43	45.45	48.29	50.06	49.60	51.25	50.83
4	27.84	46.22	42.22	46.36	49.18	50.95	50.46	52.01	51.33
5	27.93	46.13	42.75	46.94	49.76	51.53	51.03	52.49	51.51
6	26.84	42.48	37.87	41.70	44.70	46.50	46.00	47.72	47.58
7	26.79	41.70	37.62	41.46	44.37	46.18	45.67	47.25	46.84
8	27.07	42.20	38.19	42.20	45.14	46.95	46.44	48.01	47.46
9	26.97	42.47	38.83	43.01	45.94	47.75	47.21	48.68	47.75
10	27.14	43.34	39.88	44.27	47.28	49.08	48.52	49.98	48.77
11	26.37	39.76	36.60	40.45	43.38	45.22	44.65	46.15	45.59
12	26.69	40.70	37.24	41.34	44.36	46.20	45.61	47.11	46.25
13	26.85	41.36	37.86	42.11	45.16	46.99	46.39	47.88	46.86
14	27.04	42.52	39.03	43.61	46.76	48.58	47.95	49.41	48.11
15	27.43	43.81	40.24	45.10	48.37	50.19	49.54	51.04	49.54
16	26.62	39.36	37.11	41.16	44.08	45.95	45.28	46.53	45.14
17	26.81	39.59	37.12	41.38	44.40	46.27	45.59	46.86	45.29
18	26.84	39.29	36.98	41.27	44.26	46.14	45.45	46.65	44.99
19	26.96	40.44	37.74	42.31	45.42	47.29	46.58	47.80	46.01
20	27.07	41.84	38.85	43.73	46.98	48.85	48.11	49.42	47.53
21	24.19	34.43	32.97	36.54	33.52	40.74	40.05	41.64	40.70
22	24.54	34.90	33.12	36.63	33.70	40.92	40.25	41.97	41.09
23	24.79	35.50	33.07	36.48	33.80	41.05	40.39	42.46	41.62
24	24.99	35.74	33.22	36.63	34.44	41.27	40.60	42.68	41.86
25	25.10	36.02	33.37	36.85	34.59	41.53	40.86	42.97	42.14
26	25.26	35.82	33.54	36.87	34.79	41.67	40.92	43.04	42.28
27	25.42	36.00	33.62	36.98	34.52	41.84	41.09	43.20	42.45
28	25.59	36.26	33.74	37.20	34.81	42.17	41.40	43.50	42.73
29	25.61	36.25	33.67	37.14	34.75	42.13	41.36	43.42	42.70
30	25.66	36.32	33.70	37.18	34.85	42.24	41.46	43.54	42.81
31	25.56	34.79	32.67	35.55	33.63	40.57	39.80	41.72	41.18
32	26.50	36.62	33.86	36.46	38.28	40.00	39.78	40.84	40.59
33	26.42	37.13	34.38	37.14	39.06	40.77	40.53	41.65	41.40
34	26.28	37.14	34.36	37.19	39.14	40.86	40.63	41.73	41.41
35	26.10	37.07	34.38	37.22	39.19	40.91	40.66	41.78	41.44
36	25.74	35.91	33.50	36.29	38.22	39.94	39.69	40.76	40.35
37	25.63	35.78	33.47	36.25	38.19	39.90	39.65	40.71	40.27
38	25.53	35.61	33.40	36.18	38.11	39.83	39.57	40.62	40.10

# Appendix C: Single- and two-phase measured data (continued).

## Channel A: Water and helium (continued).

Data Point	Gas Flow Meter		Liquid Flow Meter		Test Fixture Press.. (Pa)		Flow Meter/Flow rates, (cc/min)			
	Temp.(°C)	Press.(Pa)	Temp.(°C)	Press.(Pa)	Inlet	Outlet	F.M. #4	F.M. #5	F.M. #6	F.M. #1
1	23.28	1,652,116	23.29	1,454,557	310,150	105,385	0.00	52.75	0.00	8.38
2	24.70	1,620,400	24.71	1,420,558	387,394	108,421	0.00	133.49	0.00	8.32
3	24.72	1,607,990	24.70	1,395,081	461,518	113,255	0.00	189.53	0.00	8.92
4	24.73	1,597,998	24.70	1,365,423	582,661	123,294	0.00	0.00	333.37	8.92
5	24.73	1,594,200	24.68	1,346,592	694,175	131,439	0.00	0.00	438.74	8.92
6	24.75	1,703,770	24.78	1,311,553	460,229	97,476	0.00	41.33	0.00	17.45
7	24.79	1,625,916	24.96	1,294,328	545,317	101,606	0.00	108.94	0.00	18.49
8	24.79	1,609,369	25.11	1,290,168	594,326	107,122	0.00	166.25	0.00	15.74
9	24.78	1,596,958	25.24	1,289,897	712,079	119,071	0.00	0.00	293.77	14.41
10	24.77	1,591,442	25.27	1,288,270	805,440	128,210	0.00	0.00	396.66	12.54
11	24.75	1,692,467	25.51	1,257,164	610,308	95,837	0.00	35.00	0.00	24.68
12	24.78	1,628,335	25.76	1,249,117	653,756	99,666	0.00	99.91	0.00	23.15
13	24.79	1,613,505	25.90	1,253,819	691,621	104,762	0.00	145.57	0.00	22.11
14	24.82	1,601,095	25.97	1,266,071	783,852	117,581	0.00	0.00	273.98	19.80
15	24.82	1,591,691	25.96	1,279,114	866,024	127,806	0.00	0.00	375.46	15.51
16	24.88	1,674,224	26.44	1,228,229	754,193	95,183	0.00	30.15	0.00	30.95
17	24.89	1,628,357	26.58	1,224,815	823,231	98,204	0.00	83.34	0.00	30.55
18	24.90	1,612,353	26.68	1,223,482	901,537	104,138	0.00	120.19	0.00	30.67
19	24.91	1,602,270	26.68	1,246,268	971,592	117,100	0.00	0.00	231.13	27.02
20	24.94	1,596,664	26.66	1,247,760	1,031,814	125,828	0.00	0.00	328.02	23.68
21	22.92	3,589,355	25.51	3,976,492	1,655,924	119,756	0.00	0.00	162.09	62.14
22	22.92	3,585,670	25.79	3,994,554	1,716,326	124,121	0.00	0.00	216.77	60.09
23	22.86	3,589,536	25.97	3,981,918	1,901,580	139,565	0.00	59.00	222.21	57.84
24	22.86	3,544,302	26.12	3,979,612	1,920,410	140,289	0.00	62.69	238.43	57.26
25	22.85	3,528,433	26.22	3,978,979	1,956,286	143,395	0.00	69.78	270.70	55.98
26	22.79	3,594,374	26.57	3,953,502	2,146,919	119,955	0.00	0.00	128.74	70.68
27	22.80	3,584,043	26.69	3,951,671	2,230,086	124,982	0.00	0.00	179.79	69.86
28	22.79	3,609,859	26.77	3,956,057	2,346,708	136,995	0.00	46.02	173.72	67.77
29	22.76	3,545,252	26.78	3,995,865	2,409,439	140,395	0.00	50.32	192.41	69.69
30	22.75	3,519,278	26.79	4,013,475	2,447,191	144,423	0.00	54.62	211.29	66.80
31	22.75	3,579,861	27.01	3,943,104	2,842,835	119,421	0.00	0.00	95.07	84.36
32	23.37	4,558,732	26.55	4,653,713	458,460	113,458	0.00	36.70	128.67	12.75
33	23.38	4,603,175	26.33	4,708,871	521,236	121,861	0.00	56.14	199.60	12.14
34	23.39	4,566,011	26.17	4,726,413	617,514	130,417	0.00	76.10	275.83	11.59
35	23.41	4,578,512	26.06	4,735,229	682,460	137,770	0.00	91.15	335.79	11.77
36	23.42	4,518,426	25.95	4,754,806	817,891	146,462	0.00	105.09	396.28	10.53
37	23.43	4,528,599	25.87	4,742,260	870,200	150,470	0.00	113.12	431.97	9.99
38	23.44	4,545,576	25.79	4,769,364	953,819	158,023	0.00	125.68	490.33	10.52



## Appendix C: Single- and two-phase measured data (continued).

Channel C1: Water and nitrogen tests. Number of channels: 5

Channel Dimensions:

Depth ( $\mu\text{m}$ ): 134.64 Hyd. Diameter ( $\mu\text{m}$ ): 127.92Width ( $\mu\text{m}$ ): 121.83 Channel Length (m): 0.0635

Data Point	Test Fixture Temperature		Test Section Temperature, ( $^{\circ}\text{C}$ )						
	Inlet	Outlet	Pos #1	Pos #2	Pos #3	Pos #4	Pos #5	Pos #6	Pos #7
1	27.01	38.98	36.01	39.03	41.41	43.23	42.82	44.10	43.61
2	27.19	40.32	36.82	40.10	42.59	44.40	43.98	45.29	44.68
3	27.40	40.91	37.53	40.97	43.49	45.30	44.86	46.16	45.39
4	27.46	41.59	38.35	41.92	44.49	46.29	45.84	47.14	46.23
5	27.37	42.27	39.04	42.79	45.41	47.22	46.76	48.06	47.06
6	27.56	43.18	39.88	43.77	46.46	48.27	47.79	49.11	48.06
7	26.37	38.23	35.53	38.92	41.50	43.36	42.84	43.99	42.78
8	26.79	39.19	36.08	39.74	42.47	44.32	43.78	45.05	43.81
9	26.94	39.89	36.78	40.62	43.41	45.26	44.71	45.97	44.62
10	27.33	40.60	37.44	41.45	44.28	46.12	45.56	46.79	45.35
11	27.41	41.49	38.29	42.47	45.35	47.19	46.62	47.85	46.37
12	27.41	42.46	39.14	43.48	46.44	48.29	47.69	48.95	47.45
13	26.80	38.42	36.39	40.27	43.03	44.92	44.26	45.23	43.24
14	26.93	39.25	36.68	40.83	43.72	45.62	44.94	45.95	44.01
15	27.18	40.16	37.44	41.77	44.74	46.63	45.94	46.96	44.98
16	27.36	41.68	38.64	43.25	46.38	48.25	47.54	48.67	46.71
17	27.51	42.74	39.37	44.18	47.42	49.28	48.56	49.74	47.86
18	24.25	34.33	32.30	35.03	36.92	38.66	38.41	39.53	39.25
19	24.26	34.11	31.84	34.52	36.39	38.13	37.89	38.99	38.73
20	24.34	34.51	32.14	34.90	36.79	38.54	38.30	39.41	39.11
21	24.45	34.98	32.57	35.40	37.33	39.07	38.81	39.92	39.56
22	24.57	35.44	33.11	35.99	37.95	39.68	39.42	40.51	40.03
23	24.83	35.89	33.60	36.52	38.49	40.22	39.96	41.04	40.52
24	24.78	35.47	33.12	35.98	37.92	39.65	39.38	40.48	39.95
25	25.29	33.12	31.59	34.52	36.79	38.37	37.85	39.21	38.81
26	25.60	33.65	31.80	34.76	37.06	38.64	38.13	39.46	39.00
27	25.76	33.87	31.97	34.91	37.23	38.82	38.31	39.62	39.14
28	25.93	34.00	32.07	35.02	37.36	38.95	38.43	39.71	39.22
29	26.02	34.03	32.04	34.97	37.31	38.90	38.38	39.62	39.11
30	26.11	34.26	32.18	35.15	37.51	39.11	38.58	39.82	39.28
31	26.13	34.27	32.19	35.16	37.53	39.13	38.60	39.84	39.29
32	26.12	34.28	32.22	35.21	37.59	39.19	38.66	39.90	39.31

## Appendix C: Single- and two-phase measured data (continued).

Channel C1: Water and nitrogen (continued).

Data Point	Gas Flow Meter		Liquid Flow Meter		Test Fixture Press., (Pa)		Flow Meter/Flow rates, (cc/min)			
	Temp.(°C)	Press.(Pa)	Temp.(°C)	Press.(Pa)	Inlet	Outlet	F.M. #4	F.M. #5	F.M. #6	F.M. #1
1	24.86	1,861,467	26.44	1,742,418	496,240	100,313	0.00	26.59	0.00	17.93
2	24.85	1,853,442	26.37	1,744,452	574,998	101,626	0.00	77.46	0.00	15.61
3	24.84	1,841,032	26.27	1,734,144	640,871	104,701	0.00	114.03	0.00	13.77
4	24.82	1,833,346	26.16	1,736,495	714,068	108,835	0.00	0.00	148.49	14.95
5	24.75	1,825,863	26.01	1,746,283	798,274	113,783	0.00	0.00	183.00	12.50
6	24.70	1,820,348	25.89	1,760,751	886,550	119,222	0.00	0.00	214.21	12.65
7	24.58	1,867,232	26.08	1,760,819	691,169	102,490	0.00	22.84	0.00	25.79
8	24.54	1,860,337	26.20	1,746,962	743,365	101,818	0.00	58.00	0.00	24.24
9	24.55	1,842,456	26.27	1,736,631	818,281	105,031	0.00	92.68	0.00	21.83
10	24.59	1,836,850	26.31	1,754,308	896,700	110,361	0.00	0.00	123.40	19.91
11	24.59	1,825,660	26.31	1,748,476	973,582	114,780	0.00	0.00	158.37	19.50
12	24.65	1,819,489	26.30	1,756,908	1,050,667	120,016	0.00	0.00	188.60	18.33
13	24.67	1,868,611	26.64	1,741,378	883,747	103,109	0.00	20.45	0.00	33.49
14	24.72	1,856,200	26.84	1,743,910	946,997	103,541	0.00	49.14	0.00	31.34
15	24.76	1,842,411	26.96	1,744,859	1,012,079	106,737	0.00	80.18	0.00	29.20
16	24.78	1,835,516	26.97	1,750,737	1,027,338	110,603	0.00	0.00	111.41	26.05
17	24.82	1,827,242	26.96	1,756,501	1,103,248	115,608	0.00	0.00	143.62	24.04
18	23.58	3,654,527	24.36	3,445,824	560,367	115,398	0.00	0.00	259.32	11.69
19	23.71	3,678,422	24.30	3,481,179	654,090	119,525	0.00	0.00	278.08	11.45
20	23.68	3,658,303	24.27	3,485,474	703,257	121,917	0.00	0.00	306.70	10.40
21	23.69	3,704,441	24.25	3,480,953	763,660	124,627	0.00	0.00	337.29	9.88
22	23.60	3,796,717	24.23	3,498,405	893,574	130,810	0.00	71.91	270.05	9.84
23	23.58	3,666,915	24.24	3,442,885	947,805	132,010	0.00	76.00	288.15	11.23
24	23.57	3,652,583	24.22	3,428,372	1,078,602	135,734	0.00	78.27	300.88	11.62
25	23.43	4,073,863	26.99	3,443,744	2,137,497	108,609	0.00	8.38	0.00	64.40
26	23.41	3,705,006	27.30	3,449,305	2,400,967	115,000	0.00	30.04	0.00	63.09
27	23.52	3,664,745	27.48	3,445,440	2,501,110	117,690	0.00	12.24	43.44	61.80
28	23.52	3,678,263	27.65	3,455,409	2,682,656	122,602	0.00	16.17	58.35	62.80
29	23.53	3,737,942	27.77	3,424,687	3,000,469	128,954	0.00	20.66	76.14	64.12
30	23.49	3,644,807	27.87	3,434,318	3,117,137	133,891	0.00	24.74	92.77	62.87
21	23.49	3,695,625	27.90	3,432,803	3,248,861	137,402	0.00	27.02	102.50	62.79
32	23.53	3,764,888	27.98	3,435,606	3,399,753	142,206	0.00	30.19	116.40	62.96

## Appendix C: Single- and two-phase measured data (continued).

Channel C2: Argon gas tests. Number of channels: 3  
Channel Dimensions:  
Depth ( $\mu\text{m}$ ): 263.73 Hyd. Diameter ( $\mu\text{m}$ ): 207.01  
Width ( $\mu\text{m}$ ): 170.37 Channel Length (m): 0.0635

Data Point	Test Fixture Temperature		Test Section Temperature, ( $^{\circ}\text{C}$ )						
	Inlet	Outlet	Pos #1	Pos #2	Pos #3	Pos #4	Pos #5	Pos #6	Pos #7
1	33.69	34.74	47.02	47.76	48.14	49.89	49.86	21.54	49.17
2	33.33	37.62	47.34	48.09	48.49	50.24	50.20	21.86	49.52
3	32.83	38.33	47.44	48.22	48.63	50.38	50.35	21.94	49.67
4	32.36	40.86	47.43	48.22	48.65	50.40	50.37	31.25	49.71
5	31.84	42.14	47.23	48.05	48.50	50.24	50.21	31.17	49.58
6	31.37	42.77	47.05	47.88	48.35	50.09	50.07	30.93	49.46
7	31.09	43.07	46.91	47.76	48.26	50.00	49.97	31.01	49.39
8	30.86	43.56	46.74	47.61	48.14	49.88	49.85	31.10	49.30
9	30.70	44.55	46.51	47.40	47.95	49.69	49.67	31.39	49.15
10	30.60	44.98	46.26	47.17	47.73	49.47	49.45	30.87	48.96
11	30.47	45.06	46.01	46.93	47.52	49.27	49.24	31.04	48.78
12	30.49	45.06	45.78	46.71	47.32	49.06	49.04	31.03	48.60
13	30.44	45.00	45.54	46.49	47.12	48.86	48.84	31.33	48.43
14	30.28	44.82	45.09	46.07	46.70	48.44	48.43	30.74	48.05
15	30.19	44.79	44.90	45.90	46.54	48.28	48.27	30.95	47.91
16	30.07	44.76	44.63	45.63	46.30	48.03	48.02	30.30	47.70
17	29.95	44.73	44.34	45.36	46.05	47.78	47.77	30.76	47.48
18	29.83	44.67	44.05	45.08	45.78	47.52	47.51	30.94	47.23

Data Point	Gas Flow Meter		Test Fixture Press., (Pa)		Gas Flow Rates, (cc/min)		
	Temp. ( $^{\circ}\text{C}$ )	Press. (Pa)	Inlet	Outlet	F.M. #4	F.M. #5	F.M. #6
1	24.03	1,375,129	13,583	3,296	28.37	0.00	0.00
2	24.07	1,343,503	49,435	3,307	0.00	129.96	0.00
3	24.10	1,335,659	94,873	3,400	0.00	249.33	0.04
4	24.06	1,315,947	140,242	3,495	0.00	345.09	0.00
5	24.03	1,331,070	191,422	3,721	0.00	0.00	404.96
6	24.02	1,300,485	252,140	3,875	0.00	0.00	460.46
7	24.02	1,310,160	319,709	4,019	0.00	0.00	484.90
8	24.04	1,300,259	392,793	4,291	0.00	0.00	502.68
9	24.04	1,300,485	450,709	4,453	0.00	0.00	524.04
10	24.08	1,296,890	512,761	4,614	0.00	0.00	545.22
11	24.06	1,296,303	571,920	4,835	0.00	0.00	561.56
12	24.07	1,300,010	628,593	5,104	0.00	0.00	575.87
13	24.09	1,297,116	687,888	5,376	0.00	0.00	587.99
14	24.08	1,312,466	754,054	5,694	0.00	0.00	599.42
15	24.09	1,322,593	791,309	5,812	0.00	130.50	485.49
16	24.10	1,326,436	846,851	6,205	0.00	132.01	494.31
17	24.13	1,330,661	905,646	6,481	0.00	133.28	502.23
18	24.13	1,327,205	963,089	6,757	0.00	134.11	508.35

## Appendix C: Single- and two-phase measured data (continued).

Channel C2: Helium gas tests.

Number of channels:

3

Channel Dimensions:

Depth ( $\mu\text{m}$ ): 263.73Hyd. Diameter ( $\mu\text{m}$ ): 207.01Width ( $\mu\text{m}$ ): 170.37

Channel Length (m): 0.0635

Data Point	Test Fixture Temperature		Test Section Temperature, ( $^{\circ}\text{C}$ )						
	Inlet	Outlet	Pos #1	Pos #2	Pos #3	Pos #4	Pos #5	Pos #6	Pos #7
1	30.69	31.75	38.29	39.38	39.69	41.48	41.45	35.20	40.61
2	31.12	31.97	41.59	42.28	42.70	44.47	44.44	22.10	43.54
3	31.65	37.10	43.43	44.19	44.68	46.45	46.41	22.04	45.59
4	31.66	37.68	44.27	45.10	45.60	47.36	47.32	21.99	46.53
5	31.43	38.50	44.89	45.75	46.28	48.04	48.00	22.00	47.23
6	31.39	40.43	45.12	46.02	46.57	48.32	48.28	22.08	47.53
7	31.34	40.56	45.22	46.15	46.72	48.47	48.43	22.11	47.70
8	31.45	37.41	45.27	46.22	46.77	48.53	48.49	22.23	47.69
9	31.45	37.59	45.11	46.05	46.62	48.37	48.34	22.16	47.55
10	31.47	41.31	45.10	46.07	46.67	48.42	48.39	22.14	47.67
11	31.75	42.48	45.11	46.12	46.74	48.49	48.46	22.24	47.80
12	28.50	38.83	40.98	42.03	42.61	44.37	44.35	21.71	43.73
13	28.80	39.57	41.28	42.32	42.93	44.69	44.67	21.76	44.07
14	28.95	39.44	41.41	42.47	43.08	44.83	44.81	21.85	44.19
15	28.97	39.87	41.46	42.54	43.16	44.91	44.89	21.96	44.27
16	28.97	40.32	41.48	42.58	43.22	44.97	44.96	21.87	44.36
17	28.90	40.62	41.37	42.47	43.14	44.89	44.87	21.81	44.31
18	28.81	40.87	41.24	42.36	43.05	44.80	44.79	21.91	44.26

Data Point	Gas Flow Meter		Test Fixture Press., (Pa)		Gas Flow Rates, (cc/min)		
	Temp. ( $^{\circ}\text{C}$ )	Press. (Pa)	Inlet	Outlet	F.M. #4	F.M. #5	F.M. #6
1	24.54	1,263,592	11,904	3,425	25.54	0.00	0.00
2	24.54	1,143,375	40,817	3,208	0.00	121.70	0.00
3	24.53	1,144,664	83,564	3,305	0.00	261.59	0.00
4	24.51	1,126,737	119,937	3,436	0.00	368.03	0.00
5	24.52	1,125,358	144,238	3,450	0.00	0.00	457.20
6	24.52	1,115,706	174,575	3,504	0.00	0.00	548.08
7	24.57	1,104,674	200,775	3,588	0.00	0.00	621.36
8	24.65	1,115,706	228,354	3,723	0.00	0.00	694.69
9	24.68	1,108,811	250,417	3,732	0.00	0.00	751.34
10	24.65	1,103,476	272,480	3,850	0.00	0.00	809.26
11	24.66	1,104,674	297,301	3,886	0.00	0.00	873.58
12	24.27	662,032	308,333	4,372	0.00	0.00	923.70
13	24.26	660,653	330,328	4,489	0.00	0.00	974.29
14	24.25	660,653	349,701	4,578	0.00	0.00	1019.32
15	24.22	659,320	370,385	4,695	0.00	222.71	835.85
16	24.22	659,274	389,690	4,781	0.00	229.37	866.93
17	24.18	660,495	408,996	4,831	0.00	237.13	903.22
18	24.14	660,653	427,216	4,964	0.00	243.97	935.99

## Appendix C: Single- and two-phase measured data (continued).

Channel C2: Nitrogen gas tests.

Channel Dimensions:

Number of channels: 3

Depth ( $\mu\text{m}$ ): 263.73Hyd. Diameter ( $\mu\text{m}$ ): 207.01Width ( $\mu\text{m}$ ): 170.37

Channel Length (m): 0.0635

Data Point	Test Fixture Temperature		Test Section Temperature, ( $^{\circ}\text{C}$ )						
	Inlet	Outlet	Pos #1	Pos #2	Pos #3	Pos #4	Pos #5	Pos #6	Pos #7
1	31.62	32.12	43.24	43.98	44.34	46.10	46.07	21.79	45.40
2	32.73	35.77	46.48	47.25	47.64	49.39	49.36	21.57	48.67
3	32.37	36.88	46.62	47.40	47.81	49.56	49.53	22.03	48.83
4	32.08	38.97	46.66	47.46	47.89	49.64	49.61	21.98	48.95
5	31.80	39.94	46.60	47.42	47.87	49.61	49.58	22.11	48.92
6	31.49	40.73	46.47	47.31	47.77	49.52	49.49	22.05	48.87
7	31.22	41.30	46.36	47.21	47.69	49.44	49.41	22.15	48.80
8	30.85	41.66	46.17	47.04	47.54	49.28	49.26	22.02	48.68
9	30.57	42.09	45.96	46.84	47.37	49.11	49.09	22.07	48.54
10	30.17	42.00	45.67	46.57	47.11	48.86	48.84	21.97	48.31
11	29.85	42.22	45.39	46.31	46.89	48.64	48.61	21.89	48.11
12	29.77	43.27	45.12	46.06	46.66	48.40	48.38	21.97	47.92
13	29.56	43.81	44.88	45.84	46.47	48.21	48.19	22.01	47.76
14	29.29	44.11	44.62	45.60	46.25	47.99	47.98	21.80	47.60
15	29.21	44.22	44.41	45.41	46.09	47.83	47.81	21.91	47.47
16	29.05	44.22	44.17	45.18	45.88	47.62	47.61	22.11	47.30
17	29.00	44.19	43.85	44.87	45.59	47.33	47.32	21.96	47.04
18	28.94	44.15	43.57	44.60	45.34	47.08	47.06	21.80	46.82

Data Point	Gas Flow Meter		Test Fixture Press., (Pa)		Gas Flow Rates, (cc/min)		
	Temp. ( $^{\circ}\text{C}$ )	Press. (Pa)	Inlet	Outlet	F.M. #4	F.M. #5	F.M. #6
1	24.13	1074337.3	10010.93	3300.43	26.34	0.00	0.00
2	24.07	952990.03	30129.98	3345.641	0.00	91.38	0.00
3	24.09	904726.9	63224.7	3397.634	0.00	201.83	0.00
4	24.08	896362.8	93561.53	3449.627	0.00	290.53	0.00
5	24.09	890937.43	122519.4	3524.226	0.00	0.00	352.28
6	24.07	884042.7	151477.3	3589.782	0.00	0.00	418.09
7	24.06	881443.05	177677.3	3691.508	0.00	0.00	466.12
8	24.07	879792.83	214908.8	3757.064	0.00	0.00	513.70
9	24.09	878526.91	246624.6	3863.311	0.00	0.00	541.09
10	24.05	877147.97	289372	3996.685	0.00	0.00	556.34
11	24.04	877147.97	340031.3	4136.84	0.00	0.00	566.37
12	24.05	877147.97	379003.5	4272.474	0.00	0.00	583.78
13	24.06	875769.02	414856.1	4392.284	0.00	0.00	599.36
14	24.05	876334.16	456224.5	4566.348	0.00	0.00	613.50
15	24.07	877147.97	489319.2	4688.419	0.00	132.64	495.00
16	24.10	877147.97	527929.7	4873.785	0.00	134.72	506.32
17	24.10	877147.97	565161.3	5018.462	0.00	136.25	515.47
18	24.11	878526.91	602392.8	5140.532	0.00	137.53	523.76

# Appendix C: Single- and two-phase measured data (continued).

Channel C2: Water tests.

Number of channels:

3

Channel Dimensions:

Depth ( $\mu\text{m}$ ): 263.73Hyd. Diameter ( $\mu\text{m}$ ): 207.01Width ( $\mu\text{m}$ ): 170.37

Channel Length (m): 0.0635

Data Point	Test Fixture Temperature		Test Section Temperature, ( $^{\circ}\text{C}$ )						
	Inlet	Outlet	Pos #1	Pos #2	Pos #3	Pos #4	Pos #5	Pos #6	Pos #7
1	23.46	34.42	30.96	33.88	36.82	38.16	38.41	26.26	39.69
2	23.40	35.30	31.87	35.50	39.06	40.22	40.58	26.93	41.56
3	23.59	35.89	32.52	36.67	40.72	41.73	42.19	27.61	42.89
4	23.86	35.97	32.86	37.40	41.85	42.74	43.28	28.18	43.91
5	24.10	35.47	32.10	36.40	40.50	41.41	41.95	28.11	40.90
6	24.27	36.35	32.86	37.54	41.93	42.68	43.31	28.02	41.96
7	24.39	37.29	33.16	37.74	42.01	42.40	43.21	28.79	42.51
8	24.71	38.62	33.81	38.44	43.01	43.24	44.17	28.86	43.39
9	24.92	39.97	34.55	39.22	43.97	44.06	45.10	29.14	44.12
10	25.22	39.77	34.14	38.51	43.32	43.39	44.44	29.09	43.49
11	25.40	41.45	35.15	39.80	45.03	44.93	46.10	30.32	45.28
12	25.65	41.23	34.68	38.84	44.48	44.54	45.68	30.22	44.90
13	25.73	40.90	34.25	38.24	43.90	43.98	45.14	30.58	44.46
14	25.80	40.34	33.71	37.59	43.15	43.24	44.43	30.52	43.77
15	25.91	41.11	34.21	38.26	44.14	44.07	45.39	30.39	44.67
16	26.02	40.71	33.92	37.84	43.67	43.59	44.94	30.47	44.19
17	26.13	40.34	33.68	37.49	43.25	43.18	44.53	30.24	43.74
18	26.19	39.65	33.22	36.85	42.50	42.43	43.79	29.64	42.92
19	26.30	39.04	32.85	36.33	41.87	41.80	43.17	29.76	42.19
20	26.42	39.63	33.33	36.96	42.93	42.65	44.17	29.72	43.00
21	26.11	37.50	31.56	34.43	39.45	39.51	40.60	34.09	39.95
22	26.15	36.60	30.96	33.61	38.48	38.55	39.64	33.30	38.85
23	26.25	35.93	30.54	33.02	37.74	37.82	38.91	32.75	38.01
24	26.31	35.40	30.21	32.54	37.18	37.25	38.35	32.27	37.36
25	26.40	35.03	29.97	32.20	36.75	36.84	37.93	31.93	36.89
26	26.42	34.68	29.73	31.87	36.36	36.44	37.54	31.73	36.45
27	26.43	34.38	29.51	31.58	35.99	36.09	37.18	34.57	36.08
28	26.42	34.12	29.34	31.34	35.69	35.78	36.88	34.43	35.76

## Appendix C: Single- and two-phase measured data (continued).

## Channel C2: Water tests (continued).

Data Point	Liquid Flow Meter		Test Fixture Press., (Pa)		Liquid Flow Rate
	Temp.(°C)	Press.(Pa)	Inlet	Outlet	F. M. #1, (cc/min)
1	23.94	1,647,979	263,990	101,796	18.29
2	24.04	1,627,860	338,566	100,975	24.95
3	24.32	1,588,119	407,378	99,056	31.30
4	24.70	1,571,165	479,875	98,423	38.83
5	25.14	1,545,937	542,877	97,340	42.26
6	25.56	1,511,283	611,847	96,104	47.34
7	25.91	1,500,568	688,661	95,412	51.65
8	26.23	1,493,243	757,902	95,294	54.77
9	26.48	1,485,693	824,363	95,025	55.72
10	26.71	1,480,335	903,392	94,935	58.41
11	26.86	1,460,488	962,596	93,868	59.38
12	27.00	1,465,077	1,039,682	94,035	62.44
13	27.12	1,461,301	1,108,878	93,694	65.51
14	27.23	1,462,160	1,214,763	93,610	68.80
15	27.35	2,176,568	1,326,932	93,194	70.59
16	27.47	2,206,837	1,433,111	93,771	75.98
17	27.62	2,225,713	1,523,647	94,623	77.88
18	27.79	2,252,478	1,690,658	95,593	84.15
19	27.99	2,240,632	1,864,495	95,561	89.42
20	28.23	2,226,617	2,075,429	95,697	92.52
21	27.32	5,094,261	1,721,729	103,656	81.22
22	27.49	5,034,966	2,060,385	103,771	89.22
23	27.78	5,018,600	2,407,947	104,011	98.75
24	27.93	4,969,523	2,763,693	103,493	108.35
25	28.06	4,916,422	3,094,663	102,795	116.16
26	28.14	4,910,686	3,477,963	103,469	121.51
27	28.23	4,894,517	3,808,121	102,356	128.71
28	28.28	4,837,099	4,126,929	102,273	135.78

# Appendix C: Single- and two-phase measured data (continued).

Channel C2: Water and argon tests.      Number of channels:      3

Channel Dimensions:

Depth ( $\mu\text{m}$ ):      263.73      Hyd. Diameter ( $\mu\text{m}$ ):      207.01

Width ( $\mu\text{m}$ ):      170.37      Channel Length (m):      0.0635

Data Point	Test Fixture Temperature		Test Section Temperature, ( $^{\circ}\text{C}$ )						
	Inlet	Outlet	Pos #1	Pos #2	Pos #3	Pos #4	Pos #5	Pos #6	Pos #7
1	28.48	46.27	37.73	41.69	45.11	46.51	46.69	28.04	48.50
2	28.09	45.18	36.88	40.83	44.21	45.63	45.81	27.89	47.47
3	27.97	44.17	36.29	40.10	43.33	44.77	44.95	28.33	46.22
4	29.04	47.61	39.68	43.60	46.88	48.33	48.48	28.07	49.64
5	26.45	37.77	31.28	34.47	37.34	38.74	38.97	28.80	40.32
6	26.71	43.02	34.74	39.43	43.53	44.78	45.07	28.51	46.61
7	26.93	43.77	35.18	39.86	43.93	45.19	45.48	28.78	46.44
8	27.27	45.64	36.36	41.01	45.06	46.33	46.61	28.62	47.87
9	26.46	43.07	35.00	40.66	45.66	46.66	47.09	28.41	48.55
10	26.86	44.57	35.68	41.48	46.67	47.67	48.11	29.20	49.30
11	27.20	46.23	36.35	41.85	46.81	47.86	48.30	29.09	49.29
12	26.67	40.76	33.82	39.16	43.95	44.94	45.40	29.16	46.33
13	27.05	43.03	34.45	39.67	44.49	45.51	45.96	28.55	46.89
14	27.29	44.57	35.30	40.47	45.19	46.24	46.70	28.87	47.53
15	26.37	38.49	32.64	36.01	41.78	41.60	42.82	37.46	43.43
16	26.37	38.62	32.70	36.11	41.95	41.76	42.99	36.94	43.55
17	26.33	39.30	33.03	36.73	42.77	42.59	43.80	37.69	44.30
18	26.23	39.02	32.76	36.41	42.40	42.22	43.43	37.33	43.87
19	26.15	39.04	32.71	36.40	42.40	42.24	43.44	37.30	43.79
20	26.12	37.12	31.72	34.77	40.35	40.18	41.41	35.35	41.70
21	26.15	37.30	31.77	34.90	40.51	40.35	41.57	35.42	41.87
22	26.15	36.78	31.51	34.46	39.95	39.79	41.02	35.00	41.29
23	26.18	36.99	31.56	34.60	40.12	39.98	41.19	35.79	41.40
24	26.14	37.58	31.87	35.15	40.83	40.68	41.89	36.22	42.03
25	26.10	37.70	31.92	35.26	40.97	40.83	42.03	36.42	42.13
26	26.07	38.02	32.11	35.56	41.36	41.22	42.41	36.63	42.48
27	24.68	36.02	29.47	32.19	34.61	36.10	36.22	36.39	37.40
28	24.70	36.06	29.50	32.18	34.59	36.05	36.16	36.48	37.31
29	24.80	36.02	29.51	32.17	34.71	36.10	36.27	36.37	37.31
30	24.74	35.99	29.28	31.88	34.25	35.73	35.85	36.28	36.98
31	24.76	35.98	29.49	32.07	34.40	35.86	35.97	36.35	36.97
32	24.78	36.19	29.38	31.94	34.32	35.79	35.91	36.24	37.05
33	24.59	35.28	28.65	31.07	33.39	34.86	34.98	35.64	36.07
34	24.58	35.13	28.78	31.21	33.50	34.97	35.09	35.66	36.01
35	24.57	35.12	29.05	31.50	33.75	35.19	35.30	35.82	36.06



## Appendix C: Single- and two-phase measured data (continued).

Channel C2: Water and argon (continued).

Data Point	Gas Flow Meter		Liquid Flow Meter		Test Fixture Press., (Pa)		Flow Meter/Flow rates, (cc/min)			
	Temp.(°C)	Press.(Pa)	Temp.(°C)	Press.(Pa)	Inlet	Outlet	F.M. #4	F.M. #5	F.M. #6	F.M. #1
1	25.30	1,667,171	26.79	1,524,996	297,847	93,526	0.00	47.60	0.00	8.96
2	25.32	1,674,654	26.71	1,517,130	555,823	100,347	0.00	131.88	0.00	11.44
3	25.31	1,670,992	26.65	1,526,760	858,242	110,013	0.00	0.00	175.22	9.95
4	25.29	1,672,868	26.55	1,538,831	1,128,018	121,289	0.00	0.00	236.31	6.49
5	25.26	1,689,574	26.68	1,572,536	535,280	98,228	0.00	38.96	0.00	18.89
6	25.26	1,679,627	26.76	1,551,784	752,560	102,503	0.00	103.53	0.00	18.73
7	25.29	1,672,416	26.85	1,562,205	1,061,761	112,246	0.00	0.00	146.20	17.76
8	25.28	1,661,452	26.87	1,554,293	1,247,896	119,204	0.00	0.00	183.07	13.02
9	25.33	1,690,772	27.21	1,585,037	764,948	102,117	0.00	33.02	0.02	26.00
10	25.32	1,677,819	27.35	1,563,833	1,018,606	104,850	0.00	84.62	0.00	24.99
11	25.32	1,670,268	27.41	1,557,458	1,269,462	113,422	0.00	0.00	127.86	21.02
12	25.32	1,661,000	27.74	1,600,025	968,354	103,303	0.00	25.74	0.00	32.38
13	25.33	1,677,412	27.85	1,518,983	1,176,281	104,029	0.00	79.16	0.00	28.97
14	25.34	1,670,947	27.82	1,576,470	1,398,766	114,613	0.00	0.00	118.80	25.04
15	22.63	3,078,648	27.51	4,876,854	1,876,666	112,515	0.00	0.00	144.05	79.72
16	22.60	2,843,571	27.45	4,832,615	2,024,440	117,025	0.00	0.00	212.55	79.15
17	22.55	2,853,179	27.37	4,708,577	2,219,933	126,002	0.00	49.68	188.08	72.12
18	22.54	2,820,581	27.29	4,691,284	2,320,529	127,810	0.00	51.08	194.59	74.12
19	22.57	2,808,171	27.21	4,668,701	2,408,714	130,627	0.00	55.40	213.45	72.77
20	22.43	3,045,101	27.34	4,882,528	2,214,576	112,484	0.00	26.21	0.00	88.53
21	22.54	2,833,534	27.35	4,832,547	2,338,772	117,480	0.00	45.23	0.00	87.82
22	22.64	3,108,532	27.40	4,915,758	2,312,888	112,165	0.00	0.00	93.40	91.68
23	22.48	2,895,225	27.43	4,782,023	2,460,119	117,701	0.00	0.00	158.10	89.94
24	22.55	2,843,503	27.36	4,667,096	2,604,434	126,221	0.00	40.76	153.70	84.60
25	22.53	2,814,048	27.30	4,672,657	2,647,565	129,189	0.00	43.92	166.82	82.77
26	22.56	2,780,094	27.25	4,609,790	2,715,134	132,300	0.00	50.75	195.87	78.52
27	23.31	4,371,489	24.74	4,650,933	639,125	124,560	0.00	66.77	240.07	10.87
28	23.28	4,268,317	24.73	4,664,428	714,560	128,886	0.00	72.44	262.64	10.18
29	23.29	4,190,373	24.84	4,594,712	911,975	132,196	0.00	74.86	275.43	13.26
30	23.29	4,232,487	24.71	4,605,993	889,370	134,513	0.00	80.85	298.06	10.30
31	23.35	4,343,888	24.70	4,627,491	935,892	138,293	0.00	85.76	318.51	11.51
32	23.28	4,269,425	24.66	4,600,952	1,051,633	141,166	0.00	87.13	326.39	9.17
33	23.28	4,265,288	24.63	4,560,533	1,182,565	144,509	0.00	87.47	330.49	11.75
34	23.27	4,258,596	24.63	4,516,067	1,247,828	147,507	0.00	91.26	347.73	10.19
35	23.26	4,259,071	24.59	4,505,420	1,322,902	151,322	0.00	93.30	357.93	9.64

# Appendix C: Single- and two-phase measured data (continued).

Channel C2: Water and helium tests. Number of channels: 3

Channel Dimensions:

Depth ( $\mu\text{m}$ ): 263.73 Hyd. Diameter ( $\mu\text{m}$ ): 207.01

Width ( $\mu\text{m}$ ): 170.37 Channel Length (m): 0.0635

Data Point	Test Fixture Temperature		Test Section Temperature, ( $^{\circ}\text{C}$ )						
	Inlet	Outlet	Pos #1	Pos #2	Pos #3	Pos #4	Pos #5	Pos #6	Pos #7
1	26.23	39.08	32.71	36.17	39.39	40.73	40.99	28.77	42.31
2	26.38	40.88	33.28	37.23	40.75	42.09	42.32	29.61	43.67
3	26.49	41.72	33.81	37.64	41.15	42.49	42.72	29.40	43.95
4	26.95	43.83	35.74	39.79	43.40	44.74	44.95	29.69	46.10
5	27.00	47.01	37.80	44.47	50.30	51.13	51.61	32.35	53.45
6	27.68	48.03	38.19	44.44	49.82	50.80	51.20	32.89	52.43
7	28.18	50.54	39.98	46.20	51.51	52.50	52.89	34.20	54.10
8	28.54	52.22	41.17	47.30	52.70	53.66	54.05	34.55	55.68
9	26.91	40.89	34.09	39.49	44.27	45.25	45.71	32.20	46.58
10	27.38	43.26	35.03	40.62	45.54	46.53	46.98	32.83	47.62
11	27.57	44.76	35.84	41.23	45.99	47.00	47.44	32.86	48.03
12	25.53	37.10	31.54	34.77	40.43	40.27	41.49	38.58	42.03
13	25.76	37.27	31.65	34.89	40.57	40.40	41.63	39.32	42.11
14	25.89	37.31	31.76	34.94	40.58	40.42	41.65	39.41	42.12
15	25.97	37.41	31.83	35.02	40.70	40.53	41.76	39.43	42.19
16	26.04	37.16	31.67	34.81	40.40	40.23	41.47	38.48	41.88
17	26.08	37.36	31.73	35.06	40.81	40.64	41.87	38.75	42.11
18	26.05	37.21	31.53	34.83	40.55	40.39	41.61	38.61	41.81
19	26.04	37.31	31.58	34.90	40.66	40.49	41.72	38.65	41.91
37	25.63	35.78	33.47	36.25	38.19	39.90	39.65	40.71	40.27
38	25.53	35.61	33.40	36.18	38.11	39.83	39.57	40.62	40.10

## Appendix C: Single- and two-phase measured data (continued).

Channel A: Water and helium (continued).

Data Point	Gas Flow Meter		Liquid Flow Meter		Test Fixture Press., (Pa)		Flow Meter/Flow rates, (cc/min)			
	Temp.(°C)	Press.(Pa)	Temp.(°C)	Press.(Pa)	Inlet	Outlet	F.M. #4	F.M. #5	F.M. #6	F.M. #1
1	24.23	1,458,996	26.60	1,598,985	343,917	101,513	0.00	49.26	0.00	19.20
2	24.24	1,431,778	26.44	1,610,039	581,435	122,068	0.00	0.00	293.54	16.69
3	24.26	1,423,256	26.34	1,623,602	790,221	138,281	0.00	0.00	442.70	12.33
4	24.28	1,413,355	26.15	1,631,062	1,076,070	153,558	0.00	111.82	430.55	10.27
5	25.38	1,472,830	27.42	1,559,334	599,881	100,041	0.00	34.60	0.00	23.71
6	25.41	1,442,516	27.42	1,562,205	802,157	119,783	0.00	0.00	238.89	17.94
7	25.44	1,425,652	27.35	1,580,697	995,684	135,797	0.00	0.00	385.01	16.17
8	25.44	1,423,143	27.23	1,582,550	1,189,279	147,018	0.00	96.25	366.47	11.13
9	25.41	1,477,012	27.76	1,515,728	886,499	99,343	0.00	28.01	0.00	32.21
10	25.42	1,446,653	27.83	1,528,681	1,029,231	119,051	0.00	0.00	196.84	27.25
11	25.42	1,431,191	27.77	1,536,638	1,201,328	134,314	0.00	0.00	328.65	21.91
12	22.75	3,463,329	26.82	4,563,358	1,730,747	109,724	0.00	17.70	0.00	83.23
13	22.77	3,046,480	26.97	4,665,423	1,831,432	118,359	0.00	41.11	0.00	82.53
14	22.80	3,236,526	27.09	4,678,331	1,818,004	115,438	0.00	0.00	92.15	85.20
15	22.78	3,014,221	27.15	4,695,285	1,891,473	120,362	0.00	0.00	141.29	83.60
16	22.83	3,026,202	27.21	4,717,371	2,087,057	126,664	0.00	0.00	191.47	85.75
17	22.79	3,049,373	27.20	4,717,484	2,201,058	139,213	0.00	48.63	183.88	82.82
18	22.79	2,979,703	27.19	4,732,449	2,340,648	143,049	0.00	52.58	201.57	83.95
19	22.79	2,957,232	27.18	4,749,584	2,383,033	146,562	0.00	57.44	223.02	85.20

# Appendix C: Single- and two-phase measured data (continued).

Channel C2: Water and nitrogen tests. Number of channels: 3

Channel Dimensions:

Depth ( $\mu\text{m}$ ): 263.73 Hyd. Diameter ( $\mu\text{m}$ ): 207.01

Width ( $\mu\text{m}$ ): 170.37 Channel Length (m): 0.0635

Data Point	Test Fixture Temperature		Test Section Temperature, ( $^{\circ}\text{C}$ )						
	Inlet	Outlet	Pos #1	Pos #2	Pos #3	Pos #4	Pos #5	Pos #6	Pos #7
1	25.68	42.92	35.40	39.29	42.88	44.21	44.43	29.25	46.12
2	25.92	42.99	35.69	39.64	43.29	44.61	44.84	29.84	46.80
3	26.08	46.16	37.38	41.93	45.87	47.22	47.41	30.48	49.30
4	26.68	48.08	38.77	43.49	47.57	48.93	49.10	31.11	50.89
5	26.30	44.83	35.82	39.94	43.67	45.02	45.24	30.27	46.83
6	25.08	39.77	33.81	38.16	42.28	43.41	43.79	29.89	45.13
7	25.31	40.91	34.24	38.80	43.11	44.22	44.60	30.13	46.18
8	25.56	44.45	35.70	40.91	45.63	46.77	47.11	30.73	48.76
9	25.97	46.65	36.93	42.17	46.91	48.04	48.38	31.17	49.91
10	26.66	49.49	38.58	43.76	48.56	49.68	50.02	31.62	52.01
11	25.17	38.35	33.83	38.87	43.80	44.67	45.23	29.72	46.13
12	25.58	39.81	34.37	39.53	44.55	45.43	45.98	30.69	46.97
13	25.95	43.02	34.71	39.72	44.66	45.54	46.08	30.87	47.13
14	26.22	45.13	35.59	40.39	45.25	46.09	46.63	31.17	48.02
15	26.60	49.08	37.96	43.26	48.56	49.37	49.92	31.90	51.94
16	25.66	39.80	34.03	38.69	43.82	44.44	45.22	30.78	45.43
17	26.07	41.13	34.53	39.31	44.46	45.08	45.85	30.95	46.19
18	26.36	44.56	35.56	40.37	45.60	46.12	46.91	31.28	48.11
19	26.71	48.39	37.43	42.74	48.43	48.93	49.71	32.58	51.63
20	26.18	37.76	32.14	35.33	40.97	40.80	42.01	39.19	42.56
21	26.27	37.89	32.25	35.45	41.13	40.95	42.17	39.99	42.70
22	26.28	37.84	32.19	35.42	41.11	40.92	42.14	39.98	42.62
23	26.30	38.26	32.40	35.83	41.66	41.47	42.68	37.24	43.10
24	26.29	38.07	32.24	35.62	41.42	41.23	42.45	37.08	42.82
25	26.25	38.16	32.25	35.66	41.50	41.31	42.52	36.56	42.88
26	26.21	36.66	31.47	34.34	39.82	39.62	40.87	35.26	41.14
27	26.28	36.88	31.62	34.55	40.05	39.87	41.11	35.49	41.39
28	26.33	36.84	31.58	34.52	40.03	39.84	41.08	35.47	41.28
29	26.33	37.26	31.76	34.87	40.48	40.30	41.53	35.87	41.69
30	26.32	37.33	31.78	34.93	40.57	40.39	41.61	35.90	41.77
31	26.24	37.19	31.66	34.81	40.45	40.27	41.50	35.85	41.59
32	24.57	34.62	28.57	31.10	33.37	34.87	34.98	35.75	36.05
33	24.62	34.92	28.67	31.24	33.53	35.01	35.12	35.87	36.26
34	24.63	35.10	28.69	31.26	33.59	35.07	35.18	35.97	36.38
35	24.64	35.38	28.85	31.44	33.80	35.29	35.41	36.02	36.61
36	24.66	35.51	28.95	31.54	33.92	35.39	35.50	36.12	36.70
37	24.60	35.36	28.75	31.31	33.69	35.16	35.28	32.32	36.49
38	24.61	35.30	28.76	31.31	33.66	35.12	35.24	32.79	36.39

## Appendix C: Single- and two-phase measured data (continued).

Channel C2: Water and nitrogen (continued).

Data Point	Gas Flow Meter		Liquid Flow Meter		Test Fixture Press., (Pa)		Flow Meter/Flow rates, (cc/min)			
	Temp.(°C)	Press.(Pa)	Temp.(°C)	Press.(Pa)	Inlet	Outlet	F.M. #4	F.M. #5	F.M. #6	F.M. #1
1	24.54	1,595,579	24.50	1,684,095	253,721	107,298	0.00	20.82	0.00	11.26
2	24.52	1,578,399	24.51	1,660,653	272,913	103,557	0.00	39.45	0.00	12.52
3	24.52	1,586,605	24.57	1,627,490	427,445	108,274	0.00	0.00	140.65	10.23
4	24.49	1,563,863	24.54	1,598,985	639,102	116,218	0.00	0.00	220.94	8.47
5	24.47	1,562,756	24.57	1,590,282	890,545	124,942	0.00	0.00	261.15	11.25
6	24.38	1,700,583	24.86	1,611,893	405,043	104,337	0.00	15.33	0.00	23.30
7	24.35	1,594,607	25.12	1,586,032	419,036	102,775	0.00	29.90	0.00	23.75
8	24.39	1,584,050	25.31	1,546,540	577,253	105,338	0.00	0.00	120.36	18.90
9	24.39	1,562,484	25.39	1,564,511	786,536	114,554	0.00	0.00	189.82	17.28
10	24.35	1,548,152	25.37	1,569,032	1,000,070	123,970	0.00	0.00	244.72	13.31
11	24.25	1,690,026	26.17	1,596,385	614,982	103,224	0.00	12.15	0.00	39.62
12	24.21	1,591,872	26.50	1,562,364	626,172	103,724	0.00	23.43	0.00	37.13
13	24.21	1,580,840	26.65	1,551,038	805,322	107,336	0.00	0.00	99.67	31.67
14	24.22	1,561,264	26.64	1,558,159	986,032	115,456	0.00	0.00	158.15	25.99
15	24.22	1,560,812	26.53	1,571,632	1,158,242	124,058	0.00	0.00	213.48	20.55
16	24.17	1,698,164	27.16	1,589,264	832,923	101,407	0.00	8.76	0.00	47.98
17	24.14	1,592,414	27.32	1,508,517	834,641	102,013	0.00	18.68	0.00	45.30
18	24.17	1,579,145	27.33	1,552,779	1,005,947	107,492	0.00	0.00	85.11	37.32
19	24.21	1,539,381	27.14	1,572,536	1,159,824	117,509	0.00	0.00	148.11	29.96
20	22.69	3,391,714	27.47	4,818,599	1,802,474	108,076	0.00	0.00	55.97	82.67
21	22.69	3,336,239	27.50	4,814,440	1,833,444	109,988	0.00	0.00	72.87	83.52
22	22.63	3,056,811	27.51	4,831,100	1,954,000	114,545	0.00	0.00	130.66	83.74
23	22.64	2,823,113	27.47	4,810,800	2,136,745	125,344	0.00	37.50	142.26	78.41
24	22.65	2,791,985	27.45	4,784,465	2,245,794	126,418	0.00	38.50	147.04	80.83
25	22.68	2,797,071	27.41	4,767,442	2,306,943	128,136	0.00	42.39	164.01	80.33
26	22.71	3,445,244	27.61	4,882,234	2,245,862	109,271	0.00	0.00	47.79	95.99
27	22.66	3,378,964	27.63	4,837,904	2,222,307	109,981	0.00	0.00	61.97	91.92
28	22.60	3,052,945	27.67	4,845,116	2,383,576	115,924	0.00	0.00	116.63	95.84
29	22.67	2,837,242	27.62	4,762,605	2,487,856	124,207	0.00	31.98	121.02	90.69
30	22.64	2,829,103	27.59	4,757,767	2,514,327	125,297	0.00	34.23	130.53	88.47
31	22.65	2,809,097	27.51	4,773,817	2,582,393	127,019	0.00	36.42	140.18	90.77
32	23.62	4,169,711	25.34	4,661,060	607,996	129,002	0.00	75.53	278.82	14.62
33	23.49	4,063,735	25.26	4,646,728	653,704	130,986	0.00	76.28	282.84	12.18
34	23.50	3,996,484	25.20	4,642,410	687,975	132,085	0.00	78.80	293.75	10.93
35	23.49	3,990,538	25.12	4,604,071	700,430	132,738	0.00	82.14	307.60	10.36
36	23.47	3,985,384	25.05	4,622,178	730,044	134,124	0.00	83.72	314.86	10.06
37	23.44	3,972,883	25.01	4,646,728	763,952	135,469	0.00	83.84	316.36	11.68
38	23.48	4,036,179	24.96	4,653,239	786,852	137,524	0.00	87.16	330.86	12.10

## Appendix C: Single- and two-phase measured data (continued).

Channel C3: Argon gas tests.

Number of channels: 7

Channel Dimensions:

Depth ( $\mu\text{m}$ ): 71.3Hyd. Diameter ( $\mu\text{m}$ ): 95.55Width ( $\mu\text{m}$ ): 144.79

Channel Length (m): 0.0635

Data Point	Test Fixture Temperature		Test Section Temperature, ( $^{\circ}\text{C}$ )						
	Inlet	Outlet	Pos #1	Pos #2	Pos #3	Pos #4	Pos #5	Pos #6	Pos #7
1	33.41	33.95	44.25	44.72	44.95	32.74	40.51	46.65	46.27
2	33.10	36.74	48.30	48.96	49.30	33.50	50.91	50.93	50.38
3	32.97	38.78	49.91	50.62	50.98	34.56	52.58	52.60	52.02
4	32.84	40.53	50.59	51.34	51.71	34.41	53.30	53.33	52.75
5	32.77	41.91	50.98	51.75	52.13	34.81	53.72	53.75	53.16
6	32.64	42.76	51.12	51.90	52.30	34.84	53.89	53.92	53.32
7	32.42	43.55	51.13	51.94	52.35	35.36	53.94	53.98	53.39
8	32.22	44.03	51.05	51.88	52.30	35.04	53.89	53.94	53.35
9	32.02	44.40	50.93	51.77	52.20	34.99	53.79	53.85	53.28
10	31.83	44.67	50.87	51.73	52.18	35.10	53.77	53.84	53.27
11	31.61	43.56	50.81	51.70	52.17	35.10	53.76	53.85	53.28
12	31.37	43.66	50.66	51.58	52.07	34.70	50.15	53.76	53.20
13	31.07	43.72	50.38	51.33	51.84	34.83	47.56	53.54	52.99
14	30.72	43.76	50.15	51.12	51.66	35.06	47.37	53.38	52.83
15	30.42	43.86	49.88	50.88	51.44	34.77	47.24	53.18	52.63
16	30.18	44.03	49.45	50.48	51.06	34.45	49.82	52.81	52.28
17	30.04	44.20	49.12	50.18	50.77	34.61	46.20	52.54	52.01
18	29.93	44.28	48.86	49.95	50.56	34.36	45.90	52.34	51.81

Data Point	Gas Flow Meter		Test Fixture Press., (Pa)		Gas Flow Rates, (cc/min)		
	Temp. ( $^{\circ}\text{C}$ )	Press. (Pa)	Inlet	Outlet	F.M. #4	F.M. #5	F.M. #6
1	24.33	1,848,266	18,340	3,269	13.73	0.00	0.00
2	24.37	1,709,625	110,729	3,257	0.00	102.49	0.00
3	24.36	1,693,371	172,782	3,307	0.00	159.64	0.00
4	24.34	1,685,211	223,803	3,312	0.00	210.82	0.00
5	24.35	1,687,539	263,793	3,418	0.00	248.20	0.00
6	24.35	1,690,320	307,919	3,493	0.00	285.98	0.06
7	24.35	1,698,955	361,720	3,619	0.00	0.00	316.55
8	24.39	1,672,687	403,066	3,725	0.00	0.00	349.20
9	24.40	1,676,417	438,919	3,861	0.00	0.00	372.92
10	24.41	1,683,493	476,896	3,999	0.00	0.00	393.14
11	24.40	1,685,505	527,533	4,137	0.00	0.00	413.40
12	24.39	1,696,627	590,987	4,413	0.00	0.00	429.56
13	24.38	1,706,505	669,971	4,551	0.00	0.00	448.46
14	24.36	1,704,629	721,829	4,688	0.00	0.00	468.98
15	24.35	1,698,345	782,819	4,826	0.00	0.00	485.85
16	24.34	1,697,734	837,412	5,382	0.00	0.00	506.12
17	24.37	1,700,080	882,917	5,346	0.00	0.00	524.52
18	24.38	1,703,137	910,519	5,439	0.00	116.94	435.33

## Appendix C: Single- and two-phase measured data (continued).

Channel C3: Helium gas tests.

Number of channels:

7

Channel Dimensions:

Depth ( $\mu\text{m}$ ):

71.3

Hyd. Diameter ( $\mu\text{m}$ ):

95.55

Width ( $\mu\text{m}$ ):

144.79

Channel Length (m):

0.0635

Data Point	Test Fixture Temperature		Test Section Temperature, ( $^{\circ}\text{C}$ )						
	Inlet	Outlet	Pos #1	Pos #2	Pos #3	Pos #4	Pos #5	Pos #6	Pos #7
1	27.02	27.14	36.62	37.11	37.35	24.69	33.21	39.07	38.63
2	26.94	29.20	37.54	38.03	38.25	24.91	39.10	39.95	39.49
3	27.78	30.45	42.78	43.52	43.89	24.27	45.53	45.47	44.76
4	28.37	33.41	45.46	46.29	46.71	24.43	48.33	48.33	47.66
5	28.63	35.14	46.93	47.80	48.25	32.49	49.86	49.90	49.25
6	29.39	36.88	47.88	48.77	49.23	32.73	50.84	50.88	50.23
7	29.85	38.69	48.53	49.43	49.89	32.85	51.49	51.54	50.88
8	30.08	39.54	48.90	49.81	50.29	33.30	51.89	51.94	51.26
9	30.26	40.32	49.33	50.26	50.75	33.92	52.35	52.39	51.71
10	30.44	40.84	49.58	50.52	51.02	33.63	52.62	52.67	51.99
11	30.59	41.20	49.69	50.63	51.14	33.80	52.74	52.80	52.12
12	30.60	41.40	49.69	50.66	51.19	34.16	52.79	52.86	52.20
13	30.45	41.98	49.67	50.66	51.21	33.78	52.81	52.89	52.25
14	30.41	41.57	48.48	49.43	49.96	34.13	51.58	51.68	51.10
15	30.42	41.28	47.90	48.85	49.39	33.53	51.01	51.13	50.57
16	30.26	41.46	47.53	48.51	49.06	33.42	50.68	50.81	50.26
17	30.08	41.88	47.15	48.14	48.71	33.36	50.34	50.48	49.93
18	29.88	42.07	46.78	47.79	48.38	33.68	50.00	50.18	49.66

Data Point	Gas Flow Meter		Test Fixture Press., (Pa)		Gas Flow Rates, (cc/min)		
	Temp. ( $^{\circ}\text{C}$ )	Press. (Pa)	Inlet	Outlet	F.M. #4	F.M. #5	F.M. #6
1	24.00	1,945,560	14,158	3,786	0.00	8.96	0.00
2	24.01	1,806,242	88,056	3,463	0.00	67.94	0.00
3	23.99	1,794,125	145,203	3,481	0.00	114.44	0.00
4	23.98	1,785,874	194,845	3,549	0.00	157.39	0.00
5	23.96	1,783,274	229,319	3,536	0.00	189.04	0.00
6	23.95	1,780,245	267,929	3,585	0.00	223.73	0.00
7	23.92	1,780,358	298,266	3,610	0.00	0.00	249.81
8	23.89	1,776,221	328,603	3,707	0.00	0.00	278.50
9	23.90	1,776,221	351,457	3,723	0.00	0.00	305.50
10	23.91	1,774,842	367,733	3,843	0.00	0.00	335.41
11	23.91	1,774,842	375,329	3,863	0.00	0.00	368.29
12	23.89	1,776,244	400,308	3,963	0.00	0.00	404.23
13	23.84	1,774,842	428,226	4,058	0.00	0.00	436.09
14	23.83	1,774,955	463,740	4,157	0.00	0.00	460.04
15	23.82	1,776,040	503,661	4,277	0.00	0.00	479.39
16	23.80	1,774,707	542,340	4,404	0.00	0.00	494.11
17	23.81	1,776,221	590,490	4,485	0.00	0.00	506.82
18	23.79	1,776,018	631,971	4,553	0.00	109.61	408.82

### Appendix C: Single- and two-phase measured data (continued).

Channel C3: Nitrogen gas tests.

Number of channels: 7

Channel Dimensions:

Depth ( $\mu\text{m}$ ): 71.3Hyd. Diameter ( $\mu\text{m}$ ): 95.55Width ( $\mu\text{m}$ ): 144.79

Channel Length (m): 0.0635

Data Point	Test Fixture Temperature		Test Section Temperature, ( $^{\circ}\text{C}$ )						
	Inlet	Outlet	Pos #1	Pos #2	Pos #3	Pos #4	Pos #5	Pos #6	Pos #7
1	27.02	27.14	36.62	37.11	37.35	24.69	33.21	39.07	38.63
2	26.94	29.20	37.54	38.03	38.25	24.91	39.10	39.95	39.49
3	27.78	30.45	42.78	43.52	43.89	24.27	45.53	45.47	44.76
4	28.37	33.41	45.46	46.29	46.71	24.43	48.33	48.33	47.66
5	28.63	35.14	46.93	47.80	48.25	32.49	49.86	49.90	49.25
6	29.39	36.88	47.88	48.77	49.23	32.73	50.84	50.88	50.23
7	29.85	38.69	48.53	49.43	49.89	32.85	51.49	51.54	50.88
8	30.08	39.54	48.90	49.81	50.29	33.30	51.89	51.94	51.26
9	30.26	40.32	49.33	50.26	50.75	33.92	52.35	52.39	51.71
10	30.44	40.84	49.58	50.52	51.02	33.63	52.62	52.67	51.99
11	30.59	41.20	49.69	50.63	51.14	33.80	52.74	52.80	52.12
12	30.60	41.40	49.69	50.66	51.19	34.16	52.79	52.86	52.20
13	30.45	41.98	49.67	50.66	51.21	33.78	52.81	52.89	52.25
14	30.41	41.57	48.48	49.43	49.96	34.13	51.58	51.68	51.10
15	30.42	41.28	47.90	48.85	49.39	33.53	51.01	51.13	50.57
16	30.26	41.46	47.53	48.51	49.06	33.42	50.68	50.81	50.26
17	30.08	41.88	47.15	48.14	48.71	33.36	50.34	50.48	49.93
18	29.88	42.07	46.78	47.79	48.38	33.68	50.00	50.18	49.66

Data Point	Gas Flow Meter		Test Fixture Press., (Pa)		Gas Flow Rates, (cc/min)		
	Temp. ( $^{\circ}\text{C}$ )	Press. (Pa)	Inlet	Outlet	F.M. #4	F.M. #5	F.M. #6
1	24.00	1,945,560	14,158	3,786	0.00	8.96	0.00
2	24.01	1,806,242	88,056	3,463	0.00	67.94	0.00
3	23.99	1,794,125	145,203	3,481	0.00	114.44	0.00
4	23.98	1,785,874	194,845	3,549	0.00	157.39	0.00
5	23.96	1,783,274	229,319	3,536	0.00	189.04	0.00
6	23.95	1,780,245	267,929	3,585	0.00	223.73	0.00
7	23.92	1,780,358	298,266	3,610	0.00	0.00	249.81
8	23.89	1,776,221	328,603	3,707	0.00	0.00	278.50
9	23.90	1,776,221	351,457	3,723	0.00	0.00	305.50
10	23.91	1,774,842	367,733	3,843	0.00	0.00	335.41
11	23.91	1,774,842	375,329	3,863	0.00	0.00	368.29
12	23.89	1,776,244	400,308	3,963	0.00	0.00	404.23
13	23.84	1,774,842	428,226	4,058	0.00	0.00	436.09
14	23.83	1,774,955	463,740	4,157	0.00	0.00	460.04
15	23.82	1,776,040	503,661	4,277	0.00	0.00	479.39
16	23.80	1,774,707	542,340	4,404	0.00	0.00	494.11
17	23.81	1,776,221	590,490	4,485	0.00	0.00	506.82
18	23.79	1,776,018	631,971	4,553	0.00	109.61	408.82



### Appendix C: Single- and two-phase measured data (continued).

Channel C3: Water tests.

Number of channels: 7

Channel Dimensions:

Depth ( $\mu\text{m}$ ): 71.3Hyd. Diameter ( $\mu\text{m}$ ): 95.55Width ( $\mu\text{m}$ ): 144.79

Channel Length (m): 0.0635

Data Point	Test Fixture Temperature		Test Section Temperature, ( $^{\circ}\text{C}$ )						
	Inlet	Outlet	Pos #1	Pos #2	Pos #3	Pos #4	Pos #5	Pos #6	Pos #7
1	23.77	38.69	33.85	36.85	40.30	29.11	41.68	43.63	44.26
2	23.84	37.13	32.35	34.86	38.08	29.33	39.45	41.16	41.72
3	23.84	37.88	32.67	35.38	39.04	29.79	40.25	42.16	42.72
4	23.80	36.08	31.46	33.83	37.29	29.57	38.58	40.18	40.65
5	23.83	34.92	30.64	32.76	36.07	29.25	37.37	38.80	39.21
6	23.99	35.21	31.00	33.29	37.02	29.55	38.22	39.83	40.52
7	24.39	36.09	31.76	34.34	38.42	29.95	39.46	41.21	41.86
8	24.70	37.15	32.46	35.25	39.76	30.15	40.66	42.54	43.21
9	24.80	38.20	33.08	36.08	40.98	30.25	41.75	43.72	44.43
10	25.08	39.05	33.54	36.79	42.03	31.10	42.66	44.72	45.44
11	25.30	38.73	33.25	36.36	41.33	30.84	41.96	43.67	43.60
12	25.30	39.67	33.83	37.33	42.70	31.17	38.44	44.97	44.77
13	25.51	39.13	33.42	36.83	42.07	31.05	37.85	44.25	44.16
14	25.66	38.50	33.14	36.47	41.50	31.06	38.09	43.58	43.45
15	25.79	38.03	32.84	36.18	41.10	30.54	37.87	43.11	42.92
16	26.01	38.74	33.21	36.91	42.08	30.63	38.00	44.03	43.78
17	26.11	38.96	33.32	37.32	42.72	31.94	36.56	44.51	44.06
18	23.75	32.68	29.37	32.26	36.97	29.00	35.53	39.57	39.36
19	24.26	31.77	28.66	31.03	35.48	29.01	34.67	37.59	36.79
20	24.85	31.45	28.48	30.52	34.45	29.15	34.00	36.21	35.83

# Appendix C: Single- and two-phase measured data (continued).

## Channel C3: Water tests (continued).

Data Point	Liquid Flow Meter		Test Fixture Press., (Pa)		liquid Flow Rate
	Temp.(°C)	Press.(Pa)	Inlet	Outlet	F. M. #1, (cc/min)
1	23.39	2,305,239	330,072	99,092	9.37
2	23.75	2,263,374	412,131	97,421	12.76
3	23.85	2,236,021	466,565	96,185	14.30
4	24.06	2,194,517	548,941	94,682	17.69
5	24.37	2,200,146	624,240	94,903	21.05
6	24.75	2,170,826	693,233	93,913	24.49
7	25.17	2,158,822	762,429	93,673	28.66
8	25.62	2,168,882	826,086	94,107	31.62
9	26.05	2,135,855	894,491	93,000	36.60
10	26.43	2,137,505	962,670	93,224	39.76
11	26.73	2,136,194	1,035,257	93,529	42.86
12	27.01	2,111,373	1,098,055	92,591	48.03
13	27.22	2,110,944	1,176,022	92,661	51.80
14	27.42	2,136,149	1,263,077	94,060	54.61
15	27.55	2,131,470	1,318,167	93,850	57.72
16	27.76	2,127,378	1,379,586	93,951	61.09
17	27.89	2,108,773	1,510,473	93,640	69.83
18	25.11	3,975,596	1,371,384	106,086	58.78
19	25.75	3,925,389	1,718,404	105,187	73.03
20	26.46	3,851,604	2,049,261	103,968	84.08

Appendix C: Single- and two-phase measured data (continued).

Channel C3: Water and argon tests. Number of channels: 7

Channel Dimensions:

Depth ( $\mu\text{m}$ ): 71.3 Hyd. Diameter ( $\mu\text{m}$ ): 95.55

Width ( $\mu\text{m}$ ): 144.79 Channel Length (m): 0.0635

Data Point	Test Fixture Temperature		Test Section Temperature, ( $^{\circ}\text{C}$ )						
	Inlet	Outlet	Pos #1	Pos #2	Pos #3	Pos #4	Pos #5	Pos #6	Pos #7
1	24.84	37.15	33.27	35.85	38.29	29.63	36.68	41.21	41.61
2	25.90	38.69	34.51	37.05	39.43	30.97	37.34	42.23	42.47
3	25.91	38.56	34.79	37.29	39.64	31.17	37.46	42.40	42.54
4	25.93	38.36	34.89	37.36	39.65	31.16	37.44	42.39	42.40
5	25.12	36.22	32.87	35.23	37.89	30.70	36.14	40.69	41.05
6	26.46	37.77	33.76	36.34	39.07	30.54	40.58	41.92	42.14
7	26.49	38.53	34.48	37.20	39.98	31.57	41.50	42.85	42.99
8	26.49	39.55	35.45	38.34	41.12	31.49	42.61	44.00	44.04
9	25.89	36.47	32.55	35.14	38.11	30.65	39.55	40.90	41.16
10	26.18	37.84	33.61	36.34	39.41	30.87	40.85	42.26	42.46
11	26.35	38.77	34.52	37.34	40.44	31.70	41.90	43.34	43.47
12	26.35	40.65	35.94	39.15	42.37	32.22	43.76	45.33	45.36

Data Point	Gas Flow Meter		Liquid Flow Meter		Test Fixture Press., (Pa)		Flow Meter/Flow rates, (cc/min)			
	Temp. ( $^{\circ}\text{C}$ )	Press. (Pa)	Temp. ( $^{\circ}\text{C}$ )	Press. (Pa)	Inlet	Outlet	F.M. #4	F.M. #5	F.M. #6	F.M. #1
1	24.27	1,166,727	24.22	1,619,646	449,339	102,580	0.00	20.49	0.00	10.02
2	25.21	1,173,599	25.21	1,560,894	591,664	102,261	0.00	77.25	0.00	10.97
3	25.17	1,171,090	25.20	1,517,130	718,256	105,110	0.00	124.89	0.00	11.94
4	25.19	1,168,467	25.28	1,519,842	889,946	112,463	0.00	0.00	165.52	9.75
5	25.15	1,178,798	25.42	1,544,957	626,409	99,137	0.00	14.73	0.00	15.91
6	25.17	1,176,379	25.56	1,526,511	713,486	101,129	0.00	71.99	0.00	15.85
7	25.15	1,170,864	25.65	1,515,547	818,874	104,999	0.00	115.61	0.00	13.23
8	25.16	1,169,485	25.72	1,518,011	953,107	112,992	0.00	0.00	158.88	13.10
9	25.11	1,172,017	26.02	1,546,585	765,705	100,607	0.00	14.72	0.00	22.15
10	25.16	1,175,000	26.19	1,520,860	837,524	101,789	0.00	65.27	0.00	19.02
11	25.14	1,169,485	26.28	1,508,268	915,830	105,851	0.00	109.63	0.00	19.11

# Appendix C: Single- and two-phase measured data (continued).

Channel C3: Water and helium tests. Number of channels: 7

Channel Dimensions:

Depth ( $\mu\text{m}$ ): 71.3 Hyd. Diameter ( $\mu\text{m}$ ): 95.55

Width ( $\mu\text{m}$ ): 144.79 Channel Length (m): 0.0635

Data Point	Test Fixture Temperature		Test Section Temperature, ( $^{\circ}\text{C}$ )						
	Inlet	Outlet	Pos #1	Pos #2	Pos #3	Pos #4	Pos #5	Pos #6	Pos #7
1	26.21	37.80	33.70	36.29	38.97	30.77	40.48	41.82	42.09
2	26.30	38.12	34.07	36.70	39.37	31.15	40.87	42.20	42.36
3	26.54	38.38	34.28	36.92	39.63	30.75	41.12	42.51	42.63
4	26.58	37.95	33.98	36.55	39.21	30.86	40.70	42.07	42.15
5	26.66	38.60	34.47	37.11	39.83	31.34	41.30	42.74	42.79
6	26.74	38.11	33.50	36.21	39.31	31.07	40.73	42.23	42.54
7	26.80	38.94	34.32	37.17	40.27	31.01	41.69	43.21	43.42
8	26.75	39.82	35.07	38.04	41.20	30.83	42.60	44.20	44.35
9	26.77	39.81	35.07	38.05	41.20	31.09	42.60	44.20	44.32
10	26.47	37.14	32.90	35.55	38.79	30.74	40.15	41.59	41.87
11	26.61	37.48	33.14	35.89	39.15	30.98	40.51	41.97	42.18
12	26.90	37.99	33.56	36.39	39.69	31.08	41.04	42.54	42.69

Data Point	Gas Flow Meter		Liquid Flow Meter		Test Fixture Press., (Pa)		Flow Meter/Flow rates, (cc/min)			
	Temp.( $^{\circ}\text{C}$ )	Press.(Pa)	Temp.( $^{\circ}\text{C}$ )	Press.(Pa)	Inlet	Outlet	F.M. #4	F.M. #5	F.M. #6	F.M. #1
1	25.03	1,186,032	26.04	1,559,515	667,165	108,173	0.00	0.00	125.03	13.12
2	25.03	1,179,137	26.06	1,548,778	768,936	118,983	0.00	0.00	224.46	14.24
3	25.00	1,177,758	26.06	1,550,902	850,248	127,137	0.00	0.00	301.10	14.15
4	24.97	1,176,221	26.06	1,540,911	941,349	133,658	0.00	0.00	366.33	14.35
5	24.95	1,174,503	26.05	1,542,425	1,009,596	140,675	0.00	0.00	440.16	12.23
6	24.89	1,197,064	26.23	1,503,950	756,932	105,103	0.00	0.00	112.38	19.22
7	24.88	1,188,722	26.26	1,507,386	832,910	116,908	0.00	0.00	212.04	17.37
8	24.84	1,185,286	26.26	1,510,936	899,438	125,658	0.00	0.00	302.78	15.23
9	24.81	1,181,488	26.25	1,509,489	979,575	132,639	0.00	0.00	368.34	14.24
10	24.77	1,209,406	26.73	1,458,016	880,608	99,090	0.00	0.00	52.73	26.27
11	24.75	1,198,307	26.81	1,477,547	920,710	104,757	0.00	0.00	97.01	25.60
12	24.75	1,191,548	26.87	1,478,022	988,640	115,404	0.00	0.00	181.81	23.91

**Appendix C: Single- and two-phase measured data (continued).**

Channel C3: Water and nitrogen tests. Number of channels: 7

Channel Dimensions:

Depth ( $\mu\text{m}$ ): 71.3 Hyd. Diameter ( $\mu\text{m}$ ): 95.55

Width ( $\mu\text{m}$ ): 144.79 Channel Length (m): 0.0635

Data Point	Test Fixture Temperature		Test Section Temperature, ( $^{\circ}\text{C}$ )						
	Inlet	Outlet	Pos #1	Pos #2	Pos #3	Pos #4	Pos #5	Pos #6	Pos #7
1	23.07	34.33	30.68	32.90	35.62	28.55	34.75	38.54	38.97
2	23.48	35.43	31.13	33.44	36.21	28.65	35.07	39.16	39.59
3	23.84	38.22	33.07	35.84	39.16	29.55	36.98	42.32	42.79
4	24.05	38.87	33.66	36.54	39.83	29.70	37.49	42.97	43.36
5	24.26	39.46	34.38	37.38	40.61	30.51	38.48	43.70	43.97
6	24.45	40.21	35.11	38.29	41.56	30.02	38.68	44.66	44.81
7	23.93	37.63	32.64	35.38	38.93	29.44	36.79	42.02	42.52
8	24.23	38.10	32.89	35.76	39.30	29.68	37.03	42.38	42.81
9	24.42	38.70	33.40	36.38	39.92	30.02	37.49	43.04	43.40
10	24.50	39.19	33.96	37.07	40.57	30.45	37.86	43.67	43.89
11	24.09	36.39	32.06	34.61	38.09	29.37	36.86	41.01	41.32
12	24.33	37.04	32.20	34.93	38.51	30.33	36.50	41.50	41.82
13	24.49	36.72	32.18	34.85	38.30	30.09	36.35	41.24	41.47

Data Point	Gas Flow Meter		Liquid Flow Meter		Test Fixture Press., (Pa)		Flow Meter/Flow rates, (cc/min)			
	Temp. ( $^{\circ}\text{C}$ )	Press. (Pa)	Temp. ( $^{\circ}\text{C}$ )	Press. (Pa)	Inlet	Outlet	F.M. #4	F.M. #5	F.M. #6	F.M. #1
1	23.52	1,232,916	23.75	1,451,641	606,776	101,701	0.00	11.88	0.00	17.09
2	23.51	1,235,629	23.88	1,433,782	609,534	100,145	0.00	23.23	0.00	15.12
3	23.51	1,217,748	24.00	1,421,417	639,848	99,569	0.00	47.04	0.00	16.16
4	23.52	1,209,474	24.08	1,413,776	714,492	102,148	0.00	86.34	0.00	16.40
5	23.50	1,210,830	24.16	1,420,332	866,425	109,950	0.00	0.00	143.22	15.11
6	23.47	1,203,958	24.20	1,426,752	973,282	117,091	0.00	0.00	191.49	14.18
7	23.46	1,228,779	24.67	1,451,867	727,558	102,813	0.00	19.89	0.00	21.52
8	23.47	1,217,748	24.78	1,434,664	772,724	101,350	0.00	41.75	0.00	20.01
9	23.50	1,212,752	24.88	1,401,999	822,728	102,790	0.00	73.73	0.00	20.15
10	23.52	1,208,547	24.91	1,422,208	958,046	111,026	0.00	0.00	133.50	19.66
11	23.53	1,223,987	25.23	1,463,034	874,563	104,215	0.00	18.31	0.00	27.27
12	23.53	1,216,052	25.35	1,458,106	906,663	103,247	0.00	37.18	0.00	26.77
13	23.56	1,210,853	25.50	1,457,722	995,752	105,923	0.00	64.20	0.00	27.39

## Appendix C: Single- and two-phase measured data (continued).

Channel D: Argon gas tests.

Number of channels: 7

Channel Dimensions:

Depth ( $\mu\text{m}$ ): 111.33      Hyd. Diameter ( $\mu\text{m}$ ): 111.86Width ( $\mu\text{m}$ ): 112.73      Channel Length (m): 0.0635

Data Point	Test Fixture Temperature		Test Section Temperature, ( $^{\circ}\text{C}$ )						
	Inlet	Outlet	Pos #1	Pos #2	Pos #3	Pos #4	Pos #5	Pos #6	Pos #7
1	29.88	32.23	39.20	42.37	42.89	44.45	44.42	44.06	41.85
2	29.73	33.93	40.80	45.23	45.74	47.28	47.20	46.70	45.68
3	30.05	34.31	40.74	46.83	47.40	48.93	48.89	48.43	48.87
4	30.32	36.08	41.83	48.01	48.63	50.15	50.16	49.77	50.08
5	30.22	38.85	42.51	48.72	49.35	50.86	50.87	50.44	50.79
6	30.53	39.31	42.86	49.08	49.71	51.23	51.23	50.78	51.16
7	30.63	39.44	42.97	49.22	49.86	51.37	51.36	50.89	51.30
8	30.68	39.96	43.06	49.33	49.97	51.48	51.46	50.98	51.42
9	30.84	40.25	42.95	49.30	49.96	51.46	51.45	50.96	51.40
10	30.87	40.47	42.75	49.19	49.87	51.37	51.36	50.88	51.30
11	30.75	40.75	42.55	49.08	49.78	51.28	51.28	50.79	51.21
12	30.78	41.06	42.45	48.98	49.69	50.88	51.14	50.72	51.12
13	30.33	41.45	42.10	48.80	49.54	51.04	51.07	50.58	50.97
14	30.25	42.90	41.74	48.52	49.29	50.80	50.85	50.39	50.72
15	30.65	43.17	41.55	48.39	49.17	50.67	50.74	50.30	50.60
16	29.47	40.98	38.15	45.01	45.82	47.30	47.43	47.15	47.19
17	29.53	41.51	38.52	45.46	46.30	47.77	47.91	47.63	47.66
18	29.51	41.74	38.56	45.56	46.42	47.89	48.04	47.77	47.77

Data Point	Gas Flow Meter		Test Fixture Press., (Pa)		Gas Flow Rates, (cc/min)		
	Temp. ( $^{\circ}\text{C}$ )	Press. (Pa)	Inlet	Outlet	F.M. #4	F.M. #5	F.M. #6
1	25.35	1,724,997	67,913	3,460.93	29.43	0.00	0.00
2	25.37	1,611,697	152,865	3,307.21	0.00	84.70	0.00
3	25.40	1,602,406	254,071	3,431.54	0.00	163.12	0.00
4	25.39	1,595,579	346,460	3,585.26	0.00	221.58	0.05
5	25.41	1,595,285	441,608	3,723.16	0.00	0.00	255.09
6	25.41	1,568,543	518,829	3,879.14	0.00	0.00	287.79
7	25.40	1,584,548	613,592	4,141.36	0.00	0.00	308.80
8	25.41	1,570,374	737,629	4,319.95	0.00	0.00	316.82
9	25.40	1,566,124	848,555	4,568.61	0.00	0.00	326.53
10	25.41	1,571,391	953,649	4,794.67	0.00	0.00	339.50
11	25.40	1,568,995	1,037,313	4,977.77	0.00	0.00	351.89
12	25.38	1,573,426	1,112,816	5,212.87	0.00	0.00	361.79
13	25.42	1,783,116	1,206,923	5,407.28	0.00	0.00	369.46
14	25.42	1,783,252	1,306,094	5,961.12	0.00	0.00	377.42
15	25.42	1,785,580	1,378,591	6,182.65	0.00	82.24	306.13
16	25.40	1,790,237	1,441,186	7,080.10	0.00	83.80	314.09
17	25.41	1,793,424	1,551,479	7,301.64	0.00	84.06	317.10
18	25.40	1,796,159	1,647,011	7,532.21	0.00	84.27	319.65

## Appendix C: Single- and two-phase measured data (continued).

Channel D: Helium gas tests.

Number of channels:

7

Channel Dimensions:

Depth ( $\mu\text{m}$ ): 111.33Hyd. Diameter ( $\mu\text{m}$ ): 111.86Width ( $\mu\text{m}$ ): 112.73

Channel Length (m): 0.0635

Data Point	Test Fixture Temperature		Test Section Temperature, ( $^{\circ}\text{C}$ )						
	Inlet	Outlet	Pos #1	Pos #2	Pos #3	Pos #4	Pos #5	Pos #6	Pos #7
1	33.13	32.92	37.02	43.71	44.31	45.79	45.82	45.54	45.68
2	33.28	34.38	37.68	44.41	45.03	46.50	46.54	46.27	46.39
3	32.87	38.71	37.92	44.68	45.31	46.78	46.83	46.55	46.67
4	32.77	40.33	37.96	44.76	45.39	46.86	46.89	46.59	46.75
5	32.79	40.64	38.00	44.81	45.45	46.91	46.93	46.60	46.80
6	32.76	40.89	37.99	44.83	45.49	46.95	46.98	46.62	46.84
7	32.70	40.72	37.98	44.84	45.52	46.97	47.00	46.65	46.86
8	32.61	42.32	37.90	44.79	45.48	46.94	46.98	46.61	46.83
9	32.52	43.08	37.81	44.72	45.43	46.88	46.94	46.57	46.78
10	32.33	43.71	37.67	44.62	45.37	46.82	46.88	46.52	46.71
11	32.17	43.89	37.49	44.47	45.23	46.68	46.76	46.39	46.57
12	31.94	43.97	37.22	44.21	44.99	46.44	46.53	46.16	46.33
13	31.70	44.02	36.94	43.95	44.76	46.21	46.31	45.95	46.10
14	31.41	44.13	36.61	43.66	44.51	45.96	46.08	45.73	45.84

Data Point	Gas Flow Meter		Test Fixture Press., (Pa)		Gas Flow Rates, (cc/min)		
	Temp. ( $^{\circ}\text{C}$ )	Press. (Pa)	Inlet	Outlet	F.M. #4	F.M. #5	F.M. #6
1	24.44	1,271,753	33,853	3,431.54	30.48	0.00	0.00
2	24.44	1,157,572	98,664	3,417.98	0.00	97.25	0.00
3	24.43	1,135,011	218,632	3,562.66	0.00	214.61	0.00
4	24.44	1,126,263	304,127	3,664.38	0.00	288.85	0.00
5	24.47	1,119,436	363,421	3,757.06	0.00	0.00	369.98
6	24.48	1,111,569	424,095	3,890.44	0.00	0.00	431.96
7	24.48	1,108,811	476,495	4,010.25	0.00	0.00	486.80
8	24.45	1,108,879	526,137	4,179.79	0.00	0.00	537.31
9	24.46	1,104,674	568,884	4,272.47	0.00	0.00	581.15
10	24.46	1,106,053	617,148	4,410.37	0.00	0.00	629.13
11	24.46	1,107,432	654,379	4,548.26	0.00	0.00	665.47
12	24.46	1,101,916	698,505	4,636.43	0.00	146.59	551.60
13	24.48	1,102,504	739,874	4,796.93	0.00	153.13	582.01
14	24.46	1,104,674	781,242	4,961.95	0.00	159.06	610.66

Appendix C: Single- and two-phase measured data (continued).

Channel D: Nitrogen gas tests.

Number of channels: 7

Channel Dimensions:

Depth ( $\mu\text{m}$ ): 111.33

Hyd. Diameter ( $\mu\text{m}$ ): 111.86

Width ( $\mu\text{m}$ ): 112.73

Channel Length (m): 0.0635

Data Point	Test Fixture Temperature		Test Section Temperature, ( $^{\circ}\text{C}$ )						
	Inlet	Outlet	Pos #1	Pos #2	Pos #3	Pos #4	Pos #5	Pos #6	Pos #7
1	31.97	32.43	33.94	40.51	40.93	42.50	42.54	42.36	42.42
2	32.03	35.67	37.15	43.91	44.47	45.95	45.99	45.76	45.85
3	31.80	37.95	38.31	45.12	45.71	47.18	47.22	46.95	47.08
4	31.39	39.75	38.50	45.37	45.98	47.45	47.50	47.21	47.35
5	31.09	42.00	38.56	45.45	46.10	47.56	47.61	47.33	47.46
6	30.88	42.93	38.55	45.48	46.15	47.61	47.68	47.39	47.51
7	30.71	43.38	38.44	45.39	46.08	47.54	47.62	47.33	47.43
8	30.48	42.91	38.18	45.13	45.84	47.30	47.38	47.09	47.19
9	30.32	42.95	37.98	44.97	45.70	47.16	47.25	46.97	47.05
10	30.12	43.13	37.87	44.82	45.59	47.04	47.15	46.86	46.93
11	29.93	43.12	37.63	44.61	45.40	46.85	46.97	46.69	46.74
12	29.72	43.12	37.33	44.31	45.13	46.59	46.72	46.46	46.47
13	29.53	43.17	37.02	44.07	44.92	46.37	46.53	46.28	46.26
14	29.26	43.11	36.68	43.74	44.62	46.07	46.26	46.02	45.96

Data Point	Gas Flow Meter		Test Fixture Press., (Pa)		Gas Flow Rates, (cc/min)		
	Temp. ( $^{\circ}\text{C}$ )	Press. (Pa)	Inlet	Outlet	F.M. #4	F.M. #5	F.M. #6
1	24.44	1,068,641	19,788	3,174	21.60	0.00	0.00
2	24.40	907,485	61,608	3,221	0.00	71.84	0.00
3	24.41	1,209,158	145,272	3,287	0.00	167.06	0.00
4	24.40	1,188,790	233,525	3,325	0.00	245.89	0.18
5	24.38	1,177,758	301,093	3,454	0.00	0.00	295.22
6	24.39	1,168,852	364,525	3,583	0.00	0.00	337.83
7	24.39	1,161,211	427,956	3,725	0.00	0.00	370.64
8	24.39	1,156,780	505,177	3,859	0.00	0.00	394.68
9	24.41	1,154,316	577,086	4,001	0.00	0.00	406.39
10	24.42	1,154,610	672,346	4,171	0.00	0.00	410.52
11	24.44	1,150,586	765,798	4,401	0.00	0.00	415.55
12	24.48	1,147,422	862,483	4,553	0.00	89.89	336.89
13	24.49	1,150,179	928,356	4,684	0.00	90.31	340.76
14	24.50	1,150,903	1,018,145	4,829	0.00	91.45	348.58



## Appendix C: Single- and two-phase measured data (continued).

Channel D: Water tests.

Number of channels:

7

Channel Dimensions:

Depth ( $\mu\text{m}$ ): 111.33Hyd. Diameter ( $\mu\text{m}$ ): 111.86Width ( $\mu\text{m}$ ): 112.73

Channel Length (m): 0.0635

Data Point	Test Fixture Temperature		Test Section Temperature, ( $^{\circ}\text{C}$ )						
	Inlet	Outlet	Pos #1	Pos #2	Pos #3	Pos #4	Pos #5	Pos #6	Pos #7
1	23.84	43.12	31.14	38.44	43.43	43.56	45.90	48.04	43.19
2	23.71	41.33	29.90	36.52	41.25	41.33	43.46	45.53	41.01
3	23.63	39.94	28.99	35.03	39.53	39.58	41.52	43.48	39.30
4	23.58	40.30	29.43	35.93	41.03	40.71	42.72	44.77	40.42
5	23.99	39.82	29.26	35.32	40.25	39.88	41.69	43.56	39.61
6	24.03	40.86	29.80	36.71	42.39	41.53	43.41	45.35	41.25
7	24.14	40.50	29.66	36.36	41.99	41.08	42.84	44.64	40.83
8	24.29	40.49	29.38	35.96	41.52	40.58	42.22	43.88	40.34
9	24.43	41.36	30.35	37.22	43.46	42.07	43.74	45.39	41.82
10	24.64	40.59	30.42	37.18	43.57	42.12	43.99	46.28	41.87
11	24.84	40.32	30.02	37.01	43.36	41.89	43.72	45.95	41.65
12	25.05	39.85	29.72	36.68	42.99	41.49	43.22	45.32	41.27
13	25.26	40.88	30.46	38.04	45.22	43.15	44.91	46.91	42.92
14	25.43	40.67	30.38	37.99	45.22	43.07	44.76	46.63	42.85
15	25.58	40.14	30.26	37.62	44.80	42.62	44.18	45.74	42.41
16	26.11	41.72	31.84	39.79	48.05	45.13	46.73	48.22	44.92
17	26.21	41.16	31.77	39.42	47.62	44.67	46.17	47.38	44.46
18	26.34	40.26	31.38	38.80	46.98	44.03	45.46	46.47	43.83
19	26.48	40.04	31.77	38.29	46.34	43.40	44.65	45.12	43.21
20	26.57	38.64	31.47	36.97	44.92	41.99	42.94	42.65	41.82
21	27.58	32.32	29.68	30.84	33.82	34.10	34.86	35.44	31.85
22	27.63	32.22	29.25	30.15	32.94	33.21	33.73	33.92	31.24
23	27.65	32.12	29.01	29.66	32.35	32.61	33.10	33.50	30.88
24	27.67	32.04	28.55	29.39	32.04	32.28	32.75	33.27	30.45
25	27.70	31.98	28.38	29.23	31.85	32.09	32.55	33.13	30.27
26	27.68	31.93	28.29	29.08	31.72	31.95	32.42	33.04	30.17

Appendix C: Single- and two-phase measured data (continued).

Channel D: Water tests (continued).

Data Point	Liquid Flow Meter		Test Fixture Press., (Pa)		liquid Flow Rate
	Temp.(°C)	Press.(Pa)	Inlet	Outlet	F. M. #1. (cc/min)
1	23.96	2,225,645	406,862	104,174	9.24
2	23.95	2,179,687	478,522	102,173	11.71
3	23.99	2,158,619	545,254	101,326	14.58
4	24.08	2,132,555	609,657	100,041	13.98
5	24.68	2,300,967	686,856	99,173	17.98
6	24.89	2,295,564	764,167	98,814	18.59
7	25.14	2,274,337	826,740	97,905	21.73
8	25.45	2,273,162	893,200	97,844	22.80
9	25.68	2,221,531	962,238	95,853	24.67
10	25.98	2,240,271	1,048,185	96,388	26.69
11	26.24	2,210,499	1,096,245	95,561	27.72
12	26.49	2,203,288	1,178,303	95,425	29.63
13	26.72	2,243,255	1,267,641	96,809	31.46
14	26.92	2,231,681	1,320,629	96,416	33.17
15	27.13	2,241,288	1,464,084	96,992	36.92
16	27.72	2,234,303	1,521,819	96,935	37.67
17	27.86	2,196,190	1,642,307	95,753	38.85
18	28.00	2,200,892	1,785,040	96,004	43.58
19	28.17	2,206,746	1,922,347	96,345	44.61
20	28.35	2,209,482	2,218,436	96,718	50.85
21	29.27	4,271,595	2,114,910	102,015	60.45
22	29.34	4,259,591	2,435,639	102,212	65.24
23	29.43	4,261,196	2,778,545	102,567	69.86
24	29.50	4,243,790	3,111,775	102,230	72.52
25	29.58	4,234,182	3,467,815	102,234	76.93
26	29.65	4,229,661	3,820,418	102,347	79.44

**Appendix C: Single- and two-phase measured data (continued).**

Channel D: Water and argon tests. Number of channels: 7

Channel Dimensions:

Depth ( $\mu\text{m}$ ): 111.33 Hyd. Diameter ( $\mu\text{m}$ ): 111.86

Width ( $\mu\text{m}$ ): 112.73 Channel Length (m): 0.0635

Data Point	Test Fixture Temperature		Test Section Temperature, ( $^{\circ}\text{C}$ )						
	Inlet	Outlet	Pos #1	Pos #2	Pos #3	Pos #4	Pos #5	Pos #6	Pos #7
1	27.03	40.71	30.19	35.66	39.53	39.88	41.52	43.00	39.64
2	27.01	40.20	29.91	35.20	39.02	39.36	40.91	42.26	39.13
3	27.25	41.44	31.17	36.59	40.47	40.84	42.37	43.57	40.59
4	27.69	43.15	32.27	38.67	42.61	42.97	44.47	45.46	42.70
5	27.66	42.82	31.53	38.49	42.39	42.79	44.19	45.02	42.55
6	26.64	41.64	30.40	36.73	41.30	41.26	43.03	44.65	41.00
7	27.14	42.90	30.97	37.73	42.42	42.37	44.18	45.73	42.09
8	27.43	43.78	31.55	38.80	43.53	43.50	45.27	46.65	43.21
9	27.90	45.61	32.52	40.78	45.60	45.57	47.31	48.48	45.26
10	27.88	45.28	32.97	40.63	45.36	45.35	46.96	47.92	45.06
11	26.49	40.75	30.12	35.77	40.23	40.15	41.79	43.30	39.92
12	26.58	40.30	29.83	35.33	39.70	39.62	41.15	42.47	39.39
13	26.88	40.77	30.23	36.11	40.51	40.44	41.92	43.12	40.20
14	27.10	42.12	30.78	37.35	41.86	41.80	43.29	44.33	41.54
15	26.53	33.88	27.65	31.17	35.08	35.00	36.03	36.63	31.36
16	26.54	33.33	27.30	30.46	34.23	34.12	35.06	35.73	30.63
17	26.57	33.51	27.35	30.46	34.22	34.10	35.04	35.78	30.63
18	26.55	33.64	27.32	30.46	34.20	34.07	34.96	35.69	30.61
19	26.47	33.21	26.48	29.80	33.44	33.29	34.13	35.01	29.89
20	26.38	33.11	26.43	29.76	33.41	33.26	34.12	34.98	29.86
21	27.61	33.90	27.39	30.44	34.38	33.88	34.71	35.94	30.60
22	27.70	34.09	27.47	30.50	34.44	33.94	34.76	36.00	30.65
23	27.71	34.30	27.52	30.65	34.65	34.14	34.98	36.18	30.82
24	27.73	34.03	27.81	30.40	34.33	33.81	34.62	35.85	30.64
25	27.75	34.10	27.85	30.47	34.42	33.92	34.72	35.92	30.72
26	25.11	36.19	28.76	32.59	35.41	36.38	37.29	37.37	36.28
27	25.13	36.41	29.46	32.85	35.69	36.64	37.56	37.57	36.50
28	25.22	36.95	29.73	33.29	36.18	37.12	38.07	38.10	36.97
29	25.38	37.36	30.02	33.93	36.80	37.78	38.68	38.63	37.67

# Appendix C: Single- and two-phase measured data (continued).

## Channel D: Water and argon (continued).

Data Point	Gas Flow Meter		Liquid Flow Meter		Test Fixture Press., (Pa)		Flow Meter/Flow rates, (cc/min)			
	Temp.(°C)	Press.(Pa)	Temp.(°C)	Press.(Pa)	Inlet	Outlet	F.M. #4	F.M. #5	F.M. #6	F.M. #1
1	25.42	1,470,977	26.48	1,555,717	688,682	96,960	0.00	15.05	0.00	11.07
2	25.47	1,479,092	26.47	1,554,881	804,062	95,954	0.00	27.96	0.00	12.99
3	25.49	1,490,282	26.46	1,544,822	883,588	97,894	0.00	54.96	0.00	12.06
4	25.46	1,467,563	26.34	1,561,640	978,442	101,920	0.00	85.11	0.00	9.45
5	25.43	1,470,095	26.29	1,558,701	1,173,597	105,914	0.00	0.00	96.44	9.60
6	25.28	1,488,270	26.36	1,620,144	811,747	101,027	0.00	13.85	0.00	15.23
7	25.32	1,497,697	26.35	1,606,196	862,000	98,525	0.00	29.22	0.00	11.95
8	25.30	1,484,540	26.32	1,596,634	955,294	99,856	0.00	49.83	0.00	12.96
9	25.29	1,482,053	26.36	1,577,713	1,056,816	102,191	0.00	74.52	0.00	12.15
10	25.34	1,456,758	26.33	1,571,067	1,231,173	105,833	0.00	90.72	0.00	12.23
11	25.32	1,472,356	26.51	1,608,750	904,273	100,093	0.00	11.00	0.00	16.74
12	25.34	1,500,432	26.57	1,603,348	1,041,964	100,304	0.00	23.81	0.00	16.80
13	25.35	1,483,342	26.60	1,604,161	1,112,855	101,387	0.00	43.91	0.00	15.10
14	25.37	1,468,716	26.60	1,594,780	1,244,872	104,484	0.00	69.13	0.00	15.29
15	24.51	3,533,225	28.10	3,984,314	1,994,489	117,100	0.00	0.00	197.97	46.32
16	24.50	3,514,508	28.13	4,040,127	2,258,094	120,791	0.00	0.00	194.64	50.99
17	24.50	3,545,591	28.14	4,069,198	2,310,743	122,717	0.00	0.00	208.81	49.67
18	24.39	3,562,635	28.10	3,958,159	2,506,666	129,203	0.00	44.70	168.81	45.25
19	24.42	3,531,372	28.08	3,967,518	2,764,574	131,495	0.00	44.56	169.65	49.85
20	24.59	3,592,407	28.05	3,914,372	2,594,806	127,024	0.00	21.03	78.36	54.56
21	25.35	3,988,323	29.33	4,101,728	2,779,675	109,423	0.00	10.54	0.00	68.22
22	25.37	3,605,586	29.39	4,157,812	2,910,155	114,050	0.00	24.72	0.00	67.02
23	25.47	3,521,131	29.39	4,068,294	3,039,166	119,507	0.00	45.42	0.00	62.79
24	25.56	3,790,184	29.43	4,172,009	3,048,502	115,058	0.00	0.00	62.22	66.69
25	25.43	3,602,738	29.43	4,045,982	3,125,678	117,206	0.00	0.00	89.14	64.03
26	23.95	2,578,248	24.82	1,996,867	1,648,274	122,645	0.00	46.76	171.88	10.14
27	23.94	2,550,601	24.82	2,030,233	1,721,675	125,706	0.00	47.89	176.74	11.31
28	23.93	2,538,033	24.78	2,049,086	1,757,663	128,355	0.00	49.80	184.51	9.41
29	23.93	2,526,933	24.75	2,047,436	1,807,870	130,582	0.00	52.46	195.50	8.86

Appendix C: Single- and two-phase measured data (continued).

Channel D: Water and helium tests. Number of channels: 7

Channel Dimensions:

Depth ( $\mu\text{m}$ ): 111.33 Hyd. Diameter ( $\mu\text{m}$ ): 111.86

Width ( $\mu\text{m}$ ): 112.73 Channel Length (m): 0.0635

Data Point	Test Fixture Temperature		Test Section Temperature, ( $^{\circ}\text{C}$ )						
	Inlet	Outlet	Pos #1	Pos #2	Pos #3	Pos #4	Pos #5	Pos #6	Pos #7
1	27.25	41.86	30.52	36.16	40.12	40.47	42.16	43.69	40.22
2	27.65	42.24	30.67	36.47	40.44	40.79	42.46	43.89	40.54
3	28.04	43.21	31.70	38.50	42.49	42.86	44.43	45.56	42.60
4	27.67	41.56	31.09	37.57	41.42	41.77	43.12	43.89	41.51
5	26.98	41.34	30.82	36.13	40.53	40.54	42.27	43.92	40.30
6	27.11	41.89	30.96	36.48	41.02	41.00	42.78	44.43	40.74
7	27.39	42.24	31.24	36.97	41.50	41.48	43.21	44.73	41.22
8	27.28	41.72	30.67	36.85	41.35	41.31	42.93	44.24	41.05
9	27.09	40.78	30.26	36.27	40.68	40.63	42.13	43.26	40.38
10	27.25	41.36	30.78	37.21	41.64	41.63	43.10	44.06	41.37
11	26.52	39.15	29.53	34.31	38.50	38.47	39.94	41.37	38.26
12	26.57	39.32	29.52	34.40	38.63	38.59	40.09	41.47	38.38
13	26.63	38.90	29.27	34.17	38.37	38.33	39.76	41.04	38.11
14	26.68	38.63	29.92	34.28	38.44	38.41	39.77	40.88	38.20
15	26.68	38.68	29.89	34.52	38.71	38.68	40.01	41.01	38.45
16	27.80	33.92	28.49	30.61	34.66	34.11	34.92	36.10	31.11
17	27.77	33.71	28.40	30.39	34.42	33.86	34.65	35.82	30.96
18	27.73	33.68	28.45	30.41	34.46	33.90	34.68	35.85	31.01
19	27.71	33.66	28.38	30.39	34.45	33.88	34.67	35.83	30.97
20	27.64	33.62	28.40	30.41	34.50	33.93	34.72	35.86	31.00

Appendix C: Single- and two-phase measured data (continued).

Channel A: Water and helium (continued).

Data Point	Gas Flow Meter		Liquid Flow Meter		Test Fixture Press., (Pa)		Flow Meter/Flow rates, (cc/min)			
	Temp.(°C)	Press.(Pa)	Temp.(°C)	Press.(Pa)	Inlet	Outlet	F.M. #4	F.M. #5	F.M. #6	F.M. #1
1	25.48	1,958,852	26.44	1,620,279	662,934	98,647	0.00	16.04	0.00	11.94
2	25.52	1,901,999	26.40	1,608,863	692,322	99,947	0.00	35.37	0.00	12.04
3	25.53	1,896,438	26.37	1,594,848	830,488	109,658	0.00	0.00	131.46	9.00
4	25.56	1,889,317	26.30	1,603,009	1,086,271	123,949	0.00	0.00	219.04	11.54
5	25.53	1,975,739	26.38	1,595,255	754,872	100,704	0.00	13.84	0.00	14.13
6	25.55	1,900,028	26.39	1,575,493	813,510	98,199	0.00	30.60	0.00	13.17
7	25.56	1,897,320	26.41	1,560,487	860,485	100,726	0.00	58.93	0.00	13.00
8	25.57	1,904,463	26.44	1,548,438	976,905	105,243	0.00	92.91	0.00	13.59
9	25.59	1,894,426	26.48	1,543,940	1,088,938	110,144	0.00	0.00	125.96	14.44
10	25.62	1,872,702	26.49	1,553,095	1,146,560	116,860	0.00	0.00	172.77	13.31
11	25.60	1,965,182	26.64	1,548,551	938,769	97,677	0.00	12.13	0.00	19.06
12	25.58	1,899,558	26.67	1,533,428	980,476	97,507	0.00	27.91	0.00	16.93
13	25.54	1,895,963	26.72	1,524,612	1,053,854	98,904	0.00	46.66	0.00	19.38
14	25.49	1,898,947	26.75	1,529,427	1,143,079	104,809	0.00	81.89	0.00	18.74
15	25.45	1,886,650	26.76	1,533,383	1,215,439	110,178	0.00	0.00	118.61	18.64
16	25.37	3,764,436	29.52	4,026,360	3,041,028	129,036	0.00	30.75	114.59	64.33
17	25.35	3,716,241	29.47	4,201,984	3,304,045	137,874	0.00	32.79	123.70	67.08
18	25.37	3,707,719	29.41	4,193,823	3,324,006	141,952	0.00	37.66	144.16	66.87
19	25.40	3,710,725	29.37	4,192,490	3,369,647	143,815	0.00	40.47	156.41	65.88
20	25.42	3,704,938	29.32	4,183,696	3,379,006	148,228	0.00	45.58	178.94	64.94

# Appendix C: Single- and two-phase measured data (continued).

Channel D: Water and nitrogen tests. Number of channels: 7

Channel Dimensions:

Depth ( $\mu\text{m}$ ): 111.33 Hyd. Diameter ( $\mu\text{m}$ ): 111.86

Width ( $\mu\text{m}$ ): 112.73 Channel Length (m): 0.0635

Data Point	Test Fixture Temperature		Test Section Temperature. ( $^{\circ}\text{C}$ )						
	Inlet	Outlet	Pos #1	Pos #2	Pos #3	Pos #4	Pos #5	Pos #6	Pos #7
1	26.36	41.91	28.36	35.89	39.93	40.30	42.07	43.66	40.04
2	26.73	41.71	28.42	36.02	40.05	40.41	42.14	43.66	40.15
3	26.51	40.46	28.00	35.40	39.31	39.66	41.25	42.66	39.42
4	26.63	40.72	27.98	36.14	40.07	40.42	41.94	43.15	40.17
5	27.03	42.30	29.45	38.07	42.06	42.42	43.90	44.87	42.14
6	25.94	41.09	28.13	36.01	40.69	40.58	42.42	44.26	40.32
7	26.38	41.29	28.72	36.16	40.82	40.72	42.52	44.28	40.46
8	26.76	41.93	29.10	36.79	41.50	41.40	43.19	44.83	41.13
9	26.87	42.09	29.30	37.18	41.88	41.79	43.51	44.98	41.51
10	27.19	43.45	29.90	38.71	43.49	43.42	45.14	46.46	43.13
11	26.01	40.91	28.30	36.23	41.34	40.85	42.63	44.45	40.60
12	26.17	41.18	28.22	36.29	41.47	40.96	42.73	44.49	40.71
13	26.70	42.22	31.16	37.33	42.59	42.09	43.86	45.45	41.81
14	25.86	30.71	24.19	27.84	30.74	31.00	31.72	32.40	27.74
15	26.01	30.80	23.91	27.81	30.69	30.95	31.64	32.35	27.72
16	26.12	30.90	23.95	27.81	30.67	30.92	31.60	32.35	27.71
17	26.17	31.07	24.01	27.86	30.74	30.98	31.66	32.44	27.76
18	26.21	31.16	24.08	27.96	30.85	31.08	31.76	32.51	27.86
19	26.21	31.31	24.15	28.07	30.97	31.20	31.91	32.67	27.97
20	25.02	36.41	28.24	32.56	35.46	36.41	37.41	37.60	36.29
21	24.98	36.24	27.56	32.57	35.44	36.38	37.36	37.51	36.25
22	25.05	36.41	25.86	32.79	35.67	36.63	37.60	37.75	36.51
23	25.09	36.42	25.96	32.79	35.67	36.62	37.58	37.68	36.49
24	25.12	36.65	26.24	33.00	35.91	36.86	37.83	37.90	36.72
25	25.09	36.46	26.11	32.88	35.77	36.71	37.65	37.69	36.57
26	25.14	36.56	26.84	33.04	35.92	36.89	37.82	37.85	36.77
27	25.16	36.60	26.72	33.07	35.95	36.89	37.82	37.82	36.75
28	25.13	36.54	26.68	33.02	35.91	36.85	37.78	37.80	36.72
29	25.13	36.45	26.67	32.90	35.81	36.72	37.66	37.64	36.57
30	25.12	36.52	26.22	33.13	36.01	36.97	37.88	37.85	36.85

## Appendix C: Single- and two-phase measured data (continued).

## Channel D: Water and nitrogen (continued).

Data Point	Gas Flow Meter		Liquid Flow Meter		Test Fixture Press., (Pa)		Flow Meter/Flow rates, (cc/min)			
	Temp.(°C)	Press.(Pa)	Temp.(°C)	Press.(Pa)	Inlet	Outlet	F.M. #4	F.M. #5	F.M. #6	F.M. #1
1	25.21	1,259,591	25.48	1,727,182	624,007	106,068	0.00	11.41	0.00	11.81
2	25.27	1,194,283	25.47	1,693,092	671,434	104,886	0.00	21.49	0.00	10.14
3	25.29	1,194,306	25.51	1,664,745	865,911	106,041	0.00	52.86	0.00	10.55
4	25.32	1,177,216	25.57	1,650,390	996,911	109,280	0.00	82.48	0.00	10.97
5	25.36	1,171,474	25.66	1,634,430	1,091,448	112,735	0.00	0.00	111.40	9.17
6	25.36	1,728,048	25.93	1,611,327	827,730	102,286	0.00	9.93	0.00	15.93
7	25.36	1,667,895	26.02	1,604,501	873,619	101,398	0.00	19.00	0.00	13.83
8	25.35	1,663,464	26.06	1,598,555	938,837	101,307	0.00	36.69	0.00	14.48
9	25.35	1,656,818	26.12	1,597,199	1,033,894	103,369	0.00	57.10	0.00	15.02
10	25.37	1,647,979	26.15	1,597,696	1,089,504	105,792	0.00	79.11	0.00	11.56
11	25.36	1,776,899	26.29	1,619,985	977,651	100,629	0.00	7.92	0.00	18.06
12	25.35	1,670,653	26.40	1,596,430	1,047,276	101,450	0.00	14.88	0.00	19.52
13	25.36	1,663,148	26.47	1,580,787	1,107,655	101,163	0.00	36.65	0.00	16.72
14	24.49	2,743,631	27.59	3,988,383	2,405,809	118,915	0.00	0.00	117.66	58.94
15	24.46	2,707,010	27.75	3,997,674	2,513,344	121,092	0.00	0.00	123.62	59.30
16	24.48	2,685,173	27.86	4,014,108	2,611,701	123,549	0.00	0.00	134.16	59.06
17	24.41	3,008,909	27.91	4,012,729	2,710,420	129,097	0.00	29.27	110.29	56.89
18	24.44	2,943,059	27.94	4,034,498	2,745,323	131,298	0.00	32.05	122.00	55.39
19	24.44	2,924,726	27.93	3,982,211	2,777,311	133,552	0.00	36.04	139.16	52.37
20	24.15	2,224,379	24.91	2,117,401	1,517,500	129,099	0.00	47.40	178.03	10.05
21	24.16	2,210,589	24.88	2,097,350	1,521,773	129,011	0.00	48.29	181.82	11.49
22	24.14	2,204,870	24.86	2,081,955	1,547,905	129,671	0.00	48.62	183.26	9.39
23	24.14	2,210,296	24.83	2,078,610	1,573,472	130,923	0.00	50.08	189.55	11.32
24	24.15	2,205,707	24.79	2,075,603	1,593,659	130,738	0.00	50.01	189.43	10.95
25	24.14	2,192,934	24.78	2,070,381	1,626,166	132,065	0.00	50.72	192.70	11.02
26	24.15	2,197,501	24.77	2,066,583	1,649,811	132,433	0.00	51.42	195.87	11.28
27	24.13	2,195,582	24.74	2,047,989	1,658,459	132,225	0.00	51.90	198.00	10.10
28	24.11	2,190,855	24.72	2,060,774	1,676,916	133,498	0.00	52.23	199.58	10.77
29	24.10	2,196,823	24.71	2,062,288	1,726,196	134,470	0.00	52.42	200.91	10.45
30	24.08	2,188,368	24.71	2,058,287	1,747,016	135,399	0.00	53.55	205.96	9.84



## Appendix C: Single- and two-phase measured data (continued).

Channel E: Argon gas tests.

Number of channels: 9

Channel Dimensions:

Depth ( $\mu\text{m}$ ): 74.91 Hyd. Diameter ( $\mu\text{m}$ ): 79.99Width ( $\mu\text{m}$ ): 58.02 Channel Length (m): 0.0635

Data Point	Test Fixture Temperature		Test Section Temperature, ( $^{\circ}\text{C}$ )						
	Inlet	Outlet	Pos #1	Pos #2	Pos #3	Pos #4	Pos #5	Pos #6	Pos #7
1	31.63	32.45	40.43	43.81	40.69	45.87	45.80	45.88	44.75
2	31.84	34.47	41.94	45.40	42.31	47.46	47.38	47.45	46.28
3	31.80	34.90	42.63	46.15	43.12	48.22	48.14	48.22	47.03
4	31.46	38.75	42.81	46.39	43.40	48.47	48.40	48.46	47.27
5	31.29	39.70	42.83	46.48	43.50	48.56	48.49	48.56	47.40
6	30.98	40.80	42.37	46.39	43.10	48.49	48.42	48.49	47.88
7	30.85	41.34	42.22	46.25	42.97	48.36	48.29	48.37	47.76
8	30.66	41.54	41.95	45.99	42.73	48.11	48.05	48.13	47.51
9	30.52	41.50	41.78	45.83	42.58	47.97	47.91	47.99	47.38
10	30.35	41.65	41.59	45.66	42.42	47.82	47.76	47.86	47.26
11	30.22	41.59	41.38	45.47	42.25	47.66	47.60	47.71	47.13
12	30.04	41.64	41.11	45.22	42.00	47.41	47.36	47.48	46.91
13	29.81	41.66	40.84	44.96	41.75	47.17	47.11	47.24	46.67
14	29.64	41.50	40.41	44.56	41.34	46.78	46.73	46.87	46.30
15	29.42	41.36	40.06	44.20	41.01	46.45	46.40	46.55	45.99
16	29.27	41.18	39.73	43.88	40.69	46.13	46.08	46.23	45.68
17	29.04	41.03	39.29	43.45	40.27	45.72	45.67	45.82	45.27
18	28.83	40.78	38.88	43.06	39.88	45.33	45.29	45.45	44.90

Data Point	Gas Flow Meter		Test Fixture Press., (Pa)		Gas Flow Rates, (cc/min)		
	Temp. ( $^{\circ}\text{C}$ )	Press. (Pa)	Inlet	Outlet	F.M. #4	F.M. #5	F.M. #6
1	23.58	3,010,695	45,781	3,138	25.60	0.00	0.00
2	23.51	2,990,779	100,939	3,122	0.00	46.31	0.00
3	23.43	2,796,190	171,921	3,126	0.00	74.14	0.00
4	23.45	2,275,897	331,246	3,190	0.00	149.53	0.00
5	23.54	2,305,669	433,265	3,312	0.00	188.69	0.00
6	23.59	2,262,696	582,191	3,456	0.00	0.00	214.67
7	23.61	2,247,776	682,854	3,603	0.00	0.00	234.80
8	23.62	2,258,853	812,521	3,757	0.00	0.00	247.93
9	23.63	2,226,775	972,682	3,906	0.00	0.00	251.99
10	23.64	2,244,656	1,129,633	4,137	0.00	0.00	257.33
11	23.64	2,230,437	1,265,448	4,275	0.00	0.00	264.43
12	23.65	2,236,902	1,393,509	4,449	0.00	0.00	272.15
13	23.66	2,225,758	1,510,222	4,679	0.00	0.00	277.69
14	23.74	2,223,000	1,640,635	4,826	0.00	0.00	282.50
15	23.80	2,236,269	1,787,391	5,102	0.00	0.00	286.56
16	23.82	2,235,885	1,870,127	5,240	0.00	62.22	231.62
17	23.85	2,234,461	1,995,046	5,516	0.00	62.67	234.77
18	23.92	2,235,410	2,115,625	5,823	0.00	63.04	237.59

# Appendix C: Single- and two-phase measured data (continued).

Channel E: Helium gas tests.

Number of channels:

9

Channel Dimensions:

Depth ( $\mu\text{m}$ ): 74.91Hyd. Diameter ( $\mu\text{m}$ ): 79.99Width ( $\mu\text{m}$ ): 58.02

Channel Length (m): 0.0635

Data Point	Test Fixture Temperature		Test Section Temperature, ( $^{\circ}\text{C}$ )						
	Inlet	Outlet	Pos #1	Pos #2	Pos #3	Pos #4	Pos #5	Pos #6	Pos #7
1	33.65	33.66	42.13	45.56	42.42	47.65	47.58	47.63	46.43
2	33.98	34.48	42.75	46.18	43.03	48.26	48.19	48.24	47.04
3	34.13	35.29	42.83	46.26	43.12	48.34	48.27	48.33	47.14
4	33.66	39.15	42.85	46.30	43.16	48.39	48.32	48.37	47.17
5	33.48	38.57	42.76	46.22	43.08	48.31	48.24	48.29	47.08
6	33.34	37.55	42.73	46.19	43.07	48.30	48.23	48.28	47.06
7	33.19	38.82	42.61	46.09	42.97	48.20	48.14	48.20	46.97
8	33.06	40.47	42.54	46.03	42.92	48.16	48.10	48.17	46.94
9	32.90	40.50	42.47	45.97	42.88	48.13	48.07	48.16	46.95
10	32.72	40.85	42.28	45.80	42.71	47.96	47.90	47.99	46.76
11	32.54	40.96	42.10	45.63	42.55	47.81	47.75	47.85	46.62
12	32.40	41.30	41.95	45.49	42.42	47.69	47.63	47.74	46.51
13	32.23	41.17	41.55	45.08	42.02	47.28	47.23	47.33	46.11
14	32.02	41.11	41.48	45.04	42.00	47.27	47.22	47.34	46.11
15	31.86	41.43	41.28	44.85	41.81	47.09	47.04	47.16	45.92
16	31.67	41.71	41.03	44.62	41.58	46.87	46.82	46.95	45.71
17	31.48	41.59	40.79	44.39	41.36	46.66	46.61	46.75	45.51
18	31.26	42.23	40.48	44.08	41.06	46.36	46.31	46.45	45.21

Data Point	Gas Flow Meter		Test Fixture Press., (Pa)		Gas Flow Rates, (cc/min)		
	Temp. ( $^{\circ}\text{C}$ )	Press. (Pa)	Inlet	Outlet	F.M. #4	F.M. #5	F.M. #6
1	23.65	2,317,695	43,340	3,149	32.21	0.00	0.00
2	23.65	2,438,048	105,550	3,135	0.00	55.97	0.00
3	23.64	2,400,115	162,991	3,135	0.00	80.20	0.00
4	23.55	1,855,318	308,210	3,248	0.00	140.02	0.00
5	23.57	1,320,965	399,922	3,346	0.00	199.79	0.00
6	23.55	1,251,882	473,254	3,450	0.00	0.00	247.10
7	23.55	1,260,495	543,581	3,554	0.00	0.00	286.02
8	23.53	1,230,158	598,739	3,603	0.00	0.00	318.82
9	23.53	1,231,537	658,033	3,707	0.00	0.00	351.59
10	23.51	1,221,726	711,812	3,795	0.00	0.00	380.85
11	23.50	1,212,232	762,833	3,881	0.00	0.00	408.77
12	23.56	1,212,232	806,643	3,994	0.00	0.00	432.10
13	23.62	1,210,853	852,261	4,107	0.00	0.00	456.75
14	23.65	1,209,474	897,970	4,178	0.00	0.00	478.37
15	23.67	1,208,479	939,338	4,282	0.00	0.00	498.70
16	23.66	1,208,095	987,602	4,406	0.00	108.56	407.62
17	23.63	1,205,880	1,030,349	4,535	0.00	111.98	423.70
18	23.59	1,208,095	1,075,854	4,598	0.00	115.18	439.12

# Appendix C: Single- and two-phase measured data (continued).

Channel E: Nitrogen gas tests. Number of channels: 9

Channel Dimensions:

Depth ( $\mu\text{m}$ ): 74.91 Hyd. Diameter ( $\mu\text{m}$ ): 79.99

Width ( $\mu\text{m}$ ): 58.02 Channel Length (m): 0.0635

Data Point	Test Fixture Temperature		Test Section Temperature, ( $^{\circ}\text{C}$ )						
	Inlet	Outlet	Pos #1	Pos #2	Pos #3	Pos #4	Pos #5	Pos #6	Pos #7
1	26.26	26.66	38.48	41.17	38.66	43.30	43.21	43.26	40.82
2	27.29	29.25	40.73	43.50	41.06	45.63	45.54	45.59	43.11
3	27.59	30.49	41.59	44.41	41.98	46.53	46.44	46.49	44.01
4	28.25	32.99	42.62	45.44	43.03	47.58	47.49	47.55	45.06
5	28.68	35.99	42.90	45.75	43.32	47.88	47.80	47.83	45.34
6	28.54	37.57	43.22	46.11	43.66	48.25	48.17	48.22	45.75
7	28.64	38.51	43.27	46.20	43.73	48.35	48.28	48.32	45.88
8	28.63	38.61	42.49	45.41	42.92	47.56	47.49	47.53	45.16
9	28.60	38.86	42.15	45.09	42.59	47.25	47.18	47.24	44.89
10	28.61	38.97	41.93	44.88	42.38	47.05	46.99	47.05	44.71
11	28.58	38.98	41.76	44.74	42.23	46.92	46.86	46.91	44.58
12	28.55	39.16	41.66	44.66	42.15	46.85	46.79	46.85	44.54
13	28.52	39.20	41.46	44.46	41.98	46.68	46.63	46.70	44.40
14	28.48	39.25	41.26	44.29	41.80	46.52	46.46	46.55	44.27
15	28.40	39.31	41.07	44.11	41.64	46.37	46.31	46.41	44.14
16	28.30	39.58	40.93	43.98	41.52	46.27	46.21	46.34	44.10
17	28.26	40.21	40.89	43.96	41.52	46.28	46.23	46.38	44.17
18	28.15	40.50	40.72	43.82	41.38	46.16	46.11	46.28	44.10

Data Point	Gas Flow Meter		Test Fixture Press., (Pa)		Gas Flow Rates, (cc/min)		
	Temp. ( $^{\circ}\text{C}$ )	Press. (Pa)	Inlet	Outlet	F.M. #4	F.M. #5	F.M. #6
1	23.60	3,902,060	43,023	3,364	21.30	0.93	0.00
2	23.57	3,913,588	84,392	3,219	0.00	37.95	0.00
3	23.50	3,808,043	142,307	3,158	0.00	61.36	0.00
4	23.40	3,166,968	256,330	3,212	0.00	105.22	0.00
5	23.55	2,883,335	338,276	3,269	0.00	155.90	0.00
6	23.53	2,723,671	422,233	3,348	0.00	0.00	182.97
7	23.54	2,700,816	507,140	3,445	0.00	0.00	214.53
8	23.55	2,711,735	557,257	3,547	0.00	0.00	232.72
9	23.54	2,689,378	638,660	3,678	0.00	0.00	256.08
10	23.56	2,685,422	703,267	3,753	0.00	0.00	270.81
11	23.55	2,682,099	788,084	3,866	0.00	0.00	279.74
12	23.54	2,668,264	854,002	3,981	0.00	0.00	285.96
13	23.52	2,682,189	966,104	4,135	0.00	0.00	292.00
14	23.52	2,659,538	1,037,334	4,173	0.00	0.00	300.51
15	23.49	2,686,326	1,107,909	4,284	0.00	0.00	306.24
16	23.48	2,672,537	1,184,407	4,422	0.00	66.24	247.38
17	23.50	2,661,550	1,258,305	4,557	0.00	67.01	251.90
18	23.54	2,674,865	1,322,957	4,673	0.00	68.06	257.49

# Appendix C: Single- and two-phase measured data (continued).

Channel E: Water tests.

Number of channels: 9

Channel Dimensions:

Depth ( $\mu\text{m}$ ): 74.91Hyd. Diameter ( $\mu\text{m}$ ): 79.99Width ( $\mu\text{m}$ ): 58.02

Channel Length (m): 0.0635

Data Point	Test Fixture Temperature		Test Section Temperature, ( $^{\circ}\text{C}$ )						
	Inlet	Outlet	Pos #1	Pos #2	Pos #3	Pos #4	Pos #5	Pos #6	Pos #7
1	22.90	39.26	32.78	36.97	34.95	41.87	42.23	44.15	45.28
2	22.88	38.09	31.19	34.90	34.05	39.44	39.85	41.44	42.45
3	22.84	36.76	30.12	33.51	32.98	37.79	38.24	39.57	40.46
4	22.84	35.75	29.34	32.48	32.16	36.55	37.02	38.14	38.92
5	22.91	35.06	28.86	31.85	30.89	35.76	36.25	37.22	37.89
6	23.15	36.99	29.99	33.46	32.14	37.64	38.25	39.31	40.26
7	23.35	40.77	31.86	36.20	34.32	40.95	41.76	42.93	43.99
8	23.74	39.87	31.60	35.72	33.76	40.20	41.04	41.85	42.40
9	24.18	39.75	31.72	35.78	33.74	40.18	41.03	41.74	42.25
10	24.48	39.17	31.56	35.48	34.18	39.75	40.61	41.20	41.64
11	26.34	39.95	32.87	36.61	35.24	40.70	41.57	42.01	42.35
12	26.64	39.61	32.81	36.46	35.07	40.45	41.32	41.67	41.97
13	26.98	39.49	32.90	36.51	34.37	40.41	41.29	41.58	41.81
14	27.30	39.26	32.92	36.47	34.32	40.29	41.18	41.37	41.56
15	27.59	39.13	32.95	36.43	34.20	40.17	41.06	41.19	41.36
16	27.86	39.05	33.00	36.47	34.30	40.17	41.07	41.12	41.24
17	28.10	40.38	33.83	37.75	35.44	41.52	42.54	42.58	42.77
18	28.32	40.24	33.82	37.74	35.40	41.57	42.61	42.45	42.57
19	28.50	40.13	33.78	37.62	35.93	41.27	42.30	42.17	42.37
20	28.71	39.89	33.64	37.47	35.87	41.05	42.09	41.91	42.08

Appendix C: Single- and two-phase measured data (continued).

---

Channel E: Water tests (continued).

Data Point	Liquid Flow Meter		Test Fixture Press., (Pa)		liquid Flow Rate
	Temp.(°C)	Press.(Pa)	Inlet	Outlet	F. M. #1, (cc/min)
1	23.38	5,335,644	834,679	104,016	10.13
2	23.40	5,309,670	1,026,194	102,892	12.74
3	23.51	5,397,968	1,213,889	103,353	16.86
4	23.73	5,396,024	1,391,886	103,111	17.02
5	24.05	5,396,725	1,543,751	102,578	19.62
6	24.53	5,421,342	1,752,741	102,381	22.09
7	24.85	5,466,848	1,862,084	102,808	24.59
8	25.36	5,492,211	2,092,775	102,980	27.55
9	25.88	5,414,877	2,212,337	101,355	28.78
10	26.28	5,427,966	2,394,765	101,362	31.45
11	28.20	5,467,141	2,612,570	101,656	34.30
12	28.59	5,521,486	2,772,732	102,397	35.67
13	28.98	5,564,346	2,944,286	102,786	36.94
14	29.32	5,604,697	3,111,749	103,333	38.43
15	29.65	5,608,246	3,267,570	103,062	40.11
16	29.94	5,631,801	3,455,378	103,297	41.67
17	30.19	5,698,285	3,640,112	104,072	44.40
18	30.42	5,683,704	3,802,308	103,961	46.55
19	30.63	5,632,728	3,943,503	102,849	48.55
20	30.88	5,709,158	4,203,061	103,903	51.11

# Appendix C: Single- and two-phase measured data (continued).

Channel E: Water and argon tests. Number of channels: 9

Channel Dimensions:

Depth ( $\mu\text{m}$ ): 74.91 Hyd. Diameter ( $\mu\text{m}$ ): 79.99

Width ( $\mu\text{m}$ ): 58.02 Channel Length (m): 0.0635

Data Point	Test Fixture Temperature		Test Section Temperature, ( $^{\circ}\text{C}$ )						
	Inlet	Outlet	Pos #1	Pos #2	Pos #3	Pos #4	Pos #5	Pos #6	Pos #7
1	26.56	38.84	31.84	34.86	33.30	38.80	39.18	40.38	41.37
2	27.03	38.88	32.09	35.15	34.32	39.10	39.44	40.64	41.51
3	27.05	39.11	32.40	35.48	34.66	39.41	39.75	40.93	41.70
4	27.23	39.77	33.25	36.49	35.21	40.48	40.81	41.99	42.63
5	27.18	39.95	33.42	36.78	34.52	40.77	41.09	42.19	42.52
6	26.97	39.76	33.82	37.19	34.69	41.12	41.42	42.40	42.47
7	26.93	39.24	33.39	36.84	34.60	40.76	41.04	41.99	41.96
8	27.15	40.50	34.65	38.43	35.68	42.51	42.77	43.77	43.52
9	26.14	39.35	31.83	35.47	35.07	39.59	40.17	41.18	42.09
10	26.32	39.49	32.00	35.67	35.21	39.79	40.38	41.36	42.23
11	26.57	39.74	32.29	36.01	35.33	40.14	40.74	41.71	42.54
12	26.87	40.28	33.07	36.81	34.93	40.97	41.54	42.51	43.14
13	27.09	41.11	33.74	37.84	35.66	42.16	42.70	43.71	44.13
14	26.99	40.73	33.65	37.83	35.51	42.10	42.64	43.53	43.78
15	27.05	40.86	33.99	38.28	35.84	42.57	43.10	43.96	44.10
16	26.67	36.57	30.84	33.98	32.93	37.60	38.25	38.76	39.44
17	26.82	36.79	31.04	34.22	33.82	37.88	38.51	39.04	39.63
18	27.03	36.94	31.04	34.27	33.73	37.94	38.58	39.10	39.69
19	27.27	37.61	31.64	35.03	34.11	38.79	39.39	39.96	40.43
20	27.34	38.15	32.01	35.63	33.66	39.45	40.04	40.57	40.91
21	27.33	38.76	32.66	36.39	34.16	40.30	40.87	41.42	41.67
22	25.88	38.52	32.82	35.78	37.50	39.59	39.77	40.81	38.07
23	25.86	38.72	32.85	35.82	36.49	39.63	39.83	40.88	37.48
24	25.87	38.77	32.95	36.00	36.69	39.84	40.03	41.08	37.65
25	25.98	39.00	33.28	36.37	37.09	40.23	40.41	41.48	37.96
26	25.90	38.81	32.95	36.01	36.78	39.86	40.05	41.12	37.69
27	26.04	39.05	33.69	36.79	37.56	40.64	40.80	41.83	38.14
28	26.22	39.74	34.11	37.30	39.23	41.21	41.38	42.45	39.65
29	25.75	38.05	32.43	35.41	35.47	39.19	39.38	40.38	37.31
30	25.92	38.60	33.35	36.44	36.41	40.25	40.43	41.40	37.95
31	26.13	39.33	34.31	37.53	37.59	41.36	41.54	42.49	38.84

Appendix C: Single- and two-phase measured data (continued).

Channel E: Water and argon (continued).

Data Point	Gas Flow Meter		Liquid Flow Meter		Test Fixture Press.. (Pa)		Flow Meter/Flow rates, (cc/min)			
	Temp.(°C)	Press.(Pa)	Temp.(°C)	Press.(Pa)	Inlet	Outlet	F.M. #4	F.M. #5	F.M. #6	F.M. #1
1	24.10	4,826.429	28.57	4,759,485	1,462,078	111,726	0.00	8.44	0.00	16.99
2	24.02	4,707.884	28.41	4,648,537	1,542,464	109,800	0.00	15.71	0.00	16.43
3	24.03	4,436.526	28.22	4,611,305	1,661,890	111,356	0.00	28.98	0.00	14.16
4	24.15	4,450.926	28.04	4,487,901	1,773,290	112,696	0.00	55.26	0.00	12.78
5	24.14	4,398.978	27.87	4,352,764	2,200,312	119,010	0.00	0.00	78.84	12.54
6	24.12	4,357.587	27.70	4,307,304	2,534,062	126,963	0.00	0.00	100.75	14.11
7	24.11	4,341.062	27.54	4,266,048	2,843,330	132,596	0.00	0.00	115.31	12.17
8	24.12	4,374.473	27.32	4,273,802	3,148,778	141,478	0.00	0.00	139.18	9.77
9	24.07	5,042.448	27.83	4,731,838	2,176,259	109,861	0.00	6.31	0.00	23.41
10	24.02	4,872.974	27.97	4,694,042	2,283,772	112,262	0.00	11.34	0.00	24.53
11	24.01	4,521.433	28.10	4,639,359	2,376,975	112,504	0.00	19.72	0.00	24.15
12	24.12	4,362.786	28.16	4,541,363	2,581,285	116,193	0.00	42.01	0.00	23.26
13	24.12	4,383.402	28.16	4,412,714	2,846,292	122,412	0.00	0.00	63.14	21.37
14	24.13	4,371.399	28.12	4,374,737	3,176,809	127,869	0.00	0.00	80.86	20.72
15	24.17	4,337.264	28.07	4,340,376	3,514,470	135,137	0.00	0.00	98.06	20.28
16	24.17	4,981.074	28.68	4,670,532	3,084,646	109,733	0.00	4.22	0.00	34.12
17	24.08	4,892.663	28.89	4,613,927	3,109,264	112,622	0.00	8.62	0.00	34.49
18	24.03	4,544.400	29.06	4,641,710	3,241,642	113,071	0.00	14.96	0.00	33.97
19	24.17	4,368.437	29.15	4,498,819	3,347,482	117,428	0.00	34.33	0.00	31.39
20	24.15	4,394.479	29.15	4,393,929	3,563,299	123,890	0.00	0.00	53.07	28.89
21	24.18	4,319.157	29.05	4,337,980	3,738,696	130,353	0.00	0.00	76.24	26.00
22	23.98	3,664.949	24.81	3,374,955	2,869,813	123,994	0.00	28.95	106.60	10.13
23	23.98	3,645.869	24.78	3,423,489	2,956,777	125,353	0.00	29.34	108.38	9.49
24	23.99	3,643.179	24.77	3,419,692	3,067,002	126,938	0.00	30.54	113.39	8.33
25	23.97	3,628.147	24.74	3,419,601	3,133,621	128,624	0.00	31.91	119.05	8.22
26	24.01	3,657.963	24.74	3,412,887	3,253,590	129,126	0.00	31.43	117.44	9.19
27	23.99	3,622.066	24.74	3,388,925	3,299,841	131,755	0.00	34.41	129.67	9.31
28	24.02	3,724.944	24.71	3,390,236	3,347,539	131,656	0.00	34.22	129.08	7.65
29	23.98	3,663.524	24.75	3,766,214	3,581,937	132,591	0.00	32.76	123.76	8.59
30	23.99	3,892.090	24.72	3,769,741	3,637,163	134,588	0.00	35.09	133.60	8.51
31	24.01	3,858.883	24.69	3,794,969	3,718,430	137,429	0.00	36.41	139.45	10.55

Appendix C: Single- and two-phase measured data (continued).

Channel E: Water and helium tests.      Number of channels:      9  
 Channel Dimensions:  
 Depth ( $\mu\text{m}$ ):      74.91      Hyd. Diameter ( $\mu\text{m}$ ):      79.99  
 Width ( $\mu\text{m}$ ):      58.02      Channel Length (m):      0.0635

Data Point	Test Fixture Temperature		Test Section Temperature, ( $^{\circ}\text{C}$ )						
	Inlet	Outlet	Pos #1	Pos #2	Pos #3	Pos #4	Pos #5	Pos #6	Pos #7
1	26.58	37.68	31.34	34.06	33.53	37.75	38.11	39.13	39.92
2	26.80	37.93	31.53	34.33	33.77	38.06	38.42	39.46	40.23
3	26.91	38.09	31.68	34.61	33.17	38.40	38.75	39.81	40.53
4	26.79	37.16	31.22	34.10	32.76	37.78	38.13	39.05	39.58
5	26.73	36.64	31.03	33.90	32.62	37.54	37.88	38.72	39.10
6	26.61	36.25	31.22	34.18	32.84	37.79	38.13	38.90	38.97
7	26.47	35.83	31.19	34.20	32.83	37.79	38.12	38.81	38.64
8	26.40	39.77	32.61	36.20	35.47	40.23	40.80	41.81	42.66
9	26.61	39.90	32.65	36.30	35.61	40.40	40.96	42.00	42.85
10	26.91	40.06	32.81	36.55	35.78	40.67	41.23	42.27	43.06
11	27.13	40.27	33.06	36.92	34.80	41.09	41.65	42.70	43.41
12	27.20	40.26	33.26	37.20	34.64	41.40	41.95	42.99	43.50
13	27.25	40.48	33.82	37.99	35.27	42.27	42.79	43.79	43.94
14	26.55	37.54	31.45	34.75	32.85	38.51	39.13	39.84	40.47
15	26.90	37.90	31.84	35.16	33.12	38.93	39.54	40.25	40.86
16	27.17	37.81	31.96	35.22	33.91	38.99	39.59	40.30	40.86
17	27.34	37.80	32.03	35.41	33.87	39.20	39.79	40.50	40.96
18	27.44	37.97	32.19	35.68	34.04	39.52	40.10	40.82	41.18
19	27.40	38.17	32.38	36.17	33.83	40.11	40.67	41.43	41.52
20	28.80	38.16	34.34	38.20	45.24	45.67	44.24	44.07	45.45
21	28.80	37.63	34.38	38.28	45.34	45.77	44.34	44.23	45.54
22	28.74	37.93	34.31	38.31	45.45	45.87	44.42	44.40	45.64
23	28.86	37.96	34.22	38.26	45.41	45.83	44.39	44.45	45.60
24	28.78	37.55	34.14	38.26	45.48	45.88	44.43	44.55	45.63
25	29.08	37.17	34.60	38.62	47.36	47.32	45.34	44.46	46.32
26	29.08	37.41	34.54	38.68	47.54	47.47	45.47	44.69	46.40
27	29.02	37.45	34.48	38.71	47.70	47.62	45.59	44.90	46.54
28	29.92	38.22	35.13	39.42	48.47	48.38	46.35	45.76	47.32
29	29.90	38.12	35.00	39.31	48.43	48.33	46.29	45.82	47.37
30	29.64	38.36	34.98	39.38	48.65	48.53	46.46	46.12	47.64
31	29.71	36.20	33.76	37.13	45.76	45.70	43.75	42.76	44.62
32	29.68	36.31	33.68	37.07	45.75	45.69	43.73	42.88	44.64
33	29.63	36.35	33.56	36.93	45.69	45.62	43.62	42.92	44.64



## Appendix C: Single- and two-phase measured data (continued).

## Channel A: Water and helium (continued).

Data Point	Gas Flow Meter		Liquid Flow Meter		Test Fixture Press., (Pa)		Flow Meter/Flow rates, (cc/min)			
	Temp.(°C)	Press.(Pa)	Temp.(°C)	Press.(Pa)	Inlet	Outlet	F.M. #4	F.M. #5	F.M. #6	F.M. #1
1	24.25	5,725,321	28.26	4,785,211	1,777,947	113,275	0.00	7.49	0.00	16.83
2	24.19	5,755,680	28.16	4,770,992	1,812,692	113,334	0.00	15.46	0.00	18.10
3	24.13	5,377,600	28.05	4,762,356	1,842,147	115,115	0.00	27.85	0.00	15.79
4	24.13	4,440,798	28.01	4,717,891	2,097,298	122,297	0.00	55.23	0.00	18.95
5	24.15	4,505,089	27.99	4,704,870	2,280,155	131,543	0.00	0.00	89.35	18.14
6	24.19	4,486,145	27.92	4,695,895	2,599,279	150,072	0.00	0.00	164.21	17.41
7	24.21	4,463,268	27.88	4,630,294	2,952,222	161,708	0.00	44.20	168.74	16.39
8	24.24	5,552,636	28.22	4,610,016	2,272,921	113,187	0.00	6.65	0.00	23.77
9	24.22	5,626,828	28.30	4,674,804	2,334,590	112,511	0.00	11.41	0.00	23.66
10	24.14	5,284,488	28.34	4,712,872	2,379,801	115,067	0.00	21.50	0.00	23.40
11	24.13	4,451,061	28.36	4,705,910	2,453,066	121,304	0.00	45.48	0.00	23.07
12	24.18	4,521,342	28.35	4,695,760	2,571,520	132,558	0.00	0.00	80.13	22.59
13	24.24	4,492,475	28.30	4,668,769	2,811,728	149,166	0.00	0.00	152.10	19.31
14	24.25	5,351,739	28.76	4,729,578	2,934,273	108,704	0.00	5.39	0.10	31.18
15	24.23	5,429,639	28.91	4,647,361	2,890,056	111,564	0.00	9.98	0.00	31.36
16	24.17	5,125,253	29.03	4,671,753	2,969,108	115,043	0.00	16.85	0.00	31.55
17	24.19	4,500,522	29.10	4,684,593	3,085,189	124,083	0.00	40.58	0.00	30.26
18	24.22	4,473,441	29.15	4,677,947	3,160,443	133,597	0.00	0.00	70.06	28.83
19	24.25	4,511,803	29.07	4,645,078	3,397,712	148,574	0.00	0.00	125.06	26.61
20	24.87	2,491,917	29.97	3,161,512	799,947	125,353	0.00	0.00	213.34	103.27
21	24.88	2,469,831	29.94	3,166,305	873,393	133,713	0.00	0.00	304.66	102.02
22	24.86	2,460,179	29.87	3,168,656	943,968	141,367	0.00	0.00	380.87	98.69
23	24.88	2,456,042	29.79	3,149,983	1,010,949	148,045	0.00	95.94	358.78	96.43
24	24.90	2,453,284	29.68	3,144,603	1,080,846	154,311	0.00	107.73	410.15	94.03
25	24.86	2,564,866	30.02	3,110,943	1,089,843	117,138	0.00	0.00	78.69	146.74
26	24.85	2,490,516	29.98	3,091,299	1,166,114	126,963	0.00	0.00	161.98	145.04
27	24.87	2,475,777	29.94	3,093,243	1,239,040	135,896	0.00	0.00	233.21	140.56
28	25.66	2,466,938	30.62	3,067,699	1,294,153	142,260	0.00	0.00	301.34	138.65
29	25.67	2,460,111	30.54	3,077,555	1,355,957	149,193	0.00	76.38	285.53	133.95
30	25.72	2,457,421	30.46	3,023,414	1,395,358	154,058	0.00	88.64	337.44	130.48
31	25.72	2,520,852	30.66	3,026,895	1,477,214	117,916	0.00	0.00	63.35	183.08
32	25.74	2,485,000	30.64	3,023,979	1,545,211	128,502	0.00	0.00	129.44	177.50
33	25.76	2,476,432	30.59	3,016,316	1,603,444	136,898	0.00	0.00	190.66	175.66

# Appendix C: Single- and two-phase measured data (continued).

Channel E: Water and nitrogen tests. Number of channels: 9

Channel Dimensions:

Depth ( $\mu\text{m}$ ): 74.91 Hyd. Diameter ( $\mu\text{m}$ ): 79.99

Width ( $\mu\text{m}$ ): 58.02 Channel Length (m): 0.0635

Data Point	Test Fixture Temperature		Test Section Temperature, ( $^{\circ}\text{C}$ )						
	Inlet	Outlet	Pos #1	Pos #2	Pos #3	Pos #4	Pos #5	Pos #6	Pos #7
1	26.51	40.40	33.28	36.39	36.96	40.42	40.76	42.13	43.06
2	27.03	40.41	33.34	36.57	37.85	40.63	40.96	42.34	43.26
3	27.21	40.50	33.31	36.64	37.89	40.72	41.04	42.40	43.22
4	27.16	39.67	32.91	36.14	36.96	40.09	40.42	41.61	42.23
5	26.97	39.97	33.45	36.78	37.08	40.73	41.04	42.18	42.57
6	27.05	40.07	33.88	37.37	37.43	41.37	41.67	42.77	42.96
7	26.08	41.27	33.26	37.27	37.92	41.64	42.19	43.51	44.51
8	26.39	40.57	32.83	36.69	37.46	40.96	41.53	42.74	43.68
9	26.65	40.89	33.13	37.08	37.77	41.36	41.91	43.12	43.94
10	26.84	41.03	33.59	37.55	38.81	41.81	42.35	43.53	44.25
11	27.01	41.30	33.73	37.91	35.61	42.24	42.76	43.95	44.46
12	27.07	41.63	34.43	38.81	35.58	43.17	43.66	44.79	45.00
13	26.43	40.00	32.71	36.68	37.32	40.87	41.60	42.56	43.49
14	26.88	40.23	32.76	36.90	37.62	41.13	41.84	42.83	43.71
15	27.03	40.36	33.06	37.23	37.79	41.46	42.15	43.13	43.88
16	27.31	40.72	33.50	37.76	38.13	42.00	42.69	43.63	44.23
17	27.46	40.82	33.75	38.19	38.44	42.48	43.15	44.07	44.40
18	27.48	41.20	34.05	38.63	39.57	43.01	43.65	44.60	44.77
19	26.65	39.86	33.70	36.73	39.10	40.59	40.80	41.92	37.19
20	26.59	39.51	33.25	36.27	38.60	40.13	40.34	41.46	37.08
21	26.36	38.86	32.82	35.76	38.04	39.56	39.77	40.84	36.58
22	26.13	38.51	32.57	35.48	37.73	39.26	39.46	40.51	36.21
23	26.12	38.71	32.67	35.64	37.93	39.45	39.64	40.72	36.38
24	26.01	38.64	32.59	35.57	37.86	39.38	39.59	40.66	36.07
25	25.96	38.38	32.48	35.43	37.70	39.22	39.42	40.48	38.25
26	25.92	38.39	32.50	35.47	37.73	39.26	39.45	40.50	38.21
27	25.80	38.08	32.36	35.28	37.53	39.05	39.25	40.29	38.12
28	25.75	38.17	32.28	35.27	37.53	39.05	39.25	40.30	38.17
29	25.77	38.43	32.43	35.46	37.76	39.30	39.49	40.58	38.37

## Appendix C: Single- and two-phase measured data (continued).

## Channel E: Water and nitrogen (continued).

Data Point	Gas Flow Meter		Liquid Flow Meter		Test Fixture Press.. (Pa)		Flow Meter/Flow rates. (cc/min)			
	Temp.(°C)	Press.(Pa)	Temp.(°C)	Press.(Pa)	Inlet	Outlet	F.M. #4	F.M. #5	F.M. #6	F.M. #1
1	24.30	5,263.600	28.19	4,810.099	1,502.135	110.191	0.00	4.87	0.00	14.63
2	24.26	5,274.609	27.99	4,763.826	1,571.896	110.571	0.00	11.19	0.00	14.46
3	24.18	5,028.230	27.81	4,770.178	1,684.812	111.338	0.00	19.44	0.00	13.14
4	24.10	4,299.332	27.69	4,779.763	1,992.588	115.960	0.00	38.96	0.00	15.10
5	24.22	4,291.375	27.60	4,747.436	2,242.064	123.059	0.00	0.00	65.29	12.97
6	24.22	4,239.856	27.43	4,723.113	2,509.218	130.704	0.00	0.00	91.02	11.71
7	24.21	5,103.190	27.66	4,826.217	2,128.516	112.368	0.00	4.39	0.00	19.98
8	24.15	5,075.001	27.77	4,775.897	2,337.008	112.038	0.00	8.89	0.00	19.76
9	24.10	4,811.486	27.90	4,776.824	2,397.976	112.373	0.00	14.42	0.00	21.69
10	24.08	4,280.388	27.96	4,758.965	2,558.024	116.415	0.00	29.04	0.00	19.82
11	24.18	4,259.704	28.02	4,771.263	2,925.999	124.453	0.00	0.00	55.09	19.88
12	24.20	4,235.493	28.00	4,726.323	3,118.555	133.245	0.00	0.00	79.27	18.78
13	24.24	5,045.796	28.50	4,832.565	2,881.263	111.230	0.00	2.92	0.00	28.72
14	24.18	5,051.988	28.69	4,784.397	2,943.293	113.472	0.00	6.55	0.00	29.05
15	24.11	4,822.088	28.82	4,749.200	3,028.584	113.044	0.00	12.00	0.00	28.41
16	24.13	4,254.460	28.92	4,729.194	3,144.777	117.593	0.00	25.60	0.00	28.41
17	24.20	4,270.871	28.96	4,691.442	3,428.750	125.403	0.00	0.00	47.90	27.10
18	24.17	4,222.970	28.92	4,692.618	3,602.813	131.823	0.00	0.00	65.35	24.98
19	23.81	3,476.462	24.90	3,302.459	2,742.204	123.425	0.00	29.23	108.66	8.63
20	24.12	3,461.136	25.10	3,352.033	2,807.670	125.091	0.00	29.05	108.92	10.92
21	24.09	3,457.044	25.06	3,354.429	2,845.489	126.013	0.00	29.40	111.13	9.11
22	24.08	3,452.975	25.03	3,362.748	2,866.987	126.836	0.00	29.51	111.80	10.53
23	24.10	3,451.664	25.03	3,376.786	2,895.538	127.923	0.00	30.34	115.37	9.66
24	24.11	3,440.904	24.97	3,395.164	2,915.657	128.385	0.00	30.41	115.73	10.38
25	24.13	3,437.038	24.94	3,389.988	2,917.556	128.690	0.00	30.97	118.08	10.35
26	24.11	3,436.383	24.90	3,400.138	2,924.451	129.234	0.00	31.76	121.44	8.75
27	24.10	3,440.339	24.87	3,422.472	2,969.481	130.616	0.00	31.66	121.20	9.38
28	24.06	3,435.094	24.84	3,426.677	2,984.401	130.485	0.00	31.94	122.45	8.85
29	24.07	3,448.296	24.81	3,452.379	3,068.155	132.164	0.00	32.68	125.97	10.48

Appendix C: Single- and two-phase measured data (continued).

Channel F: Argon gas tests.

Number of channels: 11

Channel Dimensions:

Depth ( $\mu\text{m}$ ): 54.09

Hyd. Diameter ( $\mu\text{m}$ ): 55.99

Width ( $\mu\text{m}$ ): 58.02

Channel Length (m): 0.0635

Data Point	Test Fixture Temperature		Test Section Temperature, ( $^{\circ}\text{C}$ )						
	Inlet	Outlet	Pos #1	Pos #2	Pos #3	Pos #4	Pos #5	Pos #6	Pos #7
1	32.72	33.60	46.57	47.24	47.64	49.50	49.39	49.38	43.14
2	32.62	35.40	46.96	47.64	48.04	49.90	49.79	49.77	43.52
3	32.40	38.30	47.07	47.76	48.16	50.02	49.91	49.88	43.61
4	32.12	39.82	46.93	47.63	48.04	49.90	49.79	49.75	43.47
5	31.74	40.21	46.74	47.46	47.89	49.75	49.65	49.62	43.34
6	31.77	40.65	46.57	47.31	47.76	49.62	49.51	49.49	42.31
7	31.79	40.85	46.37	47.13	47.58	49.45	49.34	49.31	41.55
8	31.70	40.89	46.20	46.97	47.42	49.29	49.19	49.16	41.41
9	31.43	40.73	46.04	46.84	47.32	49.19	49.08	49.07	41.72
10	30.91	41.01	45.78	46.60	47.09	48.96	48.86	48.85	42.58
11	30.87	41.00	45.50	46.34	46.84	48.71	48.60	48.59	41.78
12	30.93	40.95	45.21	46.06	46.57	48.44	48.34	48.34	40.62
13	30.33	40.79	44.90	45.77	46.30	48.18	48.07	48.07	41.77
14	30.13	40.69	44.56	45.45	45.99	47.87	47.77	47.77	41.49
15	29.90	40.40	44.14	45.05	45.61	47.49	47.39	47.40	41.11
16	29.66	40.28	43.72	44.64	45.19	47.08	46.98	46.97	40.62
17	29.66	39.96	43.25	44.18	44.74	46.63	46.54	46.52	39.46
18	29.23	39.58	42.70	43.63	44.19	46.09	45.99	45.98	39.69

Data Point	Gas Flow Meter		Test Fixture Press., (Pa)		Gas Flow Rates, (cc/min)		
	Temp. ( $^{\circ}\text{C}$ )	Press. (Pa)	Inlet	Outlet	F.M. #4	F.M. #5	F.M. #6
1	23.69	5,307,478	107,216	3,402	41.80	0.00	0.00
2	23.60	5,603,363	283,405	3,400	0.00	65.82	0.00
3	23.45	5,495,195	498,385	3,479	0.00	97.12	0.00
4	23.26	4,878,829	698,807	3,585	0.00	122.90	0.00
5	23.02	3,586,213	938,699	3,784	0.00	0.00	136.82
6	23.30	3,320,076	1,128,767	3,990	0.00	0.00	169.80
7	23.32	3,193,937	1,329,528	4,132	0.00	0.00	174.38
8	23.35	3,254,475	1,482,501	4,202	0.00	0.00	175.53
9	23.33	3,230,626	1,694,113	4,410	0.00	0.00	180.31
10	23.32	3,236,006	1,875,614	4,564	0.00	0.00	186.50
11	23.31	3,220,430	2,067,446	4,826	0.00	0.00	192.72
12	23.31	3,209,670	2,220,418	4,966	0.00	0.00	196.89
13	23.31	3,203,974	2,394,799	5,240	0.00	0.00	199.79
14	23.31	3,210,258	2,572,728	5,378	0.00	0.00	202.14
15	23.31	3,214,259	2,758,253	5,724	0.00	44.24	164.96
16	23.30	3,218,260	2,897,029	5,929	0.00	44.64	167.39
17	23.32	3,221,109	3,060,762	6,198	0.00	45.14	170.37
18	23.32	3,222,035	3,224,518	6,395	0.00	45.75	173.84

Appendix C: Single- and two-phase measured data (continued).

Channel F: Helium gas tests. Number of channels: 11

Channel Dimensions:

Depth ( $\mu\text{m}$ ): 54.09 Hyd. Diameter ( $\mu\text{m}$ ): 55.99

Width ( $\mu\text{m}$ ): 58.02 Channel Length (m): 0.0635

Data Point	Test Fixture Temperature		Test Section Temperature, ( $^{\circ}\text{C}$ )						
	Inlet	Outlet	Pos #1	Pos #2	Pos #3	Pos #4	Pos #5	Pos #6	Pos #7
1	30.72	29.73	46.82	48.01	48.72	50.64	50.45	50.35	43.76
2	31.93	31.65	49.23	50.47	51.21	53.12	52.92	52.85	46.24
3	32.95	33.28	49.53	50.60	51.26	53.12	52.97	52.96	46.50
4	32.42	36.18	47.19	48.13	48.70	50.58	50.44	50.39	43.97
5	32.26	36.03	46.71	47.63	48.18	50.06	49.93	49.86	43.38
6	32.34	37.12	46.74	47.66	48.21	50.09	49.95	49.88	43.39
7	32.29	38.79	46.78	47.72	48.27	50.16	50.02	49.95	43.44
8	32.24	37.62	46.79	47.74	48.31	50.19	50.06	49.99	43.47
9	32.17	39.71	46.79	47.74	48.32	50.21	50.07	50.01	43.53
10	31.83	41.06	46.71	47.71	48.31	50.20	50.06	50.02	43.55
11	32.00	41.86	46.74	47.75	48.38	50.26	50.13	50.11	43.66
12	32.07	42.28	46.78	47.82	48.45	50.35	50.20	50.20	43.78
13	31.78	42.59	46.83	47.90	48.56	50.45	50.31	50.33	43.91
14	31.95	42.78	46.80	47.89	48.57	50.46	50.32	50.34	43.91
15	31.99	42.81	46.80	47.91	48.60	50.50	50.35	50.39	43.96
16	31.96	42.98	46.75	47.88	48.59	50.49	50.34	50.39	43.94
17	31.87	43.46	46.66	47.82	48.55	50.45	50.31	50.36	43.91
18	31.74	43.38	46.46	47.63	48.37	50.27	50.13	50.20	43.77

Data Point	Gas Flow Meter		Test Fixture Press., (Pa)		Gas Flow Rates, (cc/min)		
	Temp. ( $^{\circ}\text{C}$ )	Press. (Pa)	Inlet	Outlet	F.M. #4	F.M. #5	F.M. #6
1	23.75	2,360,216	140,515	3,429	19.17	0.00	0.00
2	23.72	2,242,554	267,378	3,434	0.00	39.52	0.00
3	23.72	2,202,044	340,462	3,522	0.00	56.50	0.00
4	23.72	2,170,736	554,199	3,610	0.00	99.78	0.00
5	23.71	2,152,674	707,262	3,698	0.00	132.83	0.00
6	23.70	2,145,779	789,366	3,766	0.00	0.00	160.56
7	23.68	2,139,562	903,072	3,859	0.00	0.00	191.87
8	23.67	2,136,126	976,541	3,970	0.00	0.00	217.26
9	23.66	2,134,318	1,046,370	4,049	0.00	0.00	240.05
10	23.64	2,131,989	1,118,188	4,150	0.00	0.00	263.25
11	23.62	2,129,232	1,187,135	4,311	0.00	0.00	285.15
12	23.60	2,126,361	1,239,173	4,318	0.00	0.00	303.42
13	23.57	2,129,232	1,301,588	4,415	0.00	0.00	322.24
14	23.57	2,123,716	1,356,746	4,560	0.00	0.00	340.31
15	23.57	2,125,569	1,407,993	4,650	0.00	0.00	357.01
16	23.58	2,138,884	1,461,161	4,808	0.00	77.79	291.83
17	23.61	2,133,346	1,519,054	4,917	0.00	80.84	305.76
18	23.61	2,129,232	1,571,680	5,030	0.00	83.64	318.84

# Appendix C: Single- and two-phase measured data (continued).

Channel F: Nitrogen gas tests.

Number of channels: 11

Channel Dimensions:

Depth ( $\mu\text{m}$ ): 54.09Hyd. Diameter ( $\mu\text{m}$ ): 55.99Width ( $\mu\text{m}$ ): 58.02

Channel Length (m): 0.0635

Data Point	Test Fixture Temperature		Test Section Temperature, ( $^{\circ}\text{C}$ )						
	Inlet	Outlet	Pos #1	Pos #2	Pos #3	Pos #4	Pos #5	Pos #6	Pos #7
1	33.59	33.96	46.47	47.14	47.55	49.41	49.29	49.30	43.10
2	33.31	35.50	46.51	47.18	47.59	49.44	49.33	49.33	43.12
3	32.91	38.22	46.41	47.10	47.50	49.36	49.25	49.24	43.00
4	32.58	38.98	46.27	46.96	47.37	49.23	49.12	49.10	42.86
5	32.27	39.94	46.06	46.77	47.19	49.05	48.94	48.92	42.66
6	31.94	40.10	45.84	46.57	47.01	48.87	48.76	48.75	42.49
7	31.65	40.06	45.65	46.39	46.85	48.71	48.60	48.59	42.34
8	31.37	40.05	45.45	46.20	46.67	48.54	48.43	48.43	42.19
9	31.20	40.06	45.21	45.99	46.47	48.34	48.23	48.24	42.01
10	30.90	39.99	44.94	45.74	46.24	48.11	48.01	48.02	41.80
11	30.69	40.06	44.72	45.54	46.06	47.93	47.82	47.85	41.63
12	30.47	40.22	44.46	45.31	45.84	47.72	47.61	47.65	41.44
13	30.29	40.23	44.14	45.01	45.55	47.43	47.33	47.36	41.16
14	30.06	40.04	43.84	44.73	45.29	47.17	47.07	47.12	40.93
15	29.90	40.07	43.64	44.55	45.12	47.01	46.90	46.95	40.77
16	29.70	39.94	43.30	44.22	44.81	46.69	46.59	46.65	40.45
17	29.51	39.87	42.95	43.88	44.49	46.38	46.28	46.35	40.19
18	29.26	39.62	42.54	43.50	44.12	46.01	45.91	45.98	39.80

Data Point	Gas Flow Meter		Test Fixture Press., (Pa)		Gas Flow Rates, (cc/min)		
	Temp. ( $^{\circ}\text{C}$ )	Press. (Pa)	Inlet	Outlet	F.M. #4	F.M. #5	F.M. #6
1	23.32	2,094,509	85,153	3,429	19.02	0.00	0.00
2	23.30	1,938,462	211,564	3,411	0.00	47.95	0.00
3	23.33	1,915,789	381,717	3,429	0.00	91.31	0.00
4	23.33	1,881,021	518,414	3,493	0.00	119.24	0.00
5	23.31	1,881,021	634,291	3,585	0.00	0.00	136.61
6	23.28	1,869,673	750,009	3,651	0.00	0.00	155.95
7	23.26	1,875,505	856,188	3,737	0.00	0.00	172.11
8	23.25	1,872,928	953,980	3,827	0.00	0.00	184.92
9	23.25	1,874,126	1,053,377	3,899	0.00	0.00	192.71
10	23.25	1,870,080	1,206,440	4,010	0.00	0.00	196.43
11	23.28	1,872,250	1,345,511	4,123	0.00	0.00	198.55
12	23.30	1,875,031	1,482,456	4,254	0.00	0.00	201.09
13	23.33	1,867,887	1,601,949	4,338	0.00	0.00	205.66
14	23.38	1,872,431	1,750,311	4,551	0.00	0.00	210.32
15	23.45	2,582,882	1,806,508	4,589	0.00	45.56	170.02
16	23.44	2,564,007	1,934,524	4,743	0.00	46.26	174.01
17	23.46	2,552,093	2,051,576	4,887	0.00	46.74	177.06
18	23.46	2,557,044	2,215,264	5,068	0.00	47.34	181.10

## Appendix C: Single- and two-phase measured data (continued).

Channel F: Water tests.

Number of channels: 11

Channel Dimensions:

Depth ( $\mu\text{m}$ ): 54.09Hyd. Diameter ( $\mu\text{m}$ ): 55.99Width ( $\mu\text{m}$ ): 58.02

Channel Length (m): 0.0635

Data Point	Test Fixture Temperature		Test Section Temperature, ( $^{\circ}\text{C}$ )						
	Inlet	Outlet	Pos #1	Pos #2	Pos #3	Pos #4	Pos #5	Pos #6	Pos #7
1	24.89	42.37	35.74	38.70	42.36	44.75	44.40	46.41	40.29
2	25.04	42.65	35.73	38.62	42.26	44.64	44.31	46.31	40.22
3	25.04	42.58	35.62	38.44	42.04	44.42	44.10	46.05	40.00
4	25.02	42.46	35.49	38.25	41.82	44.20	43.88	45.81	39.80
5	24.49	42.33	35.16	37.85	41.36	43.74	43.44	45.34	40.81
6	24.80	42.24	34.93	37.56	41.02	43.41	43.11	44.97	39.23
7	24.75	41.87	34.58	37.12	40.52	42.90	42.61	44.44	38.83
8	24.51	41.36	34.25	36.71	40.05	42.43	42.15	43.93	39.03
9	24.62	40.93	33.94	36.33	39.61	41.99	41.72	43.45	38.25
10	24.61	40.53	33.69	36.02	39.24	41.62	41.36	43.05	37.91
11	24.66	40.00	33.36	35.62	38.78	41.15	40.89	42.54	37.51
12	24.67	39.22	32.95	35.09	38.15	40.52	40.27	41.84	36.91
13	24.71	38.87	32.71	34.80	37.81	40.17	39.93	41.46	36.40
14	24.68	37.90	32.43	34.45	37.38	39.74	39.51	40.98	35.87
15	24.71	37.67	32.10	34.04	36.89	39.25	39.02	40.43	35.32
16	24.72	37.35	31.88	33.76	36.54	38.90	38.67	40.05	34.94

Data Point	Liquid Flow Meter		Test Fixture Press.. (Pa)		liquid Flow Rate
	Temp.( $^{\circ}\text{C}$ )	Press.(Pa)	Inlet	Outlet	F. M. #1, (cc/min)
1	24.79	2.991.684	1.748.442	97.939	8.55
2	24.78	3.028.056	1.851.908	98.416	9.31
3	24.78	3.043.225	1.941.110	98.016	10.07
4	24.80	3.035.177	2.012.431	97.293	9.72
5	24.84	3.037.257	2.143.363	97.019	10.59
6	24.89	3.036.805	2.235.007	96.574	11.01
7	24.95	3.068.498	2.341.706	96.960	10.40
8	25.03	3.057.489	2.446.099	96.454	10.87
9	25.10	3.071.595	2.563.920	97.085	13.68
10	25.21	3.060.224	2.661.056	96.662	13.20
11	25.31	3.084.028	2.768.117	97.134	12.29
12	25.42	3.097.546	2.929.883	97.444	12.87
13	25.58	3.105.435	3.039.747	97.270	15.76
14	25.72	4.058.152	3.187.226	97.876	14.06
15	25.83	4.148.281	3.347.478	99.243	16.04
16	25.96	4.194.690	3.499.772	99.551	16.64

Appendix C: Single- and two-phase measured data (continued).

Channel F: Water and argon tests.      Number of channels:      11

Channel Dimensions:

Depth ( $\mu\text{m}$ ):      54.09      Hyd. Diameter ( $\mu\text{m}$ ):      55.99

Width ( $\mu\text{m}$ ):      58.02      Channel Length (m):      0.0635

Data Point	Test Fixture Temperature		Test Section Temperature, ( $^{\circ}\text{C}$ )						
	Inlet	Outlet	Pos #1	Pos #2	Pos #3	Pos #4	Pos #5	Pos #6	Pos #7
1	26.29	43.18	36.22	38.95	42.44	44.76	44.49	46.39	43.72
2	26.86	43.00	36.33	39.02	42.44	44.76	44.48	46.34	43.62
3	26.97	43.36	36.81	39.64	43.10	45.43	45.15	47.01	43.58
4	27.42	43.28	37.13	39.98	43.39	45.70	45.41	47.24	43.68
5	27.39	43.30	37.39	40.18	43.58	45.90	45.62	47.42	43.83
6	27.62	43.26	37.28	40.05	43.41	45.71	45.44	47.20	43.55
7	27.65	43.46	37.53	40.38	43.74	46.05	45.78	47.52	43.73
8	27.83	43.45	37.85	40.70	44.05	46.36	46.07	47.82	44.44
9	27.83	43.69	38.13	41.06	44.41	46.70	46.41	48.15	44.11
10	27.90	43.37	38.13	40.98	44.27	46.55	46.27	47.94	43.84
11	27.95	43.95	38.64	41.59	44.95	47.24	46.95	48.65	44.44
12	27.82	43.07	38.03	40.85	44.08	46.37	46.10	47.68	43.66
13	27.63	39.37	36.36	40.53	45.97	46.96	46.06	46.55	46.96
14	27.70	40.32	36.18	40.35	45.90	46.89	45.98	46.68	47.47
15	27.76	40.81	36.22	40.37	45.96	46.95	46.03	46.86	47.76
16	27.76	40.95	36.15	40.26	45.90	46.87	45.93	46.89	47.81
17	27.72	40.71	36.12	40.23	45.90	46.86	45.91	46.93	47.80
18	27.63	39.45	36.14	40.27	45.97	46.94	46.00	47.06	47.87
19	28.53	37.41	36.16	39.95	46.95	47.39	45.95	45.68	47.14
20	28.80	38.16	36.13	39.99	47.03	47.46	46.03	45.86	47.24
21	28.80	37.63	36.17	40.07	47.13	47.56	46.13	46.02	47.33
22	28.74	37.93	36.10	40.10	47.25	47.66	46.21	46.19	47.43
23	28.86	37.96	36.01	40.05	47.21	47.62	46.18	46.24	47.39
24	28.78	37.55	35.93	40.05	47.27	47.67	46.22	46.35	47.42
25	29.08	37.17	36.39	40.41	49.15	49.11	47.13	46.25	48.11
26	29.08	37.41	36.33	40.47	49.33	49.26	47.26	46.48	48.19
27	29.02	37.45	36.27	40.51	49.49	49.41	47.38	46.69	48.33
28	29.92	38.22	36.93	41.21	50.26	50.17	48.14	47.55	49.12
29	29.90	38.12	36.79	41.11	50.22	50.12	48.08	47.61	49.16
30	29.64	38.36	36.78	41.17	50.44	50.32	48.25	47.91	49.44
31	29.71	36.20	35.55	38.92	47.55	47.49	45.55	44.56	46.41
32	29.68	36.31	35.47	38.87	47.54	47.48	45.53	44.67	46.44
33	29.63	36.35	35.36	38.73	47.49	47.41	45.41	44.71	46.44



## Appendix C: Single- and two-phase measured data (continued).

## Channel F: Water and Argon tests (continued).

Data Point	Gas Flow Meter		Liquid Flow Meter		Test Fixture Press.. (Pa)		Flow Meter/Flow rates. (cc/min)			
	Temp.(°C)	Press.(Pa)	Temp.(°C)	Press.(Pa)	Inlet	Outlet	F.M. #4	F.M. #5	F.M. #6	F.M. #1
1	25.24	4.706.031	25.78	4.589.671	3,036.913	106.622	0.00	4.18	0.00	10.26
2	25.15	4.552.629	25.84	4.572.559	3,178.560	107.800	0.00	7.46	0.00	9.98
3	25.11	4.151.174	25.95	4.579.386	3,207.043	108.815	0.00	11.13	0.00	11.69
4	25.31	3.863.698	26.16	4.617.680	3,288.379	110.117	0.00	16.01	0.00	9.95
5	25.23	3.837.837	26.13	4.568.671	3,323.530	111.279	0.00	19.32	0.00	9.53
6	25.30	4.121.074	26.22	4.561.510	3,461.869	111.640	0.00	23.18	0.00	9.77
7	25.30	4.493.786	26.22	4.589.581	3,523.726	112.490	0.00	26.23	0.00	11.44
8	25.22	4.380.102	26.18	4.514.824	3,588.175	112.956	0.00	29.72	0.00	9.55
9	25.24	4.329.804	26.20	4.499.023	3,642.519	113.829	0.00	33.02	0.00	10.16
10	25.20	4.320.762	26.21	4.510.438	3,811.112	116.663	0.00	0.00	35.73	10.16
11	25.20	4.313.212	26.23	4.533.881	3,913.584	117.493	0.00	0.00	37.47	11.02
12	25.19	4.341.135	26.22	4.516.383	4,105.736	119.606	0.00	0.00	41.02	10.13
13	24.99	2.530.505	28.71	3.307.093	340.216	115.884	0.00	0.00	171.26	52.87
14	24.94	2.485.000	28.79	3.292.173	418.951	123.712	0.00	0.00	317.62	51.94
15	24.94	2.465.695	28.88	3.283.877	488.351	131.066	0.00	0.00	436.49	50.12
16	24.92	2.458.800	28.88	3.281.051	562.429	138.494	0.00	0.00	535.35	48.79
17	24.94	2.447.881	28.87	3.268.505	626.381	145.459	0.00	130.73	488.76	47.27
18	24.94	2.450.164	28.81	3.221.756	685.450	151.214	0.00	145.43	553.55	44.55
19	24.87	2.524.989	29.95	3.180.976	717.640	116.544	0.00	0.00	111.94	107.89
20	24.87	2.491.917	29.97	3.161.512	799.947	125.353	0.00	0.00	208.89	103.27
21	24.88	2.469.831	29.94	3.166.305	873.393	133.713	0.00	0.00	298.47	102.02
22	24.86	2.460.179	29.87	3.168.656	943.968	141.367	0.00	0.00	372.79	98.69
23	24.88	2.456.042	29.79	3.149.983	1,010.949	148.045	0.00	93.89	351.12	96.43
24	24.90	2.453.284	29.68	3,144.603	1,080.846	154.311	0.00	105.46	401.49	94.03
25	24.86	2.564.866	30.02	3,110.943	1,089.843	117.138	0.00	0.00	77.12	146.74
26	24.85	2.490.516	29.98	3,091.299	1,166.114	126.963	0.00	0.00	158.63	145.04
27	24.87	2.475.777	29.94	3,093.243	1,239.040	135.896	0.00	0.00	228.29	140.56
28	25.66	2.466.938	30.62	3,067.699	1,294.153	142.260	0.00	0.00	294.98	138.65
29	25.67	2.460.111	30.54	3,077.555	1,355.957	149.193	0.00	74.75	279.47	133.95
30	25.72	2.457.421	30.46	3,023.414	1,395.358	154.058	0.00	86.66	329.94	130.48
31	25.72	2.520.852	30.66	3,026.895	1,477.214	117.916	0.00	0.00	62.15	183.08
32	25.74	2.485.000	30.64	3,023.979	1,545.211	128.502	0.00	0.00	126.92	177.50
33	25.76	2.476.432	30.59	3,016.316	1,603.444	136.898	0.00	0.00	186.88	175.66

# Appendix C: Single- and two-phase measured data (continued).

Channel F: Water and helium tests.

Number of channels: 11

Channel Dimensions:

Depth ( $\mu\text{m}$ ): 54.09Hyd. Diameter ( $\mu\text{m}$ ): 55.99Width ( $\mu\text{m}$ ): 58.02

Channel Length (m): 0.0635

Data Point	Test Fixture Temperature		Test Section Temperature, ( $^{\circ}\text{C}$ )						
	Inlet	Outlet	Pos #1	Pos #2	Pos #3	Pos #4	Pos #5	Pos #6	Pos #7
1	26.72	44.20	36.71	39.48	42.99	45.30	45.04	47.01	43.40
2	27.19	43.66	36.87	39.67	43.09	45.40	45.12	47.02	43.18
3	27.45	42.93	36.45	39.16	42.50	44.81	44.55	46.37	42.20
4	27.24	42.83	36.22	38.92	42.25	44.56	44.30	46.11	42.00
5	27.50	42.59	36.45	39.17	42.48	44.78	44.52	46.32	42.13
6	27.30	42.11	36.05	38.68	41.94	44.24	43.99	45.75	41.74
7	27.32	41.29	35.70	38.25	41.41	43.70	43.47	45.13	41.40
8	27.37	41.36	35.92	38.50	41.64	43.94	43.70	45.32	42.17
9	27.39	41.17	35.89	38.48	41.61	43.90	43.65	45.25	42.02
10	27.37	40.99	35.86	38.41	41.50	43.79	43.55	45.13	42.47
11	27.34	40.62	35.74	38.28	41.32	43.60	43.37	44.89	42.26
12	27.22	40.30	35.51	38.05	41.07	43.35	43.12	44.60	41.43
13	27.31	40.35	35.89	38.45	41.47	43.75	43.51	44.97	41.63
14	27.70	40.32	36.18	40.35	45.90	46.89	45.98	46.68	47.47
15	27.76	40.81	36.22	40.37	45.96	46.95	46.03	46.86	47.76
16	27.76	40.95	36.15	40.26	45.90	46.87	45.93	46.89	47.81
17	27.72	40.71	36.12	40.23	45.90	46.86	45.91	46.93	47.80
18	27.63	39.45	36.14	40.27	45.97	46.94	46.00	47.06	47.87
19	28.53	37.41	36.16	39.95	46.95	47.39	45.95	45.68	47.14
20	28.80	38.16	36.13	39.99	47.03	47.46	46.03	45.86	47.24
21	28.80	37.63	36.17	40.07	47.13	47.56	46.13	46.02	47.33
22	28.74	37.93	36.10	40.10	47.25	47.66	46.21	46.19	47.43
23	28.86	37.96	36.01	40.05	47.21	47.62	46.18	46.24	47.39
24	28.78	37.55	35.93	40.05	47.27	47.67	46.22	46.35	47.42
25	29.08	37.17	36.39	40.41	49.15	49.11	47.13	46.25	48.11
26	29.08	37.41	36.33	40.47	49.33	49.26	47.26	46.48	48.19
27	29.02	37.45	36.27	40.51	49.49	49.41	47.38	46.69	48.33
28	29.92	38.22	36.93	41.21	50.26	50.17	48.14	47.55	49.12
29	29.90	38.12	36.79	41.11	50.22	50.12	48.08	47.61	49.16
30	29.64	38.36	36.78	41.17	50.44	50.32	48.25	47.91	49.44
31	29.71	36.20	35.55	38.92	47.55	47.49	45.55	44.56	46.41
32	29.68	36.31	35.47	38.87	47.54	47.48	45.53	44.67	46.44
33	29.63	36.35	35.36	38.73	47.49	47.41	45.41	44.71	46.44

## Appendix C: Single- and two-phase measured data (continued).

## Channel F: Water and Helium tests (continued).

Data Point	Gas Flow Meter		Liquid Flow Meter		Test Fixture Press., (Pa)		Flow Meter/Flow rates. (cc/min)			
	Temp.(°C)	Press.(Pa)	Temp.(°C)	Press.(Pa)	Inlet	Outlet	F.M. #4	F.M. #5	F.M. #6	F.M. #1
1	25.29	7,210,017	26.43	4,842,267	3,023,191	106,165	0.00	5.75	0.00	11.09
2	25.30	7,072,461	26.46	4,863,381	3,061,146	111,369	0.00	9.79	0.00	12.09
3	25.27	6,819,097	26.49	4,835,508	3,201,143	112,441	0.00	14.21	0.00	10.37
4	25.27	6,545,410	26.52	4,855,379	3,285,214	112,452	0.00	15.94	0.00	11.87
5	25.22	6,174,338	26.54	4,878,843	3,290,504	115,689	0.00	21.31	0.00	10.26
6	25.19	5,483,485	26.56	4,874,051	3,405,408	116,028	0.00	22.60	0.00	11.59
7	25.19	4,794,577	26.66	4,858,453	3,554,945	119,315	0.00	30.82	0.00	12.86
8	25.21	4,632,178	26.70	4,880,335	3,584,174	123,615	0.00	0.00	41.41	12.08
9	25.23	4,637,716	26.72	4,887,931	3,631,985	126,183	0.00	0.00	47.94	11.09
10	25.22	4,609,120	26.69	4,853,841	3,680,067	127,659	0.00	0.00	52.64	11.35
11	25.23	4,643,187	26.73	4,872,039	3,774,107	130,787	0.00	0.00	59.56	11.33
12	25.23	4,565,107	26.72	4,888,134	3,888,718	133,582	0.00	0.00	64.43	12.02
13	25.22	4,627,657	26.70	4,864,037	3,905,604	136,925	0.00	0.00	77.06	11.10
14	24.94	2,485,000	28.79	3,292,173	418,951	123,712	0.00	0.00	325.60	51.94
15	24.94	2,465,695	28.88	3,283,877	488,351	131,066	0.00	0.00	447.92	50.12
16	24.92	2,458,800	28.88	3,281,051	562,429	138,494	0.00	0.00	549.69	48.79
17	24.94	2,447,881	28.87	3,268,505	626,381	145,459	0.00	134.22	501.83	47.27
18	24.94	2,450,164	28.81	3,221,756	685,450	151,214	0.00	149.07	567.42	44.55
19	24.87	2,524,989	29.95	3,180,976	717,640	116,544	0.00	0.00	114.19	107.89
20	24.87	2,491,917	29.97	3,161,512	799,947	125,353	0.00	0.00	213.34	103.27
21	24.88	2,469,831	29.94	3,166,305	873,393	133,713	0.00	0.00	304.66	102.02
22	24.86	2,460,179	29.87	3,168,656	943,968	141,367	0.00	0.00	380.87	98.69
23	24.88	2,456,042	29.79	3,149,983	1,010,949	148,045	0.00	95.94	358.78	96.43
24	24.90	2,453,284	29.68	3,144,603	1,080,846	154,311	0.00	107.73	410.15	94.03
25	24.86	2,564,866	30.02	3,110,943	1,089,843	117,138	0.00	0.00	78.69	146.74
26	24.85	2,490,516	29.98	3,091,299	1,166,114	126,963	0.00	0.00	161.98	145.04
27	24.87	2,475,777	29.94	3,093,243	1,239,040	135,896	0.00	0.00	233.21	140.56
28	25.66	2,466,938	30.62	3,067,699	1,294,153	142,260	0.00	0.00	301.34	138.65
29	25.67	2,460,111	30.54	3,077,555	1,355,957	149,193	0.00	76.38	285.53	133.95
30	25.72	2,457,421	30.46	3,023,414	1,395,358	154,058	0.00	88.64	337.44	130.48
31	25.72	2,520,852	30.66	3,026,895	1,477,214	117,916	0.00	0.00	63.35	183.08
32	25.74	2,485,000	30.64	3,023,979	1,545,211	128,502	0.00	0.00	129.44	177.50
33	25.76	2,476,432	30.59	3,016,316	1,603,444	136,898	0.00	0.00	190.66	175.66

# Appendix C: Single- and two-phase measured data (continued).

Channel F: Water and nitrogen tests. Number of channels: 11

Channel Dimensions:

Depth ( $\mu\text{m}$ ): 54.09 Hyd. Diameter ( $\mu\text{m}$ ): 55.99

Width ( $\mu\text{m}$ ): 58.02 Channel Length (m): 0.0635

Data Point	Test Fixture Temperature		Test Section Temperature, ( $^{\circ}\text{C}$ )						
	Inlet	Outlet	Pos #1	Pos #2	Pos #3	Pos #4	Pos #5	Pos #6	Pos #7
1	26.85	44.87	37.17	39.96	43.46	45.78	45.51	47.47	44.04
2	27.17	43.98	36.83	39.58	42.97	45.29	45.02	46.91	43.61
3	27.39	44.07	37.02	39.83	43.27	45.57	45.32	47.20	43.78
4	27.35	44.06	37.10	39.89	43.32	45.62	45.36	47.24	44.38
5	27.66	43.85	36.97	39.79	43.17	45.48	45.21	47.06	44.05
6	27.76	44.04	37.38	40.25	43.65	45.95	45.67	47.51	43.78
7	27.78	43.44	37.06	39.75	43.00	45.29	45.04	46.74	43.17
8	27.89	43.88	37.76	40.59	43.90	46.19	45.92	47.65	43.77
9	27.63	42.97	36.94	39.66	42.86	45.15	44.89	46.55	42.86
10	27.51	42.88	36.83	39.53	42.75	45.05	44.78	46.46	42.79
11	27.26	42.38	36.06	38.66	41.85	44.14	43.88	45.56	42.25
12	26.86	40.06	34.96	38.72	43.56	44.73	43.99	45.28	45.99
13	27.63	39.37	36.36	40.53	45.97	46.96	46.06	46.55	46.96
14	27.70	40.32	36.18	40.35	45.90	46.89	45.98	46.68	47.47
15	27.76	40.81	36.22	40.37	45.96	46.95	46.03	46.86	47.76
16	27.76	40.95	36.15	40.26	45.90	46.87	45.93	46.89	47.81
17	27.72	40.71	36.12	40.23	45.90	46.86	45.91	46.93	47.80
18	27.63	39.45	36.14	40.27	45.97	46.94	46.00	47.06	47.87
19	28.53	37.41	36.16	39.95	46.95	47.39	45.95	45.68	47.14
20	28.80	38.16	36.13	39.99	47.03	47.46	46.03	45.86	47.24
21	28.80	37.63	36.17	40.07	47.13	47.56	46.13	46.02	47.33
22	28.74	37.93	36.10	40.10	47.25	47.66	46.21	46.19	47.43
23	28.86	37.96	36.01	40.05	47.21	47.62	46.18	46.24	47.39
24	28.78	37.55	35.93	40.05	47.27	47.67	46.22	46.35	47.42
25	29.08	37.17	36.39	40.41	49.15	49.11	47.13	46.25	48.11
26	29.08	37.41	36.33	40.47	49.33	49.26	47.26	46.48	48.19
27	29.02	37.45	36.27	40.51	49.49	49.41	47.38	46.69	48.33
28	29.92	38.22	36.93	41.21	50.26	50.17	48.14	47.55	49.12
29	29.90	38.12	36.79	41.11	50.22	50.12	48.08	47.61	49.16
30	29.64	38.36	36.78	41.17	50.44	50.32	48.25	47.91	49.44
31	29.71	36.20	35.55	38.92	47.55	47.49	45.55	44.56	46.41
32	29.68	36.31	35.47	38.87	47.54	47.48	45.53	44.67	46.44
33	29.63	36.35	35.36	38.73	47.49	47.41	45.41	44.71	46.44

## Appendix C: Single- and two-phase measured data (continued).

## Channel F: Water and Nitrogen tests (continued).

Data Point	Gas Flow Meter		Liquid Flow Meter		Test Fixture Press., (Pa)		Flow Meter/Flow rates, (cc/min)			
	Temp.(°C)	Press.(Pa)	Temp.(°C)	Press.(Pa)	Inlet	Outlet	F.M. #4	F.M. #5	F.M. #6	F.M. #1
1	25.02	4,918,841	26.60	4,944,807	3,267,039	108,724	0.00	3.74	0.00	9.79
2	24.98	4,811,238	26.59	4,908,185	3,405,227	107,305	0.00	5.51	0.00	9.91
3	24.94	4,639,480	26.61	4,895,458	3,411,738	108,553	0.00	8.04	0.00	10.29
4	24.90	4,433,881	26.57	4,931,288	3,513,486	110,002	0.00	10.46	0.00	10.64
5	24.91	4,331,907	26.59	4,937,008	3,628,933	111,044	0.00	13.37	0.00	10.22
6	24.91	4,290,041	26.57	4,917,748	3,679,073	111,317	0.00	15.70	0.00	18.93
7	24.95	4,250,752	26.61	4,936,646	3,895,771	114,930	0.00	21.21	0.00	9.54
8	24.97	4,198,895	26.57	4,894,939	4,096,215	117,299	0.00	0.00	29.32	10.10
9	25.01	4,391,721	26.59	4,898,895	4,094,226	117,005	0.00	0.00	26.78	12.05
10	24.99	4,447,264	26.56	4,903,551	4,082,155	115,563	0.00	0.00	23.56	11.96
11	24.98	4,571,346	26.61	4,953,894	4,063,008	113,793	0.00	0.00	17.14	10.10
12	25.08	2,448,582	28.03	3,254,557	611,325	150,513	0.00	114.32	435.15	32.54
13	24.99	2,530,505	28.71	3,307,093	340,216	115,884	0.00	0.00	124.69	52.87
14	24.94	2,485,000	28.79	3,292,173	418,951	123,712	0.00	0.00	231.62	51.94
15	24.94	2,465,695	28.88	3,283,877	488,351	131,066	0.00	0.00	318.58	50.12
16	24.92	2,458,800	28.88	3,281,051	562,429	138,494	0.00	0.00	390.90	48.79
17	24.94	2,447,881	28.87	3,268,505	626,381	145,459	0.00	95.44	356.81	47.27
18	24.94	2,450,164	28.81	3,221,756	685,450	151,214	0.00	105.98	403.39	44.55
19	24.87	2,524,989	29.95	3,180,976	717,640	116,544	0.00	0.00	81.17	107.89
20	24.87	2,491,917	29.97	3,161,512	799,947	125,353	0.00	0.00	151.63	103.27
21	24.88	2,469,831	29.94	3,166,305	873,393	133,713	0.00	0.00	216.49	102.02
22	24.86	2,460,179	29.87	3,168,656	943,968	141,367	0.00	0.00	270.61	98.69
23	24.88	2,456,042	29.79	3,149,983	1,010,949	148,045	0.00	68.16	254.88	96.43
24	24.90	2,453,284	29.68	3,144,603	1,080,846	154,311	0.00	76.52	291.33	94.03
25	24.86	2,564,866	30.02	3,110,943	1,089,843	117,138	0.00	0.00	55.89	146.74
26	24.85	2,490,516	29.98	3,091,299	1,166,114	126,963	0.00	0.00	115.03	145.04
27	24.87	2,475,777	29.94	3,093,243	1,239,040	135,896	0.00	0.00	165.60	140.56
28	25.66	2,466,938	30.62	3,067,699	1,294,153	142,260	0.00	0.00	213.95	138.65
29	25.67	2,460,111	30.54	3,077,555	1,355,957	149,193	0.00	54.22	202.70	133.95
30	25.72	2,457,421	30.46	3,023,414	1,395,358	154,058	0.00	62.92	239.53	130.48
31	25.72	2,520,852	30.66	3,026,895	1,477,214	117,916	0.00	0.00	44.96	183.08
32	25.74	2,485,000	30.64	3,023,979	1,545,211	128,502	0.00	0.00	91.85	177.50
33	25.76	2,476,432	30.59	3,016,316	1,603,444	136,898	0.00	0.00	135.28	175.66

## APPENDIX D

# Appendix D: Single- and two-phase calculated data.

Channel A: Argon gas tests.

Number of channels:

3

Channel Dimensions:

Depth ( $\mu\text{m}$ ): 255.80

Hyd. Diameter ( $\mu\text{m}$ ): 256.91

Width ( $\mu\text{m}$ ): 258.03

Channel Length (m): 0.0635

Data Point	Heat Trans.								Uncertainty	
	Re	f	Velocity (m/s)	Q (Watts)	coeff. W/m <sup>2</sup> -K	Heat Flux (W/m <sup>2</sup> )	Nu		U-f	U-Nu
1										
2										
3	413.0	0.1543	20.94	0.0178	7.765	121.63	0.110417		0.031	0.225
4	633.0	0.1095	30.94	0.0320	14.344	217.93	0.203729		0.031	0.196
5	867.0	0.0868	40.68	0.0495	22.360	337.39	0.317345		0.031	0.177
6	1,079.5	0.0768	48.93	0.0968	34.265	660.17	0.483840		0.031	0.118
7	1,255.9	0.0758	54.47	0.1246	41.641	849.67	0.586697		0.031	0.108
8	1,483.3	0.0720	61.15	0.1621	53.869	1105.34	0.757696		0.031	0.101
9	1,699.8	0.0692	66.73	0.2025	66.870	1381.43	0.939469		0.031	0.095
10	1,923.7	0.0681	71.48	0.2352	76.532	1604.32	1.075018		0.031	0.093
11	2,101.3	0.0683	74.68	0.2766	90.836	1886.32	1.274359		0.031	0.089
12	2,308.3	0.0669	78.48	0.3224	108.074	2199.18	1.513778		0.031	0.086
13	3,030.7	0.0624	89.49	0.5053	179.677	3446.59	2.511865		0.031	0.080
14	3,726.9	0.0597	97.55	0.7314	285.312	4988.49	3.977011		0.031	0.078
15	4,407.0	0.0569	104.20	0.9077	370.116	6190.79	5.155816		0.031	0.079
16	5,082.5	0.0557	108.95	1.0864	459.665	7409.76	6.401325		0.031	0.080

Appendix D: Single- and two-phase calculated data (continued).

Channel A: Helium gas tests. Number of channels: 3

Channel Dimensions:

Depth ( $\mu\text{m}$ ): 255.80 Hyd. Diameter ( $\mu\text{m}$ ): 256.91

Width ( $\mu\text{m}$ ): 258.03 Channel Length (m): 0.0635

Data Point	Re	f	Velocity	Q	Heat Trans. coeff.	Heat Flux	Nu	Uncertainty	
			(m/s)	(Watts)	W/m <sup>2</sup> -K	(W/m <sup>2</sup> )		U-f (%)	U-Nu (%)
1									
2									
3	72.7	0.8569	32.28	0.0200	10.730	136.71	0.0176525	0.031	0.305
4	95.7	0.6968	41.33	0.0387	20.598	264.30	0.0337881	0.031	0.216
5	121.7	0.5860	50.71	0.0563	30.520	383.98	0.0500165	0.031	0.193
6	149.8	0.4724	60.89	0.0803	33.172	547.83	0.0542253	0.031	0.164
7	171.1	0.4269	67.95	0.0960	37.040	654.64	0.0604353	0.031	0.156
8	197.5	0.3787	76.35	0.1211	46.402	825.68	0.0755812	0.031	0.145
9	223.8	0.3403	84.49	0.1640	64.542	1118.72	0.1048675	0.031	0.126
10	247.8	0.3114	91.64	0.2068	83.395	1410.24	0.1352209	0.031	0.115
11	274.6	0.2856	99.12	0.2405	97.834	1640.55	0.1584963	0.031	0.112
12	360.8	0.2238	121.49	0.3970	172.375	2707.56	0.2786209	0.031	0.099
13	456.1	0.1835	143.18	0.5820	266.539	3969.59	0.4302420	0.031	0.094
14	547.6	0.1609	160.40	0.7424	349.572	5063.88	0.5643628	0.031	0.093
15	643.8	0.1426	176.93	0.8884	425.075	6059.35	0.6869200	0.031	0.093



Appendix D: Single- and two-phase calculated data (continued).

Channel A: Nitrogen gas tests.

Number of channels: 3

Channel Dimensions:

Depth ( $\mu\text{m}$ ): 255.80

Hyd. Diameter ( $\mu\text{m}$ ): 256.91

Width ( $\mu\text{m}$ ): 258.03

Channel Length (m): 0.0635

Data Point					Heat Trans.		Nu	Uncertainty	
	Re	f	Velocity (m/s)	Q (Watts)	coeff. W/m <sup>2</sup> -K	Heat Flux (W/m <sup>2</sup> )		U-f (%)	U-Nu (%)
1									
2									
3									
4									
5	537.7	0.1307	31.16	0.0637	30.923	434.34	0.295	0.031	0.145
6	673.4	0.1103	38.04	0.0848	40.794	578.63	0.389	0.031	0.138
7	819.0	0.0971	44.94	0.1104	52.846	752.87	0.504	0.031	0.132
8	959.8	0.0859	51.38	0.1373	66.127	936.45	0.631	0.031	0.127
9	1,084.2	0.0784	56.78	0.1612	78.161	1099.80	0.746	0.031	0.124
10	1,221.1	0.0722	62.43	0.1907	93.531	1300.81	0.893	0.031	0.121
11	1,351.9	0.0690	67.61	0.2610	102.434	1780.29	0.976	0.031	0.098
12	1,480.9	0.0665	72.38	0.3182	118.987	2170.12	1.131	0.031	0.091
13	1,963.9	0.0638	86.03	0.4600	177.026	3137.45	1.681	0.031	0.087
14	2,417.5	0.0632	95.72	0.6278	254.355	4281.83	2.411	0.031	0.085
15	2,856.4	0.0619	103.48	0.7976	335.670	5439.91	3.179	0.031	0.084
16	3,332.6	0.0609	110.18	0.9777	423.995	6668.32	4.016	0.031	0.084

Appendix D: Single- and two-phase calculated data (continued).

Channel A: Water tests.                      Number of channels:                      3  
 Channel Dimensions:  
 Depth ( $\mu\text{m}$ ):                      255.80                      Hyd. Diameter ( $\mu\text{m}$ ):                      256.91  
 Width ( $\mu\text{m}$ ):                      258.03                      Channel Length (m):                      0.0635

Data Point	Re	f	Velocity	Q	h - overall	Heat Flux	Nu	Uncertainty	
								U-f	U_Nu
			(m/s)	(Watts)	W/m <sup>2</sup> -K	(W/m <sup>2</sup> )		(%)	(%)
1	292.67	2.1342	0.90	11.550	8493.92472	78779	3.481	0.031	0.127
2	452.76	0.8574	1.45	14.937	11248.3605	101878	4.629	0.031	0.137
3	813.40	0.2748	2.65	22.172	15561.9094	151230	6.419	0.031	0.143
4	1,102.66	0.1611	3.58	27.525	19263.5396	187738	7.941	0.031	0.149
5	1,400.19	0.1123	4.45	37.885	26172.7978	258395	10.765	0.031	0.141
6	1,574.26	0.0980	4.91	46.113	30587.2304	314519	12.554	0.031	0.132
7	1,747.58	0.0847	5.44	47.464	35593.8189	323735	14.607	0.031	0.146
8	1,928.25	0.0759	5.92	56.149	39977.6314	382968	16.379	0.031	0.137
9	2,023.96	0.0722	6.24	56.697	42232.7974	386707	17.313	0.031	0.143
10	2,321.62	0.0590	7.22	59.001	47542.2493	402422	19.507	0.031	0.156
11	2,576.36	0.0531	7.94	68.972	51061.7059	470433	20.929	0.031	0.145
12	2,935.60	0.0467	8.99	78.895	55422.8406	538115	22.701	0.031	0.140
13	3,289.14	0.0411	10.15	80.828	60242.4717	551297	24.696	0.031	0.151
14	3,581.78	0.0383	11.02	85.446	63062.8762	582797	25.843	0.031	0.152
15	3,866.52	0.0356	11.96	86.012	66318.4592	586652	27.195	0.031	0.161
16	4,111.17	0.0338	12.81	88.658	69882.3194	604702	28.679	0.031	0.166
17	4,332.16	0.0328	13.57	88.002	71787.1406	600227	29.477	0.031	0.175
18	4,778.31	0.0294	15.06	90.839	76777.31	619579	31.547	0.031	0.185
19	5,011.42	0.0285	15.89	90.786	79303.327	619218	32.607	0.031	0.193
20	5,309.29	0.0274	16.91	91.119	82474.3963	621488	33.926	0.031	0.202
21	5,426.25	0.0278	17.33	87.572	82283.6312	597293	33.858	0.031	0.213

Appendix D: Single- and two-phase calculated data (continued).

Channel A: Water-argon tests.

Number of channels: 3

Channel Dimensions:

Depth ( $\mu\text{m}$ ): 255.80 Hyd. Diameter ( $\mu\text{m}$ ): 256.91

Width ( $\mu\text{m}$ ): 258.03 Channel Length (m): 0.0635

Data Point	G	x	f	Two-phase	Q	h - overall	Heat Flux	Nu	Uncertainty	
									U f	U Nu
	kg/s-m <sup>2</sup>	Quality		Re-avg	(Watts)	W/m <sup>2</sup> -K	(W/m <sup>2</sup> )		(%)	(%)
1	1.255	0.05901	0.3038	527	15.666	13.367	106853	5.483	0.031	0.143
2	1.387	0.116672	0.1675	591	18.483	18.799	126062	7.704	0.031	0.163
3	1.345	0.180881	0.1269	574	18.724	19.060	127708	7.816	0.031	0.162
4	1.378	0.235876	0.1071	590	19.241	19.507	131232	8.001	0.031	0.161
5	1.398	0.292012	0.1208	600	19.566	19.617	133451	8.048	0.031	0.160
6	1.301	0.377753	0.1100	561	18.347	17.718	125136	7.272	0.031	0.155
7	3.980	0.017952	0.3905	1,624	41.428	34.528	282563	14.201	0.031	0.147
8	3.662	0.043857	0.2087	1,510	39.578	35.723	269943	14.680	0.031	0.154
9	3.196	0.075929	0.1318	1,367	34.441	33.171	234910	13.583	0.031	0.162
10	3.446	0.093957	0.1324	1,424	36.756	31.774	250700	13.061	0.031	0.150
11	3.340	0.12225	0.1466	1,371	33.637	26.997	229424	11.108	0.031	0.145
12	3.176	0.154612	0.1329	1,324	36.018	30.648	245666	12.594	0.031	0.146
13	8.483	0.009105	0.5808	3,406	61.586	45.628	420051	18.796	0.031	0.159
14	8.380	0.015089	0.3790	3,402	66.534	50.514	453800	20.786	0.031	0.154
15	8.076	0.021849	0.2887	3,288	65.494	49.066	446706	20.184	0.031	0.151
16	7.656	0.034562	0.2094	3,134	65.603	48.705	447450	20.027	0.031	0.147
17	7.159	0.051604	0.1637	2,938	63.138	45.039	430636	18.518	0.031	0.142
18	6.659	0.073816	0.1691	2,736	60.102	40.977	409935	16.850	0.031	0.137
19	11.739	0.006417	0.7974	4,737	83.240	58.195	567748	23.959	0.031	0.157
20	11.525	0.010913	0.4955	4,662	83.791	57.781	571508	23.783	0.031	0.154
21	11.028	0.015786	0.3683	4,475	84.298	57.187	574967	23.532	0.031	0.149
22	10.477	0.025034	0.2591	4,281	85.792	58.482	585156	24.049	0.031	0.144
23	9.642	0.038722	0.1923	3,961	83.784	55.420	571461	22.780	0.031	0.138
24	9.048	0.052643	0.1994	3,733	82.676	54.281	563904	22.305	0.031	0.134

Appendix D: Single- and two-phase calculated data (continued).

Channel A: Water-helium tests. Number of channels: 3

Channel Dimensions:

Depth ( $\mu\text{m}$ ): 255.80 Hyd. Diameter ( $\mu\text{m}$ ): 256.91

Width ( $\mu\text{m}$ ): 258.03 Channel Length (m): 0.0635

Data Point	G	x	f	Two-phase	Q	h - overall	Heat Flux	Nu	Uncertainty	
									U <sub>f</sub>	U <sub>Nu</sub>
	kg/s-m <sup>2</sup>	Quality		Re-avg	(Watts)	W/m <sup>2</sup> -K	(W/m <sup>2</sup> )		(%)	(%)
1	2.372	0.0033	0.0858	952.56	17.966	18687.6	122538	7.698	0.031	0.206
2	2.277	0.0070	0.0890	922.15	17.477	20749.5	119205	8.540	0.031	0.227
3	2.244	0.0107	0.0905	910.06	16.928	22811.4	115458	9.387	0.031	0.233
4	2.197	0.0149	0.0933	886.69	16.138	22317.5	110072	9.189	0.031	0.238
5	2.158	0.0189	0.0959	865.97	16.144	23092.7	110113	9.514	0.031	0.240
6	2.125	0.0230	0.0982	849.85	15.579	22331.9	106257	9.205	0.031	0.157
7	4.046	0.0019	0.0489	1,670.00	36.260	30870.6	247318	12.679	0.031	0.167
8	3.868	0.0041	0.0512	1,599.67	35.096	33158.3	239379	13.616	0.031	0.174
9	3.881	0.0062	0.0509	1,610.98	34.681	34616.3	236545	14.209	0.031	0.176
10	3.800	0.0086	0.0521	1,577.11	34.542	35022.3	235599	14.376	0.031	0.175
11	3.728	0.0109	0.0534	1,544.07	34.867	35620.1	237814	14.625	0.031	0.173
12	3.549	0.0138	0.0563	1,469.08	33.124	33276.7	225924	13.664	0.031	0.181
13	8.178	0.0009	0.0443	3,310.06	55.722	50198.0	380059	20.659	0.031	0.180
14	8.051	0.0020	0.0444	3,264.47	55.635	50501.2	379463	20.780	0.031	0.164
15	7.827	0.0031	0.0446	3,224.33	60.275	49963.8	411115	20.525	0.031	0.163
16	7.594	0.0043	0.0449	3,132.15	59.695	49717.4	407160	20.421	0.031	0.159
17	7.422	0.0055	0.0452	3,060.64	61.565	51284.1	419910	21.065	0.031	0.158
18	7.272	0.0067	0.0454	3,008.38	63.134	53609.4	430611	22.013	0.031	0.174
19	11.287	0.0007	0.0408	4,576.26	76.296	62966.5	520382	25.908	0.031	0.171
20	10.972	0.0015	0.0411	4,463.80	77.157	64218.6	526259	26.414	0.031	0.173
21	10.640	0.0023	0.0414	4,344.92	73.849	62382.2	503692	25.649	0.031	0.173

Appendix D: Single- and two-phase calculated data (continued).

Channel A: Water-Nitrogen tests.      Number of channels:      3  
 Channel Dimensions:  
 Depth ( $\mu\text{m}$ ):      255.80      Hyd. Diameter ( $\mu\text{m}$ ):      256.91  
 Width ( $\mu\text{m}$ ):      258.03      Channel Length (m):      0.0635

Data Point	G	x	f	Two-phase	Q	h - overall	Heat Flux	Nu	Uncertainty	
	kg/s-m <sup>2</sup>	Quality		Re-avg	(Watts)	W/m <sup>2</sup> -K	(W/m <sup>2</sup> )		U <sub>f</sub>	U <sub>Nu</sub>
									(%)	(%)
1	1.865	0.0210	0.1050	809.20	21.601	16.521	147333	6.903	0.031	0.134
2	1.795	0.0448	0.1113	801.24	20.783	17.799	141756	7.611	0.031	0.145
3	1.868	0.0650	0.1090	853.55	21.586	21.426	147229	9.348	0.031	0.162
4	1.852	0.0876	0.1123	869.52	21.329	21.879	145475	9.767	0.031	0.166
5	1.771	0.1155	0.1210	857.54	20.019	21.565	136539	9.916	0.031	0.173
6	1.810	0.1354	0.1213	895.18	19.953	21.762	136094	10.226	0.031	0.175
7	3.222	0.0118	0.0608	1,373.08	32.516	24.046	221778	9.967	0.031	0.137
8	3.165	0.0253	0.0622	1,378.77	32.552	29.747	222025	12.481	0.031	0.157
9	3.074	0.0395	0.0645	1,366.89	32.173	30.986	219437	13.177	0.031	0.162
10	3.043	0.0533	0.0658	1,379.89	32.483	32.754	221555	14.115	0.031	0.167
11	2.986	0.0683	0.0681	1,375.87	31.488	32.150	214764	14.066	0.031	0.169
12	2.935	0.0836	0.0706	1,371.68	30.131	30.416	205513	13.522	0.031	0.168
13	4.407	0.0086	0.0434	1,910.47	42.640	34.934	290833	14.405	0.031	0.149
14	4.370	0.0183	0.0437	1,932.08	45.138	39.317	307867	16.347	0.031	0.152
15	4.260	0.0284	0.0451	1,913.20	45.153	40.239	307974	16.886	0.031	0.153
16	4.193	0.0389	0.0463	1,905.03	44.565	40.342	303961	17.105	0.031	0.154
17	4.108	0.0496	0.0479	1,881.39	42.638	37.985	290816	16.283	0.031	0.153
18	3.927	0.0624	0.0515	1,797.50	36.696	29.853	250291	12.983	0.031	0.148
19	8.959	0.0044	0.0428	3,824.74	65.731	50.904	448323	20.928	0.031	0.161
20	8.614	0.0092	0.0431	3,733.10	66.425	54.313	453060	22.409	0.031	0.162
21	8.554	0.0142	0.0433	3,705.02	61.945	48.632	422506	20.174	0.031	0.163
22	8.319	0.0194	0.0437	3,630.20	62.464	49.522	426043	20.643	0.031	0.161
23	8.174	0.0249	0.0439	3,591.24	60.536	48.689	412894	20.402	0.031	0.163
24	8.018	0.0306	0.0442	3,525.12	57.016	44.591	388883	18.799	0.031	0.163

Appendix D: Single- and two-phase calculated data (continued).

Channel B: Argon gas tests. Number of channels: 3

Channel Dimensions:

Depth ( $\mu\text{m}$ ): 211.140 Hyd. Diameter ( $\mu\text{m}$ ): 210.051

Width ( $\mu\text{m}$ ): 208.97 Channel Length (m): 0.0635

Data Point	Heat Trans.								
	Re	f	Velocity	Q	coeff.	Heat Flux	Nu	Uncertainty	
			(m/s)	(Watts)	W/m <sup>2</sup> -K	(W/m <sup>2</sup> )		U-f	U-Nu
1	260.3	0.2402	16.09	0.0086	2.935	71.92	0.034098	0.031	0.232
2	706.1	0.0923	39.59	0.0407	14.391	338.48	0.166318	0.031	0.140
3	1.026.7	0.0671	53.88	0.0798	28.189	663.86	0.324900	0.031	0.109
4	1.422.6	0.0576	67.98	0.1450	54.637	1205.39	0.625138	0.031	0.091
5	1.790.1	0.0510	78.83	0.1977	75.734	1644.17	0.864497	0.031	0.087
6	2.250.5	0.0510	86.91	0.2810	105.909	2337.13	1.209111	0.031	0.080
7	2.524.3	0.0506	90.97	0.3163	120.034	2630.08	1.369598	0.031	0.080
8	2.953.7	0.0487	97.08	0.3971	151.371	3302.39	1.726652	0.031	0.077
9	3.310.3	0.0469	101.84	0.4615	179.546	3837.38	2.046069	0.031	0.077
10	3.631.2	0.0456	105.63	0.5272	209.444	4384.24	2.385056	0.031	0.076
11	3.979.8	0.0445	109.47	0.6449	270.952	5362.90	3.078541	0.031	0.074
12	4.354.6	0.0392	117.29	0.7213	306.381	5997.93	3.480945	0.031	0.074
13	4.664.1	0.0393	119.18	0.7957	342.464	6616.97	3.890101	0.031	0.073
14	5.007.0	0.0378	122.91	0.8770	383.340	7293.29	4.352510	0.031	0.073
15	5.380.8	0.0377	124.94	0.9647	427.681	8022.28	4.856246	0.031	0.073
16	5.692.9	0.0375	126.65	1.0388	465.965	8638.64	5.291541	0.031	0.074
17	5.930.5	0.0373	127.98	1.0935	496.640	9093.22	5.640217	0.031	0.074

Appendix D: Single- and two-phase calculated data (continued).

Channel B: Helium gas tests.

Number of channels: 3

Channel Dimensions:

Depth ( $\mu\text{m}$ ): 211.140

Hyd. Diameter ( $\mu\text{m}$ ): 210.051

Width ( $\mu\text{m}$ ): 208.97

Channel Length (m): 0.0635

Data Point	Re	f	Velocity (m/s)	Q (Watts)	Heat Trans.	Heat Flux (W/m <sup>2</sup> )	Nu	Uncertainty	
					coeff. W/m <sup>2</sup> -K			U-f (%)	U-Nu (%)
1	31.2	1.9987	16.85	0.0033	1.149	27.33	0.0015622	0.031	0.625
2	79.3	0.7799	39.75	0.0360	13.232	299.74	0.0178406	0.031	0.153
3	121.7	0.5066	57.64	0.0936	36.918	778.19	0.0495003	0.031	0.100
4	172.6	0.3585	76.66	0.1342	54.630	1115.96	0.0730729	0.031	0.099
5	218.5	0.2838	92.39	0.1934	82.515	1607.99	0.1100241	0.031	0.092
6	258.8	0.2408	105.37	0.2537	111.804	2109.54	0.1487222	0.031	0.087
7	312.5	0.2016	121.16	0.3360	152.173	2793.88	0.2020723	0.031	0.084
8	362.5	0.1767	134.15	0.3827	170.479	3182.52	0.2264976	0.031	0.084
9	409.6	0.1593	145.18	0.3984	170.227	3313.23	0.2265631	0.031	0.086
10	458.5	0.1446	156.36	0.4639	201.180	3857.48	0.2676377	0.031	0.084
11	510.4	0.1319	167.44	0.5484	244.260	4560.55	0.3247277	0.031	0.082
12	556.9	0.1227	176.82	0.6306	286.242	5244.07	0.3802599	0.031	0.081
13	604.5	0.1148	186.19	0.7055	325.961	5866.39	0.4328321	0.031	0.080
14	649.7	0.1099	193.52	0.7705	361.113	6407.34	0.4794401	0.031	0.080
15	709.0	0.1026	203.38	0.8665	413.591	7205.32	0.5489410	0.031	0.080
16	755.4	0.0977	211.26	0.9368	455.488	7790.53	0.6044350	0.031	0.080
17	815.8	0.0920	220.54	1.0180	509.119	8465.36	0.6753118	0.031	0.081

Appendix D: Single- and two-phase calculated data (continued).

Channel B: Nitrogen gas tests. Number of channels: 3

Channel Dimensions:

Depth ( $\mu\text{m}$ ): 211.140 Hyd. Diameter ( $\mu\text{m}$ ): 210.051

Width ( $\mu\text{m}$ ): 208.97 Channel Length (m): 0.0635

Data Point	Heat Trans.								
	Re	f	Velocity	Q	coeff.	Heat Flux	Nu	Uncertainty	
			(m/s)	(Watts)	W/m <sup>2</sup> -K	(W/m <sup>2</sup> )		U-f (%)	U-Nu (%)
1	160.5	0.3662	11.96	0.01258	4.504	104.62	0.03503	0.031	0.161
2	404.9	0.1488	28.65	0.0493	17.652	410.29	0.137	0.031	0.110
3	676.0	0.0935	45.15	0.1042	37.722	866.67	0.292	0.031	0.092
4	910.7	0.0752	57.68	0.1694	63.308	1408.56	0.488	0.031	0.082
5	1,173.1	0.0615	70.35	0.2330	87.502	1937.33	0.675	0.031	0.079
6	1,414.6	0.0535	81.11	0.3278	129.840	2725.75	0.999	0.031	0.074
7	1,647.6	0.0489	90.06	0.3989	159.972	3317.35	1.230	0.031	0.073
8	1,874.4	0.0484	96.24	0.4444	178.696	3695.42	1.374	0.031	0.074
9	2,139.9	0.0483	102.27	0.5113	207.960	4252.22	1.600	0.031	0.074
10	2,359.9	0.0489	106.15	0.5830	241.269	4848.20	1.855	0.031	0.074
11	2,592.0	0.0488	110.06	0.6614	275.103	5499.96	2.116	0.031	0.073
12	2,846.2	0.0402	120.99	0.7268	305.258	6044.32	2.349	0.031	0.073
13	3,049.6	0.0401	123.96	0.7875	334.974	6548.45	2.578	0.031	0.073
14	3,323.8	0.0395	128.32	0.8694	375.705	7230.10	2.892	0.031	0.074
15	3,533.1	0.0394	130.94	0.9363	408.970	7785.83	3.149	0.031	0.074
16	3,761.7	0.0394	133.37	1.0115	446.545	8411.75	3.439	0.031	0.074
17	4,055.6	0.0394	136.10	1.1063	496.146	9199.65	3.823	0.031	0.074



# Appendix D: Single- and two-phase calculated data (continued).

Channel B: Water tests.

Number of channels:

3

Channel Dimensions:

Depth ( $\mu\text{m}$ ): 211.140Hyd. Diameter ( $\mu\text{m}$ ): 210.051Width ( $\mu\text{m}$ ): 208.97

Channel Length (m): 0.0635

Data Point	Re	f	Velocity	Q	h - overall	Heat Flux	Nu	Uncertainty	
								U-f	U Nu
			(m/s)	(Watts)	W/m <sup>2</sup> -K	(W/m <sup>2</sup> )		(%)	(%)
1	345.07	0.8484	1.28	12.186	6360.797	101335	2.129	0.031	0.148
2	485.95	0.4370	1.84	14.394	9096.572	119696	3.050	0.031	0.178
3	637.37	0.2506	2.52	14.942	11030.43	124255	3.716	0.031	0.225
4	882.72	0.1395	3.48	19.060	13276.27	158497	4.472	0.031	0.234
5	1.131.56	0.0914	4.44	23.331	14994.44	194012	5.048	0.031	0.237
6	1.388.62	0.0656	5.41	29.418	18079.26	244632	6.081	0.031	0.228
7	1.597.12	0.0549	6.11	34.530	20832.44	287144	6.993	0.031	0.221
8	1.676.50	0.0537	6.34	38.646	23754.35	321370	7.964	0.031	0.209
9	1.861.79	0.0479	6.89	42.566	27317.14	353971	9.137	0.031	0.210
10	1.991.82	0.0450	7.30	48.239	30081.47	401146	10.050	0.031	0.198
11	2.068.42	0.0437	7.59	46.785	30860.81	389055	10.312	0.031	0.212
12	2.239.66	0.0400	8.17	54.618	34068.53	454192	11.376	0.031	0.197
13	2.308.60	0.0387	8.45	54.417	34749.22	452520	11.608	0.031	0.203
14	2.433.41	0.0360	8.94	53.436	35709.09	444365	11.933	0.031	0.217
15	2.532.57	0.0343	9.35	54.109	36802.77	449957	12.306	0.031	0.223
16	2.583.10	0.0345	9.47	59.227	37403.22	492521	12.496	0.031	0.207
17	2.750.13	0.0316	10.13	60.312	39082.49	501544	13.065	0.031	0.216
18	2.778.45	0.0314	10.26	59.793	39104.31	497230	13.075	0.031	0.220
19	3.134.97	0.0281	11.30	64.865	39626.15	539402	13.214	0.031	0.218
20	3.348.11	0.0261	12.14	67.385	43498.36	560358	14.515	0.031	0.227
21	3.472.80	0.0254	12.66	66.481	44264.47	552842	14.779	0.031	0.239
22	3.633.99	0.0242	13.29	66.742	45600.65	555015	15.231	0.031	0.248
23	3.784.38	0.0233	13.86	64.607	45832.62	537259	15.311	0.031	0.265
24	4.014.68	0.0222	14.80	64.345	48072.2	535079	16.070	0.031	0.283
25	4.220.39	0.0213	15.62	64.294	50157.4	534659	16.774	0.031	0.298
26	4.413.17	0.0204	16.38	66.000	53329.03	548845	17.840	0.031	0.306
27	4.761.85	0.0187	17.75	66.366	56722.1	551888	18.985	0.031	0.328
28	5.000.88	0.0176	18.71	66.567	59219.85	553558	19.828	0.031	0.344
29	5.201.20	0.0171	19.50	62.378	58978.7	518719	19.752	0.031	0.379
30	5.517.87	0.0161	20.79	62.372	61343.81	518676	20.555	0.031	0.403
31	5.930.67	0.0144	22.44	63.536	64313.03	528350	21.560	0.031	0.425
32	6.066.64	0.0140	23.32	79.414	76942.38	660391	25.838	0.031	0.363
33	6.693.65	0.0124	25.91	80.591	82255.85	670179	27.643	0.031	0.394
34	6.555.81	0.0124	25.41	61.541	53642.82	511763	18.030	0.031	0.337
35	7.181.26	0.0118	27.90	62.617	56712.47	520710	19.066	0.031	0.361
36	7.852.99	0.0111	30.56	64.856	60340.83	539326	20.290	0.031	0.380
37	8.336.22	0.0108	32.49	66.378	62592.93	551986	21.050	0.031	0.393
38	8.770.81	0.0107	34.26	67.700	65125.45	562983	21.906	0.031	0.406
39	9.305.06	0.0104	36.42	69.715	68204.63	579733	22.946	0.031	0.418

Appendix D: Single- and two-phase calculated data (continued).

Channel B: Water-argon tests.

Number of channels: 3

Channel Dimensions:

Depth ( $\mu\text{m}$ ): 211.140 Hyd. Diameter ( $\mu\text{m}$ ): 210.051

Width ( $\mu\text{m}$ ): 208.97 Channel Length (m): 0.0635

Data Point	G	x	f	Two-phase	Q	h - overall	Heat Flux	Nu	Uncertainty	
	kg/s-m <sup>2</sup>	Quality		Re-avg	(Watts)	W/m <sup>2</sup> -K	(W/m <sup>2</sup> )		U f (%)	U Nu (%)
1	1119.036	0.026055	0.1881	444.94	13.767	7067.0	114487	2.333	0.031	0.079
2	1159.937	0.147082	0.2004	477.44	16.084	9045.4	133751	2.979	0.031	0.081
3	1296.409	0.236895	0.2002	534.66	17.783	11009.2	147883	3.628	0.031	0.087
4	1439.653	0.312862	0.1999	595.12	19.534	12318.3	162442	4.062	0.031	0.088
5	1576.583	0.372584	0.1995	653.25	20.824	13279.3	173165	4.380	0.031	0.090
6	1774.711	0.410118	0.1977	701.46	20.249	15479.9	168389	5.134	0.031	0.106
7	4306.38	0.006831	0.0543	1,509.76	28.333	18166.2	235613	6.076	0.031	0.116
8	4301.51	0.039199	0.0547	1,551.60	31.989	28079.1	266011	9.366	0.031	0.131
9	4585.722	0.066148	0.0534	1,635.35	29.874	30491.0	248422	10.186	0.031	0.151
10	4492.317	0.100768	0.0565	1,604.12	29.375	30782.6	244276	10.285	0.031	0.153
11	4386.938	0.135326	0.0602	1,567.96	30.202	30909.8	251151	10.330	0.031	0.148
12	4630.725	0.156665	0.0590	1,639.45	29.702	32582.1	246992	10.903	0.031	0.159
13	7914.442	0.003503	0.0293	2,793.20	45.398	36273.5	377523	12.123	0.031	0.138
14	7661.691	0.021702	0.0302	2,755.53	48.453	41668.9	402922	13.901	0.031	0.137
15	7525.456	0.040567	0.0316	2,691.56	47.614	42258.7	395948	14.108	0.031	0.140
16	7797.694	0.057872	0.0311	2,778.87	48.232	44944.5	401086	15.013	0.031	0.145
17	7706.493	0.076753	0.0322	2,744.62	47.999	46703.4	399152	15.604	0.031	0.148
18	7363.327	0.100529	0.0345	2,625.19	47.389	46683.7	394075	15.600	0.031	0.148
19	13066.54	0.002237	0.0408	4,596.96	65.751	51015.5	546769	17.054	0.031	0.146
20	12170.27	0.013526	0.0415	4,340.07	69.465	55057.2	577659	18.381	0.031	0.138
21	11566.02	0.026938	0.0421	4,142.69	71.391	57025.3	593674	19.032	0.031	0.133
22	11327.35	0.040092	0.0425	4,053.72	69.548	57980.8	578343	19.355	0.031	0.136
23	11294.71	0.05425	0.0437	3,698.98	52.517	63892.5	436722	21.533	0.031	0.190
24	16176.9	0.002208	0.0396	5,181.88	48.575	65459.5	403939	22.101	0.031	0.246
25	16195.23	0.010464	0.0396	5,202.39	48.184	68089.7	400689	22.984	0.031	0.253
26	10698.79	0.002722	0.0436	3,522.45	58.637	52174.7	487614	17.565	0.031	0.149
27	10050.67	0.011714	0.0442	3,356.62	58.863	52340.6	489493	17.596	0.031	0.144
28	9951.487	0.020386	0.0442	3,395.53	59.327	52509.5	493354	17.614	0.031	0.143
29	14219.87	0.027385	0.0402	5,007.53	102.978	56964.4	856347	19.046	0.031	0.103
30	12661.34	0.013561	0.0416	4,311.50	59.073	46350.4	491239	15.550	0.031	0.153
31	12793.79	0.017224	0.0415	4,357.86	60.138	47474.2	500094	15.927	0.031	0.153
32	12521.8	0.023576	0.0418	4,277.61	61.288	48056.7	509661	16.118	0.031	0.149
33	12329.61	0.029245	0.0420	4,217.64	62.200	48732.5	517240	16.343	0.031	0.146
34	12052.65	0.040635	0.0423	4,135.38	63.522	49290.3	528234	16.527	0.031	0.142
35	12092.46	0.041628	0.0422	4,177.76	63.362	49796.7	526902	16.684	0.031	0.143

Appendix D: Single- and two-phase calculated data (continued).

Channel B: Water-helium tests.

Number of channels: 3

Channel Dimensions:

Depth ( $\mu\text{m}$ ): 211.140 Hyd. Diameter ( $\mu\text{m}$ ): 210.051

Width ( $\mu\text{m}$ ): 208.97 Channel Length (m): 0.0635

Data Point	G	x	f	Two-phase	Q	h - overall	Heat Flux	Nu	Uncertainty	
									U f	U Nu
	kg/s-m <sup>2</sup>	Quality		Re-avg	(Watts)	W/m <sup>2</sup> -K	(W/m <sup>2</sup> )		(%)	(%)
1	1925.433	0.001616	0.1220	668.94	17.025	10872.1	141573	3.640	0.031	0.101
2	1445.991	0.014185	0.1610	513.64	14.243	9578.9	118441	3.199	0.031	0.101
3	1584.227	0.027938	0.1479	566.83	16.344	11518.6	135914	3.845	0.031	0.102
4	1424.962	0.052327	0.1688	509.63	14.500	10424.6	120580	3.480	0.031	0.104
5	4089.663	0.000726	0.0619	1,317.19	23.857	15700.3	198389	5.298	0.031	0.125
6	3495.863	0.005978	0.0706	1,161.60	24.695	17342.5	205358	5.833	0.031	0.117
7	2871.775	0.015743	0.0845	979.60	23.592	17619.1	196190	5.910	0.031	0.114
8	1966.268	0.036654	0.1217	695.25	18.836	13683.2	156639	4.573	0.031	0.107
9	6228.61	0.000453	0.0405	2,011.02	33.443	23056.3	278107	7.779	0.031	0.134
10	5193.128	0.003972	0.0472	1,732.72	34.658	25632.8	288212	8.618	0.031	0.123
11	4114.761	0.010955	0.0579	1,423.19	34.208	24484.5	284463	8.201	0.031	0.111
12	2720.373	0.026821	0.0849	986.17	28.797	18530.4	239474	6.176	0.031	0.096
13	7637.554	0.000383	0.0329	2,479.00	38.434	31333.5	319605	10.565	0.031	0.149
14	6864.585	0.00294	0.0360	2,269.63	39.248	32010.0	326379	10.772	0.031	0.139
15	5938.165	0.007488	0.0411	1,999.71	38.721	30864.4	321993	10.366	0.031	0.130
16	13161.86	0.000907	0.0420	4,100.71	60.056	44617.5	499416	15.109	0.031	0.152
17	12820.03	0.002373	0.0421	4,042.58	60.649	45038.1	504345	15.231	0.031	0.149
18	12636.8	0.003469	0.0422	4,018.78	61.229	45405.7	509165	15.342	0.031	0.146
19	12506.09	0.004765	0.0423	3,998.08	61.647	45980.2	512641	15.527	0.031	0.145
20	12252.61	0.006004	0.0425	3,930.02	60.746	45295.5	505150	15.291	0.031	0.145
21	15970.44	0.000913	0.0398	5,075.27	67.673	50760.3	562755	17.151	0.031	0.160
22	16488.13	0.001836	0.0394	5,253.31	69.225	52962.4	575657	17.890	0.031	0.162
23	16458.79	0.002765	0.0395	5,256.12	70.612	53698.9	587198	18.135	0.031	0.160
24	15869.9	0.003733	0.0398	5,083.90	69.787	52782.1	580332	17.819	0.031	0.157
25	15566.99	0.004725	0.0400	4,989.15	70.168	52830.2	583503	17.834	0.031	0.154
26	19028.62	0.000708	0.0381	6,025.35	71.399	56929.5	593739	19.242	0.031	0.177
27	19177.27	0.001689	0.0380	6,086.84	73.309	58465.7	609624	19.756	0.031	0.175
28	18750.7	0.002425	0.0382	5,958.07	72.386	57796.7	601950	19.528	0.031	0.174
29	18449.6	0.003327	0.0384	5,864.52	72.496	57464.1	602862	19.415	0.031	0.171
30	18670.39	0.003893	0.0383	5,927.24	73.133	58151.4	608159	19.649	0.031	0.172

# Appendix D: Single- and two-phase calculated data (continued).

Channel B: Water-Nitrogen tests. Number of channels: 3

Channel Dimensions:

Depth ( $\mu\text{m}$ ): 211.140 Hyd. Diameter ( $\mu\text{m}$ ): 210.051

Width ( $\mu\text{m}$ ): 208.97 Channel Length (m): 0.0635

Data Point	G	x	f	Two-phase	Q	h - overall	Heat Flux	Nu	Uncertainty	
									U <sub>f</sub>	U <sub>Nu</sub>
	kg/s-m <sup>2</sup>	Quality,		Re-avg	(Watts)	W/m <sup>2</sup> -K	(W/m <sup>2</sup> )		(%)	(%)
1	2853.194	0.005711	0.0856	962.78	20.123	14211.4	168139	4.763	0.031	0.116
2	2431.893	0.051424	0.1023	883.91	19.797	15456.8	165415	5.402	0.031	0.115
3	2367.315	0.099361	0.1087	921.14	20.071	16505.3	167707	6.050	0.031	0.117
4	1954.428	0.151837	0.1389	811.14	16.446	13456.6	137414	5.219	0.031	0.115
5	2241.605	0.164679	0.1232	942.30	18.410	15268.4	153829	6.009	0.031	0.117
6	5861.516	0.002646	0.0443	1,849.45	25.585	21191.6	213773	7.130	0.031	0.161
7	4753.687	0.026787	0.0532	1,617.12	30.229	27128.6	252579	9.292	0.031	0.138
8	4191.489	0.056571	0.0609	1,501.35	29.924	25817.7	250026	9.089	0.031	0.128
9	3799.817	0.078729	0.0679	1,411.02	29.187	23323.2	243875	8.388	0.031	0.118
10	3413.208	0.109726	0.0771	1,328.33	27.847	21338.6	232675	7.917	0.031	0.112
11	8015.253	0.001973	0.0319	2,562.27	37.293	31555.3	311599	10.594	0.031	0.156
12	7168.526	0.018019	0.0352	2,402.90	41.909	35957.5	350170	12.219	0.031	0.139
13	5623.413	0.043522	0.0451	1,972.15	37.863	30660.1	316365	10.662	0.031	0.126
14	4992.725	0.060721	0.0511	1,802.81	35.569	27870.1	297195	9.849	0.031	0.121
15	9327.963	0.00165	0.0454	2,990.44	41.194	35142.9	344197	11.790	0.031	0.162
16	7827.603	0.016263	0.0323	2,609.36	43.425	36078.4	362835	12.244	0.031	0.141
17	6393.225	0.038788	0.0396	2,225.19	41.744	32191.6	348793	11.145	0.031	0.125
18	17102.02	0.004605	0.0387	5,721.42	72.231	56127.3	603525	18.801	0.031	0.160
19	16840.63	0.009309	0.0389	5,673.28	73.178	56967.9	611436	19.164	0.031	0.157
20	17107.14	0.013422	0.0388	5,778.79	74.268	57946.1	620543	19.573	0.031	0.157
21	16888.56	0.018246	0.0389	5,726.90	73.273	57639.6	612236	19.562	0.031	0.157
22	12775.58	0.004641	0.0415	4,324.66	54.833	44127.6	458156	14.765	0.031	0.161
23	12819.26	0.013709	0.0415	4,403.96	57.676	46124.8	481914	15.559	0.031	0.155
24	12753.15	0.01774	0.0416	4,406.07	58.810	47056.3	491384	15.932	0.031	0.153
25	12678.43	0.02364	0.0417	4,411.94	60.561	48635.7	506018	16.559	0.031	0.149
26	12103.35	0.031425	0.0422	4,250.12	59.909	47466.9	500567	16.283	0.031	0.145

Appendix D: Single- and two-phase calculated data (continued).

Channel C1: Argon gas tests.                      Number of channels:                      5  
 Channel Dimensions:  
 Depth ( $\mu\text{m}$ ):                      134.640                      Hyd. Diameter ( $\mu\text{m}$ ):                      127.92  
 Width ( $\mu\text{m}$ ):                      121.83                      Channel Length (m):                      0.0635

Data Point	Re	f	Velocity (m/s)	Q (Watts)	Heat Trans.	Heat Flux (W/m <sup>2</sup> )	Nu	Uncertainty	
					coeff. W/m <sup>2</sup> -K			U-f	U-Nu
1	53.4	1.1009	5.48	0.0002	0.273	1.93	0.001927	0.031	1.722
2	246.6	0.2478	21.26	0.0044	3.566	35.23	0.025198	0.031	0.449
3	631.6	0.1006	44.00	0.0286	14.928	230.43	0.105073	0.031	0.186
4	1.000.2	0.0680	59.98	0.0681	32.504	548.58	0.227941	0.031	0.132
5	1.390.3	0.0576	71.06	0.1354	67.096	1090.06	0.468532	0.031	0.105
6	1.740.3	0.0505	79.44	0.1901	95.079	1530.48	0.662900	0.031	0.099
7	2.076.5	0.0507	82.76	0.2297	112.734	1849.67	0.785977	0.031	0.099
8	2.378.2	0.0509	84.97	0.2531	120.080	2038.42	0.837660	0.031	0.101
9	2.687.0	0.0495	87.94	0.2961	138.557	2384.62	0.966646	0.031	0.100
10	2.989.2	0.0480	90.78	0.3536	166.361	2847.23	1.159983	0.031	0.097
11	3.235.7	0.0466	93.15	0.4053	192.530	3263.68	1.341784	0.031	0.095
12	3.515.7	0.0452	95.75	0.5273	269.391	4246.39	1.872281	0.031	0.091
13	3.738.8	0.0443	97.57	0.6060	321.515	4880.32	2.231997	0.031	0.090
14	3.959.6	0.0438	98.97	0.6706	365.836	5400.14	2.538045	0.031	0.091
15	4.172.5	0.0421	101.42	0.7322	403.897	5896.45	2.801572	0.031	0.091
16	4.365.0	0.0418	102.52	0.8007	449.148	6447.90	3.114988	0.031	0.091
17	4.531.2	0.0416	103.19	0.8621	490.450	6942.47	3.401878	0.031	0.092
18	4.698.6	0.0415	103.85	0.9281	538.762	7473.93	3.737730	0.031	0.093

Appendix D: Single- and two-phase calculated data (continued).

Channel C1: Helium gas tests. Number of channels: 5

Channel Dimensions:

Depth ( $\mu\text{m}$ ): 134.640 Hyd. Diameter ( $\mu\text{m}$ ): 127.92

Width ( $\mu\text{m}$ ): 121.83 Channel Length (m): 0.0635

Data Point	Re	f	Velocity (m/s)	Q (Watts)	Heat Trans.	Heat Flux (W/m <sup>2</sup> )	Nu	Uncertainty	
					coeff. W/m <sup>2</sup> -K			U-f (%)	U-Nu (%)
1	7.7	8.5782	6.65						
2	31.3	2.2071	22.68	0.0015	0.719	12.08	0.0005979	0.031	1.370
3	79.6	0.9175	45.34	0.0110	9.647	88.84	0.0080457	0.031	0.474
4	127.1	0.5950	62.59	0.0496	28.055	399.36	0.0232386	0.031	0.178
5	180.9	0.4048	80.23	0.0836	41.360	673.30	0.0341347	0.031	0.150
6	227.7	0.3236	93.11	0.1111	53.807	894.59	0.0442757	0.031	0.142
7	280.9	0.2655	105.93	0.1498	70.227	1205.99	0.0576794	0.031	0.131
8	332.0	0.2243	117.73	0.1904	90.235	1532.99	0.0739434	0.031	0.123
9	385.8	0.1953	128.59	0.2337	111.429	1882.19	0.0911686	0.031	0.118
10	437.1	0.1733	138.47	0.2860	137.413	2303.03	0.1122417	0.031	0.111
11	487.9	0.1565	147.48	0.3446	167.269	2774.95	0.1364453	0.031	0.106
12	543.4	0.1426	156.11	0.3867	208.373	3114.43	0.1700141	0.031	0.109
13	599.3	0.1310	164.39	0.4380	244.412	3527.45	0.1994393	0.031	0.108
14	658.8	0.1204	172.90	0.5010	283.835	4034.43	0.2316009	0.031	0.106
15	707.5	0.1148	178.48	0.5624	326.201	4528.91	0.2661107	0.031	0.105
16	770.9	0.1072	186.02	0.6251	365.869	5034.05	0.2985233	0.031	0.104
17	825.2	0.1011	192.61	0.6771	396.265	5452.42	0.3233312	0.031	0.103
18	883.5	0.0957	199.11	0.7385	434.934	5947.37	0.3549218	0.031	0.102

Appendix D: Single- and two-phase calculated data (continued).

Channel C1: Nitrogen gas tests.      Number of channels:      5  
 Channel Dimensions:  
 Depth ( $\mu\text{m}$ ):      134.640      Hyd. Diameter ( $\mu\text{m}$ ):      127.92  
 Width ( $\mu\text{m}$ ):      121.83      Channel Length (m):      0.0635

Data Point					Heat Trans.					Uncertainty	
	Re	f	Velocity	Q	coeff.	Heat Flux	Nu	U-f	U-Nu		
			(m/s)	(Watts)	W/m <sup>2</sup> -K	(W/m <sup>2</sup> )		(%)	(%)		
1	37.5	1.7984	4.37	0.00018	0.169	1.45	0.00082	0.031	2.523		
2	172.8	0.3747	17.80	0.0048	3.819	38.27	0.018	0.031	0.453		
3	407.4	0.1602	36.05	0.0180	14.119	145.16	0.068	0.031	0.293		
4	647.1	0.1069	50.69	0.0502	25.879	404.23	0.125	0.031	0.172		
5	897.6	0.0845	62.70	0.1052	50.181	847.46	0.241	0.031	0.123		
6	1,140.9	0.0691	73.21	0.1641	78.100	1321.21	0.374	0.031	0.107		
7	1,357.5	0.0603	81.39	0.2289	111.389	1843.49	0.531	0.031	0.098		
8	1,597.4	0.0541	88.91	0.2941	144.717	2368.55	0.690	0.031	0.094		
9	1,807.1	0.0519	93.50	0.3479	170.778	2801.52	0.813	0.031	0.093		
10	2,013.0	0.0526	95.35	0.3414	156.800	2749.15	0.748	0.031	0.098		
11	2,215.4	0.0528	97.47	0.4157	196.209	3347.37	0.935	0.031	0.094		
12	2,420.9	0.0523	99.94	0.5321	266.603	4285.28	1.267	0.031	0.089		
13	2,604.2	0.0514	102.04	0.5687	278.781	4579.42	1.326	0.031	0.089		
14	2,793.0	0.0503	104.44	0.6706	342.857	5400.21	1.628	0.031	0.088		
15	2,978.1	0.0487	107.12	0.7418	388.335	5973.90	1.843	0.031	0.088		
16	3,150.3	0.0481	108.83	0.8140	428.703	6554.81	2.034	0.031	0.088		
17	3,319.6	0.0477	110.14	0.8776	469.790	7067.07	2.229	0.031	0.088		
18	3,484.3	0.0472	111.48	0.9520	515.596	7666.50	2.446	0.031	0.088		

Appendix D: Single- and two-phase calculated data (continued).

Channel C1: Water tests.                      Number of channels:                      5  
 Channel Dimensions:  
 Depth ( $\mu\text{m}$ ):                      134.640                      Hyd. Diameter ( $\mu\text{m}$ ):                      127.92  
 Width ( $\mu\text{m}$ ):                      121.83                      Channel Length (m):                      0.0635

Data Point	Re	f	Velocity	Q	h - overall	Heat Flux	Nu	Uncertainty	
								U-f	U_Nu
			(m/s)	(Watts)	W/m <sup>2</sup> -K	(W/m <sup>2</sup> )		(%)	(%)
1	302.26	0.3442	1.77	10.153	7567.223	81765	1.535	0.031	0.111
2	353.68	0.2586	2.12	10.929	9472.409	88013	1.926	0.031	0.128
3	523.85	0.1273	3.23	13.720	14597.34	110489	2.978	0.031	0.156
4	613.52	0.1064	3.72	17.487	15206.55	140822	3.097	0.031	0.131
5	804.55	0.0699	4.79	25.492	17949.92	205283	3.647	0.031	0.110
6	896.27	0.0598	5.38	27.287	19510.71	219742	3.969	0.031	0.113
7	978.30	0.0533	5.93	27.664	20658.77	222775	4.206	0.031	0.119
8	1,074.41	0.0468	6.55	28.382	22089.32	228559	4.501	0.031	0.126
9	1,259.71	0.0380	7.51	37.443	24537.53	301525	4.987	0.031	0.108
10	1,290.56	0.0390	7.72	36.699	24727.53	295535	5.028	0.031	0.112
11	1,364.59	0.0364	8.20	36.357	25025.44	292782	5.091	0.031	0.116
12	1,522.45	0.0323	8.92	46.580	28809	375111	5.844	0.031	0.102
13	1,605.43	0.0306	9.43	48.788	30544.46	392886	6.197	0.031	0.103
14	1,656.56	0.0304	9.75	48.762	31332.94	392677	6.359	0.031	0.106
15	1,711.65	0.0294	10.10	49.201	32227.02	396214	6.542	0.031	0.109
16	1,708.89	0.0295	10.09	49.130	32177.99	395644	6.532	0.031	0.109
17	1,754.68	0.0307	10.40	48.460	34008.4	390244	6.907	0.031	0.115
18	1,844.43	0.0286	10.95	49.490	35839.51	398546	7.280	0.031	0.119
19	1,387.56	0.0358	8.83	35.112	21738.79	282753	4.450	0.031	0.116
20	1,660.17	0.0310	10.61	38.372	29312.42	309008	6.003	0.031	0.135
21	1,794.17	0.0316	11.46	39.526	35230.72	318302	7.214	0.031	0.149
22	1,948.20	0.0316	12.45	40.551	40157.43	326555	8.224	0.031	0.162
23	2,079.52	0.0318	13.27	42.144	46524.47	339383	9.525	0.031	0.175
24	2,268.77	0.0300	14.51	43.278	49932.66	348521	10.225	0.031	0.184
25	2,435.56	0.0289	15.60	44.228	52647.56	356165	10.783	0.031	0.191
26	2,751.78	0.0269	17.70	46.258	57814.36	372513	11.846	0.031	0.203



Appendix D: Single- and two-phase calculated data (continued).

Channel C1: Water-argon tests.

Number of channels: 5

Channel Dimensions:

Depth ( $\mu\text{m}$ ): 134.640

Hyd. Diameter ( $\mu\text{m}$ ): 127.92

Width ( $\mu\text{m}$ ): 121.83

Channel Length (m): 0.0635

Data Point	G	x	f	Two-phase	Q	h - overall	Heat Flux	Nu	Uncertainty	
	kg/s-m <sup>2</sup>	Quality		Re-avg	(Watts)	W/m <sup>2</sup> -K	(W/m <sup>2</sup> )		U f	U Nu
									(%)	(%)
1	3.300	0.015222	0.1173	707.57	14.754	13943.4	118817	2.840	0.031	0.142
2	3.224	0.047053	0.1218	704.34	15.994	13690.1	128797	2.783	0.031	0.128
3	2.813	0.085278	0.1427	626.47	15.261	11803.5	122901	2.396	0.031	0.117
4	2.537	0.130342	0.1664	565.12	13.598	10501.0	109507	2.132	0.031	0.117
5	2.067	0.252469	0.2282	480.08	12.828	8537.8	103305	1.728	0.031	0.101
6	5.164	0.01009	0.0760	1,085.91	20.036	18806.5	161347	3.838	0.031	0.148
7	4.775	0.028589	0.0827	1,016.78	20.094	17964.9	161821	3.662	0.031	0.139
8	4.659	0.050585	0.0856	1,005.22	21.705	17867.7	174789	3.638	0.031	0.128
9	4.144	0.080309	0.0979	907.90	21.000	16328.6	169113	3.320	0.031	0.120
10	5.771	0.008604	0.0661	1,247.42	27.698	21093.6	223055	4.292	0.031	0.120
11	5.360	0.021277	0.0710	1,175.15	27.597	20426.7	222235	4.150	0.031	0.115
12	5.065	0.03847	0.0753	1,129.03	27.362	19490.2	220344	3.954	0.031	0.111
13	4.758	0.055227	0.0803	1,076.92	27.861	18847.4	224368	3.818	0.031	0.104
14	4.410	0.075967	0.0873	1,013.46	27.794	17838.6	223822	3.608	0.031	0.099
15	2.765	0.172805	0.1721	574.63	10.403	11121.9	83775	2.276	0.031	0.162
16	2.523	0.239492	0.2052	524.59	9.528	9984.3	76726	2.045	0.031	0.160
17	2.994	0.243694	0.1748	619.35	11.080	11685.4	89230	2.395	0.031	0.162
18	3.233	0.260412	0.1682	658.13	11.110	12714.6	89466	2.610	0.031	0.175
19	3.506	0.272107	0.1594	706.10	11.392	13502.7	91740	2.776	0.031	0.182
20	3.578	0.299363	0.1626	719.21	11.548	13662.3	92994	2.810	0.031	0.182
21	3.275	0.37127	0.1979	658.86	10.670	12428.2	85928	2.558	0.031	0.180
22	13.427	0.003895	0.0311	2,638.05	34.156	40705.8	275054	8.365	0.031	0.201
23	12.944	0.015069	0.0323	2,569.79	34.826	40997.9	280451	8.416	0.031	0.195
24	13.241	0.025609	0.0318	2,638.45	35.483	41868.2	285741	8.592	0.031	0.196
25	13.252	0.036678	0.0319	2,655.55	37.049	43208.9	298354	8.863	0.031	0.191
26	13.183	0.05564	0.0327	2,650.39	37.203	42801.7	299599	8.778	0.031	0.189
27	12.746	0.070491	0.0341	2,577.73	37.958	42439.2	305678	8.699	0.031	0.182
28	12.055	0.085515	0.0365	2,451.28	37.725	41036.9	303799	8.408	0.031	0.175
29	10.730	0.116418	0.0420	2,201.32	36.475	37688.4	293736	7.717	0.031	0.165

Appendix D: Single- and two-phase calculated data (continued).

Channel C1: Water-helium tests. Number of channels: 5

Channel Dimensions:

Depth ( $\mu\text{m}$ ): 134.640 Hyd. Diameter ( $\mu\text{m}$ ): 127.92

Width ( $\mu\text{m}$ ): 121.83 Channel Length (m): 0.0635

Data Point	G	x	f	Two-phase	Q	h - overall	Heat Flux	Nu	Uncertainty	
	kg/s-m <sup>2</sup>	Quality		Re-avg	(Watts)	W/m <sup>2</sup> -K	(W/m <sup>2</sup> )		U f (%)	U Nu (%)
1	1.676	0.003086	0.2204	371.86	10.251	8001.3	82553	1.623	0.031	0.114
2	1.670	0.008804	0.2148	383.78	10.553	7865.5	84982	1.590	0.031	0.109
3	1.798	0.012926	0.2005	412.76	11.387	8418.6	91702	1.702	0.031	0.109
4	1.822	0.026202	0.2001	419.29	11.515	8016.7	92727	1.621	0.031	0.104
5	1.846	0.038525	0.2001	424.69	11.546	7715.7	92981	1.560	0.031	0.102
6	3.483	0.001433	0.1070	764.86	18.733	15710.4	150853	3.191	0.031	0.124
7	3.701	0.003978	0.1018	805.93	18.977	15881.1	152825	3.229	0.031	0.125
8	3.161	0.007552	0.1186	693.82	16.437	13321.2	132363	2.706	0.031	0.122
9	2.920	0.016516	0.1294	641.84	15.556	11911.1	125273	2.419	0.031	0.117
10	2.569	0.027806	0.1473	570.64	14.305	10274.2	115197	2.085	0.031	0.110
11	4.931	0.00103	0.0780	1048.55	22.680	18757.3	182639	3.823	0.031	0.129
12	4.634	0.003284	0.0821	997.96	22.321	18050.4	179754	3.674	0.031	0.125
13	4.433	0.005219	0.0853	962.58	22.118	17337.8	178119	3.526	0.031	0.121
14	3.994	0.012023	0.0941	878.93	21.243	15505.8	171068	3.149	0.031	0.113
15	3.161	0.022493	0.1182	707.45	17.807	12276.8	143400	2.489	0.031	0.107
16	6.182	0.000819	0.0623	1312.26	27.067	21307.6	217974	4.343	0.031	0.127
17	6.112	0.002445	0.0629	1302.90	26.844	21111.1	216177	4.301	0.031	0.127
18	6.145	0.003772	0.0628	1306.14	26.289	20749.9	211709	4.229	0.031	0.128
19	5.438	0.008741	0.0704	1170.82	25.178	19105.5	202761	3.889	0.031	0.122
20	4.793	0.014789	0.0792	1047.66	24.334	17313.3	195959	3.518	0.031	0.113
21	12.493	0.004144	0.0334	2454.66	43.945	42845.4	353889	8.805	0.031	0.157
22	12.099	0.005901	0.0343	2397.88	43.061	42963.8	346766	8.821	0.031	0.158
23	11.675	0.008698	0.0353	2334.40	42.941	44205.5	345803	9.068	0.031	0.160
24	11.565	0.009477	0.0355	2322.78	42.700	43654.4	343864	8.950	0.031	0.159
25	11.323	0.011125	0.0362	2283.84	42.474	43291.7	342045	8.872	0.031	0.158
26	14.189	0.0036	0.0287	2859.77	51.479	51609.6	414561	10.577	0.031	0.158
27	14.047	0.005257	0.0289	2841.06	51.044	51809.5	411054	10.614	0.031	0.159
28	13.647	0.00694	0.0297	2772.27	50.016	50518.0	402782	10.345	0.031	0.158
29	14.045	0.007632	0.0289	2853.02	51.331	52243.3	413369	10.698	0.031	0.159
30	13.477	0.008842	0.0301	2741.20	49.365	50117.9	397533	10.261	0.031	0.158
31	16.930	0.002857	0.0441	3384.05	53.640	59592.3	431960	12.223	0.031	0.177
32	2.569	0.008001	0.1555	529.78	8.930	10671.2	71916	2.182	0.031	0.179
33	2.461	0.014094	0.1626	509.66	9.047	10048.2	72859	2.054	0.031	0.168
34	2.370	0.022635	0.1705	490.24	8.842	9667.7	71208	1.976	0.031	0.165
35	2.421	0.028933	0.1685	499.50	9.122	9756.6	73457	1.995	0.031	0.162
36	2.199	0.042781	0.1912	446.57	7.684	8465.8	61877	1.734	0.031	0.170
37	2.105	0.050947	0.2019	426.46	7.338	8005.4	59096	1.641	0.031	0.169
38	2.234	0.058314	0.1923	451.30	7.737	8388.9	62303	1.720	0.031	0.168

Appendix D: Single- and two-phase calculated data (continued).

Channel C1: Water-Nitrogen tests. Number of channels: 5  
 Channel Dimensions:  
 Depth ( $\mu\text{m}$ ): 134.640 Hyd. Diameter ( $\mu\text{m}$ ): 127.92  
 Width ( $\mu\text{m}$ ): 121.83 Channel Length (m): 0.0635

Data Point	G	x	f	Two-phase	Q	h - overall	Heat Flux	Nu	Uncertainty	
	kg/s-m <sup>2</sup>	Quality		Re-avg	(Watts)	W/m <sup>2</sup> -K	(W/m <sup>2</sup> )		U <sub>f</sub>	U <sub>Nu</sub>
									(%)	(%)
1	3.602	0.006603	0.1075	769.92	14.741	14536.5	118706	2.982	0.031	0.150
2	3.191	0.023836	0.1216	704.30	14.136	13412.6	113840	2.793	0.031	0.142
3	2.868	0.042052	0.1368	649.80	12.889	11646.1	103793	2.467	0.031	0.136
4	3.150	0.05385	0.1252	727.75	14.690	12489.8	118295	2.676	0.031	0.129
5	2.719	0.083488	0.1488	651.62	13.048	10474.3	105075	2.312	0.031	0.122
6	2.808	0.102413	0.1456	693.99	13.914	10698.4	112052	2.406	0.031	0.117
7	5.176	0.004933	0.0758	1,088.49	21.021	19619.7	169282	4.024	0.031	0.145
8	4.907	0.013869	0.0795	1,055.71	20.696	18867.3	166662	3.898	0.031	0.140
9	4.472	0.026091	0.0876	982.37	19.512	16957.1	157134	3.542	0.031	0.134
10	4.137	0.040276	0.0951	931.86	18.294	15484.8	147319	3.276	0.031	0.131
11	4.115	0.055374	0.0961	950.35	19.083	15307.4	153674	3.285	0.031	0.124
12	3.942	0.073116	0.1013	936.00	19.279	14655.8	155256	3.199	0.031	0.117
13	6.714	0.004061	0.0580	1,419.59	26.734	22757.2	215290	4.661	0.031	0.138
14	6.325	0.0109	0.0614	1,359.48	26.557	22289.0	213862	4.590	0.031	0.134
15	5.943	0.01992	0.0652	1,303.96	26.115	21107.4	210307	4.380	0.031	0.128
16	5.360	0.031051	0.0719	1,209.33	25.760	19431.7	207448	4.069	0.031	0.119
17	5.018	0.045245	0.0770	1,162.34	25.387	18484.4	204445	3.921	0.031	0.114
18	2.598	0.09936	0.1776	565.58	8.322	8793.7	67014	1.997	0.031	0.166
19	2.600	0.118395	0.1817	576.43	8.018	8959.1	64570	2.077	0.031	0.173
20	2.439	0.146448	0.1991	560.69	7.580	8305.2	61040	1.985	0.031	0.169
21	2.394	0.173978	0.2083	571.54	7.523	8022.7	60585	1.977	0.031	0.164
22	2.443	0.19429	0.2080	600.70	7.787	8010.1	62709	2.019	0.031	0.159
23	2.774	0.19018	0.1809	683.83	9.030	9097.6	72717	2.281	0.031	0.156
24	2.932	0.207194	0.1757	733.65	9.088	9531.0	73185	2.439	0.031	0.162
25	12.920	0.001803	0.0323	2,536.11	34.670	38480.2	279196	7.923	0.031	0.189
26	12.721	0.00728	0.0327	2,531.71	34.987	39786.0	281750	8.228	0.031	0.189
27	12.548	0.014192	0.0333	2,523.42	34.577	39480.1	278446	8.216	0.031	0.189
28	12.822	0.019808	0.0327	2,600.11	34.997	40223.7	281833	8.413	0.031	0.190
29	13.199	0.027693	0.0320	2,698.72	35.529	41597.0	286112	8.767	0.031	0.193
230	13.041	0.035252	0.0325	2,694.11	35.523	41443.6	286063	8.797	0.031	0.191
31	13.091	0.040224	0.0325	2,717.32	35.523	41455.0	286064	8.843	0.031	0.191
32	13.222	0.04704	0.0324	2,761.49	35.746	41440.7	287859	8.900	0.031	0.190

Appendix D: Single- and two-phase calculated data (continued).

Channel C2: Argon gas tests. Number of channels: 3

Channel Dimensions:

Depth ( $\mu\text{m}$ ): 263.730 Hyd. Diameter ( $\mu\text{m}$ ): 207.01

Width ( $\mu\text{m}$ ): 190.37 Channel Length (m): 0.0635

Data Point					Heat Trans.		Nu	Uncertainty	
	Re	f	Velocity	Q	coeff.	Heat Flux		U-f	U-Nu
			(m/s)	(Watts)	W/m <sup>2</sup> -K	(W/m <sup>2</sup> )			
1	53.8	1.4968	3.51	0.0004	0.235	3.33	0.002683	0.031	0.957
2	284.0	0.3274	16.07	0.0096	5.459	72.37	0.062066	0.031	0.246
3	638.8	0.1505	30.83	0.0279	15.802	209.83	0.179611	0.031	0.198
4	1.006.4	0.1012	42.67	0.0684	41.949	514.47	0.475537	0.031	0.145
5	1.344.4	0.0866	50.07	0.1116	71.580	839.39	0.810644	0.031	0.131
6	1.745.8	0.0754	56.93	0.1619	105.988	1217.75	1.200066	0.031	0.125
7	2.085.6	0.0739	59.96	0.2059	136.091	1548.50	1.540876	0.031	0.123
8	2.427.3	0.0728	62.15	0.2575	174.170	1936.70	1.971372	0.031	0.121
9	2.735.8	0.0688	64.79	0.3208	229.653	2413.21	2.596582	0.031	0.121
10	3.069.2	0.0648	67.41	0.3790	281.691	2851.02	3.183585	0.031	0.123
11	3.373.1	0.0616	69.43	0.4291	324.999	3227.91	3.673283	0.031	0.123
12	3.657.3	0.0586	71.20	0.4715	365.051	3546.85	4.125885	0.031	0.125
13	3.936.6	0.0561	72.70	0.5152	405.323	3875.88	4.581664	0.031	0.127
14	4.232.5	0.0538	74.12	0.5639	455.135	4241.80	5.147022	0.031	0.129
15	4.469.1	0.0501	76.16	0.6049	493.993	4549.96	5.587245	0.031	0.130
16	4.717.4	0.0478	77.44	0.6537	544.094	4917.17	6.155084	0.031	0.131
17	4.961.1	0.0458	78.58	0.7050	598.279	5303.08	6.769494	0.031	0.133
18	5.176.8	0.0441	79.44	0.7527	652.223	5662.27	7.381554	0.031	0.135

Appendix D: Single- and two-phase calculated data (continued).

Channel C2: Helium gas tests.

Number of channels: 3

Channel Dimensions:

Depth ( $\mu\text{m}$ ): 263.730

Hyd. Diameter ( $\mu\text{m}$ ): 207.01

Width ( $\mu\text{m}$ ): 190.37

Channel Length (m): 0.0635

Data Point	Re	f	Velocity (m/s)	Q (Watts)	Heat Trans.		Nu	Uncertainty	
					coeff. W/m <sup>2</sup> -K	Heat Flux (W/m <sup>2</sup> )		U-f (%)	U-Nu (%)
1	5.6	14.0952	3.16	0.0004	0.352	3.05	0.0004753	0.031	0.948
2	30.7	3.0777	15.05	0.0017	1.147	13.03	0.0015476	0.031	1.189
3	77.3	1.2372	32.34	0.0279	20.048	210.19	0.0268562	0.031	0.208
4	123.9	0.7973	45.51	0.0489	33.162	367.81	0.0443897	0.031	0.190
5	166.5	0.5720	56.53	0.0766	50.230	576.04	0.0671842	0.031	0.167
6	218.1	0.4379	67.77	0.1272	88.634	957.11	0.1182625	0.031	0.146
7	266.6	0.3604	76.83	0.1571	108.513	1181.78	0.1447691	0.031	0.144
8	324.1	0.2999	85.89	0.1219	73.595	916.98	0.0985731	0.031	0.187
9	370.8	0.2626	92.90	0.1428	87.967	1074.40	0.1177945	0.031	0.183
10	417.3	0.2315	100.06	0.2567	185.835	1931.25	0.2476487	0.031	0.141
11	475.6	0.2023	108.01	0.3171	245.024	2385.48	0.3259174	0.031	0.140
12	526.7	0.1768	114.21	0.3341	277.058	2513.34	0.3718284	0.031	0.148
13	581.7	0.1599	120.47	0.3824	324.296	2876.20	0.4346357	0.031	0.147
14	634.3	0.1458	126.03	0.4035	337.260	3034.93	0.4520013	0.031	0.148
15	686.7	0.1345	130.89	0.4514	383.936	3395.24	0.5142531	0.031	0.147
16	738.3	0.1246	135.55	0.5027	436.072	3781.83	0.5837435	0.031	0.147
17	796.9	0.1142	141.00	0.5575	494.975	4193.43	0.6623978	0.031	0.147
18	853.2	0.1054	145.90	0.6114	554.161	4599.01	0.7414481	0.031	0.148

Appendix D: Single- and two-phase calculated data (continued).

Channel C2: Nitrogen gas tests. Number of channels: 3

Channel Dimensions:

Depth ( $\mu\text{m}$ ): 263.730 Hyd. Diameter ( $\mu\text{m}$ ): 207.01

Width ( $\mu\text{m}$ ): 190.37 Channel Length (m): 0.0635

Data Point					Heat Trans.		Nu	Uncertainty	
	Re	f	Velocity	Q	coeff.	Heat Flux		U-f	U-Nu
			(m/s)	(Watts)	W/m <sup>2</sup> -K	(W/m <sup>2</sup> )		(%)	(%)
1	44.5	1.3940	3.26	0.00028	0.164	2.09	0.00129	0.031	1.968
2	166.5	0.5681	11.30	0.0062	3.447	46.99	0.027	0.031	0.338
3	417.2	0.2353	24.95	0.0233	13.091	175.55	0.102	0.031	0.235
4	662.8	0.1532	35.92	0.0569	34.004	428.10	0.264	0.031	0.167
5	876.7	0.1238	43.56	0.0893	55.025	671.70	0.427	0.031	0.149
6	1,126.4	0.0986	51.69	0.1309	82.896	984.34	0.643	0.031	0.139
7	1,341.8	0.0854	57.63	0.1708	110.460	1284.94	0.857	0.031	0.133
8	1,612.8	0.0763	63.52	0.2213	144.945	1664.59	1.125	0.031	0.129
9	1,816.3	0.0721	66.90	0.2672	178.974	2010.31	1.388	0.031	0.126
10	2,030.3	0.0717	68.79	0.3090	207.284	2324.78	1.609	0.031	0.125
11	2,255.6	0.0723	70.03	0.3627	247.416	2728.51	1.921	0.031	0.123
12	2,464.1	0.0694	72.18	0.4365	318.576	3283.34	2.470	0.031	0.124
13	2,660.9	0.0664	74.11	0.5022	379.942	3777.58	2.945	0.031	0.124
14	2,876.1	0.0639	75.86	0.5701	441.647	4288.83	3.423	0.031	0.125
15	3,063.4	0.0607	77.61	0.6203	490.152	4665.83	3.799	0.031	0.126
16	3,270.3	0.0580	79.26	0.6761	541.519	5086.12	4.198	0.031	0.127
17	3,458.3	0.0557	80.58	0.7235	595.438	5442.12	4.616	0.031	0.129
18	3,640.2	0.0536	81.77	0.7706	648.743	5796.80	5.030	0.031	0.131

Appendix D: Single- and two-phase calculated data (continued).

Channel C2: Water tests.

Number of channels: 3

Channel Dimensions:

Depth ( $\mu\text{m}$ ): 263.730

Hyd. Diameter ( $\mu\text{m}$ ): 207.01

Width ( $\mu\text{m}$ ): 190.37

Channel Length (m): 0.0635

Data Point	Re	f	Velocity	Q	h - overall	Heat Flux	Nu	Uncertainty	
								U-f	U_Nu
			(m/s)	(Watts)	W/m <sup>2</sup> -K	(W/m <sup>2</sup> )		(%)	(%)
1	551.40	0.1402	2.26	13.773	14772.61	103606	4.917	0.031	0.171
2	758.47	0.1163	3.08	20.396	18342.2	153428	6.099	0.031	0.148
3	959.11	0.0981	3.87	26.457	21498.35	199023	7.143	0.031	0.137
4	1,194.11	0.0798	4.80	32.307	24431.23	243026	8.114	0.031	0.132
5	1,296.19	0.0791	5.23	32.999	28918.3	248227	9.607	0.031	0.147
6	1,467.33	0.0732	5.85	39.304	32107.47	295659	10.654	0.031	0.138
7	1,618.07	0.0709	6.39	45.759	38739.26	344216	12.839	0.031	0.138
8	1,743.94	0.0704	6.77	52.297	44186.04	393399	14.618	0.031	0.135
9	1,801.99	0.0747	6.89	57.547	48399.02	432893	15.984	0.031	0.132
10	1,890.38	0.0753	7.22	58.305	52929.43	438594	17.479	0.031	0.140
11	1,956.88	0.0781	7.34	65.342	55551.08	491525	18.308	0.031	0.131
12	2,058.55	0.0766	7.72	66.700	60625.72	501745	19.979	0.031	0.138
13	2,154.26	0.0745	8.10	68.135	65015.79	512537	21.432	0.031	0.144
14	2,251.24	0.0743	8.51	68.621	69165.71	516195	22.812	0.031	0.152
15	2,329.78	0.0775	8.73	73.560	70735.6	553348	23.308	0.031	0.145
16	2,500.38	0.0723	9.39	76.571	76327.6	575999	25.158	0.031	0.150
17	2,556.20	0.0731	9.63	75.912	78204.2	571041	25.784	0.031	0.155
18	2,744.80	0.0696	10.41	77.704	84287.04	584516	27.808	0.031	0.163
19	2,901.66	0.0681	11.06	78.152	88873.67	587887	29.338	0.031	0.172
20	3,022.74	0.0709	11.44	83.882	89456.6	630990	29.507	0.031	0.162
21	2,591.73	0.0742	10.04	63.528	88701.25	477884	29.336	0.031	0.206
22	2,821.63	0.0743	11.03	64.062	97672.05	481896	32.333	0.031	0.225
23	3,104.54	0.0712	12.21	65.603	108344.8	493489	35.889	0.031	0.244
24	3,389.45	0.0680	13.40	67.633	119119.8	508761	39.478	0.031	0.260
25	3,622.32	0.0663	14.36	68.873	128312.2	518093	42.539	0.031	0.274
26	3,775.56	0.0680	15.02	68.974	135026.4	518848	44.781	0.031	0.288
27	3,987.14	0.0662	15.91	70.327	144549	529025	47.954	0.031	0.302
28	4,193.15	0.0643	16.79	71.845	152991.8	540445	50.771	0.031	0.312

Appendix D: Single- and two-phase calculated data (continued).

Channel C2: Water-argon tests. Number of channels: 3

Channel Dimensions:

Depth ( $\mu\text{m}$ ): 263.730 Hyd. Diameter ( $\mu\text{m}$ ): 207.01

Width ( $\mu\text{m}$ ): 190.37 Channel Length (m): 0.0635

Data Point	G	x	f	Two-phase	Q	h - overall	Heat Flux	Nu	Uncertainty	
	kg/s-m <sup>2</sup>	Quality		Re-avg	(Watts)	W/m <sup>2</sup> -K	(W/m <sup>2</sup> )		U f (%)	U Nu (%)
1	1.112	0.02509	0.2009	436.25	11.181	12809.2	84111	4.188	0.031	0.164
2	1.497	0.074837	0.1597	578.81	14.452	16963.2	108711	5.557	0.031	0.168
3	1.408	0.144303	0.1856	538.74	12.873	15859.8	96839	5.205	0.031	0.176
4	1.124	0.301427	0.2726	449.90	11.767	12077.8	88517	3.951	0.031	0.148
5	2.328	0.013916	0.1055	821.71	14.882	25632.6	111945	8.473	0.031	0.246
6	2.380	0.045749	0.1008	888.38	21.920	23530.3	164890	7.734	0.031	0.157
7	2.353	0.085078	0.1054	886.69	22.374	24644.7	168304	8.096	0.031	0.159
8	1.862	0.153367	0.1408	717.68	19.306	20966.1	145225	6.876	0.031	0.156
9	3.188	0.011032	0.0728	1,187.20	29.903	26079.2	224942	8.571	0.031	0.132
10	3.140	0.035546	0.0744	1,191.36	31.413	27686.5	236304	9.083	0.031	0.132
11	2.747	0.073375	0.0868	1,063.12	29.527	28460.7	222117	9.321	0.031	0.140
12	3.963	0.008236	0.0596	1,444.89	31.531	29579.6	237188	9.743	0.031	0.145
13	3.630	0.03216	0.0650	1,358.91	32.759	33996.3	246425	11.169	0.031	0.153
14	3.237	0.062607	0.0739	1,233.58	31.577	33415.0	237531	10.961	0.031	0.153
15	10.004	0.031524	0.0444	3,550.31	68.421	74508.3	514685	24.616	0.031	0.168
16	10.116	0.049216	0.0444	3,595.46	69.960	75581.6	526268	24.971	0.031	0.166
17	9.368	0.064688	0.0454	3,350.98	68.564	70545.3	515766	23.294	0.031	0.158
18	9.658	0.067482	0.0451	3,441.00	69.716	73334.7	524430	24.226	0.031	0.162
19	9.580	0.077047	0.0454	3,411.22	69.671	73254.3	524093	24.203	0.031	0.161
20	10.833	0.006126	0.0434	3,779.19	67.247	79413.9	505860	26.276	0.031	0.183
21	10.799	0.011149	0.0435	3,775.25	68.014	79940.0	511629	26.446	0.031	0.181
22	11.396	0.021555	0.0430	3,963.46	68.398	83264.9	514516	27.564	0.031	0.188
23	11.378	0.038684	0.0432	3,966.72	69.390	84335.3	521980	27.916	0.031	0.187
24	10.858	0.052633	0.0438	3,806.93	70.139	81253.3	527615	26.883	0.031	0.178
25	10.692	0.058851	0.0441	3,752.14	69.977	80263.9	526391	26.555	0.031	0.176
26	10.300	0.073213	0.0446	3,625.48	69.420	77528.1	522206	25.645	0.031	0.172
27	1.620	0.183173	0.1898	552.19	10.352	21446.2	77870	7.128	0.031	0.290
28	1.590	0.220733	0.2026	542.29	10.174	21423.8	76533	7.123	0.031	0.294
29	2.051	0.213258	0.1555	699.88	12.963	27237.6	97509	9.054	0.031	0.294
30	1.719	0.270832	0.2004	586.28	10.881	24915.3	81853	8.288	0.031	0.318
31	1.918	0.269597	0.1793	654.24	12.109	26706.6	91087	8.884	0.031	0.307
32	1.694	0.341368	0.2246	579.54	10.872	25304.6	81781	8.421	0.031	0.322
33	2.072	0.309509	0.1771	700.56	12.468	32416.4	93790	10.797	0.031	0.359
34	1.944	0.361954	0.2047	656.56	11.546	28347.8	86853	9.449	0.031	0.341
35	1.934	0.392685	0.2163	652.94	11.465	26225.7	86246	8.744	0.031	0.319



# Appendix D: Single- and two-phase calculated data (continued).

Channel C2: Water-helium tests.

Number of channels: 3

Channel Dimensions:

Depth ( $\mu\text{m}$ ): 263.730Hyd. Diameter ( $\mu\text{m}$ ): 207.01Width ( $\mu\text{m}$ ): 190.37

Channel Length (m): 0.0635

Data Point	G	x	f	Two-phase	Q	h - overall	Heat Flux	Nu	Uncertainty	
	kg/s-m <sup>2</sup>	Quality		Re-avg	(Watts)	W/m <sup>2</sup> -K	(W/m <sup>2</sup> )		U f (%)	U Nu (%)
1	2335.125	0.00133	0.1026	833.65	16.948	22544.4	127488	7.442	0.031	0.194
2	2051.618	0.012572	0.1159	746.93	16.797	21708.7	126354	7.152	0.031	0.186
3	1544.808	0.031375	0.1554	567.77	13.289	17377.2	99963	5.720	0.031	0.187
4	1320.407	0.056688	0.1820	497.88	12.595	14337.9	94745	4.708	0.031	0.164
5	2873.113	0.001043	0.0765	1,118.19	32.491	23220.3	244410	7.595	0.031	0.109
6	2195.576	0.011701	0.0995	868.63	25.268	20301.3	190079	6.629	0.031	0.119
7	2002.183	0.024408	0.1075	815.23	25.316	19897.0	190440	6.478	0.031	0.115
8	1411.218	0.047842	0.1533	585.77	18.908	14518.7	142233	4.718	0.031	0.112
9	3911.848	0.000824	0.0597	1,431.35	30.892	28579.1	232380	9.409	0.031	0.144
10	3329.527	0.007698	0.0687	1,253.31	29.869	28678.0	224683	9.414	0.031	0.144
11	2703.382	0.017972	0.0841	1,034.58	26.253	26188.8	197486	8.582	0.031	0.146
12	10126.57	0.000349	0.0441	3,511.98	66.113	73790.4	497324	24.431	0.031	0.173
13	10045.39	0.000859	0.0442	3,497.89	65.291	73812.5	491144	24.428	0.031	0.175
14	10379.44	0.001848	0.0438	3,620.98	66.911	76191.3	503328	25.210	0.031	0.176
15	10195.35	0.00299	0.0440	3,563.23	65.860	74998.7	495426	24.811	0.031	0.176
16	10473.39	0.004304	0.0437	3,652.46	65.782	76752.6	494840	25.397	0.031	0.180
17	10127.64	0.005685	0.0441	3,540.22	64.494	73509.4	485151	24.317	0.031	0.177
18	10275.68	0.006471	0.0440	3,585.01	64.762	75661.9	487164	25.034	0.031	0.180
19	10435.3	0.007151	0.0438	3,643.87	66.372	77039.8	499273	25.488	0.031	0.171

Appendix D: Single- and two-phase calculated data (continued).

Channel C2: Water-Nitrogen tests. Number of channels: 3

Channel Dimensions:

Depth ( $\mu\text{m}$ ): 263.730 Hyd. Diameter ( $\mu\text{m}$ ): 207.01

Width ( $\mu\text{m}$ ): 190.37 Channel Length (m): 0.0635

Data Point	G	x	f	Two-phase	Q	h - overall	Heat Flux	Nu	Uncertainty	
									U f	U Nu
	kg/s-m <sup>2</sup>	Quality		Re-avg	(Watts)	W/m <sup>2</sup> -K	(W/m <sup>2</sup> )		(%)	(%)
1	1.374	0.005791	0.1695	509.95	13.321	13678.6	100208	4.525	0.031	0.299
2	1.534	0.010093	0.1520	573.51	14.681	14531.9	110433	4.825	0.031	0.290
3	1.309	0.053491	0.1803	528.20	14.256	12986.3	107237	4.485	0.031	0.264
4	1.167	0.121811	0.2127	518.62	12.819	11228.9	96433	4.155	0.031	0.253
5	1.578	0.136169	0.1657	687.61	14.834	16555.9	111584	6.246	0.031	0.318
6	2.839	0.002623	0.0849	1.011.03	23.501	21520.0	176785	7.126	0.031	0.281
7	2.899	0.005088	0.0822	1.049.59	25.427	23118.5	191268	7.662	0.031	0.276
8	2.363	0.030507	0.0997	911.36	24.641	21501.7	185359	7.275	0.031	0.257
9	2.234	0.063207	0.1064	913.45	24.867	21884.0	187056	7.630	0.031	0.255
10	1.828	0.119015	0.1336	820.23	21.482	18984.4	161596	6.993	0.031	0.253
11	4.824	0.001586	0.0506	1.692.98	35.883	27516.1	269924	9.115	0.031	0.256
12	4.526	0.003291	0.0530	1.621.64	36.269	28456.9	272830	9.423	0.031	0.254
13	3.917	0.019242	0.0601	1.477.79	37.214	35107.5	279941	11.761	0.031	0.279
14	3.290	0.042344	0.0715	1.300.21	34.038	34143.5	256044	11.672	0.031	0.289
15	2.699	0.078777	0.0869	1.154.62	32.268	28608.5	242732	10.104	0.031	0.254
16	5.835	0.001164	0.0410	2.087.63	46.531	40197.0	350022	13.282	0.031	0.272
17	5.513	0.002625	0.0427	2.010.40	46.797	41561.7	352024	13.727	0.031	0.273
18	4.600	0.016459	0.0500	1.764.32	46.706	44780.4	351340	14.930	0.031	0.280
19	3.773	0.039003	0.0599	1.541.19	44.884	40015.7	337631	13.581	0.031	0.256
20	10.131	0.007988	0.0441	3.588.65	65.840	74675.9	495276	24.879	0.031	0.350
21	10.260	0.010426	0.0439	3.650.58	66.806	75398.7	502538	25.173	0.031	0.348
22	10.382	0.019554	0.0439	3.725.20	66.771	75733.6	502281	25.511	0.031	0.350
23	9.833	0.030806	0.0446	3.582.04	64.913	71238.1	488298	24.252	0.031	0.339
24	10.152	0.032189	0.0443	3.694.54	65.906	73628.5	495772	25.105	0.031	0.344
25	10.137	0.036736	0.0443	3.707.07	66.278	73762.3	498571	25.263	0.031	0.343
26	11.759	0.007129	0.0426	4.113.91	69.011	85172.5	519130	28.386	0.031	0.382
27	11.286	0.00954	0.0430	3.969.55	67.045	81785.6	504342	27.312	0.031	0.378
28	11.871	0.018198	0.0425	4.209.62	69.473	85497.2	522603	28.792	0.031	0.381
29	11.322	0.026056	0.0431	4.062.48	68.460	82148.4	514985	27.865	0.031	0.370
30	11.077	0.028958	0.0434	3.988.10	67.374	80375.3	506812	27.339	0.031	0.368
31	11.390	0.030941	0.0431	4.098.51	68.730	82218.7	517015	28.028	0.031	0.369
32	2.010	0.114131	0.1433	757.26	10.420	24326.6	78380	9.077	0.031	0.655
33	1.727	0.141331	0.1714	673.27	8.978	21118.9	67535	8.115	0.031	0.658
34	1.593	0.164619	0.1906	638.94	8.255	19682.1	62097	7.761	0.031	0.666
35	1.539	0.180481	0.2005	630.66	8.067	18907.0	60685	7.590	0.031	0.654
36	1.518	0.192729	0.2061	631.92	7.954	18477.0	59830	7.523	0.031	0.648

Appendix D: Single- and two-phase calculated data (continued).

Channel C3: Argon gas tests.

Number of channels: 7

Channel Dimensions:

Depth ( $\mu\text{m}$ ): 71.30

Hyd. Diameter ( $\mu\text{m}$ ): 55.55

Width ( $\mu\text{m}$ ): 144.79

Channel Length (m): 0.0635

Data Point	Re	f	Velocity	Q	Heat Trans. coeff.	Heat Flux	Nu	Uncertainty	
			(m/s)	(Watts)	W/m <sup>2</sup> -K	(W/m <sup>2</sup> )		U-f	U-Nu
1	23.0	2.5728	3.17	0.0001	0.081	0.88	0.000427	0.031	1.862
2	238.3	0.2341	23.64	0.0080	4.207	62.57	0.022108	0.031	0.284
3	438.2	0.1276	36.82	0.0237	11.905	185.47	0.062408	0.031	0.185
4	649.1	0.0841	48.62	0.0469	23.720	367.31	0.124087	0.031	0.147
5	827.2	0.0657	57.24	0.0716	36.799	560.73	0.192182	0.031	0.129
6	1.033.3	0.0529	65.97	0.1000	52.029	782.54	0.271469	0.031	0.121
7	1.249.1	0.0460	73.01	0.1343	70.996	1051.22	0.370164	0.031	0.114
8	1.465.3	0.0393	80.54	0.1685	90.292	1319.09	0.470596	0.031	0.111
9	1.644.1	0.0355	86.01	0.1997	108.360	1563.44	0.564650	0.031	0.108
10	1.819.9	0.0328	90.67	0.2314	126.120	1811.16	0.657126	0.031	0.106
11	2.038.5	0.0304	95.34	0.2438	127.098	1908.37	0.663358	0.031	0.109
12	2.266.6	0.0291	99.07	0.2833	154.147	2217.70	0.804670	0.031	0.109
13	2.548.0	0.0275	103.43	0.3347	188.855	2619.92	0.986149	0.031	0.109
14	2.783.4	0.0256	108.16	0.3824	216.240	2993.70	1.129602	0.031	0.107
15	3.019.5	0.0242	112.05	0.4353	248.078	3407.82	1.296257	0.031	0.106
16	3.265.1	0.0226	116.73	0.4938	278.566	3865.75	1.455689	0.031	0.104
17	3.480.0	0.0213	120.97	0.5460	328.302	4274.01	1.715531	0.031	0.106
18	3.723.6	0.0193	127.37	0.5974	365.422	4676.64	1.909577	0.031	0.107
19	3.970.8	0.0179	132.67	0.6559	408.406	5134.69	2.134301	0.031	0.107
20	4.173.4	0.0169	137.04	0.6978	442.499	5462.45	2.313306	0.031	0.108
21	4.388.8	0.0158	142.02	0.7528	485.628	5893.06	2.539338	0.031	0.108

Appendix D: Single- and two-phase calculated data (continued).

Channel C3: Helium gas tests. Number of channels: 7

Channel Dimensions:

Depth ( $\mu\text{m}$ ): 71.30 Hyd. Diameter ( $\mu\text{m}$ ): 55.55

Width ( $\mu\text{m}$ ): 144.79 Channel Length (m): 0.0635

Data Point					Heat Trans.				
	Re	f	Velocity	Q	coeff.	Heat Flux	Nu	U-f	U-Nu
			(m/s)	(Watts)	W/m <sup>2</sup> -K	(W/m <sup>2</sup> )		(%)	(%)
1	2.2	31.5231	3.27E-08	2.59					
2	28.9	2.1990	4.26E-07	24.01	0.0030	1.858	23.63	0.031	0.737
3	68.2	0.9329	9.78E-07	43.99	0.0164	8.887	128.68	0.031	0.317
4	109.7	0.5799	1.55E-06	60.14	0.0475	26.622	371.88	0.031	0.185
5	152.8	0.3926	2.13E-06	75.73	0.0768	43.648	601.49	0.031	0.162
6	199.7	0.2946	2.74E-06	89.83	0.0944	52.422	739.24	0.031	0.168
7	242.2	0.2367	3.3E-06	102.12	0.1419	82.845	1110.50	0.031	0.143
8	287.5	0.1957	3.88E-06	114.01	0.1834	109.546	1436.04	0.031	0.135
9	334.1	0.1653	4.47E-06	125.58	0.2235	136.782	1749.37	0.031	0.132
10	378.3	0.1443	5.03E-06	135.71	0.2702	168.507	2115.54	0.031	0.127
11	427.4	0.1260	5.64E-06	146.50	0.3191	213.415	2498.20	0.031	0.127
12	473.0	0.1123	6.21E-06	156.26	0.3627	247.995	2838.86	0.031	0.126
13	523.6	0.1003	6.83E-06	166.45	0.4185	293.253	3275.75	0.031	0.125
14	569.8	0.0915	7.4E-06	175.44	0.4711	346.263	3687.71	0.031	0.126
15	618.2	0.0847	7.98E-06	183.28	0.5152	373.457	4032.89	0.031	0.124
16	669.7	0.0779	8.59E-06	191.98	0.5639	382.351	4413.89	0.031	0.119
17	716.5	0.0725	9.15E-06	199.66	0.6150	459.044	4814.35	0.031	0.124
18	768.1	0.0673	9.76E-06	207.89	0.6680	502.371	5228.94	0.031	0.124

Appendix D: Single- and two-phase calculated data (continued).

Channel C3: Nitrogen gas tests.

Number of channels: 7

Channel Dimensions:

Depth ( $\mu\text{m}$ ): 71.30

Hyd. Diameter ( $\mu\text{m}$ ): 55.55

Width ( $\mu\text{m}$ ): 144.79

Channel Length (m): 0.0635

Data Point					Heat Trans.			Uncertainty	
	Re	f	Velocity	Q	coeff.	Heat Flux	Nu	U-f	U-Nu
			(m/s)	(Watts)	W/m2-K	(W/m^2)		(%)	(%)
1	13.7	5.8976	2.07	0.00002	0.018	0.18	0.00007	0.031	8.572
2	136.3	0.6298	15.67	0.0044	3.227	34.40	0.012	0.031	0.452
3	270.6	0.3125	26.39	0.0104	5.346	81.32	0.020	0.031	0.381
4	417.6	0.1965	36.30	0.0306	14.753	239.55	0.054	0.031	0.209
5	538.7	0.1485	43.60	0.0515	24.020	402.95	0.087	0.031	0.166
6	684.8	0.1145	51.60	0.0760	36.039	594.86	0.130	0.031	0.148
7	804.2	0.0965	57.62	0.1062	51.895	831.49	0.187	0.031	0.131
8	942.2	0.0809	64.23	0.1341	66.135	1049.76	0.238	0.031	0.125
9	1.069.9	0.0691	70.46	0.1628	80.462	1274.17	0.289	0.031	0.120
10	1.202.8	0.0584	77.36	0.1899	94.347	1486.54	0.338	0.031	0.117
11	1.334.3	0.0488	84.94	0.2154	107.934	1686.55	0.387	0.031	0.116
12	1.518.1	0.0415	93.23	0.2512	126.332	1966.04	0.453	0.031	0.114
13	1.700.2	0.0365	100.58	0.3020	153.837	2363.86	0.551	0.031	0.110
14	1.879.6	0.0336	106.10	0.3261	177.493	2553.05	0.636	0.031	0.115
15	2.055.4	0.0317	110.56	0.3509	196.743	2746.62	0.705	0.031	0.118
16	2.210.7	0.0305	113.96	0.3930	225.913	3076.72	0.810	0.031	0.117
17	2.379.3	0.0297	116.89	0.4519	269.163	3537.78	0.965	0.031	0.116
18	2.529.2	0.0289	119.57	0.5024	306.761	3932.85	1.099	0.031	0.115
19	2.685.9	0.0285	121.51	0.5472	338.194	4283.28	1.213	0.031	0.115
20	2.830.2	0.0280	123.50	0.6004	381.194	4700.03	1.367	0.031	0.115
21	2.970.2	0.0273	125.64	0.6351	441.417	4971.35	1.583	0.031	0.121

Appendix D: Single- and two-phase calculated data (continued).

Channel C3: Water tests. Number of channels: 7

Channel Dimensions:

Depth ( $\mu\text{m}$ ): 71.30 Hyd. Diameter ( $\mu\text{m}$ ): 55.55

Width ( $\mu\text{m}$ ): 144.79 Channel Length (m): 0.0635

Data Point	Re	f	Velocity	Q	h - overall	Heat Flux	Nu	Uncertainty	
								U-f	U_Nu
			(m/s)	(Watts)	W/m <sup>2</sup> -K	(W/m <sup>2</sup> )		(%)	(%)
1	254.69	0.2071	2.16	9.591	8468.662	75076	1.294	0.031	0.133
2	341.83	0.1257	2.94	11.646	12234.65	91167	1.873	0.031	0.155
3	385.83	0.1076	3.30	13.793	13767.28	107970	2.106	0.031	0.147
4	468.67	0.0777	4.08	14.930	16558.81	116870	2.538	0.031	0.165
5	551.18	0.0597	4.85	16.045	19521.7	125605	2.996	0.031	0.181
6	644.23	0.0474	5.65	18.901	21001.17	147962	3.222	0.031	0.169
7	763.63	0.0370	6.61	23.054	23742.47	180468	3.637	0.031	0.158
8	854.14	0.0323	7.29	27.039	26285.4	211666	4.020	0.031	0.149
9	1,000.06	0.0255	8.44	33.672	30974.09	263591	4.731	0.031	0.141
10	1,098.57	0.0229	9.17	38.108	33916.48	298314	5.174	0.031	0.136
11	1,182.92	0.0209	9.88	39.485	38567.01	309096	5.885	0.031	0.147
12	1,337.81	0.0174	11.08	47.330	47155.65	370504	7.188	0.031	0.147
13	1,438.24	0.0158	11.95	48.405	50899.79	378922	7.761	0.031	0.154
14	1,508.83	0.0151	12.59	48.099	51655.53	376527	7.881	0.031	0.159
15	1,589.52	0.0139	13.31	48.488	53528.29	379570	8.169	0.031	0.164
16	1,697.54	0.0129	14.09	53.361	57251.29	417716	8.729	0.031	0.159
17	1,946.58	0.0107	16.11	61.544	66809.04	481774	10.182	0.031	0.160
18	1,501.90	0.0140	13.56	36.140	38767.2	282911	5.966	0.031	0.178
19	1,857.84	0.0109	16.84	37.719	49054.06	295271	7.552	0.031	0.214
20	2,144.59	0.0096	19.39	38.184	58684.94	298906	9.032	0.031	0.249

Appendix D: Single- and two-phase calculated data (continued).

Channel C3: Water-argon tests.

Number of channels: 7

Channel Dimensions:

Depth ( $\mu\text{m}$ ): 71.30

Hyd. Diameter ( $\mu\text{m}$ ): 55.55

Width ( $\mu\text{m}$ ): 144.79

Channel Length (m): 0.0635

Data Point	G	x	f	Two-phase	Q	h - overall	Heat Flux	Nu	Uncertainty	
	$\text{kg/s-m}^2$	Quality		Re-avg	(Watts)	$\text{W/m}^2\text{-K}$	$(\text{W/m}^2)$		U f (%)	U Nu (%)
1	2.302	0.012523	0.2361	395.25	8.571	9829.1	67095	1.503	0.031	0.169
2	2.615	0.049224	0.2101	461.41	10.116	12101.4	79191	1.846	0.031	0.173
3	2.944	0.080939	0.1934	518.86	11.266	13003.9	88192	1.985	0.031	0.169
4	2.582	0.143713	0.2371	454.43	9.703	11044.2	75956	1.687	0.031	0.167
5	3.637	0.007007	0.1496	620.26	12.226	14409.2	95708	2.205	0.031	0.177
6	3.729	0.036448	0.1460	655.30	12.767	14579.5	99940	2.225	0.031	0.172
7	3.240	0.074612	0.1735	574.26	11.807	12620.8	92425	1.925	0.031	0.161
8	3.343	0.111996	0.1735	598.69	13.203	13066.3	103354	1.991	0.031	0.149
9	5.054	0.00579	0.1064	870.89	16.188	18841.9	126718	2.880	0.031	0.177
10	4.451	0.031121	0.1219	780.34	15.703	17194.1	122927	2.624	0.031	0.165
11	4.579	0.054454	0.1201	812.12	17.200	17694.6	134645	2.698	0.031	0.155
12	4.102	0.097137	0.1377	741.82	17.748	16381.3	138932	2.494	0.031	0.139

# Appendix D: Single- and two-phase calculated data (continued).

Channel C3: Water-helium tests.      Number of channels:      7  
Channel Dimensions:  
Depth ( $\mu\text{m}$ ):      71.30      Hyd. Diameter ( $\mu\text{m}$ ):      55.55  
Width ( $\mu\text{m}$ ):      144.79      Channel Length (m):      0.0635

Data Point	G	x	f	Two-phase	Q	h - overall	Heat Flux	Nu	Uncertainty	
	kg/s-m <sup>2</sup>	Quality		Re-avg	(Watts)	W/m <sup>2</sup> -K	(W/m <sup>2</sup> )		U f	U Nu
									(%)	(%)
1	2.996	0.00742	0.1768	525.25	10.513	11953.6	82294	1.824	0.031	0.194
2	3.273	0.013586	0.1621	576.26	11.713	13009.5	91692	1.984	0.031	0.186
3	3.271	0.019718	0.1625	578.68	11.722	13006.3	91759	1.983	0.031	0.187
4	3.337	0.025468	0.1608	588.08	11.488	13132.3	89928	2.003	0.031	0.164
5	2.879	0.037514	0.1874	511.16	10.409	11515.0	81482	1.755	0.031	0.109
6	4.378	0.004962	0.1196	774.05	15.068	17707.1	117955	2.699	0.031	0.119
7	3.979	0.011132	0.1313	709.92	14.624	16016.8	114475	2.440	0.031	0.115
8	3.516	0.019138	0.1485	632.60	13.910	14282.7	108890	2.174	0.031	0.112
9	3.312	0.026466	0.1589	595.99	13.079	13444.4	102382	2.046	0.031	0.144
10	5.969	0.0019	0.0886	1,041.91	19.277	22632.4	150904	3.455	0.031	0.144
11	5.826	0.003717	0.0905	1,021.83	19.180	22208.1	150141	3.388	0.031	0.146
12	5.462	0.007894	0.0962	965.98	18.336	20896.3	143539	3.186	0.031	0.173



Appendix D: Single- and two-phase calculated data (continued).

Channel C3: Water-Nitrogen tests.

Number of channels: 7

Channel Dimensions:

Depth ( $\mu\text{m}$ ): 71.30

Hyd. Diameter ( $\mu\text{m}$ ): 55.55

Width ( $\mu\text{m}$ ): 144.79

Channel Length (m): 0.0635

Data Point	G	x	f	Two-phase	Q	h - overall	Heat Flux	Nu	Uncertainty	
	kg/s-m <sup>2</sup>	Quality		Re-avg	(Watts)	W/m <sup>2</sup> -K	(W/m <sup>2</sup> )		U <sub>f</sub>	U <sub>Nu</sub>
									(%)	(%)
1	3.898	0.003579	0.1450	639.90	13.236	15835.0	103616	2.442	0.031	0.178
2	3.462	0.00787	0.1614	579.96	12.440	15428.7	97379	2.386	0.031	0.180
3	3.724	0.015218	0.1462	649.47	16.026	17121.8	125452	2.657	0.031	0.155
4	3.832	0.029329	0.1429	683.72	16.806	17506.3	131557	2.752	0.031	0.151
5	3.643	0.059135	0.1539	675.23	16.017	15884.5	125383	2.570	0.031	0.144
6	3.530	0.089339	0.1625	681.80	15.715	15019.9	123019	2.505	0.031	0.139
7	4.911	0.005354	0.1104	843.71	20.281	21857.2	158759	3.361	0.031	0.157
8	4.597	0.012501	0.1178	801.64	19.112	20784.8	149613	3.216	0.031	0.158
9	4.676	0.022712	0.1161	830.49	19.868	21095.2	155525	3.294	0.031	0.154
10	4.676	0.046326	0.1183	855.12	20.069	20521.2	157101	3.278	0.031	0.149
11	6.219	0.00446	0.0881	1,055.34	23.063	25481.0	180542	3.920	0.031	0.164
12	6.133	0.009414	0.0890	1,055.36	23.424	26596.2	183365	4.107	0.031	0.166
13	6.323	0.016965	0.0871	1,094.49	23.110	26650.4	180905	4.146	0.031	0.170

## Appendix D: Single- and two-phase calculated data (continued).

Channel D: Argon gas tests.                      Number of channels:                      7  
Channel Dimensions:  
Depth ( $\mu\text{m}$ ):                      111.330                      Hyd. Diameter ( $\mu\text{m}$ ):                      111.88  
Width ( $\mu\text{m}$ ):                      112.43                      Channel Length (m):                      0.0635

Data Point					Heat Trans.				
	Re	f	Velocity	Q	coeff.	Heat Flux	Nu	Uncertainty	
			(m/s)	(Watts)	W/m <sup>2</sup> -K	(W/m <sup>2</sup> )		U-f	U-Nu
1	58.7	3.3451	5.60	0.0013	0.770	8.72	0.004785	0.031	0.435
2	218.2	0.7173	16.11	0.0087	4.412	58.71	0.027371	0.031	0.250
3	529.8	0.2529	31.03	0.0218	10.060	146.68	0.062344	0.031	0.246
4	845.5	0.1565	42.16	0.0480	21.842	322.55	0.135005	0.031	0.188
5	1,110.7	0.1292	48.52	0.0967	45.952	649.31	0.283043	0.031	0.137
6	1,375.0	0.1068	54.74	0.1242	59.131	833.79	0.363849	0.031	0.136
7	1,627.7	0.0971	58.74	0.1513	71.962	1015.55	0.442667	0.031	0.135
8	1,854.1	0.0964	60.27	0.1883	90.734	1264.27	0.557738	0.031	0.131
9	2,061.8	0.0935	62.11	0.2197	107.940	1475.13	0.663109	0.031	0.131
10	2,275.8	0.0885	64.58	0.2563	128.131	1720.45	0.786900	0.031	0.130
11	2,456.0	0.0835	66.94	0.2966	150.431	1991.22	0.923672	0.031	0.127
12	2,605.3	0.0800	68.82	0.3325	172.898	2232.12	1.061144	0.031	0.126
13	2,752.9	0.0776	70.28	0.3935	206.376	2641.98	1.266700	0.031	0.121
14	2,891.3	0.0753	71.79	0.4887	276.694	3281.34	1.695315	0.031	0.117
15	3,027.6	0.0717	73.88	0.5211	307.172	3498.25	1.880421	0.031	0.120
16	3,162.0	0.0683	75.69	0.5134	353.991	3446.84	2.176506	0.031	0.136
17	3,249.6	0.0678	76.31	0.5743	389.913	3855.97	2.395539	0.031	0.133
18	3,315.6	0.0674	76.83	0.6220	422.455	4176.18	2.594776	0.031	0.132

Appendix D: Single- and two-phase calculated data (continued).

Channel D: Helium gas tests.

Number of channels: 7

Channel Dimensions:

Depth ( $\mu\text{m}$ ): 111.330

Hyd. Diameter ( $\mu\text{m}$ ): 111.88

Width ( $\mu\text{m}$ ): 112.43

Channel Length (m): 0.0635

Data Point	Re	f	Velocity (m/s)	Q (Watts)	Heat Trans.	Heat Flux (W/m <sup>2</sup> )	Nu	Uncertainty	
					coeff. W/m <sup>2</sup> -K			U-f (%)	U-Nu (%)
1	6.1	16.8991	5.80						
2	25.4	4.1034	18.50	0.0022	1.429	14.88	0.0010358	0.031	0.913
3	80.5	1.3737	40.82	0.0359	27.583	240.80	0.0198963	0.031	0.207
4	133.2	0.8840	54.94	0.0749	62.608	503.06	0.0450715	0.031	0.183
5	193.7	0.5781	70.38	0.1112	94.419	746.64	0.0679435	0.031	0.181
6	254.7	0.4479	82.17	0.1488	127.660	998.79	0.0918378	0.031	0.179
7	315.7	0.3660	92.60	0.1792	151.275	1202.89	0.1088589	0.031	0.178
8	377.3	0.3101	102.21	0.2565	241.071	1722.08	0.1731385	0.031	0.175
9	435.9	0.2712	110.55	0.3187	316.914	2139.75	0.2274170	0.031	0.177
10	506.7	0.2366	119.67	0.3949	411.565	2651.33	0.2951677	0.031	0.180
11	565.2	0.2145	126.59	0.4496	479.984	3018.81	0.3442281	0.031	0.182
12	630.1	0.1979	132.81	0.5090	558.547	3417.14	0.4006518	0.031	0.185
13	700.6	0.1808	139.84	0.5743	645.429	3855.78	0.4630899	0.031	0.187
14	772.7	0.1668	146.42	0.6487	752.082	4355.47	0.5397323	0.031	0.191
15	643.8	0.1426	176.93	0.8884	425.075	6059.35	0.6869200	0.031	0.191

Appendix D: Single- and two-phase calculated data (continued).

Channel D: Nitrogen gas tests.      Number of channels:      7  
 Channel Dimensions:  
 Depth ( $\mu\text{m}$ ):      111.330      Hyd. Diameter ( $\mu\text{m}$ ):      111.88  
 Width ( $\mu\text{m}$ ):      112.43      Channel Length (m):      0.0635

Data Point					Heat Trans.				
	Re	f	Velocity	Q	coeff.	Heat Flux	Nu	U-f	U-Nu
			(m/s)	(Watts)	W/m <sup>2</sup> -K	(W/m <sup>2</sup> )		(%)	(%)
1	31.6	2.7850	4.11	0.00021	0.175	1.42	0.00074	0.031	2.208
2	123.2	0.7501	13.67	0.0067	4.542	44.84	0.019	0.031	0.293
3	370.1	0.2578	31.78	0.0343	22.899	230.19	0.096	0.031	0.192
4	670.3	0.1543	46.81	0.0858	59.938	575.91	0.252	0.031	0.160
5	911.9	0.1205	56.16	0.1545	118.912	1037.28	0.498	0.031	0.148
6	1,156.7	0.0992	64.26	0.2195	175.207	1473.38	0.733	0.031	0.146
7	1,389.0	0.0872	70.50	0.2812	230.763	1888.02	0.966	0.031	0.147
8	1,629.9	0.0809	75.08	0.3301	267.535	2216.17	1.121	0.031	0.146
9	1,812.4	0.0792	77.30	0.3803	311.593	2553.29	1.305	0.031	0.147
10	1,996.0	0.0807	78.09	0.4441	369.164	2981.71	1.547	0.031	0.147
11	2,170.1	0.0810	79.05	0.5041	424.130	3384.22	1.777	0.031	0.148
12	2,371.0	0.0787	81.18	0.5791	497.651	3887.71	2.086	0.031	0.150
13	2,483.3	0.0782	82.00	0.6321	554.603	4243.71	2.325	0.031	0.151
14	2,646.2	0.0763	83.70	0.7075	632.410	4749.75	2.652	0.031	0.153

Appendix D: Single- and two-phase calculated data (continued).

Channel D: Water tests.

Number of channels: 7

Channel Dimensions:

Depth ( $\mu\text{m}$ ): 111.330 Hyd. Diameter ( $\mu\text{m}$ ): 111.88

Width ( $\mu\text{m}$ ): 112.43 Channel Length (m): 0.0635

Data Point	Re	f	Velocity	Q	h - overall	Heat Flux	Nu	Uncertainty	
								U-f	U_Nu
			(m/s)	(Watts)	W/m <sup>2</sup> -K	(W/m <sup>2</sup> )		(%)	(%)
1	253.61	0.4144	1.76	12.216	11086.42	82016	1.974	0.031	0.146
2	315.30	0.2832	2.23	14.150	14989.65	95000	2.675	0.031	0.169
3	386.91	0.1980	2.77	16.316	19955.32	109541	3.567	0.031	0.193
4	372.09	0.2313	2.66	16.035	17059.65	107658	3.048	0.031	0.171
5	478.25	0.1515	3.42	19.532	23338.2	131133	4.171	0.031	0.190
6	499.75	0.1528	3.54	21.467	22222.78	144123	3.967	0.031	0.167
7	582.68	0.1183	4.13	24.400	26450.31	163814	4.722	0.031	0.174
8	612.39	0.1137	4.34	25.359	30201.02	170253	5.391	0.031	0.189
9	668.95	0.1027	4.69	28.657	29717.12	192398	5.299	0.031	0.167
10	719.88	0.0937	5.08	29.223	28203.05	196193	5.032	0.031	0.158
11	747.00	0.0899	5.27	29.452	29399.86	197735	5.246	0.031	0.163
12	796.45	0.0833	5.64	30.090	31314.47	202015	5.589	0.031	0.170
13	856.01	0.0785	5.99	33.708	31303.81	226307	5.580	0.031	0.154
14	902.12	0.0730	6.31	34.680	32648.08	232835	5.820	0.031	0.156
15	1,000.25	0.0641	7.02	36.872	36049.17	247553	6.429	0.031	0.162
16	1,041.60	0.0637	7.17	40.326	33565.31	270737	5.972	0.031	0.141
17	1,069.31	0.0638	7.39	39.818	34029.8	267331	6.058	0.031	0.145
18	1,190.55	0.0544	8.29	41.605	36750.92	279327	6.547	0.031	0.151
19	1,217.63	0.0553	8.49	41.501	39271.36	278629	6.997	0.031	0.160
20	1,370.01	0.0482	9.67	42.114	44373.74	282741	7.917	0.031	0.179
21	1,544.59	0.0327	11.50	19.728	54468.39	132446	9.776	0.031	0.463
22	1,665.79	0.0318	12.41	20.612	84942.1	138387	15.246	0.031	0.652
23	1,781.85	0.0312	13.29	21.454	115172.8	144035	20.674	0.031	0.831
24	1,848.16	0.0321	13.80	21.801	156643.4	146367	28.119	0.031	1.095
25	1,959.30	0.0315	14.63	22.665	195107.6	152169	35.025	0.031	1.304
26	2,021.15	0.0323	15.11	23.158	221995	155478	39.855	0.031	1.448
27	2,152.49	0.0313	16.12	24.324	267507.7	163304	48.033	0.031	1.656

# Appendix D: Single- and two-phase calculated data (continued).

Channel D: Water-argon tests.

Number of channels: 7

Channel Dimensions:

Depth ( $\mu\text{m}$ ): 111.330 Hyd. Diameter ( $\mu\text{m}$ ): 111.88Width ( $\mu\text{m}$ ): 112.43 Channel Length (m): 0.0635

Data Point	G	x	f	Two-phase	Q	h - overall	Heat Flux	Nu	Uncertainty	
	$\text{kg/s-m}^2$	Quality		Re-avg	(Watts)	$\text{W/m}^2\text{-K}$	$(\text{W/m}^2)$		U f	U Nu
									(%)	(%)
1	2.089	0.010879	0.2092	393.82	10.488	18.501	70416	3.292	0.031	0.274
2	2.473	0.019053	0.1791	463.81	11.976	22.525	80402	4.011	0.031	0.291
3	2.350	0.0423	0.1903	447.37	12.235	19.518	82141	3.471	0.031	0.249
4	1.929	0.086342	0.2378	375.39	10.946	14.708	73490	2.611	0.031	0.211
5	2.009	0.108608	0.2349	389.53	11.180	15.522	75060	2.757	0.031	0.218
6	2.867	0.008244	0.1512	543.40	15.792	22.709	106027	4.039	0.031	0.225
7	2.281	0.022761	0.1895	440.14	13.199	18.628	88615	3.307	0.031	0.221
8	2.512	0.038094	0.1729	490.26	15.076	19.693	101215	3.493	0.031	0.205
9	2.418	0.063983	0.1804	482.85	15.724	18.302	105564	3.239	0.031	0.183
10	2.492	0.085507	0.1798	495.99	15.918	18.412	106868	3.260	0.031	0.183
11	3.147	0.006462	0.1390	590.19	16.472	26.123	110592	4.651	0.031	0.247
12	3.187	0.015389	0.1390	595.63	16.049	27.724	107751	4.939	0.031	0.268
13	2.914	0.032671	0.1535	548.97	14.859	23.801	99760	4.237	0.031	0.250
14	3.018	0.054392	0.1493	577.41	16.637	24.557	111695	4.365	0.031	0.231
15	9.379	0.075048	0.0538	1.639.05	25.307	78.799	169907	14.144	0.031	0.484
16	10.324	0.074836	0.0491	1.793.54	25.729	100.909	172739	18.124	0.031	0.603
17	10.151	0.083385	0.0503	1.767.26	25.802	106.564	173226	19.137	0.031	0.632
18	9.410	0.099106	0.0552	1.640.06	24.478	106.964	164337	19.209	0.031	0.666
19	10.363	0.098665	0.0504	1.796.23	25.587	163.369	171787	29.355	0.031	0.963
20	10.671	0.041946	0.0461	1.845.36	26.333	159.679	176793	28.683	0.031	0.916
21	12.822	0.003898	0.0361	2.263.41	29.610	221.563	198792	39.695	0.031	1.126
22	12.669	0.009661	0.0367	2.242.86	29.715	244.239	199503	43.747	0.031	1.235
23	11.989	0.019546	0.0391	2.127.16	28.979	226.844	194556	40.625	0.031	1.176
24	12.806	0.025104	0.0369	2.266.55	29.576	242.217	198569	43.392	0.031	1.231
25	12.458	0.037847	0.0384	2.207.01	29.019	228.972	194827	41.020	0.031	1.186
26	2.564	0.259557	0.2434	453.17	10.399	19.229	69815	3.454	0.031	0.291
27	2.827	0.251281	0.2178	500.87	11.679	20.470	78408	3.676	0.031	0.277
28	2.516	0.300019	0.2601	448.83	10.803	18.321	72530	3.289	0.031	0.267
29	2.477	0.330442	0.2746	444.65	10.859	17.222	72903	3.091	0.031	0.251
30	2.757	0.306307	0.2376	495.91	12.245	19.622	82210	3.520	0.031	0.253
31	2.371	0.37896	0.3069	429.03	10.731	17.145	72044	3.076	0.031	0.252
32	2.366	0.393901	0.3138	429.98	10.928	16.653	73371	2.987	0.031	0.241
33	2.497	0.398719	0.2967	458.52	11.989	18.426	80488	3.301	0.031	0.242
34	2.679	0.380372	0.2685	491.55	12.804	20.061	85962	3.594	0.031	0.246
35	2.848	0.374718	0.2553	512.17	12.377	22.515	83095	4.042	0.031	0.285

Appendix D: Single- and two-phase calculated data (continued).

Channel D: Water-helium tests.

Number of channels: 7

Channel Dimensions:

Depth ( $\mu\text{m}$ ): 111.330 Hyd. Diameter ( $\mu\text{m}$ ): 111.88

Width ( $\mu\text{m}$ ): 112.43 Channel Length (m): 0.0635

Data Point	G	x	f	Two-phase	Q	h - overall	Heat Flux	Nu	Uncertainty	
	kg/s-m <sup>2</sup>	Quality		Re-avg	(Watts)	W/m <sup>2</sup> -K	(W/m <sup>2</sup> )		U f	U Nu
									(%)	(%)
1	2.231	0.001031	0.1913	426.51	11.970	21975.3	80364	3.905	0.031	0.283
2	2.251	0.002322	0.1884	433.58	12.061	22957.7	80974	4.076	0.031	0.292
3	1.700	0.013091	0.2487	332.01	9.473	13764.5	63596	2.440	0.031	0.227
4	2.200	0.020904	0.1977	420.98	11.224	16564.4	75355	2.943	0.031	0.232
5	2.641	0.000826	0.1629	500.70	13.924	22348.6	93484	3.974	0.031	0.250
6	2.463	0.002059	0.1737	470.15	13.365	21247.7	89727	3.776	0.031	0.247
7	2.436	0.004182	0.1748	468.04	13.283	20663.3	89179	3.670	0.031	0.242
8	2.555	0.006948	0.1683	487.70	13.544	21047.3	90933	3.740	0.031	0.242
9	2.723	0.009657	0.1601	513.92	13.685	21719.1	91876	3.864	0.031	0.248
10	2.522	0.014943	0.1726	479.40	13.060	18631.3	87683	3.313	0.031	0.225
11	3.564	0.00063	0.1240	657.80	16.526	31265.0	110954	5.576	0.031	0.293
12	3.168	0.001686	0.1393	586.10	14.820	28210.7	99497	5.030	0.031	0.295
13	3.632	0.002604	0.1221	669.36	16.360	32135.2	109839	5.732	0.031	0.304
14	3.521	0.005046	0.1265	647.41	15.441	28175.1	103665	5.027	0.031	0.285
15	3.512	0.007718	0.1271	646.01	15.467	27105.7	103845	4.836	0.031	0.275
16	12.117	0.006072	0.0383	2,143.26	27.175	149225.5	182449	26.729	0.031	0.835
17	12.645	0.00677	0.0368	2,230.58	27.565	161444.8	185066	28.926	0.031	0.889
18	12.621	0.007934	0.0369	2,224.57	27.543	151802.9	184917	27.201	0.031	0.838
19	12.446	0.008825	0.0375	2,192.62	27.186	151164.9	182522	27.088	0.031	0.845
20	12.287	0.010233	0.0381	2,162.37	26.976	140769.3	181108	25.228	0.031	0.795

Appendix D: Single- and two-phase calculated data (continued).

Channel D: Water-Nitrogen tests.      Number of channels:      7  
 Channel Dimensions:  
 Depth ( $\mu\text{m}$ ):      111.330      Hyd. Diameter ( $\mu\text{m}$ ):      111.88  
 Width ( $\mu\text{m}$ ):      112.43      Channel Length (m):      0.0635

Data Point	G	x	f	Two-phase	Q	h - overall	Heat Flux	Nu	Uncertainty	
	kg/s-m <sup>2</sup>	Quality		Re-avg	(Watts)	W/m <sup>2</sup> -K	(W/m <sup>2</sup> )		U <sub>f</sub>	U <sub>Nu</sub>
									(%)	(%)
1	2.215	0.005014	0.1950	422.01	12.598	29001.3	84582	5.182	0.031	0.350
2	1.914	0.011472	0.2268	367.57	10.433	24109.1	70047	4.334	0.031	0.351
3	2.035	0.031934	0.2212	392.73	10.172	23154.1	68293	4.254	0.031	0.347
4	2.162	0.052226	0.2118	427.48	10.742	22184.2	72119	4.157	0.031	0.316
5	1.874	0.087209	0.2488	391.77	9.819	16317.7	65924	3.163	0.031	0.257
6	2.988	0.003938	0.1463	561.31	16.569	29811.0	111241	5.329	0.031	0.277
7	2.606	0.008974	0.1675	495.20	14.168	26176.3	95121	4.699	0.031	0.284
8	2.750	0.017302	0.1584	532.33	15.117	27534.2	101490	4.977	0.031	0.280
9	2.883	0.027687	0.1524	565.18	15.774	27644.6	105904	5.047	0.031	0.270
10	2.271	0.050656	0.1948	463.24	13.048	20351.4	87602	3.794	0.031	0.241
11	3.383	0.003138	0.1293	634.36	18.466	30998.2	123979	5.537	0.031	0.260
12	3.666	0.005736	0.1191	692.02	20.117	35408.3	135059	6.338	0.031	0.271
13	3.175	0.017002	0.1369	615.51	17.864	26372.5	119933	4.764	0.031	0.230
14	11.399	0.030025	0.0440	1,966.22	19.820	232363.5	133070	43.100	0.031	1.759
15	11.496	0.032527	0.0436	1,992.63	19.680	376414.8	132129	69.973	0.031	2.857
16	11.498	0.036541	0.0437	2,004.72	19.602	531532.8	131602	99.179	0.031	4.045
17	11.121	0.040682	0.0453	1,951.09	19.364	641054.1	130008	120.078	0.031	4.936
18	10.892	0.0464	0.0464	1,924.04	19.072	564549.6	128046	106.339	0.031	4.415
19	10.402	0.055856	0.0490	1,857.64	18.648	483437.1	125196	91.915	0.031	3.867
20	2.323	0.189694	0.2452	501.63	8.321	18697.1	55867	4.094	0.031	0.347
21	2.602	0.17327	0.2150	550.13	9.353	21649.7	62795	4.652	0.031	0.357
22	2.219	0.20768	0.2625	489.58	7.804	20722.9	52396	4.635	0.031	0.406
23	8.174	0.0249	0.0439	3,591.24	60.536	48,689	412894	20.402	0.031	0.409
24	8.018	0.0306	0.0442	3,525.12	57.016	44,591	388883	18.799	0.031	0.393



Appendix D: Single- and two-phase calculated data (continued).

Channel E: Argon gas tests.                      Number of channels:                      9  
 Channel Dimensions:  
 Depth ( $\mu\text{m}$ ):                      74.910                      Hyd. Diameter ( $\mu\text{m}$ ):                      79.991  
 Width ( $\mu\text{m}$ ):                      85.81                      Channel Length (m):                      0.0635

Data Point					Heat Trans.			Uncertainty	
	Re	f	Velocity	Q	coeff.	Heat Flux	Nu	U-f	U-Nu
			(m/s)	(Watts)	W/m2-K	(W/m^2)			
1	56.9	0.7871	8.30	0.0004	0.250	3.02	0.001107	0.031	1.220
2	124.1	0.4542	15.01	0.0026	1.698	21.32	0.007506	0.031	0.388
3	242.2	0.2484	24.03	0.0059	3.763	49.27	0.016621	0.031	0.333
4	670.4	0.0839	48.46	0.0396	28.604	331.19	0.125786	0.031	0.163
5	984.3	0.0581	61.15	0.0686	50.870	573.26	0.223470	0.031	0.150
6	1,330.2	0.0490	69.58	0.1123	86.576	938.01	0.379936	0.031	0.139
7	1,595.3	0.0427	76.10	0.1480	117.783	1236.17	0.516616	0.031	0.136
8	1,857.5	0.0397	80.35	0.1857	151.493	1551.63	0.664470	0.031	0.136
9	2,074.2	0.0398	81.67	0.2206	180.918	1842.54	0.793715	0.031	0.135
10	2,270.6	0.0391	83.40	0.2629	218.840	2196.08	0.960098	0.031	0.135
11	2,443.7	0.0376	85.70	0.2996	251.080	2503.03	1.101827	0.031	0.135
12	2,601.3	0.0360	88.21	0.3423	292.292	2859.95	1.282884	0.031	0.135
13	2,718.5	0.0349	90.00	0.3830	331.911	3199.55	1.457166	0.031	0.135
14	2,822.1	0.0340	91.56	0.4199	372.545	3508.08	1.636273	0.031	0.137
15	2,907.7	0.0333	92.87	0.4636	418.266	3873.20	1.837930	0.031	0.138
16	3,000.0	0.0318	95.24	0.4943	453.425	4129.74	1.993284	0.031	0.140
17	3,054.3	0.0312	96.40	0.5343	502.941	4464.03	2.212036	0.031	0.142
18	3,094.4	0.0307	97.44	0.5686	545.138	4750.35	2.399041	0.031	0.143
19	3,115.5	0.0303	98.14	0.6030	588.852	5037.59	2.592562	0.031	0.145

Appendix D: Single- and two-phase calculated data (continued).

Channel E: Helium gas tests.      Number of channels:      9  
 Channel Dimensions:  
 Depth ( $\mu\text{m}$ ):      74.910      Hyd. Diameter ( $\mu\text{m}$ ):      79.991  
 Width ( $\mu\text{m}$ ):      85.81      Channel Length (m):      0.0635

Data Point	Re	f	Velocity (m/s)	Q (Watts)	Heat Trans.	Heat Flux (W/m <sup>2</sup> )	Nu	Uncertainty	
					coeff. W/m <sup>2</sup> -K			U-f (%)	U-Nu (%)
1	8.2	4.7520	10.44	0.0000	0.004	0.05	0.0000021	0.031	93.291
2	18.2	3.2159	18.14	0.0006	0.398	4.88	0.0002063	0.031	2.022
3	31.4	2.0670	25.99	0.0023	1.644	19.51	0.0008500	0.031	0.862
4	79.4	0.9333	45.38	0.0266	21.738	221.99	0.0111929	0.031	0.208
5	137.5	0.5052	64.75	0.0416	33.034	347.14	0.0170264	0.031	0.219
6	195.4	0.3484	80.08	0.0477	36.032	398.68	0.0185993	0.031	0.255
7	253.6	0.2713	92.70	0.0813	65.293	679.45	0.0336546	0.031	0.203
8	306.3	0.2247	103.33	0.1278	111.144	1067.59	0.0571766	0.031	0.172
9	368.1	0.1891	113.95	0.1551	134.506	1295.99	0.0692060	0.031	0.169
10	428.6	0.1643	123.43	0.1909	170.121	1594.71	0.0875112	0.031	0.164
11	491.1	0.1448	132.48	0.2240	202.283	1871.33	0.1040654	0.031	0.162
12	547.1	0.1311	140.04	0.2619	242.418	2187.79	0.1246809	0.031	0.159
13	610.3	0.1186	148.03	0.2906	276.671	2427.36	0.1423544	0.031	0.161
14	547.6	0.1609	160.40	0.7424	349.572	5063.88	0.5643628	0.031	0.159
15	672.9	0.1092	155.04	0.3228	303.508	2696.40	0.1562152	0.031	0.158
16	732.6	0.1013	161.63	0.3675	356.285	3070.11	0.1833413	0.031	0.157
17	796.1	0.0954	167.29	0.4160	416.391	3475.62	0.2142466	0.031	0.157
18	862.0	0.0892	173.61	0.4504	453.954	3762.95	0.2336700	0.031	0.159
19	929.3	0.0840	179.65	0.5242	563.300	4378.90	0.2897979	0.031	0.160

Appendix D: Single- and two-phase calculated data (continued).

Channel E: Nitrogen gas tests.      Number of channels:      9  
 Channel Dimensions:  
 Depth ( $\mu\text{m}$ ):      74.910      Hyd. Diameter ( $\mu\text{m}$ ):      79.991  
 Width ( $\mu\text{m}$ ):      85.81      Channel Length (m):      0.0635

Data Point				Heat Trans.				Uncertainty	
	Re	f	Velocity	Q	coeff.	Heat Flux	Nu	U-f	U-Nu
			(m/s)	(Watts)	W/m2-K	(W/m^2)		(%)	(%)
1	45.1	1.3736	7.21	0.00022	0.121	1.81	0.00037	0.031	5.006
2	88.4	0.8327	12.30	0.0021	1.136	17.55	0.003	0.031	1.032
3	169.3	0.4564	19.89	0.0060	3.224	50.18	0.010	0.031	0.705
4	374.9	0.2138	34.10	0.0223	12.371	185.92	0.038	0.031	0.444
5	637.6	0.1101	50.53	0.0594	36.477	496.33	0.110	0.031	0.313
6	844.3	0.0867	59.30	0.0992	62.504	828.46	0.189	0.031	0.270
7	1.096.7	0.0669	69.53	0.1442	93.936	1205.09	0.284	0.031	0.258
8	1.255.5	0.0584	75.43	0.1693	117.794	1414.74	0.356	0.031	0.263
9	1,491.6	0.0500	83.00	0.2120	152.776	1770.95	0.461	0.031	0.262
10	1,663.3	0.0458	87.77	0.2436	179.600	2035.44	0.542	0.031	0.264
11	1.825.8	0.0440	90.67	0.2759	205.738	2305.18	0.621	0.031	0.265
12	1.943.9	0.0428	92.68	0.3070	232.004	2564.57	0.700	0.031	0.263
13	2,105.6	0.0420	94.64	0.3490	267.851	2915.57	0.808	0.031	0.264
14	2.236.0	0.0401	97.40	0.3841	299.654	3209.15	0.904	0.031	0.265
15	2.341.3	0.0391	99.25	0.4195	331.761	3504.29	1.001	0.031	0.266
16	2,458.7	0.0376	101.64	0.4700	378.093	3926.13	1.140	0.031	0.264
17	2.550.9	0.0368	103.36	0.5325	440.377	4449.02	1.327	0.031	0.261
18	2.644.9	0.0355	105.51	0.5866	495.384	4900.63	1.493	0.031	0.261
19	2,737.8	0.0347	107.25	0.6434	555.359	5374.75	1.673	0.031	0.263

Appendix D: Single- and two-phase calculated data (continued).

Channel E: Water tests.

Number of channels: 9

Channel Dimensions:

Depth ( $\mu\text{m}$ ): 74.910 Hyd. Diameter ( $\mu\text{m}$ ): 79.991

Width ( $\mu\text{m}$ ): 85.81 Channel Length (m): 0.0635

Data Point	Re	f	Velocity	Q	h - overall	Heat Flux	Nu	Uncertainty	
								U-f	U_Nu
			(m/s)	(Watts)	W/m <sup>2</sup> -K	(W/m <sup>2</sup> )		(%)	(%)
1	322.80	0.1357	3.28	11.378	10410.22	95051	1.333	0.031	0.127
2	401.18	0.1000	4.13	13.315	15030.75	111235	1.926	0.031	0.152
3	523.65	0.0651	5.46	16.133	20767.85	134778	2.666	0.031	0.171
4	523.12	0.0713	5.52	15.107	21801.61	126207	2.802	0.031	0.190
5	599.17	0.0585	6.36	16.398	25710.04	136992	3.306	0.031	0.206
6	689.54	0.0513	7.16	21.014	28933.08	175557	3.712	0.031	0.181
7	798.70	0.0437	7.97	29.405	34474.82	245652	4.403	0.031	0.153
8	890.00	0.0385	8.93	30.500	38928.53	254804	4.975	0.031	0.166
9	932.80	0.0370	9.33	30.777	40368.2	257119	5.157	0.031	0.171
10	1.016.27	0.0333	10.19	31.711	43412.88	264917	5.548	0.031	0.179
11	1.137.37	0.0303	11.12	32.042	46454.04	267685	5.919	0.031	0.190
12	1.181.94	0.0295	11.56	31.728	47760.01	265062	6.086	0.031	0.197
13	1.226.75	0.0291	11.97	31.726	49018.13	265044	6.245	0.031	0.203
14	1.276.90	0.0283	12.45	31.534	50241.68	263439	6.400	0.031	0.209
15	1.334.82	0.0271	13.00	31.735	52399.8	265123	6.674	0.031	0.217
16	1.388.89	0.0264	13.50	31.982	54001.98	267186	6.877	0.031	0.222
17	1.502.67	0.0245	14.39	37.381	57361.04	312292	7.292	0.031	0.202
18	1.575.97	0.0232	15.09	38.036	59343.02	317763	7.543	0.031	0.206
19	1.644.87	0.0220	15.74	38.709	63047.47	323381	8.014	0.031	0.214
20	1.730.75	0.0211	16.57	39.196	66401.86	327449	8.440	0.031	0.223

Appendix D: Single- and two-phase calculated data (continued).

Channel E: Water-argon tests.

Number of channels: 9

Channel Dimensions:

Depth ( $\mu\text{m}$ ): 74.910 Hyd. Diameter ( $\mu\text{m}$ ): 79.991

Width ( $\mu\text{m}$ ): 85.81 Channel Length (m): 0.0635

Data Point	G	x	f	Two-phase	Q	h - overall	Heat Flux	Nu	Uncertainty	
	kg/s-m <sup>2</sup>	Quality		Re-avg	(Watts)	W/m <sup>2</sup> -K	(W/m <sup>2</sup> )		U f (%)	U Nu (%)
1	6.228	0.007187	0.1002	822.96	14.410	28950.8	137581	3.693	0.031	0.454
2	6.067	0.014325	0.1031	805.91	13.550	27260.6	129370	3.476	0.031	0.457
3	5.325	0.032079	0.1193	709.20	12.103	23568.4	115553	3.004	0.031	0.443
4	4.994	0.068938	0.1311	670.93	11.795	20587.1	112611	2.623	0.031	0.401
5	5.155	0.115199	0.1336	693.52	12.394	21238.0	118337	2.707	0.031	0.394
6	5.998	0.143928	0.1192	803.58	14.450	22849.5	137964	2.914	0.031	0.369
7	5.527	0.198647	0.1390	736.41	12.800	20704.3	122207	2.644	0.031	0.378
8	5.010	0.290717	0.1707	677.91	12.578	17791.7	120087	2.270	0.031	0.334
9	8.568	0.005491	0.0727	1,132.51	21.338	38521.1	203731	4.913	0.031	0.410
10	9.015	0.009792	0.0692	1,195.45	22.365	40258.2	213532	5.133	0.031	0.409
11	8.948	0.017771	0.0699	1,192.59	22.217	39415.9	212120	5.023	0.031	0.404
12	8.827	0.041314	0.0720	1,186.50	22.306	37192.7	212971	4.737	0.031	0.382
13	8.370	0.071618	0.0776	1,137.07	22.117	33965.9	211169	4.322	0.031	0.354
14	8.385	0.101394	0.0804	1,133.47	21.704	32778.8	207226	4.174	0.031	0.351
15	8.510	0.133176	0.0820	1,152.65	22.144	31916.1	211424	4.065	0.031	0.337
16	12.474	0.003446	0.0510	1,609.79	23.268	49284.1	222157	6.301	0.031	0.490
17	12.653	0.006997	0.0503	1,639.25	23.785	49852.5	227088	6.371	0.031	0.486
18	12.533	0.012729	0.0509	1,629.50	23.418	50513.3	223584	6.454	0.031	0.498
19	11.806	0.031952	0.0546	1,549.54	22.999	46433.0	219582	5.928	0.031	0.468
20	11.136	0.055562	0.0590	1,470.72	22.683	43557.5	216569	5.558	0.031	0.445
21	10.392	0.089591	0.0652	1,380.98	22.365	39208.6	213536	5.001	0.031	0.409
22	4.992	0.260945	0.1699	653.61	11.871	21748.2	113340	2.784	0.031	0.418
23	4.815	0.282549	0.1811	631.72	11.644	22060.6	111174	2.824	0.031	0.429
24	4.505	0.326471	0.2061	591.49	10.923	20120.4	104292	2.576	0.031	0.418
25	4.566	0.344577	0.2082	601.61	11.168	19835.1	106626	2.539	0.031	0.405
26	4.955	0.324258	0.1866	650.85	12.024	22214.8	114804	2.844	0.031	0.419
27	5.184	0.346127	0.1837	683.62	12.672	21314.2	120991	2.729	0.031	0.387
28	4.592	0.3938	0.2217	611.17	11.665	18661.0	111377	2.388	0.031	0.369
29	4.979	0.371236	0.2016	647.92	11.513	21789.2	109923	2.794	0.031	0.431
30	5.119	0.394619	0.2021	671.24	12.201	20735.2	116493	2.657	0.031	0.392

## Appendix D: Single- and two-phase calculated data (continued).

Channel E: Water-helium tests.      Number of channels:      9  
Channel Dimensions:  
Depth ( $\mu\text{m}$ ):      74.910      Hyd. Diameter ( $\mu\text{m}$ ):      79.991  
Width ( $\mu\text{m}$ ):      85.81      Channel Length (m):      0.0635

Data Point	G	x	f	Two-phase	Q	h - overall	Heat Flux	Nu	Uncertainty	
	kg/s-m <sup>2</sup>	Quality		Re-avg	(Watts)	W/m <sup>2</sup> -K	(W/m <sup>2</sup> )		U f (%)	U Nu (%)
1	6.134	0.000746	0.1023	800.92	12.841	28451.7	122601	3.633	0.031	0.250
2	6.599	0.001452	0.0947	865.77	13.844	30312.1	132181	3.869	0.031	0.247
3	5.766	0.003037	0.1082	758.60	12.143	25734.9	115937	3.284	0.031	0.240
4	6.939	0.00562	0.0912	902.95	13.570	29642.2	129565	3.787	0.031	0.249
5	6.677	0.010206	0.0958	863.64	12.470	27242.6	119062	3.483	0.031	0.251
6	6.485	0.021816	0.1004	834.13	11.774	23485.9	112410	3.004	0.031	0.234
7	6.182	0.033362	0.1072	790.35	10.909	20924.0	104151	2.679	0.031	0.228
8	8.655	0.000578	0.0711	1,151.87	21.823	37094.5	208363	4.727	0.031	0.194
9	8.618	0.001019	0.0712	1,150.75	21.588	36906.1	206113	4.702	0.031	0.195
10	8.530	0.001972	0.0717	1,144.30	21.139	36123.5	201828	4.600	0.031	0.196
11	8.427	0.004342	0.0724	1,135.46	20.894	34785.8	199486	4.427	0.031	0.191
12	8.284	0.008146	0.0739	1,116.68	20.386	32778.9	194639	4.172	0.031	0.186
13	7.160	0.019455	0.0863	967.63	17.857	26219.7	170495	3.336	0.031	0.173
14	11.360	0.000457	0.0554	1,479.04	23.534	45278.4	224693	5.783	0.031	0.222
15	11.427	0.000814	0.0547	1,498.86	23.693	45206.5	226210	5.770	0.031	0.221
16	11.504	0.0014	0.0542	1,511.48	23.076	44250.8	220322	5.647	0.031	0.223
17	11.058	0.003639	0.0565	1,455.32	21.808	41253.1	208217	5.263	0.031	0.221
18	10.568	0.006733	0.0591	1,394.47	20.961	38689.9	200132	4.935	0.031	0.216
19	9.822	0.013858	0.0640	1,298.01	19.948	34416.8	190453	4.389	0.031	0.204
20	37.627	0.001858	0.0399	5,055.33	66.396	78629.4	633927	10.012	0.031	0.165
21	37.218	0.002879	0.0400	4,972.80	61.903	70146.1	591031	8.937	0.031	0.165
22	36.041	0.003956	0.0404	4,827.05	62.405	71215.5	595827	9.071	0.031	0.163
23	35.254	0.005103	0.0406	4,728.15	60.463	69852.0	577281	8.896	0.031	0.165
24	34.423	0.006289	0.0409	4,593.99	56.931	63749.6	543558	8.123	0.031	0.165
25	53.416	0.000604	0.0366	7,122.66	81.433	85108.0	777496	10.845	0.031	0.166
26	52.832	0.001333	0.0367	7,061.31	82.945	86925.6	791932	11.074	0.031	0.164
27	51.241	0.002087	0.0370	6,846.96	81.473	84418.4	777875	10.755	0.031	0.162
28	50.549	0.002832	0.0369	6,869.00	79.115	82722.3	755366	10.520	0.031	0.164
29	48.880	0.003665	0.0373	6,633.22	75.715	78941.3	722902	10.041	0.031	0.165
30	47.653	0.004541	0.0375	6,465.20	78.338	80115.9	747941	10.190	0.031	0.158
31	66.651	0.000497	0.0346	8,853.35	81.637	99461.4	779448	12.679	0.031	0.201
32	64.656	0.001092	0.0349	8,595.13	80.782	98923.3	771278	12.609	0.031	0.199
33	64.025	0.001682	0.0350	8,509.78	81.183	100085.8	775113	12.758	0.031	0.198

Appendix D: Single- and two-phase calculated data (continued).

Channel E: Water-Nitrogen tests.      Number of channels:      9  
 Channel Dimensions:  
 Depth ( $\mu\text{m}$ ):      74.910      Hyd. Diameter ( $\mu\text{m}$ ):      79.991  
 Width ( $\mu\text{m}$ ):      85.81      Channel Length (m):      0.0635

Data Point	G	x	f	Two-phase	Q	h - overall	Heat Flux	Nu	Uncertainty	
	kg/s-m <sup>2</sup>	Quality		Re-avg	(Watts)	W/m <sup>2</sup> -K	(W/m <sup>2</sup> )		U f (%)	U Nu (%)
1	5.339	0.003374	0.1147	718.78	13.955	23791.7	133237	3.039	0.031	0.194
2	5.300	0.008109	0.1154	720.61	13.281	23017.2	126804	2.952	0.031	0.197
3	4.858	0.016291	0.1267	667.43	12.027	21252.8	114830	2.747	0.031	0.201
4	5.678	0.032358	0.1112	784.97	13.069	24073.6	124777	3.164	0.031	0.210
5	5.058	0.06762	0.1294	724.77	11.772	19820.9	112395	2.699	0.031	0.193
6	4.787	0.110264	0.1431	717.11	10.776	16831.6	102888	2.396	0.031	0.182
7	7.290	0.002999	0.0836	984.75	20.836	31271.8	198938	3.992	0.031	0.172
8	7.236	0.006644	0.0849	976.75	19.249	31126.2	183788	3.989	0.031	0.185
9	7.968	0.010006	0.0769	1,085.26	21.237	34036.9	202760	4.373	0.031	0.183
10	7.377	0.023078	0.0839	1,020.52	19.405	29828.0	185277	3.880	0.031	0.177
11	7.593	0.048074	0.0833	1,079.83	19.721	29869.2	188291	3.981	0.031	0.175
12	7.386	0.075474	0.0879	1,082.40	19.133	26499.5	182677	3.630	0.031	0.162
13	10.469	0.00182	0.0587	1,398.47	26.738	42193.0	255289	5.385	0.031	0.182
14	10.611	0.004108	0.0577	1,430.27	26.633	43035.6	254286	5.501	0.031	0.186
15	10.415	0.007857	0.0588	1,412.61	26.013	41018.3	248363	5.260	0.031	0.183
16	10.510	0.017202	0.0585	1,446.98	26.224	40338.7	250375	5.216	0.031	0.179
17	10.219	0.035881	0.0612	1,434.49	25.034	37126.8	239013	4.889	0.031	0.174
18	9.607	0.054546	0.0661	1,377.33	23.837	34120.1	227589	4.576	0.031	0.168
19	4.004	0.215805	0.1953	668.82	8.354	16709.2	79762	2.683	0.031	0.224
20	4.858	0.182026	0.1550	777.08	10.215	21268.0	97525	3.283	0.031	0.232
21	4.230	0.215897	0.1874	696.82	8.350	17712.5	79720	2.849	0.031	0.237
22	4.759	0.1945	0.1631	760.42	9.479	20204.1	90506	3.170	0.031	0.238
23	4.482	0.214879	0.1773	734.24	8.923	18700.2	85193	3.005	0.031	0.234
24	4.753	0.204562	0.1653	767.93	9.577	20172.1	91439	3.203	0.031	0.235
25	4.764	0.208432	0.1663	770.64	9.413	17964.9	89868	2.866	0.031	0.216
26	4.208	0.243076	0.1969	708.73	8.085	15338.5	77197	2.553	0.031	0.215
27	4.452	0.232695	0.1844	737.05	8.503	15966.6	81181	2.625	0.031	0.214
28	4.275	0.245873	0.1954	719.04	8.157	15409.0	77877	2.575	0.031	0.215
29	4.925	0.224881	0.1645	809.63	9.766	18184.4	93242	2.960	0.031	0.211

Appendix D: Single- and two-phase calculated data (continued).

Channel F: Argon gas tests.                      Number of channels:                      11  
 Channel Dimensions:  
 Depth ( $\mu\text{m}$ ):                      54.090                      Hyd. Diameter ( $\mu\text{m}$ ):                      55.99  
 Width ( $\mu\text{m}$ ):                      58.02                      Channel Length (m):                      0.0635

Data Point					Heat Trans.				
	Re	f	Velocity	Q	coeff.	Heat Flux	Nu	U-f	U-Nu
			(m/s)	(Watts)	W/m <sup>2</sup> -K	(W/m <sup>2</sup> )			
1	145.7	0.1223	24.67	0.0008	0.551	8.28	0.001706	0.031	1.137
2	347.7	0.0853	38.84	0.0061	4.396	63.99	0.013568	0.031	0.367
3	701.6	0.0483	57.31	0.0273	21.578	287.59	0.066371	0.031	0.187
4	1.078.9	0.0330	72.52	0.0579	48.464	609.87	0.148828	0.031	0.154
5	1.410.0	0.0283	80.73	0.0897	76.046	944.59	0.233531	0.031	0.144
6	1.907.0	0.0190	100.20	0.1361	118.997	1432.59	0.365207	0.031	0.141
7	2.087.5	0.0184	102.90	0.1640	146.931	1726.11	0.450804	0.031	0.141
8	2.174.9	0.0184	103.58	0.1842	167.045	1939.67	0.512552	0.031	0.140
9	2.306.9	0.0177	106.40	0.2159	194.249	2273.51	0.596349	0.031	0.139
10	2.423.4	0.0167	110.05	0.2660	241.600	2800.32	0.741957	0.031	0.133
11	2.521.8	0.0158	113.72	0.3013	279.402	3171.87	0.858105	0.031	0.134
12	2.576.9	0.0152	116.18	0.3248	308.825	3419.38	0.948449	0.031	0.136
13	2.604.6	0.0149	117.89	0.3697	348.375	3892.05	1.070968	0.031	0.133
14	2.613.0	0.0146	119.28	0.4038	386.212	4251.42	1.187753	0.031	0.133
15	2.670.9	0.0137	123.44	0.4438	429.733	4672.60	1.322483	0.031	0.134
16	5.082.5	0.0557	108.95	1.0864	459.665	7409.76	6.401325	0.031	0.135
17	2.676.9	0.0133	125.11	0.4768	472.083	5019.47	1.453480	0.031	0.139
18	2.680.5	0.0129	127.17	0.4950	504.079	5211.54	1.552640	0.031	0.139
19	2.686.9	0.0125	129.58	0.5337	551.076	5618.95	1.699199	0.031	0.139



Appendix D: Single- and two-phase calculated data (continued).

Channel F: Helium gas tests.

Number of channels: 11

Channel Dimensions:

Depth ( $\mu\text{m}$ ): 54.090

Hyd. Diameter ( $\mu\text{m}$ ): 55.99

Width ( $\mu\text{m}$ ): 58.02

Channel Length (m): 0.0635

Data Point	Re	f	Velocity (m/s)	Q (Watts)	Heat Trans.	Heat Flux (W/m <sup>2</sup> )	Nu	Uncertainty	
					coeff. W/m <sup>2</sup> -K			U-f (%)	U-Nu (%)
1	9.2	6.8701	11.31						
2	26.7	2.2902	23.32						
3	44.7	1.2444	33.34	0.0007	0.396	7.30	0.0001439	0.031	3.030
4	115.8	0.4706	58.88	0.0193	13.787	203.61	0.0049957	0.031	0.275
5	192.3	0.2823	78.38	0.0310	22.614	326.18	0.0081979	0.031	0.275
6	256.9	0.1983	94.74	0.0517	39.278	544.46	0.0142169	0.031	0.222
7	347.8	0.1431	113.22	0.0933	74.924	982.58	0.0270628	0.031	0.173
8	426.5	0.1130	128.20	0.0934	71.515	983.37	0.0258719	0.031	0.201
9	501.2	0.0940	141.65	0.1528	126.215	1608.59	0.0455413	0.031	0.155
10	584.7	0.0791	155.34	0.2166	186.704	2280.65	0.0672798	0.031	0.137
11	669.6	0.0681	168.26	0.2632	235.164	2771.07	0.0846366	0.031	0.134
12	741.6	0.0606	179.04	0.3002	272.230	3160.98	0.0979149	0.031	0.132
13	825.5	0.0541	190.15	0.3522	317.155	3708.04	0.1140706	0.031	0.128
14	905.9	0.0488	200.81	0.3860	353.058	4063.47	0.1269252	0.031	0.128
15	983.7	0.0446	210.66	0.4182	382.957	4402.76	0.1376618	0.031	0.129
16	1.053.5	0.0418	218.11	0.4552	420.105	4792.10	0.1509887	0.031	0.128
17	1.140.2	0.0384	228.13	0.5178	488.405	5451.28	0.1754492	0.031	0.126
18	1.224.0	0.0356	237.50	0.5582	530.240	5876.87	0.1905295	0.031	0.126
19	1.297.5	0.0334	245.52	0.6142	597.175	6466.18	0.2145224	0.031	0.126

Appendix D: Single- and two-phase calculated data (continued).

Channel F: Nitrogen gas tests.      Number of channels:      11  
 Channel Dimensions:  
 Depth ( $\mu\text{m}$ ):      54.090      Hyd. Diameter ( $\mu\text{m}$ ):      55.99  
 Width ( $\mu\text{m}$ ):      58.02      Channel Length (m):      0.0635

Data Point	Re	f	Velocity (m/s)	Q (Watts)	Heat Trans.	Heat Flux (W/m <sup>2</sup> )	Nu	Uncertainty	
					coeff. W/m <sup>2</sup> -K			U-f (%)	U-Nu (%)
1	55.0	0.7152	5.07E-07	11.22	0.00020	0.145	2.08	0.031	2.675
2	194.5	0.2003	1.83E-06	28.30	0.0042	3.197	43.84	0.031	0.464
3	501.1	0.0716	4.89E-06	53.88	0.0270	22.831	284.57	0.031	0.206
4	778.8	0.0464	7.86E-06	70.36	0.0524	45.597	552.20	0.031	0.178
5	999.7	0.0373	1.04E-05	80.61	0.0834	75.777	878.47	0.031	0.158
6	1,252.1	0.0298	1.36E-05	92.02	0.1152	105.620	1213.18	0.031	0.152
7	1,481.4	0.0251	1.66E-05	101.56	0.1459	133.787	1536.01	0.031	0.149
8	1,678.1	0.0222	1.95E-05	109.12	0.1766	162.516	1859.72	0.031	0.146
9	1,828.3	0.0208	2.21E-05	113.71	0.2040	189.818	2148.03	0.031	0.145
10	1,966.4	0.0204	2.53E-05	115.91	0.2395	224.041	2521.75	0.031	0.143
11	2,059.9	0.0203	2.81E-05	117.16	0.2742	259.282	2887.32	0.031	0.141
12	2,140.1	0.0200	3.1E-05	118.66	0.3147	302.902	3313.19	0.031	0.139
13	2,223.9	0.0193	3.39E-05	121.36	0.3514	344.821	3699.41	0.031	0.139
14	2,303.8	0.0186	3.76E-05	124.10	0.3909	385.943	4115.64	0.031	0.139
15	2,368.9	0.0178	3.96E-05	127.21	0.4199	419.024	4421.19	0.031	0.138
16	2,430.3	0.0172	4.31E-05	129.97	0.4595	465.332	4837.73	0.031	0.139
17	2,470.5	0.0167	4.62E-05	132.06	0.4987	514.966	5250.84	0.031	0.139
18	2,512.6	0.0161	5.06E-05	134.80	0.5464	571.531	5752.65	0.031	0.140

Appendix D: Single- and two-phase calculated data (continued).

Channel F: Water tests.

Number of channels: 11

Channel Dimensions:

Depth ( $\mu\text{m}$ ): 54.090      Hyd. Diameter ( $\mu\text{m}$ ): 55.99

Width ( $\mu\text{m}$ ): 58.02      Channel Length (m): 0.0635

Data Point	Re	f	Q	h - overall	Heat Flux	Nu	Uncertainty	
							U-f	U_Nu
			(Watts)	W/m <sup>2</sup> -K	(W/m <sup>2</sup> )		(%)	(%)
1	364.88	0.0723	10.245	15,046	107865	1.340	0.031	0.152
2	398.96	0.0641	11.237	17,194	118310	1.531	0.031	0.157
3	431.38	0.0570	12.115	18,967	127553	1.689	0.031	0.161
4	415.62	0.0631	11.621	18,533	122346	1.651	0.031	0.163
5	450.05	0.0561	12.956	20,932	136404	1.866	0.031	0.165
6	468.74	0.0539	13.164	22,716	138591	2.024	0.031	0.175
7	441.04	0.0629	12.216	21,959	128611	1.958	0.031	0.182
8	457.32	0.0599	12.562	22,796	132250	2.034	0.031	0.183
9	574.01	0.0394	15.313	29,028	161218	2.591	0.031	0.191
10	551.25	0.0438	14.411	27,937	151722	2.495	0.031	0.196
11	511.03	0.0523	12.944	25,983	136279	2.321	0.031	0.203
12	530.98	0.0502	12.858	26,750	135370	2.392	0.031	0.210
13	648.20	0.0346	15.320	32,911	161294	2.944	0.031	0.217
14	572.29	0.0454	12.758	26,782	134314	2.398	0.031	0.214
15	651.52	0.0365	14.272	32,113	150261	2.876	0.031	0.228
16	674.09	0.0353	14.434	33,609	151966	3.011	0.031	0.236

Appendix D: Single- and two-phase calculated data (continued).

Channel F: Water-argon tests.      Number of channels:      11  
 Channel Dimensions:  
 Depth ( $\mu\text{m}$ ):      54.090      Hyd. Diameter ( $\mu\text{m}$ ):      55.99  
 Width ( $\mu\text{m}$ ):      58.02      Channel Length (m):      0.0635

Data Point	G	x	f	Two-phase	Q	h - overall	Heat Flux	Nu	Uncertainty	
	kg/s-m <sup>2</sup>	Quality		Re-avg	(Watts)	W/m <sup>2</sup> -K	(W/m <sup>2</sup> )		U f (%)	U Nu (%)
1	6.009	0.011125	0.1432	576.32	12.011	18469.8	126450	1.642	0.031	0.159
2	5.904	0.021073	0.1467	568.39	11.283	17774.6	118785	1.580	0.031	0.163
3	6.953	0.0269	0.1247	672.58	13.488	20120.2	142003	1.787	0.031	0.156
4	6.032	0.045597	0.1460	585.69	11.318	16633.3	119153	1.477	0.031	0.155
5	5.847	0.057341	0.1525	567.75	11.008	15708.6	115895	1.395	0.031	0.151
6	6.072	0.068745	0.1484	590.64	11.238	16621.6	118312	1.476	0.031	0.156
7	7.098	0.067649	0.1265	691.92	13.273	19097.9	139739	1.696	0.031	0.152
8	6.078	0.091009	0.1513	593.58	11.229	15676.4	118219	1.392	0.031	0.149
9	6.501	0.095887	0.1419	636.35	12.194	16565.5	128379	1.471	0.031	0.145
10	6.582	0.106942	0.1423	642.75	12.043	16334.5	126791	1.451	0.031	0.146
11	7.132	0.10611	0.1304	700.62	13.500	17586.2	142127	1.561	0.031	0.140
12	6.727	0.128932	0.1433	654.23	12.127	16392.9	127677	1.457	0.031	0.146
13	31.165	0.017103	0.0284	2,923.20	43.282	50059.2	455682	4.462	0.031	0.141
14	31.196	0.035853	0.0286	2,956.84	46.586	57607.9	490467	5.130	0.031	0.143
15	30.715	0.055196	0.0295	2,927.99	47.424	60080.0	499285	5.348	0.031	0.144
16	30.535	0.074868	0.0303	2,914.96	47.661	61297.7	501778	5.457	0.031	0.145
17	30.226	0.094422	0.0313	2,877.65	46.443	58768.9	488954	5.234	0.031	0.144
18	29.246	0.117489	0.0337	2,747.15	40.863	47466.4	430207	4.234	0.031	0.141
19	63.081	0.008676	0.0385	5,851.46	66.229	74780.1	697268	6.672	0.031	0.157
20	60.942	0.01822	0.0388	5,712.27	67.491	80039.2	710560	7.134	0.031	0.157
21	60.823	0.027982	0.0390	5,670.12	63.486	72318.4	668390	6.450	0.031	0.158
22	59.453	0.038084	0.0393	5,556.20	64.597	74126.5	680093	6.611	0.031	0.155
23	58.733	0.048643	0.0395	5,496.93	63.203	73330.6	665407	6.539	0.031	0.157
24	57.933	0.059349	0.0398	5,395.78	60.110	67800.5	632849	6.050	0.031	0.158
25	85.558	0.005987	0.0356	7,958.35	81.870	86958.5	861937	7.756	0.031	0.161
26	85.171	0.01313	0.0357	7,941.59	83.927	89335.7	883594	7.967	0.031	0.158
27	83.159	0.02042	0.0360	7,752.45	82.982	87501.9	873651	7.804	0.031	0.157
28	82.574	0.02753	0.0359	7,828.88	81.104	86317.9	853881	7.685	0.031	0.159
29	80.429	0.035373	0.0363	7,615.76	78.179	83158.8	823081	7.405	0.031	0.160
30	79.007	0.043493	0.0365	7,479.80	81.496	85378.5	858001	7.604	0.031	0.153
31	106.654	0.004932	0.0337	9,882.57	81.998	99551.4	863285	8.883	0.031	0.193
32	104.011	0.010782	0.0340	9,645.79	81.565	99557.5	858731	8.883	0.031	0.191
33	103.536	0.01652	0.0341	9,600.53	82.396	101355.0	867479	9.044	0.031	0.190

# Appendix D: Single- and two-phase calculated data (continued).

Channel F: Water-helium tests.

Number of channels: 11

Channel Dimensions:

Depth ( $\mu\text{m}$ ): 54.090Hyd. Diameter ( $\mu\text{m}$ ): 55.99Width ( $\mu\text{m}$ ): 58.02

Channel Length (m): 0.0635

Data Point	G	x	f	Two-phase	Q	h - overall	Heat Flux	Nu	Uncertainty	
	kg/s-m <sup>2</sup>	Quality		Re-avg	(Watts)	W/m <sup>2</sup> -K	(W/m <sup>2</sup> )		U f (%)	U Nu (%)
1	6.427	0.001368	0.1306	625.35	13.300	21013.8	140020	1.865	0.031	0.162
2	7.013	0.002162	0.1199	681.76	13.673	21116.2	143948	1.874	0.031	0.160
3	6.023	0.003809	0.1405	582.73	11.036	17843.0	116188	1.584	0.031	0.168
4	6.898	0.003821	0.1231	665.34	12.727	20883.4	133992	1.855	0.031	0.170
5	5.976	0.005908	0.1424	576.54	10.681	16951.1	112447	1.506	0.031	0.166
6	6.748	0.005732	0.1269	646.62	11.828	19234.0	124523	1.710	0.031	0.170
7	7.506	0.007325	0.1152	713.35	12.405	20446.1	130601	1.819	0.031	0.173
8	7.071	0.010534	0.1226	672.77	11.704	18795.8	123224	1.672	0.031	0.170
9	6.508	0.013425	0.1338	618.23	10.619	16936.2	111802	1.507	0.031	0.169
10	6.672	0.014565	0.1309	632.41	10.756	17105.9	113238	1.522	0.031	0.169
11	6.675	0.016876	0.1317	630.25	10.490	16618.4	110437	1.480	0.031	0.170
12	7.090	0.01769	0.1247	666.33	10.981	17478.0	115607	1.557	0.031	0.171
13	6.580	0.0229	0.1348	619.37	10.158	15424.7	106941	1.374	0.031	0.165
14	30.189	0.003716	0.0286	2,860.57	45.098	55767.7	474800	4.965	0.031	0.143
15	29.190	0.005826	0.0295	2,781.26	45.091	57124.9	474727	5.082	0.031	0.144
16	28.479	0.008052	0.0303	2,716.86	44.480	57207.4	468295	5.089	0.031	0.145
17	27.658	0.01035	0.0313	2,631.05	42.533	53822.2	447798	4.790	0.031	0.144
18	26.155	0.013177	0.0337	2,454.29	36.582	42494.1	385141	3.787	0.031	0.141
19	62.589	0.000877	0.0385	5,805.35	65.717	74202.2	691879	6.620	0.031	0.157
20	59.943	0.001858	0.0388	5,617.75	66.396	78740.1	699027	7.017	0.031	0.157
21	59.292	0.002879	0.0390	5,526.04	61.903	70515.5	651727	6.288	0.031	0.158
22	57.416	0.003956	0.0393	5,364.07	62.405	71611.2	657015	6.384	0.031	0.155
23	56.162	0.005103	0.0395	5,254.17	60.463	70152.1	636565	6.253	0.031	0.157
24	54.839	0.006289	0.0398	5,105.08	56.931	64214.5	599378	5.727	0.031	0.158
25	85.097	0.000604	0.0356	7,915.08	81.433	86494.8	857340	7.714	0.031	0.161
26	84.165	0.001333	0.0357	7,846.90	82.945	88290.8	873259	7.873	0.031	0.158
27	81.632	0.002087	0.0360	7,608.70	81.473	85910.1	857758	7.661	0.031	0.157
28	80.529	0.002832	0.0359	7,633.20	79.115	84200.8	832938	7.495	0.031	0.159
29	77.869	0.003665	0.0363	7,371.19	75.715	80537.9	797140	7.170	0.031	0.160
30	75.915	0.004541	0.0365	7,184.48	78.338	82069.7	824751	7.306	0.031	0.153
31	106.181	0.000497	0.0337	9,838.31	81.637	99114.1	859493	8.843	0.031	0.193
32	103.002	0.001092	0.0340	9,551.36	80.782	98601.4	850484	8.797	0.031	0.191
33	101.997	0.001682	0.0341	9,456.52	81.183	99863.4	854712	8.909	0.031	0.190

# Appendix D: Single- and two-phase calculated data (continued).

Channel F: Water-Nitrogen tests. Number of channels: 11

Channel Dimensions:

Depth ( $\mu\text{m}$ ): 54.090 Hyd. Diameter ( $\mu\text{m}$ ): 55.99

Width ( $\mu\text{m}$ ): 58.02 Channel Length (m): 0.0635

Data Point	G	x	f	Two-phase	Q	h - overall	Heat Flux	Nu	Uncertainty	
	kg/s-m <sup>2</sup>	Quality		Re-avg	(Watts)	W/m <sup>2</sup> -K	(W/m <sup>2</sup> )		U f (%)	U Nu (%)
1	5.707	0.00757	0.1469	563.39	12.111	18931.9	127509	1.691	0.031	0.160
2	5.799	0.011406	0.1460	571.21	11.444	18317.7	120489	1.643	0.031	0.165
3	6.052	0.015963	0.1401	600.45	11.806	18617.0	124295	1.677	0.031	0.163
4	6.287	0.020555	0.1356	625.96	12.244	19072.0	128909	1.726	0.031	0.161
5	6.083	0.027987	0.1411	610.28	11.410	18289.9	120130	1.667	0.031	0.166
6	11.154	0.018141	0.0760	1112.10	21.195	32464.9	223147	2.929	0.031	0.159
7	5.806	0.049745	0.1517	592.21	10.364	16531.9	109114	1.540	0.031	0.166
8	6.262	0.066768	0.1424	651.93	11.259	16544.1	118535	1.567	0.031	0.154
9	7.358	0.051975	0.1207	746.93	12.840	19938.1	135182	1.863	0.031	0.163
10	7.257	0.046232	0.1219	731.37	12.743	19811.3	134163	1.841	0.031	0.163
11	6.092	0.039917	0.1454	605.95	10.579	17727.7	111381	1.638	0.031	0.174
12	20.576	0.083603	0.0462	2098.13	30.131	42521.8	317227	4.120	0.031	0.155
13	30.899	0.008625	0.0284	2922.27	42.640	49316.8	448925	4.432	0.031	0.141
14	30.636	0.018254	0.0286	2955.33	45.138	55816.9	475218	5.057	0.031	0.143
15	29.868	0.028381	0.0295	2926.44	45.153	57203.8	475383	5.231	0.031	0.144
16	29.392	0.03889	0.0303	2913.94	44.565	57316.6	469189	5.296	0.031	0.145
17	28.799	0.04955	0.0313	2877.79	42.638	53954.3	448898	5.040	0.031	0.144
18	27.528	0.062411	0.0337	2749.46	36.696	42626.9	386345	4.040	0.031	0.141
19	62.807	0.004357	0.0385	5850.35	65.731	74217.6	692023	6.649	0.031	0.157
20	60.387	0.009194	0.0388	5710.17	66.425	78774.8	699335	7.083	0.031	0.157
21	59.972	0.01419	0.0390	5667.23	61.945	70563.7	652172	6.379	0.031	0.158
22	58.321	0.019412	0.0393	5552.78	62.464	71678.4	657632	6.511	0.031	0.155
23	57.304	0.024928	0.0395	5493.19	60.536	70237.0	637336	6.414	0.031	0.157
24	56.214	0.030582	0.0398	5392.04	57.016	64310.4	600272	5.908	0.031	0.158
25	85.301	0.003003	0.0356	7957.17	81.445	86507.2	857463	7.738	0.031	0.161
26	84.612	0.006608	0.0357	7939.12	82.971	88318.7	873535	7.925	0.031	0.158
27	82.310	0.010316	0.0360	7748.88	81.513	85952.6	858182	7.741	0.031	0.157
28	81.438	0.013957	0.0359	7824.23	79.168	84257.3	833497	7.601	0.031	0.159
29	79.006	0.018005	0.0363	7610.33	75.781	80607.9	797833	7.302	0.031	0.160
30	77.289	0.02223	0.0365	7473.77	78.422	82158.1	825638	7.473	0.031	0.153
31	106.391	0.002472	0.0337	9881.21	81.647	99125.7	859594	8.865	0.031	0.193
32	103.450	0.00542	0.0340	9642.96	80.803	98626.9	850704	8.845	0.031	0.191
33	102.680	0.008329	0.0341	9596.33	81.216	99903.3	855054	8.984	0.031	0.190

## BIBLIOGRAPHY

- Anderson, T.M., and I. Mudawar, 1989, "Microelectronic Cooling by Enhanced Pool Boiling of a Dielectric Fluorocarbon Liquid," *J Heat Transfer*, v111, August, pp. 752-759.
- Babin, B.R., G.P. Peterson, and D. Wu, 1990, "Steady-State Modeling and Testing of a Micro Heat Pipe," *J Heat Transfer*, v112, pp. 595-601.
- Badran, B., J.M. Albayyari, F.M. Gerner, P. Ramadas, T. Henderson, and K.W. Baker, 1993, "Liquid-Metal Micro Heat Pipes," *Heat Pipes and Capillary Pumped Loops*, ASME HTD-v236, pp. 71-85.
- Bailey, Darin K., 1996, "An Apparatus for the Study of Friction and Heat Transfer in Microchannels," Masters of Science Thesis, Louisiana Tech University.
- Baker, Ovid, 1954, "Simultaneous Flow of Oil and Gas," *The Oil and Gas Journal*, July 26, pp. 185-195.
- Barron, Randall F., 1985, *Cryogenic Systems*, 2nd ed., Oxford Univ. Press, New York.
- Bowers, M.B., and I. Mudawar, 1994, "High Flux Boiling Low Flow Rate, Low Pressure Drop Mini-Channel and Micro-Channel Heat Sinks," *Int J Heat Mass Transfer*, v37, n2, pp. 321-332.
- Cao, Y., A. Faghri, and E.T. Mahefkey, 1993, "Micro/Miniature Heat Pipes and Operating Limitations," *Heat Pipes and Capillary Pumped Loops*, ASME HTD-v236, pp. 55-62.
- Chapra, Steven C., and Raymond P. Canale, 1985, *Numerical Methods for Engineers*, McGraw-Hill, New York.
- Choi, S.B., 1991, "Friction Factors and Heat Transfer in Microtubes," Doctor of Engineering Dissertation, Louisiana Tech University.
- Collier, J. G., 1981, *Convective Boiling and Condensation*, McGraw-Hill, New York NY.

- Cotter, T.P., 1984, "Principles and Prospects for Micro Heat Pipes," *Proc 5th Int Heat Pipe Conf*, Tsukuba, Japan, pp. 328-335.
- Drost, M.K., M.R. Beckett, and R.S. Wegeng, 1994, "Thermodynamic Evaluation of a Microscale Heat Pump," *Microscale Heat Transfer*, ASME HTD-Vol. 291, pp. 35-43.
- Duncan, A.B., and G.P. Peterson, 1994, "Review of Microscale Heat Transfer," *Appl Mech Rev*, v47, n9, September, pp. 397-428.
- Gerner, F.M., J.P. Longtin, H.T. Henderson, W.M. Hsieh, P. Ramadas, and S. Chang, 1992, "Flow and Heat Transfer Limitations in Micro Heat Pipes," *Topics in Heat Transfer - v3*, ASME HTD-v206-3, pp. 99-104.
- Harley, J., J. Pfahler, H. Bau, and J. Zemel, 1989a, "Transport Processes in Micron and Submicron Channels," *Convection Heat Transfer and Transport Processes*, ASME HTD - Vol. 116, pp. 1-5.
- Harley, J., and H. Bau, 1989b, "Fluid Flow in Micron and Submicron Size Channels," *Proceedings of the 1989 Micro Electro Mechanical Systems Workshop*, Salt Lake City, Utah, February 20-22, pp. 25-28.
- Hartnett, J. P., and M. Kostic, 1989, "Heat Transfer in Newtonian and Non-Newtonian Fluids in Rectangular Channels," *Adv Heat Transfer*, v19, pp. 247-356.
- Hayduk, W., 1981, *Encyclopedia of Fluid Mechanics, Vol. 1: Flow Phenomena and Measurement; Chapter 3: Correlation for Molecular Diffusivities in Liquids*, Gulf Press, Houston, Texas.
- He, J.G., 1988, "Experimental Investigation for Enhancing Effect of Polymeric Additives on Subcooled Nucleate Flow Boiling with Higher Velocity," Master of Science Thesis, Tsinghua University, Beijing, China.
- Holman, Jack Phillip, 1984, *Experimental Methods for Engineers*, 4<sup>th</sup> ed., McGraw-Hill, New York.
- Incropera, Frank W., and David P. DeWitt, 1985, *Fundamentals of Heat and Mass Transfer*, 2<sup>nd</sup> ed., John Wiley and Sons, New York.
- Khrustalev, D., and A. Faghri, 1994, "Thermal Analysis of a Micro Heat Pipe," *J Heat Transfer*, v116, February, pp. 189-198.



- Lockhart, R. W., and R. C. Martinelli, 1949, "Proposed Correlation of Data for Isothermal Two-Phase, Two-Component Flow in Pipes," *Chem Engr Progress*, v45, n1, pp. 41-48.
- Little, W.A., 1990a, "Advances in Joule-Thompson Cooling," *Adv Cryo Engr*, v35, Plenum Press, New York, pp. 1305-1314.
- Little, W.A., 1990b, "Microminiature Refrigerators for Joule-Thompson Cooling of Electronic Chips and Devices," *Adv Cryo Engr*, v35, Plenum Press, New York, pp. 1325-1333.
- Little, W.A., 1984, "Microminiature Refrigeration," *Rev Sci Instrum*, v55, n5, pp. 661-680.
- Longtin, J.P., Badran, B., and F.M. Gerner, 1992, "A One-Dimensional Model of a Micro Heat Pipe during Steady-State Operation," *Heat Transfer on the Microscale*, ASME HTD - v 200, pp. 23-33.
- Mallik, A.K., G.P. Peterson, and M.H. Weichold, 1992, "On the Use of Micro Heat Pipes as Integral Part of Semiconductor Devices," *J Elec Packaging*, v114, pp. 436-442.
- Martinelli, R. C., L. M. K. Boelter, T. H. M. Taylor, E. G. Thomsen, and E. H. Morrin, 1944, "Isothermal Pressure Drop for Two-Phase Two-Component flow in a Horizontal Pipe," *Trans ASME*, February, pp.139-151.
- Martinelli, R. C., and D. B. Nelson, 1948, "Prediction of Pressure Drop During Forced Circulation Boiling of Water," *Trans ASME*, August, pp. 695-702.
- Marto, P.J., and Lt. V.J. Lepere, USN, 1982, "Pool Boiling Heat Transfer From Enhanced Surfaces to Dielectric Fluids," *J Heat Transfer*, v104, pp. 292-299.
- McAdams, W. H., W. K. Woods, and L. C. Heroman, Jr., 1942, "Vaporization Inside Horizontal Tubes - II - Benzene-Oil Mixtures," *Trans ASME*, v64, pg. 193.
- Mudawar, I., and T.M. Anderson, 1993, "Optimization of Enhanced Surfaces for High Flux Chip Cooling by Pool Boiling," *J Electronic Packaging*, v115, pp. 89-100.
- Mudawar, I., and T.M. Anderson, 1990, "Parametric Investigation Into the Effects of Pressure, Subcooling, Surface Augmentation and Choice of Coolant on Pool Boiling in the Design of Cooling Systems for High-Power-Density Electronic Chips," *J Electronic Packaging*, v112, pp. 375-382.

- Mudawar, I., and M.B. Bowers, 1995, "Parametric Study of Ultra-High CHF in Highly Subcooled Water Flow Inside Small Diameter Tubes," Engineering Foundation Conference on Convective Flow Boiling, Banff, Alberta, April 30 - May 5, Paper II-9.
- Peng, X.F., and B.-X. Wang, 1993, "Forced Convection and Flow Boiling Heat Transfer for Liquid Flowing through Microchannels," *Int J Heat Mass Transfer*, v36, n14, pp. 3421-3427.
- Peterson, G.P., 1992, "Overview of Micro Heat Pipe Research and Development," *Appl Mech Rev*, v45, n5, pp. 175-189.
- Peterson, G.P., A.B. Duncan, and M.H. Weichold, 1993, "Experimental Investigation of Micro Heat Pipes Fabricated in Silicon Wafers," *J Heat Transfer*, v115, August, pp. 751-756.
- Peterson, G.P., A.B. Duncan, A.S. Ahmed, A.K. Mallik, and M.H. Weichold, 1991, "Experimental Investigation of Micro Heat Pipes in Silicon Wafers," *Micromechanical Sensors, Actuators, and Systems*, ASME DSC-v32, pp. 341-348.
- Pfahler, J., J. Harley, H. Bau, and J.N. Zemel, 1991, "Gas and Liquid Flow in Small Channels," *Micromechanical Sensors, Actuators, and Systems*, ASME DSC - v 32, 49-60.
- Pfahler, J., J. Harley, H. Bau, and J.N. Zemel, 1990a, "Liquid and Gas Transport in Small Channels," *Microstructures, Sensors and Actuators*, ASME DSC-v19, Dallas, Texas, Nov. 25-30, 149-157.
- Pfahler, J., J. Harley, H. Bau, and J.N. Zemel, 1990b, "Liquid Transport in Micron and Submicron Channels," *Sensors and Actuators*, A21-23, 431-434.
- Reid, Robert C., John M. Prausnitz, and Bruce E. Poling, 1987, *The Properties of Gases and Liquids*, 4<sup>th</sup> ed., McGraw-Hill, New York.
- Schenck, Hilbert Jr., 1968, *Theories of Engineering Experimentation*, 2<sup>nd</sup> ed., McGraw-Hill, New York.
- Sonntag, Richard E., and Gordon J. Van Wylen, 1991, *Introduction to Thermodynamics: Classical and Statistical*, 3rd ed., John Wiley and Sons, New York.

- Stanley, R. S., T. A. Ameel, and R.O. Warrington, 1996, "Convective Flow Boiling in Microgeometries: A Review and Applications," *Convective Flow Boiling*, Proceedings of the First International Conference on Convective Flow Boiling, Ed. John Chen, pp. 305-310.
- Suo, M., and P. Griffith, 1964, "Two-Phase Flow in Capillary Tubes," *J Basic Engr*, September, pp. 576-582.
- Swanson, L.W., and G.P. Peterson, 1995, "The Interfacial Thermodynamics of Micro Heat Pipes," *J Heat Transfer*, v117, February, pp. 195-201.
- Swanson, L.W., and G.P. Peterson, 1993, "The Interfacial Thermodynamics of the Capillary Structures in Micro Heat Pipes," *Heat Transfer on the Microscale*, ASME HTD - v253, pp.45-51.
- White, Frank M., 1986, *Fluid Mechanics*, 2<sup>nd</sup> ed., McGraw-Hill, New York.
- Wright, N., and B. Gebhart, 1989, "Enhanced Boiling on Microconfigured Surfaces," *J Electronic Packaging*, v111, pp. 112-120.
- Wu, P., and W.A. Little, 1983, "Measurement of Friction Factor for the Flow of Gases in Very Fine Channels Used for Microminature Joule-Thompson Refrigerators," *Cryogenics*, May, pp. 273-277.
- Wu, D., and G.P. Peterson, 1991a, "Transient Experimental Investigation of Micro Heat Pipes," *AIAA J ThermoPhysics*, v5, n4, Oct.-Dec., pp. 539-544.
- Wu, D., and G.P. Peterson, 1991b, "Investigation of the Transient Characteristics of a Micro Heat Pipe," *AIAA J Thermophysics*, v5, n2, April-June, pp. 129-134.
- Yu, D., R.O. Warrington, R.F. Barron, and T.A. Ameel, 1995, "An Experimental and Theoretical Investigation of Fluid Flow and Heat Transfer in Microtubes," 4th ASME/JSME Thermal Engineering Joint Conference, March, Maui, Hawaii.
- Zhukov, V.M., and I.L. Yarmak, 1990, "Transient Heat Transfer in Two-Phase Cryogenic Liquid Forced Flows Under Step Heat Flux in Narrow Channels," *Cryogenics*, v30, pp. 82-286.

## VITA

Mr. Stanley is a life long native of Louisiana, originally from Winnsboro. He graduated in 1984 from Airline High School in Bossier City. As an undergraduate at Louisiana Tech, he was active in the student chapter of the American Society of Mechanical Engineers and the Tau Beta Pi Engineering Honor Society. Mr. Stanley received his Bachelor of Science in 1989 and his Master of Science in 1992, from Louisiana Tech. As a graduate student, Mr. Stanley participated in numerous research projects, had several publications, and was an instructor for the Department of Mechanical and Industrial Engineering. Currently, Mr. Stanley is an instructor at Louisiana Tech and conducting research in the micro thermal fluids area at the Institute for Micromanufacturing.